

GEOLOGICAL FIELDWORK 2009

A SUMMARY OF FIELD ACTIVITIES AND CURRENT RESEARCH





GEOLOGICAL FIELDWORK 2009

A Summary of Field Activities and Current Research

**Ministry of Energy, Mines
and Petroleum Resources**
British Columbia Geological Survey

Paper 2010-1

Ministry of Energy, Mines and Petroleum Resources

Mining and Minerals Division

British Columbia Geological Survey

Parts of this publication may be quoted or reproduced if source and authorship are acknowledged.
The following is the recommended format for referencing individual works contained in this publication:

Schiarizza, P. and Massey, N.W.D. (2010): Geochemistry of volcanic and plutonic rocks of the Sitlika assemblage, Takla Lake area, central British Columbia (NTS 093N/04, 05, 12, 13); in *Geological Fieldwork 2009, BC Ministry of Energy Mines and Petroleum Resources*, Paper 2010-1, pages 55–68.

COVER PHOTO: *Campsite located at the western contact of the Aley carbonatite. Fieldwork conducted during the summer of 2009 forms part of an MSc study by Duncan McLeish of the University of Victoria. This work is partially funded by the UVic-MEMPR partnership agreement. Photo by Mitch Mihalynuk, project geologist.*

This publication is also available, free of charge, as colour digital files, in Adobe Acrobat PDF format, from the BC Ministry of Energy, Mines and Petroleum Resources website at:

<http://www.empr.gov.bc.ca/Mining/Geoscience/PublicationsCatalogue/Fieldwork/Pages/default.aspx>

British Columbia Cataloguing in Publication Data

Main entry under title:

Geological Fieldwork: - 1974 -

Annual.

Issuing body varies

Vols. For 1978-1996 issued in series: Paper / British Columbia. Ministry of Energy, Mines and Petroleum Resources; vols for 1997- 1998, Paper / British Columbia. Ministry of Employment and Investment; vols for 1999-2004, Paper / British Columbia Ministry of Energy and Mines; vols for 2005- , Paper / British Columbia Ministry of Energy, Mines and Petroleum Resources.

Includes Bibliographical references.

ISSN 0381-243X=Geological Fieldwork

1. Geology - British Columbia - Periodicals. 2. Mines and mineral resources - British Columbia - Periodicals. 3. Geology - Fieldwork - Periodicals. 4. Geology, Economic - British Columbia - Periodicals. 5. British Columbia. Geological Survey Branch - Periodicals. I. British Columbia. Geological Division. II. British Columbia. Geological Survey Branch. III. British Columbia. Geological Survey Branch. IV. British Columbia. Dept. of Mines and Petroleum Resources. V. British Columbia. Ministry of Energy, Mines and Petroleum Resources. VI. British Columbia. Ministry of Employment and Investment. VII. British Columbia Ministry of Energy and Mines. VIII. Series: Paper (British Columbia. Ministry of Energy, Mines and Petroleum Resources). IX. Series: Paper (British Columbia. Ministry of Employment and Investment). X. Series: Paper (British Columbia Ministry of Energy and Mines). XI. Series: Paper (British Columbia Ministry of Energy, Mines and Petroleum Resources).

QE187.46 622.1'09711 C76-083084-3 (Rev.)

VICTORIA
BRITISH COLUMBIA
CANADA

JANUARY 2010

FOREWORD

Geological Fieldwork 2009

The provision of accessible, new geoscience data about British Columbia is aimed primarily at increasing mineral tenure acquisition and mineral exploration activity in the province. The British Columbia Geological Survey (BCGS) presents here the results of field surveys and geoscience research for 2009 in a thirty-fifth edition of *Geological Fieldwork*. Most articles are contributions by survey staff to the understanding of the geology, geochemistry and mineral deposits of the province. The volume also includes contributions about collaborative research with other organizations and projects completed by other professional geoscientists.

British Columbia Geological Survey Successes

The BCGS, in partnership with Geoscience BC, Smithers Exploration Group and the Northwest Community College, began a surficial geology and till sampling program southeast of Houston. Preliminary work indicates that cover by glacial deposits in this part of the Nechako Plateau is not as extensive as previously thought.

The first season of the north coast project, carried out jointly with the Geological Survey of Canada (GSC), covered an area of 30 by 50 km. Mapping on Porcher Island and along the adjacent Grenville Channel found geological indicators commonly associated with volcanogenic massive sulphide deposits.

The Iskut River project commenced in the fall with a 10-day field season. A partnership with the University of Victoria, Pacific North West Capital Corp and the GSC, the objective is to investigate mineralization within the Coast Belt of northwestern British Columbia.

Our online interface MapPlace and its supporting site now exceed 11 000 web pages. Used 24 hours a day, 7 days a week by the exploration community worldwide, this interface plays an essential and growing role in attracting investment to the province.

Numerous mineral resource assessments to facilitate government land use planning were completed.

The Property File database captured 2860 new documents and maps for the QUEST area and 1540 for other areas, while 481 MINFILE occurrences were updated and 17 new ones identified. Contracts for both projects were funded by Geoscience BC.

BCGeology Map, BC's digital geology map, is undergoing its first major update since release in 2005. Throughout 2009, a team from the BCGS, Geoscience BC and the GSC worked to update the Quesnel Trough geology for the QUEST geophysical area.

Survey staff updated our website and moved servers as part of a government-wide initiative.

The BC Mineral Development Office in Vancouver hosted national and international delegations of potential investors and was a key player in organizing the Asia Investment Mission.

Survey geologists were organizers and presenters at conferences and workshops around the province, and led industry field trips in the northeastern coalfields and the Merritt and Princeton areas, as well as a copper-gold mine tour.

The BCGS hosted its first Open House of the 21st century in Victoria in the fall. The event was a success, with more than 85 participants, and will be continued in 2010.

D.V. Lefebure
Chief Geologist
British Columbia Geological Survey

CONTENTS

Demchuk, T., Fredericks, J., Jones, L., Lefebure, D.V. and Rowins, S.: British Columbia Geological Survey activities in 2009 1

NORTHERN BRITISH COLUMBIA

Mihalynuk, M.G. Stier, T.J., Jones, M.I. and Johnston, S.T.: Stratigraphic and structural setting of the Rock and Roll deposit, northwestern British Columbia (NTS 104B/11). 7

Nelson, J.L., Mahoney, J.B., Gehrels, G.E., van Staal, C. and Potter, J.J.: Geology and mineral potential of Porcher Island, northern Grenville Channel and vicinity, northwestern British Columbia 19

CENTRAL BRITISH COLUMBIA

Ferbey, T.: Quaternary geology and till geochemistry of the Nadina River map area (NTS 093E/15), west-central British Columbia 43

Schiarizza, P. and Massey, N.W.D.: Geochemistry of volcanic and plutonic rocks of the Sitlika assemblage, Takla Lake area, central British Columbia (NTS 093N/04, 05, 12, 13). 55

Paradis, S., Simandl, G.J., Bradford, J., Leslie, C. and Brett, C.: Carbonate-hosted lead-zinc mineralization on the Cariboo Zinc property, Quesnel Lake area, east-central British Columbia (NTS 093A/14E, 15W). 69

Simandl, G.J., Paradis, S., Simandl, L. and Dahrouge, J.: Vermiculite in the Blue River area, east-central British Columbia, Canada (NTS 083D/06). 83

Hora, Z.D., Langrová, A., Pivec, E. and Žák, K.: Niobium-thorium-strontium-rare earth element mineralogy and preliminary sulphur isotope geochemistry of the Eaglet property, east-central British Columbia (NTS 093A/10W) . 93

SOUTHERN BRITISH COLUMBIA

Soloviev, S.G.: Evaluation of 'reduced' intrusive-related gold mineralization in the area west of Cranbrook, southeastern British Columbia (NTS 082F/08, 16) 97

Massey, N.W.D. and Oliver, S.L.: Southern Nicola Project: Granite Creek area, southern British Columbia (parts of 92H/07, 10), 113

Massey, N.W.D., Gabites, J.E., Mortensen, J.K. and Ullrich, T.D.: Boundary Project: geochronology and geochemistry of Jurassic and Eocene intrusions, southern British Columbia (NTS 082E). 127

Massey, N.W.D.: Boundary Project: Geochemistry of volcanic rocks of the Wallace Formation, Beaverdell area, south-central British Columbia (NTS 082E/06E, 07W, 10W, 11W) 143

Oliver, S.L., Hickey, K.A. and Russell, J.K.: Redefining the southern Nicola Group: petrographic and structural characterization of the Eastgate-Whipsaw metamorphic belt, southern British Columbia (NTS 092H/02E) 153

Mihalynuk, M.G., Logan, J., Friedman, R.M. and Preto, V.A.: Age of mineralization and 'Mine Dykes' at Copper Mountain alkaline copper-gold-silver porphyry deposit (NTS 092H/07), south-central British Columbia. 163

PROVINCE-WIDE

Hancock, K.D. and Barlow, N.D.: British Columbia's Property File: project update and a case study of an integrated MapPlace analysis of a target hidden in the files 173

Lett, R.E. and Jackaman, W.: Preliminary review of the effect of analytical method variability on regional geochemical survey data, British Columbia 179

GEOLOGICAL SURVEY BRANCH STAFF AND CONTRACTORS

Ministry of Energy, Mines and Petroleum Resources

Name	Title	Phone	E-Mail
Dave Lefebure	Chief Geologist	250-952-0374	Dave.Lefebure@gov.bc.ca
Jay Fredericks	Director, BC Mineral Development Office	604-660-3332	Jay.Fredericks@gov.bc.ca
Larry Jones	Director, Resource Information	250-952-0386	Larry.Jones@gov.bc.ca
Stephen Rowins	Director, Geoscience Initiatives	250-952-0454	Stephen.Rowins@gov.bc.ca
Yao Cui	Geomatics Geoscientist	250-952-0440	Yao.Cui@gov.bc.ca
Laura de Groot	Database Manager	250-952-0387	Laura.deGroot@gov.bc.ca
Tania Demchuk	Manager, Geoscience Marketing and Partnerships	250-952-0417	Tania.Demchuk@gov.bc.ca
Pat Desjardins	GIS Geologist	250-952-0425	Pat.Desjardins@gov.bc.ca
Larry Diakow	Metals Senior Project Geologist	250-952-0430	Larry.Diakow@gov.bc.ca
Travis Ferbey	Quaternary Geologist	250-953-3773	Travis.Ferbey@gov.bc.ca
Kirk Hancock	MapPlace Resource Geoscientist	250-952-0433	Kirk.Hancock@gov.bc.ca
Andrew Legun	Coal Project Geologist	250-952-0446	Andrew.Legun@gov.bc.ca
Ray Lett	Geochemist	250-952-0396	Ray.Lett@gov.bc.ca
Jim Logan	Metals Senior Project Geologist	250-952-0436	Jim.Logan@gov.bc.ca
Nick Massey	Mapping Project Geoscientist (Southeast)	250-952-0428	Nick.Massey@gov.bc.ca
Sarah Meredith-Jones	Mineral Inventory Geologist	250-387-5261	Sarah.MeredithJones@gov.bc.ca
Mitch Mihalynuk	Mapping Senior Project Geologist (Central)	250-952-0431	Mitch.Mihalynuk@gov.bc.ca
JoAnne Nelson	Mapping Senior Project Geologist (Northwest)	250-952-0438	JoAnne.Nelson@gov.bc.ca
Graham Nixon	Mapping Senior Project Geologist (Southwest)	250-952-0448	Graham.Nixon@gov.bc.ca
Bruce Northcote	Regional Geologist	604-660-2713	Bruce.Northcote@gov.bc.ca
Patrick Saunders	Geoscience Assistant, Vancouver office	604-660-2708	Patrick.Saunders@gov.bc.ca
Paul Schiarizza	Mapping Senior Project Geologist (Central)	250-952-0434	Paul.Schiarizza@gov.bc.ca
George Simandl	Industrial Minerals Specialist	250-952-0413	George.Simandl@gov.bc.ca
Arlene Veenhof	Finance and Management (A/Section) Admin Assistant	250-952-0372	Arlene.Veenhof@gov.bc.ca
Allan Wilcox	Assessment Report Geologist	250-952-0390	Allan.Wilcox@gov.bc.ca

British Columbia Geological Survey Activities in 2009

by T. Demchuk, J. Fredericks, L. Jones, D.V. Lefebure and S. Rowins

INTRODUCTION

The British Columbia Geological Survey (BCGS) is committed to supporting a thriving, safe and responsible mining industry for the benefit all British Columbians. We accomplish this by providing expert advice to government on mineral resources, globally competitive geoscience expertise, data to attract mineral industry investment, and geoscience information to the public.

The BCGS focused on creating new products from existing data, completing five significant field projects (four with partners), delivering key programs like MapPlace and the BC Mineral Development Office, and working to support a wide variety of clients. Many of our programs involve co-operative partnerships with universities, other government agencies, First Nations, local communities and industry.

The BCGS continued its long collaboration with the Geological Survey of Canada (GSC) with the start of a new major program in the north, called 'Edges'. It was the last year of the GSC's Targeted Geoscience Initiative in southern and central BC. Geoscience BC, a key partner of the BCGS, had another very active year contributing new geophysical, geochemical and other geoscience data. Projects with Geoscience BC in 2009 included a surficial mapping and till sampling program southwest of Houston, MINFILE and Property File updates in the QUEST area (Quesnel Trough), and uploading Geoscience BC data on MapPlace. The BCGS worked with the Resource Development and Geoscience Branch, its sister branch in the Ministry of Energy, Mines and Petroleum Resources (MEMPR), on several projects. The BCGS also continued its active support of the National Geological Surveys Committee and the Committee of Provincial Geologists.

The BCGS and its staff were recognized by both industry and government for the successful delivery of programs and results. The Fraser Institute, in its annual 'Survey of Mining Companies 2008/2009', ranked British Columbia seventh globally with regards to the quality of our geological database. Geoscience results from west of Williams Lake and northern Vancouver Island, released at Mineral Exploration Roundup in January 2009, led to 2800 and 1500 hectares of staking of BCGS mineralization discoveries, respectively. The Geoscience Assistant Program was a finalist for a Premier's Award in the partnerships category and received an honourable mention.

This publication is also available, free of charge, as colour digital files in Adobe Acrobat® PDF format from the BC Ministry of Energy, Mines and Petroleum Resources website at <http://www.empr.gov.bc.ca/Mining/Geoscience/PublicationsCatalogue/Fieldwork/Pages/default.aspx>.

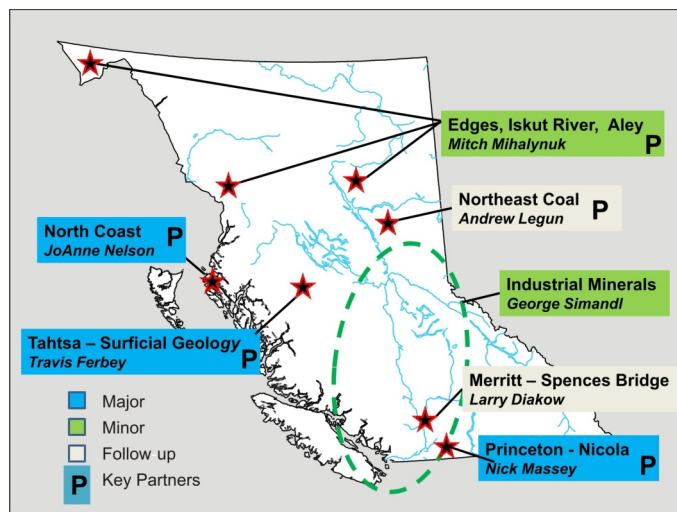


Figure 1: British Columbia Geological Survey field project areas, 2009.

BCGS FIELD ACTIVITIES

The British Columbia Geological Survey makes it a priority to generate new geoscience data and products, including bedrock and surficial geology maps and deposit studies. The survey collaborated with a number of partners, including the GSC, Geoscience BC and several companies, to deliver most of the field surveys. The location of the 2009 field projects are shown in Figure 1. Our objective is to help diversify local economies by attracting mineral exploration activity that may lead to new mines. In all parts of the province, both mineral exploration and mining are essential drivers of local employment and tax revenue, and directly support the development of regional infrastructure.

Field mapping and mineral deposit studies (Figure 1) were continued in the Merritt area, the Peace River coalfields and the Princeton area (Massey et al., Massey and Oliver, Oliver et al., this volume), and on industrial minerals in east-central BC (Simandl, this volume). The Edges project in northern BC started in 2009 with the primary fieldwork in the north coast (Nelson et al., this volume) and Iskut River areas (Mihalynuk et al., this volume). The other new field project was the Tahtsa Lake area Quaternary geology and till geochemistry survey in the region southwest of Houston and northeast of the Huckleberry mine (Ferbey, this volume).

In addition to these 2009 projects, several other projects were brought to completion. These include age determinations of mineralization and 'Mine Dykes' at the Copper Mountain alkalic porphyry Cu-Au-Ag deposit (Mihalynuk et al., this volume), and a discussion of the geochemistry of Permo-Triassic volcanic and plutonic rocks of

the Sitlika assemblage near Takla Lake (Schiarizza and Massey, this volume). Several follow-up studies were also completed on BC mineral properties and regions. These include investigations of the Nb–Th–Sr–rare earth element mineralogy and sulphur isotope geochemistry of the Eaglet property (Hora et al., this volume); a geological characterization of carbonate-hosted Pb–Zn mineralization at the Cariboo Zinc property in the Quesnel Lake area (Paradis et al., this volume); and an evaluation of reduced intrusion-related gold mineralization west of Cranbrook (Soloviev, this volume). A technical paper on the effects of analytical method on regional geochemical surveys (Lett and Jackaman, this volume) rounds out the contributions.

Ongoing Projects

Geological highlights from Massey and Oliver (2009) included mapping northwards from Whipsaw Creek into the Granite Creek and Tulameen River areas, concentrating on the Nicola Group rocks. Field observations confirmed that the Eastgate–Whipsaw metamorphic belt is lithologically distinct from the Nicola Group to the east. The presence of volcanogenic massive sulphide (VMS) mineral prospects (e.g., Redstar) reinforces the necessity of understanding the geological differences between the Eastgate–Whipsaw metamorphic belt and the Nicola Group rocks for effective exploration. Shelley Oliver, a graduate student completing an MSc thesis at The University of British Columbia, further redefined the geology of the Eastgate–Whipsaw metamorphic belt through a petrographic and structural study (Figure 2).

Major New Projects

EDGES: MODELLING THE EVOLUTION OF THE NORTHERN CORDILLERA RESOURCE ENVIRONMENT FROM THE EDGES OF EXOTIC TERRANES

Edges is a highly focused multiyear geological mapping initiative involving formal collaboration between the Government of Canada, the Province of British Columbia, the Yukon Territory, Geoscience BC, the United States Geological Survey and the Alaska Department of Geological and Geophysical Surveys. A key project in the federal Geoscience for Energy and Minerals (GEM) program, it began field operations in 2009 in BC and will last until 2013. Support is being contributed by all participating agencies.

The ultimate goal of the initiative is to improve the effectiveness of resource exploration and discovery in the northern cordillera by outlining resource-rich environments in British Columbia, the Yukon and Alaska. The geological targets are the exotic outer terranes with their enclosed pre-accretionary syngenetic and epigenetic deposits, and the metal-rich Triassic through Paleogene magmatic arcs and associated accretion zones that resulted from interaction of the terranes with the western margin of ancient North America. The target areas include parts of northern and central BC where the geological map base is either several decades out of date or at a scale insufficient to evaluate mineral potential using modern tectonic interpretations.



Figure 2: Shelley Oliver and Nick Massey during fieldwork in the Whipsaw Creek area, southern British Columbia.

NORTH COAST PARTNERSHIP PROJECT (EDGES)

JoAnne Nelson completed a successful initial field season mapping on Porcher Island and the adjacent Grenville Channel south of Prince Rupert (Figure 3). Her activities were carried out with help from Brian Mahoney (and his graduate students) from the University of Wisconsin, George Gehrels of the University of Arizona, Cees van Stahl from the GSC and Richard Bryant from the Lax Kw'alaams First Nation. The north coast project team

completed geological mapping of an area measuring 30 by 50 km;

traced rock units of the Alexander terrane of southeastern Alaska into northwestern BC, including those that are known to host VMS mineralization; and

determined that geological indicators of VMS-style systems occur in two trends, one on northeastern Porcher Island and, offset across the Salt Lagoon fault, on northeastern Pitt Island, and the other on the mainland coast east of the Grenville Channel fault and Telegraph Passage.

ISKUT RIVER PARTNERSHIP PROJECT

Mitch Mihalynuk, along with University of Victoria graduate student Toby Stiers and Murray Jones of Equity Exploration Consultants Ltd, spent ten days last fall studying precious-metal-rich, polymetallic massive sulphide mineralization at the Rock and Roll deposit, within the Coast Belt of northwestern BC. The short-term goal of the project is to determine the stratigraphic and structural setting of the Rock and Roll deposit. The longer term goal is to evaluate the potential for similar mineralization within the Iskut and adjacent regions. This work was the initial phase of a BCGS partnership with the University of Victoria and

Pacific North West Capital Corp (and field representatives, Equity Exploration Consultants Ltd).

TAHTSA LAKE PARTNERSHIP PROJECT

Travis Ferbey, in partnership with Geoscience BC, the Northwest Community College and the Smithers Exploration Group, completed a till geochemistry survey northeast of the Huckleberry mine and southwest of the past-producing Equity Silver mine, in NTS 093E/15 (west-central BC). This is an area that has high potential to host porphyry $\text{Cu}\pm\text{Mo}\pm\text{Au}$ and polymetallic vein occurrences, and possibly VMS-type deposits. Quaternary till cover presents a challenge to traditional prospecting and makes the area ideally suited for a mineral potential assessment using till geochemistry. In total, 100 till samples were collected for analysis (Figure 4). Samples were collected regionally and near known metallic mineral occurrences to characterize detrital dispersal and to document precious metal, base metal and pathfinder element values.

Observations made at 164 field stations suggest that Quaternary sediments within the study area are less areally extensive and thinner than anticipated, and therefore may not be as significant a hindrance to mineral exploration as previously thought.

BCGEOLOGY MAP QUEST AREA UPDATE

The BCGS, Geoscience BC and the GSC are collaborating to update the province's digital geology map at 1:100 000 scale for the Quesnel Trough area in central BC. The update area corresponds to Geoscience BC's QUEST Project geophysical survey footprint, which extends from Williams Lake to Mackenzie. Jim Logan is leading the project with help from Colin Barnett (Geoscience BC) and Bert Struik (GSC).

A workshop was held on March 11–13, 2009 to bring Travis Ferbey, Ray Lett, Jim Logan, Mitch Mihalyuk, JoAnne Nelson and Paul Schiarizza from the BCGS together with Fil Ferri (Resource Development and Geoscience Branch of MEMPR), Bert Struik and geophysicists from the GSC, and Colin Barnett, Peter Kowalczyk and other contractors from Geoscience BC.

The workshop was the first step in integrating all bedrock mapping and geophysical and geochemical data for the region. Subsequent work by geology team members was required to determine the final map pattern. A key objective is to interpret and update bedrock geology in areas with significant glacial overburden, particularly in the Prince George region. Initial results were released in poster format at the Kamloops Exploration Group (KEG) annual conference in April 2009. The final map will be integrated into MapPlace by Pat Desjardins and Yao Cui, and released as a Geoscience Map early in 2010.



Figure 3: JoAnne Nelson, mapping on Porcher Island, western British Columbia.

MAPPLACE AND DATABASE ACTIVITIES

MapPlace

MapPlace, our internet portal and one of the most effective geoscience online map systems globally, continues to improve with the addition of new data layers and improved interface tools. MapPlace has provided clients with efficiencies in research time, data costs and analysis. Data themes and applications available on MapPlace include mineral potential, bedrock and surficial geology, publications, mineral and petroleum tenure, MINFILE, assessment reports, and geochemical and geophysical surveys. Yao Cui



Figure 4: Russ Gawa, a graduate from the Reclamation and Prospecting Program at the Northwest Community College, collecting a till sample, west-central British Columbia.

and Pat Desjardins contributed geomatics expertise to MapPlace data and application enhancements and integration of servers.

New data and updates on MapPlace in 2009 include regional geochemistry catchment basins and regional geochemistry survey (RGS) locations snapped to 1:20 000 scale rivers;
mineral tenure archives for January 2007 and January 2008;
physiographic subdivisions and volcanic centres;
wildlife habitat areas, ungulate winter range, fish-sensitive watersheds and guide outfitters;
MapPlace2Go updates with current mines and exploration properties;
reanalysis of 3479 archived stream and lake sediment samples that cover parts of NTS areas 093E, F, L and M (Geoscience BC Report 2009-5); and
infill stream sediment and water geochemical data for 1007 samples from NTS areas 093F and K (Geoscience BC Report 2009-11).

Property File and Databases

Property File, a collection of an estimated 100 000 unique industry documents and maps, continued to grow during 2009. Recent Property File donations were made by Ken Dawson and the families of Cam Stephens and Dennis Groc. As of December 2009, 9598 Property File documents were available online, including 396 documents from the Falconbridge Collection, 1649 documents from the Cyprus-Anvil Collection, 304 documents from Chevron Collection, 476 documents from the Placer Dome Collection, 1328 documents from the Rimfire Collection, 2969 Mine Plans and 2070 documents from the Library Collection. These are retrieved through the Property File search application or through links from MINFILE. This volume includes an update on the Property File project (Hancock and Barlow, this volume) and a case study on using the database in conjunction with MapPlace.

Geoscience BC funding for two QUEST projects contributed to updates to Property File and MINFILE. The QUEST Property File project added 2619 new Property File items and new information to 481 MINFILE occurrences, and created 17 new occurrences. The QUEST MINFILE update included updates to 497 occurrences, including 135 new ones. Sarah Meredith-Jones is the MINFILE contact.

Users can now access more than 30 000 company mineral assessment reports using the Assessment Report Indexing System (ARIS) database over the web. Allan Wilcox works with clients to approve reports. An initiative is underway to encourage the mining industry to submit assessment reports in digital form to the Mineral Titles Branch. Benefits include higher quality, more efficient digital reports; quicker approval; and lower costs for printing, mailing, storage, scanning and processing.

Other database activity included standardizing data tables for efficient tracking of exploration activity in the province, moving all database applications to new servers, adding 18 new Mineral Deposit Profiles, updates to the publication catalogue, and an enhanced scale-based density display of RGS and MINFILE in KML format, with links to detailed reports.

Yao Cui developed a high-performance algorithm for delineating catchment basins and presented dynamic spatial data on Google™ Earth using free and open-source tools. Laura de Groot contributed to the conversion of more than 11 000 web pages to the new government standard and keeps staff on track with database management plans.

Mineral Resource Evaluations

The Level 2 Mineral Resource Assessment of the Atlin-Taku Land Planning Area, conducted in 2008, resulted in the publication of GeoFile 2009-5 (Atlin-Taku Mineral Resource Assessment), which included methodology; data tables; a Manifold® map; metallic and industrial mineral potential maps in PDF; a geology map in PDF; a geology map with tracks and geology legend; workshop photos; shape files; MINFILE, ARIS and RGS tables and reports; and an interactive map on MapPlace.

During the past year, Kirk Hancock, Sarah Meredith-Jones and Allan Wilcox provided 15 assessments of the mineral resource potential of different areas of BC for the Ministry of Aboriginal Relations and Reconciliation, to assist with treaty negotiations.

BCGeology Map: BC's Digital Bedrock Geology Map

The province's bedrock geology map for industry and government clients is a critical source of information for deciding on areas for exploration and assessing mineral potential. Updating is an important, ongoing task to weave the new data into the digital provincial product, BCGeology Map. The data-specification model and maintenance strategy are being developed and implemented by Yao Cui.

The Geology Map of BC (Geoscience Map 2009-1) is available on one sheet at 1:1 500 000 or 1:2 000 000 scale and as a Manifold® map file. The cartographically correct map has a simplified legend.

BC MINERAL DEVELOPMENT OFFICE

The role of the BC Mineral Development Office (MDO) in Vancouver is to promote investment in the province's mineral exploration and mining, both domestically and internationally. This includes delivering a multifaceted technical campaign to highlight the province's superior coal and mineral potential, renowned geoscience database and expertise, and attractive business climate. The MDO interacts with decision-makers in industry, including executive management, geologists and prospectors, and forms part of the wider marketing efforts of the Ministry of Energy, Mines and Petroleum Resources (MEMPR). The MDO also hosts incoming national and international companies and government representatives, and provides leadership for government trade missions. Some examples of MDO activities in the past year include

acting as a key player to profile information on BC's mineral resources, investment procedures and specific mineral commodities to Asian investors, including the Asia Investment Mission to China, Japan and Korea in October and the first provincial Virtual Trade Mission in June, presented via video-conferencing facilities to BC's trade offices in Beijing, Shanghai and Guangzhou;

preparing articles on BC's mineral resources and exploration and mining activity for numerous ministry and industry publications to promote the province;
 profiling BC mineral industry investment opportunities at numerous conferences, including the Mineral Exploration Roundup, the Prospectors and Developers Association of Canada (PDAC) Convention and the KEG annual meeting;
 responding on a daily basis to requests for assistance from prospectors, geologists, companies and the public;
 working on various land-use issues, including those associated with referrals from Mineral Titles; and
 helping co-ordinate a field tour and a forum on exploration and mining updates.



Figure 5: Business meetings between Canadian and Chinese companies in Beijing, organized by MEMPR as part of the 2009 Asia Investment Mission.

Marketing Coal and Minerals to the Asia-Pacific Region

The MEMPR continued an active Asia-Pacific marketing strategy to attract direct investment from Asia in BC exploration and mining projects (Figure 5). Asian countries are leading consumers of the province's coal and metal ores, and have a record of investment in BC's mineral industry. Key selling points are BC's rich geology, expert geoscience information, interactive online databases, continuing demand for commodities such as copper and coal, a Pacific Rim gateway, modern infrastructure and a skilled workforce. The BCGS provides the MEMPR with most of the technical expertise and professional delegates for international presentations and meetings with Asian companies. It is the point of contact for incoming international investors through the BC Mineral Development Office in Vancouver.

Regional Geologists

Regional Geologists play a vital role in providing detailed geological knowledge of the region in which they live and work, and gathering information on industry exploration and mining activity.

Regional Geologist	Office	Region
Paul Wojdak	Smithers	Northwest
Vacant	Prince George	North-Central and Northeast
Bruce Madu	Kamloops	South-Central
Dave Grieve	Cranbrook	Southeast
Bruce Northcote	Vancouver	Southwest

The MDO works closely with the regional geologists in attracting mineral investment to BC and in preparing publications such as *Exploration and Mining in British Columbia* and the *British Columbia Mines and British Columbia Mines and Mineral Exploration Overview*.

TECHNICAL MARKETING

BCGS Open House

The BCGS hosted its first open house of the 21st century on November 13, 2009. This successful event, hosted



Figure 6: British Columbia Geological Survey open house crowd in discussions during a break.

in Victoria, drew a crowd of more than 85 participants (Figure 6). Ten MEMPR geologists and two professors from the School of Earth and Ocean Sciences at the University of Victoria presented technical talks on subjects that included epithermal gold and silver veins in the Toadoggonne area; geology and mineral deposits of the Spences Bridge Group; geochemistry; geological database innovation; Cache Creek oroclinal entrapment; geology of northern Vancouver Island; the Wingdam Conglomerate; and the NEPTUNE Canada Ocean Observatory.

The open house was made possible thanks to sponsorship from the Pacific Section of the Geological Association of Canada. Planning for next year's Open House (November 10, 2010) is underway.

Conferences, Workshops and Field Trips

Staff participated in numerous conferences and workshops during 2009, as organizers, speakers and attendees. Highlights from conferences included
 presentations by Graham Nixon and Paul Schiarizza, and participation by many staff at the Mineral Exploration Roundup 2009 (Figure 7);
 participation in the PDAC Convention, at the MEMPR booth, on the trade show floor and helping host an Asian investor luncheon;
 presentations by Nick Massey, Bruce Northcote, Yao Cui and Larry Jones at the KEG annual meeting in Kamloops;

a presentation at the Smithers Exploration Group Rock Talk, delivered jointly by Ray Lett and JoAnne Nelson;

Geological Society of America presentations and coordination of one session in Kelowna by Nick Massey, Mitch Mihalynuk, JoAnne Nelson, Paul Schiarizza and George Simandl;

a Geological Association of Canada–Mineralogical Association of Canada presentation by Steve Rowins; an overview of exploration activities presented at Minerals North by Jay Fredericks; and

presentations by Larry Diakow and Kirk Hancock at Minerals South.

Staff also shared their expertise by leading four field trips in 2009. Mitch Mihalynuk led a trip in northwestern BC at the request of Edges project leaders from the GSC and Yukon Geoscience Office. Steve Rowins and Graham Nixon led a two-day trip for 25 industry participants to the Merritt and Princeton areas to examine a variety of mineral deposits. Andrew Legun and retired MEMPR coal geologist Barry Ryan led a field trip and workshop in the northeastern BC coalfield (Figure 8). The trip was sponsored by Peace River Coal Inc and Western Coal Corp. Dave Lefebure, Bruce Madu and Bruce Northcote led a field trip through BC for 11 Japanese senior executives. The trip was funded by the Japanese Oil, Gas and Mineral National Development Corporation (JOGMEC) and is a good example of BCGS technical marketing work being facilitated by Jay Fredericks and the British Columbia MDO.

Publications

During the past year, the BCGS published *Geological Fieldwork 2008*, 12 Open File maps and reports, 2 Geoscience Maps, 18 new industrial mineral deposit profiles, 10 GeoFile maps, reports and data files, and 2 Information Circulars. Staff published several articles in external journals. The BCGS also processed more than 600 company assessment reports for tenure maintenance and updated more than 1900 mineral occurrences.

With the Regional Geologists as principal authors, the BCGS published *Exploration and Mining in British Columbia 2008* and *British Columbia Mines and Mineral Exploration Overview 2008*, and co-ordinated articles on provincial industry activities in the Canadian Institute of Mining, Metallurgy and Petroleum *Mineral Exploration Review* and *The Northern Miner*.

All geoscience publications are available online at the BCGS website:

<http://www.empr.gov.bc.ca/Mining/Geoscience>

STAFF UPDATE

Sarah Meredith-Jones started as the new permanent Mineral Inventory Geologist in February. Sarah fills the position left open by Kirk Hancock as he moved to the MapPlace Geologist position left by Larry Jones, who became Director of the Resource Information Section of the BCGS.

The position of Director, Geoscience Initiatives, vacated by Brian Grant in early 2008 and filled in the interim on a part-time basis by Phillippe Erdmer, was filled by Ste-

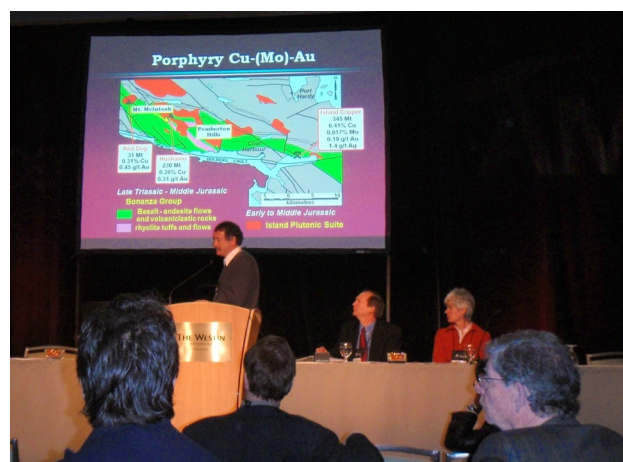


Figure 7: Graham Nixon presenting at Roundup 2009 in Vancouver.



Figure 8: Andrew Legun explaining regional geology near Bullmoose Mine, on a field trip in the northeast BC coalfield.

phen (Steve) Rowins, who joined the branch in May of 2009. Arlene Veenhof, the new Administrative Assistant for the BCGS, started in June of 2009.

NEED MORE INFORMATION? WANT TO COMMENT?

The BCGS staff have considerable expertise and welcome the chance to share it. Our contact list is online at:

<http://www.empr.gov.bc.ca/Mining/Geoscience/Staff/Pages/default.aspx>.

We always appreciate your input regarding our many programs and activities. Please e-mail us at Geological.Survey@gov.bc.ca or call (250) 952-0429.

To learn about new publications, data releases and upcoming events, join the BCGS release notification list by e-mailing Geological.Survey@gov.bc.ca. Approximately 15–20 e-mail updates are sent per year.

Stratigraphic and Structural Setting of the Rock and Roll Deposit, Northwestern British Columbia (NTS 104B/11)

by M.G. Mihalynuk, T.J. Stier¹, M.I. Jones² and S.T. Johnston¹

KEYWORDS: volcanic-hosted massive sulphide, sulphide, replacement sulphide, Rock and Roll, Stikine assemblage, Stuhini Group, Iskut River, Craig River, Bronson, Monsoon Lake, Hoodoo Mountain

INTRODUCTION

Precious-metal-rich polymetallic massive sulphide deposits are attractive exploration targets because of the high value of the ore and economic resilience from individual commodity price volatility. Precious-metal-rich polymetallic massive sulphide (PMPMS) mineralization at the Rock and Roll deposit (BC Geological Survey, 2009; MINFILE 104B 377), located within the Coast Belt of northwestern British Columbia, is stratiform and is interpreted as volcanogenic. However, the PMPMS mineralization is spatially associated with a diorite sill and dike complex, which is locally characterized by wispy veinlets and disseminations of the same sulphide mineral assemblage. Resolving the primary control on mineralization is imperative for successful targeting of exploration efforts, both on the property and regionally. To this end, geological mapping and sampling was conducted around the Rock and Roll deposit in mid-October 2009. This one-week reconnaissance program in the Iskut River area of northwestern BC (Figure 1) is the initial phase of a partnership between the University of Victoria; the BC Ministry of Energy, Mines and Petroleum Resources; and Pacific North West Capital Corp (and field representatives, Equity Exploration Consultants Ltd). Our aim is to establish the mode of occurrence and to determine the stratigraphic and structural setting of the Rock and Roll deposit. Our longer term goal is to evaluate the potential for similar PMPMS mineralization within the Iskut and adjacent regions (Figure 1).

LOCATION AND ACCESS

Access to the region around the Rock and Roll deposit is via the Bronson airstrip, located 300 km north-northwest of Terrace, 330 km northwest of Smithers and 75 km east-northeast of Wrangell, Alaska. Both Terrace and Smithers

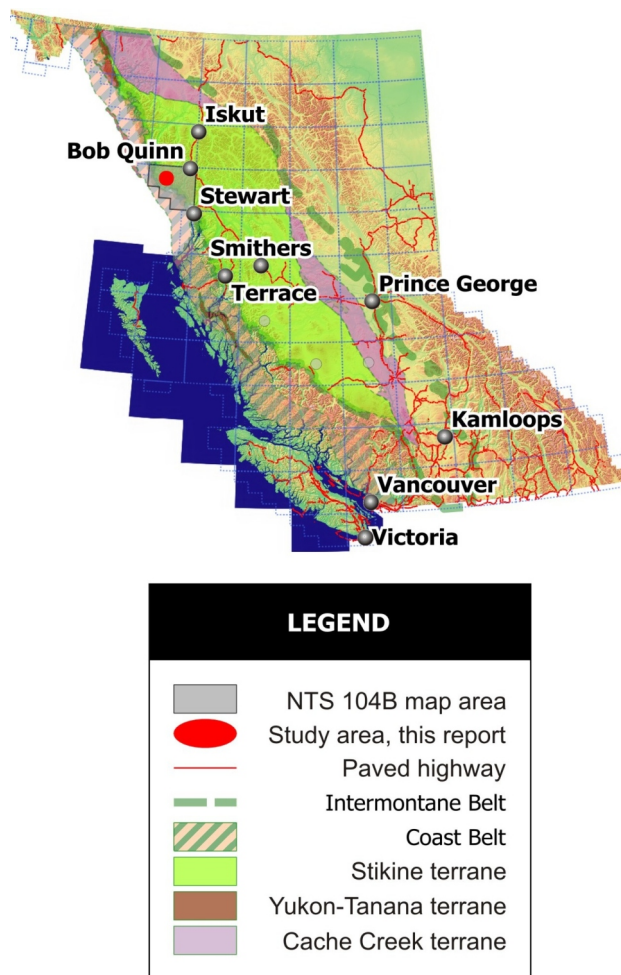


Figure 1. Location of the study area within the Iskut NTS area (104B) near the boundary of the Coast Belt and western Stikine terrane.

are serviced by scheduled commercial flights from Vancouver and both are approximately 400 km by road (~5 hour drive) from Bob Quinn airstrip. A 60 km flight southwest from Bob Quinn brings you to the Bronson airstrip, located on the south bank of the west-flowing Iskut River, at its confluence with Bronson Creek. The main showing on the Rock and Roll property, the Black Dog occurrence, is 10 km west of Bronson camp. Helicopter landing spots are limited to riverbanks, a few swampy openings and newly cut pads; old helicopter pads are overgrown and unserviceable.

The Iskut River valley is a U-shaped glacial valley; it has a relatively flat bottom and steep sides. Alpine glaciers,

¹University of Victoria, Victoria, BC

²Equity Exploration Consultants Ltd, Vancouver, BC (for Pacific North West Capital Corp)

This publication is also available, free of charge, as colour digital files in Adobe Acrobat® PDF format from the BC Ministry of Energy, Mines and Petroleum Resources website at <http://www.empr.gov.bc.ca/Mining/Geoscience/PublicationsCatalogue/Fieldwork/Pages/default.aspx>.

relicts of the once extensive Cordilleran Ice Sheet, extend down to treeline at approximately 1000 m elevation. Our work focused near the Rock and Roll property, beneath the dense hemlock-fir-spruce canopy between 60 m and 300 m elevation, east of the confluence of the Craig and Iskut rivers. Outcrop is plentiful, but is covered in moss and an understory of devil's club. Work in this rainy coastal region benefitted greatly from logistical support provided by a well-provisioned base camp at Bronson airstrip and daily helicopter set-outs for drilling crews overseen by Equity Exploration Consultants Ltd.

REGIONAL GEOLOGY AND PREVIOUS WORK

Rocks between the west-flowing Iskut and Craig rivers have not been mapped as part of a systematic regional program since fieldwork done in the late 1920s by Kerr (1935, 1948; Figure 2). Thus, the most recent compilation map (e.g., Massey et al., 2005; Figure 2) reproduces the geological contacts presented by Kerr, with slight modification of unit assignments. Accordingly, the area is underlain by a northwestward-tapering wedge of Stuhini Group arc volcanic and sedimentary rocks. On the northeast side of the

wedge, Stuhini Group rocks are shown in contact with a unit of Permian limestone, minor chert, argillite and metamorphosed equivalents. Mineralization at the Rock and Roll property is apparently located within Stuhini Group rocks along this contact. On the west side of the wedge, Stuhini Group rocks are shown in contact with a unit of 'pre-Permian' quartzite, argillite, limestone, tuff, intrusive and metamorphosed equivalents. Both Permian and pre-Permian units have been assigned to the Devonian to Permian Stikine assemblage by Massey et al. (2005). Along the Craig River, the wedge is intruded by an arcuate diorite body of the John Peaks stock or Unuk metadiorite (Massey et al., 2005).

The area is peripheral to later regional mapping by Grove (1986), Lefebure and Gunning (1989; NTS 104B/10W, 11E; Figure 2), Alldrick et al. (1990; NTS 104B/06E, 07W, 10W, 11E), Kirkham et al. (1991; NTS 104B/08) and Kirkham (1992; NTS 104B/08, 09). Fillipone and Ross (1989) mapped immediately north of the Iskut River in the Twin and Hoodoo glaciers areas (NTS 104B/14S; Figure 2). Logan and Koyanagi (1994) mapped the Galore Creek area ~30 km to the north (NTS 104G/03, 04) and Logan et al. (2000) mapped the Forrest Kerr–Mess Creek area ~15 km to the east (NTS 104B/10, 15, 104G/02, 07W; Figure 2). Edwards et al. (2000) produced a map of the Quater-

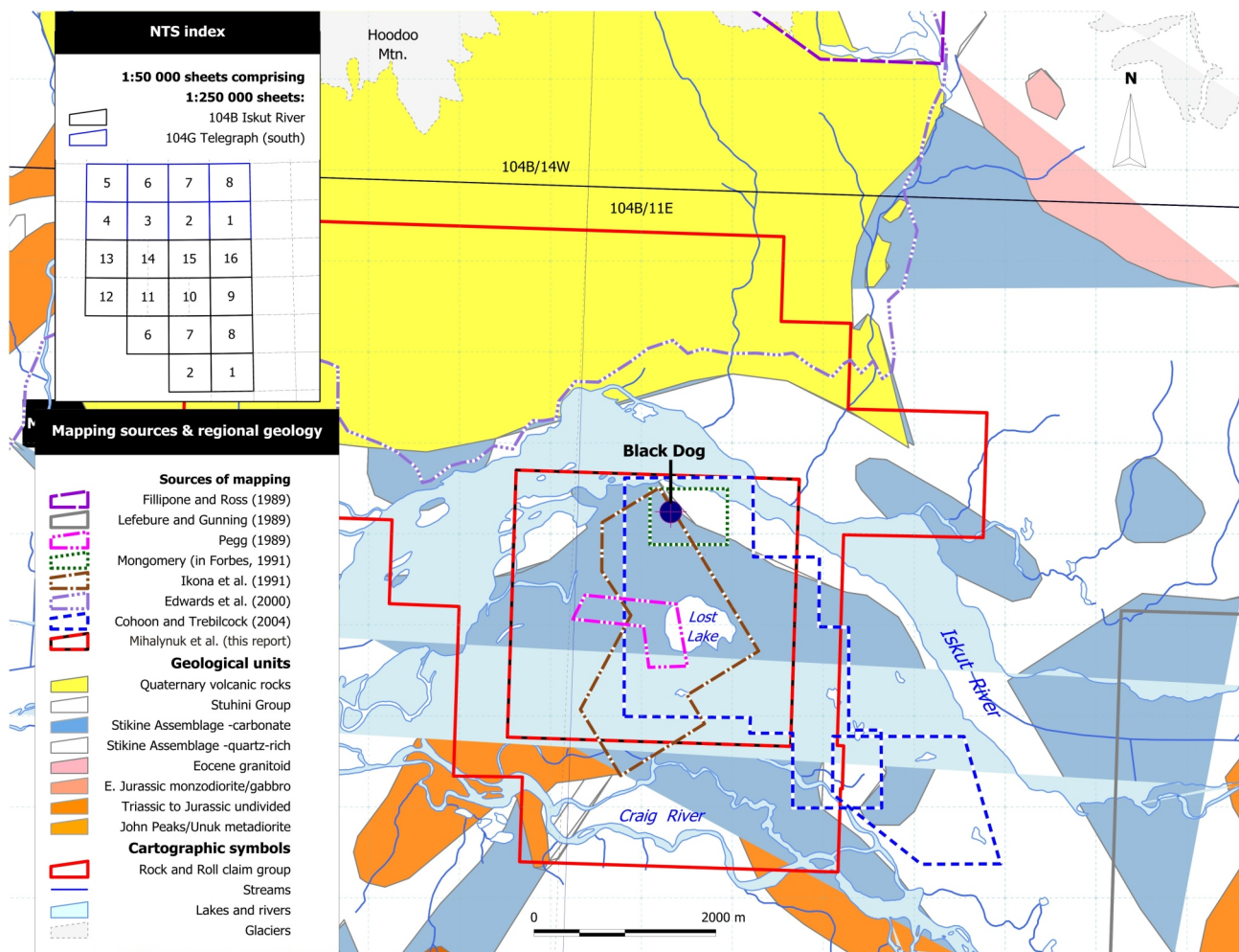


Figure 2. Location of the Rock and Roll property, NTS areas and sources of geological map data. The regional geology shown is after Kerr (1935) as compiled by Massey et al. (2005).

nary Hoodoo Mountain volcano, including the immediately surrounding basement rocks previously mapped by Phillipone and Ross (1989). Many other parts of the Iskut map area (NTS 104B) were mapped as part of Geological Survey of Canada projects (e.g., Anderson, 1989; Anderson and Thorkelson, 1990), culminating in a program under the direction of Anderson in 1991 (Anderson, 1993).

Property-scale mapping reported by Montgomery et al. (1991) covers about 3.25 km² around and west of Lost Lake (Figure 2), including much of a ~0.5 km² area previously mapped by Pegg (1989). Montgomery (*in Forbes, 1991*) covered ~0.5 km² around surface mineralization at the main Black Dog trenches. Much of the Rock and Roll property (~6.5 km²) was mapped at 1:2500 scale as reported by Cohoon and Trebilcock (2004b), as was the adjacent Phiz property (Rob claims; Cohoon and Trebilcock, 2004a). Reconnaissance mapping reported here aims to test and extend the available historical mapping in order to provide a structural and stratigraphic setting for the Rock and Roll deposit and evaluate regional potential for this deposit type.

Exploration Work at Rock and Roll

Exploration at the Rock and Roll property began with staking the Rob and Rock and Roll claims in 1986 and 1988. From 1987 to 1989, preliminary assessment work was done on the claims, including reconnaissance geological mapping, soils and silt sampling (Todoruk and Ikona, 1988a, b; Montgomery and Ikona, 1989; Pegg, 1989). In 1990, the program was expanded to include petrographic work and ground geophysical surveys (Montgomery et al., 1991), all of which contributed to the discovery of polymetallic Ag-Au-Zn-Cu-Pb massive sulphide mineralization at the Black Dog zone. This discovery was immediately followed up with a trenching program (110 m) and in late 1990, a nine hole, diamond-drill program totalling 675 m, which tested the mineralization over a strike length of 50 m (Montgomery et al., 1991).

Work in 1991 focused on a major drill program of at least 86 drillholes (10 525 m) on the Rock and Roll property and five drillholes (373 m) on the Rob claims. Additional line cutting, plugger soil sampling, mapping, prospecting and petrographic work was done. Most of this early exploration work was conducted by the Prime Resources Group ('Prime') and was not filed for assessment. Fortunately, drill logs have been recovered (Dunning and Scott, 1997), but reports documenting other aspects of exploration at the Rock and Roll and the Rob claims in 1991 have apparently been lost.

In 1997, a third drill campaign was conducted by Redstar Resources Corp. Preparatory work combined a comprehensive review of previous work including a re-examination of old drillcore and lithochemical and petrographic analyses, followed by a ten drillhole program (2203 m) that tested along strike and downdip extensions of the known mineralization (Dunning and Scott, 1997). By the end of this campaign, sulphide mineralization had been intersected for over 650 m along strike and between 40 and 200 m downdip. Based on 104 holes completed on the Black Dog and adjacent zones, Redstar Resources Corp calculated a pre-43-101 resource of 675 000 t grading 1.75 g/t Au, 233.8 g/t Ag, 0.40% Cu, 0.50% Pb and 2.20% Zn (Becherer, 1997; *in* Dunning and Scott, 1997).

In 2004, a program of geological mapping, mobile metal ion and conventional soil sample geochemistry, and minor rock sampling was conducted (Cohoon and Trebilcock, 2004). Exploration efforts were renewed in 2009 with a 350 line km airborne electromagnetic and magnetic survey and drilling campaign (five holes totalling 540 m) by Pacific North West Capital Corp (Jones, 2009).

PROPERTY GEOLOGY

We report here on the results of a six day reconnaissance field mapping program. Units were defined during the course of mapping (Figure 3) on the basis of distinctive lithological characteristics. They are described here, ordered by their presumed age. They apparently young towards the northeast, from carbonate units near Craig River, through volcanic units near Lost Lake, to sediment-dominated units nearer to the Iskut River (Figure 3). However, both depositional and structural interleaving has occurred and neither fossils nor direct isotopic age determinations are available to conclusively constrain the ages of any of the units.

Carbonate Units

Carbonate outcrops extensively in the southwestern part of the mapped area. There are at least three variants: homogeneous relatively pure limestone/marble, well-bedded limestone with or without tuffaceous interlayers and sooty- and flaggy-weathering limestone. Macrofossils are conspicuously absent, possibly having been destroyed during deformation and recrystallization.

MARBLE

White crystalline marble is the most common carbonate. It is typically strongly foliated and buff-weathering. However, colour changes with the degree of recrystallization—with less intensely foliated limestone, it is more commonly medium to dark grey. Compositional layering tends to be strongly transposed. Where relict bedding is well displayed, massive carbonate beds range from 5 to ~100 cm thick.

TUFFACEOUS CARBONATE

Tuffaceous carbonate is green, rust or, less commonly, brown-weathering. Tuffaceous layers tend to be more competent and resistant to weathering than the enclosing carbonate, but pyritic tuff layers can weather recessively (Figure 4). Volcanic clasts vary in proportion from a few percent to packed with a carbonate matrix. In one tuffaceous horizon, quartz grains were identified in hand specimen. This volcanic material is suspected to be of dacitic composition and was sampled for U-Pb age determination.

Open to isoclinal folds are outlined by compositional layering caused by variations in tuff content. In regions of high strain, folds are preserved only as hinges of rootless isoclinal folds.

Tuffaceous carbonate is sporadically exposed and, as a result, is not represented as a separate map unit in Figure 3.

TUFF-QUARTZITE UNIT

Beneath root masses of trees blown down near the Craig River, outcrops of decimetre-thick beds of alternat-

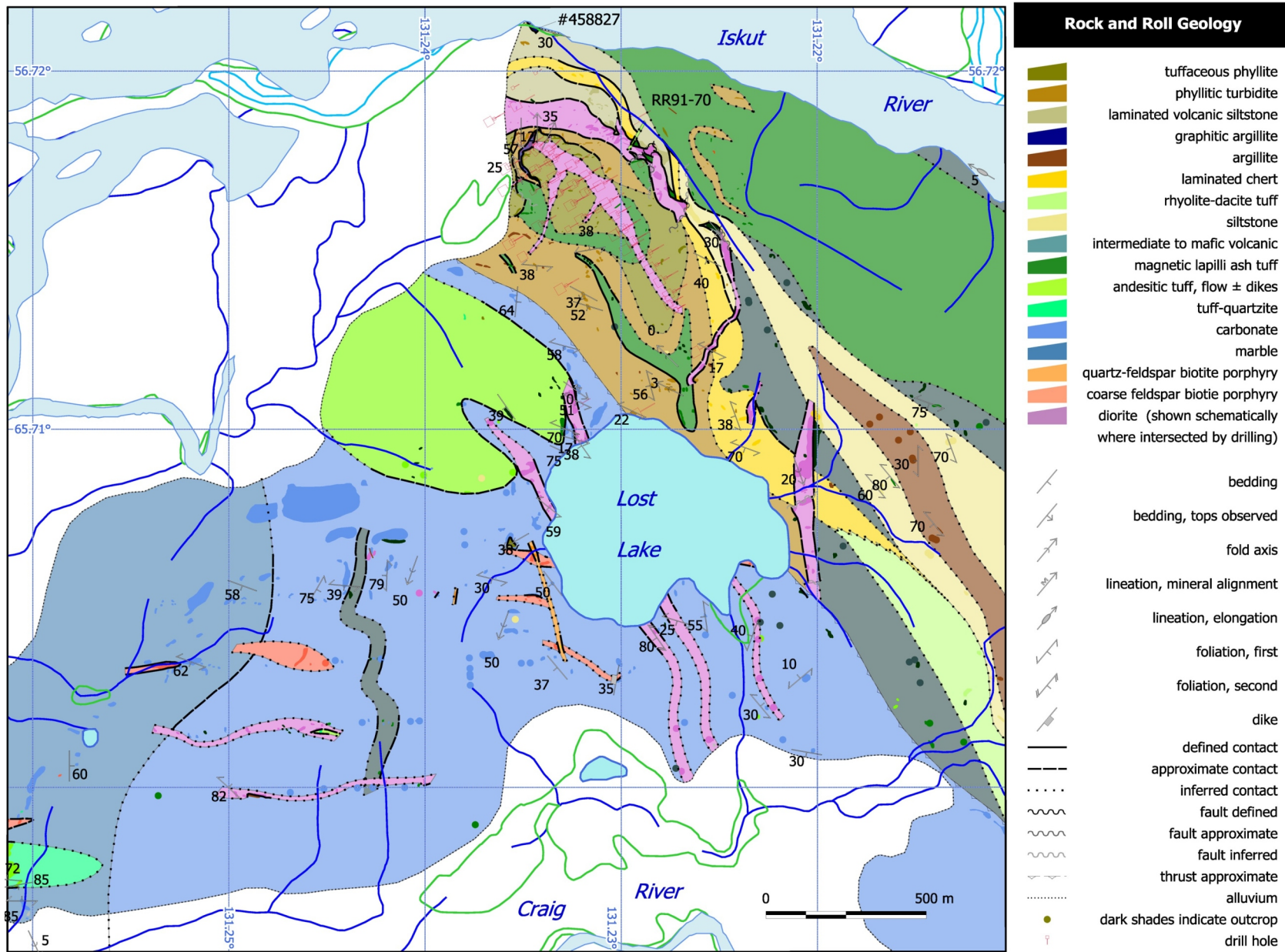


Figure 3. Geology between the Iskut and Craig rivers, based on reconnaissance mapping during this study and a compilation of mapping by Montgomery (*in Forbes*, 1991), Montgomery et al. (1991) and Cohoon and Trebilcock (2004a, b).

ing green tuff and ‘quartzite’ are freshly exposed over several hectares. This unit passes across strike into more typical tuff-carbonate interbeds and the ‘quartzite’ is interpreted as a product of carbonate replacement. Silicification and the occurrence of grossular garnet and abundant epidote within the tuff-quartzite are interpreted as the product of contact metamorphism. This metamorphism is attributed to a several square kilometre intrusive body, which is incorrectly shown on compilation maps (e.g., Massey et al., 2005) as underlying the same area, but the main mass of intrusion must lie farther to the south. No significant base-metal mineralization was observed.

SOOTY LIMESTONE

Black, sooty limestone was mapped at two localities equidistant from the southern and western shores of Lost Lake. Relict beds or folia form continuous layers of uniform thickness. These layers are typically 1–2 cm thick (and up to 15 cm). Slaty parting and sooty black weathering are characteristic. This unit is combined with the main carbonate unit in Figure 3.

Volcanic and Volcaniclastic Units

MAFIC VOLCANIC ROCKS

Light green- to rusty-weathering mafic volcanic rocks are exposed in rounded, glaciated outcrops. Fresh surfaces are dark green, predominantly due to pervasive chlorite and minor epidote alteration. Iron oxides are not as abundant as is to be expected in a mafic volcanic rock. This is reflected in the magnetic susceptibilities, which are approximately 0.5×10^{-3} SI. Volcanic clasts are rarely visible on the outcrop surface, but ash-sized, microporphyrific grains are evident in hand sample. Compositional layering can be observed locally. Outcrops of this unit appear massive and featureless, or rarely, display vague breccia textures. These rare outcrops are interpreted as autobrecciated flow units. Intercalated sedimentary layers point to submarine deposition, although pillows were not conclusively identified. Fragments and layering are obscured by the typical moderate to strong foliation developed within this unit. Gradational contacts with sediment-dominated units may be due to both sedimentary and structural interleaving.

TUFFACEOUS PHYLLITE

Light to dark green-grey-weathering, platy outcrops of phyllitic tuffaceous siltstone crop out on the forested ridge along which most exploration has been conducted (herein called ‘Sulphide ridge’). Tuffaceous phyllite interfingers with phyllitic turbidite (see below), but can be resolved into a mappable unit as shown on Figure 3. Although this unit tends to be recessive, it underlies much of ‘Sulphide ridge’ where it is extensively intruded by diorite dikes. Volcanic siltstone with argillaceous partings and quartz-poor, thin greywacke beds are locally well preserved.

Protolith textures in both units are commonly obscured by moderate to intense foliation and cataclasis. Both units probably grade into cherty siltstone and graphitic argillite.

MAGNETIC LAPILLI ASH TUFF

Light green and rust-weathering, strongly foliated, fine feldspar crystal (20%) lapilli ash tuff is exposed in the Iskut River bed about 450 m northeast of the Black Dog trench. Feldspar and light green-grey ash fragments are elongated towards 120° . Scattered, flattened and elongated

light-coloured felsic lapilli contain 20% fine- to medium-grained feldspar phenocrysts and sparse quartz eyes. A dusting of 1–2% fine-grained magnetite (probably metamorphic) generates a moderately high average magnetic susceptibility of $26 (\times 10^{-3})$ SI. This unit is likely responsible for the elevated aeromagnetic response over areas along strike from these outcrops (Jones, 2009). Unfortunately, our mapping did not include tracing out this unit to verify correlation with the aeromagnetic high.

Fine-grained Sedimentary Rocks

PHYLLITIC TURBIDITE

Low, platy outcrops of grey to brown and rust-coloured argillaceous siltstone are widespread on the flanks of ‘Sulphide ridge’. Thin, graded siltstone to laminated siliceous argillite couplets (0.5–3 cm thick) are interpreted as AE turbidite beds. Coarser layers of medium sand to rare volcanic pebble conglomerate have been intersected in drillcore (e.g., DDH RR97-103, 0.5 m sampled for detrital zircons), but were not observed in outcrop. Thin quartz-feldspar tuff layers (1–3 cm thick; Figure 5) occur within the turbiditic siltstone at one locality where they were sam-

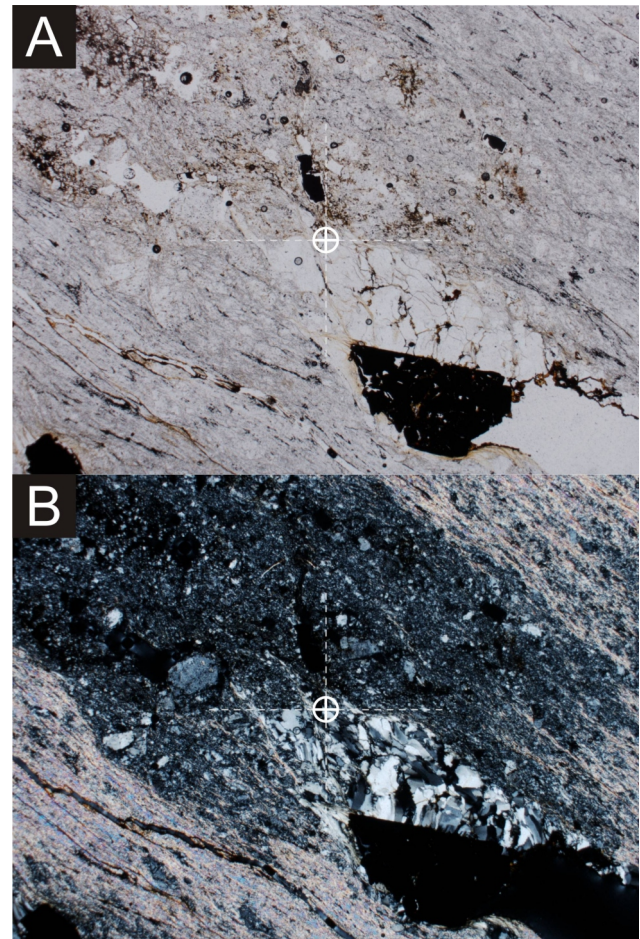


Figure 4. Thin section of tuffaceous carbonate schist, northwestern British Columbia in: **A)** plane-polarized light and **B)** cross-polarized light. Feldspar and quartz grains dominate the central 40% as a diagonal domain, extending from the top left to the bottom right. Secondary quartz fibres have grown in the pressure shadow of a rotated pyrite grain (opaque, bottom right).

pled for U-Pb age determination. Phyllitic turbidite is commonly interleaved with tuffaceous phyllite.

RIBBED CHERTY SILTSTONE/ARGILLITE

Resistant, laminated argillaceous to cherty siltstone beds 0.5–2 cm thick alternate with recessive, featureless silt-poor argillaceous beds 1–5 cm thick to produce the conspicuous ribbed appearance of this unit. It is siliceous and translucent, with a conchoidal fracture. It is best exposed near the north end of ‘Sulphide ridge’ where clean exposures are light green to green-grey weathering. Rhythmic layering within this unit is interpreted as stacked AE turbidite beds.

Locally the unit is chaotically folded and beds are segmented. Such disruption may be due to soft-sediment deformation and the formation of rip-up clasts. Elsewhere, folding caused by regional strain is well developed, except where the primary layering is obscured by strong foliation. This unit has been included with the phyllitic turbidite unit in Figure 3.

GRAPHITIC ARGILLITE (± SILTSTONE)

Dark grey to black, commonly rusty, moderately siliceous to friable graphitic argillite and siltstone is calcareous in many localities. It generally contains up to several percent disseminated pyrite and pyrrhotite and may be bleached as a result of sulphide weathering. This unit grades into the ribbed cherty siltstone-argillite unit, with feathery intercalations observed in drillcore.

Near the Black Dog showing, graphitic argillite is the layered rock most commonly associated with massive sulphide mineralization. It is also the unit in which Zn-Cu mineralization was observed along the bank of the Iskut River about 330 m north of the Black Dog trenches (Table 1, Figure 3).

LAMINATED VOLCANIC SILTSTONE

Dark to light green and locally orange, indurated volcanic siltstone forms the upper northeast flank of ‘Sulphide ridge’. Very well displayed, disrupted laminae are characteristic, although some outcrops are massive. Microporphyrific ash fragments can be observed in hand sample. The unit grades into laminated chert, which lacks volcanic clasts.

LAMINATED CHERT

Creamy white- to rusty-weathering, very well laminated chert occurs in at least one layer >3 m thick on the north side of the ‘Sulphide ridge’. However, multiple exposures closer to the Iskut River suggest structural repetition or a total composite thickness on the order of 100 m. Locally the unit appears flow banded, with sparse, very fine grained feldspar phenocrysts. However, synsedimentary faults with displacement of several millimetres can be observed and a volcanic flow or pyroclastic texture could not be verified petrographically. Instead, it appears to be a siliceous argillite with less than 1% silt grains that are subround and not angular as would be expected of ash content. Fine- to very fine grained white crystals that were interpreted as feldspar microlites in hand sample could be metamorphic minerals.

This unit is interpreted as sedimentary in origin, but may include a significant dust tuff component. It probably grades to the southeast into a felsic lapilli tuff unit (Fig-

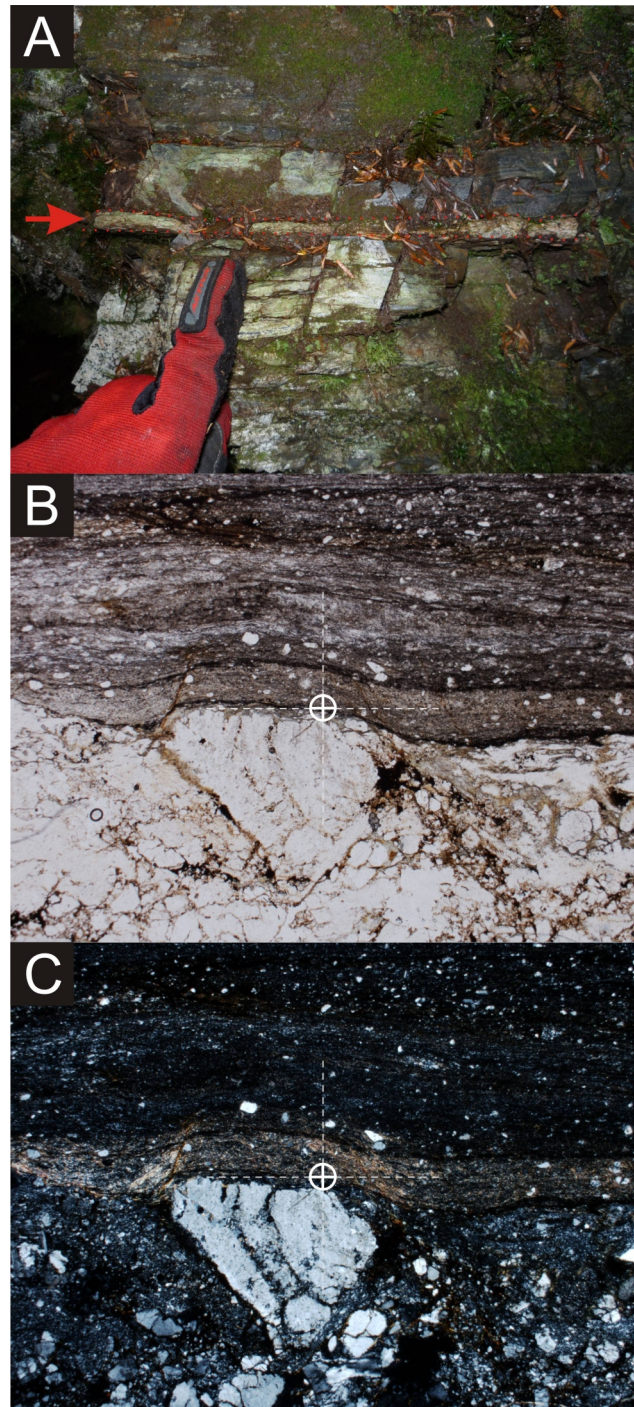


Figure 5. Layers of quartz-feldspar crystal-ash tuff within phyllitic turbidite, northwestern British Columbia: **A**) the outcrop habit of light to dark grey-weathering, well-bedded and moderately to weakly foliated silty argillite turbidite with a 2 cm thick tuff band (red arrow); dotted lines highlight the contacts of the tuff band; **B**) plane-polarized light view of contact between medium-grained felsic tuff and silty argillite; the circle at the crosshairs has a radius of 100 μ m; **C**) cross-polarized light view of contact between medium-grained felsic tuff and silty argillite; note angular crystal fragments produced by cataclasis of original angular feldspar and quartz crystal pyroclasts within the tuff band; the circle at the crosshairs has a radius of 100 μ m.

ure 3) on the adjacent Phiz property where it forms a distinctive marker horizon containing up to 50% subrounded felsic lapilli-sized clasts (Cohoon and Trebilcock, 2004a).

Rhyodacitic flows were intersected by drilling in hole RR91-70. A 5 m sample of split core (sample TST09-7-01) was collected for U-Pb age determination. Possible age equivalence of tuffaceous layers sampled from carbonate and turbiditic argillite will be tested.

Intrusive Rocks

DIORITE

Dark green, rounded to blocky and resistant diorite sills and dikes up to 50 m in width are common. Most are steeply dipping and trend perpendicular to or parallel with the dominant northwest-trending structural grain within the country rocks (Figures 3, 6). Texture is variable on a hand-sample scale, ranging from coarse grained holocrystalline and equigranular, to fine grained and porphyritic. A typical diorite outcrop is medium grained, with felted pyroxene, hornblende and feldspar and <5% interstitial quartz. The dikes are altered everywhere: hornblende is strongly chloritized and feldspar grains are turbid with epidote-calcite alteration (Figure 7). Leucoxene is a common alteration product after titanium oxides (rutile, sphene). Embayed magnetite (Figure 7) can range up to several percent by volume, although measured magnetic susceptibilities are comparatively low, between 0.8 and 0.95 ($\times 10^{-3}$ SI). There is no apparent relationship between magnetic susceptibility and degree of fabric development.

The holocrystalline plagioclase-rich diorite matrix can be used to distinguish this unit from andesite and basalt, except where this texture is obliterated by foliation and local mylonite development. Dike margins can be difficult to define where the foliation is produced by slip and cataclasis, which causes structural interleaving over a metre or more.

POSTDEFORMATIONAL INTRUSIONS

Potassium-Feldspar Biotite Porphyry

Resistant, blocky, reddish-weathering, porphyritic quartz monzonite is medium grey on fresh surfaces. Coarse feldspar phenocrysts are characteristic and appear to be orthoclase and minor plagioclase, ranging in size up to 25 mm. Medium-grained, euhedral, strongly chlorite-altered biotite booklets comprise 5% of the intrusion. Clots of chlorite may replace fine-grained prismatic to interstitial hornblende in the feldspar-quartz matrix. Quartz content is variable, but is generally less than 10% of the fine-grained matrix.

Quartz Feldspar Biotite Porphyry

Orange, blocky weathering, quartz-feldspar porphyry crops out west and south of Lost Lake. It contains 40% medium-grained, subidiomorphic, white feldspar crystals in a fine-grained to aphanitic orange matrix. Quartz eyes may be present up to 5% and are typically embayed square - quartz <5 mm in diameter. Sparse, fine- to medium-grained biotite booklets are chloritized. At one locality, about 300 m southwest of Lost Lake, the unit can be mapped as a north-trending, near-vertical dike cutting carbonate rocks.

Table 1. Analysis performed on a ~4 m chip sample (#458827) collected oblique to the strike of a foliated outcrop (~1.5 m true width) along the southern bank of the Iskut River, northwestern British Columbia. Analyses performed at ALS Chemex Laboratories (Vancouver) by aqua regia digestion and inductively coupled plasma-mass spectroscopy, except for Au, which was analyzed by fire assay atomic absorption spectroscopy.

Element	Unit	Value	Element	Unit	Value
Au	ppm	0.24	Mg	%	3.59
Ag	ppm	14.7	Mn	ppm	1160
Al	%	4.13	Mo	ppm	16
As	ppm	496	Na	%	0.02
B	ppm	<10	Ni	ppm	62
Ba	ppm	140	P	ppm	980
Be	ppm	<0.5	Pb	ppm	571
Bi	ppm	<2	S	%	1.77
Ca	%	1.27	Sb	ppm	11
Cd	ppm	7.9	Sc	ppm	13
Co	ppm	29	Sr	ppm	40
Cr	ppm	93	Th	ppm	<20
Cu	ppm	656	Ti	%	0.24
Fe	%	9.03	Tl	ppm	<10
Ga	ppm	10	U	ppm	<10
Hg	ppm	1	V	ppm	223
K	%	0.05	W	ppm	<10
La	ppm	10	Zn	ppm	1720

MINERALIZATION

During the course of this study, we observed mineralization on the surface at two localities: the main Black Dog occurrence and about 330 m farther to the north, at outcrops along the south bank of the Iskut River. Mineralization at the Black Dog is part of a multi-layered, stratiform zone that has been traced more than 650 m, mainly to the south-east. Representative analyses of massive sulphide where intersected by drilling at the Black Dog are 1.1 and 3.8 g/t Au, 27 and 308 g/t Ag, 0.85 and 2.44% Pb, 4.19 and 9.98% Zn, and 0.01 and 0.24% Cu from intervals 19.4–20.2 m and 18.0–18.3 m in hole RR90-3. Mineralization along the Iskut River bank has not been drill tested; however, we collected a ~4.0 m chip sample oblique to the strike (1.5 m true thickness) of the enclosing graphitic argillaceous strata that yielded 14.7 ppm Ag, 0.24 ppm Au, 0.066% Cu and 0.17% Zn (Table 1).

These two areas of surface mineralization are representative of the two distinct styles of mineralization comprising the Rock and Roll deposit: massive pyrrhotite(+pyrite)-sphalerite-chalcopryrite±galena and stringer and wispy pyrrhotite-chalcopryrite±sphalerite-galena.

Massive pyrrhotite-sphalerite-chalcopryrite forms banded layers (Figure 8) in both outcrop and drillcore that are up to ~10 m thick (e.g., drillhole RR91-037), where they are associated with graphitic argillaceous siltstone. Massive sulphide commonly forms a matrix to clasts of argillite or, as at the main Black Dog showing, diorite (Figure 9). Clasts of apparent felsic volcanic material have also been observed at the Black Dog, but these could be altered diorite fragments (Figure 9), although they lack both mafic minerals and the high degree of alteration typical of diorite



Figure 6. Rose diagram of diorite dike orientations, northwestern British Columbia. The mean orientation is 012° (N = 9).

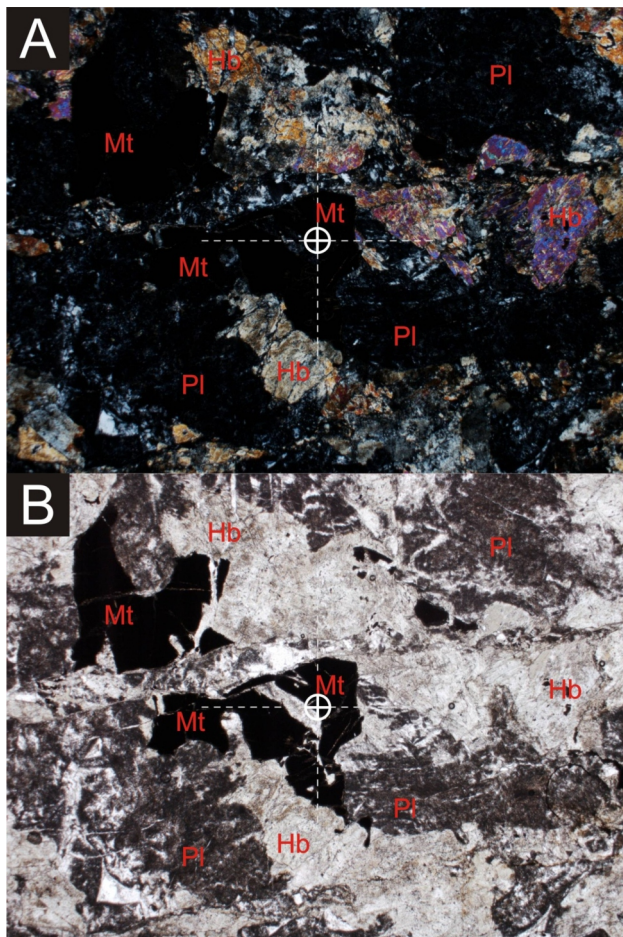


Figure 7. A) Altered, nonfoliated hornblende diorite in cross-polarized light. **B)** The same field of view in plane-polarized light with very weakly pleochroic hornblende (probably low-Fe). Abbreviations: Mt, embayed opaque (resorbed magnetite?); Pl, strongly turbid plagioclase; Hb, hornblende. The circle at the crosshairs has a radius of 100 μm.

(e.g., Figure 7). At the Black Dog occurrence, a diorite dike is cut by moderately to steeply dipping brittle faults to produce blocks several metres long. Graphitic argillite is folded around the blocks and sulphide has flowed between them (Figure 10). Folds in sulphide and argillite are tight and hinges plunge in opposite directions, both north and south, within the 15 m length of the main exploration trench. Veins of sphalerite–pyrrhotite±chalcopyrite extend into the diorite and surround breccia fragments near the faults (Figures 9, 11).

Wispy trains and disseminations of sulphides outline folded foliation within the diorite and graphitic argillite. Mineralization along the Iskut River (Table 1) is of this type. Pyrite–chalcopyrite–galena is most notable within the argillite and pyrrhotite–chalcopyrite–sphalerite is a common assemblage within the diorite. Sphalerite also outlines foliation in a siliceous tuff or sediment where intersected by drilling below the massive sulphide horizon. Wispy and disseminated sulphide predates folding and could be syngenetic; however, a predeformational intrusive-related source cannot be ruled out on this basis, particularly given the occurrence of this mineralization within foliated diorite. Some late stringers of pyrrhotite–chalcopyrite cut the fabric and are likely remobilized.

STRUCTURE

The predominant fabric throughout the ‘Sulphide ridge’ area is south- to southwest-dipping bedding and foliation that is moderately well developed within volcano-sedimentary strata (Figure 12) and variably developed within diorite dikes. In places, the foliation is demonstrably axial planar to overturned folds, which range from open to tight. Rootless isoclinal folds are common where foliation is most strongly developed, particularly within carbonate-rich rock types.

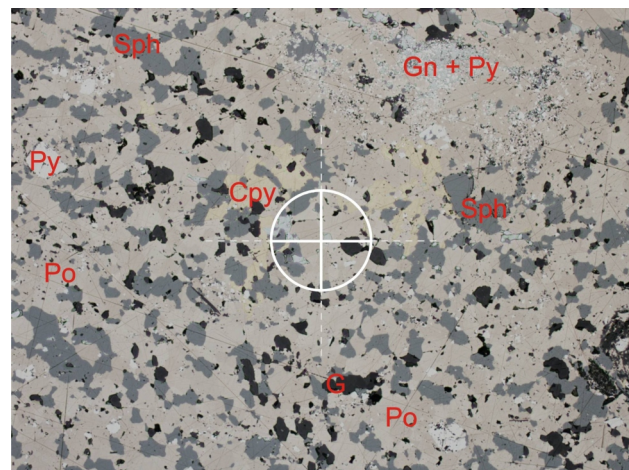


Figure 8. Polished section of a representative sample of massive, pinkish, pyrrhotite-rich (Po) sulphide from interval 19.4–20.2 m of drillhole RR90-3, Rock and Roll deposit, northwestern British Columbia. Yellow chalcopyrite (Cpy) comprises ~10% of the field of view, and medium-grey sphalerite (Sph) comprises ~20%. Bluish-white tabular galena (Gn) is subordinate to granular yellowish-white pyrite (Py), which together comprise ~5%. Dark grey to black gangue (G) is mainly carbonate. The radius of the circle at the crosshairs is 100 μm.

Outcrop to map-scale folds can be traced northwest of Lost Lake where foliated diorite crosscuts mafic volcanic and carbonate rocks. Within one of these fold closures, intrafolial isoclinal folds plunge shallowly towards 120° (Figures 3, 12, 13).

Strain associated with southwest-dipping foliation may have thickened northeast-trending diorite dikes, while dissecting thin dikes not within, or orthogonal to, the flattening fabric.

Repetition of a mineralized horizon is seen in drill sections, with up to four layers observed (M. Jones, pers comm, 2009). This repetition may result from tight to isoclinal folding about shallowly southeast plunging fold axes. Such folding would necessarily predate intrusion of the diorite dikes as they have not been observed to outline isoclinal folds. Moderate to shallow dips in the region of 'Sulphide ridge' (Figure 13) are consistent with the possi-

bility of stratiform sulphide layers repeated by early folds with shallow axial surfaces. This pattern is observed at outcrop scale in other rock types.

DISCUSSION

Interlayered sedimentary and volcanic sequences of Triassic and late Paleozoic age, which are ideal candidates for stratiform mineralization, are regionally extensive in the Iskut area. A volcano-sedimentary succession, including a felsic volcanic marker horizon, hosts the Rock and Roll mineralization. This host stratigraphy may be used to (1) unravel the complex crustal structure in the area and (2) constrain the age of the mineralizing environment through isotopic age determination.

Age of Host Strata

Geochronological constraints on the age of the Rock and Roll deposit host strata are lacking. One unpublished isotopic age determination from a sample of volcanic strata north of the Iskut River is reported by Edwards et al. (2000) as ">190 Ma based on 2 discordant zircon fractions (P. van der Heyden, written communication, 1987)" (see Figure 2) is not reliable. Strata from which the zircons were extracted were interpreted as the oldest Stuhini Group rocks in the immediate area (Phillipone and Ross, 1989).

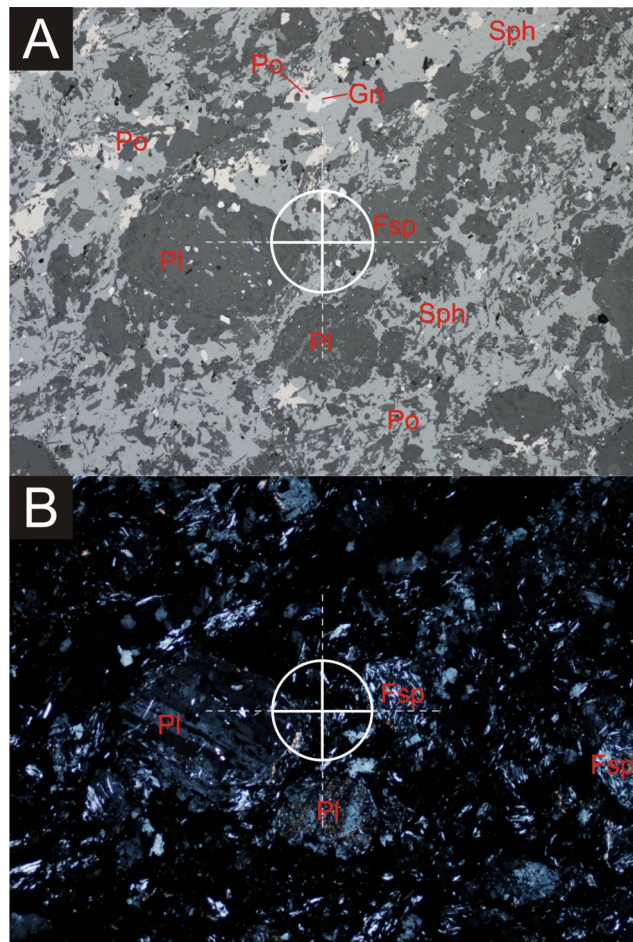


Figure 9. Mineralization from the Rock and Roll deposit, northwestern British Columbia: **A)** reflected light view of sphalerite-rich mineralization; **B)** transmitted light view of sphalerite-rich mineralization. Clasts comprised mainly of plagioclase (Pl) and unidentified feldspar (Fsp) float in a matrix of sphalerite (Sph), which is medium grey in reflected light, and minor flesh to light tan-coloured pyrrhotite (Po) and galena (Gn). Some feldspar clasts are relatively fresh plagioclase (Pl); others are much more altered. These clasts might have originated as diorite, and were subsequently fragmented and milled during brittle deformation. However, a lack of mafic minerals and the relatively fresh plagioclase are both inconsistent with this interpretation. The circle at the crosshairs has a radius of 100 μm.



Figure 10. Massive sulphide at the main trench, Black Dog occurrence, northwestern British Columbia. The view is east-southeast. A very rusty massive sulphide layer appears to have been 'squeezed up' between diorite blocks.

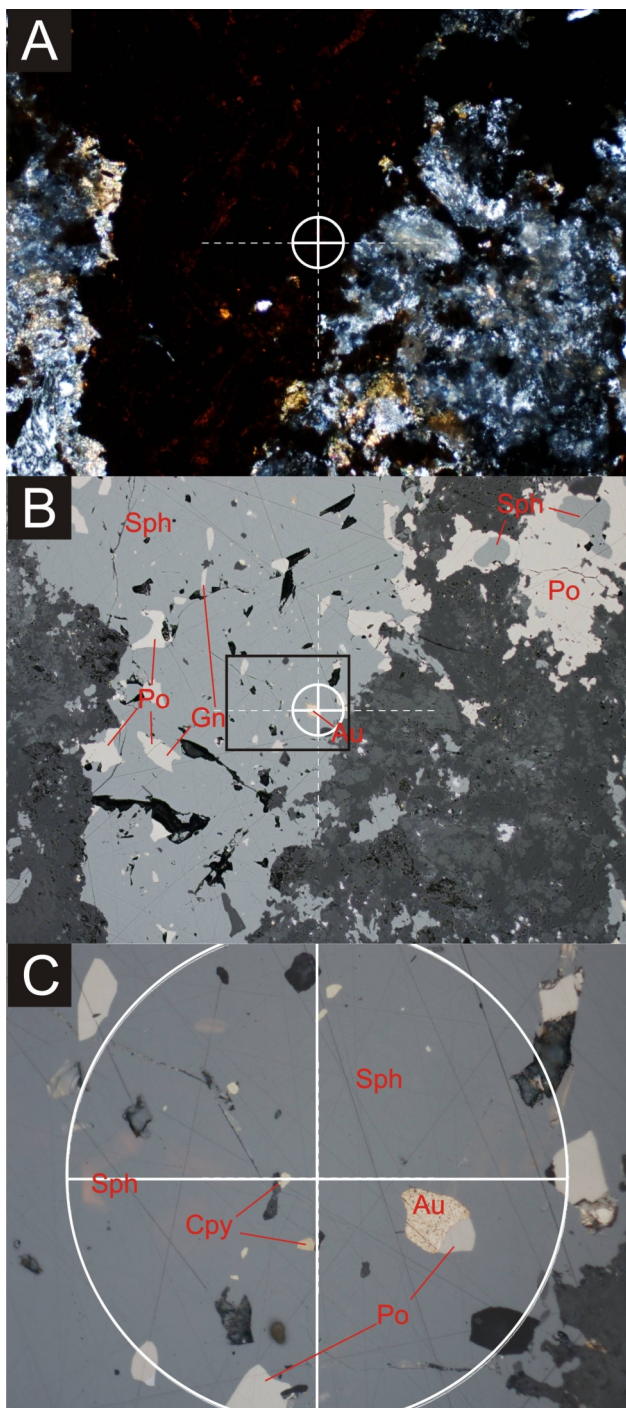


Figure 11. Sphalerite-rich massive sulphide in contact with diorite, northwestern British Columbia; the circle at the crosshairs in A and B has a radius of 50 μm , and in C has a radius of 100 μm : **A)** transmitted plane-polarized view of irregular brown-orange sphalerite vein within altered diorite; **B)** same field of view as A under reflected light; medium-grey sphalerite (Sph) encloses xenomorphic pyrrhotite (Po) and bladed galena (Gn); the highly reflective yellow grain at the crosshairs is gold (Au); top right of photo shows flesh to light tan-coloured pyrrhotite enclosing xenomorphic sphalerite; **C)** higher magnification of gold grain (Au) and less reflective yellow chalcopyrite (Cpy); internal reflections in sphalerite are well displayed.

About 7 km east of Lost Lake, Stuhini Group strata are mapped as intruded by ca. 193 Ma plutons, including the 193.9 $\pm 6/-0.6$ Ma (U-Pb zircon; Lewis et al., 2001) Iskut River stock and the 195 ± 1 Ma Red Bluff porphyry (U-Pb zircon; Macdonald et al., 1992). Near this locality, the Stuhini Group is mapped as overlain by a coeval, discontinuous blanket of dacite-rhyolite flow rocks belonging to the Betty Creek Formation of the Early Jurassic Hazelton Group, dated at 193 ± 1 Ma and 194 ± 3 Ma (Lewis et al., 2001). However, none of these magmatic units are known to extend onto the Rock and Roll property (the John Peaks/Unuk metadiorite body along the Craig River is undated).

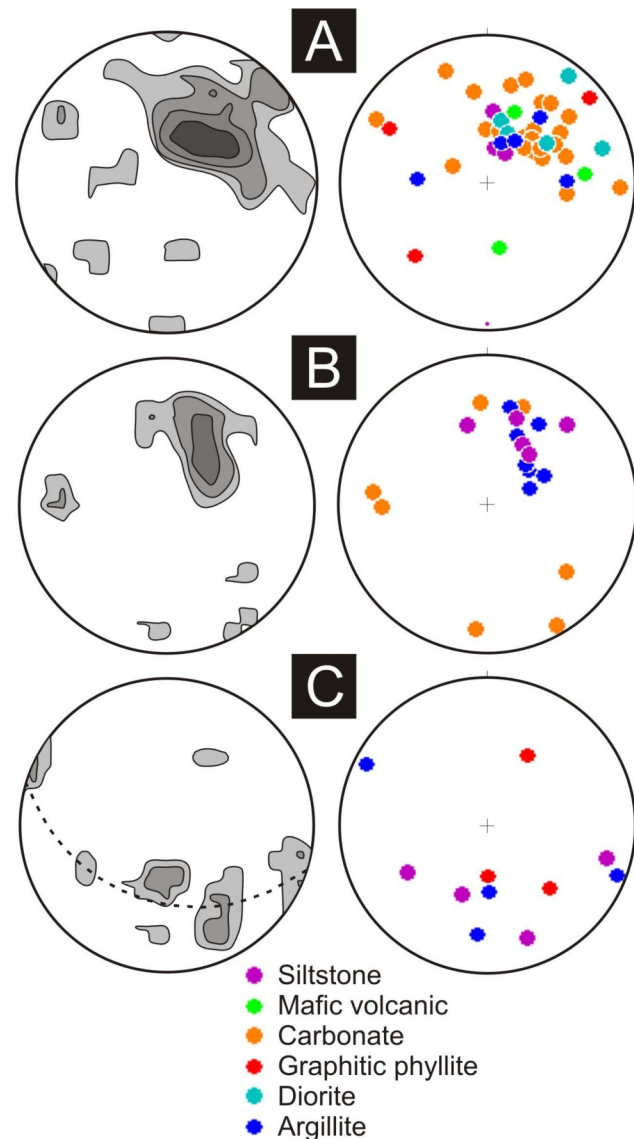


Figure 12. **A)** Poles to foliation, all rock types, Rock and Roll property, northwestern British Columbia. The mean orientation is 130/39; N = 46; contours at 2%, 4%, 8% and 16%. **B)** Poles to bedding, all rock types. The mean orientation is 115/43; N = 19; contours at 5%, 10% and 20%. **C)** Fold hinges, all rock types. Plane of best fit is 107/46; N = 13; contours at 7% and 14%.

Deposit Model and Age of Mineralization

Two models are proposed to explain the origin of massive sulphide mineralization observed at the Rock and Roll deposit: (1) skarn mineralization attributable to metasomatism, coeval with, and generated by, intrusion of dikes and sills of diorite; and (2) syngenetic mineralization attributable to hydrothermal cells, driven by submarine volcanism. Skarn mineralization is consistent with the close spatial relationship between diorite and massive sulphide at the main Black Dog occurrence, with sulphide veins cutting the dikes and with possible diorite fragments within the massive sulphide. In this model, metasomatism and mineralization is attributed to the expulsion of reduced, sulphide and metal-rich fluids from the intruding diorite magmas. Replacement of reactive graphitic argillite layers explains the stratiform nature of the mineralized layers. This model requires that the diorite intrusions were reduced and metal rich, characteristics that can be tested through geochemical analysis.

Syngenetic mineralization is consistent with the spatial association of massive sulphides and graphitic argillite, the occurrence of multiple horizons that can be traced at approximately the same stratigraphic horizon from drillhole to drillhole, the lack of diorite association with mineralization in some drillholes, and the presence of a distal felsic volcanic horizon within the productive part of the stratigraphy. In addition, sparse geochemical data from the sulphide-bearing zones reveal elevated Mn, Co and V typical of other PMPMS deposits of syngenetic origin.

We prefer a model of syngenetic mineralization because of the strong apparent stratigraphic control of the mineralization and evidence for remobilization where the sulphide mineral suite is hosted by diorite. The PMPMS association with graphitic argillite is consistent with a reducing and sulphide-preserving environment (versus oxidizing, sulphide-destroying). The association of felsic volcanic rocks within the section is consistent with a corresponding high Cu-Zn tenor of the mineralization (e.g., Kuroko style). However, the expectation of increased sulphide nearer to an intrusive centre has not been borne out by preliminary drilling on the Phiz property where strata containing the most proximal felsic volcanic rocks in the local area have not yet revealed PMPMS mineralization. Clear evidence for synchronicity of mineralization and host strata is required. Uranium-lead zircon dating of the host strata and the diorite, as well as direct Re-Os dating of the sulphide mineralization, is needed to unequivocally demonstrate whether or not the Rock and Roll deposit is syngenetic.

ACKNOWLEDGMENTS

The authors acknowledge the assistance of our project partners: Pacific Northwest Capital and the University of Victoria (BC Ministry of Energy, Mines and Petroleum Resources Partnership Fund). This project is also funded in part by a Natural Science and Engineering Research Council (NSERC) grant to Stephen T. Johnston. Paul Wojdak provided background information and logistical support.

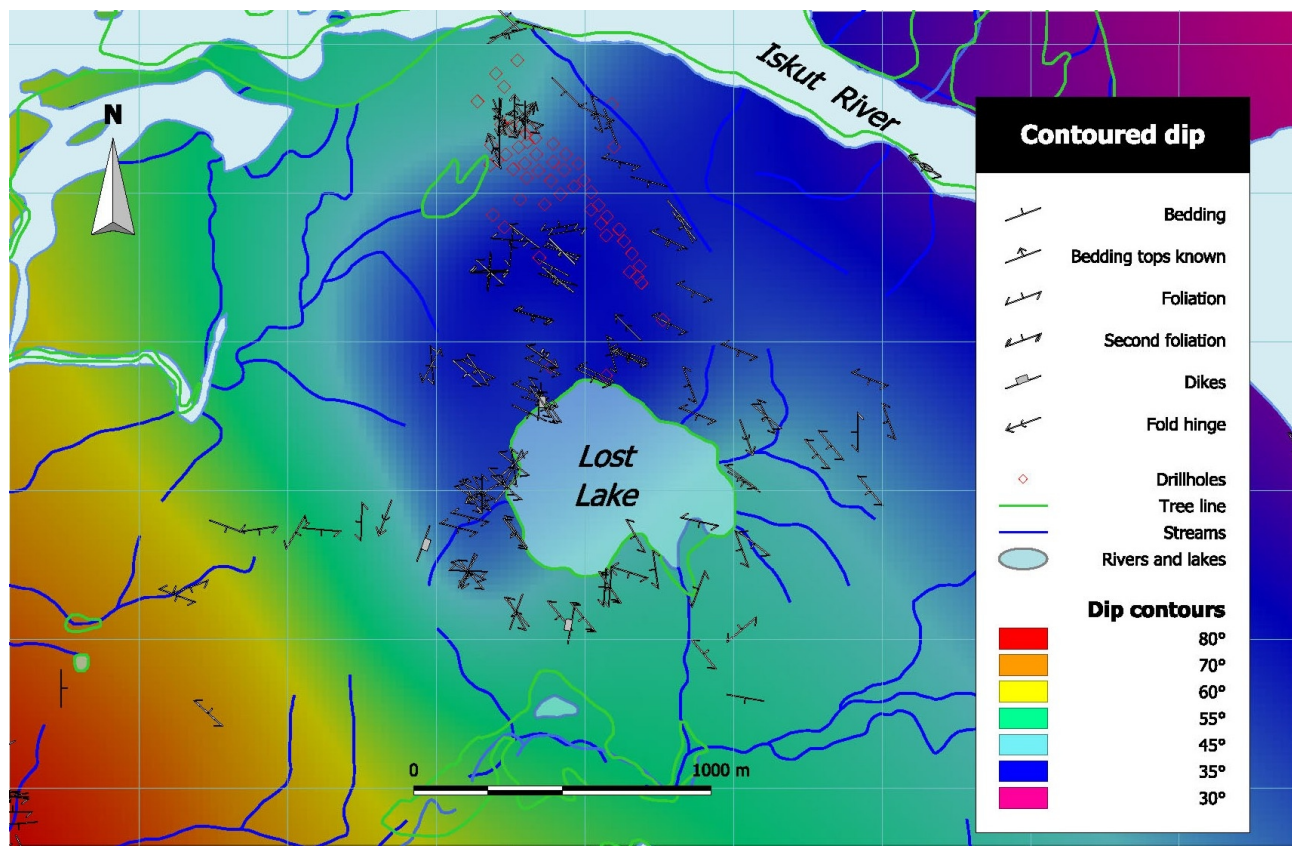


Figure 13. Contoured dips (isogons) for bedding and foliation data collected during this study around the Rock and Roll property. Dike orientations and fold hinges are shown for reference. Dense distribution of drillholes corresponds to mineralization in the subsurface of 'Sulphide ridge'. Grid is 500 m, UTM WGS84.

Pete and Kathy Kossey, proprietors of Bronson Bistro, bestowed warm and inviting camp facilities. Punctual transportation by Lars Helgesen (Quantum Helicopters Ltd), master of the approach, was appreciated. Steve Rowins reviewed an earlier draft of the manuscript.

REFERENCES

- Alldrick, D.J., Britton, J.M., MacLean, M.E., Hancock, K.D., Fletcher, B.A. and Hiebert, S.D. (1990): Geology and mineral deposits of the Snippaker area (NTS 104B/6E, 7W, 10W, 11E); *BC Ministry of Energy, Mines and Petroleum Resources*, Open File 1990-16, scale 1:50 000.
- Anderson, R.G. (1989): A stratigraphic, plutonic, and structural framework for the Iskut River map area, northwestern British Columbia; in *Current Research Part E, Geological Survey of Canada*, Paper 89-1E, pages 143–151.
- Anderson, R.G. (1993): A Mesozoic stratigraphic and plutonic framework for northwestern Stikinia (Iskut River area), northwestern British Columbia, Canada; in *Mesozoic Paleogeography of the Western United States – II*, Dunne, G. and McDougall, K., Editors, *Society of Economic Paleontologists and Mineralogists*, Volume 71, pages 477-494.
- Anderson, R.G. and Thorkelson, D.J. (1990): Mesozoic stratigraphy and setting for some mineral deposits in Iskut map area, northwestern British Columbia; in *Current Research Part E, Geological Survey of Canada*, Paper 90-1E, pages 131–139.
- BC Geological Survey (2009): MINFILE BC mineral deposits database; BC Ministry of Energy, Mines and Petroleum Resources, URL <<http://www.minfile.ca>> [December 2009].
- Becherer, M.P.E. (1997): Mineral resource estimate, Black Dog and SRV zones, Rock and Roll project; unpublished company report, *Red Star Resources Ltd*.
- Cohoon, G.A. and Trebilcock, D.A. (2004a): Phiz Property geology and geochemistry surveys; submitted by Newcastle Minerals Ltd, *BC Ministry of Energy, Mines and Petroleum Resources*, Assessment Report 27 555, 73 pages plus appendices and maps.
- Cohoon, G.A. and Trebilcock, D.A. (2004b): Rock and Roll project, geology and geochemical surveys; submitted by Conquest Resources Limited, *BC Ministry of Energy, Mines and Petroleum Resources*, Assessment Report 27 582, 84 pages plus maps.
- Dunning, J.K. and Scott, T.C. (1997): 1997 Diamond drilling assessment report on the Rock and Roll mineral claims; submitted by Redstar Resources Corp, *BC Ministry of Energy, Mines and Petroleum Resources*, Assessment Report 25 221, 31 pages plus appendices with maps.
- Edwards, B.R., Anderson, R.G., Russell, J.K., Hastings, N.L. and Guo, Y.T. (2000): Geology, the Quaternary Hoodoo Mountain volcanic complex and Paleozoic and Mesozoic basement rocks, parts of Hoodoo Mountain (NTS 104B/14) and Craig River (NTS 104B/11) map areas, northwestern British Columbia; *Geological Survey of Canada*, Map 3721, scale 1:20 000.
- Fillipone, J.A. and Ross, J.V. (1989): Stratigraphy and structure in the Twin Glacier–Hoodoo Mountain area, northwestern British Columbia (104B/14); in *Geological Fieldwork 1988, BC Ministry of Energy, Mines and Petroleum Resources*, Paper 1989-1, pages 285–293.
- Forbes, J.R. (1991): Field work summary report on the Rock & Rock and Bornagay properties; unpublished company report, *Prime Equities Inc*.
- Grove, E.W. (1986): Geology and mineral deposits of the Unuk River–Salmon River–Anyox area; *BC Ministry of Energy, Mines and Petroleum Resources*, Bulletin 63, 152 pages.
- Jones, M.I. (2009): 2009 geophysical report on the Rock and Roll claims; submitted by Pacific North West Capital Corp, *BC Ministry of Energy, Mines and Petroleum Resources*, Assessment Report 31 158 (off confidential August 6, 2010).
- Kerr, F.A. (1935): Stikine River area, south sheet, Cassiar district, British Columbia; *Geological Survey of Canada*, Map 311A, scale 1:126 720.
- Kerr, F.A. (1948): Lower Stikine and western Iskut River areas, British Columbia; *Geological Survey of Canada*, Memoir 246, 94 pages plus maps.
- Kirkham, R.V. (1992): Preliminary geological map of the Brucejack Creek area, British Columbia (part of 104B/8), *Geological Survey of Canada*, Map 2550, scale 1:50 000.
- Kirkham, R.V. (1991): Provisional geology of the Mitchell-Sulphurets region, northwestern British Columbia (104 B/8, 9); *Geological Survey of Canada*, Map 2416, scale 1:50 000.
- Lefebure, D.V. and Gunning, M.H. (1989): Geology of the Bronson Creek area, NTS 104B/10W, 11E (in part); *BC Ministry of Energy, Mines and Petroleum Resources*, Open File 1989-28, 2 sheets, scale 1:25 000.
- Lewis, P.D., Mortensen, J.K., Childe, F., Friedman, R.M., Gabites, J., Ghosh, D. and Bevier, M.L. (2001): Geochronology data set; metallogenesis of the Iskut River area, northwestern BC, *Mineral Deposits Research Unit*, Miscellaneous Report, pages 89–96.
- Logan, J.M. and Koyanagi V.M. (1994): Geology and mineral deposits of the Galore Creek area (104G/3, 4); *BC Ministry of Energy, Mines and Petroleum Resources*, Bulletin 92, 96 pages plus map.
- Macdonald, A.J., van der Heyden, P., Lefebure, D.V. and Alldrick, D.J. (1992): Geochronometry of the Iskut River area—an update (104A and B); in *Geological Fieldwork 1991, BC Ministry of Energy, Mines and Petroleum Resources*, Paper 1992-1, pages 495–501.
- Massey, N.W.D., MacIntyre, D.G., Desjardins, P.J. and Cooney, R.T. (2005): Digital geology map of British Columbia: whole province; *BC Ministry of Energy, Mines and Petroleum Resources*, GeoFile 2005-1, scale 1:250 000, URL <<http://www.empr.gov.bc.ca/Mining/Geoscience/PublicationsCatalogue/GeoFiles/Pages/2005-1.aspx>>.
- Montgomery, A.T. and Ikona, C.K. (1989): Geological report on the Rob 17, 19, 20, 21 mineral claims; submitted by Consolidated Bel Air Resources Ltd, *BC Ministry of Energy, Mines and Petroleum Resources*, Assessment Report 18 462, 14 pages plus appendices and maps.
- Montgomery, A.T., Todoruk, S.L. and Ikona, C.K. (1991): Assessment report on the Rock and Roll Project; submitted by Eurus Resources Corporation, *BC Ministry of Energy, Mines and Petroleum Resources*, Assessment Report 20 884, 18 pages plus figures, appendices and maps.
- Pegg, R. (1989): Geological and geochemical report on the 1989 exploration program of the Rock and Roll property; submitted by Nick C. Carter, *BC Ministry of Energy, Mines and Petroleum Resources*, Assessment Report 19 566, 8 pages plus appendices and maps.
- Todoruk, S.L. and Ikona, C.K. (1988a): Geological report on the Rob 17 & 18 and Win 1 & 2 mineral claims; submitted by Northwest Gold Syndicate, *BC Ministry of Energy, Mines and Petroleum Resources*, Assessment Report 17 209, 35 pages plus appendices and maps.
- Todoruk, S.L. and Ikona, C.K. (1988b): Geological report on the Rob 19, 20, 21 mineral claims; submitted by New Alster Energy Ltd, *BC Ministry of Energy, Mines and Petroleum Resources*, Assessment Report 17 219, 15 pages plus appendices.

Geology and Mineral Potential of Porcher Island, Northern Grenville Channel and Vicinity, Northwestern British Columbia

by J.L. Nelson, J.B. Mahoney¹, G.E. Gehrels², C. van Staal³ and J.J. Potter²

KEYWORDS: Alexander terrane, Porcher Island, Grenville Channel, Coast Mountains, Wales Group, Descon Formation, iron formation

INTRODUCTION

The mineral potential of a significant number of tracts in the northern coastal area of British Columbia is assessed as high (Categories 1 and 2 out of 10; BC Mineral Potential Assessment Program; MapPlace, 2009; Kilby, 1995), but active mineral exploration has been low, as indicated by the relatively low number of assessment reports and recorded mineral showings. Just as it has received comparatively little exploration interest, this area has also not seen systematic public geological mapping since the original Geological Survey of Canada work in the 1960s (Roddick, 1970; Hutchison 1982).

This is year 1 of a planned three year activity to examine the bedrock geology of the north coast area of BC and its potential for hosting significant mineral deposits (Figure 1). The north coast bedrock mapping and mineral deposit study is part of a larger co-operative, National Resources Canada-led endeavour, the Edges (Multiple Metals-Northwest Canadian Cordillera (Yukon, BC)) project. The Edges project aims to increase our understanding of the far-travelled terranes that make up the outer accreted margin of the Canadian Cordillera and of their metallic mineral potential (for a detailed project description see http://gsc.nrcan.gc.ca/gem/min/edges_e.php). Edges is a contribution to the GEM (Geo-mapping for Energy and Minerals) program, a federal program that was initiated in 2008 to enhance public geoscience knowledge in northern Canada to stimulate economic activity in the energy and mineral sectors. The Edges project is a collaboration between the Geological Survey of Canada, the BC Geological Survey and the Yukon Geological Survey, and involves the United States Geological Survey and Canadian and American academic contributors.

The northern coastal area of BC is underlain in part by rocks of the southern Alexander terrane, a large composite crustal fragment that underlies part of the St. Elias Mountains on the Yukon-Alaska border and most of southeastern

Alaska (Figure 1; Wheeler et al., 1991). It is of considerable exploration interest because of the volcanogenic massive sulphide (VMS) deposits that it hosts, including Niblack and others on southern Prince of Wales Island just north of the BC-Alaska border, as well as a trend of Triassic deposits, notably Windy Craggy and the Greens Creek mine (Figure 1). In this first year of the north coast project, we began geological mapping on and near Porcher Island (NTS 103J/01, 02, 103G/15, 16, 103H/12), at the northern end of the Alexander terrane in BC to take advantage of the proximity of these rocks to the much better known stratigraphy in southeastern Alaska, as well as to the known volcanogenic deposits there.

PREVIOUS WORK

The northern coastal region of BC was first mapped systematically, at 1:250 000 scale, as part of Geological Survey of Canada regional coverage of the entire Coast Mountains batholith and its surrounding rocks. The Porcher Island-Grenville Channel area was covered as part of the Prince Rupert-Skeena map area (Hutchison, 1982) and the Douglas Channel-Hecate Strait map area (Roddick, 1970). The focus of these studies was on the plutonic rocks; at that time, the necessary tools for the analysis of metamorphosed volcanic and sedimentary sequences, U-Pb dating and trace-element geochemistry, were not yet available.

More recent geological work in the northern coastal region of BC has focused on understanding the structural and igneous history of the Coast Mountains orogen; Porcher Island and Grenville Channel have been visited by many researchers in the course of much broader studies (Chardon et al., 1999; Chardon, 2003; Butler et al., 2006; Gehrels et al., 2009). Overall, the details of its geology and of the prebatholithic Alexander terrane rocks in particular have not been investigated. The sole exception to this has been the ongoing, mostly unpublished work of G. Gehrels, part of which is summarized in Gehrels (2001) and Gehrels and Boghossian (2000).

REGIONAL GEOLOGICAL SETTING

Northern coastal BC is underlain by a wide variety of metasedimentary and metavolcanic rocks that have been assigned to several tectonic assemblages. From west to east, these include the Banks Island assemblage, the Alexander terrane, the Gravina belt and the Yukon-Tanana terrane (Figure 2). With the exception of the Banks Island assemblage, which has only been recognized along the outer coast of northern BC, most of these units can be traced northward into adjacent portions of southeastern Alaska, where their lithic components, structural and metamorphic

¹ University of Wisconsin at Eau Claire, WI

² University of Arizona, Tucson, AZ

³ Geological Survey of Canada, Vancouver, BC

This publication is also available, free of charge, as colour digital files in Adobe Acrobat® PDF format from the BC Ministry of Energy, Mines and Petroleum Resources website at <http://www.empr.gov.bc.ca/Mining/Geoscience/PublicationsCatalogue/Fieldwork/Pages/default.aspx>.

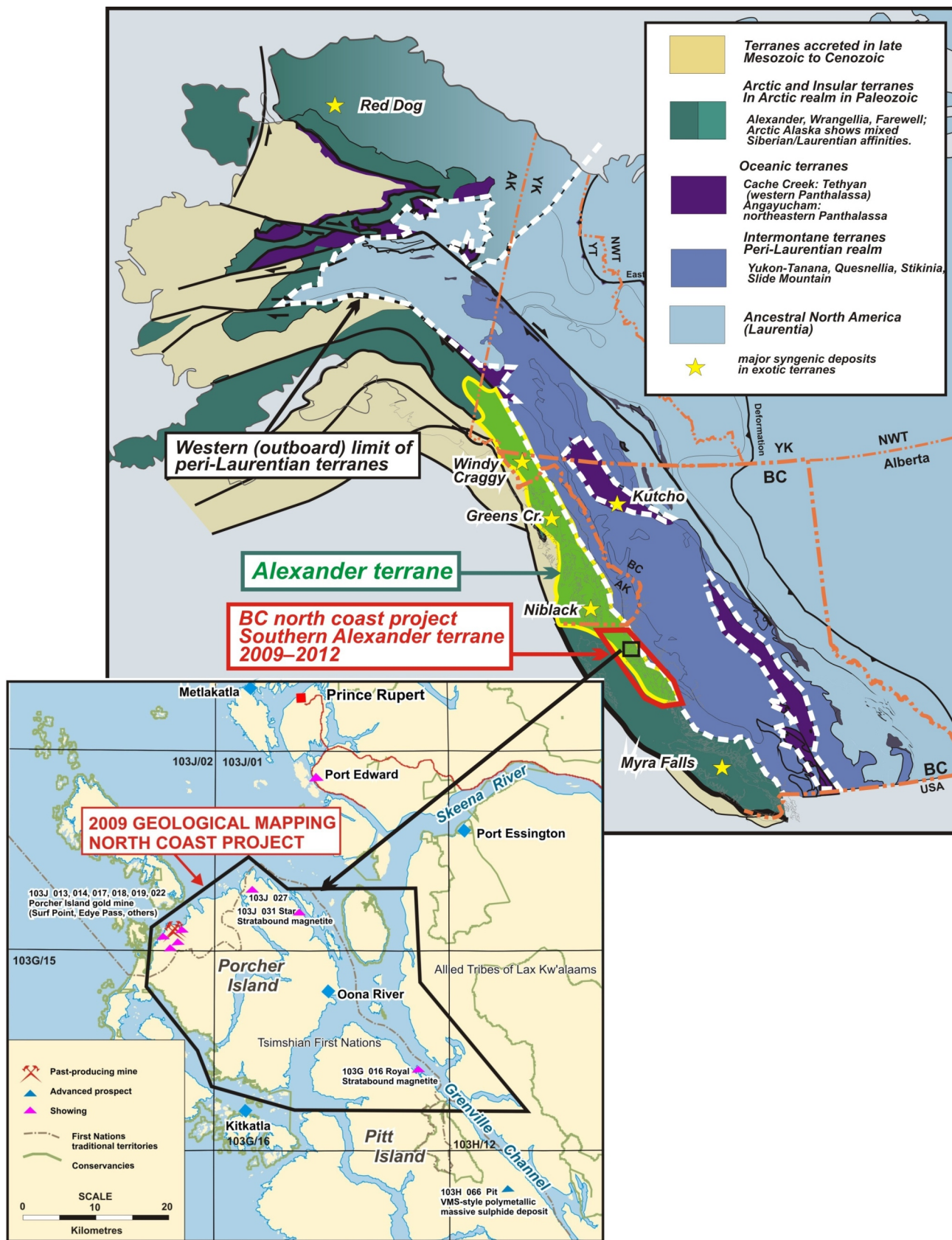


Figure 1. Location of the north coast project, British Columbia, in the context of northern Cordilleran terranes and in terms of local geography.

characteristics, and ages have been described by Gehrels et al. (1987, 1996), Rubin and Saleeby (1992), Saleeby (2000) and Gehrels (2001).

Alexander Terrane

The Alexander terrane in the southern part of southeastern Alaska and northern coastal BC consists of a broad range of volcanic, sedimentary and plutonic rocks, and their metamorphic equivalents, which are primarily of early Paleozoic age (Figure 3). These rocks underlie most of southern part of southeastern Alaska, where they have experienced only minor younger metamorphism, deformation and plutonism. Farther to the southeast, Cretaceous plutons become more widespread and the degree of younger deformation and metamorphism increases. In spite of this younger overprint, it is possible to correlate geological units from southeastern Alaska into northwestern coastal BC, and accordingly we use the nomenclature established in the adjacent Alaskan panhandle. The following unit descriptions are taken from the well-preserved portion of the Alexander terrane in southern part of southeastern Alaska (from Gehrels and Saleeby, 1987; Gehrels et al., 1996).

The oldest rocks recognized in the Alexander terrane consist of Late Proterozoic to Cambrian metavolcanic and metasedimentary assemblages of the Wales Group (Figure 3). Metavolcanic components range from mafic to felsic in composition, with lithic units ranging from metres to hundreds of metres in thickness. Protolith features indicate that these rocks were originally pillow flows, flow breccia, tuffaceous breccia and tuff. Metasedimentary components, similar in abundance to metavolcanic rocks, consist of metagreywacke rich in volcanic detritus, phyllite or schist derived from mudstone and shale, and massive marble. Intrusive into these assemblages are bodies of complexly interlayered gabbro, diorite, tonalite and granodiorite, with layering commonly on a 1–10 m scale. All rocks of the Wales Group have a strong foliation and lineation that is commonly folded around outcrop-scale open folds. Metamorphism ranges from greenschist (rich in actinolite, chlorite and epidote) to amphibolite facies (rich in amphibole, biotite, muscovite and rare garnet).

Rocks of the Wales Group in southeastern Alaska are overlain by a younger suite of lower grade and less deformed volcanic and sedimentary rocks referred to as the Descon Formation. Protoliths of these rocks are very similar to those in the Wales Group, with the

only significant difference being a scarcity of marble in the Descon Formation. Rocks of the Descon Formation generally lack a metamorphic foliation and lineation and are greenschist or lower in metamorphic grade. The age of these strata is constrained by fossils and U-Pb geochronology as Early Ordovician–Late Silurian. Plutons that are coeval (and probably cogenetic) with volcanic rocks of the Descon Formation are widespread and range from diorite to granite in composition.

These early Paleozoic assemblages are overlain unconformably by a variety of Devonian strata that commonly include a basal clastic sequence (conglomerate and sandstone) of the Karheen Formation; mafic volcanic rocks of the Coronados, St Joseph Islands and Port Refugio formations; and limestone of the Wadleigh Formation. The basal conglomerate is interpreted to represent a major phase of uplift and erosion, the Klakas orogeny, as it overlies and contains clasts of a wide variety of older rocks (Gehrels and Saleeby, 1987).

Younger strata in the Alexander terrane include fine- to medium-grained clastic strata, carbonate rocks and minor

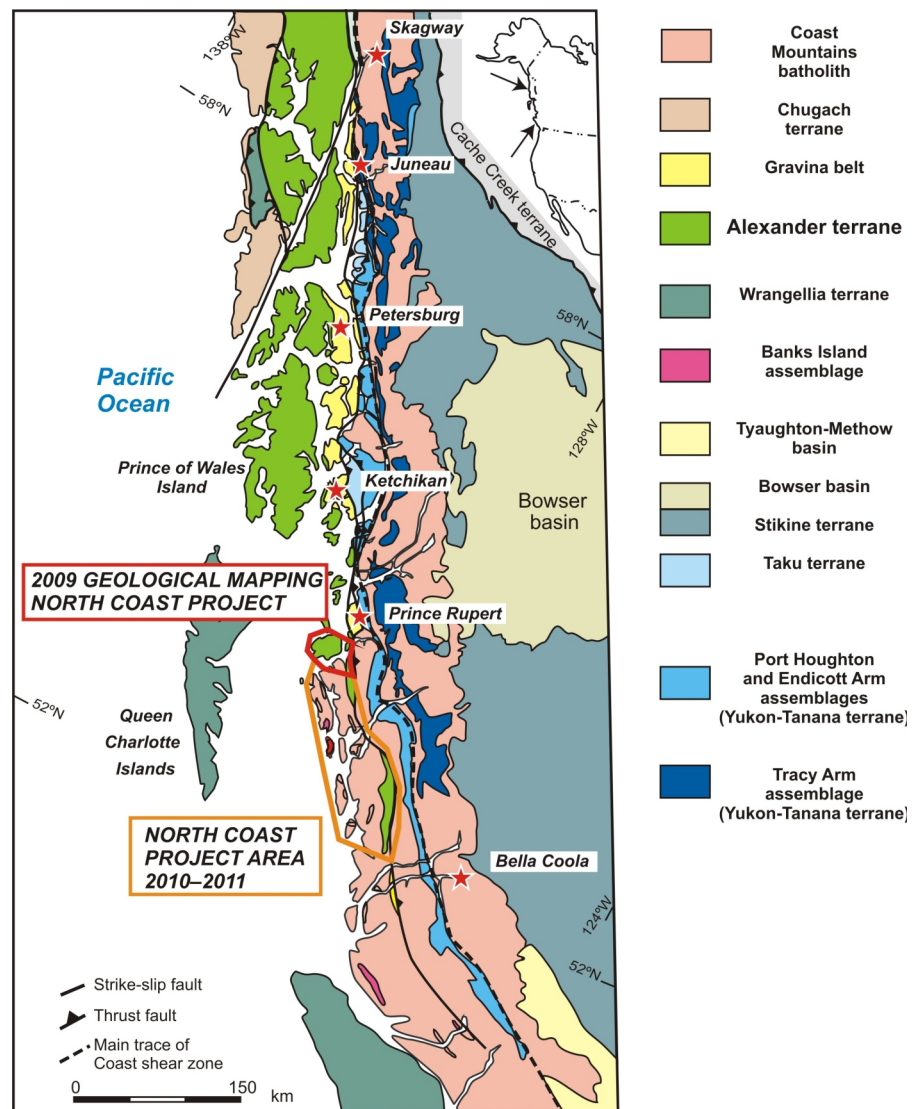


Figure 2. Regional geology of northern coastal British Columbia and southeastern Alaska and setting of the Alexander terrane.

basalt of Carboniferous and Permian age, a Triassic basal conglomerate overlain by bimodal volcanic rocks, carbonate rocks and rare conglomeratic strata of Triassic through Middle Jurassic age.

The Niblack prospect on southern Prince of Wales Island (Figure 1), acquired by CBR Gold Corporation in 2009, is a Cu-Zn-Au-Ag-rich, Kuroko-type VMS deposit with an estimated resource of 2.59 million tonnes at 1.2% Cu, 2.2% Zn, 33.2 g/t Ag and 2.3 g/t Au (CBR Gold Corp., 2009). It is located within a tightly folded pyroclastic rhyolite unit, the Lookout rhyolite, which lies above a bimodal felsic and mafic sequence and below a section of mafic volcanic rocks. It has been regarded as hosted within the Wales Group (Gehrels et al., 1996). Recently, an Ordovician date of ca. 478 Ma has been obtained from the Lookout rhyolite (Karl et al., 2009); this suggests that it is coeval with the Descon Formation, rather than with the Neoproterozoic–Cambrian Wales Group. Ayuso et al. (2005) and Slack et al. (2005) assigned these rocks to the informal Moira Sound unit. They, as well as Gehrels et al. (1983), point out that volcanogenic deposits are known both in this unit and within the Wales Group proper and that both Neoproterozoic and Ordovician volcanic sequences are prospective for syngenetic mineralization.

Other Terranes and Assemblages

BANKS ISLAND ASSEMBLAGE

The Banks Island assemblage (Figures 2, 3) has been recognized as a distinct unit based on the predominance of interlayered metaclastic quartzite and marble in it, which are rare in the generally more primitive Paleozoic arc-related assemblages of the Alexander terrane; it appears to have a continental margin affinity (Gehrels and Boghossian, 2000). These rocks are exposed on the southern shore of Banks Island and can be traced northward to western Porcher Island, west of the 2009 map area. The dominant lithic components are strongly deformed and regionally

metamorphosed metaclastic quartzite that commonly occur in centimetre-scale bands, marble layers with thicknesses of several centimetres to several tens of metres, and phyllite and schist derived from shale and mudstone. These rocks have a well-developed foliation everywhere, which is commonly folded into tight, outcrop-scale isoclinal folds. Pelitic components have been metamorphosed to biotite phyllite or schist, and garnet is present in some regions.

The age of the Banks Island assemblage is constrained only by the following relations: a maximum age of deposition is indicated by detrital zircons recovered from two quartzite rocks, which are as young as ca. 415 Ma (Silurian; G. Gehrels, pers comm, 2009). A minimum age for the assemblage can be inferred from an orthogneiss, which has yielded a U-Pb age of 357 Ma (Early Mississippian), and which appears to have experienced the same regional deformation and metamorphism as surrounding marble. A broader minimum age constraint is provided by plutons of Late Jurassic age that are emplaced into these rocks (Gehrels et al., 2009) and at least locally intrude across the regional foliation and folds. Together, these constraints suggest that at least some portions of the Banks Island assemblage accumulated during mid-Paleozoic time.

GRAVINA BELT

Rocks of the Alexander terrane are overlain by Upper Jurassic and Lower Cretaceous clastic strata—commonly conglomeratic turbidites—and mafic volcanic rocks of the Gravina belt. These rocks can be traced, generally along the inboard margin of the Alexander terrane, for the length of southeastern Alaska (Berg et al., 1972) and into northern coastal BC (Figure 2). On Tongass Island in southeastern Alaska and on the mainland east of Port Simpson (Lax Kw’alaams), these rocks also overlie a sequence of meta-volcanic and metasedimentary rocks that have been assigned to the Yukon-Tanana terrane (Gehrels, 2001).

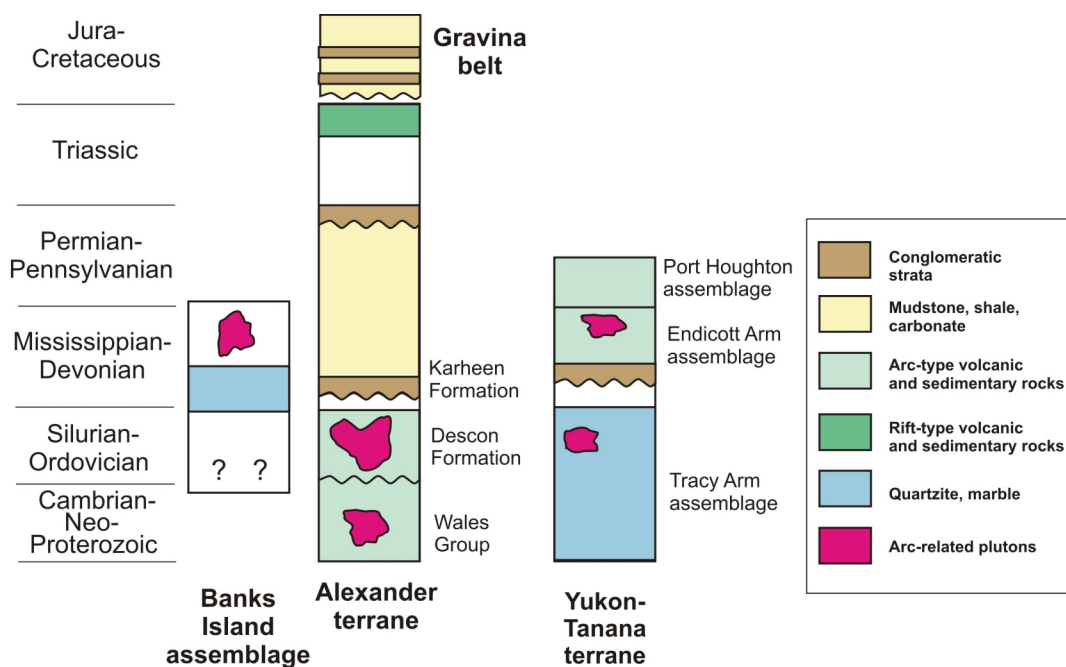


Figure 3. Stratigraphic columns for major terranes of southeastern Alaska.

YUKON-TANANA TERRANE

East of the Alexander terrane and Gravina belt are metavolcanic and metasedimentary rocks of the Yukon-Tanana terrane that underlie the western margin of the Coast Mountains, along the length of southeastern Alaska and northern coastal BC (Figure 2). In general, these rocks form a panel that dips eastward and young westward, suggesting that the overall stratigraphy is inverted. Using the nomenclature defined in southeastern Alaska, the Yukon-Tanana terrane includes the following (Figure 3):

Tracy Arm assemblage: Marble, quartzite, pelitic schist and orthogneiss are migmatitic and commonly high in metamorphic grade.

Endicott Arm assemblage: This unit has a distinctive basal conglomerate containing clasts derived from the Tracy Arm assemblage. Overlying strata include greenschist- to amphibolite-facies felsic to mafic metavolcanic rocks, pelitic schist and minor marble. Available faunal and U-Pb geochronological constraints suggest that most strata are Devonian–Mississippian in age.

Port Houghton assemblage: These strata gradationally overlie the Endicott Arm assemblage and consist of greenschist- to amphibolite-facies metaturbidite, pelitic schist and metabasalt. Available faunal constraints suggest that most strata are late Paleozoic in age.

In northwestern BC, the Ecstall belt (Alldrick, 2001; Alldrick et al., 2001; see also Gareau and Woodsworth, 2000), with its enclosed Devonian volcanogenic deposits, is also assigned to the Yukon-Tanana terrane. The host units are equivalent to the middle Endicott Arm assemblage of southeastern Alaska.

Plutons of the Western Coast Plutonic Complex

Tonalitic to granodioritic plutons of the Coast Plutonic Complex, or the Coast Mountains batholith, occur as isolated bodies in northern and western portions of northern coastal BC, and increase in extent southeastward to form huge continuous bodies of plutonic rock (Figure 2; Gehrels et al., 2009). Compositionally, most bodies are tonalite and granodiorite, with subordinate diorite and minor gabbro and leucogranodiorite. Most bodies have more hornblende than biotite and abundant titanite, and some plutonic suites contain euhedral epidote that is interpreted to be magmatic in origin. Plutons west of the main batholith are generally undeformed, whereas a subsolidus foliation and lineation are more strongly developed toward the east into the core of the Coast Mountains orogen.

According to a recent comprehensive geochronological summary (Gehrels et al., 2009), plutonic U-Pb ages record a history of eastward migration across the Coast Mountains: westernmost are 160–140 Ma (Late Jurassic) tonalite and granodiorite, there are few plutons in the area that are 140–120 Ma, 120–100 Ma (Early Cretaceous) tonalite and granodiorite occur directly east of the Late Jurassic bodies, a nearly continuous band of 100–85 Ma plutons (e.g., Ecstall pluton of Hutchison, 1982) underlies the western margin of the Coast Mountains, mainly tonalitic sills of ca. 70–60 Ma (latest Cretaceous–earliest Tertiary age) occur to the east, and the central and eastern

portions of the Coast Mountains are underlain by huge 60–50 Ma (Eocene) granodiorite bodies.

The depth of emplacement of these plutons also changes eastward across the Coast Mountains. Hornblende barometric studies of the plutons, conducted by Butler et al. (2006), suggest that westernmost Late Jurassic bodies were emplaced at depths of ~15 km. The Early Cretaceous plutons to the east were slightly deeper, ~20 km, whereas mid-Cretaceous plutons of the Ecstall belt were emplaced at significantly greater depths, perhaps 25–30 km. This increase in depth of emplacement correlates well with the eastward increase in metamorphic grade.

LOCAL GEOLOGY

The 2009 map area, comprising the vicinity of Porcher Island, northwestern Pitt Island and Grenville Channel, is underlain by a series of northwest-striking panels of metamorphosed supracrustal and metaplutonic rocks, intruded by late synkinematic, Cretaceous plutons (Figure 4). Although they are metamorphosed and in some cases strongly deformed, we have tentatively correlated the stratified units with known stratigraphic units of the Alexander terrane of southeastern Alaska. We recognize the Wales Group, the Descon Formation and the Karheen Formation. Pre-Cretaceous plutonic bodies include the Ordovician McMicking pluton, the Devonian (?) Swede Point pluton and the possibly Silurian Hunt Inlet pluton. Southwest of the metamorphosed supracrustal units, two metamorphosed igneous complexes, the Ogden Channel and Billy Bay complexes, are recognized. They may be intrusive equivalents of the Wales and/or the Descon volcanic sequences.

Because of lack of bedrock exposure and difficult access to the island interiors, most of the observations that form the basis of our mapping were made along shorelines. These were supplemented with logging road traverses where such access existed, helicopter spot checking and image analysis of 5 m resolution SPOT-5 satellite data from 2004 to 2006.

The geology in Figure 4 is based on a 1:50 000 open file map in preparation that will be available in early 2010 (Nelson et al., in press).

Stratified Units

WALES GROUP (?)

The Wales Group was named for a succession of greenschist- to amphibolite-facies metavolcanic and metasedimentary rocks exposed on Prince of Wales Island in southeastern Alaska (Buddington and Chapin, 1929; Gehrels and Saleeby, 1987). The protoliths include basaltic to andesitic flows, breccia and tuff, rhyolite tuff, greywacke, mudstone and limestone. Metasedimentary and metavolcanic rocks occur in subequal proportions, and the rocks are characterized by well-developed foliation and lineation (Gehrels and Saleeby, 1987). The Wales Group is Late Proterozoic to Cambrian in age, based on a ca. 554 Ma U-Pb date on a crosscutting pluton on Dall Island (Gehrels, 1990) and on a small population of ca. 595 Ma, probably inherited zircons in the Ordovician Lookout rhyolite, which overlies the Wales Group on southern Prince of Wales Island.

In the 2009 map area, the Wales Group is exposed on the eastern side of Porcher Island, on the west coast of the

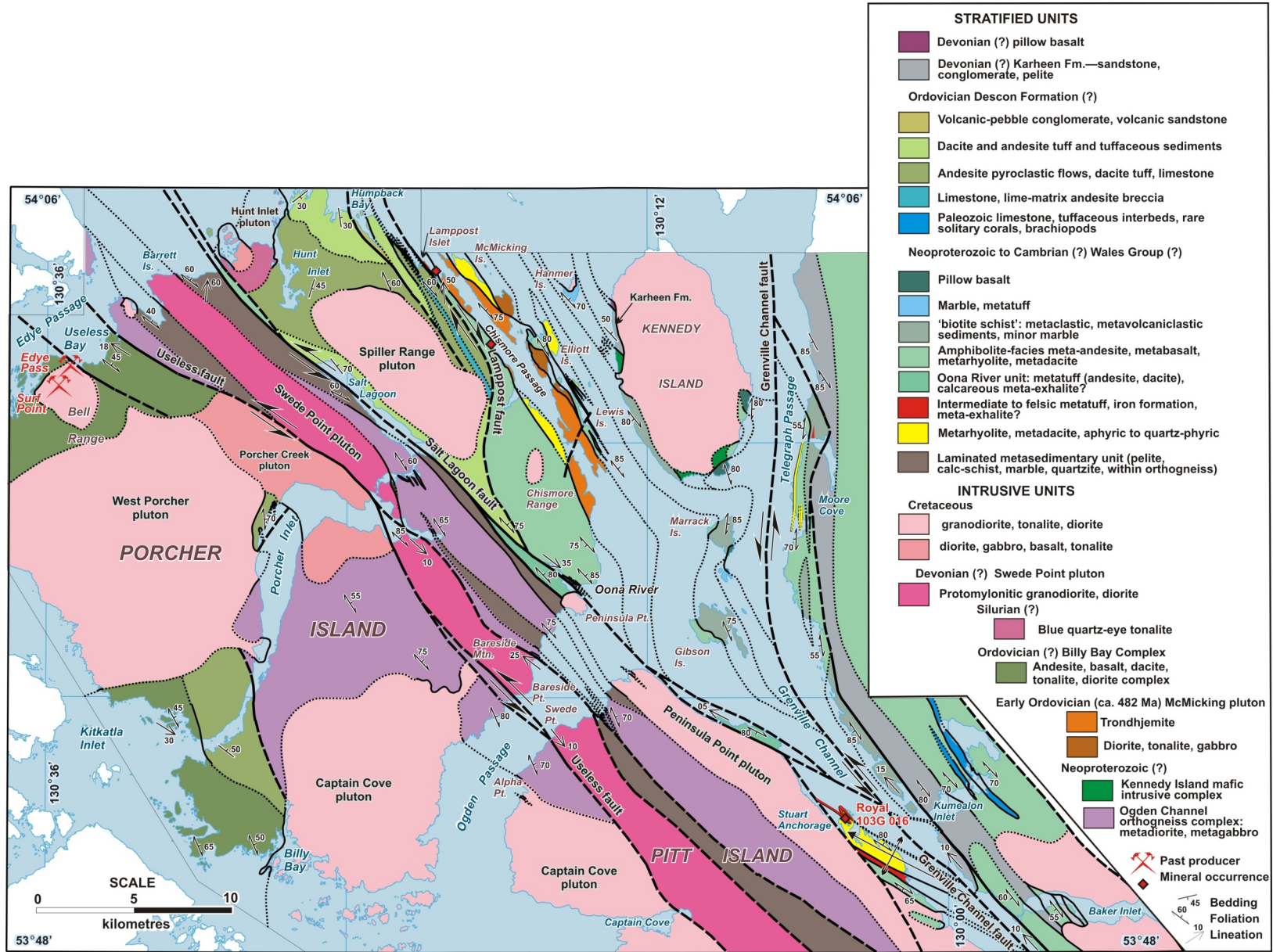


Figure 4. Geology of Porcher Island and Grenville Channel area, northwestern British Columbia. Geological mapping done in 2009 by J. Nelson, J.B. Mahoney, G. Gehrels and C. van Staal; with added information from Roddick (1970), Hutchison (1982) and G. Gehrels, pers comm (2009).

mainland east of Telegraph Passage and Grenville Channel, and on the islands in between (Figure 4). The outcrop belt contains several subparallel lithostratigraphic facies belts exposed between the Useless fault on central Porcher Island and the eastern side of Grenville Channel. The different facies are structurally and stratigraphically interdigitated on a variety of scales, but an overall regional map pattern can be discerned (Figure 4). Wales Group facies belts are described here from southwest to northeast. Note that all of these rocks are in amphibolite grade and in many parts of the area are highly strained, with sporadic and incomplete preservation of protolith textures and features. Nevertheless, enough diagnostic outcrops are present to allow confidence in characterizing the units.

Central Porcher Island

A metasedimentary unit forms the westernmost facies belt, occupying a faulted panel between the Useless and Salt Lagoon faults. It is well exposed along both the north and south coasts of Porcher Island. It consists of rusty-weathering, dark-coloured, thin-bedded metaclastic rocks, including thinly layered to laminated phyllite, biotite schist, marble, calcsilicate, lesser amphibolite and minor quartzite and metagreywacke (Figure 5). Light grey to tan coarse-grained marble successions are generally 1–10 m in thickness, but range locally up 30 m; they are intercalated with thin phyllite, biotite schist and green metatuff units. All primary layering in the unit is transposed into foliation. Intrafolial folds are particularly evident in the more calcareous intervals. Similar rocks form septa within the Ogden Channel Complex (see below). If the intrusions of the Ogden Channel Complex were feeders to volcanic successions of the Wales Group, then this metasedimentary unit contains the oldest supracrustal rocks exposed locally.

Northeastern Porcher–Chismore Passage Section

A meta-andesite unit, consisting of resistant, blocky-weathering, dark green metavolcanic rocks is exposed along the eastern coast of Porcher Island and on Elliott and Lewis islands (Figures 4, 6). The succession is dominated by dark green, massive andesite to basaltic andesite with interbedded thin- to medium-bedded tuff, tuff breccia, metaclastic rocks and marble. The resistant, blocky nature of the exposures results in prominent ribs of metavolcanic rock standing in bold relief against less resistant, finer-grained interbeds. Flow-top (?) breccias are locally preserved. The rocks are generally aphanitic to locally small plagioclase-phyric, and chloritically altered mafic minerals and centimetre-scale lapilli are locally evident. Marble layers within the andesite unit consist of thin layers and laminae of marble, interlayered with green metatuff.

A succession (>100 m) of light grey to greenish grey rhyolitic aphanitic to quartz-phyric crystal tuff and vitric crystal lapilli tuff is exposed on the eastern side of Elliott and Lewis islands. Rhyolite and dacite are interlayered with andesitic tuff and in some areas with thin marble units. Felsic rocks are recrystallized and display a distinct sugary texture, but primary quartz phenocrysts and white, aphanitic lapilli clasts are well preserved. Quartz veins (2–15 cm) are abundant within the unit on eastern Elliott Island. On Elliott Island, the unit appears tabular and laterally continuous, but thins to the south. On the eastern side of Lewis Island, rhyolitic intervals form 5–15 m successions intercalated within andesitic metavolcanic rocks. On McMicking



Figure 5. Typical thinly laminated metamorphosed clastic rocks of the Wales Group on central Porcher Island, northwestern British Columbia; rock hammer for scale.



Figure 6. Typical Wales Group meta-andesite tuff with intrafolial folds, Elliott Island, northwestern British Columbia; rock hammer for scale.

Island, similar rhyolite or dacite forms a large, coherent-textured single body that may be a cryptodome rather than a surface flow.

Gibson, Marrack, Hanmer and Kennedy Islands

This section consists of three units. From southwest to northeast they include meta-andesite/metabasalt, a mixed metasedimentary unit and metamorphosed basalt and pillow basalt.

The meta-andesite/metabasalt unit is indistinguishable from the meta-andesite section on northeastern Porcher Island (see above), except that it is of higher metamorphic grade. It passes northeastward through a transitional contact into the metasedimentary unit. In most exposures, this consists of biotite schist, laminated pelite and metatuff, and minor thin marble and calcsilicate rocks. Thicker marble bodies occur on Hanmer Island (Figure 7) and on Lamb Island, an islet south of Marrack Island. They contain clasts and interbeds of fragmental volcanic origin, a feature that links them to the rest of the Wales Group.

A distinctive succession of stretched pillow basalt occurs on Daring Point, on the southeastern tip of Kennedy Island, and extends to the south to the southeastern tip of Marrack Island and the northeastern tip of Bedford Island (Figure 4). The basalt is aphanitic, locally amygdaloidal, and occurs in thick, homogeneous successions of up to 20–30 m thick. The diagnostic characteristic of the unit is stretched pillows, which display length to width ratios of 10:1 to 30:1, forming long, thin tubes that dominate the exposure.

Stuart Anchorage–Northeastern Pitt Island–Oona River

The Wales Group (?) section exposed on the small peninsula south of Stuart Anchorage on northeastern Pitt Island forms a tight anticline, truncated to the southwest by a fault that juxtaposes it with a body of unfoliated Cretaceous granodiorite. The stratigraphically lowest unit is a white, quartz-rich metadacite, consisting mostly of quartz with lesser biotite and muscovite in discontinuous trains. Colour laminations in some places appear to reflect original depositional layering in tuff; elsewhere, more even, coarse-grained textures may be derived from a coherent volcanic or hypabyssal protolith. One outcrop at the top of the dacite shows volcanic breccia textures (Figure 8). The sparse vegetation pattern on the rocky crest of the peninsula is very similar to that developed on the trondhemite on McMicking, Elliott and Lewis islands. This pattern is probably due to similar, nutrient-poor bedrock chemistry. It is possible that the Stuart Anchorage metadacite is a high-level equivalent of the McMicking trondhemite, and thus would be part of the Ordovician Descon Formation rather than the Wales Group. This suggested correlation will be tested by U-Pb dating.

The dacite is overlain gradationally by very biotite rich laminated tuff, which passes upward into a sequence of green andesitic thin-bedded to laminated tuff and tuffaceous sedimentary beds, cherty, fine-grained metadacite tuff and impure metachert. A notable feature within the thin-bedded tuffaceous unit is the presence of iron formation—fine-grained magnetite in layers and laminae, with some associated epidote-garnet concentrations. Metachert within this unit contains unusual metamorphic assemblages, including manganian zoisite and axinite, as well as disseminations and laminae of sulphide minerals



Figure 7. Wales Group marble on Hanmer Island, with thin interlayers of andesitic metatuff, northwestern British Columbia; rock hammer for scale.

and magnetite. This unit is described in detail in the section on volcanogenic occurrences. The mixed laminated unit in turn grades upward into typical, less distinctly bedded green andesitic metatuff and lapilli tuff of the Wales Group. Facing directions determined from graded bedding and basal scours show original sedimentary tops facing towards the overlying andesitic section.

A continuation of the laminated metatuff unit outcrops in the valley around the village of Oona River, where it is used for road metal because of its susceptibility to fracture into centimetre-size blocks. It is both colour- and compositionally laminated on scales ranging from millimetres to decimetres, with alternation of hornblende-, plagioclase-quartz- and biotite-rich laminae; the latter give it a strong cleavage.

Eastern Grenville Passage

Rocks assigned to the Wales Group on the mainland coast east of Grenville Channel are, like the exposures on the nearby islands, for the most part amphibolite-facies andesite metatuff and breccia. These dark green rocks form monotonous sequences along the coast. Protoliths also include subvolcanic (?) intrusions—diorite, andesite and basalt, now metamorphosed to amphibolite facies—which are difficult in many cases to distinguish from extrusive rocks. Within this predominantly intermediate section, there are discrete bodies of potassium feldspar-rich metarhyolite and thin sequences of pelitic metasedimentary strata, particularly in the area around Moore Cove. Of particular interest are quartz-sericite schist and magnetite-bearing chert, described in the section on economic geology.

Metavolcanic rocks correlated with the Wales Group also occur in Kumealon and Baker inlets. They are mostly monotonous meta-andesite typical of the Wales Group. However, in both areas, protolith compositions are indicative of at least local bimodal volcanism. One example in Kumealon Inlet is of a basaltic pillow breccia (Figure 9), now a garnet-chloritoid amphibolite, in contact with a metamorphosed felsic breccia containing an assemblage of garnet, biotite, sillimanite and cordierite. At such high metamorphic grade, the preservation of primary igneous textures is remarkable.



Figure 8. Dacite peperitic breccia at top of metadacite in Wales Group, Stuart Anchorage, northwestern British Columbia; rock hammer for scale.

DESCON FORMATION (?)

The Descon Formation was named by Eberlein et al. (1983) for a succession of basaltic-andesitic pillow flows and breccia, rhyolitic-dacitic tuff and breccia, greywacke and mudstone with subordinate conglomerate and limestone that underlies much of central Prince of Wales Island in southern Alaska (Gehrels and Saleeby, 1987). It is interpreted to be Early Ordovician to Early Silurian in age in southeastern Alaska, based on the occurrence of Middle Ordovician graptolites, 480–438 Ma plutons, and detrital zircon geochronology that ranges from ca. 490 to 460 Ma (Gehrels and Saleeby, 1987; Gehrels et al, 1996). The Descon Formation is interpreted to unconformably overlie deformed volcanic strata of the Late Proterozoic to Cambrian Wales Group, based on the greater degree of deformation and metamorphism in the Wales Group and the presence of a thick sedimentary breccia with deformed Wales Group clasts at the base of the Descon Formation on southern Prince of Wales Island.

In the 2009 map area, the Descon Formation is exposed in two outcrop belts along the northeastern and northwestern coasts of Porcher Island. As in southeast Alaska, the Descon Formation is differentiated from the older Wales Group by a lower degree of deformation and metamorphism and a lack of the striped marble-tuff units present in the Wales Group. In contrast to the Wales Group, the Descon Formation lacks penetrative cleavage and abundant intrafolial folds, does not exceed upper-greenschist metamorphic grade and displays well-preserved volcanic and sedimentary textures.

Eastern Facies

On northeast Porcher Island, the Descon Formation is exposed in a fault panel bounded on the east by the Lamppost fault, a sinistral oblique fault that juxtaposes Wales Group strata with the Descon Formation, and on the west by the Salt Lagoon fault, a sinistral transcurrent fault (Figure 4). The Descon Formation on northeast Porcher Island forms a gently dipping panel of rocks that generally dips to the west, but is folded into a series of gentle folds with an amplitude of hundreds of metres. The northeastern side of the outcrop belt is moderately foliated, with a lithologically controlled distribution of shear zones, and foliation decreases markedly to the west. The rocks in this area are generally lower-greenschist facies with readily identifiable sedimentary and volcanic textures. Regional mapping suggests the entire fault panel forms a broad, north-plunging synclinorium in which a crude stratigraphy youngs upsection from the eastern edge of the outcrop belt near Lamppost Islet to the centre of the synclinorium near Humpback Bay (Figure 4).

The lower portion of the stratigraphy consists of thin-bedded andesitic tuff and volcanic breccia (0.5–2 m) intercalated with brown marble (1–2 m) and thin- to medium-bedded green volcanoclastic arenite and wacke. Marble locally contains rhythmic intercalations (centimetre-scale) of thin green tuff. A striking component of this part of the sequence is andesite breccia beds with limestone matrix (Figure 10).

On the west side of the synclinorium, thin marble beds are intercalated with thin-bedded black argillite and thin- to medium-bedded volcanic lithic arenite on the shores of Salt Lagoon.



Figure 9. Basalt pillow breccia in amphibolite facies, Kumealon Inlet, northwestern British Columbia; pen magnet for scale.

Interbedded tuff, volcanoclastic sedimentary rocks and marble near the base of the succession give way up to epiclastic strata with interbedded very finely laminated felsic tuff (Figure 11). Rhyolitic lapilli tuff (0.5–2 m) with distinct white angular lapilli clasts forms a minor but distinctive part of the thin-bedded succession, and becomes volumetrically more important upward. Rhyolitic to dacitic lapilli tuff and tuff breccia units up to several metres thick are interbedded with thin bedded, fine-grained sedimentary successions north of Lamppost Islet.

The primary volcanic character of the Descon Formation decreases upsection, and the unit becomes increasingly epiclastic in character. South of Mason Point, the section is dominated by medium- to thick-bedded, fine- to medium-grained volcanic lithic arenite to wacke that is locally coarse-grained, moderately well sorted, subangular to subrounded and intercalated with thin-bedded siltstone to mudstone. Sedimentary structures include parallel to wavy laminations, graded bedding, crosslaminations and basal scour surfaces. Thin brown marble is locally rhythmically interbedded within the clastic sedimentary succession. The succession coarsens upward, and near Humpback Bay, medium- to thick-bedded, locally massive, medium- to coarse-

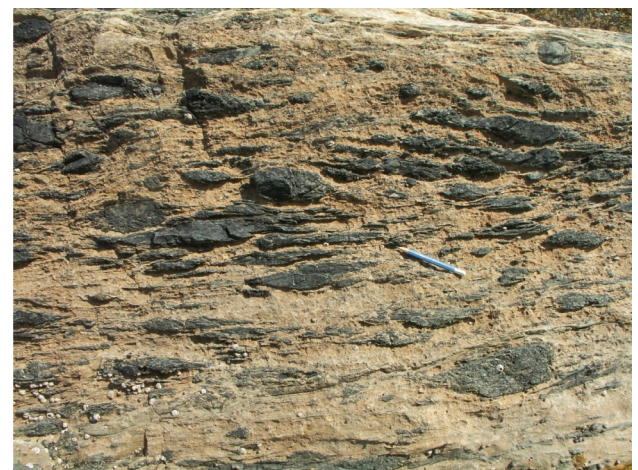


Figure 10. Lime-matrix andesitic breccia, lower Descon Formation, northeastern Porcher Island, northwestern British Columbia; pencil for scale.

grained volcanic lithic arenite/wacke interbedded with crudely stratified volcanic pebble conglomerate dominate the sequence (Figure 12). Conglomerate beds are 10–40 cm thick, tabular and laterally continuous. Thin (10–30 cm) marble beds are locally evident. Thick (1–3 m) quartz-bearing rhyolitic lapilli tuff with abundant angular white lapilli clasts form less than 10% of the succession.

The stratigraphically highest part of the Descon Formation in this area is exposed in the islands northeast of Hunt Inlet. This portion of the section is dominated by dark grey to dark green, thin- to medium-bedded, fine-grained lithic arenite, siltstone and argillite interbedded with distinctive intervals of resistant, thin-bedded green siliceous vitric tuff.

Western Facies

Exposures of the Descon Formation on western Porcher Island are concentrated around Useless Bay and at the mouth of Porcher Inlet (Figure 4). The unit is widely exposed to the west on the Porcher Peninsula and to the north on Stephens Island, but these exposures were not examined during the 2009 field season. In general, the western facies of the Descon Formation represents a proximal facies dominated by coarse fragmental volcanic rocks and associated hypabyssal intrusions, in sharp contrast to more well-bedded, sediment-dominated successions of the eastern, distal facies.

At Useless Bay, the unit is dominated by dark green to dark grey andesitic tuff breccia, breccia and lesser lava flows. Andesitic dikes locally cut the fragmental rocks. Thin- to medium-bedded volcanoclastic sedimentary successions are locally interbedded within pyroclastic successions. Exposures are massive, and bedding is difficult to discern. To the south, near the mouth of Porcher Inlet, the Descon Formation is contained within two fault panels between the Billy Bay Complex on the west and a fault on the east that separates it from the orthogneiss of the Ogden Channel Complex (Figure 4). The easternmost of these two fault panels contains a moderately east-dipping succession of thick-bedded to massive andesitic lapilli tuff and tuff breccia overlain by a thick sequence (hundreds of metres) of medium- to thick-bedded volcanic lithic arenite and wacke and thin- to medium-bedded volcanic sandstone, siltstone and argillite. This succession may represent a transitional facies between the proximal western facies and the more distal eastern facies. The westernmost fault panel contains mafic, intermediate and felsic volcanic, hypabyssal and plutonic rocks of the Billy Bay Complex (described below), which is interpreted as vent-proximal to subvolcanic facies of the Descon Group.

KARHEEN FORMATION

The Karheen Formation was named for a succession of conglomerate, sandstone, siltstone, shale and minor limestone exposed on Prince of Wales Island (Eberlein and Churkin, 1970; Gehrels and Saleeby, 1987). Conodont and brachiopod biostratigraphy indicate the formation is middle Early Devonian (Pragian) in age. The formation overlies Silurian and older rocks, and is interpreted as part of a subaerial to shallow marine clastic wedge that coarsens and thickens to the southeast (Eberlein and Churkin, 1970; Gehrels and Saleeby, 1987). Detrital zircon geochronology from the Karheen Formation includes a ca. 450–420 Ma dominant population, apparently derived from Late Ordovician and Silurian plutonic rocks of the southern Alex-



Figure 11. Well-bedded crystal-ash tuff, upper Descon Formation, northeastern Porcher Island, northwestern British Columbia; rock hammer for scale.



Figure 12. Descon conglomerate, near Humpback Bay, northeastern Porcher Island, northwestern British Columbia; rock hammer handle for scale.

ander terrane, and a diverse Middle Proterozoic–Late Archean population of unknown cratonic derivation (Gehrels et al., 1996).

In the 2009 map area, the Karheen Formation is exposed on the western side of Kennedy Island and on the eastern shore of the Grenville Channel (Figure 4). On western Kennedy Island, the unit is steeply dipping, with tops to the east, and is presumed to unconformably overlie the Wales Group. The Karheen Formation is intruded by the Kennedy Island pluton, which also intrudes the Wales Group on its southern end. On western Kennedy Island, the Karheen Formation consists of medium- to thick-bedded, medium- to coarse-grained lithic feldspathic arenite, polymict matrix- to clast-supported pebble to cobble conglomerate, and thin- to medium-bedded intervals of fine-grained sandstone, siltstone and shale. The unit contains abundant sedimentary structures, including trough cross-stratification, graded bedding, basal scour surfaces and crude channel structures, typical of the Karheen in its type exposures in southeastern Alaska (Figure 13). The conglomerate contains distinctive clasts of blue quartz-eye plutonic rocks that resemble Silurian trondhjemite exposed

in southeast Alaska, and potentially to the west in the McMicking pluton (Gehrels and Boghossian, 2000) and the Hunt Inlet pluton, which may be Silurian (see below). The southern end of the Kennedy Island exposures become finer grained, with interbedded sandstone, siltstone and mudstone/shale (pelite). The sedimentary succession is overlain by a volcanic package containing pillow basalt that displays bulbous pillow outlines and amygdaloidal rinds (Figure 14). They may represent the mafic part of the bimodal volcanic sequence that in places overlies the Karheen Formation in southeastern Alaska. In contrast to the highly deformed pillow basalt in the Wales Group on nearby Murrack Island, this basalt shows no evidence of flattening.

On the eastern shore of Grenville Channel, grey thin- to medium-bedded, well-sorted, in places cross-stratified sandstone, siltstone, shale and minor matrix-supported plutonic and quartz pebble conglomerate occur in two structural panels. Near the mouth of Kumealon Inlet, plutonic-cobble conglomerate and sandstone overlie amphibolite of the Wales Group across a sharp, apparently unfaulted, unconformable (?) contact in the core of a regional fold. The more extensive panel of Karheen-equivalent strata, the Kumealon clastic unit, extends over 35 km, from Telegraph Passage to Baker Inlet, in fault contact with Wales Group metavolcanic rocks to the west (Figure 4). This succession is inferred to be correlative with the Karheen Formation on Kennedy Island, although the precise stratigraphic relation between the two packages is uncertain. The Kumealon clastic unit is a sequence of grey, thick-bedded, well-sorted sandstone interbedded with thin-bedded sandstone, siltstone and pelite. In one outcrop near the western end of Kumealon Inlet, texturally pristine cross-stratified quartz-pebble conglomerate and sandstone (Figure 15) are interlayered with highly foliated pelite crowded with garnet porphyroblasts up to 1 cm across—a dramatic instance of compositional control on the preservation of primary features during high-grade dynamothermal metamorphism. Sparse top directions suggest overall eastward younging in this sequence; however, west-facing beds are also observed and the prevalence of isoclinal folding in the area makes stratigraphic facing directions difficult to determine.

A detrital zircon sample from the Karheen Formation on Kennedy Island yielded a population dominated by Silurian, 435–430 Ma zircons (Gehrels and Boghossian, 2000). This signature, typical of the Karheen in southeastern Alaska, represents erosion of Silurian plutons. A quartz-pebble conglomerate in Kumealon Inlet yields a similar Silurian detrital peak, with a scattering of Precambrian grains (G. Gehrels, pers comm, 2009). This similarity in detrital zircon signatures supports the correlation of the Kumealon clastic unit east of Grenville Channel with the Karheen Formation on Kennedy Island.

PALEOZOIC LIMESTONE IN KUMEALON INLET

Two bands of marble and calcsilicate outcrop near the head of Kumealon Inlet and extend north along Kumealon Lagoon. The more easterly body is dominated by pure, well-bedded marble; the more westerly body shows interlayering on a centimetre to metre scale with metatuff and clastic (?) metasedimentary layers. Above a thin contact zone of intercalation with metavolcanic laminae, the eastern unit comprises a thick basal succession (10–50 m)

of thin- to medium-bedded, brown-weathering, light brown, coarse-grained marble with local relict fossil material. Recrystallized fossil material, including apparent solitary (Rugosan) corals, trace fossils (fine worm tubes) and bioclastic hash suggest the protolith was a late Paleozoic fossiliferous rudstone to floatstone (Figure 16). The marble becomes intercalated towards the west with thin-bedded,



Figure 13. Cross-stratification in Karheen metasandstone, western Kennedy Island, northwestern British Columbia; rock hammer for scale.



Figure 14. Undeformed pillow basalt stratigraphically above the Karheen Formation, western Kennedy Island, northwestern British Columbia; rock hammer for scale.



Figure 15. Quartz-pebble conglomerate in the Kumealon clastic unit, northwestern British Columbia; rock hammer for scale.

greenish-grey volcanoclastic (?) fine-grained sandstone and siltstone, and gradationally passes into thin- to medium-bedded volcanoclastic strata, which then passes westward into the thinly layered marble-metavolcanic unit.

The structural and stratigraphic relationships between the marble and the metavolcanic rocks around it are not known. Both the marble and the rocks around it are isoclinally folded with transposed layering. The discontinuity of the marble unit was noted by Roddick (1970): it does not outcrop to the south on the shores of Baker Inlet, nor to the north in the mountains east of Moore Cove. We have thus interpreted it as occupying the core of a doubly plunging synform that ‘airs’ —is eroded away in both up-plunge directions—to the northwest and southeast of Kumealon Inlet. We have assumed, because of continuity and resemblance to Wales Group exposures elsewhere, that the metavolcanic unit here also belongs to the Wales Group. However, the field relationships, in which there are apparently transitional contacts between the metavolcanic unit and the coral-bearing Paleozoic limestone (Figure 17), are not compatible with this interpretation.

Plutonic/Metamorphic Complexes

OGDEN CHANNEL COMPLEX

The Ogden Channel Complex comprises both orthogneiss and the older metasedimentary septa that it intrudes. It outcrops in two adjacent, northwest-striking belts that span both sides of Ogden Channel on Pitt and Porcher islands, separated from each other by the Useless fault and the Swede Point pluton (Figure 4). The orthogneiss consists of many small bodies with intricate crosscutting original relationships. It is dominantly mafic, consisting of variable-textured metadiorite and gabbro with subordinate smaller bodies of quartz diorite and tonalite. It is locally and regionally heterogeneous, both in composition and texture. Compositional bands occur typically on 1–10 m scales; textures vary from coarse to fine grained. The orthogneiss is an intrusive complex, strongly deformed throughout and metamorphosed to amphibolite grade.

The metasedimentary septa within the orthogneiss consist of laminated pelite, siliceous pelite, calcsilicate, lesser pure marble, quartzite, meta-greywacke with quartz-rich layers and amphibolite sills (?). Thin layering typifies



Figure 16. Solitary coral, marble unit, Kumealon Inlet, northwestern British Columbia; pencil for scale.

the unit—both as compositional layering such as pelite-quartzite or calcsilicate-marble, and also within lithologic units, which can be finely colour laminated. Like the enclosing orthogneiss, the metasedimentary units have been metamorphosed at amphibolite grade. Isoclinal folding is common. We interpret these as remnants of country rock that were intruded by the orthogneiss.

BILLY BAY COMPLEX

The Billy Bay Complex is exposed on the western shore of Porcher Island from Billy Bay, where it is truncated by the Captain Cove pluton, to Kitkatla Inlet, where it is cut off by the West Porcher pluton. It is a mafic, intermediate and felsic extrusive/intrusive complex in which volcanic and subvolcanic components are mixed on scales of 1–50 m, including basalt and andesite flows, tuff and breccia; plagioclase-phyric granodiorite; diorite; and very minor meta-argillite, metachert and metasandstone. It has the character of a complex volcanic centre consisting of many mutually crosscutting intrusive and hypabyssal phases as well as extrusive remnants. Most units of the Billy Bay Complex have undergone amphibolite-facies metamorphism. Unlike the Ogden Channel Complex, primary igneous textures are preserved in spite of strong shearing, as are other features such as chilled dike margins and flow-breccia transitions. Fabric development is strongly lithologically partitioned. Foliation is strongest in mafic tuff, which are now highly foliated amphibolite. By contrast, the interiors of some dikes and sills show original plagioclase-phyric textures, and diorite show pseudomorphed salt-and-pepper plagioclase-augite intergrowths, without any superimposed foliation.

Provisionally, we regard the Billy Bay Complex as a vent-proximal facies of the Descon Formation, based on the comparable preservation of primary textures compared to those in the Wales Group. This assertion will be tested by U-Pb dating. The complex may well be a composite of igneous units of several ages; the granodiorite in particular are compositionally dissimilar to Descon felsic units, which tend to contain less potassium feldspar.



Figure 17. Gradational contact between metavolcanic unit and Paleozoic marble, Kumealon Inlet, northwestern British Columbia; rock hammer for scale.

Intrusive Units

ORDOVICIAN

McMicking Pluton

The McMicking pluton is a northwesterly elongate body that outcrops on McMicking, Elliott and Lewis islands (Figure 4). Most of the body consists of coarse-grained equigranular to somewhat inequigranular white to pale grey trondhjemite. It is quartz-rich, with blobby quartz grains studding many exposures. Sodic plagioclase is the dominant mineral; potassium feldspar is absent. Minor mafic minerals have been recrystallized to chlorite, epidote, sericite and actinolite. It is variably foliated; the degree of foliation increases strongly southwest towards the Lampost fault. The border phase of the McMicking pluton contrasts strongly with its uniform, felsic interior. It consists of crosscutting phases of variably textured tonalite and diorite. Foliation is less pronounced in the pluton than in the main trondhjemite, probably due to a lack of easily deformed minerals such as quartz and mica.

The McMicking pluton cuts across layering and foliations in the Wales Group (Figure 18), indicating that it was emplaced after an episode of regional metamorphism and deformation. This relationship is overprinted by younger, lower-grade metamorphism and shearing of both the pluton and the older metavolcanic rocks that it intrudes.

The McMicking pluton has been dated by U-Pb methods on zircon as 482 ± 15 Ma (Early Ordovician; Gehrels and Boghossian, 2000). It is coeval with the oldest known Ordovician plutons in the Alexander terrane of southeastern Alaska (Gehrels and Saleeby, 1987; S. Karl, pers comm, 2009). It was probably a feeder to Descon-aged volcanism. Its trondhjemitic composition and lack of older zircon inheritance are consistent with intrusion in a primitive arc environment.

SILURIAN (?)

Hunt Inlet Pluton

The Hunt Inlet pluton outcrops on the shores of far northern Porcher Island and adjacent islands near Hunt Inlet. Its characteristic and unique outcrop style is expressed as a horde of tiny islets and subtidal rocks that pose a dis-



Figure 18. Trondhjemite of the McMicking pluton intrudes metaandesite tuff, northwestern Elliott Island, northwestern British Columbia; pencil for scale.

ting hazardous to small-boat navigation. The body consists of weakly foliated lower-greenschist grade metatonalite with blue quartz eyes. Primary mafic minerals are recrystallized to fuzzy clots of epidote, chlorite, biotite and possibly actinolite. It intrudes the deformed and somewhat foliated Descon Formation, and is cut by Cretaceous (?) unfoliated, fresh diorite. It physically resembles granitoid rocks of Silurian age on Prince of Wales Island (Gehrels and Saleeby, 1987), and this is offered as a tentative correlation pending U/Pb geochronology.

DEVONIAN (?)

Swede Point Pluton

The Swede Point pluton forms a northwesterly trending belt of light-coloured exposures that extends across central Pitt and central Porcher Island. These outcrops are much more devoid of vegetation than other plutonic units: Bareside Mountain on southeastern Porcher Island is a particularly prominent example. The body consists of very strongly foliated granodiorite, granite, tonalite and diorite. Small plagioclase-phyric textures are very common. In parts it is compositionally heterogeneous on a metre scale; elsewhere it is more uniform. One of the distinguishing characteristics of the Swede Point pluton is the common presence of synkinematic to postkinematic garnet, which may indicate a relatively aluminous composition. Its degree of protomylonitic deformation is also distinctive, compared to the less-foliated but presumably older McMicking pluton.

The Swede Point pluton intrudes rocks of the Ogden Channel Complex. Intrusive relationships are clearly shown in outcrops near Bareside Point (Figure 19), Barrett Point, and in the channel leading to Salt Lagoon. The Swede Point phases crosscut early foliation in the Ogden Channel Complex. Near Barrett Island, east of Useless Bay, some dikes are mylonitized whereas others crosscut the foliation, which suggests synkinematic emplacement (see discussion in 'Structure').

The Swede Point pluton has been dated as 382 ± 14 Ma by U-Pb methods (van der Heyden, 1989); however, because of complicated systematics, this date is considered approximate and we have collected samples for reanalysis. Middle Devonian plutons are rare in the Alexander terrane.

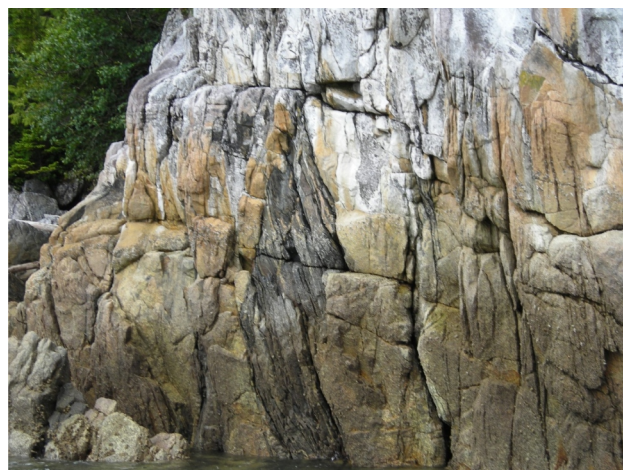


Figure 19. Swede Point pluton intruding amphibolite-facies orthogneiss of the Ogden Channel Complex, near Bareside Point, northwestern British Columbia; field of view is 20 m.

CRETACEOUS INTRUSIONS

Typical of the western reaches of the Coast Plutonic Complex, the Porcher Island–Pitt Island area is host to a number of individual plutons. In map view, they are equant and irregular in shape, except for the tabular, elongate Peninsula Point pluton (Figure 4). They crosscut foliation in the older rocks and some faulted unit contacts, but are offset and locally deformed by the major faults in the area, including the Salt Lagoon and Useless faults (Figure 4) and farther west, the Kitkatla shear zone (Chardon et al., 1999). The Cretaceous suite includes granodiorite, tonalite, diorite and minor true granite, along with swarms of pegmatite near pluton margins. Although these are not dated on Porcher Island, U–Pb dates from similar bodies on Pitt, McCauley and Stephens islands are in the range of 113–101 Ma (Butler et al., 2006; Gehrels 2001).

Captain Cove Pluton

The Captain Cove pluton is exposed on southeastern Porcher Island and across Ogden Channel on Pitt Island (Figure 4). Except for some diorite-gabbro border phases near Alpha Point, it is a voluminous body of granodiorite, quartz diorite and quartz monzonite (Roddick, 1970). Butler et al. (2006) report three U–Pb ages from the Captain Cove pluton of 108.5–107 Ma. One of their samples is from a dike that crosscuts fabrics of the Kitkatla shear zone on Pitt Island southwest of the present map area. On the other hand, Chadron et al. (1999) describe gneissic foliations within the Captain Cove body that are deflected into the shear zone, suggesting that it was emplaced at a late stage of motion.

West Porcher Pluton

This large, equant body outcrops on the western coast of Porcher Island in Kitkatla Inlet and extends into the Bell Range (contacts on Figure 4 partly based on Roddick, 1970). It is homogeneous over a broad area, consisting of fresh, coarse-grained granodiorite with scattered black mafic restite inclusions. It resembles the Captain Cove pluton in igneous composition and texture, overall shape and appearance; they are probably related. Minerals include plagioclase, quartz, hornblende, biotite and traces of magnetite. In its westernmost exposures it shows a mainly magmatic to subsolidus (?) foliation characterized by weak alignment of mafic minerals and possibly quartz. Late pegmatite and aplite dikes both follow and cut across this fabric. At its southern contact north of the entrance to Porcher Inlet, it hornfelses rocks of the Billy Bay Complex and truncates both layering and a local mylonitic foliation.

Porcher Creek Pluton (Cretaceous? Jurassic?)

Unlike the other known or assumed Cretaceous intrusions, which tend to be uniform in composition and texture over broad areas, the Porcher Creek pluton is highly variable. On the southern side of Porcher Inlet it is essentially a dike complex, consisting of crosscutting diorite, andesite, tonalite and leucotonalite phases. Emplacement coincided with shearing and cataclasis, as shown by numerous chloritic shears and minor faults. North of the inlet it is more uniform in composition, a diorite that is intruded by younger granodiorite of the West Porcher pluton.

Peninsula Point Pluton

The Peninsula Point pluton is a northwesterly elongate body that outcrops near Oona River on Porcher Island, and continues southeast along the northeastern shores of Pitt Island. It is a fresh, undeformed granodiorite with clear euhedral titanite grains. Early crystallizing hornblende prisms and oscillatory/normal-zoned plagioclase grains are surrounded by matrix quartz and orthoclase. Early brown biotite is succeeded in a few areas by late-stage green biotite, with secondary interstitial epidote.

On the northeastern coast of Pitt Island, small offshoots of the Peninsula pluton and pegmatite within its margin show minor offsets and boudinage; these are related to a continuation of the Salt Lagoon fault that is inferred to lie offshore. We interpret this to show that the pluton was emplaced during the later stages of motion on the fault.

Other Bodies

Undeformed, fresh plutonic bodies of probable mid-Cretaceous age outcrop in the Spiller Range, the Chismore Range, northwest of Hunt Inlet and Kennedy Island. A subsurface northern extension of the Spiller Range pluton was responsible for extensive hornfelsing of the Descon Formation east of Hunt Inlet. Highly deformed granitoid bodies outcrop in Baker Inlet east of Grenville Channel, where Mansfield (2004) interpreted them to be infolded with schist. Although undated, they may be related to the ca. 90 Ma Ecstall pluton, which outcrops extensively farther east; this will be tested geochronologically.

Structural Geology

CRETACEOUS SINISTRAL-OBLIQUE FAULTS

The large-scale map pattern of the Porcher Island–Grenville Channel area, as shown on Figure 4, is dominated by a set of regional, north- to northwest-striking, mainly sinistral transcurrent faults. They form part of a zone of sinistral shearing that affected the entire northwestern Coast Mountains in Cretaceous time (Chardon et al., 1999). Locally, these faults offset and create local zones of tectonite in otherwise undeformed plutons, which are assumed to be of late Early Cretaceous age, based on similarities with nearby dated bodies (ca. 114–107 Ma; Butler et al., 2006). Thus, at least the later stages of motion on the faults took place during the late Early Cretaceous. Their earlier history is unconstrained at present, due to lack of age control on older rock units.

The major mapped transcurrent faults include, from northeast to southwest, the Grenville Channel and the Lamppost, Salt Lagoon and Useless faults. All correspond to strong topographic lineaments, and one is a shipping channel. Except for the Grenville Channel fault, they are defined by outcropping tectonite zones characterized by well-developed L–S fabrics, which commonly culminate in the development of banded mylonite. On approaching the west-northwest-trending shear zones, the regional foliations progressively become more intense and deflect into parallelism; the sense of deflection suggests sinistral shear. The lineations in the tectonite commonly plunge shallowly to moderately, which, combined with ample mesoscale shear-sense indicators such as C–S structures, shear bands, intrafolial drag folds with curvilinear axial surfaces, asymmetric fragments, boudins and tails around

porphyroclasts, consistently indicate sinistral transcurrent shear (Figures 20–22), commonly with an oblique, normal component.

The Grenville Channel fault is not exposed on land within the mapped area. Tectonite exposed on the north-eastern coast of Grenville channel shows strong rodding, boudinage and local development of L>S fabrics. Shear-sense indicators are consistently sinistral (Figure 23).

Plunges of mylonitic lineations in the northwest-trending shear zones range from moderate to shallow north-west, to less commonly moderate southeast, suggesting a combination of sinistral-normal and sinistral-reverse motion, with the oblique-normal motion being dominant. Fabrics are generally much better developed in the pre-Cretaceous metamorphic units than in the plutonic rocks. Whether this indicates that there were extensive pre-Cretaceous movements on the faults, or whether the plutons were intruded late during a single episode of Cretaceous sinistral regional shear is not clear at present.

Our interpretation of the trajectory of the Grenville Channel fault (Figure 4) differs from that of Chardon et al. (1999). In their interpretation, it tracks straight onto north-eastern Porcher Island, where it connects with the Lampost fault. However, detailed geological relationships indicate that the Lampost fault, which forms the structural boundary between rocks of the Descon Formation and Wales Group, is deflected southward to merge with the Salt Lagoon fault. We have chosen instead to curve the Grenville Channel fault into Telegraph Passage, such that it acquires a northerly strike. Such a fault trajectory is attractive for two reasons. First, such a structure accommodates a logical break between the highly tectonized domain on the mainland from the less deformed and metamorphosed rocks to the west; for example, well-preserved crossbedded Karheen-equivalent sandstone on western Kennedy Island, immediately west of the Telegraph Passage, shows much less strain. Second, the northerly deflection of the fault mirrors that displayed by the foliations and major lithologic contacts on the east side of Telegraph Passage.

The dominantly sinistral movement on the fault zones had a major influence on the regional map patterns shown in Figure 4. The Useless fault offsets the Swede Point pluton by several kilometres in a sinistral sense. The deflec-



Figure 20. Sinistral offset on granodiorite sill (shown by arrows) within Wales Group metatuff near Salt Lagoon fault, Oona River, northwestern British Columbia. The left-hand dike is 10 cm wide.



Figure 21. Sinistral clast asymmetry in actinolite-chlorite schist near Useless fault, northwestern British Columbia; rock hammer for scale.



Figure 22. Sinistral entrainment of earlier foliation: looking north-east, hammer head to the northwest. Swede Point pluton and septum of Ogden Channel metadiorite, next to the Useless fault along Ogden Channel, British Columbia; rock hammer for scale.



Figure 23. Sinistral-sense asymmetric boudins in metamorphosed felsic volcanic rock, Kumealon Inlet, northwestern British Columbia. The field of view is 2 m wide.

tion of the Grenville Channel fault from a northwesterly to northerly trend is interpreted as a restraining bend in the overall fault array. The northeast-trending fold outlined by strata on Gibson and Marrack islands (Figure 4) could represent shortening associated with the formation of the restraining bend. The deflection of the Lamppost fault may represent a smaller-scale restraining structure associated with the Telegraph Passage bend. Mapping suggests that the Lamppost fault and adjacent units are cut off by the Salt Lagoon fault. A second block with northerly internal foliations is seen southwest of the Useless fault. Its southwestern boundary is the Kitkatla shear zone, a major sinistral fault located southwest of Kitkatla Inlet, outside of the map area, described by Chardon et al. (1999). This may represent a second restraining bend within the fault system. This block is invaded by large, unfoliated Cretaceous plutons, the Captain Cove and West Porcher plutons. Although these bodies are cut off by the Kitkatla shear zone (Chardon et al., 1999; Butler et al., 2006), they are postkinematic to foliation development and their deflection within the block, suggesting that most of the motion accommodated by this fault predates emplacement of the plutons.

BARRETT ISLAND SHEAR ZONE

The Barrett Island shear zone is well exposed within the metasedimentary unit of the Wales Group on the north coast of Porcher Island, between the Salt Lagoon fault and the Devonian (?) Swede Point pluton. The metasedimentary unit comprises metagreywacke, phyllite, biotite schist, marble, amphibolite and minor quartzite. These rocks display a well-developed transposition foliation with abundant interfolial folds. They are in structurally modified intrusive contact with the Swede Point pluton, a coarse-grained biotite granodiorite to diorite with a strong protomylonitic foliation defined by the alignment of wispy biotite around plagioclase porphyroclasts. Tight to isoclinal folds are cut by both undeformed and mylonitized dikes, suggesting that pluton emplacement was synkinematic (Figure 24a). The shear zone is a distinct 80–100 m wide ductile deformation zone, characterized by abundant tight to isoclinal, macroscopic folds with amplitudes ranging from 0.25 to 2 m, locally greater than 5 m and well-developed foliation and lineation. The deformational style is lithologically controlled, with carbonate units containing well-developed, large-amplitude refolded isoclinal folds (Figure 24b), whereas deformation within the plutonic unit is characterized by discrete mylonite zones.

Structural analysis of foliation, lineation and folds constrains fault kinematics. The primary foliation, parallel to transposed compositional layering within the metasedimentary units, strikes northwest and dips moderately northeast (Figures 24c, d). The majority of intersection lineations have an approximate downdip plunge with a slight northwesterly bias, supporting approximately dip-parallel to sinistral-normal oblique motion on the shear zone (Figure 24c). Sinistral oblique sense of shear is shown by asymmetric tails on rotated porphyroblasts (Figure 24e). Fold axes of macroscopic, tight to isoclinal folds generally plunge downdip (Figure 24d). All observed asymmetric folds have a counterclockwise sense of vergence, also suggesting oblique sinistral shear; although they were probably rotated into the direction of tectonic transport parallel to L_1 stretching lineations (Figure 24b). The age of deformation will be constrained by geochronological analysis of

both the pluton and a mylonitized dike crosscutting F_1 folds (Figure 24a). If the Swede Point pluton is Paleozoic, as suggested by the preliminary U-Pb date of van der Heyden (1989), then this shear zone retains the record of much earlier deformation than the main, Early Cretaceous, sinistral event. The highly elongated shape of the pluton (Figure 4) may have been due to emplacement into an active shear zone.

FOLIATIONS, LINEATIONS AND FOLDS

The effects of strong deformation, although not as intense as within the shear zones, are nevertheless seen throughout pre-Cretaceous units of the map area. Transposition of compositional layering into foliation is nearly universal, the sole exceptions being the Karheen Formation on Kennedy Island, and parts of the Descon Formation on northeastern Porcher Island, where bedding-cleavage relationships are seen. The Wales Group on Elliott and Lewis islands shows intrafolial isocline development. Isoclinal folding is particularly well developed in intervals of thin-layered marble and metatuff. Here, the contrast in deformational styles between Wales and Descon rocks is interpreted as being due to the Wales orogeny (Gehrels and Saleeby, 1987). Farther east on the mainland coast, deformation is clearly younger, as the Paleozoic (?) Kumealon marble unit is involved in isoclinal folding. Tonalitic dikes and sills that cut diorite in the Ogden Channel Complex are tightly folded in some places. They are interpreted as relatively felsic components of the original intrusive complex. Therefore, the deformation could have been as old as the protolith, or as young as Early Cretaceous.

Mesoscopic folds are uncommon in the area. The Descon Formation on northeastern Porcher Island is folded into an open syncline between the Lamppost and Salt Lagoon faults. Wales Group (?) units near Stuart Anchorage on the northeastern coast of Pitt Island form a tight, upright anticline. The two marble exposures in Kumealon Inlet are interpreted as synformal keels. In Baker Inlet, Mansfield (2004) mapped second-phase folds involving panels of metaplutonic and metavolcanic/metasedimentary rock. As noted in the discussion of sinistral faults, the panel immediately northeast of the Grenville Channel fault near Kumealon and Baker inlets is an L-S tectonite that defines the core of a regional fold that developed during sinistral motion on the Grenville Channel fault. Karheen-equivalent strata occur in its core, indicating that it is a syncline.

Although both moderately plunging and shallow mineral and stretching lineations are observed in the major shear zones, in other areas moderate plunges are both to the northwest and to the southeast; this may indicate folding of an earlier set of lineations.

Metamorphism

Metamorphic grades and histories in the Porcher Island–Grenville Channel area are to some extent unit specific. There are also regional metamorphic gradients due to the location of this area on the western flank of the Coast Mountains orogen. The complex variations in metamorphism are probably due to the combined effects of Paleozoic events and Cretaceous dynamothermal overprinting.

The Wales Group, the inferred oldest supracrustal unit in the area, displays a variable metamorphic character that probably resulted from several stages of regional metamorphism. On eastern and northern Porcher Island, the Wales

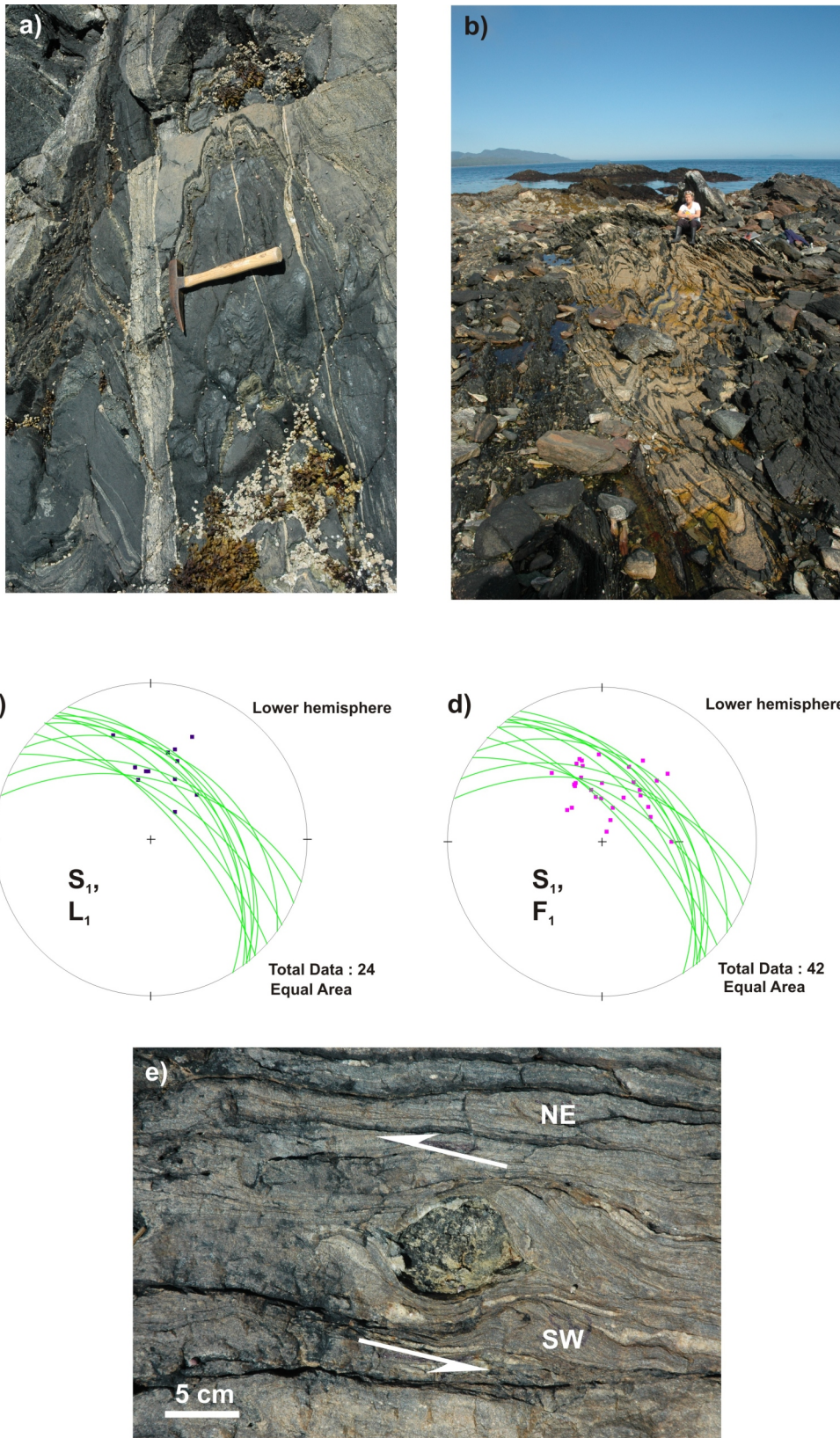


Figure 24. Barrett Island shear zone, northwestern British Columbia: **a)** Swede Point dikelet cuts isoclinally folded Wales Group schist and amphibolite; rock hammer for scale; **b)** refolded isoclines in laminated marble/metatuff; rock hammer for scale; **c)** stereonet plot of S_1 (great circles) and L_1 stretching lineations; **d)** stereonet plot of S_1 (great circles) and F_1 isoclinal fold axes; **e)** rotated (-shaped) clast, showing oblique-sinistral sense of shear. The arrow is 10 cm long.

Group is at middle-amphibolite grade. Intermediate and mafic rocks contain assemblages of blue-green pleochroic hornblende, plagioclase, brown or less commonly green biotite, titanite and quartz, with cummingtonite in some localities. This stands in strong contrast to greenschist metamorphic assemblages that are developed in the Ordovician McMicking pluton, and in structurally juxtaposed Descon strata. This early metamorphism of the Wales Group is interpreted to reflect the Cambrian–Ordovician Wales orogeny. It has also been affected by extensive synkinematic retrograde metamorphism, both on northern Lewis Island and on northeastern Porcher Island near the Lamppost fault. The chlorite schist and retrograded amphibolite on Lewis Island are cut by the McMicking pluton (Figure 18). Hornblende garbenschiefer and spongy, postkinematic garnets show static thermal metamorphism related to its emplacement. Retrograde metamorphism in rocks situated along the Lamppost fault, on the other hand, is probably related to exhumation during late motion on the Lamppost fault.

The Wales Group in the Stuart Anchorage area contains a number of assemblages developed in highly variable tuffaceous, siliciclastic and possible exhalative protoliths. The magnetite iron formations consist of laminae or bands of magnetite interlayered with hornblende-plagioclase and in some cases epidote. The hornblende is dark forest green, perhaps evidence of a more iron-rich composition, compared to the blue-green pleochroism that is common elsewhere. In some cases, titanite mantles magnetite, suggesting that the magnetite grains were not of late-kinematic, contact skarn-related origin. In this unit, there is also schist that contains assemblages of pink-violet pleochroic manganous zoisite and axinite (?) with quartz, plagioclase, biotite and opaque minerals: these could be metamorphosed calcareous exhalite.

Metamorphic grade in the Wales Group increases to the east and south across the Grenville Channel towards the core of the Coast Mountains orogen. Garnet amphibolite occurs in Kumealon and Baker inlets, as well as along the adjacent mainland coast. A few instances of sillimanite were found on the shores of these inlets, in assemblages with red-brown biotite, plagioclase, orthoclase, muscovite and quartz, in metamorphosed felsic hosts. Wolf et al. (2009) reported a mid-Cretaceous (108–102 Ma) Lu-Hf age on syntectonic garnet growth in this area. This age is slightly younger than the existing constraints on shear zone movement farther west (114–106 Ma; Butler et al., 2006), and supports the interpretation that all of the rocks in the map area were involved as a series of panels in mid-Cretaceous sinistral shearing and transpression.

Mafic to intermediate orthogneisses of the Ogden Channel Complex all contain assemblages of amphibolite to epidote amphibolite facies. They are truly orthogneisses, in the sense that primary mafic minerals are obliterated; not even relict crystal outlines remain. Instead, clumps of coarse, idiomorphic, metamorphic hornblende approximate the locations of individual original grains. Areas within these aggregates populated with dense masses of tiny opaque minerals are probably original clinopyroxenes; the clearer areas are probably after igneous hornblende. Normal-zoned plagioclases have been recrystallized to finer grain sizes, except for remaining porphyroclasts. Many of the Ogden Channel orthogneiss samples contain clear, well-formed epidote crystals, which appear to have grown in equilibrium with hornblende, calcic plagioclase,



Figure 25. Pyritic quartz veins from near the Surf Point adit, north-western British Columbia; pen knife for scale.

biotite, titanite and magnetite. Protomylonitic foliations within the complex have been overprinted by regional metamorphic recrystallization: this indicates an early (pre-peak metamorphism) episode of shearing.

The screens of pre-orthogneiss metasedimentary, metavolcanic and meta-intrusive rocks within the complex, also at amphibolite grade, consist of hornblende-plagioclase assemblages in metatuff, biotite–quartz–plagioclase±garnet in pelitic rocks and diopside±clinzoisite in calcisilicate rocks.

The Devonian (?) Swede Point pluton, which intrudes the Ogden Channel orthogneiss, has been metamorphosed to epidote to possibly garnet amphibolite grade: epidote and in some cases garnet porphyroblasts seem to grow in equilibrium with metamorphic hornblende. The body is also protomylonitic, perhaps due to its proximity to the Useless fault. Compared to the surrounding orthogneiss, it displays igneous artifacts such as plagioclase phenocrysts. The orthogneiss complex underwent an episode of metamorphism and deformation prior to the intrusion of the Swede Point pluton; at some later time both were sheared and metamorphosed in epidote amphibolite facies in a higher pressure–lower temperature environment than the Wales Group.

The Descon Formation on northeastern Porcher Island, the Silurian (?) pluton that intrudes it and most of the McMicking pluton contain greenschist-facies metamorphic assemblages of chlorite, epidote and actinolite; original plagioclases have been albitized and are spotted with saussurite and sericite. These rocks are also much less deformed than the Wales Group and the Ogden Channel Complex. The Descon Formation shows a transposition foliation along the eastern coast of Porcher Island, but with preservation of protolith textures such as clasts and phenocrysts. Farther to the west, the foliation is very weak, except within discrete shear zones.

Farthest west, the Billy Bay Complex shows amphibolite, greenschist-amphibolite transitional, possible epidote-amphibolite, and strong retrograde greenschist assemblages, all developed at high strain rates. It is lower grade than the Ogden Channel Complex, but higher grade than the Descon Formation, to which it is inferred to form the

subvolcanic roots. Its amphibolite grade may represent comparatively deep crustal levels during the same metamorphic event; or a later metamorphism related to proximity to the Kitkatla shear zone.

MINERAL OCCURRENCES AND MINERAL POTENTIAL

Two major types of metallic mineral deposits are well represented and/or indicated in the north coastal region of BC. A significant past gold producer with substantial current reserves, the combined Surf Point–Edye Pass mines, are located on northwestern Porcher Island (Figures 1, 4). More regionally, Prince of Wales Island in southeastern Alaska is well known for its VMS deposits, as is the Ecstall mineral belt in the Coast Mountains, east of the present map area (Alldrick, 2001; Alldrick et al., 2001). The Prince of Wales deposits, including the Niblack (Figure 1), are hosted by rocks of the southern Alexander terrane (Ayuso et al., 2005; Slack et al., 2005). The present map area lies within the southern extension of this belt. This observation, along with the presence of local favourable rock types, alteration patterns, and prospects and showings, supports the potential for VMS-style deposits in the Alexander terrane of coastal BC.

Surf Point–Edye Pass Mines

The Surf Point and Edye Pass mines were in operation between 1919 and 1939, when they produced 61 567 t of ore, yielding 639 914 g Au, 225 994 t Ag and 4161 kg Cu (BC Geological Survey, 2009; MINFILE 103J 017; Figures 1, 4). The orebodies are a set of pyritiferous quartz veins hosted in a northeasterly zone of fracturing and weak brittle shearing within an undeformed Cretaceous stock that underlies the western part of the Bell Range (Figure 4). The Surf Point and Edye Pass adits are located about 1 km apart along this trend. Exploration work in 1979–1980 by Banwan Gold Mines extended the Edye Pass adit 1 km southwest below the Surf Point workings (Scott, 1997). Work on the deposit by Cathedral Gold Corporation resulted in the discovery of the AT zone, about 50 m west of adit no 4 portal. Mineralization is persistent to a depth of 550 m and remains open. The zone also remains open along strike. Based on 66 holes totalling 12 192 m, the AT zone contains 544 300 t of indicated reserves grading 6.86 g/t Au, plus an additional 816 500 t of inferred reserves at the same grade. (pre NI 43-101; Anonymous, 1997; Scott, 1997) Property ownership is currently split between Imperial Metals Corporation and the former Cross Lake Minerals. The underground workings are in good condition, the trail and boardwalk connecting the workings have been rehabilitated, and there is a well-maintained exploration camp located near tidewater next to the Edye Pass adit.

The zone hosting the two mines and associated showings displays a 20° (north-northeasterly) structural trend. Its northeastern end abuts against a zone of strong ductile shearing exposed along the shore near the Edye Pass mine. This zone could be a splay of the Useless fault (Figure 4). Throughout the rest of its length, hostrocks are undeformed and unaltered granodiorite and tonalite. The veins themselves are pyritic quartz (Figure 25). They have narrow selvages of sericite-chlorite alteration in the host granodiorite. Individual veins, well-exposed in the roof and floor of the Surf Point adit, range in thickness from 5 to



Figure 26. Pyritic, siliceous quartz-sericite schist (metamorphosed altered rhyolite) in Wales Group near Moore Cove, northwestern British Columbia. The field of view is 3 m wide.



Figure 27. Layer of magnetite in thinly laminated Wales Group metatuff, northeastern Porcher Island, northwestern British Columbia; rock hammer for scale.



Figure 28. Magnetite laminations in siliceous, iron-rich metatuff, Wales Group, Stuart Anchorage, northwestern British Columbia; pencil for scale.

30 cm, and appear to be continuous over up to a few tens of metres. Their strikes are somewhat more northeasterly than the overall trend of the mineralized zone (40–90°; 2009 observations and MINFILE 103J 017). Latest motion on their enclosing surfaces was transcurrent, as shown by gently plunging slickenlines and chlorite streaks. The northeasterly orientation of the controlling structure is consistent with a zone of extension related to late dextral motion on the northwesterly bounding faults.

In summary, the Porcher Island gold mine shows continuity of mineralization and grade over 1 km in strike length; it has a considerable unmined resource and potential for expansion. The lack of continuity of individual veins and the resulting wallrock dilution impacts its mineable grade at present; however, larger individual veins may be found, and the potential for stockwork-style bulk mineable targets offers interesting possibilities to future explorers.

Indications of Volcanogenic Potential: Quartz-Sericite Schist and Iron Formation

The idea of projecting Paleozoic and older volcanogenic potential south from southeastern Alaska into far northwestern BC is not new to this project. It generated a few industry projects in the 1980s and early 1990s (cf. Franzen, 1984; Bohme, 1993), and has intrigued some government geologists (P. Wojdak and M. Mihalynuk, pers comm, 1990–2007). Until now, however, no detailed, systematic geological work has been done to test the relevant rock correlations and document likely hostrocks.

We have described here mixed volcanic successions assigned provisionally to both the Wales Group (Neoproterozoic–Cambrian) and Descon Formation (Ordovician–Early Silurian). Both of them are dominated by andesite volcanoclastic protoliths with minor rhyolite, dacite and basalt. Laminated tuff sequences are indicative of primarily subaqueous deposition. Some of the dacite is lensoid in shape and forms bodies that are typically 100–300 m thick and up to 1 km long with coherent textures including aphyric and quartz phyric. These probably originated as domes or cryptodomes at small volcanic centres. Felsic tuff forms discrete beds in the metre to decimetre range, as well as sets of laminae in dominantly andesite volcanoclastic sequences. These rocks are overall plausible as hosts for Kuroko-style volcanogenic occurrences.

More specific indicators of VMS environments were noted, all of them within rocks assigned to the Wales Group. Near Moore Cove on the eastern side of Telegraph Passage, there are a number of small bodies of quartz-sericite schist, pyritic quartz-sericite schist and metamorphosed silicified rhyolite (Figures 4, 26). This sequence passes eastward into a metasedimentary package that includes an unusual magnetite-rich metachert, possibly an iron formation.

Stratabound, stratiform magnetite occurs at a number of widely scattered sites along the northeastern side of Porcher Island immediately northeast of the Lamppost fault, and on the eastern side of Pitt Island near Stuart Anchorage (Figure 4). Two of these occurrences have been previously documented as MINFILE localities: Royal (MINFILE 103G 016) and Star (MINFILE 103J 031; Figure 1). The bodies are continuous over tens to hundreds of metres, enclosed in highly strained metatuff. The Royal occurrence and its southern extension lie immediately above a

felsic metatuff body (Figure 4). Individual layers vary in thickness from tens of centimetres to a maximum at the Royal showing of several metres, which is interpreted as a thickened fold axial zone. The most common mineralization consists of pure, fine-grained magnetite with shiny grey specular hematite partings (Figure 27). Magnetite also forms fine laminae and blebs within metatuff (Figure 28). Schist containing manganoan zoisite and axinite occurs in association with the iron formation in Stuart Anchorage, and also within the Oona River unit on the northeastern shoulder of Pitt Island. Because of its unusual compositions and association with felsic metatuff and iron formation, it is interpreted as metamorphosed exhalite. Epidote and epidote-garnet metazones accompany the magnetite in a few cases. Overall, however, calcsilicate rocks are minor compared to the magnetite, a feature atypical of skarn associations. Although limy layers occur within the volcanic sequences, there is no marble in direct association with the magnetite bodies. Instead, the texture of magnetite laminated in siliceous, intermediate tuff is more amenable to interpretation as original stratabound exhalative deposits, as opposed to metamorphic replacements. We consider these to represent regional iron formation, and thus to be distal indicators of sulphide-dominated volcanogenic deposits.

The best currently known example of such a deposit is the Pit prospect or Pitt/Trinity property (MINFILE 103H 066), located on central Pitt Island 10 km south of the current map area (Figure 1). This belt of VMS-style mineralization was explored between 1980 and 1993 (Figure 2; Lo, 1992; Bohme, 1993). As shown in the Figure 1 inset, it is approximately on strike with the zone of stratabound magnetite and metamorphosed calcareous exhalite (?) on east Porcher and east Pitt islands. On the property, a number of separate showings have been identified in two separate trends parallel to regional northwest strike, within two metamorphic inliers that are interlayered with tabular Cretaceous intrusive bodies (Bohme, 1993). The Pyrite Creek trend is 1.7 km long; two other showings (Pitt zone) lie along strike 3 km to the northwest. The B Creek zone is a separate inlier 2 km to the northeast. In both, pyrite-rich semimassive to massive sulphide bodies are hosted by metavolcanic and metasedimentary rocks including quartz-muscovite schist, pyritic quartz-biotite schist and carbonaceous argillite. True thicknesses are on the order of 0.2–1.6 m. Principal sulphide minerals are pyrite, chalcopyrite, sphalerite, pyrrhotite, galena, covellite and possibly bornite; barite is inferred based on values of 1.0–5.5% Ba in assays. Drill intersections of the Pyrite Creek zone returned 0.94–2.2% Cu, 0.41–1.2% Pb and 1.5–4.9% Zn over 2 m widths. Reported values of precious metals are low (Bohme, 1993).

In summary, the Pitt/Trinity VMS-style sulphide trends are of interest because of their significant extent along regional strike. This area is targeted for detailed map coverage in year 3 of the north coast project, in 2011.

Other Showings

We examined the Etta showing (MINFILE 103J 027; Figure 1) near Hunt Inlet to evaluate the type of mineralization present. Patchy zones of epidote skarn that contain scattered pyrite, chalcopyrite and sphalerite concentrations occur in greenschist-grade andesite pyroclastic hostrock near and at a contact with limestone. A surface sample assayed 8.0% Zn, 0.11% Cu and 1.37 g/t Ag (Freberg, 1974). The exposure was trenched and drilled in 1974, although no

assay values were reported (Freberg, 1974); some of the core is still on site. In the northern part of Porcher Island, metavolcanic and metasedimentary rocks assigned to the Descon Formation are intruded by numerous dikes and plugs too small to map. Hornfelsing is common and the large Spiller Range pluton outcrops several kilometres to the south. The Jifney Etta small past producer (MINFILE 103J 028), the Por showing (MINFILE 103J 023) and other small skarn showings (not located) are similar to Etta. All of them are probably best interpreted as skarns associated with small limestone bodies in the Descon volcanic-sedimentary sequence.

DISCUSSION

Significance of New Porcher Island/Grenville Channel Results for Understanding the Southward Extension of the Alexander Terrane

The Alexander terrane south of the BC-Alaska border is now better understood. The detailed field mapping of this project in 2009 follows up the earlier intimations of Gehrels and Boghossian (2000) and Gehrels (2001) that individual map units of the Alexander terrane can be traced and correlated from southeastern Alaska into the northern and even central coastal areas of BC. We can with some certainty recognize the Wales Group on and near Porcher Island, as a deformed metavolcanic sequence intruded postkinematically by the ca. 482 Ma McMicking pluton. The existence of a less-deformed and less-metamorphosed Descon Formation on northern Porcher Island has been proposed. Felsic units both within the presumed Wales and Descon units have been collected for U-Pb dating—because at least some of the amphibolite-grade metamorphism in this area is of Cretaceous age, it follows that more certain indicators than the relative degree of metamorphism and deformation must be used. The metamorphosed Ogdan Channel and Billy Bay complexes may be intrusive equivalents of the Wales and Descon supracrustal units. This also will be tested by U-Pb geochronology. Other plutons that have been interpreted as Paleozoic—the Hunt Inlet and Swede Point bodies—will also be dated. Finally, equivalents of the Devonian Karheen Formation are now known to occur on Kennedy Island and on the mainland coast, as shown by sedimentological observations and detrital zircon geochronology. The continued unravelling of Alexander terrane stratigraphy and history will provide a useful context for geological studies and regional mineral exploration in this area.

Regional Significance of Cretaceous Sinistral/Oblique Faults

The newly identified Salt Lagoon, Useless and Lamp-post faults on Porcher Island, along with the Grenville Channel, Kitkatla and Principe-Laredo faults (Chardon et al., 1999), define a regime of large-scale, Early to mid-Cretaceous sinistral displacements within the coastal region of BC. It has been interpreted as the cause of apparent duplication of the Late Jurassic to Early Cretaceous proto-Coast Mountains arc (Gehrels et al., 2009), and closure of the Tyaughton Basin in the southern Coast Mountains (Monger et al., 1994). Estimated total displacement across this zone was at least 800 km. Prior to this event, but after mid-Juras-

sic accretion to Stikinia and the outer Yukon-Tanana terrane, the southern Alexander terrane of Porcher Island may have lain at the latitude of the present-day western Yukon, across the Denali fault from the Kluane schist and Nisling terrane. Trajectories of the regional sinistral faults have not yet been traced with certainty into southeastern Alaska, in large part because of the masking effects of later dextral structures such as the Denali fault.

New Mineral Potential Outlined in this Project

Deformed and metamorphosed volcanic sequences in the Grenville Channel–eastern Porcher Island area contain geological features that are indicative of the existence of syngenetic submarine hot-spring systems. These include many small rhyolite and dacite volcanic centres; local premetamorphic clay sericitization and silicification of rhyolite; magnetite iron formation, and metachert with magnetite, sulphides, manganous zoisite and axinite that we interpret as metamorphosed exhalite. Although no new sulphide showings were found in 2009, it is considered highly encouraging that extensive volcanogenic mineralization has been identified on the Pitt property, located on Pitt Island 10 km to the south along strike from the zone of stratabound magnetite on east Porcher and east Pitt islands. The presence of magnetite iron formation makes regional airborne magnetometer surveys a potentially effective and cost-effective tool in locating targets in the generally vegetation-covered interiors of the islands.

Future Research Directions and Mapping Plans

Mapping in 2010 for the north coast project will target the southernmost part of the belt of Alexander exposures west of Bella Coola. This area has the second highest percentage of Paleozoic exposures in the belt, after Porcher Island. By that time, data provided by U-Pb and geochemical studies at the University of Wisconsin at Eau Claire and the University of Arizona will help to guide our developing understanding of the southern Alexander terrane, its relationship to better-known exposures in Alaska and its potential to host as-yet-undiscovered metallic deposits.

SUMMARY AND CONCLUSIONS

The north coast project can list the following accomplishments after its first year of operation:

Completion of geological map coverage of an area of 30 by 50 km, including Porcher Island, the adjacent mainland coast and smaller islands in between.

Rock units of the Alexander terrane of southeastern Alaska can be traced into northwestern BC, including those that are known to host VMS mineralization.

Geological indicators of VMS-style systems occur in two trends, one on northeastern Porcher Island and, offset across the Salt Lagoon fault, on northeastern Pitt Island; the other east of the Grenville Channel fault on the mainland coast east of Telegraph Passage.

ACKNOWLEDGMENTS

We first acknowledge the key role of our captain, Don Willson and his boat, the *Phoebe*, in providing a convenient logistical base of operations and safe co-ordination of our daily zodiac traverses. The project was also greatly enhanced by our partnership with the Lax Kw'alaams First Nation, in whose traditional territory part of the mapped area is located (Figure 1). Their Project Observer, Richard Bryant, contributed nautical skills and insights into his nation's history that were much appreciated. Brennan Kadulski, University of Wisconsin, gave excellent assistance in the field. Martin Pepper and Jim Gehrels each brought unique contributions to the project. The residents of Oona River, especially Jan Lemon, Karl Bergman, Lutz Budde and Bobby Letts, offered us welcome, good advice and directions. A word of thanks to the Gulf of Alaska must be included here. In 2009, it took a long summer break from its customary storm-brewing activities to give us a season of sun and light breezes. The north coast project is part of Edges (Multiple Metals)—Northwest Canadian Cordillera (Yukon, BC): financial and logistical support from the Geological Survey of Canada made it all possible; we thank our Canadian and American colleagues in the Edges project for their ideas and insights. Larry Diakow's careful review improved the accuracy and clarity of the manuscript.

REFERENCES

- Alldrick, D.J. (2000): Geology and mineral deposits of the Ecstall belt, northwest BC; in *Geological Fieldwork 1999, BC Ministry of Energy, Mines and Petroleum Resources*, Paper 2000-1, pages 279–306.
- Alldrick, D.J., Friedman, R.M. and Childe, F.C. (2000): Age and geologic history of the Ecstall greenstone belt, northwest BC; in *Geological Fieldwork 1999, BC Ministry of Energy, Mines and Petroleum Resources*, Paper 2000-1, pages 269–278.
- Anonymous (1997): Cathedral puts Sterling gold mine on hiatus; *Northern Miner*, April 21, 1997, page 14.
- Ayuso, R.A., Karl, S.M., Slack, J.F., Haeussler, P.J., Bittenbender, P.E., Wandless, G.A. and Colvin, A.S. (2005): Oceanic Pb-isotopic sources of Proterozoic and Paleozoic volcanogenic massive sulphide deposits on Prince of Wales Island and vicinity, southeastern Alaska; in *Studies by the U.S. Geological Survey in Alaska 2005, United States Geological Survey, Professional Paper 1732-E*, pages 1–20.
- BC Geological Survey (2009): MINFILE BC mineral deposits database; *BC Ministry of Energy, Mines and Petroleum Resources*, URL <<http://minfile.ca>> [November 2009].
- Berg, H.C., Jones, D.L. and Richter, D.H. (1972): Gravina-Nutzotin belt—tectonic significance of an upper Mesozoic sedimentary and volcanic sequence in southern and southeastern Alaska; *United States Geological Survey, Professional Paper 800-D*, pages D1–D24.
- Bohme, D.W. (1993): Geological, geochemical and geophysical report on the Pitt/Trinity claim group, Skeena Mining Division, NTS 103H/12W; submitted by Inco Ltd., *BC Ministry of Energy, Mines and Petroleum Resources*, Assessment Report 22 912, 138 pages.
- Buddington, A.F. and Chapin, T. (1929): Geology and mineral deposits of southeastern Alaska; *US Geological Survey, Bulletin 800*, 398 pages.
- Butler, R.F., Gehrels, G.E., Hart, W., Davidson, C. and Crawford, M.L. (2006): Paleomagnetism of Late Jurassic to mid-Cretaceous plutons near Prince Rupert, British Columbia, in *Paleogeography of the North American Cordillera: Evidence For and Against Large-Scale Displacements*, Haggart, J.W., Enkin, R.J. and Monger, J.W.H., Editors, *Geological Association of Canada, Special Paper 46*, pages 171–200.
- CBR Gold Corp. (2009): Resource summary; *CBR Gold Corp.*, URL <http://www.cbrgoldcorp.com/project_areas/overview/> [December 2009].
- Chardon, D. (2003): Strain partitioning and batholith emplacement at the root of a transpressive magmatic arc; *Journal of Structural Geology*, Volume 25, pages 91–108.
- Chardon, D., Andronicos, C.L. and Hollister, L.S. (1999): Large-scale transpressive shear zone patterns and displacements within magmatic arcs: the Coast Plutonic Complex, British Columbia; *Tectonics*, Volume 18, pages 278–292.
- Eberlein, G.D. and Churkin, M. Jr. (1970): Paleozoic stratigraphy in the northwest coastal area of Prince of Wales Island, southeastern Alaska; *United States Geological Survey, Bulletin 1284*, 67 pages, 2 sheets, 1:125 000 scale.
- Eberlein, G.D., Churkin, M. Jr., Carter, C., Berg, H.C. and Ovenshine, A.T. (1983): Geology of the Craig quadrangle, Alaska; *United States Geological Survey, Open File Report 83-91*, 28 pages, 1:250 000 scale.
- Franzen, J.P. (1984): Geochemical report, Por 1-8 mineral claims, Skeena Mining Division, NTS 103J/1W; submitted by Billiton Canada Limited, *BC Ministry of Energy, Mines and Petroleum Resources*, Assessment Report 13 051, 33 pages.
- Freberg, R.A. (1974): Report on diamond drilling 1974, Yukonadian Explorations Limited, Hunt Inlet, Porcher Island, B.C.; submitted by Yukonadian Mineral Exploration, *BC Ministry of Energy, Mines and Petroleum Resources*, Assessment Report 5027, 31 pages.
- Gareau, S.A. and Woodsworth, G.J. (2000): Yukon-Tanana terrane in the Scotia-Quaal belt, Coast Plutonic Complex, central-western British Columbia, in *Tectonics of the Coast Mountains, Southeastern Alaska and British Columbia*, Stowell, H.H. and McClelland, W.C., Editors, *Geological Society of America, Special Paper 343*, pages 23–44.
- Gehrels, G.E. (1990): Late Proterozoic to Cambrian metamorphic basement to the Alexander terrane on Long and Dall islands, southeastern Alaska; *Geological Society of America Bulletin*, Volume 102, pages 760–767.
- Gehrels, G.E. (2001): Geology of the Chatham Sound region, southeast Alaska and coastal British Columbia; *Canadian Journal of Earth Sciences*, Volume 38, pages 1579–1599.
- Gehrels, G.E. and Boghossian, N.D. (2000): Reconnaissance geology and U-Pb geochronology of the west flank of the Coast Mountains between Bella Coola and Prince Rupert, coastal British Columbia; in *Tectonics of the Coast Mountains, Southeastern Alaska and British Columbia*, Stowell, H.H. and McClelland, W.C., Editors, *Geological Society of America, Special Paper 343*, pages 61–76.
- Gehrels, G.E. and Saleeby, J.B. (1987): Geologic framework, tectonic evolution and displacement history of the Alexander terrane; *Tectonics*, Volume 6, pages 151–174.
- Gehrels, G.E., Berg, H.C. and Saleeby, J.B. (1983): Ordovician-Silurian volcanogenic massive sulfide deposits on southern Prince of Wales Island and the Barrier Islands, southeastern Alaska; *United States Geological Survey, Open File Report 83-318*, 11 pages.
- Gehrels, G.E., Butler, R.F. and Bazard, D.R. (1996): Detrital zircon geochronology of the Alexander terrane, southeastern Alaska; *Geological Society of America Bulletin*, Volume 108, pages 722–734.
- Gehrels, G., Rusmore, M., Woodsworth, G., Crawford, M., Andronicos, C., Hollister, L., Patchett, J., Ducea, M., Butler, R., Klepeis, K., Davidson, C., Friedman, R., Haggart, J., Mahoney, B., Crawford, W., Pearson D. and Girardi, J. (2009): U-Th-Pb geochronology of the Coast Mountains batholith in north-coastal British Columbia: constraints on

- age and tectonic evolution; *Geological Society of America Bulletin*, Volume 121, pages 1341–1361.
- Hutchison, W.W. (1982): Geology of the Prince Rupert–Skeena map area, British Columbia; *Geological Survey of Canada*, Memoir 394, 115 pages.
- Karl, S.M., Ayuso, R.A., Slack, J.F. and Friedman, R.M. (2009): Neoproterozoic to Triassic rift-associated VMS deposits in the Alexander composite oceanic arc terrane, southeast Alaska; in *Mining: Modern Mine Reclamation*, Morris, H., Editor, *Alaska Miners Association*, 2009 Annual Convention, Abstracts, page 9.
- Kilby, W.E. (1995): Mineral potential project—overview; in *Geological Fieldwork 1994*, *BC Ministry of Energy, Mines and Petroleum Resources*, Paper 1995-1, pages 411–416.
- Lo, B.B.H. (1992): Geophysical report on a helicopter-borne electromagnetic and magnetometer survey at the Pitt/Trinity property, British Columbia, NTS 103H/12; submitted by Inco Ltd., *BC Ministry of Energy, Mines and Petroleum Resources*, Assessment Report 22 475, 45 pages.
- MapPlace (2009): Mineral resource assessment layer; British Columbia Geological Survey MapPlace website; BC Ministry of Energy, Mines and Petroleum Resources, URL <<http://mapplace.ca>> [December 2009].
- Mansfield, M.R. (2004): Thermal and structural evolution of the Grenville Channel shear zone, Coast Plutonic Complex, British Columbia; unpublished MSc thesis, *University of Texas*, 61 pages.
- Monger, J.W.H., van der Heyden, P., Journeay, J.M., Evenchick, C.A. and Mahoney, J.B.M. (1994): Jurassic-Cretaceous basins along the Canadian Coast Belt: their bearing on pre-mid-Cretaceous sinistral displacements; *Geology*, Volume 22, pages 175–178.
- Nelson, J.L., Mahoney, J.B. and Gehrels, G.E. (in press): Geology and mineral potential of the Porcher Island–Grenville Channel area, northwestern British Columbia; *BC Ministry of Energy, Mines and Petroleum Resources*, Open File 2010-03, scale 1:50 000.
- Roddick, J.A. (1970): Douglas Channel–Hecate Strait map-area, British Columbia; *Geological Survey of Canada*, Paper 70-41, 70 pages.
- Rubin, C.M. and Saleeby, J.B. (1992) Tectonic history of the eastern edge of the Alexander terrane, southeast Alaska; *Tectonics*, Volume 11, pages 586–602.
- Saleeby, J.B. (2000): Geochronologic investigations along the Alexander-Taku terrane boundary, southern Revillagigedo Island to Cape Fox areas, southeast Alaska; in *Tectonics of the Coast Mountains, Southeastern Alaska and British Columbia*, Stowell, H.H. and McClelland, W.C., Editors, *Geological Society of America*, Special Paper 343, pages 107–143.
- Scott, T.C. (1997): 1996–1997 diamond drilling assessment report on the Tob 1, L6513, L6515, L6516, L6517 and L7191 mineral claims located on Porcher Island, Skeena Mining Division, NTS 103J/2E; submitted by Cathedral Gold Corp., *BC Ministry of Energy, Mines and Petroleum Resources*, Assessment Report 25 073, 298 pages.
- Slack, J.F., Shanks, W.C., Karl, S.M., Gemery, P.A., Bitterbender, P.E. and Ridley, W.I. (2005): Geochemical and sulphur-isotopic signatures of volcanogenic massive sulphide deposits on Prince of Wales Island and vicinity, southeastern Alaska; in *Studies by the U.S. Geological Survey in Alaska 2005*, *United States Geological Survey*, Professional Paper 1732-C, 37 pages.
- van der Heyden, P. (1989): U-Pb and K-Ar geochronometry of the Coast Plutonic complex, 53°N to 54°N, British Columbia, and implications for the Insular-Intermontane terrane boundary; unpublished PhD thesis, *The University of British Columbia*, 392 pages.
- Wheeler, J.O., Brookfield, A.J., Gabrielse, H., Monger, J.W.H., Tipper, H.W. and Woodsworth, G.J. (1991): Terrane map of the Canadian Cordillera; *Geological Survey of Canada*, Map 1713A, scale 1:2 000 000.
- Wolf, D.E., Andronicus, C.L., Vervoort, J.D., Mansfield, M.R. and Chardon, D. (2009): Application of Lu-Hf garnet dating to unravel the relationships between deformation, metamorphism and plutonism: an example from the Prince Rupert area, British Columbia; *Geological Society of America*, Abstracts with Programs, Volume 41, Number 7, page 223.

Quaternary Geology and Till Geochemistry of the Nadina River Map Area (NTS 093E/15), West-Central British Columbia

T. Ferbey

KEYWORDS: Tahtsa Lake district, Quaternary geology, surficial mapping, till geochemical survey, till geochemistry, trace-element geochemistry, heavy minerals, gold grain counts, porphyry Cu, porphyry Cu-Mo, polymetallic vein, volcanogenic massive sulphide

INTRODUCTION

The Tahtsa Lake district has high potential to host new porphyry Cu±Mo and polymetallic vein-style (including Au) mineralization. Centred on Tahtsa Lake (approximately 100 km south of Houston, British Columbia; Figure 1), this district, and areas immediately adjacent to it, have a rich mineral exploration history and at present host a producing porphyry Cu-Mo mine (Huckleberry mine) and numerous developed Cu±Mo prospects (e.g., Berg, Lucky Ship, Whiting Creek; MacIntyre, 1985). This district also hosts epithermal vein and perhaps volcanogenic massive sulphide (VMS)-style mineralization, as suggested by past producers such as Equity Silver and Emerald Glacier (MacIntyre, 1985; MacIntyre et al., 2004; Alldrick et al., 2007; Figure 2).

Currently there are large areas of unstaked ground within, and adjacent to, the northern and northeastern portion of the Tahtsa Lake district. Much of this area is covered with glacial drift and continuous bedrock outcrop is limited to the higher peaks and their steep flanks. Till geochemical surveys are an effective method for assessing the metallic mineral potential of areas covered with glacial drift and are ideally suited to assessing the potential for new mineralization in this area. Till geochemical surveys are also well suited for following up on airborne geophysical data recently acquired by Geoscience BC for the QUEST-West Project area (Kowalczyk, 2009), where drift can cover electrically anomalous bedrock.

A two-year Quaternary geology and till geochemistry program is currently underway within the northern portion of the Tahtsa Lake district, and adjacent areas (NTS map areas 093E/15, 16, 093L/01, 02; Figure 2). The objectives of this program are to

- 1) characterize and delineate the Quaternary materials that occur in the study area and reconstruct the region's glacial and ice-flow history; and
- 2) assess the economic potential of covered bedrock (subcrop) by conducting till geochemistry surveys.

This publication is also available, free of charge, as colour digital files in Adobe Acrobat® PDF format from the BC Ministry of Energy, Mines and Petroleum Resources website at <http://www.empr.gov.bc.ca/Mining/Geoscience/PublicationsCatalogue/Fieldwork/Pages/default.aspx>.

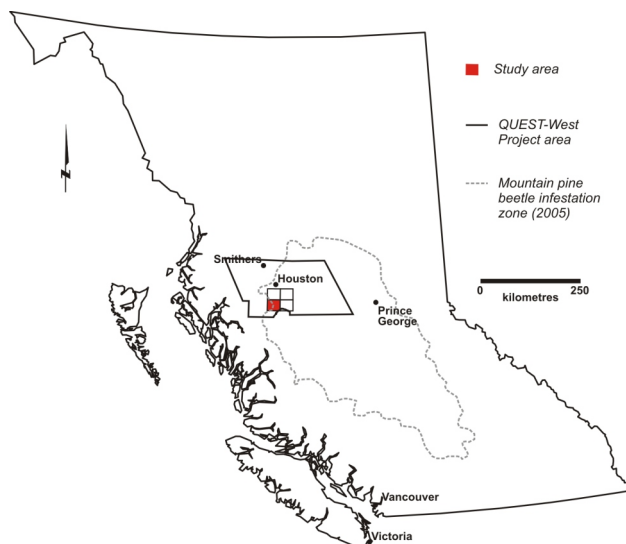


Figure 1. Location of study area in west-central British Columbia.

The study area falls within the mountain pine beetle-impacted zone and Geoscience BC's QUEST-West Project area. The goal of this project is to provide to the mineral exploration community high-quality, regional-scale, geochemical data that will help guide exploration efforts. Integrating interpretations of these data with other geochemical and geophysical data being collected by Geoscience BC in the QUEST-West Project area, and historic data that have been collected by the British Columbia Geological Survey (BCGS) and the Geological Survey of Canada (GSC), will provide a powerful tool for companies exploring in this drift-covered area.

The focus of this paper is surficial geology mapping and the sampling component of a till geochemical survey completed within the Nadina River map area (NTS 093E/15) during the 2009 field season.

STUDY AREA

The study area is located in west-central BC, approximately 100 km southwest of Houston, in NTS map area 093E/15 (Figures 1, 2). It is accessible by Forest Service, private and abandoned mine and mineral exploration roads. Quaternary sediments were studied in detail within NTS 093E/15 while a regional-scale glacial history and ice-flow study was conducted within NTS 093E/15 and 16. The primary objective of this year's till geochemistry survey is to assess the mineral potential of NTS 093E/15. To do this, ad-

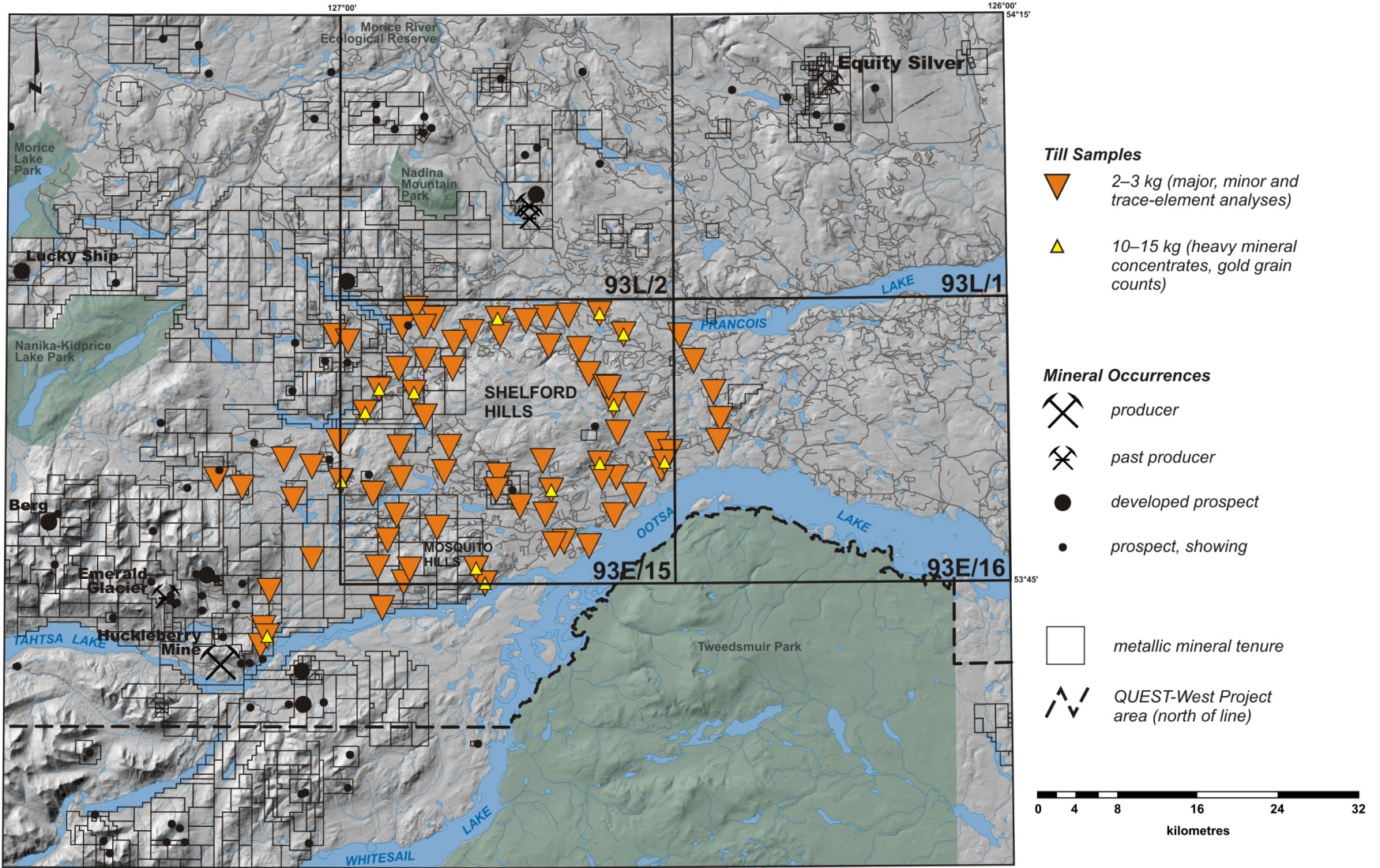


Figure 2. Study area including locations of mineral occurrences, west-central British Columbia. Also shown are locations of till samples collected during the 2009 field season.

ditional till samples were collected within portions of NTS 093E/11, 14 and 16 to take into account the study area's complex ice-flow history.

The majority of the study area is situated in the Nechako Plateau, a subdivision of the Interior Plateau. The Nechako Plateau is an area of low relief with flat or gently rolling topography (within the study area, 880–944 m asl) most of which is covered by a package of glacial sediments (Figure 2; Holland, 1976). Although bedrock outcrop is relatively uncommon, some exposures can be found at the stoss (i.e., up-ice) end of crag-and-tail forms, along lake shorelines, on higher ground within Shelford (1494 m asl) and Mosquito (1402 m asl) hills, and on local small-scale erosional remnants that stand above the plateau surface to the west and northwest of Shelford Hills (Figure 3). Bedrock outcrop can also be found in the upper reaches of the Nadina River valley and within roadcuts associated with newly constructed forestry roads. The very southwest corner of the study area is situated in the Tahtsa Ranges, a northwest-trending belt of nongranitic mountains that range in elevation from 2100 to 2431 m asl (Holland, 1976). These mountains are situated between the Nechako Plateau to the east and the Coast Mountains to the west. While the majority of hills and mountains within the Nechako Plateau are forested, the Tahtsa Ranges extend up into subalpine and alpine environments.

Small lakes are common within the study area and can be interconnected forming lake chains. The largest lake within the study area is Ootsa Lake, which is part of an interconnected series of large lakes (i.e., Tahtsa, Ootsa, Whitesail, Eutsuk, Tetachuk, Natalkuz lakes) that make up the Nechako Reservoir. Nadina River flows in an arc through the north-central part of the study area, connecting Nadina Lake to Francois Lake, and is the largest river in the study area.



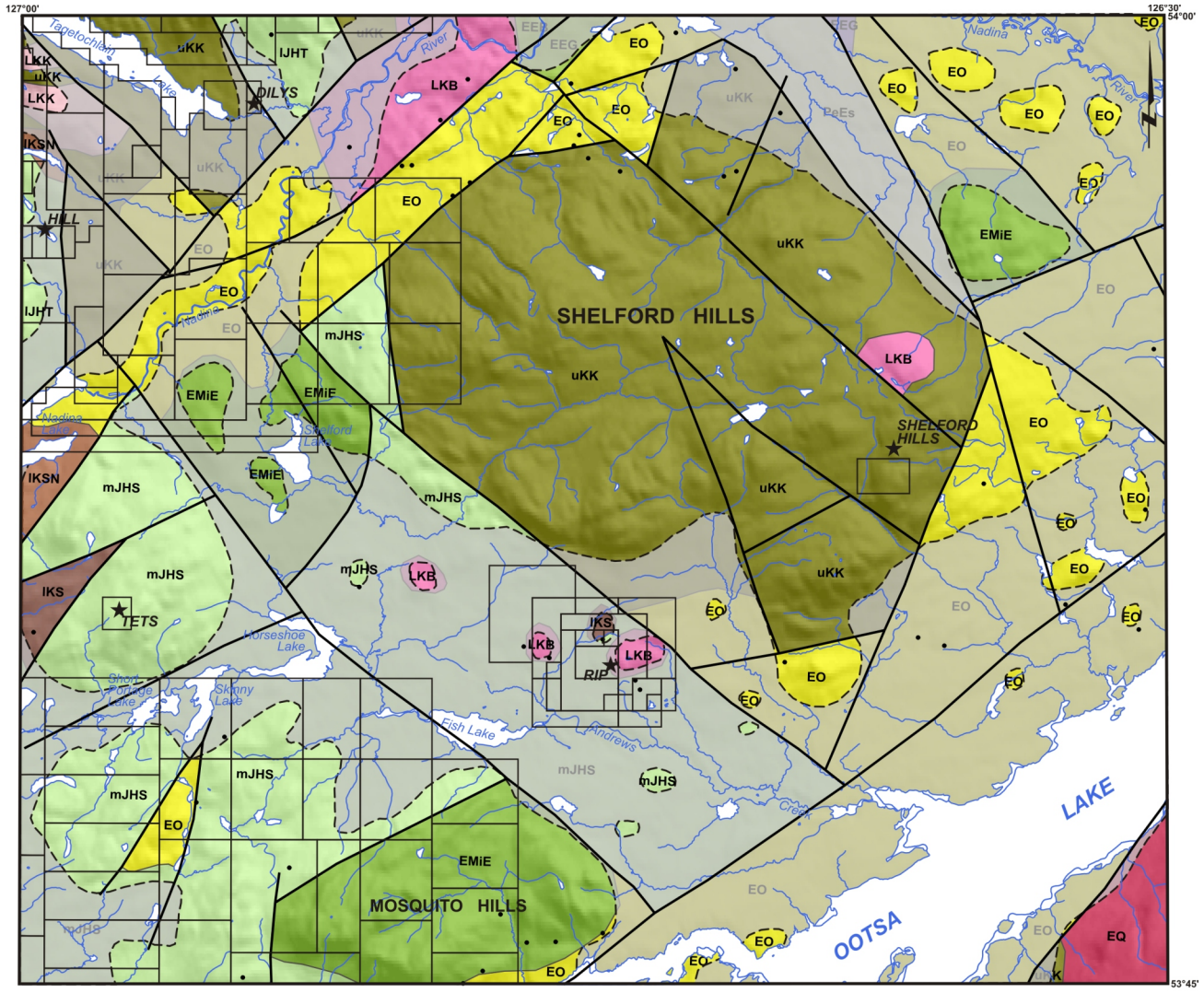
Figure 3. Subdued topography of the southwest corner of the study area, west-central British Columbia. View is towards the east with Mosquito Hills in the background. Note red-coloured pine trees in middle of photograph, indicating that mountain pine beetles have moved through the area.

BEDROCK GEOLOGY

The bedrock geology of the study area was first described and mapped by Hedley (1935) and was included in subsequent mapping by Duffell (1959). The main geological subdivisions found in the study area, as summarized from Woodsworth (1980), MacIntyre (1985), MacIntyre et al. (1994) and Diakow (2006), are as follows. The Tahtsa Lake district lies within the Stikine terrane, just east of the Coast Crystalline Belt (Monger et al., 1991). The western part of the study area is underlain mainly by Early to Middle Jurassic Hazelton Group volcanic and sedimentary rocks (Figure 4). In places, these rocks are unconformably overlain by Early Cretaceous Skeena Group marine sedimentary rocks and local basalt to andesite flows. These rocks are in turn unconformably overlain by felsic pyroclastics, felsic flows and younger basaltic flows of the Early to Late Cretaceous Kasalka Group volcanic rocks. Small- to medium-sized, Late Cretaceous to Early Tertiary stocks have intruded these volcanic piles and sedimentary packages. Elsewhere in the region, there is a strong positive relationship between the location of intrusive rock types (in particular porphyritic intrusions like those of the Late Cretaceous Bulkley suite) and the locations of Cu, Mo, Au, Pb, Zn and/or Ag mineralization (Carter, 1981; MacIntyre, 1985).

In the most eastern part of the study area, Eocene Ootsa Lake Group felsic to mafic volcanic rocks dominate. Younger, and less widespread, Eocene to Lower Miocene Endako Group basaltic and alkaline volcanic rocks do also occur locally. An approximation of the areal extent of Quaternary sediment cover has been included in Figure 4 and is represented by a light grey transparent overlay and black dashed line.

Significant contributions towards the understanding of the region's metallogensis, in particular porphyry Cu-Mo deposits, have been made by Carter (1981) and MacIntyre (1985). Other detailed work has been conducted on specific metallic mineral deposits adjacent to the study area (e.g., Panteleyev, 1981; Cyr et al., 1984; Jackson and Illerbrun, 1995) and additional geological information on local mineral occurrences and claims is available in the BCGS Assessment Report Indexing System (ARIS). More recently, MacIntyre (2001), MacIntyre et al. (2004), Alldrick (2007a, b) and Alldrick et al. (2007) have investigated the mineral potential of mid-Cretaceous rhyolites of the Rocky Ridge Formation. This work suggests that these rhyolites have potential to host VMS-type deposits. While rhyolites do occur within the study area, they have been assigned to the younger, Eocene Ootsa Lake Group. Limited outcrop and a lack of observable field relationships make it difficult to assess whether these rhyolites are



GEOLOGY

(Duffell, 1959; modified from Massey et al., 2005)

- Quaternary deposits
till, glaciofluvial, fluvial, colluvium, organics
- EEB** Eocene Endako Group Buck Creek Formation
basaltic volcanic rocks
- EEG** Eocene Endako Group Goosly Lake Formation
alkaline volcanic rocks
- EmiE** Eocene to Lower Miocene Endako Group
basaltic volcanic rocks
- EO** Eocene Ootsa Lake Group
rhyolite, felsic volcanic rocks
- PeEs** Paleocene to Eocene, undivided sedimentary rocks
- uKK** Cretaceous Kasalka Group
andesitic volcanic rocks
- IKS** Lower Cretaceous Skeena Group
undivided sedimentary rocks
- IKSN** Lower Cretaceous Skeena Group Mt. Ney Volcanics
undivided volcanic rocks
- mJHS** Middle Jurassic Hazelton Group Smithers Formation
undivided sedimentary rocks
- IJHT** Lower Jurassic Hazelton Group Telkwa Formation
calc-alkaline volcanic rocks
- EQ** Eocene Quanchus Plutonic Suite
feldspar porphyritic intrusive rocks
- LKB** Late Cretaceous Bulkley Plutonic Suite
intrusive rocks
- LKK** Late Cretaceous Kasalka Plutonic Suite
granodioritic intrusive rocks

- metallic mineral tenure
- ★ metallic mineral occurrence (showing)
- bedrock outcrop observed in roadcut during 2009 field season



Figure 4. Bedrock geology of the study area, west-central British Columbia. Quaternary sediment cover is approximated by the light grey transparent overlay and black dashed line. Bedrock contacts have been extended beneath this transparent overlay.

in fact Eocene in age or older and perhaps equivalent to Rocky Ridge Formation rhyolites.

Mineral Occurrences

There are five documented mineral occurrences within the study area (Figure 4). Tets (MINFILE 093E 084; MINFILE, 2009; Cu, Zn, Pb, Ag veins) and Sheldford Hills (MINFILE 093E 085; Zn, Pb, Au epithermal veins) are vein-type showings while Rip (MINFILE 093E 092; Cu and Mo calcalkaline porphyry), Dilys (MINFILE 093E 094; Cu mineralization) and Hill (MINFILE 093E 097; Cu, Au, Zn alkalic porphyry) are porphyry-type showings. Although there is no MINFILE occurrence associated with it, there is a claim block in the southwest corner of the study area, centred on Mosquito Hills (Figure 4). Known as the Rox claims, mineralization here consists of sulphide and precious metal-bearing veinlets, predominantly hosted in Middle Jurassic Smithers Formation sedimentary rocks. Mineralization is likely associated with either a porphyry, polymetallic vein or epithermal system (Ogryzlo, 2003; Lane, 2008). Immediately west of Tahtsa Reach Road, this claim block butts against a claim block held by Huckleberry Mine Ltd. This adjacent block extends to the west and is continuous from the mineral lease that covers the Huckleberry minesite.

The region has a rich exploration history and is well endowed with metallic mineral deposits. Adjacent to the study area are noteworthy past-producing mines and one still in operation (Figure 2). Approximately 13 km to the southwest of the study area is Huckleberry mine, a producing porphyry Cu-Mo mine with a production rate of approximately 17 000 tonnes of ore per day. Average grades for 2008 were 0.316% Cu and 0.006% Mo. Mine life is expected to extend to the end of 2011 (Imperial Metals Corporation, 2009). Another 9 km northwest of Huckleberry mine is the past-producing Emerald Glacier mine, a Pb, Zn, Ag and Au vein deposit. This mine operated intermittently between 1951 and 1968 and produced 2.6 million g of Ag, 1524 g of Au, 891 t of Zn, and 766 t of Pb (MINFILE 093E 001). Approximately 26 km to the northeast of the study area is Equity Silver, a past-producing Cu-Ag-Au mine, which was in production from 1980 to 1994. Combined mine production here was 33.8 million tonnes grading at 64.9 g/t Ag, 0.4% Cu and 0.46 g/t Au (MINFILE 093L 001). Developed prospects in the region such as Berg (porphyry Cu-Mo), Whiting Creek (porphyry Cu-Mo), and Lucky Ship (porphyry Mo) also demonstrate the potential for ore-grade bedrock to occur within the region (Figure 2). In all instances mentioned here, ore-grade bedrock is closely associated with Late Cretaceous and younger plutonic rocks. Intrusive suites of similar age and composition do exist within the study area.

QUATERNARY GEOLOGY

Previous Quaternary geology work conducted within the study area is limited to soils and terrain mapping. Researchers with the BC Ministry of Environment were the first to map the area, producing a 1:50 000 scale soil and landform map (Young, 1976). Singh (1998) has completed the most recent mapping within the study area, a terrain classification map. Directly south and adjacent to the study area, Ferbey and Levson (2001a, b, 2003) and Ferbey (2004) conducted a detailed study of the Quaternary geol-

ogy and till geochemistry of the Huckleberry mine region. Included in this work was surficial geology mapping and detailed sedimentological descriptions for Quaternary sediments in the vicinity of Huckleberry mine. Also included in work was an investigation into the region's ice-flow history.

Quaternary geological studies have been conducted in areas adjacent to the study area. To the north and northwest, Clague (1984), Tipper (1994) and Levson (2001a, 2002) discuss the Quaternary geology and geomorphological features of portions of NTS 093L, M and 103I, P. To the northeast, Plouffe (1996a, b) mapped the surficial deposits, and described the Quaternary stratigraphy, of the west half of NTS 093K. Mate (2000) conducted a similar study to the southeast in NTS map area 093F/12.

Surficial Geology

During the 2009 field season surficial materials were described at 131 sites within the study area. Observations were made at roadcuts and streamcuts, discontinuous exposures along Ootsa Lake and in hand-dug pits. Data collected at each site included map unit, topographic position, slope aspect and angle, and sedimentological characteristics, such as texture, structure, lateral and vertical variability, lower contacts and relationships with adjacent sediment types.

The dominant surficial material found in the study area is an overconsolidated, grey to brown diamicton with a silt-rich matrix. It is typically massive and matrix supported, and in many examples vertical jointing and subhorizontal fissility is well developed (Figure 5). Matrix proportion varies from 70 to 80% and modal clast size is small pebble but locally can include boulder-sized material and larger. Clast shape is typically subangular to subrounded. In lower valley settings, it occurs as thick units (>2 m thick) that typically overlie glacially eroded and polished bedrock. On hill flanks and in higher elevation settings, it occurs as thinner units (<2 m thick), including veneers (<1 m thick), that are closely associated, and discontinuous, with locally derived diamicton (e.g., colluvium) and bedrock. The surface expression of this diamicton most often conforms to underlying bedrock topography but also can be streamlined, as seen in the drumlinized and fluted terrain between the south



Figure 5. Silt- and clay-rich, overconsolidated diamicton, interpreted as a basal till (west-central British Columbia). Moderately well developed vertical jointing and subhorizontal fissility give this basal till a blocky appearance. Pick for scale (65 cm long).

and southeast flanks of Shelford Hills and the northern shore of Ootsa Lake. These characteristics are consistent with those of a subglacially derived diamicton (Dreimanis, 1989). This unit is interpreted to be a basal till, the ideal sample medium for a till geochemistry survey.

Glaciofluvial sand and gravel can also be found within the study area. Sandy, pebble- to cobble-sized gravels occur in fan-like features at the mouths of gulleys that head in higher ground, such as Shelford and Mosquito hills, and are related to meltwater draining off this high ground from stagnant ice. Similar sized gravels also occur within late-glacial to deglacial drainage systems (now abandoned) as outwash plains and esker-like ridges (e.g., in the Fish Lake area and south through the Andrews Creek area towards Ootsa Lake). Silt- and clay-rich glaciolacustrine and lacustrine sediments only rarely occur within the study area. Thick organic units are, however, common along the shorelines of smaller lakes and in low-lying areas that separate these smaller lakes when they occur in chains.

Surficial mapping is currently in progress for NTS 093E/15. This mapping is being conducted at a scale of 1:50 000, using aerial photographs (1:40 000 scale, black and white), digital orthophotographs and other available remotely sensed imagery (e.g., Landsat). An integral part of this mapping is the reconstruction of the region's glacial and ice-flow history using macro-scale landforms (e.g., drumlins, flutes, crag-and-tail forms) identifiable in remotely sensed imagery.

Ice-Flow History

Ferbey and Levson (2001a, b) and Ferbey (2004) built on previous work by Stumpf et al. (2000) that indicated there was an ice-flow reversal in west-central BC during the Late Wisconsinan glacial maximum. During the onset of glaciation, ice flowed radially from accumulation centres, such as the Coast Mountains, towards central BC. Sometime during the glacial maximum, however, the ice divide over the Coast Mountains migrated east into central BC resulting in an ice-flow reversal. Glaciers were then flowing west across some parts of the western Nechako Plateau, over the Coast Mountains and towards the Pacific Ocean. Eastward ice flow resumed once the ice divide migrated back over the axis of the Coast Mountains, and continued until the close of the Late Wisconsinan glaciation.

Evidence for this ice-flow reversal in the Huckleberry mine region is seen in macro-scale glacial landforms (e.g., crag-and-tail forms, roches moutonnées) and micro-scale ice-flow indicators (e.g., rat tails, roches moutonnées) on bedrock outcrop in valley bottoms and at higher elevation sites (i.e., >1500 m asl; Figure 6). This ice-flow reversal is also detectable in trace-element till geochemical data from Huckleberry mine (Ferbey and Levson, 2007). One of the challenges of interpreting till geochemical data collected as part of this project, and other similar projects being conducted within the region, will be determining transport direction of basal till and conversely the direction to a bedrock source of till samples elevated in elements of interest.

During the 2009 field season, ice-flow data were observed and recorded at 33 field stations. These data were used to supplement an additional 120 field stations, and 207 moderately well to well preserved streamlined landforms measured in aerial photographs, presented and discussed by Ferbey and Levson (2001b). The majority of bedrock outcrop studied in the field is located on the lower flanks of

hillslopes exposed in roadcuts. In these exposures, outcrop-scale features such as striations, grooves and rat tails were studied and measured (Figure 7). Landform-scale features such as crag-and-tail ridges and roches moutonnées were also measured. Orientations of these features indicate that there are two dominant ice-flow directions in the region, 054–096° and 252–306°. These values are in agreement with those presented by Ferbey and Levson (2001a, b) and Ferbey (2004) and confirm that there was an ice-flow reversal within the study area during the Late Wisconsinan.

TILL GEOCHEMISTRY SURVEY

Till geochemical surveys can detect known sources of mineralization and identify new geochemical exploration targets (e.g., Levson et al., 1994; Cook et al., 1995; Sibbick and Kerr, 1995; Plouffe, 1997; Levson, 2002; Ferbey, 2009). Till geochemical surveys are well suited to assessing the mineral potential of ground covered by glacial drift. Basal till, the sample medium used in these surveys, is ideal for these assessments as in most cases it has a relatively simple transport history, is deposited directly down-ice of its source, and produces a geochemical signature that is areally more extensive than its bedrock source and therefore, at a regional scale, can be more easily detected (Levson, 2001b).

Directly south and adjacent to the study area, Ferbey and Levson (2001a) and Ferbey (2004) conducted a detailed till geochemistry survey of the Huckleberry mine region. These studies demonstrate a clear relationship between till samples elevated in Cu, Mo, Au, Ag and Zn and Cu-Mo ore zones at Huckleberry mine and smaller scale polymetallic vein occurrences on the mine property. Lateral and vertical variability in trace-element concentrations in till at Huckleberry mine provide further evidence for an ice-flow reversal in the region during the Late Wisconsinan glacial maximum (Ferbey and Levson, 2007). These results suggest that interpreting trace-element geochemical data from tills or soils in this region can be complex, in particular when considering transport direction.

Plouffe and Ballantyne (1993), Plouffe (1995), Plouffe et al. (2001) and Levson and Mate (2002) have also conducted till geochemistry surveys to the east of the study area, in NTS map areas 093F and K. Using percentile plots of precious-metal, base-metal and pathfinder element concentrations, and/or gold grain counts, each of these surveys identifies prospective ground where there are no known mineral occurrences.

Sample Media

During the 2009 field season, 2–3 kg till samples were collected at 84 sample sites for major, minor and trace-element geochemical analyses (Figures 2, 8). An additional 16 till samples, each weighing 10–15 kg, were collected for heavy mineral separation and gold grain counts (Figure 2). These larger samples were collected at sites where an adequate amount of sample material was exposed. Given that net transport direction in the study area was likely affected by an ice-flow reversal during the Late Wisconsinan glacial maximum, till samples were collected outside of NTS 093E/15 to take into account possible east and west transport of basal till. Till sample density for this survey is one sample per 14 km². For simplicity, areas inaccessible by truck (e.g., Shelford Hills), and areas where till does not oc-

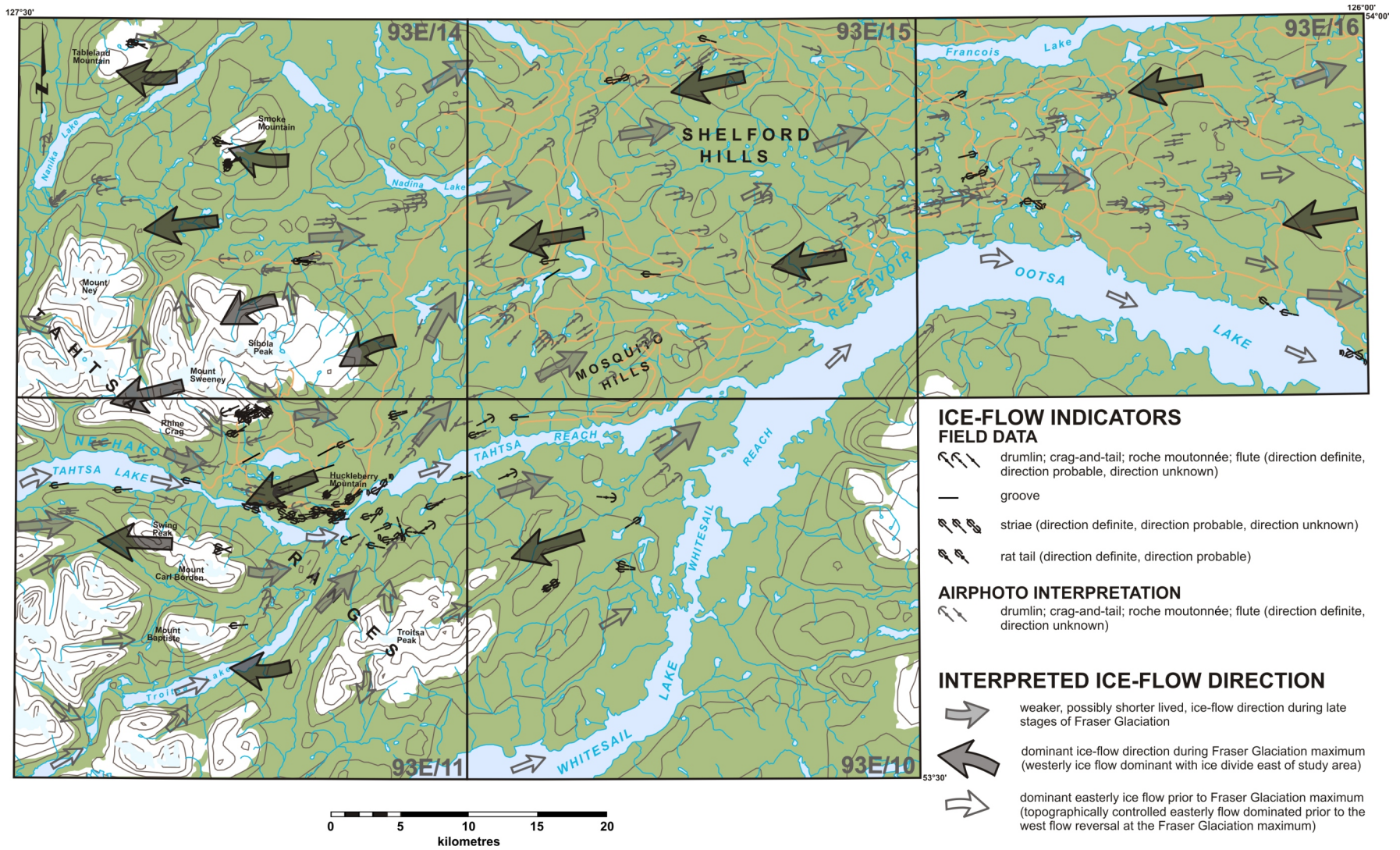


Figure 6. Ice-flow history of the Tahtsa Lake–Ootsa Lake region, west-central British Columbia (after Ferbey and Levson, 2001b).

cur, were included in this calculation. The majority of unweathered till in the study area occurs >1 m below surface and so most till samples were collected at this depth or lower.

Till samples collected for major, minor and trace-element analyses are being sieved, and decanted and centrifuged, to produce a silt- plus clay-sized (<0.063 mm) and clay-sized (<0.002 mm) fraction. This sample preparation is being conducted at Acme Analytical Laboratories Ltd. (Vancouver, BC). Heavy mineral samples have been sent to Overburden Drilling Management (ODM; Nepean, ON), where heavy mineral (0.25–2.0 mm) and gold grain (<2.0 mm) concentrates are being produced using a combination of gravity tabling and heavy liquids.

On the 2–3 kg samples, minor and trace-element analyses (37 elements) will be conducted on splits of the silt- plus clay- and clay-sized fractions, respectively, by inductively coupled plasma-mass spectrometry (ICP-MS), following an aqua-regia digestion. Major element analyses will be conducted on a split of the silt- plus clay-sized fraction only using inductively coupled plasma-emission spectrometry (ICP-ES), following a lithium metaborate/tetraborate fusion and dilute nitric acid digestion. This analytical work will be conducted at Acme Analytical Laboratories Ltd. (Vancouver, BC).

Also as part of this project, a split of the silt- plus clay-sized fraction (<0.063 mm) will be analyzed for 35 elements by instrumental neutron activation analysis (INAA) at Becquerel Laboratories Inc. (Mississauga, ON). INAA for elements such as Au, Ba and Cr complement those produced by aqua-regia digestion followed by ICP-MS as they are considered to be a near-total determination and hence more representative of rock-forming and economic mineral geochemistry. Additionally, INAA determinations will be conducted on bulk heavy mineral concentrates produced from the 10–15 kg samples. Heavy mineral picking, scanning electron microscopy analyses on difficult-to-identify heavy mineral grains, and pebble counts may be conducted on these samples at a later date. Instrumental neutron acti-



Figure 7. Moderately well preserved rat tails on an outcrop of Skeena Group conglomerate, west-central British Columbia. In the centre of this photograph is a large rat tail indicating ice flow towards the west-southwest. Note that just above it and to the right is a smaller rat tail indicating ice flow towards the east. This outcrop is located on the southern flank of Shelford Hills, north of Andrews Creek, and is the only outcrop of Skeena Group conglomerate observed within the study area.

vation analysis will dictate for which samples, if any, these additional and costly analyses are warranted.

Quality Control

Quality control measures for analytical determinations include the use of field duplicates, analytical duplicates and reference standards. For each block of 20 samples submitted for analysis, one field duplicate (taken at a randomly selected sample site), one analytical duplicate (a sample split after sample preparation but before analysis) and one reference standard will be included in INAA and ICP-MS analysis. Reference standards used will be a combination of certified Canada Centre for Mineral and Energy Technology (CANMET) and in-house BCGS geochemical reference materials. Duplicate samples will be used to measure sampling and analytical variability, whereas reference standards will be used to measure the accuracy and precision of the analytical methods.

QUATERNARY DRIFT COVER AND MINERAL EXPLORATION

Observations made during the 2009 field season suggest that drift cover within the study area may not be a significant hindrance to mineral exploration. In general, drift appears to be less areally extensive than was once thought. Also, a recent increase in logging activity has not only resulted in improved access to the study area, through the building of new roads, but has also resulted in the creation of new bedrock exposures. For example, a previously unmapped quartz diorite ridge was observed in a roadcut on the southeast flank of Shelford Hills (Figure 9). Similar observations were made by Mihalynuk et al. (2008, 2009) while conducting bedrock mapping and resource potential studies in NTS map areas 093C/1, 8 and 9, areas that had received little attention by the mineral exploration industry because of a perceived problem with thick and continuous Late Oligocene to Pleistocene Chilcotin Group basalt and Quaternary drift cover. Mihalynuk et al. determined that this perception was unfounded and that bedrock exposures do exist. While conducting foot traverses at sufficient enough density for 1:50 000 scale bedrock mapping, they described ten new metallic mineral occurrences. A similar



Figure 8. Typical till sample site (west-central British Columbia). Shown is a 2–3 kg sample collected for major, minor and trace-element geochemical analyses. Pick for scale (65 cm long).



Figure 9. New forestry roads have created new bedrock exposures. Shown here is an unmapped quartz diorite ridge observed in a roadcut on the southeast flank of Shelford Hills, approximately 6 km south-southeast of Shelford Hills mineral occurrence, west-central British Columbia. Pick for scale (65 cm long).

approach to bedrock mapping and prospecting within NTS map area 093E/15 could result in similar success.

Within the study area, not only is drift less areally extensive than was once thought, it is also likely not as thick. It is relatively common to see small bedrock knobs (metres to a couple tens of metres across) extending through Quaternary cover to surface. Additionally, as observed in roadcuts, Quaternary cover may only be 1–2 m thick, with basal till directly overlying glacially eroded and polished bedrock. Exceptions can be found in some of the larger valleys like Nadina River valley, or in abandoned late-glacial and deglacial drainages, such as the one that extends south from Fish Lake, down Andrews Creek to Ootsa Lake. In these examples, valley fill and glaciofluvial sequences are typically thick and blanket much if not all underlying bedrock units. These general observations could prove useful in guiding and interpreting data from future geological, geophysical and/or geochemical surveys.

SUMMARY

The 2009 field season saw the completion of fieldwork for year one of a two-year Quaternary geology program that is designed to assess the mineral potential of the northern portion of the Tahtsa Lake district and adjacent areas (NTS 093E/15, 16, 093L/01, 02). This study area falls within Geoscience BC's QUEST-West Project area where additional geochemical data have been compiled and collected, mineral occurrence data have been updated (i.e., MINFILE, 2009), and helicopter-borne time domain electromagnetic and gravity data have been acquired. The focus of this year's work is the Nadina River map area (NTS 093E/15) where 84 basal till samples, each weighing 2–3 kg, were collected for major, minor and trace-element geochemical analyses, and an additional 16 till samples, each weighing 10–15 kg, were collected for separation and analysis of heavy mineral concentrates and gold grain counts. Ongoing and complementary to this till geochemical survey, is a 1:50 000 scale surficial geology mapping and regional ice-flow study. Given that the study area experienced an ice-flow reversal during the Late Wisconsinan glacial maximum, assessing and quantifying net transport

direction of basal till in the study area will be a significant contribution to the understanding of detrital dispersion for the region. An understanding of these variables must exist prior to further investigation of any till samples, collected as part of this study, that are elevated in an element(s) of interest. An assessment of net transport direction will also be of interest to mineral exploration companies working in the area, who are conducting their own surficial sediment geochemistry surveys. Observations made during the 2009 field season suggest that Quaternary sediments within the study area are not necessarily as areally extensive nor thick as was once thought, and therefore may not be a significant hindrance to mineral exploration.

Till geochemical data for the Nadina River map area (NTS 093E/15) will be the topic of a combined BCGS Open File and Geoscience BC Report to be released in late spring 2010. Field crews will return to the study area during the 2010 summer field season and complete data and till sample collection for the Wistaria, Colleymount and Owen Lake map areas (NTS 093E/16, L/01, 02).

ACKNOWLEDGMENTS

This year's program has truly been a collaborative effort and the author would like to gratefully acknowledge Geoscience BC for analytical support; the Smithers Exploration Group (C. Ogryzlo and J. L'Orsa) and Northwest Community College (T. Reedy and R. Maurer) for sponsoring a graduate of their Reclamation and Prospecting Program to assist with fieldwork; and Huckleberry Mine Ltd. (B. Mracek, W. Curtis and F. Sayeed) for allowing the field crew to stay at the minesite. R.E. Gawa is thanked for his assistance in the field. The author would also like to thank L.J. Diakow and D.G. MacIntyre for discussions on, and their insight into, local bedrock lithologies. R.E. Lett is thanked for assistance with geochemical reference standards. The author would also like to thank P.L. Ogryzlo for so freely sharing his ideas on porphyry Cu deposits and how and where he believes the next ones will be found. T.E. Demchuk is thanked for her review of an earlier version of this manuscript.

REFERENCES

- Alldrick, D.J. (2007a): Geology of the Skeena Group, central British Columbia (NTS 93E, 93F, 93K, 93L, 93M, 103I, 103P); *BC Ministry of Energy, Mines and Petroleum Resources*, Open File 2007-8, scale 1:250 000.
- Alldrick, D.J. (2007b): Geology of the Equity Silver mine area; *BC Ministry of Energy, Mines and Petroleum Resources*, Open File 2007-9, scale 1:10 000.
- Alldrick, D.J., MacIntyre, D.G. and Villeneuve, M.E. (2007): Geology, mineral deposits, and exploration potential of the Skeena Group (NTS 093E, L, M; 103I), central British Columbia; in *Geological Fieldwork 2006*, *BC Ministry of Energy, Mines and Petroleum Resources*, Paper 2007-1, pages 1–17.
- Carter, N.C. (1981): Porphyry copper and molybdenum deposits, west-central British Columbia; *BC Ministry of Energy, Mines and Petroleum Resources*, Bulletin 64, 150 pages.
- Clague, J.J. (1984): Quaternary geology and geomorphology, Smithers-Terrace-Prince Rupert area, British Columbia; *Geological Survey of Canada*, Memoir 413, 71 pages.
- Cook, S.J., Levson, V.M., Giles, T.R. and Jackaman, W. (1995): A comparison of regional lake sediment and till geochemistry surveys: a case study from the Fawnie Creek area, central

- British Columbia; *Exploration Mining Geology*, Volume 4, pages 93–101.
- Cyr, J.B., Pease, R.B. and Schroeter, T.G. (1984): Geology and mineralization at Equity Silver mine; *Economic Geology*, Volume 29, pages 947–968.
- Diakow, L.J. (2006): Geology of the Tahtsa Ranges between Eutsuk Lake and Morice Lake, Whitesail Lake map area, west-central British Columbia (parts of NTS 93E/5, 6, 7, 10, 11, 12, 13, 14, and 15); *BC Ministry of Energy, Mines and Petroleum Resources*, Geoscience Map 2006-5, scale 1:150 000.
- Dreimanis, A. (1989): Tills: their genetic terminology and classification; in Genetic Classification of Glacigenic Deposits, Goldthwait, R.P. and Matsch, C.L., Editors, *A.A. Balkema*, Rotterdam, pages 17–83.
- Duffel, S. (1959): Whitesail Lake, Coast District; *Geological Survey of Canada*, Map 1064A, scale 1 in. to 4 mi.
- Ferbey, T. (2004): Quaternary geology, ice-flow history and till geochemistry of the Huckleberry mine region, west-central British Columbia; MSc thesis, *University of Victoria*, 301 pages.
- Ferbey, T. (2009): Till geochemical exploration targets, Redstone and Loomis Lake map areas (NTS 93B/04 and 05), central British Columbia; *BC Ministry of Energy, Mines and Petroleum Resources*, Open File 2009-9, 52 pages.
- Ferbey, T. and Levson, V.M. (2001a): Quaternary geology and till geochemistry of the Huckleberry mine area; in Geological Fieldwork 2000, *BC Ministry of Energy, Mines and Petroleum Resources*, Paper 2001-1, pages 397–410.
- Ferbey, T. and Levson, V.M. (2001b): Ice flow history of the Tahtsa Lake–Ootsa Lake region; *BC Ministry of Energy, Mines and Petroleum Resources*, Open File 2001-8, scale 1:110 000.
- Ferbey, T. and Levson, V.M. (2003): Surficial geology of the Huckleberry mine area; *BC Ministry of Energy, Mines and Petroleum Resources*, Open File 2003-2, scale 1:15 000.
- Ferbey, T. and Levson, V.M. (2007): The influence of ice-flow reversals on the vertical and horizontal distribution of trace elements in tills, Huckleberry mine area, west-central British Columbia; in Application of Till and Stream Sediment Heavy Mineral and Geochemical Methods to Mineral Exploration in Western and Northern Canada, Paulen, R.C. and McMartin, I., Editors, *Geological Association of Canada*, Short Course Notes 18, pages 145–151.
- Hedley, M.S. (1935): Tahtsa-Morice area; *Geological Survey of Canada*, Map 367A, scale 1 in. to 4 mi.
- Holland, S.S. (1976): Landforms of British Columbia: a physiographic outline; *BC Ministry of Energy, Mines and Petroleum Resources*, Bulletin 48, 138 pages.
- Imperial Metals Corporation (2009): Annual report 2008; *Imperial Metals Corporation*, 48 pages.
- Jackson, A. and Illerbrun, K. (1995): Huckleberry porphyry copper deposit, Tahtsa Lake District, west-central British Columbia; in Porphyry Deposits of the Northwestern Cordillera of North America, Schroeter, T.G., Editor, *Canadian Institute of Mining, Metallurgy and Petroleum*, Special Volume 46, pages 313–321.
- Kowalczyk, P.K. (2009): QUEST-West geophysics in central British Columbia (NTS 093E, F, G, K, L, M, N, 103I): new regional gravity and helicopter time-domain electromagnetic data; in Geoscience BC Summary of Activities 2008, *Geoscience BC*, Report 2009-1, pages 1–6.
- Lane, R.A. (2008): A geological report on the Rox property, Omineca Mining Division, British Columbia; submitted by Lowprofile Ventures Ltd., *BC Ministry of Energy, Mines and Petroleum Resources*, Assessment Report 30342, 86 pages.
- Levson, V.M. (2001a): Quaternary geology of the Babine porphyry copper district: implications for geochemical exploration; *Canadian Journal of Earth Sciences*, Volume 38, pages 733–749.
- Levson, V.M. (2001b): Regional till geochemical surveys in the Canadian Cordillera: sample media, methods, and anomaly evaluation; in Drift Exploration in Glaciated Terrain, McClenaghan, M.B., Bobrowsky, P.T., Hall, G.E.M. and Cook, S.J., Editors, *Geological Society*, Special Publication, Number 185, pages 45–68.
- Levson, V.M. (2002): Quaternary geology and till geochemistry of the Babine porphyry copper belt, British Columbia (NTS 93 L/9, 16, M/1, 2, 7, 8); *BC Ministry of Energy, Mines and Petroleum Resources*, Bulletin 110, 278 pages.
- Levson, V.M. and Mate, D.J. (2002): Till geochemistry of the Tetachuck Lake and Marilla map areas (NTS 93F/5 and F/12); *BC Ministry of Energy, Mines and Petroleum Resources*, Open File 2002-11, 180 pages.
- Levson, V.M., Giles, T.R., Cook, S.J. and Jackaman, W. (1994): Till geochemistry of the Fawnie Creek area (93F/03); *BC Ministry of Energy, Mines and Petroleum Resources*, Open File 1994-18, 40 pages.
- MacIntyre, D.G. (1985): Geology and mineral deposits of the Tahtsa Lake District, west-central British Columbia; *BC Ministry of Energy, Mines and Petroleum Resources*, Bulletin 75, 82 pages.
- MacIntyre, D.G. (2001): The mid-Cretaceous Rocky Ridge Formation – a new target for subaqueous hot-spring deposits (Eskay Creek type) in central British Columbia; in Geological Fieldwork 2000, *BC Ministry of Energy, Mines and Petroleum Resources*, Paper 2001-1, pages 253–268.
- MacIntyre, D.G., Ash, C.H. and Britton, J. (1994): Skeena Arcview data (NTS 93E,L,M; 94D; 104A,B; 103G,H; 103 I,P); *BC Ministry of Energy, Mines and Petroleum Resources*, Open File 1994-14, digital data.
- MacIntyre, D.G., McMillan, R.H. and Villeneuve, M.E. (2004): The mid-Cretaceous Rocky Ridge Formation – important host rocks for VMS and related deposits in central British Columbia; in Geological Fieldwork 2003, *BC Ministry of Energy, Mines and Petroleum Resources*, Paper 2004-1, pages 231–247.
- Massey, N.W.D., MacIntyre, D.G., Desjardins, P.J. and Cooney, R.T. (2005): Digital geology map of British Columbia: whole province; *BC Ministry of Energy, Mines and Petroleum Resources*, GeoFile 2005-1, 1:250 000 scale, URL <<http://www.empr.gov.bc.ca/Mining/Geoscience/PublicationsCatalogue/Geofiles/Pages/2005-1.aspx>> [December 2009].
- Mate, D.J. (2000): Quaternary geology, stratigraphy and applied geomorphology in southern Nechako Plateau, central British Columbia; MSc thesis, *University of Victoria*, 253 pages.
- Mihalynuk, M.G., Peat, C.R., Terhune, K. and Orovan, E.A. (2008): Regional geology and resource potential of the Chezacut map area, central British Columbia (NTS 093/08); in Geological Fieldwork 2007, *BC Ministry of Energy, Mines and Petroleum Resources*, Paper 2008-1, pages 117–134.
- Mihalynuk, M.G., Orovan, E.A., Larocque, J.P., Friedman, R.M. and Bachiu, T. (2009): Geology, geochronology and mineralization of the Chilanko Forks to southern Klusko River area, British Columbia (NTS 93C/01, 08, 09S); in Geological Fieldwork 2008, *BC Ministry of Energy, Mines and Petroleum Resources*, Paper 2009-1, pages 81–100.
- MINFILE (2009): MINFILE BC mineral deposits database; *BC Ministry of Energy, Mines and Petroleum Resources*, URL <<http://minfile.ca>> [November 2009].
- Monger, J.W.H., Wheeler, J.O., Tipper, H.W., Gabrielse, H., Harms, T., Struik, L.C., Campbell, R.B., Dodds, C.J., Gehrels, G.E. and O'Brien, J. (1991): Cordilleran terranes (Chapter 8: Upper Devonian to Middle Jurassic assemblages); in *Geology of the Cordilleran Orogen in Canada*,

- Gabrielse, H. and Yorath, C.J., Editors, *Geological Survey of Canada*, Geology of Canada Series, Number 4, pages 281–327.
- Ogryzlo, P.L. (2003): Geophysical surveying and diamond drilling on the Rox 1 mineral claim, Omnicca Mining Division; submitted by Gary Thompson, *BC Ministry of Energy, Mines and Petroleum Resources*, Assessment Report 27050, 48 pages.
- Panteleyev, A. (1981): Berg porphyry copper-molybdenum deposit; *BC Ministry of Energy, Mines and Petroleum Resources*, Bulletin 66, 158 pages.
- Plouffe, A. (1995): Geochemistry, lithology, mineralogy, and visible gold grain content of till in the Manson River and Fort Fraser map areas, central British Columbia (NTS 93K and N); *Geological Survey of Canada*, Open File 3194, 119 pages.
- Plouffe, A. (1996a): Surficial geology, Cunningham Lake, British Columbia (NTS 93K/NW); *Geological Survey of Canada*, Open File 3183, scale 1:50 000.
- Plouffe, A. (1996b): Surficial geology, Burns Lake, British Columbia (NTS 93K/SW); *Geological Survey of Canada*, Open File 3184, scale 1:50 000.
- Plouffe, A. (1997): Reconnaissance till geochemistry on the Chilcotin Plateau (92O/5 and 12); in Interior Plateau Geoscience Project: Summary of Geological, Geochemical and Geophysical Studies (092N, 092O, 093B, 093C, 093F, 093G, 093G), Diakow, L.J., Metcalfe, P. and Newell, J., Editors, *BC Ministry of Energy, Mines and Petroleum Resources*, Paper 1997-2, pages 145–157.
- Plouffe, A. and Ballantyne, S.B. (1993): Regional till geochemistry, Manson River and Fort Fraser area, British Columbia (93K, 93N), silt plus clay and clay size fractions; *Geological Survey of Canada*, Open File 2593, 210 pages.
- Plouffe, A., Levson, V.M. and Mate, D.J. (2001): Till geochemistry of the Nechako River map area (NTS 93F), central British Columbia; *Geological Survey of Canada*, Open File 4166, 66 pages.
- Sibbick, S.J. and Kerr, D.E. (1995): Till geochemistry of the Mount Milligan area, north-central British Columbia; recommendations for drift exploration for porphyry copper-gold mineralization; in Drift Exploration in the Canadian Cordillera, Bobrowsky, P.T., Sibbick, S.J., Newell, J.M. and Matysek, P., Editors, *BC Ministry of Energy, Mines and Petroleum Resources*, Paper 1995-2, pages 167–180.
- Singh, N. (1998): Terrain classification map phase 3, 93E.076, 077, 086, 087, 088, 096, 097, 098; *BC Ministry of Forests*, scale 1:20 000.
- Stumpf, A.J., Broster, B.E. and Levson, V.M. (2000): Multiphase flow of the Late Wisconsinan Cordilleran Ice Sheet in western Canada; *Geological Society of America Bulletin*, Volume 112, pages 1850–1863.
- Tipper, H.W. (1994): Preliminary interpretations of glacial and geomorphic features of Smithers map area (93L), British Columbia; *Geological Survey of Canada*, Open File 2837, 7 pages.
- Woodsworth, G.J. (1980): Geology of Whitesail Lake (93E) map area, British Columbia; *Geological Survey of Canada*, Open File 708, scale 1:250 000.
- Young, G. (1976): 93E/15 soils and landforms, Nadina River; *BC Department of Lands and Forests*, scale 1:50 000.

Geochemistry of Volcanic and Plutonic Rocks of the Sitlika Assemblage, Takla Lake Area, Central British Columbia (NTS 093N/04, 05, 12, 13)

by P. Schiarizza and N.W.D. Massey

KEYWORDS: Sitlika assemblage, Cache Creek terrane, island-arc basalt, ocean-floor basalt, within-plate basalt, rhyolite, dacite, tonalite, diorite

INTRODUCTION

The Sitlika assemblage comprises a belt of Permo-Triassic volcanic, sedimentary and plutonic rocks, which crop out in the Takla Lake area of central British Columbia. It includes rocks that correlate with the Kutcho assemblage of northern BC, which hosts the Kutcho Creek Cu-Zn volcanogenic massive sulphide deposit. The Sitlika belt was mapped by the BC Geological Survey between 1995 and 1998, as part of the Nechako NATMAP federal-provincial geoscience program. Samples of representative volcanic and plutonic rocks were analyzed for whole-rock geochemistry during this program, but only some of this data has previously been presented (Childe and Schiarizza, 1997; Schiarizza and Massey, 2000). In this paper, we present, and briefly discuss, the geochemistry of the full suite of Sitlika samples collected during the NATMAP program.

The Takla Lake map area is located along the western edge of NTS map sheet 093N. The most direct access is via networks of logging and forest service roads that originate near the town of Fort St. James, which is located 125 km southeast of Takla Narrows. Access from Fort St. James is also provided by the CN Rail line which, in part, follows the eastern shore of Takla Lake.

REGIONAL GEOLOGY

The Sitlika assemblage is generally included in the oceanic Cache Creek terrane. It comprises a Permo-Triassic volcanic unit and an overlying Late Triassic-Early Jurassic (?) clastic sedimentary unit, and two small tonalite to diorite plutons of Early Triassic age (Figure 1). The main stratigraphic units of the Sitlika assemblage are folded and structurally overlain by higher elements of the Cache Creek terrane across a system of mainly east-dipping, Early-Middle Jurassic thrust faults (Struik et al., 2001). These higher units of the Cache Creek terrane include, in ascending order, a tectonically disrupted Late Paleozoic ophiolite succession and a structurally imbricated assemblage of Carboniferous-Early Mesozoic chert, argillite, phyllite, limestone and basalt (Figures 1, 2). All units of the Cache Creek terrane, including the Sitlika assemblage, commonly

display a penetrative foliation and lower greenschist-facies metamorphic mineral assemblages.

The Sitlika assemblage is flanked to the west by rocks of the Stikine terrane, which includes arc-derived volcanic and sedimentary rocks of the Late Paleozoic Asitka Group, the Late Triassic Takla Group, the Early-Middle Jurassic Hazelton Group and Late Triassic-Middle Jurassic arc-related plutonic suites (MacIntyre et al., 2001). These rocks are separated from the Sitlika assemblage mainly by a system of steeply dipping, north-striking faults, which are, at least in part, related to a regional dextral strike-slip fault system of Late Cretaceous-Early Tertiary age. Older, east-dipping thrust faults are preserved locally within the Stikine terrane and relationships beyond the Takla Lake area suggest that Stikine terrane was the footwall to the Early-Middle Jurassic west-directed thrust system documented in the adjacent Cache Creek terrane (Struik et al., 2001).

Younger rocks exposed in the Takla Lake map area include several large granitic plutons in the southeast and Late Cretaceous sedimentary rocks of the Sustut Group along the western boundary of the area. The mainly Early Cretaceous granitic plutons cut various units of the Cache Creek terrane and the thrust faults separating them. The Sustut Group comprises conglomerate and sandstone that is in fault contact with various units of the Stikine terrane (Figure 1).

THE SITLIKA ASSEMBLAGE

The Sitlika assemblage was named by Paterson (1974) for greenschist-facies metavolcanic and metasedimentary rocks on the eastern side of Takla Lake, which had previously been included in the Cache Creek and Takla groups by Armstrong (1949). He subdivided the assemblage into three divisions: a central volcanic division, a greywacke division to the east and a narrow argillite division to the west. Monger et al. (1978) correlated the Sitlika assemblage with the Kutcho Formation, host to the Kutcho Creek volcanogenic massive sulphide deposit, which occurs in the eastern part of the King Salmon allochthon in northern BC. They suggested that the Kutcho and Sitlika assemblages might have been contiguous prior to dispersion along Late Cretaceous or Early Tertiary dextral strike-slip faults.

The distribution and subdivisions of the Sitlika assemblage shown on Figure 1 are based on 1995-1998 geological mapping by the BC Geological Survey (Schiarizza and Payie, 1997; Schiarizza et al., 1998; Schiarizza and MacIntyre, 1999). This continuous belt is offset by a northeast-striking fault about 7 km northwest of Mount Olson, but a narrow sliver of volcanic and sedimentary rocks correlated with the Sitlika assemblage extends an additional 35 km

This publication is also available, free of charge, as colour digital files in Adobe Acrobat® PDF format from the BC Ministry of Energy, Mines and Petroleum Resources website at <http://www.empr.gov.bc.ca/Mining/Geoscience/PublicationsCatalogue/Fieldwork/Pages/default.aspx>.

northwestward into the southern part of the McConnell Creek map area (Monger, 1977; Richards, 1990). The southern end of the belt is likewise truncated by a northeast-striking fault just beyond the southern boundary of Fig-

ure 1, although several fault-bounded blocks of sedimentary rocks correlated with the Sitlika clastic sedimentary unit have been mapped southward from there to the vicinity of Babine Lake (MacIntyre and Schiarizza, 1999). A belt of

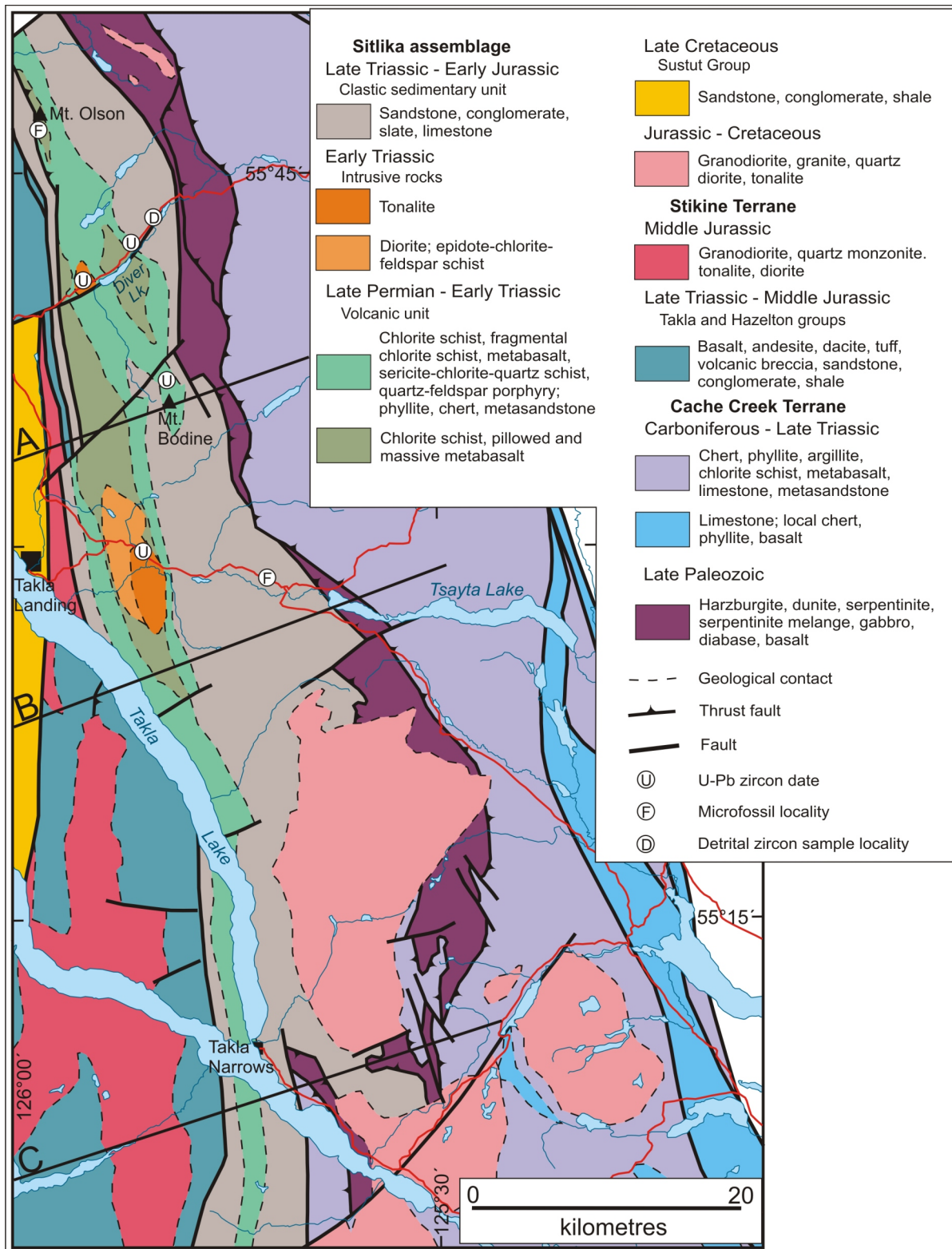


Figure 1. Generalized geology of the Takla Lake area, central British Columbia (after Schiarizza, 2000; Schiarizza et al., 2000).

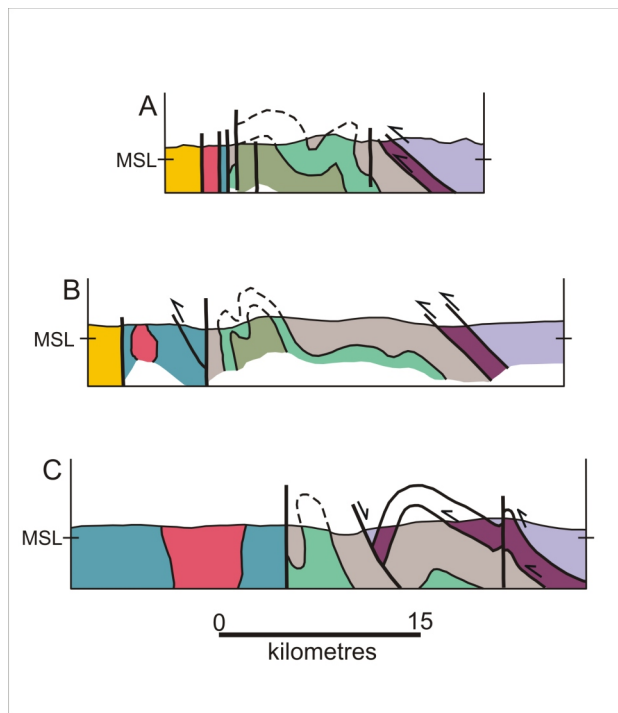


Figure 2. Schematic vertical cross-sections through the western part of the Takla Lake area, central British Columbia. See Figure 1 for legend and location of section lines. Abbreviation: MSL, mean sea level.

volcanic rocks exposed near Cunningham Lake in this southern area was provisionally correlated with the Sitlika volcanic unit, but subsequently yielded a Middle Jurassic U-Pb zircon date, which demonstrates that it is not actually part of the Sitlika assemblage (Mihalynuk et al., 2008).

The Sitlika assemblage is currently divided into two main units: a volcanic unit and an unconformably overlying clastic sedimentary unit. The volcanic unit corresponds to the volcanic division originally defined by Paterson (1974). The clastic sedimentary unit forms a wide belt to the east of the volcanic unit, where it corresponds to the greywacke division of Paterson. The clastic sedimentary unit is structurally repeated as a narrow belt to the west of the volcanic unit (Figure 2), where it corresponds, in part, to Paterson's argillite division. However, part of Paterson's argillite division has been reassigned to the adjacent Stikine terrane, where it is included in a sedimentary unit in the upper part of the Takla Group (Schiarizza and MacIntyre, 1999).

Volcanic Unit

The volcanic unit of the Sitlika assemblage is separated into two subunits: a mafic volcanic subunit and an overlying mixed volcanic subunit. The mafic volcanic subunit comprises a monotonous succession of plagioclase-epidote-actinolite-chlorite schist, semischist and greenstone that locally displays relict volcanic features such as pillows, pillow breccias, amygdules and relict phenocrysts of plagioclase, and, less commonly, pyroxene. The mixed volcanic subunit includes similar mafic schist, intercalated with felsic volcanic rocks and sedimentary rocks. The felsic units include quartz-sericite schist, with or without relict quartz and feldspar phenocrysts, and massive

to flow-banded feldspar porphyry and quartz-feldspar porphyry. Fragmental sericite-chlorite schist is also common and contains flattened fragments of felsic and mafic volcanic rock, locally accompanied by relict crystals of feldspar, quartz and pyroxene, and, rarely, clasts of dioritic to tonalitic plutonic rock. Sedimentary rocks within the mixed volcanic subunit include black phyllite, siltstone, feldspathic sandstone, green siliceous phyllite and chert.

A massive, quartz-plagioclase-phyric rhyolite unit within the mixed volcanic subunit on the northeastern flank of Mount Bodine has yielded a U-Pb zircon date of 258 ± 10 Ma (Childe and Schiarizza, 1997). A sample of flow-banded rhyolite from near the top of the mixed volcanic subunit northeast of Diver Lake appears to be from about the same stratigraphic level (Figure 1), but yielded a younger U-Pb zircon date of 248.4 ± 0.3 Ma (M. Villeneuve, in Struik et al., 2007). Despite the range, both samples indicate a Late Permian age, which is corroborated by Permian radiolarians (*Latentibifistula* sp.) extracted from a narrow chert interval intercalated with volcanic rocks of the mixed subunit south of Mount Olson (F. Cordey, in Struik et al., 2007).

Intrusive Rocks

Dikes and sills of variably foliated diorite, feldspar-chlorite schist and quartz-feldspar porphyry are widespread within the Sitlika volcanic unit, which also hosts two mappable plutons. The composite Maclaing Creek pluton, east of Takla Landing, includes a mafic component consisting of foliated diorite and epidote-chlorite-feldspar schist, and a younger felsic component consisting of massive to weakly foliated chlorite-epidote-altered tonalite (Schiarizza et al., 1998). The smaller Diver Lake stock, west of Diver Lake, consists mainly of massive to weakly foliated tonalite, which displays several textural variations (Schiarizza and Payie, 1997). Zircons from the Diver Lake pluton yielded a U-Pb date of 241 ± 1 Ma (Childe and Schiarizza, 1997) and tonalite from the Maclaing Creek pluton yielded a U-Pb zircon date of 243 Ma (M. Villeneuve, in Struik et al., 2007). These dates indicate that magmatism within the Sitlika assemblage continued into the Early Triassic.

Clastic Sedimentary Unit

The clastic sedimentary unit of the Sitlika assemblage consists of slate, siltstone and sandstone, with local intercalations of conglomerate and limestone. Where observed, the base of the unit is in abrupt stratigraphic contact with the volcanic unit, and commonly includes a basal conglomerate that contains clasts of felsic to mafic volcanic and plutonic rocks, which may have been derived from the underlying volcanic unit (Schiarizza and Payie, 1997; Schiarizza et al., 1998). Higher stratigraphic levels consist largely of thin-bedded slate and siltstone, commonly intercalated with thin to thick, massive to graded beds of fine- to coarse-grained sandstone and granule conglomerate. Sandstones range from schistose wacke, containing quartz, feldspar and lithic grains, to quartz-rich wacke and arenite. Calcareous rocks, including thin layers and lenses of calcareous sandstone, calcarenite and impure marble, are scattered throughout the unit, but may be most common in the lower part.

The clastic sedimentary unit is dated at a single locality, 3 km west of Tsayta Lake, where Late (?) Norian conodonts were extracted from a schistose calcarenite bed (M.J. Orchard, *in* Struik et al., 2007). In addition, a sandstone sample from northeast of Diver Lake was analyzed for detrital zircons (Figure 1) and yielded grains as young as 202 Ma (latest Triassic; M. Villeneuve, *in* Struik et al., 2007).

GEOCHEMISTRY OF THE SITLIKA ASSEMBLAGE

The samples analyzed from the Sitlika assemblage are listed in Table 1 and their locations are shown on Figure 3. The geochemical data are listed in Tables 2, 3 and 4. Major elements and Rb, Sr, Ba, Y, Zr, Nb, V, Cr, Ni, Cu and Zn were determined by X-ray fluorescence (majors on fused disc, traces on pressed powder pellet) at McGill University. Rare earth elements (REE), Hf, Ta and Th were determined by peroxide-fusion inductively coupled plasma–mass spectrometry at the Memorial University of Newfound-

land, except for samples PSC95-16-4 and PSC95-18-6-1, (originally reported by Childe and Schiarizza, 1997), which were determined by instrumental neutron activation analysis at Activation Laboratories Ltd.

The Sitlika rocks have been subject to varying degrees of chemical alteration accompanying low-grade metamorphism, a process which particularly affects the alkali and alkaline earth elements. Despite this alteration, the mafic volcanic rocks can be shown to consist of three geochemically distinct types, which define two belts within the Sitlika volcanic unit: an eastern belt containing type 1 volcanic rocks, of mid-ocean-ridge basalt (MORB) affinity, and a western belt containing a mixture of type 2 volcanic rocks, of volcanic-arc affinity, and type 3 volcanic rocks, of alkaline within-plate character. Felsic samples are mainly from the eastern belt and show an affinity with the type 1 mafic volcanic rocks. A single felsic sample that comes from the western belt is geochemically similar to the type 2 mafic volcanic rocks. A dividing line between the eastern and western belts is shown on Figure 3, based purely on geochemistry as there is no mapped structural or stratigraphic

Table 1. Geochemical samples from the Sitlika volcanic unit and associated intrusions. Easting and northing refer to UTM Zone 10 coordinates (NAD 83). Abbreviations: v1, mafic volcanic subunit; v2, mixed volcanic subunit; M, Maclaing Creek pluton; D, Diver Lake stock; d, diorite; t, tonalite; f, felsic.

Sample	Easting	Northing	Unit	Type	Description
96GPA-9-6-1	318924	6176524	v1	1	pillowed metabasalt
96GPA-14-1-1	318279	6168448	v2	1	pale greenstone
96GPA-14-4	317641	6168228	v2	1	feldspar-phyric chloritic schist
96GPA-14-10	316121	6168238	v1	2	feldspar-phyric chloritic schist
96GPA-18-3-1	319810	6158630	v1	2	amygdaloidal chloritic schist
96GPA-21-5	313882	6186742	v1	1	pillowed chloritic semischist
96PSC-7-9	315726	6174187	v1	3	chloritic greenstone; possible pillows
96PSC-7-11	315835	6174040	v1	1	greenstone; possible pillows
96PSC-15-14	320165	6172334	v1	1	epidote-chlorite semischist; pillows
97NMA-8-14	321280	6144558	v1	2	massive feldspar-phyric greenstone
97NMA-14-1-4	326233	6131109	v1	3	pillowed chlorite schist
97NMA-14-7-2	325314	6132537	v1	2	weakly foliated pyroxene-phyric metabasalt
97NMA-17-4	324212	6136182	v2	2	massive pyroxene (?) feldspar phyric metabasalt
97NMA-23-16	326557	6113236	v1	2	massive feldspar-phyric greenstone; up to 50% 1–2 mm phenocrysts
97NMA-24-8-1	321719	6140425	v2	3	aphyric weakly foliated greenstone; hints of pillows
97NMA-28-4-2	318304	6146063	v2	3	massive feldspar basalt
PSC95-16-9-3	318986	6174937	v2	1	massive pyritic metavolcanic; pillows
PSC95-17-7-2	321478	6172109	v2	1	chlorite schist with relict feldspar and mafic phenocrysts
PSC95-17-11	320711	6171937	v1	1	calcite-epidote-chlorite schist; hints of pillows
PSC95-18-6-1	319514	6175597	v1	1	pillowed metabasalt
PSC95-22-3	320530	6176518	v2	1	pillowed calcite-epidote-chlorite schist
96PSC-15-15-3	320005	6172450	v1	f1	massive quartz porphyry; grades to sericite-quartz semischist; dike?
96PSC-18-17	315627	6184358	v2	f1	feldspar-phyric siliceous semischist; thick flow or sill
96PSC-28-1-1	322188	6163803	v2	f1	fragmental felsic semischist with quartz, feldspar and felsic lithic fragments
96PSC-31-8	321569	6166314	v2	f1	quartz-feldspar-phyric semischist
97NMA-25-6-2	319790	6143795	v2	f2	quartz-feldspar crystal tuff
97PSC-22-2	320395	6176435	v2	f1	flow-banded quartz-feldspar-phyric rhyolite
PSC95-22-2	320459	6176430	v2	f1	chlorite-sericite-quartz semischist; rare tiny feldspar phenocrysts
96PSC-12-1	319072	6154388	M	d	epidote-chlorite-feldspar semischist (metadiorite)
96PSC-12-3-1	317636	6154515	M	d	epidote-chlorite-feldspar semischist (metadiorite)
97PSC-2-3-1	319393	6152476	M	t	medium-grained, weakly foliated, chlorite-epidote–altered tonalite
97PSC-2-6	319923	6153763	M	t	medium-grained, massive, chlorite-epidote–altered tonalite
97NMA-30-2	317864	6153531	M	d	chlorite-feldspar semischist (metadiorite)
PSC95-16-1-1	316835	6174320	D	t	quartz-phyric tonalite
PSC95-16-1-2	316835	6174320	D	t	quartz-feldspar porphyry; more mafic, older phase than 16-1-1
PSC95-16-2	316686	6174143	D	t	crowded feldspar porphyry
PSC95-16-4	316721	6173971	D	t	medium-grained tonalite

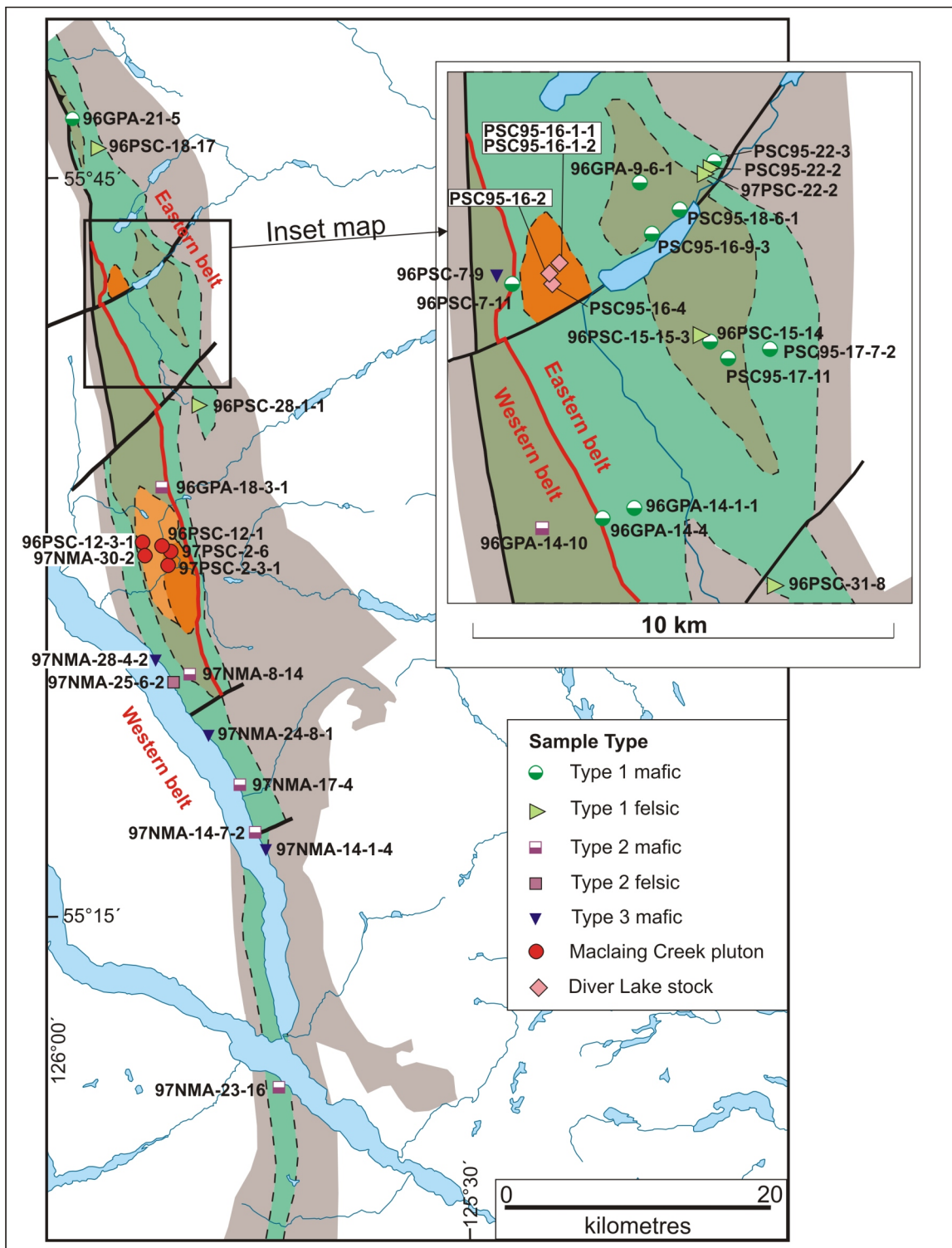


Figure 3. Locations of samples listed in Table 1. See Figure 1 for legend.

divide between the two belts. There is little lithological difference between mafic volcanic rocks in the two belts, although relict pyroxene phenocrysts are more common, and locally very abundant, within western belt basalt.

Type 1 volcanic rocks are a subalkaline, bimodal basalt and rhyolite series (Figures 4a, c). Rare earth element (REE) patterns are mid-ocean-ridge basalt (MORB)-like

light rare earth element (LREE)-depleted for mafic rocks (Figure 5a) and flat for felsic rocks (Figure 5d). Similar MORB characteristics are seen for both mafic and felsic rocks in the various tectonic discrimination diagrams (Figures 6–8).

Type 2 volcanic rocks are subalkaline, basalt to dacite (Figures 4b, d). Rare earth element patterns show a moder-

Table 2. Whole-rock chemical analyses for Sitlika volcanic rocks of the eastern belt. Dashes indicate element determinations below detection limit; blank values indicate elements not analyzed. Abbreviation: LOI, loss-on-ignition.

Sample	Units	Mafic intermediate										Felsic						
		PSC95-16-9-3	PSC95-17-7-2	PSC95-17-11	PSC95-18-6-1	PSC95-22-3	96PSC-7-11	96PSC-15-14	96GPA-9-6-1	96GPA-14-1-1	96GPA-14-4	96GPA-21-5	97PSC-22-2	PSC95-22-2	96PSC-31-8	96PSC-18-17	96PSC-28-1-1	96PSC-15-3
SiO ₂	%	49.00	62.09	46.98	49.89	43.91	47.90	49.38	50.77	47.05	49.13	49.63	83.12	74.14	72.90	73.98	76.62	82.16
TiO ₂	%	2.17	1.38	1.53	1.42	1.35	1.29	1.58	1.58	1.35	1.51	1.40	0.09	0.12	0.50	0.56	0.35	0.21
Al ₂ O ₃	%	16.40	15.02	16.15	15.64	17.13	16.59	17.34	14.65	15.00	17.02	18.86	9.48	14.68	13.63	13.32	11.42	7.48
Fe ₂ O ₃ ^t	%	12.62	8.18	12.36	13.91	11.78	8.66	10.34	14.47	9.79	13.16	9.79	0.81	1.29	4.09	3.23	3.16	2.30
MnO	%	0.19	0.17	0.19	0.22	0.18	0.13	0.20	0.23	0.19	0.22	0.14	0.02	0.04	0.08	0.07	0.06	0.06
MgO	%	4.79	2.53	5.04	4.92	6.84	8.80	6.29	6.39	9.23	3.99	5.05	0.29	0.35	1.19	0.26	0.86	0.49
CaO	%	5.08	2.68	9.05	7.70	7.89	11.78	7.04	4.45	13.17	8.94	7.09	0.09	0.31	0.44	0.50	0.82	5.08
Na ₂ O	%	5.38	7.23	4.24	4.38	4.20	2.97	5.01	5.76	1.95	3.95	5.03	4.68	7.05	6.18	7.13	5.31	0.67
K ₂ O	%	0.04	0.18	0.07	0.12	0.22	0.20	0.10	0.08	0.04	0.16	0.47	0.73	1.28	0.20	0.37	0.37	0.17
P ₂ O ₅	%	0.24	0.20	0.28	0.14	0.18	0.08	0.22	0.17	0.09	0.21	0.28	0.01	0.02	0.09	0.12	0.06	0.02
LOI	%	3.85	0.98	4.70	2.56	6.68	2.17	3.12	2.25	2.82	2.50	3.00	0.42	0.82	1.19	0.75	1.18	1.51
Total	%	99.76	100.64	100.59	100.90	100.36	100.58	100.61	100.80	100.68	100.78	100.74	99.74	100.10	100.49	100.29	100.21	100.15
Rb	ppm	-	1	-	-	3	3	1	-	1	2	6	5	9	1	2	3	1
Sr	ppm	106	74	133	125	74	212	194	38	257	94	71	22	26	28	48	31	41
Ba	ppm	191	132	135	138	119	125	139	129	100	158	198	80	125	63	87	78	77
Y	ppm	44	53	38	37	28	26	40	27	26	30	28	48	86	51	53	51	57
Zr	ppm	121	268	110	107	75	76	146	73	99	87	71	155	234	220	331	183	242
Nb	ppm	4	4	3	3	4	2	4	3	2	4	4	8	8	4	4	4	3
V	ppm	402	164	253	391	288	221	227	368	192	326	302	-	-	38	20	32	13
Cr	ppm	66	-	217	-	271	436	288	62	553	31	320	-	-	-	19	-	-
Ni	ppm	11	-	45	3	62	169	137	17	254	5	37	-	9	5	-	3	-
Cu	ppm	46	12	27	53	89	30	45	63	13	48	13	12	23	31	14	29	6
Zn	ppm	136	111	118	126	124	85	118	158	96	139	121	24	60	75	106	89	85
Hf	ppm				2.9		2.240	3.703	2.000			2.043				7.374	4.362	
Ta	ppm				0.3		1.054	1.214	1.257			1.252				4.486	5.120	
Th	ppm						0.089	0.247	0.226			0.152				1.320	1.020	
La	ppm				4.3		1.944	5.975	2.637			3.967				10.662	8.154	
Ce	ppm				1.0		7.443	19.316	8.962			11.606				29.756	21.658	
Pr	ppm						1.423	3.291	1.617			1.968				4.369	3.256	
Nd	ppm				16.0		8.069	16.534	8.819			10.496				20.920	15.524	
Sm	ppm				3.6		2.985	5.061	3.111			3.471				6.418	4.816	
Eu	ppm				1.4		1.083	1.752	1.093			1.380				1.496	1.084	
Gd	ppm						3.817	6.443	3.930			4.534				7.497	6.100	
Tb	ppm				0.9		0.645	1.091	0.672			0.783				1.260	1.045	
Dy	ppm						4.205	7.062	4.507			4.906				8.548	7.262	
Ho	ppm						0.839	1.463	0.932			1.040				1.866	1.661	
Er	ppm						2.565	4.470	2.770			3.129				5.631	5.365	
Tm	ppm						0.333	0.629	0.394			0.423				0.845	0.804	
Yb	ppm				3.6		2.218	4.190	2.546			2.508				5.924	5.584	
Lu	ppm				0.5		0.329	0.656	0.372			0.390				0.965	0.855	

Table 3. Whole-rock chemical analyses for Sitlika volcanic rocks of the western belt. Dashes indicate element determinations below detection limit; blank values indicate elements not analyzed. Abbreviation: LOI, loss-on-ignition.

Sample	Units	Type 2 mafic - intermediate						Type 2	Type 3 mafic			
		97NMA- 8-14	96GPA- 14-10	96GPA- 18-3-1	97NMA- 14-7-2	97NMA- 17-4	97NMA- 23-16	97NMA- 25-6-2	97NMA- 24-8-1	97NMA- 28-4-2	97NMA- 14-1-4	96PSC- 7-9
SiO ₂	%	56.53	63.80	46.94	51.89	48.60	48.66	66.00	46.51	51.70	40.41	47.08
TiO ₂	%	0.84	0.55	1.08	0.71	1.01	0.75	0.48	2.31	1.04	1.97	2.29
Al ₂ O ₃	%	17.08	16.97	18.81	14.11	18.03	22.02	15.37	17.50	19.14	15.45	16.81
Fe ₂ O ₃ ^t	%	7.66	5.69	11.92	10.02	9.46	8.56	4.21	9.08	8.21	8.52	9.29
MnO	%	0.17	0.10	0.16	0.17	0.16	0.19	0.09	0.15	0.16	0.15	0.14
MgO	%	4.23	1.69	6.84	6.91	6.68	3.88	1.37	8.75	3.15	3.60	7.87
CaO	%	6.20	3.53	4.85	8.74	10.86	9.48	4.36	5.69	8.81	14.27	10.32
Na ₂ O	%	5.20	5.80	4.16	3.14	2.32	3.54	3.32	4.10	3.14	4.18	3.36
K ₂ O	%	0.36	0.61	1.24	1.27	0.04	0.39	1.91	0.91	0.83	1.01	0.36
P ₂ O ₅	%	0.12	0.12	0.17	0.36	0.15	0.12	0.10	0.50	0.22	0.45	0.31
LOI	%	2.20	1.55	4.52	2.67	3.66	3.22	2.96	4.77	3.70	9.79	2.83
Total	%	100.59	100.40	100.70	99.99	100.97	100.81	100.24	100.27	100.10	99.80	100.66
Rb	ppm	6	10	17	25	3	7	33	11	13	18	5
Sr	ppm	173	106	151	283	480	416	265	179	344	276	164
Ba	ppm	102	178	239	358	-	248	506	200	283	157	297
Y	ppm	30	22	21	23	23	20	19	31	24	28	38
Zr	ppm	114	100	46	70	71	51	119	259	135	214	233
Nb	ppm	6	6	4	4	7	4	7	25	13	28	6
V	ppm	161	111	263	225	273	197	79	220	180	212	248
Cr	ppm	105	24	285	337	143	17	22	188	29	259	222
Ni	ppm	18	6	42	64	19	7	4	72	6	135	100
Cu	ppm	93	22	52	338	25	197	32	53	71	40	9
Zn	ppm	67	69	124	64	68	91	39	68	67	58	75
Hf	ppm				2.152		1.374	2.707	5.015		4.224	
Ta	ppm				0.153		0.182	0.511	1.587		1.807	
Th	ppm				1.333		0.424	2.266	1.422		2.137	
La	ppm				9.200		4.476	9.088	20.290		15.952	
Ce	ppm				20.205		10.473	18.423	46.763		34.939	
Pr	ppm				2.756		1.490	2.206	5.907		4.445	
Nd	ppm				12.547		7.349	8.798	24.724		18.916	
Sm	ppm				2.987		2.028	1.952	5.155		4.349	
Eu	ppm				0.895		0.809	0.701	1.726		1.463	
Gd	ppm				3.405		2.615	2.240	5.536		4.274	
Tb	ppm				0.494		0.419	0.346	0.791		0.669	
Dy	ppm				3.121		2.740	2.271	4.726		4.126	
Ho	ppm				0.696		0.615	0.515	0.993		0.945	
Er	ppm				2.183		1.931	1.638	2.934		2.916	
Tm	ppm				0.300		0.259	0.235	0.379		0.392	
Yb	ppm				1.898		1.665	1.600	2.319		2.465	
Lu	ppm				0.283		0.239	0.241	0.336		0.332	

Table 4. Whole-rock chemical analyses for intrusive rocks from the Diver Lake stock and the Maclaing Creek pluton. Dashes indicate element determinations below detection limit; blank values indicate elements not analyzed. Abbreviation: LOI, loss-on-ignition.

Sample	Units	Maclaing Creek pluton					Diver Lake stock			
		96PSC-12-1	96PSC-12-3-1	97PSC-2-3-1	97PSC-2-6	97NMA-30-2	PSC95-16-1-1	PSC95-16-1-2	PSC95-16-2	PSC95-16-4
SiO ₂	%	60.68	54.58	61.81	67.91	53.42	74.47	66.42	48.53	74.43
TiO ₂	%	0.72	1.00	0.68	0.42	1.05	0.30	0.65	1.81	0.31
Al ₂ O ₃	%	16.60	16.59	16.34	15.60	16.37	13.45	16.01	14.64	13.92
Fe ₂ O ₃ ^t	%	5.75	9.04	5.54	3.80	9.26	2.55	4.72	15.65	2.09
MnO	%	0.08	0.16	0.09	0.07	0.18	0.05	0.11	0.24	0.03
MgO	%	2.59	3.62	2.74	1.34	3.60	0.65	1.35	5.56	0.71
CaO	%	6.59	6.96	5.30	4.43	5.18	1.95	3.66	6.37	2.45
Na ₂ O	%	4.99	4.55	4.32	4.22	4.98	5.09	5.56	3.79	5.16
K ₂ O	%	0.25	0.18	1.17	0.45	0.49	0.69	0.30	0.45	0.62
P ₂ O ₅	%	0.15	0.18	0.13	0.09	0.16	0.06	0.18	0.11	0.06
LOI	%	1.93	3.72	1.85	1.45	5.81	0.99	1.34	3.42	0.87
Total	%	100.32	100.57	99.97	99.78	100.50	100.25	100.30	100.57	100.65
Rb	ppm	5	4	20	7	10	9	3	6	5
Sr	ppm	146	266	161	256	149	133	200	119	111
Ba	ppm	110	69	360	702	169	181	170	257	258
Y	ppm	33	33	30	19	34	27	40	31	29
Zr	ppm	156	104	130	135	106	139	131	47	127
Nb	ppm	6	5	7	7	5	4	4	3	4
V	ppm	108	184	115	63	209	25	56	490	27
Cr	ppm	28	63	72	25	23	-	-	35	-
Ni	ppm	10	14	15	7	7	-	-	-	-
Cu	ppm	21	76	33	26	104	5	4	32	4
Zn	ppm	17	61	27	7	92	57	60	117	43
Hf	ppm									4.5
Ta	ppm									1.6
La	ppm									5.8
Ce	ppm									1.0
Nd	ppm									16.0
Sm	ppm									2.3
Eu	ppm									0.9
Tb	ppm									0.6
Yb	ppm									3.1
Lu	ppm									0.5

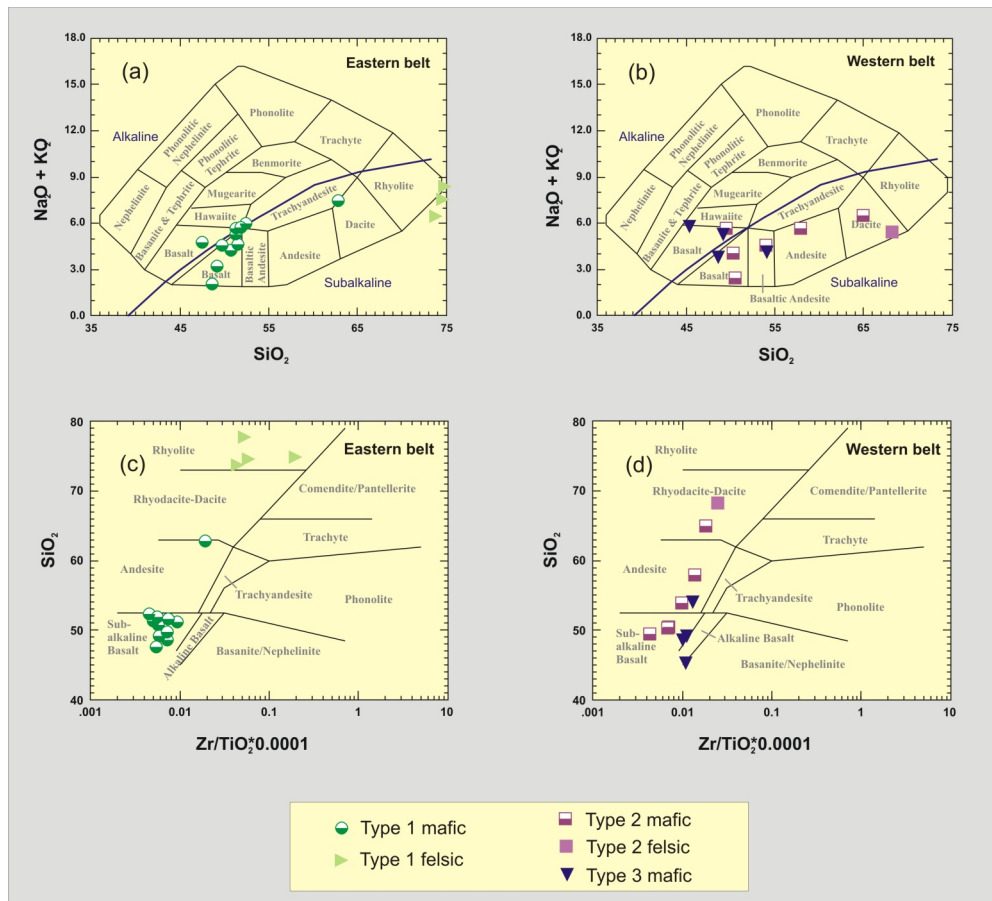


Figure 4. Geochemical classification of Sitlika volcanic rocks from the eastern and western belts: **a)** and **b)** alkali-silica diagrams, fields after Cox et al. (1979), with alkaline-subalkaline dividing line after Irvine and Baragar (1971); **c)** and **d)** silica versus zirconium-titania ratio, fields after Winchester and Floyd (1977).

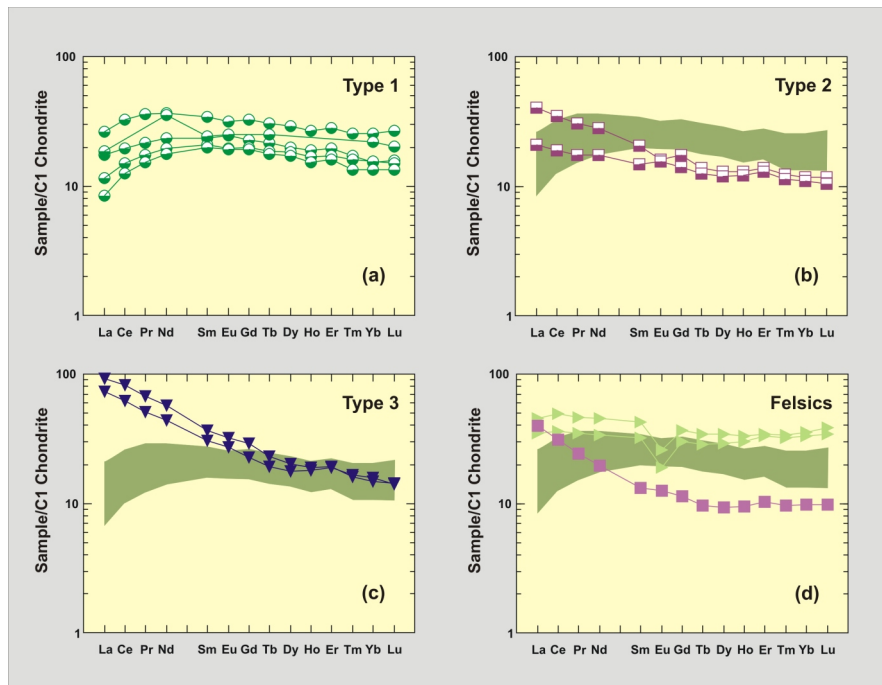


Figure 5. Rare earth element plots for Sitlika volcanic rocks. Normalizing values from Sun and McDonough (1989). Type 1 basalt in a) is repeated as the shaded area in b)–d) for reference. Symbols as in Figure 4.

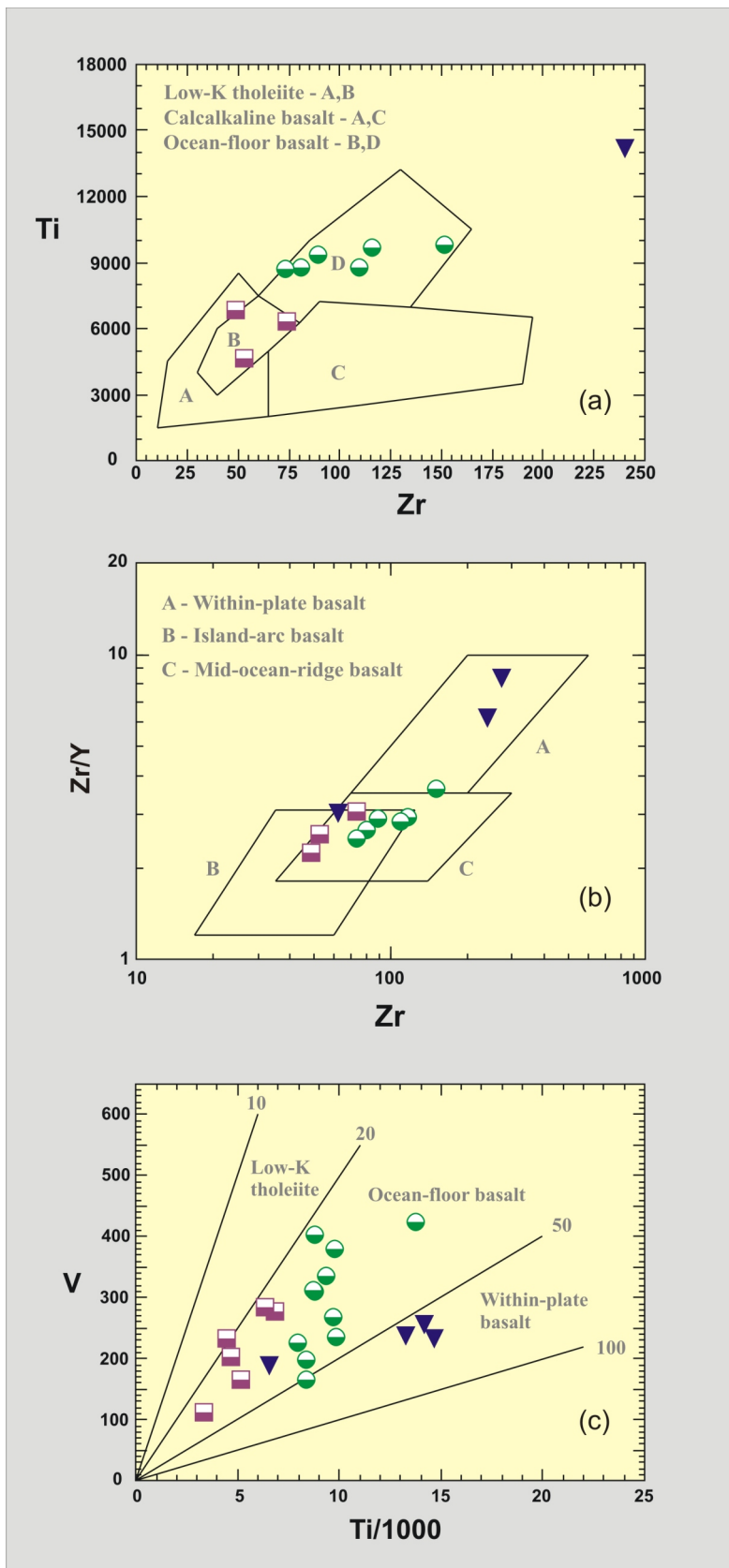


Figure 6. Tectonic discrimination diagrams for Sitlika basalts: **a)** Ti-Zr diagram, fields after Pearce and Cann (1973); **b)** Zr/Y-Zr diagram, fields after Pearce and Norry (1979); **c)** Ti-V diagram, fields after Shervais (1982). Symbols as in Figure 4.

ate LREE enrichment for both mafic and felsic rocks (Figures 5b, d). Heavy rare earth elements (HREE) have lower concentrations than in type 1 basalt. An oceanic-arc signature is apparent in the various tectonic discrimination diagrams (Figures 6–8).

Type 3 volcanic rocks are alkaline in character (Figures 4b, d). Only mafic rocks have been analyzed and it is unclear if felsic members are present. Rare earth element patterns in these rocks show much more LREE enrichment than in type 2 samples, and HREE have higher concentrations than in type 2 samples, comparable to those in type 1 basalt (Figure 5c). A within-plate character is suggested by discrimination diagrams (Figures 6, 7).

Intrusive rocks from the Diver Lake stock and the Maclaing Creek pluton are calcalkaline intermediate to felsic (Figure 9). They plot in the volcanic-arc field on discrimination diagrams (Figure 8) and are similar to the type 2 felsic volcanic sample. They are inferred to be related to the type 2 volcanic rocks, although the Diver Lake stock is located in the eastern belt (but at its western edge).

DISCUSSION

The volcanic rocks of the Sitlika assemblage have an oceanic signature. The western belt includes mafic and felsic rocks with a volcanic-arc signature, but also includes alkaline basalt of within-plate character. Intrusive rocks of the Maclaing Creek pluton and Diver Lake stock have a volcanic-arc signature, consistent with their location within and along the margin of the western belt. In contrast, volcanic rocks in the eastern belt have MORB characteristics. They may have formed in a back-arc setting, behind the western belt arc.

Comparison to the Kutcho Assemblage

The Sitlika volcanic unit is reasonably correlated with the Kutcho assemblage (Childe and Thompson, 1997) on the basis of general mafic to felsic volcanic character, the presence of associated tonalitic intrusive units, the age of the volcanic and intrusive units, comparable primitive Nd-isotopic signatures, and structural and tectonic setting (Monger et al., 1978; Childe et al., 1998). Although they both represent intraoceanic arc systems (and probably parts of the same system), there are distinctions between volcanic rocks of the Kutcho assemblage, as represented by analyses presented by Barrett et al. (1996) and Childe et al. (1998), and the Sitlika volcanic unit. Kutcho volcanic rocks are tholeiitic, with characteristics of low-K island-arc basalt. Contents of the immobile

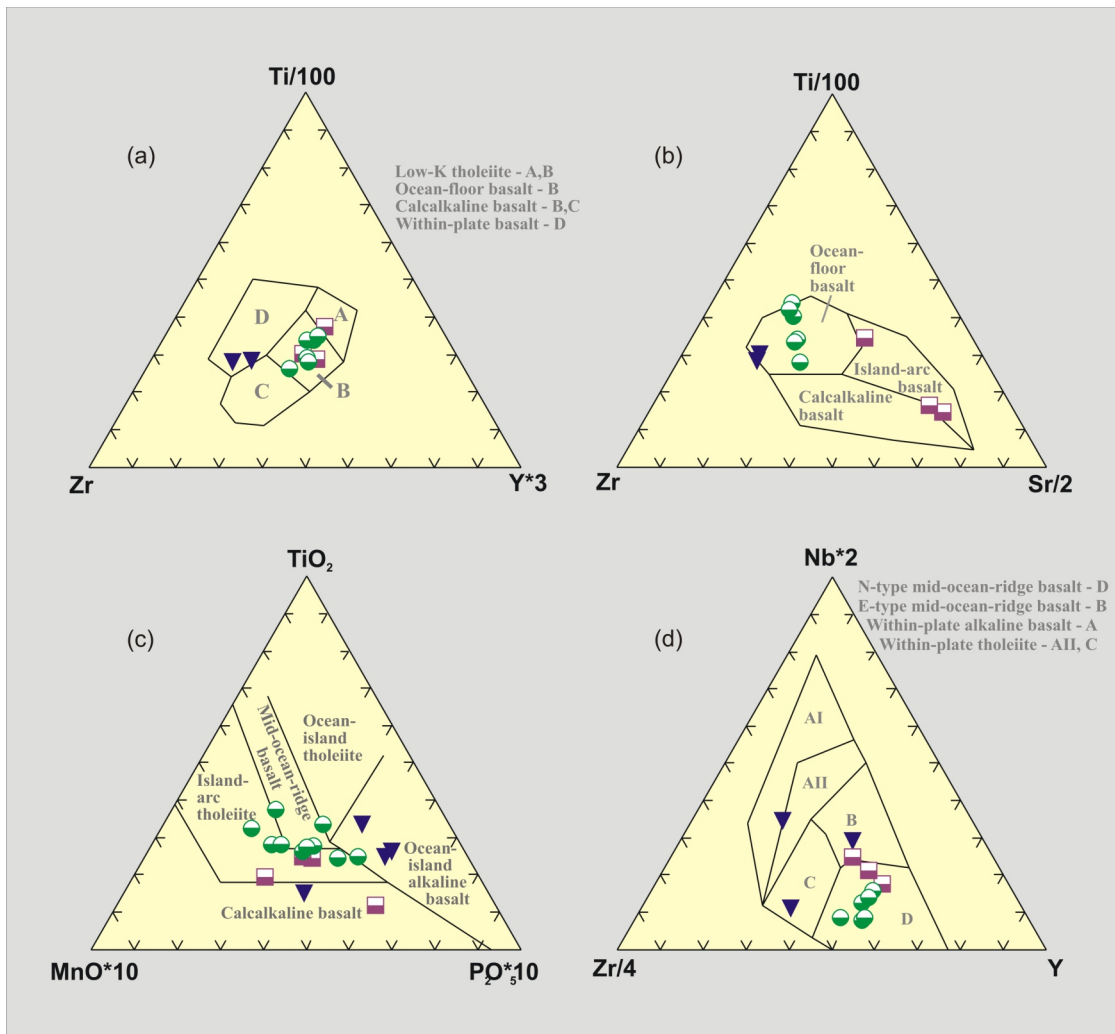


Figure 7. Triangular tectonic discrimination diagrams for Sitlika basalts: **a)** Ti-Zr-Y diagram, fields after Pearce and Cann (1973); **b)** Ti-Zr-Sr diagram, fields after Pearce and Cann (1973). **c)** Ti-Mn-P diagram, fields after Mullen (1983). **d)** Nb-Zr-Y diagram, fields after Meschede (1986). Symbols as in Figure 4.

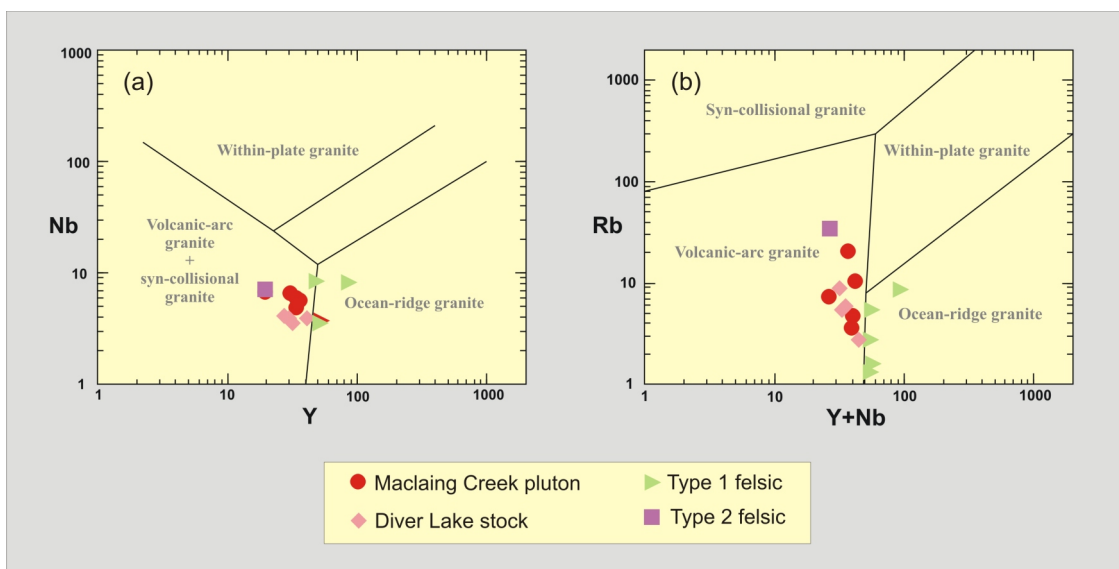


Figure 8. Tectonic discrimination diagrams for Sitlika intrusive and felsic volcanic rocks: **a)** Nb-Y tectonic discrimination diagram, fields after Pearce et al. (1984); **b)** Rb-(Y+Nb) tectonic discrimination diagram, fields after Pearce et al. (1984).

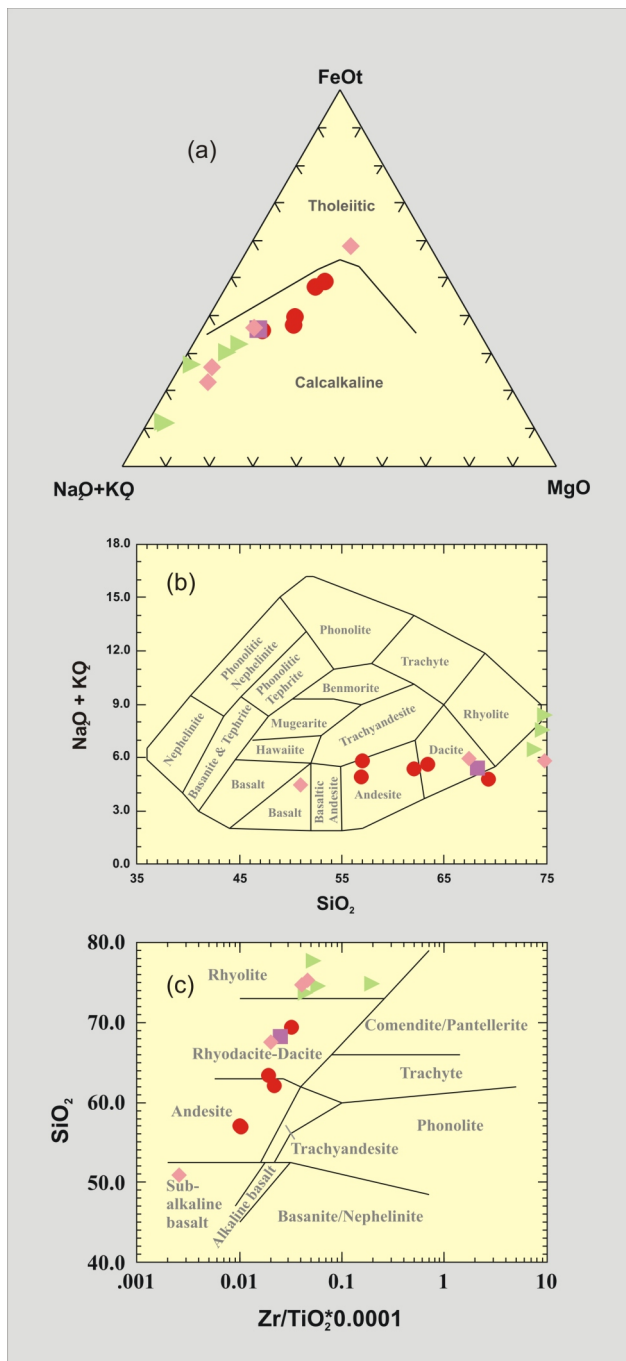


Figure 9. Geochemical classification of rocks from the Maclaing Creek pluton and the Diver Lake stock, with Sitlika felsic volcanic rocks included for comparison: **a)** AFM triangle diagram, tholeiitic-calcalkaline divide after Irvine and Baragar (1971); **b)** alkali-silica diagram, fields after Cox et al. (1979); **c)** silica versus zirconium-titanium ratio, fields after Winchester and Floyd (1977). Symbols as in Figure 8.

high-field strength elements, such as Zr and Y, and the rare-earth elements, are significantly lower in the Kutcho basalt than in the Sitlika lavas, even the similarly LREE-depleted type 1 flows. The LREE-enriched patterns of types 2 and 3 Sitlika flows are not reported from the Kutcho area. However, gabbro intrusions within the Kutcho assemblage are

calcalkaline in character, with REE patterns showing moderate LREE enrichment very similar to that of the Sitlika type 2 volcanic rocks.

ACKNOWLEDGMENTS

We thank the many people who contributed to our work in the Sitlika belt, and in particular Don MacIntyre, Bert Struik, Fiona Childe, Mike Villeneuve, Mike Orchard, Fabrice Cordey and Garry Payie.

REFERENCES

- Armstrong, J.E. (1949): Fort St. James Map-Area, Cassiar and Coast Districts, British Columbia; *Geological Survey of Canada*, Memoir 252, 210 pages.
- Barrett, T.J., Thompson, J.F.H. and Sherlock, R.L. (1996): Stratigraphic, lithogeochemical and tectonic setting of the Kutcho Creek massive sulphide deposit, northern British Columbia; *Exploration and Mining Geology*, Volume 5, pages 309–338.
- Childe, F.C. and Schiarizza, P. (1997): U-Pb geochronology, geochemistry and Nd isotopic systematics of the Sitlika assemblage, central British Columbia; in *Geological Fieldwork 1996, BC Ministry of Energy, Mines and Petroleum Resources*, Paper 1997-1, pages 69–77.
- Childe, F.C. and Thompson, J.F.H. (1997): Geological setting, U-Pb geochronology, and radiogenic isotopic characteristics of the Permo-Triassic Kutcho assemblage, north-central British Columbia; *Canadian Journal of Earth Sciences*, Volume 34, pages 1310–1324.
- Childe, F.C., Thompson, J.F.H., Mortensen, J.K., Friedman, R.M., Schiarizza, P., Bellefontaine, K. and Marr, J.M. (1998): Primitive Permo-Triassic volcanism in the Canadian Cordillera: tectonic and metallogenic implications; *Economic Geology*, Volume 93, pages 224–231.
- Cox, K.G., Bell, J.D. and Pankhurst, R.J. (1979): The Interpretation of Igneous Rocks; *G. Allen and Unwin*, London, 450 pages.
- Irvine, T.N. and Baragar, W.R.A. (1971): A guide to the chemical classification of the common volcanic rocks; *Canadian Journal of Earth Sciences*, Volume 8, pages 523–548.
- MacIntyre, D.M. and Schiarizza, P. (1999): Bedrock geology, Cunningham Lake (93K/11, 12, 13, 14); *BC Ministry of Energy, Mines and Petroleum Resources*, Open File 1999-11, 1:100 000 scale.
- MacIntyre, D.G., Villeneuve, M.E. and Schiarizza, P. (2001): Timing and tectonic setting of Stikine terrane magmatism, Babine-Takla lakes area, central British Columbia; *Canadian Journal of Earth Sciences*, Volume 38, pages 579–601.
- Meschede, M. (1986): A method of discriminating between different types of mid-ocean ridge basalts and continental tholeiites with the Nb-Zr-Y diagram; *Chemical Geology*, Volume 56, pages 207–218.
- Mihalynuk, M.G., Friedman, R.M. and Ullrich, T.D. (2008): Geochronological results from reconnaissance investigations in the beetle infested zone, south-central British Columbia; in *Geological Fieldwork 2007, BC Ministry of Energy, Mines and Petroleum Resources*, Paper 2008-1, pages 135–145.
- Monger, J.W.H. (1977): The Triassic Takla Group in McConnell Creek map-area, north-central British Columbia; *Geological Survey of Canada*, Paper 76-29, 45 pages.
- Monger, J.W.H., Richards, T.A. and Paterson, I.A. (1978): The hinterland belt of the Canadian Cordillera: new data from northern and central British Columbia; *Canadian Journal of Earth Sciences*, Volume 15, pages 823–830.

- Mullen, E.D. (1983): MnO/TiO₂/P₂O₅: a minor element discriminant for basaltic rocks of oceanic environments and its implications for petrogenesis; *Earth and Planetary Science Letters*, Volume 62, pages 53–62.
- Paterson, I.A. (1974): Geology of Cache Creek Group and Mesozoic rocks at the northern end of the Stuart Lake belt, central British Columbia; in Report of Activities, *Geological Survey of Canada*, Paper 74-1, Part B, pages 31–42.
- Pearce, J.A. and Cann, J.R. (1973): Tectonic setting of basic volcanic rocks determined using trace element analyses; *Earth and Planetary Science Letters*, Volume 19, pages 290–300.
- Pearce, J.A. and Norry, M.J. (1979): Petrogenetic implications of Ti, Zr, Y, and Nb variations in volcanic rocks; *Contributions to Mineralogy and Petrology*, Volume 69, pages 33–47.
- Pearce, J.A., Harris, N.B.W. and Tindle, A.G. (1984): Trace element discrimination diagrams for the tectonic interpretation of granitic rocks; *Journal of Petrology*, Volume 25, pages 956–983.
- Richards, T.A. (1990): Geology of Hazelton map area (93M); *Geological Survey of Canada*, Open File 2322, 1:250 000 scale.
- Schiarizza, P. (2000): Bedrock geology, Old Hogem (western part) (93N/11, 12, 13); *BC Ministry of Energy, Mines and Petroleum Resources*, Open File 2000-33, 1:100 000 scale.
- Schiarizza, P. and MacIntyre, D. (1999): Geology of the Babine Lake–Takla Lake area, central British Columbia (93K/11, 12, 13, 14; 93N/3, 4, 5, 6); in Geological Fieldwork 1998, *BC Ministry of Energy, Mines and Petroleum Resources*, Paper 1999-1, pages 33–68.
- Schiarizza, P. and Massey, N. (2000): Volcanic facies and geochemistry of the Sitlika assemblage, central British Columbia: part of a primitive intra-oceanic arc in western Cache Creek terrane; *Geological Society of America*, 96th Annual Meeting, Cordilleran Section, Vancouver, BC, Abstracts with Programs, page A-66.
- Schiarizza, P. and Payie, G. (1997): Geology of the Sitlika assemblage in the Kenny Creek – Mount Olson area (93N/12, 13), central British Columbia; in Geological Fieldwork 1996, *BC Ministry of Energy, Mines and Petroleum Resources*, Paper 1997-1, pages 79–100.
- Schiarizza, P., Massey, N. and MacIntyre, D. (1998): Geology of the Sitlika assemblage in the Takla Lake area (93N/3, 4, 5, 6, 12), central British Columbia; in Geological Fieldwork 1997, *BC Ministry of Energy, Mines and Petroleum Resources*, Paper 1998-1, pages 4-1–4-19.
- Schiarizza, P., Massey, N. and MacIntyre, D.M. (2000): Bedrock geology, Tsayta Lake (93N/3, 4, 5, 6); *BC Ministry of Energy, Mines and Petroleum Resources*, Open File 2000-19, 1:100 000 scale.
- Shervais, J.W. (1982): Ti-V plots and the petrogenesis of modern and ophiolitic lavas; *Earth and Planetary Science Letters*, Volume 59, pages 101–118.
- Struik, L.C., MacIntyre, D.G. and Williams, S.P. (2007): Nechako NATMAP project: a digital suite of geoscience information for central British Columbia (NTS map sheets 093N, 093K, 093F, 093G/W, 093L/9, 16, and 093M/1, 2, 7, 8); *BC Ministry of Energy, Mines and Petroleum Resources*, Open File 2007-10 and *Geological Survey of Canada*, Open File 5623, CD-ROM.
- Struik, L.C., Schiarizza, P., Orchard, M.J., Cordey, F., Sano, H., MacIntyre, D.G., Lapierre, H. and Tardy, M. (2001): Imbricate architecture of the upper Paleozoic to Jurassic oceanic Cache Creek Terrane, central British Columbia; *Canadian Journal of Earth Sciences*, Volume 38, pages 495–514.
- Sun, S.S. and McDonough, W.F. (1989): Chemical and isotopic systematics of oceanic basalts: implications for mantle composition and processes; in *Magmatism in the Ocean Basins*, *Geological Society of London*, Special Publication 42, pages 313–345.
- Winchester, J.A. and Floyd, P.A. (1977): Geochemical discrimination of different magma series and their differentiation products using immobile elements; *Chemical Geology*, Volume 20, pages 325–343.

Carbonate-Hosted Lead-Zinc Mineralization on the Cariboo Zinc Property, Quesnel Lake Area, East-Central British Columbia (NTS 093A/14E, 15W)

by S. Paradis^{1,3}, G.J. Simandl^{2,3}, J. Bradford⁴, C. Leslie⁵ and C. Brett⁶

KEYWORDS: Cariboo terrane, carbonate-hosted, non-sulphide, oxide, vein, breccia, sphalerite, galena, cerussite, smithsonite, hemimorphite

INTRODUCTION

The carbonate-hosted sulphide and nonsulphide deposits on the Cariboo Zinc property are located north of Quesnel Lake in east-central British Columbia (NTS 93A/14E, 15W), at a latitude of approximately 52°49'N and longitude 120°55'W (Figure 1). They are hosted by rocks of the Cariboo terrane, which represents a displaced segment of the ancestral North American margin (Struik, 1988). The Cariboo terrane is known to host a wide variety of metallic deposits, including polymetallic Ag-Pb-Zn (\pm Au) veins, carbonate- and sediment-hosted massive sulphides (i.e., Zn-Pb Mississippi Valley type, sedimentary exhalative Zn-Pb-Ag Besshi type), Au placers and nonsulphide deposits (Struik, 1988; Höy and Ferri, 1998).

Individual carbonate-hosted Pb-Zn occurrences on the Cariboo Zinc property crop out along a northwest-trending belt about 8 km long. They comprise pervasive fine-grained sulphide and nonsulphide disseminations and aggregates forming pods, sulphide- and nonsulphide-bearing quartz veins, and crackle breccias similar to those found in Mississippi Valley-type deposits. This paper, based on our 2009 field observations and previous work by Teck Corporation and Pembroke Mining Corporation, provides a basis for ongoing laboratory investigations of sulphide and nonsulphide minerals from the Cariboo Zinc deposits. It also contributes to a better understanding of geological constraints on nonsulphide deposits of southern BC.

BACKGROUND INFORMATION ON NONSULPHIDE DEPOSITS

Nonsulphide deposits were the main source of Zn prior to the 1930s. However, the mining industry turned its atten-

tion to sulphide ore following the development of differential flotation and breakthroughs in smelting technology. Today, most Zn derives from sulphide ore (Hitzman et al., 2003; Simandl and Paradis, 2009). Nevertheless, the successful operation of a dedicated processing plant to extract Zn metal at the Skorpion mine in Namibia demonstrates that deposits containing nonsulphide and mixed Zn-Pb ores represent valid exploration targets.

Carbonate-hosted, nonsulphide base-metal deposits form in supergene environments from sulphide deposits (such as Mississippi Valley-type [MVT], sedimentary exhalative [SEDEX], Irish-type and vein-type deposits and, to a lesser extent, skarns). Several carbonate-hosted sulphide deposits in the Kootenay terrane and elsewhere in BC have near-surface Zn- and Pb-bearing iron-oxide gossans (Simandl and Paradis, 2009; Paradis and Simandl, work in progress, 2010). Such gossans form when carbonate-hosted, base-metal sulphide mineralization is subject to intense weathering and metals are liberated by the oxidation of sulphide minerals. Liberated metals can be trapped locally, forming direct-replacement, nonsulphide ore deposits, or they can be transported by percolating waters down and away from the sulphide protore, forming wallrock-replacement carbonate-hosted nonsulphide base-metal deposits (Heyl and Bozion, 1962; Hitzman et al., 2003; Simandl and Paradis, 2009). The direct-replacement nonsulphide deposits, also known as 'red ores', consist commonly of Fe-oxyhydroxides (red in colour), goethite and hematite, with lesser concentrations of hemimorphite, smithsonite, hydrozincite and cerussite; they typically contain >20% Zn, >7% Fe and Pb \pm As. Wallrock-replacement deposits can be located in proximity to protore or several hundreds of metres away (Heyl and Bozion, 1962; Hitzman et al., 2003; Reichert and Borg, 2008). The wallrock-replacement deposits, also known as 'white ores', consist of smithsonite, hydrozincite and minor Fe-hydroxides, and contain <40% Zn, <7% Fe and very low concentrations of Pb. Wallrock-replacement deposits are commonly rich in Zn and poor in Pb relative to the direct-replacement carbonate-hosted nonsulphide base-metal deposits (Simandl and Paradis, 2009). From the metallurgical and environmental perspectives, the 'white ores' are simpler and preferable.

REGIONAL GEOLOGY

The Cariboo Zinc sulphide and nonsulphide occurrences occur within the Cariboo terrane of central BC (Figure 2). To the east, the Cariboo terrane is in fault contact with the western margin of the North American miogeocline along the Rocky Mountain Trench (Figure 1). To the west, it is in fault contact (along the westerly-verging Pleasant Valley thrust) with rocks of the Barkerville subterrane (Figure 2), which corresponds to a northern extension of the Kootenay terrane. Rocks of the Barkerville

¹ Geological Survey of Canada–Pacific, Sidney, BC

² British Columbia Ministry of Energy, Mines and Petroleum Resources, Victoria, BC

³ School of Earth and Ocean Sciences, University of Victoria, Victoria, BC

⁴ Pembroke Mining Corporation, Vancouver, BC

⁵ Richfield Ventures Corporation, Quesnel, BC

⁶ RebelEX Resources Corporation, Vancouver, BC

This publication is also available, free of charge, as colour digital files in Adobe Acrobat® PDF format from the BC Ministry of Energy, Mines and Petroleum Resources website at <http://www.empr.gov.bc.ca/Mining/Geoscience/PublicationsCatalogue/Fieldwork/Pages/default.aspx>.

subterranean are interpreted as an outboard facies of the North American continental margin (Struik, 1988; Colpron and Price, 1995), whereas rocks of the Cariboo terrane contain facies that suggest a more proximal continental-shelf setting (Struik, 1988; Ferri and O'Brien, 2002; Schiarizza and Ferri, 2003). Rocks of the Cariboo and Barkerville terranes are structurally overlain, across the gently dipping Pundata thrust fault, by Lower Mississippian to Lower Permian basalts and chert of the Antler Formation of the Slide Mountain terrane (Struik, 1988).

The Cariboo terrane comprises thick sequences of Precambrian to Early Mesozoic siliciclastic and carbonate rocks that show similarities with rocks of the North American miogeocline. In the Quesnel Lake area, the Cariboo terrane is represented by the Late Proterozoic Kaza Group, the Late Proterozoic to Late Cambrian Cariboo Group and

the Ordovician to Mississippian Black Stuart Group (Figure 2).

The Cariboo Group includes argillite, slate and phyllite of the Isaac Formation; carbonate of the Cunningham Formation; argillite and phyllite of the Yankee Belle Formation; white quartzite of the Yanks Peak Formation; shale, phyllite and micaceous quartzite of the Midas Formation; carbonate of the Mural Formation; and slate, phyllite and minor limestone of the Dome Creek Formation (Struik, 1988). Sedimentary rocks of the Isaac, Cunningham and Yankee Belle formations correlate with those of the Windermere Supergroup, and the quartzite of the Yanks Peak Formation correlates with that of the Hamill Group in southern BC (Struik, 1988). The archaeocyathid-bearing carbonate of the Mural Formation is biostratigraphically correlative with the Badshot Formation of the

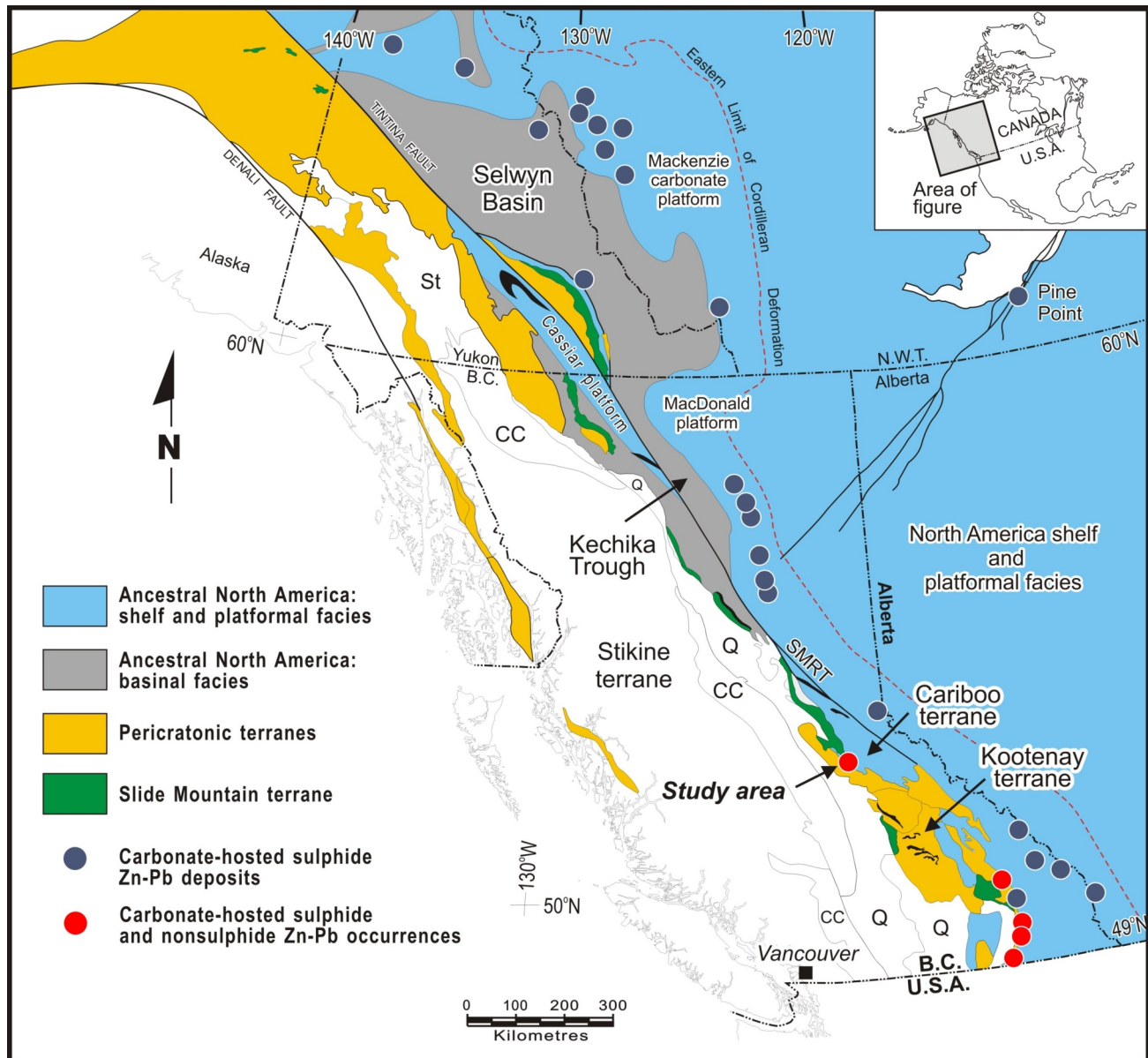


Figure 1. Location of the Cariboo Zinc property study area with respect to other significant carbonate-hosted sulphide and nonsulphide occurrences in the northern cordillera (modified from Nelson et al., 2002, 2006). Abbreviations: St, Stikine terrane; CC, Cache Creek terrane; Q, Quesnel terrane; SRMT, southern Rocky Mountain Trench.

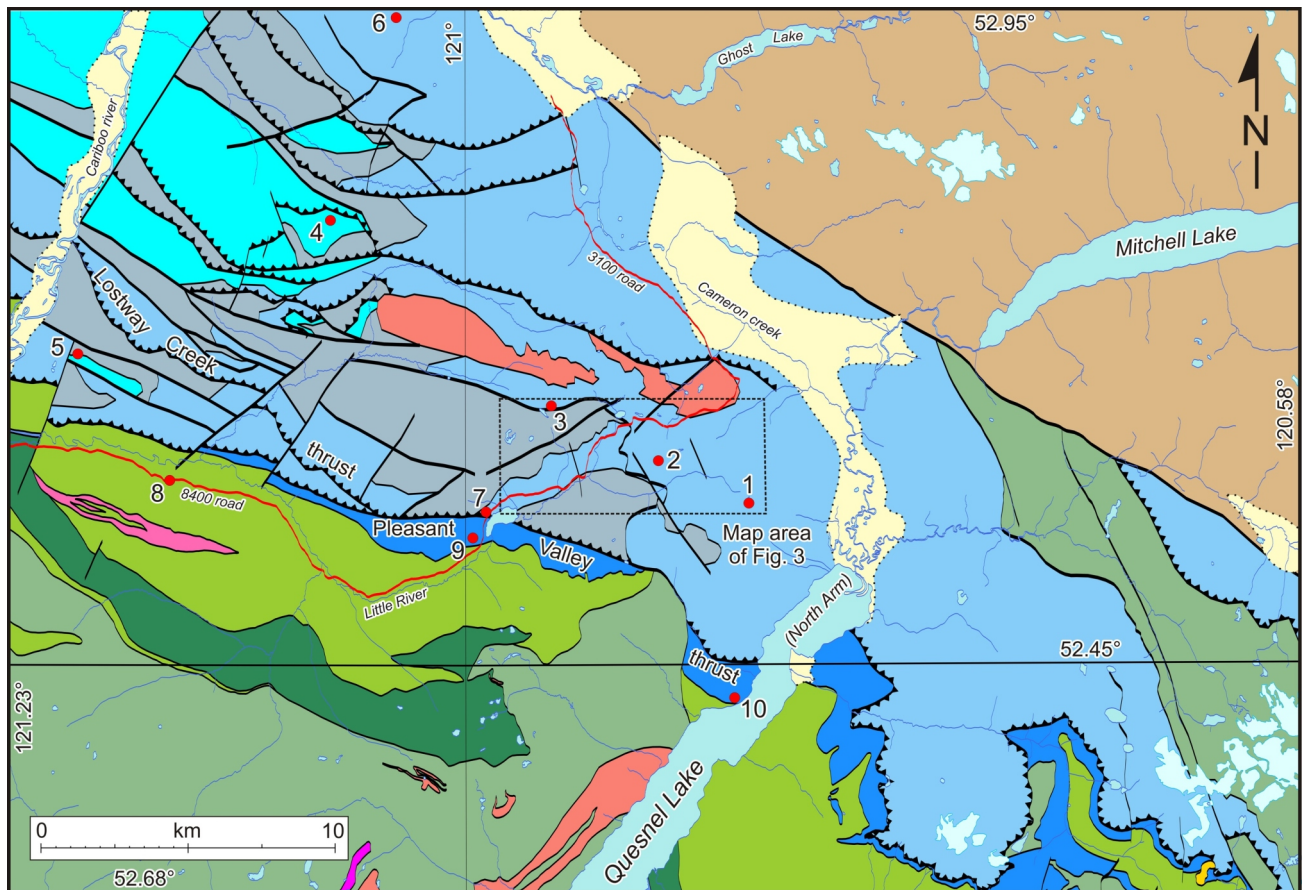
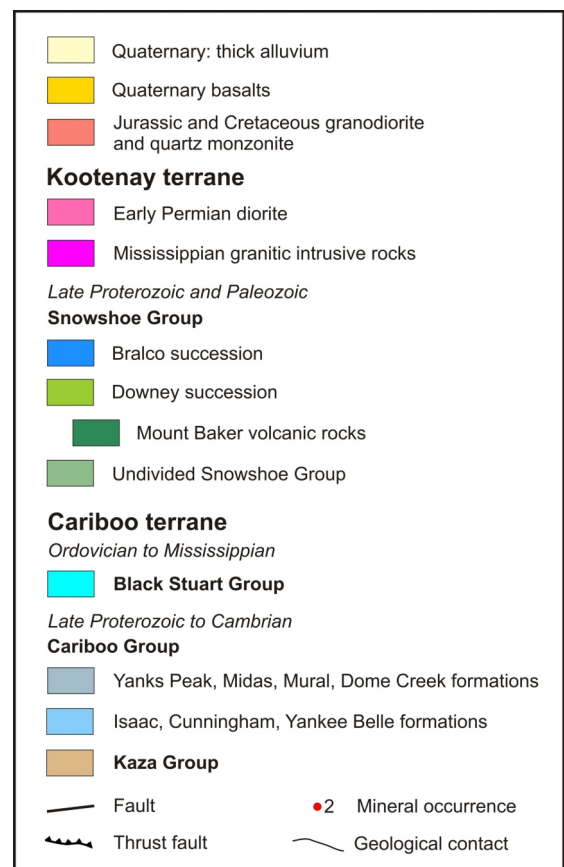


Figure 2. General bedrock geology between the Cariboo River and Mitchell Lake (after Campbell, 1978; Struik, 1983a, b, 1988; Ferri and O'Brien, 2003), east-central British Columbia. The dotted rectangle is the area covered by Figure 3. Mineral occurrences, according to BC MINFILE (BC Geological Survey, 2009): 1, Sil; 2, Grizzly Lake; 3, Lam; 4, Comin Throu Bear; 5, Maybe; 6, Mt. Kimball; 7, Maeford Lake; 8, Ace; 9, Mae; 10, Cariboo Scheelite. Occurrences 1, 2, and 3 form the Cariboo Zinc property.

Kootenay Arc, which hosts numerous stratabound carbonate-hosted Zn-Pb sulphide and nonsulphide deposits and polymetallic Pb-Zn (\pm Ag) veins (Struik, 1988; Paradis, 2007).

The carbonate-hosted sulphide and nonsulphide occurrences (Flipper Creek, Dolomite Flats, Main, Gunn and Que) of the Cariboo Zinc property (Figure 3) belong to a number of stratabound Zn-Pb occurrences in Late Proterozoic to Early Paleozoic platform carbonates and carbonaceous shale of the Cariboo terrane. These include the Maybe (MINFILE 093A 110; BC Geological Survey, 2009), Vic (MINFILE 093A 070), Cunning (MINFILE 093A 222), and Comin Throu Bear (MINFILE 093A 158) stratabound massive sulphide deposits (Höy and Ferri, 1998). Numerous polymetallic Zn-Pb (\pm Ag \pm Au) veins crosscut sedimentary rocks of the Cariboo and Black Stuart groups; some examples include the Joy (MINFILE 093A 049), MB (MINFILE 093A 68), and VIP (MINFILE 093 162) showings.



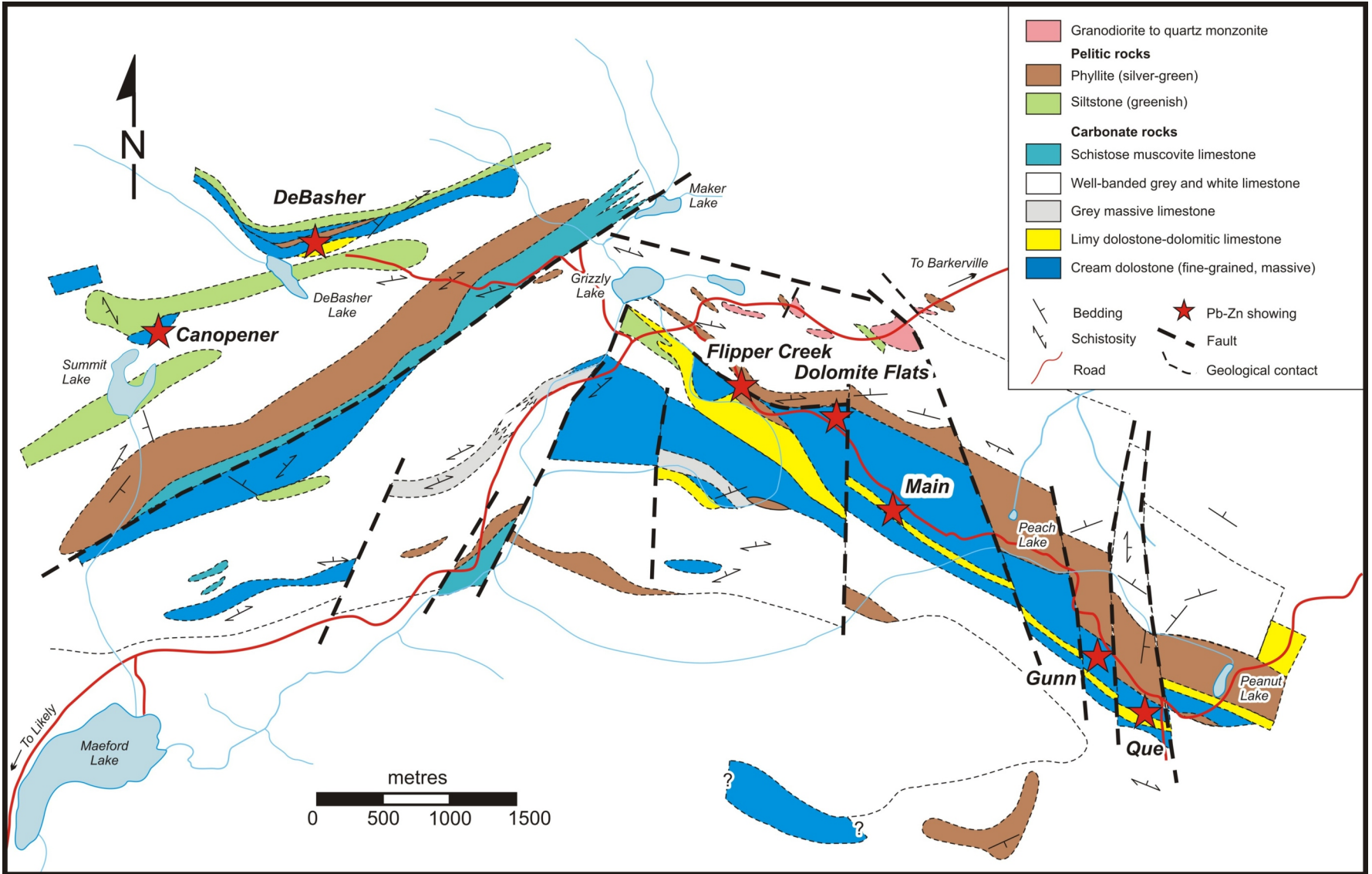


Figure 3. Regional geology of the Cariboo Zinc property area, east-central British Columbia (from Lormand and Alford, 1990).

GEOLOGY OF THE CARIBOO ZINC PROPERTY

Based on the regional mapping of Struik (1983b, 1988), the property is underlain by Late Proterozoic carbonate and pelitic metasedimentary rocks of the Cunningham and Isaac formations of the Cariboo Group (Figure 2).

The carbonate hosting the Zn-Pb sulphide and non-sulphide mineralization was designated by Murrell (1991) as the Isaac Formation; however, Höy and Ferri (1998) referred to it as the Cunningham Formation. Bradford and Hocking (2008) favoured the interpretation of Höy and Ferri (1998), based on the extrapolation of geological mapping done west of the Cariboo Zinc deposit area by Struik (1988).

A geological map of the study area (Figure 3), produced by Lormand and Alford (1990), outlines folded sequences consisting of interlayered carbonate and metapelitic sediments. The metasedimentary rocks strike 240° and dip to the northwest in the northern part of the property, and strike 310° and dip to the northeast in the southern part (Murrell, 1991; McLeod, 1995). This suggests the presence of a major open fold, with a hinge located near the Grizzly Lake area. A strong southwest- to northwest-striking foliation is present in metapelitic units on the eastern limb of the fold. The western limb is characterized by a southwest-striking foliation that generally dips northwest. Several north- to northeast-trending faults are interpreted to crosscut the metasedimentary rocks (Figure 3).

Three main varieties of carbonate rocks encountered during our visit are

light to medium grey, mottled dolomitic limestone or limy dolostone, commonly with rounded, distinct to diffuse 'fragments' of white dolomite and locally appearing brecciated (e.g., Main prospect);

creamy white, fine-grained dolostone that is locally silicified; and

thinly bedded/layered grey limestone.

The interlayered metapelite consists of fine-grained medium to dark silver-grey and green phyllite, siltstone and garnet-muscovite schist, the latter representing a more highly metamorphosed equivalent of the phyllite (Murrell, 1991).

Most of the Pb-Zn mineralization seems to be associated with the dolostone–dolomitic limestone interval adjacent to the 'phyllite' unit (Figure 3). We do not have detailed information to determine if this generalization is correct for the Canopener occurrence. At the Main prospect, the separation between the dolostone–dolomitic limestone interval and the phyllite appears wider (Figure 3) because the contact between the dolostone and the phyllite (largely eroded) is interpreted to be subhorizontal.

Intrusive rocks, mainly granodiorite and quartz monzonite, crop out north and southeast of the mineralized belt but have not been observed on the Cariboo Zinc property. The presence of similar intrusive rocks at depth is suggested by geophysical data (Figure 4).

CARBONATE-HOSTED SULPHIDE AND NONSULPHIDE MINERALIZATION

The Cariboo Zinc property encompasses several Zn-Pb sulphide and nonsulphide occurrences in a southeast-trending belt about 8 km long. The main occurrences, from west to east, are Canopener, DeBasher, Flipper Creek, Dolomite Flats, Main, Gunn and Que (Figure 3). In the BC MINFILE database, DeBasher corresponds to the LAM showing (MINFILE 093A 050), Flipper Creek, Dolomite Flats, and Main are encompassed by the Grizzly Lake prospect (MINFILE 093A 065), and Gunn and Que correspond to the Sil showing (MINFILE 093A 062).

Descriptions of the occurrences visited (i.e., Flipper Creek, Dolomite Flats, Main, and Gunn) are based on our field observation and the reports of Murrell (1991) and Bradford and Hocking (2008). The description of the DeBasher showing is summarized from Murrell (1991) and Bradford and Hocking (2008). No description of the Canopener (also known as Summit Lake) occurrence is given in BC MINFILE or in assessment reports.

DeBasher

The DeBasher showing is located on the west side of road 8400 and northeast of DeBasher Lake (Figure 3). Sulphide mineralization consists of quartz veins and mosaic breccias containing erratically distributed galena and sphalerite. Patches of orange oxide boxwork (after sphalerite) were the only nonsulphides observed by Bradford and Hocking (2008). The hostrocks are siliceous limy dolostone overlain by cream dolostone. These rocks are overlain by phyllite along a faulted contact (Murrell, 1991). Mineralization seems to be preferentially located at the faulted dolostone-phyllite contact.

Flipper Creek

The Flipper Creek prospect was discovered during road building in 1989 (Murrell, 1991). It is located 650 m southeast of the 8400 road and extends for 240 m in a north-westerly direction along the south bank of Flipper Creek. This mineralization coincides with a 100 m by 350 m Pb-Zn soil anomaly outlined by Teck Corporation during follow-up work (Bradford and Hocking, 2008).

Mineralization, hosted by medium-grained white dolostone, consists of sphalerite clots and pods, veins and distinctive breccia zones approximately 0.5 m thick containing barite, galena and sphalerite. The breccia is crosscut by a white, fine- to coarse-grained barite vein trending 185°. The seams and pods of galena and sphalerite occur within and along the margin of the vein (Figure 5). Barite-associated mineralization may postdate some earlier sphalerite- and galena-bearing veinlets.

According to Murrell (1991), mineralization is preferentially located at the contact between phyllite to the north and underlying cream dolostone to the south. This contact may correspond to a northwest-trending fault along Flipper creek¹ (Figure 3).

Murrell (1991) reported patchy green sphalerite hosted within the cream dolostone and associated with

¹ unofficial place name

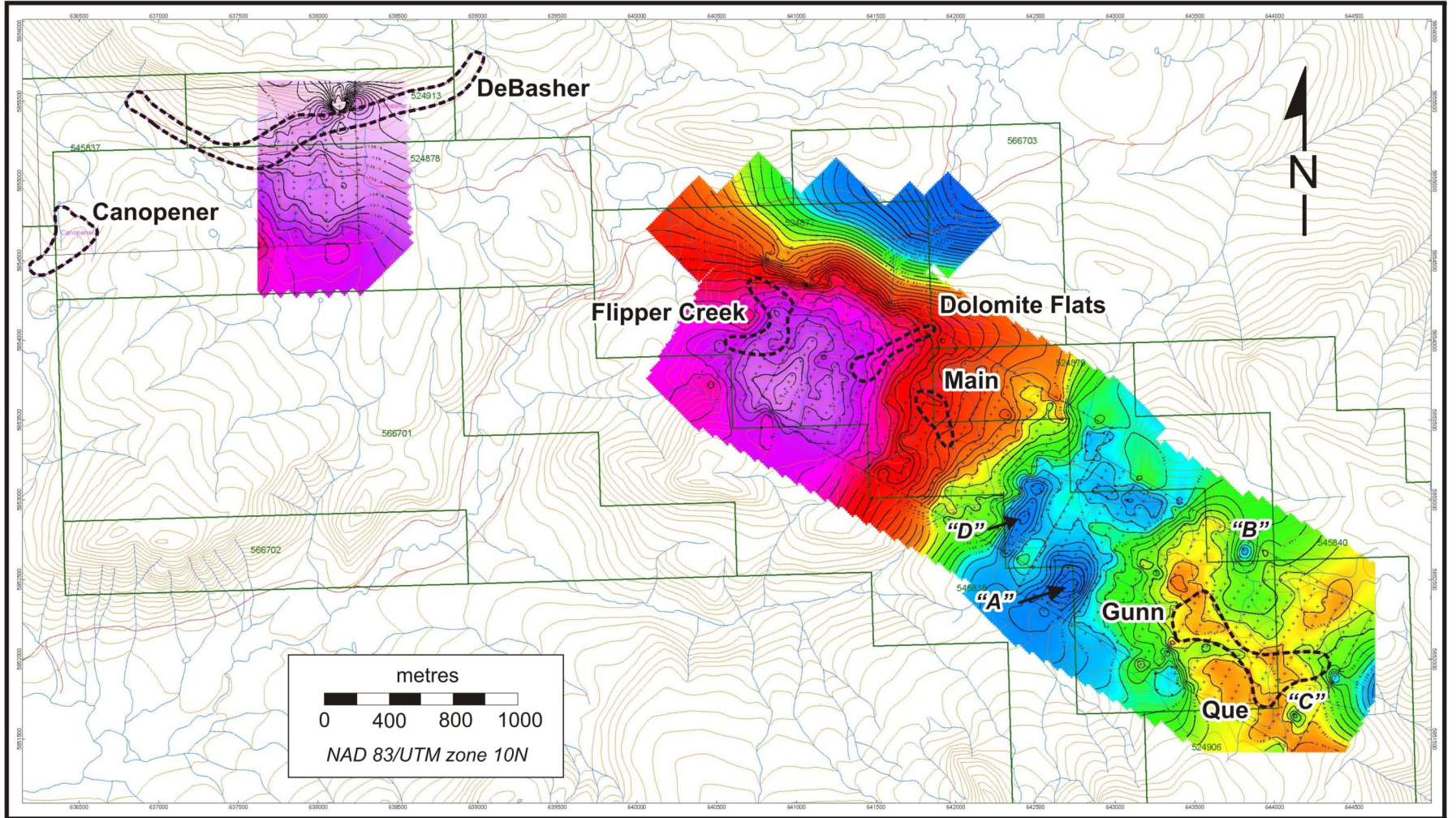


Figure 4. Cariboo Zinc property, east-central British Columbia, showing ground gravity contours of calculated Bouguer gravity anomalies (Luckman, 2008). Anomalies A, B, C, and D are discussed in the text.

white barite in proximity to the fault. Irregular disseminated blebs, wisps and veinlets of galena were uncovered during our visit, and orange-red sphalerite was observed within a dark grey brecciated dolostone (Murrell, 1991).

Dolomite Flats

The Dolomite Flats prospect is located approximately 800 m east-southeast of the Flipper Creek occurrence and 600 m northwest of the Main prospect (Figure 3). The mineralization is present in several low-relief dome-shaped outcrops, up to 40 m by 20 m in size, along the main access road (Figure 6A). The two main rock types present in this area are limestone and dolostone.

The limestone crops out on the side of the road between the Main and Dolomite Flats occurrences. It is beige to medium grey and pitted on weathered surfaces, and pale grey on fresh surfaces. Subtle layering that is locally discernible may represent relicts of original bedding or metamorphic layering. This rock reacts well with HCl and does not appear to be mineralized.

White- to cream-coloured, fine- to medium-grained crystalline dolostone is the dominant lithology at the Dolo-



Figure 5. Barite vein with seams of galena at the border and in the middle of the vein, Flipper Creek prospect, Cariboo Zinc property, east-central British Columbia.

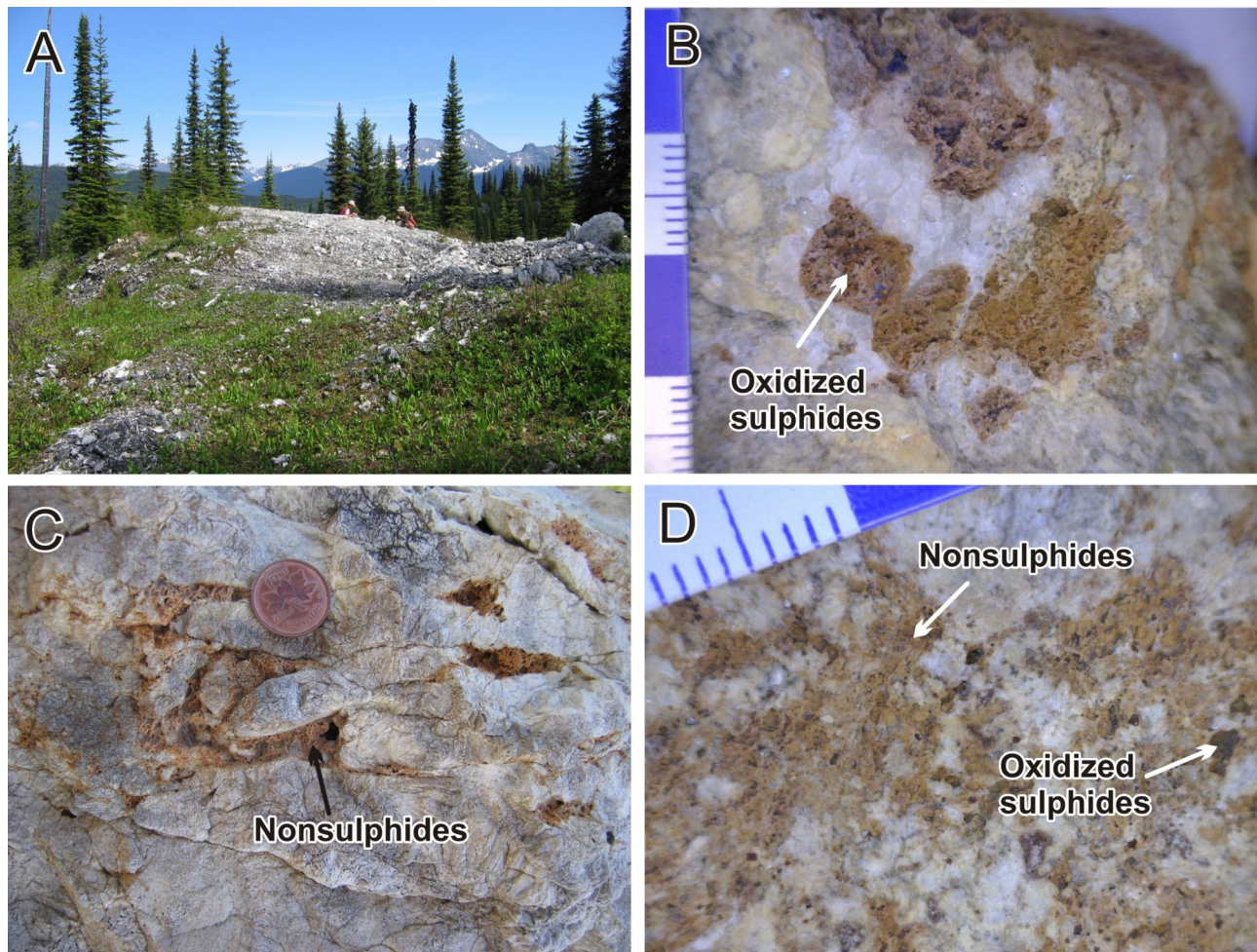


Figure 6. Dolomite Flats prospect, Cariboo Zinc property, east-central British Columbia: **A)** typical outcrop exposure in the Dolomite Flats prospect area; **B)** orange-brown patches corresponding to oxidized sulphides disseminated in the dolostone; **C)** fracture-filling oxidized sulphides occasionally forming boxwork texture in the dolostone; **D)** close-up of fine grains and aggregates of nonsulphides and oxidized sulphides in the dolostone.

mite Flats prospect. The dolostone is characterized by low response to 'Zinc Zap' (Zn indicator solution) and weak acid reaction (largely limited to calcite microfracture coatings). It commonly contains less than 1% millimetre-size grains of a soft grey to black mineral, and locally contains white mica and possibly clinopyroxene, preferentially concentrated along hairline fractures (microscope study is needed to confirm the mineralogy).

Base-metal (Zn-Pb) sulphide and nonsulphide mineralization appears to be confined to the dolostone. In proximity to mineralization, the dolostone host rock is generally medium- to coarse-grained, with crystals up to 1 cm in size. The main sulphide minerals are orange-brown to dark grey sphalerite and pyrite that are commonly (at least partially) oxidized and accompanied by some quartz and talc grains. These are disseminated within the dolostone or occur as fracture fillings (Figure 6B, C). No obvious structural control for the disseminated sphalerite mineralization is visible on the scale of the outcrop; however, at hand-specimen scale, sphalerite appears to be partially controlled by hairline fractures.

Nonsulphide minerals are typically soft reddish brown to orange, probably dominated by smithsonite or hemimorphite; however, the mineralogy has yet to be confirmed. These minerals are widespread throughout the fine-grained cream-coloured dolostone (characterized by a weak response to Zinc Zap) in low concentrations as fine aggregates or minute specks (Figure 6D). Where present in above-average concentrations, they form dull fracture coatings and/or sugary textured and porous pods with strong Zinc Zap response. Locally, the nonsulphides are associated with quartz grains, and visible relicts of sphalerite and pyrite crystals. The most spectacular occurrences of nonsulphides at this locality consist of radiating nonsulphide needles lining cavities.

An exploration hole, drilled with a hand-held Pack-sack drill in 1998, reached a depth of 34 m in dolostone breccia and ended in mineralization (hole 98-2; McLeod, 1999). The anomalous samples from this hole (Table 1) are considered to be generally representative of the known mineralization.

Diamond-drill hole 94-1 (length 92.4 m), collared 380 m southeast of hole 98-2 (halfway between the Main and Dolomite Flats zones), returned anomalous Pb and Zn in interlayered limestone, phyllite and dolostone between 63.7 m and the end of the hole. Several samples returned up to 2.21% Zn over 0.6 m intervals (e.g., sample G12 [79.86–80.47 m] returned 0.01% Pb and 2.21% Zn; McLeod, 1995). This hole also ended in galena-sphalerite mineralization. Additional drilling took place in 1999 within the general area of the Dolomite Flats prospect; however, it targeted a gravity anomaly rather than geochemical anomalies. Pembroke Mining now believes that the 1999 drill-holes were collared below the most favourable contact, which is located within the dolostone near the phyllite contact.

Lead is present in the form of galena as isolated short (<5 cm) and narrow (<2 mm) fracture fillings and small pods (<3 cm). These galena fillings are not common in the outcrops and are rather irregularly distributed.

Results of chemical analyses of samples collected during the 2009 visit were not available at the time of writing.

Table 1. Zn and Pb content of samples from drillhole 98-2 (McLeod, 1999; Bradford and Hocking, 2008), Dolomite Flats prospect, Cariboo Zinc property, east-central British Columbia.

Sample no.	Zn (wt.%)	Pb (wt.%)	Width (m)	Recovery (%)
GL2 #1	1.34	0.01	0–2.5	40
GL2#2	5.95	0.03	2.5–3.5	60
GL2#7	1.00	0.42	16.6–27.4	90
GL2#8	1.06	0.35	27.4–28.2	90
GL2#9	0.90	0.31	28.2–31.4	75
GL2#10	3.75	0.50	31.4–34	60

Main

The Main prospect, discovered in 1989, is exposed in a trench approximately 48 m long and 28 m wide (Figure 7A). Another smaller trench is located 230 m northwest of the main trench.

Mineralization consists of numerous intersecting 2–3 cm wide quartz veins containing galena and lesser sphalerite (Figure 7B, C). Mineralization is largely fracture controlled. The main quartz-galena (\pm sphalerite) vein system strikes 300–360° and dips east at 60–90°. It crosscuts barren quartz veins (2–3 cm wide) with orientations of 150°/80°W, 135°/50°S and 120°/45°S.

Areas (up to 1 m by 0.5 m) consisting largely of massive galena (\pm euhedral sphalerite) are present along exposed faces of major fractures within the principal trench of the Main prospect (Figure 7D); in most cases, however, these fractures are less than 5 cm thick and, as the galena content decreases, quartz content increases.

Mapping has shown that phyllite is present in the area; however, unlike elsewhere on the property, it is flat lying or dips gently to the south (Murrell, 1991).

Teck Corporation drilled two Winkie holes, GL90-1 and GL90-2 oriented at 307° and 288°, respectively, and plunging 45°, directly beneath the main trench to test for possible vertical extensions of the surface mineralization (Murrell, 1991). Both drillholes were anomalous in Zn throughout, with values up to 3.9% Zn and 1.1% Pb over 0.5 m. Lead values were lower than expected, based on the spectacular nature of the galena-rich surface exposures.

Gunn

The Gunn showing is associated with an extensive Zn-Pb soil anomaly (Cannon, 1970; Bradford, 2006). One large outcrop of dolostone with numerous small trenches occurs adjacent to the dirt road. Several outcrops and numerous larger trenches occur over a 250 m by 125 m area south of the dirt road, approximately 150 m southeast of the Main prospect (Figure 3).

Mineralization consists of quartz-galena (\pm sphalerite) veins and fracture fillings, barite-galena-sphalerite veins, pods of oxidized sulphides, and disseminated fresh and oxidized sphalerite. The carbonate host is a fine- to medium-grained recrystallized white dolostone (Figure 8A). The dolostone weathers pale to medium grey with an occasional pinkish tint, appears beige adjacent to the veins and is white on fresh surfaces. Adjacent to the mineralized veins, the dolostone occasionally contains fine-grained disseminated

dark grey– and honey-coloured, partially oxidized sphalerite (Figure 8B–D).

A white to pale grey–weathering silicified knob located immediately south of the road contains galena-bearing veins with variably weathered sphalerite, and barite-galena-sphalerite veins (Figure 8E). Trenching in the vicinity of the knob has revealed several additional showings over an area measuring 250 m by 125 m (Murrell, 1991; Bradford and Hocking, 2008).

The principal Gunn excavation (Figure 8F), located 250 m west of the road, shows a complex network of quartz-galena (\pm sphalerite \pm nonsulphides) veins enclosed in siliceous cream-coloured dolostone that also locally hosts fine-grained, disseminated, dark grey sphalerite and encloses irregular zones of nonsulphide Zn-Pb mineralization. The veins generally trend northwest or north ($280^{\circ}/67^{\circ}\text{S}$, $300^{\circ}/80\text{--}90^{\circ}\text{N}$ to $110\text{--}130^{\circ}/46^{\circ}\text{S}$ and $000^{\circ}/45^{\circ}\text{E}$). One set of mineralized veins trends 040° and dips 60°SE . Most of the veins are less than 5 cm thick and vary in mineralogy and mineral proportions along strike. They consist of quartz and galena with subordinate amounts of calcite, sphalerite and nonsulphide minerals. The nonsulphides include white to pale grey, translucent to transparent radiating crystals, 2–3 mm in length (probably

cerussite; Figure 9A), and stubby white transparent crystals, 1.5 mm in length and 0.5 mm in diameter (Figure 9B) that are tentatively identified as anglesite. Other nonsulphides observed are hydrozincite and hemimorphite. At two locations within the main excavation, Pembrook Mining Corporation and Zincore Metals Inc. geologists reported 16–30% Zn with much lower Pb values across widths of 3–6 m. These zones most likely sampled a combination of vein-type and nonsulphide replacement-type mineralization.

Que

The Que showing comprises a large number of shallow exploratory trenches and stripped outcrops and subcrops (Figure 10A) located at the extreme southeast corner of the Cariboo Zinc property, approximately 750 m south of the Gunn zone (Figure 3). The showing consists of irregularly distributed dolostone-hosted sphalerite, galena and nonsulphide mineralization. The area of known mineralization outlined between 1981 and 2008 by various operators continues to expand, as Pembrook Mining Corporation located several new mineralized outcrops during our 2009 field visit.

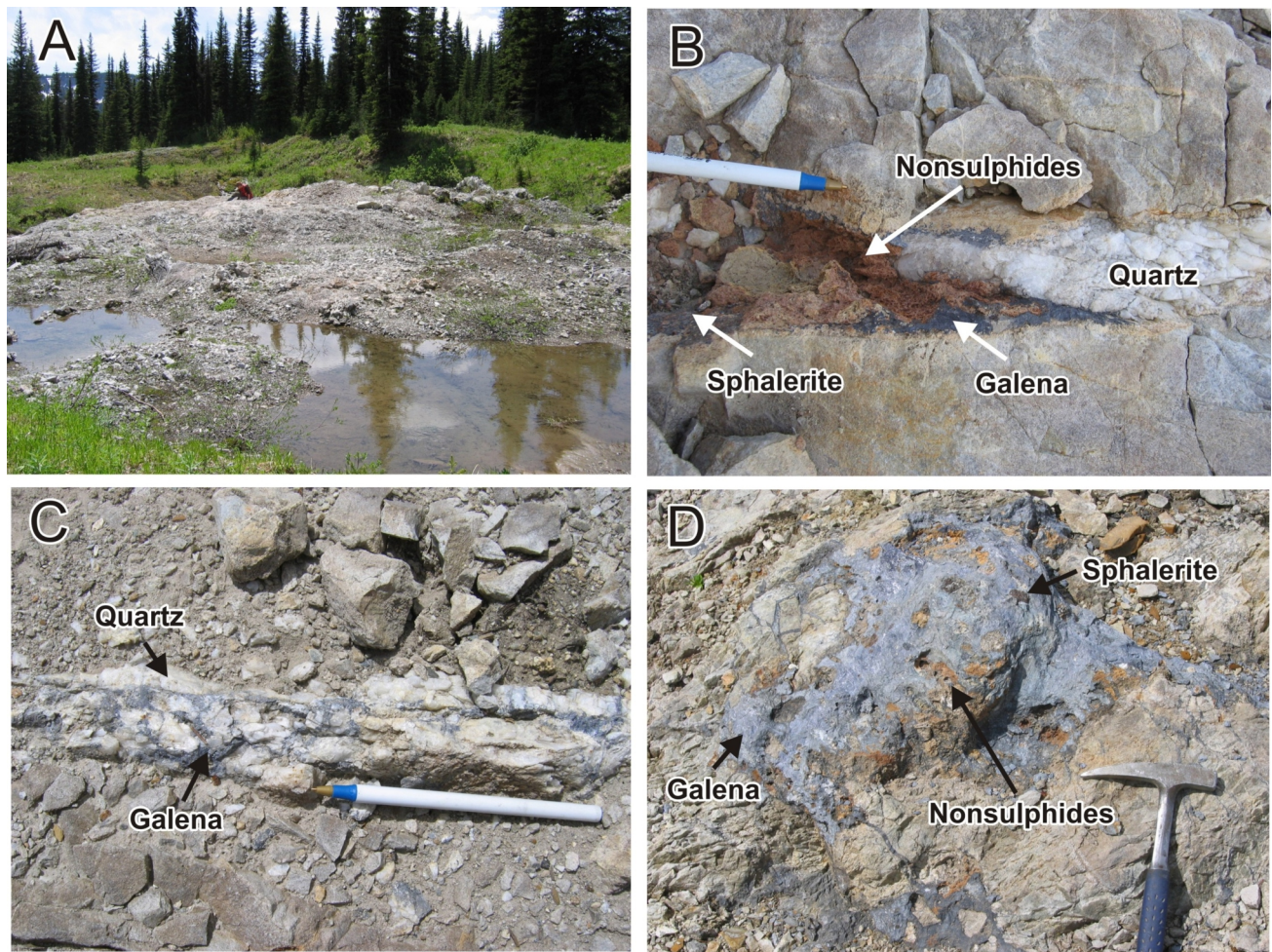


Figure 7. Main prospect, Cariboo Zinc property, east-central British Columbia: **A)** main trench; **B)** quartz-sphalerite-galena-nonsulphide (after sphalerite) vein; **C)** quartz-galena vein; **D)** pod of galena, nonsulphides (cerussite) and sphalerite that form part of a vein-breccia system.

Boulders of nonsulphide mineralization are scattered throughout the area. At least at one locality, the presence of several large angular and friable nonsulphide-bearing blocks (>1 m in diameter), which strongly react to ‘Zinc Zap’, suggests a local origin (Figure 10B, 10C). One of the

main base-metal nonsulphide minerals is probably cerussite (Figure 10D), but detailed mineralogical investigation is required.

During our 2009 property visit, white-coated galena (sphalerite-free) nodules up to 4–5 cm across (Figure 11)

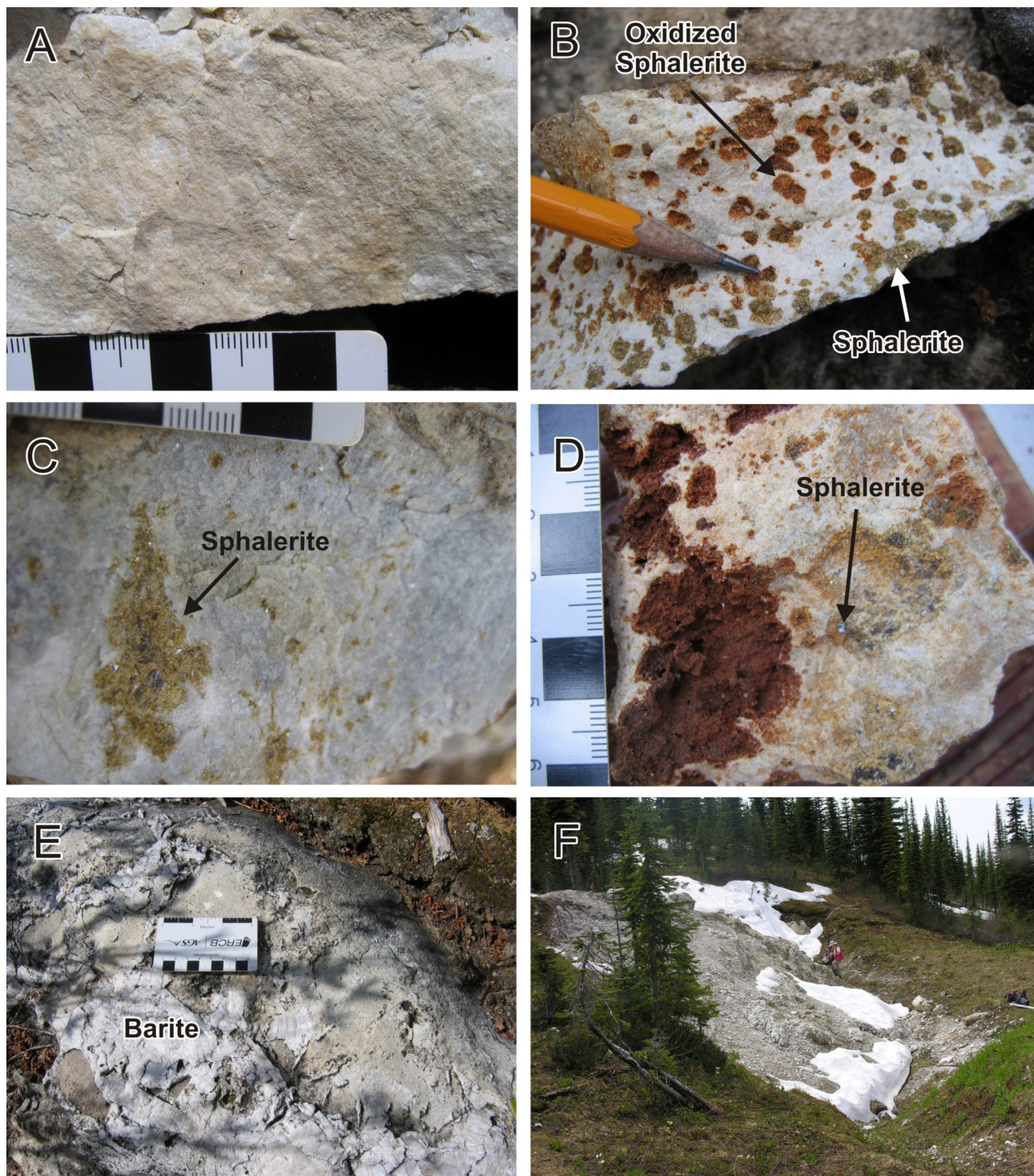


Figure 8. Gunn showing, Cariboo Zinc property, east-central British Columbia: **A)** fine-grained recrystallized white dolostone; **B)** disseminated oxidized (orange) and fresh (yellowish) sphalerite in the fine-grained white dolostone; **C)** aggregates of fresh yellow sphalerite in the fine-grained white dolostone; **D)** oxidized reddish brown sulphides (presumably sphalerite) in the white dolostone; **E)** barite-galena-sphalerite vein crosscutting the dolostone (only barite is clearly visible in the photograph); **F)** main Gunn excavation.

were uncovered in a north-flowing stream less than 50 m upstream from an occurrence of high-grade nonsulphide-rich boulders. These rounded nodules may be important because the creek bed consists exclusively of flat, coarse, angular dolostone fragments, indicating a proximal origin. No rounded exotic pebbles, commonly observed in the nearby overburden, were seen in the stream. These galena nodules may have formed by dissolution of the surrounding hostrocks and partial conversion of galena to anglesite. This would be consistent with the process described by Heyl and Bozion (1962), Reichert and Borg (2008) and Simandl and Paradis (2009). Cavities within the rounded nodules still contain remnants of the host dolostone and orange-coloured nonsulphide minerals. These cavities formed by partial dissolution of the host dolostone and sphalerite crystals. Sharp and angular quartz grains protruding from the galena would have broken off or separated from the galena if the nodules had been transported downstream for any significant distance. The presence of quartz suggests a type of mineralization (or protore) similar to that observed in the Main and Gunn occurrences. One of the nodules contains 'striated' relicts of amphibole crystals or stacked sericite sheets. Both amphibole and sericite were observed locally, adjacent to galena-rich veins at or near the Main prospect.

DISCUSSION

This discussion is based on the 2009 field observations and previous investigations by the industry. No results of chemical analyses, thin section petrography or powder x-ray diffraction on samples collected during 2009 were available at the time of writing.

Field Observations

All the mineralization observed during our field visit is stratabound, hosted by Mg-bearing carbonates (i.e., limy dolostone–dolomitic limestone and fine-grained creamy dolostone). It seems to be located close to the contact between the cream dolostone and the limy dolostone (Figure 3) and, according to company reports, near the contact between the dolomitic carbonate rocks and the overlying phyllite. Although overall the mineralization is stratabound, it is in part structurally controlled on the outcrop scale. It occurs as disseminations of fine specks and centimetre-size aggregates, irregular replacement zones, veins and fracture fillings locally forming narrow breccia zones. Sphalerite occurs mostly as pervasive fine- to medium-grained, low-grade disseminations in dolostone; aggregates forming centimetre-size clots; and, less frequently, fracture and breccia fillings. Galena occurs mainly as fracture and vein fillings in association with quartz and/or calcite, sphalerite and barite. Galena-rich crackle and mosaic dolostone breccias (\pm sphalerite) are less common. In all of the occurrences, galena and sphalerite are at least partially transformed into Zn-Pb nonsulphides. Smithsonite, hemimorphite, cerussite, hydrozincite and possibly anglesite are probably the main nonsulphide Zn and Pb minerals. They form millimetre-scale orange patches, oxide boxworks (after sphalerite), open-space fillings and irregular replacement pods and masses with or without remnants of sphalerite and galena. The best Zn-Pb nonsulphide mineralization was observed as blocks or subcrops within the Que zone (Figure 10c). The friable nature of the nonsulphide blocks indicates a proximal source.

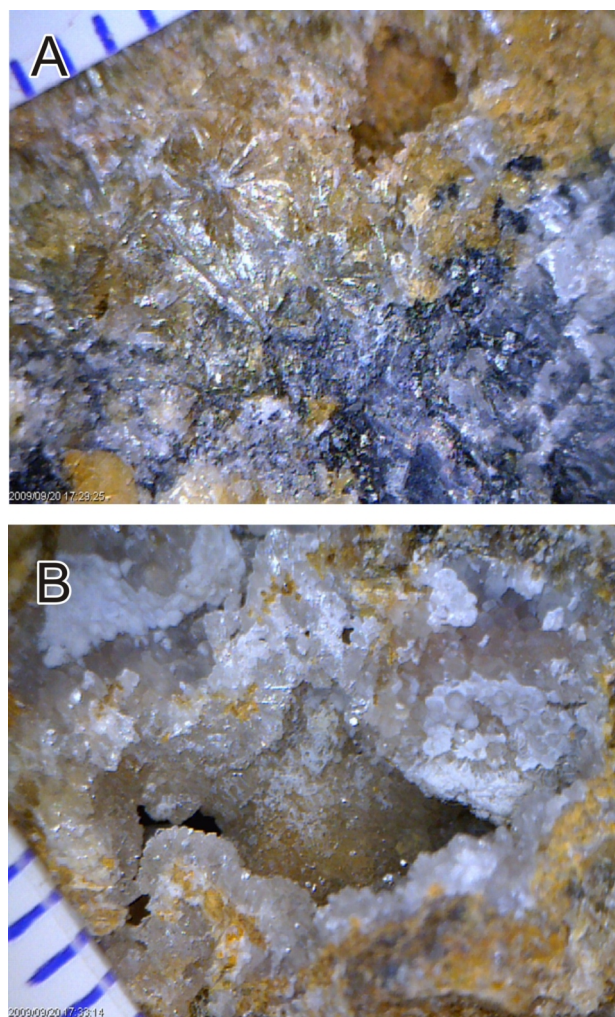


Figure 9. Gunn showing, Cariboo Zinc property, east-central British Columbia: **A**) white to pale grey, translucent to transparent radiating crystals, 2–3 mm in length (probably cerussite); **B**) stubby white transparent crystals (probably anglesite) lining cavities.

The presence of galena nodules covered by a white coating (Figure 11), within the same area, is consistent with near-surface oxidation of sulphide ores (Simandl and Paradis, 2009).

Surprisingly, Fe-sulphides (pyrite and/or marcasite) are absent (or present in low concentrations) throughout the area, with the exceptions of the DeBasher and Dolomite Flats occurrences, where pyrite is found associated with aggregates of sphalerite. This is significant because pyrite is more reactive in surface environments than sphalerite or galena. The destabilization of pyrite is expected to result in the formation of acidic solutions that are then able to attack sphalerite and, to some extent, galena. This means that either pyrite already reacted or it was never present in the system. If pyrite was originally present but later destroyed, then its oxidation may have resulted in the formation of solutions with a capacity to transport Zn. Such solutions favour the formation of 'white' Zn-rich nonsulphide deposits in the area. This aspect must be followed up by detailed petrographic studies.

Several minerals tentatively identified during this study, or reported in previous studies, are known to gener-



Figure 10. Que showing, Cariboo Zinc property, east-central British Columbia: **A)** shallow exploratory trenches (arrow) and stripped out-crops and subcrops; **B)** close-up of aggregates of nonsulphide minerals (orange and white); **C)** large, angular nonsulphide-bearing blocks; **D)** radiating, tabular translucent crystals of cerussite in cavity.

ate distinct infrared spectral responses that, under favourable conditions, may be detectable by remote sensing, a relatively new and probably underutilized exploration tool in British Columbia. The vegetation cover, however, may reduce the effectiveness of such an approach.

The significance of galena nodules remains to be confirmed. They may be relicts of primary sulphide mineralization, partially rounded by interaction with supergene fluids (as described by Reichert and Borg, 2008) and subject to additional rounding during short downstream transport.

Review of Existing Data with Focus on Pb-Zn Nonsulphides

Exploration in the area has consisted of traditional prospecting, geological mapping, geophysical and geochemical surveys, trenching and limited drilling. Both geochemical and geophysical methods are effective exploration tools in selecting Pb-Zn sulphide targets on the Cariboo Zinc property (Cannon, 1970; Murrell, 1991; Bradford, 2006). Additional information may be extracted from existing surveys, if the nonsulphide Pb-Zn mineralization is also targeted. For example, the ground gravity

contours of the calculated Bouguer anomaly (Figure 4) represents results of the most recent gravity survey. It shows a general trend of increasing gravity to the northwest and de-



Figure 11. Galena nodules, Que showing, Cariboo Zinc property, east-central British Columbia.

creasing gravity to the southeast (Luckman, 2008). The gravity highs superimposed on this trend may reflect the presence of Pb-Zn mineralization or localities where minor igneous intrusions approach the surface. General spatial association of relatively discrete gravity highs with known Zn-Pb sulphide mineralization is observed at the Gunn and Que showings (Figure 4). The main exploration target was the Pb-Zn sulphide mineralization (either Irish-type or MVT); therefore, the interpretation was geared towards the selection and testing of gravity highs. Numerous drill targets were previously identified by Paget Resources Corporation or the predecessor companies, based on gravity highs (Luckman, 2008). As a byproduct of the search for gravity highs, the surveys also commonly identified gravity lows. Figure 4 provides few examples of gravity lows that were not previously discussed. Some of them are located at the edge of the surveyed area and may be an artifact of the data processing. Others, including anomalies A, B, C and D, may require closer attention. They may possibly correspond to karst features or the presence of porous (vuggy) nonsulphide mineralization.

The large, nearly circular negative anomaly (Figure 4, anomaly A) is not associated with a strong geochemical signature, but it coincides with the projected location of the strata hosting the main occurrence. It may also be an expression of a karst structure. Anomalies B and C have a much smaller footprint. The lowest value of these anomalies corresponds to one or two gravity readings. They could 1) represent operational glitches during the survey; 2) reflect the difficulty of obtaining the proper inner terrain corrections using the clinometers at those particular locations; or 3) be mineralization related. Anomaly B is located near the historical borehole 98-01, which tested a gravity anomaly detected during the 1996 survey. This short vertical borehole intersected a 4 m section of 3.26% Zn and 97 ppm Pb near the surface (McLeod, 1999). Low core recovery, no mention of sulphides in the company's core log and very low Pb values strongly suggest that this may be direct-replacement-type nonsulphide Zn mineralization. Two critical gravity readings on the survey line adjacent to anomaly B are missing, complicating the assessment of this anomaly. Anomaly C corresponds to a single anomalous reading. It is located within the Que showing area. Historical chemical analyses of at least three samples collected within 100 m of this anomaly returned between 400 and 5000 ppm Pb. Anomaly D is a multistation type. The lowest Bouguer values are concentrated along a single traverse, cutting across the projection of the favourable carbonate horizon that hosts the Main prospect. This gravity low may coincide with the trace of a north-northeast-trending fault (with or without associated karst), with probable graben- or half-graben-style down-drop east of the fault.

Karst features, such as sinkholes, caverns and solution-collapse breccias and other structures, are recognized to be important controls on MVT mineralization in several Pb-Zn districts (e.g., Pine Point, Tri-State, east and central Tennessee, upper Mississippi Valley). In the Cariboo Zinc area, the karst structures may also provide the channels for downward migration of supergene Zn-bearing fluids and/or result in depressions of the water table. Both of these possibilities are important for the genesis of nonsulphide wallrock-replacement Zn-Pb deposits (Simandl and Paradis, 2009). Furthermore, the karst structures and related topographic depressions are also known to control the distribution of 'residual- and karst-fill-' types of nonsulphide deposits, as defined by Heyl and Bozion,

(1962) and Hitzman et al. (2003). We had no strong reasons to consider this category of nonsulphide Pb-Zn deposits in the Salmo area of southern BC (Simandl and Paradis, 2009); however, this category of mineralization could be encountered in the Cariboo district. Knowledge of physical properties of nonsulphide mineralization in the Cariboo Zinc district would greatly improve the quality of the interpretation, but such data are not presently available.

CONCLUSION

The area is characterized by a large number of strata-bound Pb-Zn occurrences hosted by dolomitic carbonates along a northwest-trending belt about 8 km long. Both Pb-Zn sulphide and nonsulphide types of mineralization are present at the Flipper Creek, Dolomite Flats, Main, Gunn and Que occurrences. The continuity of sulphide and nonsulphide mineralization exposed within the Cariboo Zinc property is not well constrained.

Modern exploration programs are typically integrated (i.e., combining traditional prospecting and mapping with geophysical and geochemical methods). The area was investigated to some extent in terms of its Zn-Pb massive sulphide potential but remains nearly virgin in terms of exploration aimed at nonsulphide base-metal deposits. Existing surveys could be reinterpreted to identify areas favourable for nonsulphide mineralization. For example, the possible significance of the positive Bouguer anomalies was previously addressed. Negative Bouguer anomalies were not discussed. They should be carefully assessed to determine if they reflect karst structures, which could be potential controls on nonsulphide Pb-Zn ores. Estimates of physical properties of nonsulphide and sulphide mineralization (based on samples collected in 2009) will facilitate future interpretation of the geophysical surveys done on the Cariboo Zinc property.

Detailed laboratory work, including microscopy, scanning electron microscopy, powder x-ray diffraction, and geochemical and isotopic analyses will help develop customized genetic and exploration models for sulphide and nonsulphide Pb-Zn mineralization within the Cariboo terrane. It may also open the door for use of cutting-edge exploration technologies. For example, depending on vegetation cover, the short-wave infrared spectral response of some nonsulphide base-metal ore minerals (e.g., hydrozincite and smithsonite) may make remote sensing a potentially cost-effective exploration method that has yet to be tested in British Columbia.

ACKNOWLEDGMENTS

The authors extend their appreciation to Pembroke Mining Corporation for giving us access to their property, permitting us to sample surface exposures and sharing their knowledge of the area. Earlier versions of this manuscript benefited from reviews by Paul Schiarizza and Tania Demchuk of the BC Ministry of Energy, Mines and Petroleum Resources, and Jan Bednarski of the Geological Survey of Canada. The authors were assisted in the field by Laura Simandl from St. Michaels University School, Victoria. This project is being done under the umbrella of the Cordilleran Targeted Geoscience Initiative Program (TGI-3) of the Geological Survey of Canada, in collaboration with the BC Ministry of Energy, Mines and Petroleum Resources.

REFERENCES

- BC Geological Survey (2009): MapPlace GIS internet mapping system; *BC Ministry of Energy, Mines and Petroleum Resources*, MapPlace website, URL <<http://www.MapPlace.ca>> [November 2009].
- Bradford, J. (2006): Rock geochemistry and geological mapping on the Cariboo Zinc property (GR 1–4 mineral claims); *BC Ministry of Energy, Mines and Petroleum Resources*, Assessment Report 28732, 35 pages.
- Bradford, J. and Hocking, M. (2008): Cariboo Zinc property; report on geological mapping (GR 1–13 mineral claims) 93A/14E and 93A/15W, UTM Zone 10, NAD83, 641000E, 5854000N; *Pembroke Mining Corporation*, internal report, 33 pages.
- Campbell, R.B. (1978): Geological map of the Quesnel Lake map-area, British Columbia; *Geological Survey of Canada*, Open File 574.
- Cannon, R.W. (1970): Geochemical report, geochemical soil survey, Quesnel Lake area; *BC Ministry of Energy, Mines and Petroleum Resources*, Assessment Report 2366, 13 pages.
- Colpron, M. and Price, R.A. (1995): Tectonic significance of the Kootenay terrane, southeastern Canadian Cordillera: an alternate model; *Geology*, Volume 23, pages 25–28.
- Ferri, F. and O'Brien, B.H. (2002): Preliminary geology of the Cariboo Lake area, central British Columbia (093A/11, 12, 13, and 14); in *Geological Fieldwork 2001*, *BC Ministry of Energy, Mines and Petroleum Resources*, Paper 2002-1, pages 59–79.
- Ferri, F., and O'Brien, B.H. (2003): Geology of the Cariboo Lake area, central British Columbia; *BC Ministry of Energy, Mines and Petroleum Resources*, Open File 2003-1, pages 77–96.
- Heyl, A.V. and Bozion, C.N. (1962): Oxidized zinc deposits of the United States, part 1, general geology; *United States Geological Survey*, Bulletin 1135-A, 52 pages.
- Hitzman, M.W., Reynolds, N.A., Sangster, D.F., Cameron, R.A. and Carman, C.E. (2003): Classification, genesis, and exploration guides for nonsulphide zinc deposits; *Economic Geology*, Volume 98, pages 685–714.
- Höy, T., and Ferri, F. (1998): Zn-Pb deposits in the Cariboo subterranean, central British Columbia (93A/NW); in *Geological Fieldwork 1997*, *BC Ministry of Energy, Mines and Petroleum Resources*, Paper 1998-1, pages 14-1–14-10.
- Lormand, C. and Alford, C. (1990): Grizzly Lake project, regional geology of Fog claims: geological map, scale 1:10 000; *BC Ministry of Energy, Mines and Petroleum Resources*, Assessment Report 21038, Figure GL 90-3b.
- Luckman, N. (2008): 2008 assessment report, ground gravity survey on the Cariboo property, Cariboo Mining Division, central British Columbia, 52°48'54"N, 120°54'30"W, NTS 93A/15; *Paget Resources Corporation*, internal report, 54 pages.
- McLeod, J.W. (1995): Report on the Grizzly Lake zinc-lead property, Cariboo Mining District; *BC Ministry of Energy, Mines and Petroleum Resources*, Assessment Report 23995, 33 pages.
- McLeod, J.W. (1999): Report on the Grizzly Lake zinc-lead property, lat. 52°48'N, long. 120°58'W, NTS 93A/14E and 15W; *BC Ministry of Energy, Mines and Petroleum Resources*, Assessment Report 25824, 25 pages.
- Murrell, M.R. (1991): Geological, geochemical, and prospecting report on the Fog 1, Fog 2, and Fog 3 claim groups, Cariboo Mining District, NTS 93A/15; *BC Ministry of Energy, Mines and Petroleum Resources*, Assessment Report 21038, 69 pages.
- Nelson, J.L., Colpron, M., Piercey, S.J., Dusel-Bacon, C., Murphy, D.C. and Roots, C.F. (2006): Paleozoic tectonic and metallogenetic evolution of pericratonic terranes in Yukon, northern British Columbia and eastern Alaska; in *Paleozoic Evolution and Metallogeny of Pericratonic Terranes at the Ancient Pacific Margin of North America, Canadian and Alaskan Cordillera*, Colpron, M. and Nelson, J.L., Editors, *Geological Association of Canada*, Special Paper 45, pages 323–360.
- Nelson, J.L., Paradis, S., Christensen, J. and Gabites, J. (2002): Canadian Cordilleran Mississippi Valley-type deposits: a case for Devonian–Mississippian back-arc hydrothermal origin; *Economic Geology*, Volume 97, pages 1013–1036.
- Paradis, S. (2007): Carbonate-hosted Zn-Pb deposits in southern British Columbia – potential for Irish-type deposit; *Geological Survey of Canada*, Current Research 2007-A10, 7 pages.
- Reichert, J. and Borg, G. (2008): Numerical simulation and geochemical model of supergene carbonate-hosted non-sulphide zinc deposits; *Ore Geology Reviews*, Volume 33, pages 134–151.
- Schiarizza, P. and Ferri, F. (2003): Barkerville terrane, Cariboo Lake to Wells: a new look at stratigraphy, structure, and regional correlations of the Snowshoe Group; in *Geological Fieldwork 2002*, *BC Ministry of Energy, Mines and Petroleum Resources*, Paper 2003-1, pages 77–96.
- Simandl, G.J. and Paradis, S. (2009): Carbonate-hosted, nonsulphide, zinc-lead deposits in the southern Kootenay Arc, British Columbia (NTS 082F/03); in *Geological Fieldwork 2008*, *BC Ministry of Energy, Mines and Petroleum Resources*, Paper 2009-1, pages 205–218.
- Struik, L.C. (1983a): Bedrock geology of Spanish Lake (93A/11) and parts of adjoining map areas, central British Columbia; *Geological Survey of Canada*, Open File 920, 1:50 000.
- Struik, L.C. (1983b): Bedrock geology of Quesnel Lake (93A/10) and part of Mitchell Lake (93A/15) map areas, central British Columbia; *Geological Survey of Canada*, Open File 962, 1:50 000.
- Struik, L.C. (1988): Structural geology of the Cariboo gold mining district, east-central BC; *Geological Survey of Canada*, Memoir 421, 100 pages.

Vermiculite in the Blue River Area, East-Central British Columbia, Canada (NTS 083D/06)

by G.J. Simandl^{1,2}, S. Paradis^{2,3}, L. Simandl⁴ and J. Dahrouge⁵

KEYWORDS: vermiculite, market, deposit, exfoliation, physical properties, carbonatite, rare earth elements, economic potential

ABSTRACT

There is currently no vermiculite produced within the Province of British Columbia. Only four localities in the BC MINFILE list vermiculite as a commodity. High concentrations of vermiculite were encountered in semiconsolidated outcrops during a hike to examine the Hodgie rare earth zone in the Blue River area. Follow-up bibliographic research indicates that this is probably a new occurrence, although similar occurrences were described in the Blue River area by McCammon (1950). Based on our observations and on the data of McCammon (1950), the occurrences located in the Blue River area have above-average vermiculite content and are certainly of higher grade than other known vermiculite occurrences in the province. Reconnaissance-level field observations, in-house particle-size analyses and rudimentary laboratory-scale exfoliation tests are encouraging. They indicate that detailed chemical and mineralogical studies are the next logical step in the assessment of this and other vermiculite occurrences in the Blue River area. Chemical analyses are required to establish trace-element levels of vermiculite-bearing material, to ensure that it does not contain elevated levels of environmentally sensitive substances. Mineralogical follow-up should establish the absence or presence of asbestiform particles. The presence of such particles would negatively impact the development of this vermiculite resource. If the outcomes of the above-recommended tests justify more rigorous laboratory and field investigations, then these occurrences of the Blue River area have the potential to become significant commercial sources of vermiculite. The closest operating vermiculite exfoliation plant is in Edmonton, Alberta, a relatively good location. This plant belongs to Grace Canada Inc.

¹ British Columbia Ministry of Energy Mines and Petroleum Resources, Victoria, BC

² Centre for Earth and Ocean Sciences, University of Victoria, Victoria, BC

³ Geological Survey of Canada–Pacific, Sidney, BC

⁴ St. Michaels University School, Victoria, BC

⁵ Commerce Resources Corp., Vancouver, BC

This publication is also available, free of charge, as colour digital files in Adobe Acrobat® PDF format from the BC Ministry of Energy, Mines and Petroleum Resources website at <http://www.empr.gov.bc.ca/Mining/Geoscience/PublicationsCatalogue/Fieldwork/Pages/default.aspx>.

INTRODUCTION

Vermiculite is a sheet silicate with variable chemical composition. The following formula is considered representative: $Mg_{1.8}Fe^{2+}_{0.9}Al_{4.3}SiO_{10}(OH)_2 \cdot 2O$. Vermiculite is commonly bronze coloured, but it can be grey-white, greenish, brown or colourless. It is characterized by a scaly appearance, low density (2.3–2.7 g/cm³), a micaceous habit and perfect basal cleavage. Individual flakes split with ease, are soft (1.5 to 2 on the Mohs scale of hardness) and pliable, but inelastic.

Vermiculite has a high total water content that can reach up to 20%, but commercial products contain from 6 to 17 wt. % H₂O. When heated to temperatures not exceeding 500°C, the water can be driven out from the vermiculite, but the mineral rehydrates readily on exposure to humidity in the air. When heated quickly to temperatures in the 870–1100°C range, vermiculite particles exfoliate by expanding at right angles to their basal cleavage. The increase in volume expected from commercial products is 8 to 12 times the original volume. On a laboratory scale, selected individual flakes may expand up to 30 times their original volume. This expansion is believed to result from the separation of the layers due to the conversion of contained interlaminar water into steam. Expanded vermiculite is a pale-coloured, low-density, porous material that is chemically inert and adsorbent. It has excellent thermal and acoustic insulation properties and high fire resistance.

Vermiculite Deposits

Economic concentrations of vermiculite are believed to form by weathering or near-surface alteration of biotite or phlogopite minerals within carbonatite bodies, ultramafic complexes or mafic gneiss units. They may also form residual deposits associated with these rock types (Birkett and Simandl, 1999; Simandl et al., 1999). Given favourable physical and chemical conditions, vermiculite also forms within a variety of intermediate and felsic rocks; however, in these settings, mafic minerals (vermiculite precursors) are present in lower concentrations. It is therefore less likely that the vermiculite occurrences hosted by intermediate and felsic rocks will have grades of economic interest. Typical vermiculite ore grades range from 20% to 35%, and processed products consist of 90% vermiculite (Hindman, 2006).

Carbonatite complexes may also contain niobium, rare earth elements (REE), phosphate, fluorite, zirconium, uranium, thorium, titanium, copper and iron mineralization (Mariano, 1989; Modreski et al., 1995; Armbrustmacher et al., 1996; Richardson and Birkett, 1996; Birkett and Simandl, 1999; Simandl et al., 1999; Simandl, 2002). With the exception of copper, these commodities have been previously reported in the Blue River area.

Market

Vermiculite is used as a lightweight aggregate in concrete; as an additive in a variety of acoustic, thermal and fire insulation products; in soil conditioning; as a fertilizer or insecticide carrier; and in absorbent packing, paints and sealants (Simandl et al., 1999; Hindman, 2006; Potter, 2009). It is also used in refractory gunning and castable mixes, in vermiculite dispersions and in replacing asbestos in brake linings, primarily for the automotive market. Recent interest in vermiculite-related nanotechnology (e.g., Weiss et al., 2006) may ultimately result in new, highly specialized but significant vermiculite markets.

Vermiculite substitutes in lightweight concrete and plaster are expanded perlite, clay, shale, slag and slate. In loose-fill thermal and fireproofing insulations, competing materials are fibreglass, perlite and rock wool. Peat, perlite, sawdust, tree bark and synthetic soil conditioners compete with vermiculite as soil-enhancement products.

World vermiculite annual production (Figure 1) is approximately 500 000 tonnes (t; Simandl et al., 1999; Potter, 2009). In 2008, the main vermiculite-producing countries were South Africa (200 000 t), China (110 000 t), United States (100 000 t), Russia (25 000 t), Brazil (15 000 t), Australia (15 000 t) and Zimbabwe (15 000 t). All remaining countries combined to account for the balance, which is less than 30 000 t (Potter, 2009).

American imports, excluding any material from Canada and Mexico, were about 54 000 tonnes for the first 8 months of 2008. China provided 70% and South Africa provided 25% of these exports (Potter, 2009).

Vermiculite concentrate (before exfoliation) is a moderately priced product that is shipped close to the market before being expanded. During 2008, depending on specifications, prices for American vermiculite concentrate, ex-plant (i.e., cost not including transportation and insurance; in bulk) ranged from US\$95 to US\$180 per tonne (Moeller, 2008). The average unit value of exfoliated vermiculite in the United States for 2008 was estimated at US\$430 per tonne (Potter, 2009).

Because most vermiculite production is confined to only three countries, transportation costs may represent a large proportion of the selling price. For example, the June 2009 prices of South African vermiculite concentrate (FOB, bulk, Rotterdam) ranged from US\$280 to US\$450 per tonne (Anonymous, 2009).

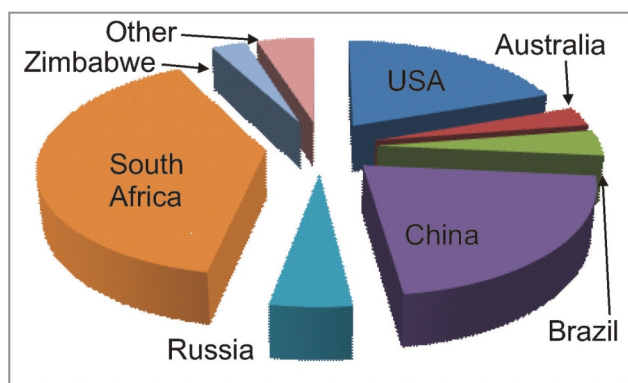


Figure 1. Main vermiculite-producing countries; total production for 2008 is approximately 510 000 tonnes (Potter, 2009).

Mining and Processing Market

Vermiculite is normally mined by open pit and, in some cases, blasting may be required. Processing of primary vermiculite ores consists of screening, blending and dry or wet beneficiation. Beneficiation may involve crushing; air classification or other methods sensitive to particle density/morphology (such as winnowing); electrostatic or high-intensity magnetic separations; and, in some cases, even flotation (Hindman, 2006). Concentrates are typically transported as close as possible to markets before being thermally or chemically exfoliated.

Vermiculite in British Columbia

There is currently no vermiculite production within the province and there are only four occurrences listed with vermiculite as a commodity in the BC MINFILE database (BC Geological Survey, 2009). Two of these occurrences were described by White (1990) and tested by Morin and Lamothe (1991). The Joseph Lake occurrence (MINFILE 093K 077) has very low vermiculite content (5.6%) and is of no of economic interest (Morin and Lamothe, 1991). The Sowchea Creek showing (MINFILE 093K 083) has a slightly higher vermiculite content; however, it does not exfoliate enough to be of economic interest (Morin and Lamothe, 1991). At the Shuttleworth Creek occurrence (MINFILE 082ESW110), vermiculite is reported to be associated with asbestiform anthophyllite. Based on this association, it is unlikely that this occurrence would be considered for follow-up work as a source of vermiculite in the foreseeable future. The Verity occurrence, in the Blue River area (MINFILE 083D 005), is carbonatite related. There is no detailed description of the vermiculite mineralization in MINFILE, but brief descriptions of vermiculite-bearing outcrops were provided by McCammon (1950). One of these occurrences could correspond to the coarse mineralization (vermiculite flakes reaching more than 15 cm across) associated with the Upper Fir carbonatite, as described by Simandl et al. (2007).

VERMICULITE IN THE BLUE RIVER AREA

During a hike to examine the newly discovered Hodgie rare earth zone in the Blue River area, anomalous concentrations of vermiculite were encountered along the access road. The fine-grained, unconsolidated vermiculite-bearing exposures, containing flakes less than 6 mm across, are the main subject of this paper. They were most likely exhumed during construction of the access road to the Hodgie rare earth zone. They may represent a new discovery, but there is a possibility that this occurrence coincides with one of the showings described by McCammon (1950).

Location

The carbonatite-related tantalum, niobium, REE and vermiculite deposits of the Blue River area (McCammon, 1953; Dahrouge, 2002; Simandl et al., 2002; Commerce Resources Corp., 2008) are spatially and genetically associated. Most of them are accessible by an extensive network of logging roads that connect to Highway 5 at the Lem-priere train station, and are located approximately 40 km

north of the municipality of Blue River (Simandl et al., 2002).

The vermiculite occurrence described in this paper is located adjacent to the three diamond-drill holes that intersected the Hodgie rare earth zone, investigated for its REE content by Commerce Resources Corp. (2008). The Hodgie zone itself is located approximately 2 km southeast and uphill from the Fir carbonatite (Commerce Resources Corp., 2008). The Fir carbonatite is the main target of drilling and bulk-sampling efforts carried out by Commerce Resources

(Figure 2). The UTM (Zone 11, NAD 83) co-ordinates of the main vermiculite occurrence, sampled and described in this document, are 354137E and 5795372N at an elevation of approximately 1760 m above sea level.

Geological Setting of Blue River Carbonatites and Fenites

Vermiculite was discovered in the Blue River area in 1950 (McCammon, 1950), before the carbonate rocks

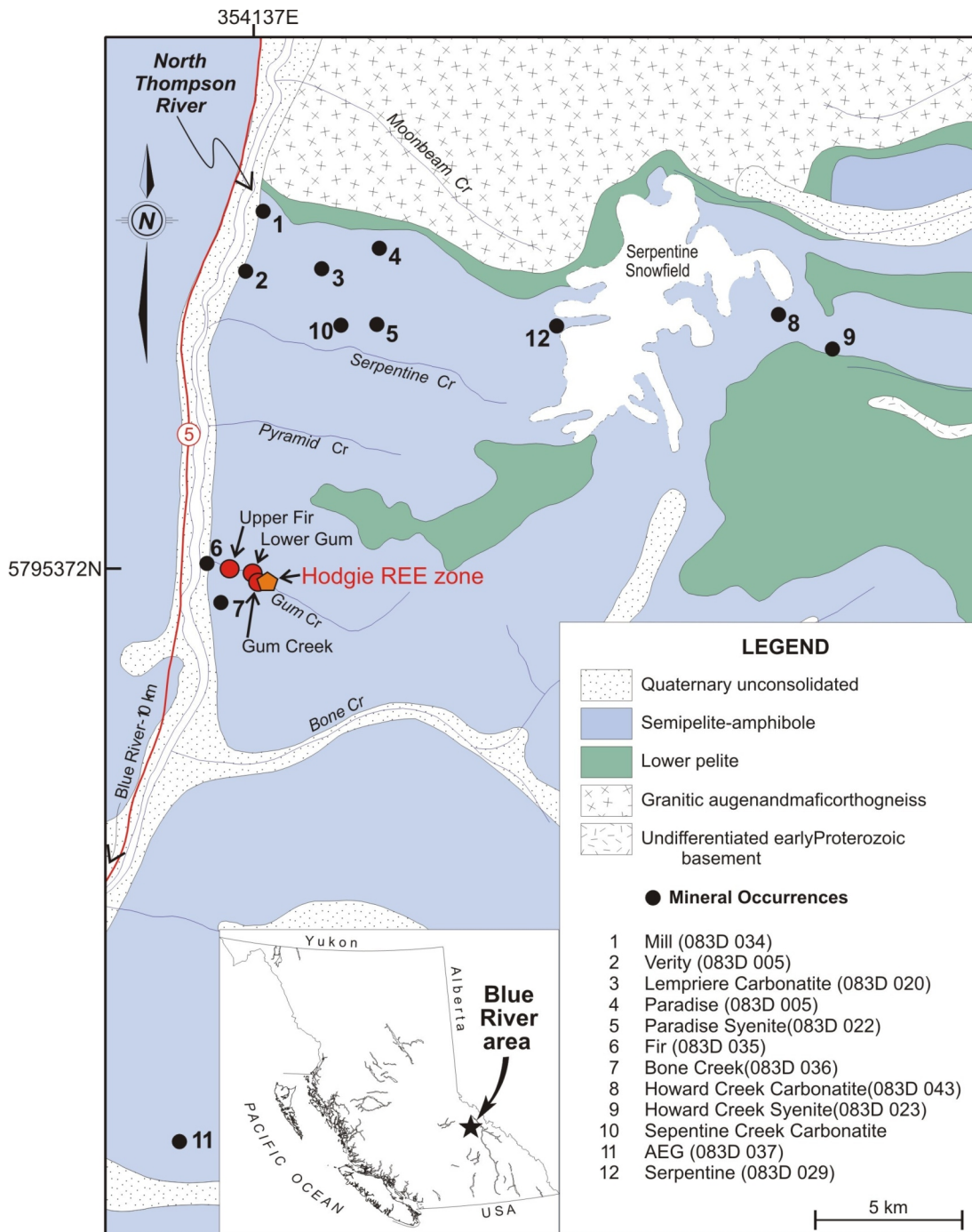


Figure 2. Location of vermiculite and carbonatite occurrences in the Blue River area, east-central British Columbia (modified from Simandl et al., 2002).

closely associated with vermiculite occurrences were recognized to be carbonatites. The carbonatites with associated fenite zones, and the related vermiculite occurrences, are part of a broad alkaline belt that follows the Rocky Mountain Trench (Pell, 1994). The Blue River carbonatites are part of the central portion of this belt and are located within the northeastern margin of the Shuswap Metamorphic Complex mapped by Campbell (1967). These carbonatites are hosted by the semipelite-amphibolite unit (Figure 1) of the Hadrynian Horsethief Creek Group (Mountjoy, 1992). Dominant rock types in the area that host carbonatites are amphibolite and biotite-feldspar-quartz (\pm garnet \pm kyanite) gneiss. Rocks within the semipelite-amphibolite unit have reached amphibolite-facies metamorphism. Sillimanite and kyanite are reported to coexist in some of the metapelite layers in this area (Campbell, 1967; Digel, 1989). The carbonatites are deformed and locally mylonitized, and appear to follow general trends observed in the hostrocks. The potassium-argon dates (White, 1982; Pell, 1994) obtained on richterite from the dolomitic Verity carbonatite are probably metamorphic (92.5 ± 3.2 and 80.2 ± 2.8 Ma). Uranium-lead dating on zircon from the same deposit indicates 325 Ma, probably the emplacement age of the carbonatite. This zircon date is more compatible with the slightly older dates from the nearby Mud Lake carbonatite and Paradise Lake syenite (363–340 Ma), also obtained on zircons (Pell, 1994). Gneisses and amphibolites host numerous crosscutting or concordant pegmatites. A number of these pegmatites are exposed in roadcuts of the deactivated access road leading to the Hodgie rare earth zone.

Vermiculite Mineralization

Vermiculite is exposed in a roadcut (break in slope) for nearly 80 m from the road fork that leads to three drillholes intersecting the Hodgie rare earth zone (Figure 3), approximately 2 km southeast and upslope of the Upper Fir carbonatite. The company reported that 84 grab samples were collected from float and outcrops in the area. Seven

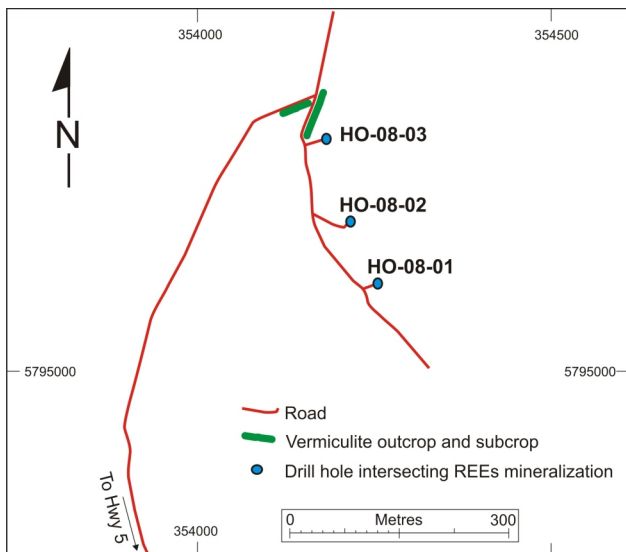


Figure 3. Sketch showing the position of the vermiculite occurrence relative to diamond-drill holes HO-08-01, HO-08-02 and HO-08-03, which intersected the Hodgie rare earth zone, Blue River area, east-central British Columbia.

samples returned total REEs + yttrium greater than 2.0%, with a high value of 11.1% (Commerce Resources Corp., 2008). The main vermiculite exposure is vertical, 0.5–3 m in height and continuous for 80 m (Figure 4). It is heterogeneous, highly friable to semiconsolidated and characterized by a layered texture that represents the original gneissic layering of the protolith (Figures 5, 6). The mineralization is unconformably overlain by overburden containing clasts of local and exotic rock types. The unconformity is sharp and irregular, and the bottom portion of the overburden has some regolith-like characteristics. The size of the vermiculite particles is equivalent to the size of the biotite flakes in the surrounding gneiss.

Unconsolidated, soil-contaminated subcrop material within the ‘lower’ roadcut (Figure 3) also contains some vermiculite. This material does not show the well-preserved primary textural features that were observed within the upper roadcut, raising the possibility that it may have slumped to its current position from the upper roadcut area.



Figure 4. An 80 m long vermiculite-bearing outcrop, adjacent to the Hodgie rare earth zone, Blue River area, east-central British Columbia.



Figure 5. Vermiculite zone showing layering inherited from the protolith (mafic biotite gneiss/amphibolite), adjacent to the Hodgie rare earth zone, Blue River area, east-central British Columbia; layers dominated by amphibole are dark grey and those dominated by vermiculite are greenish and pale brown.

SAMPLING PROCEDURE AND LABORATORY WORK

Reconnaissance-type laboratory examination covers two vertical channel samples (2 and 1.5 m in length, weighing 912 and 610 g, respectively) and a grab sample (weighing 492 g) of unconsolidated, vermiculite-bearing material. Channel samples 09-SP-306 and 09-SP-307 were taken perpendicular to the layering and are considered to be representative. Grab sample 09-SP-305 represents one of the soft, high-grade mineralized layers, approximately 30 cm thick.

The samples were air dried (24 hours at 40°C) in a Despatch Industries (USA) LLB Series bench oven, weighed and screened for 2 minutes using a CE Tyler Combustion Engineering Inc. portable sieve shaker (model RX). No crushing, attrition milling or other processing-enhancing vermiculite particle liberation was done.

Grain-Size Distribution and Mineralogy

Most of the particles within the three samples that were collected are finer than 2 mm (Table 1). Macroscopic examination indicates that the main constituents of the unconsolidated mineralization are vermiculite, medium and dark green amphiboles (possibly richterite and hornblende), and feldspar (probably plagioclase). A green, vitreous, translucent mineral (probably clinopyroxene) and white, translucent, glassy mineral (most likely apatite) are the less common constituents. These minerals are present in all size fractions, but their proportions vary from sample to sample. Variations are also observed from one size fraction to the next within individual samples. Dark amphibole is most abundant in sample 09-SP-307, where the green pyroxene and plagioclase are minor non-vermiculite constituents. The dark green amphibole is also the main non-vermiculite constituent of sample 09-SP-306; however, the feldspar and the green pyroxene are significant constituents in this sample. The green, vitreous, semitransparent mineral, tentatively identified as clinopyroxene, is the main non-vermiculite constituent of sample 09-SP-305.



Figure 6. Sharp, irregular contact between amphibole-rich (dark green-grey) and vermiculite-dominated (beige to pale brown) semiconsolidated layers, vermiculite zone adjacent to the Hodgie rare earth zone, Blue River area, east-central British Columbia.

Table 1. Description and grain-size fractions of vermiculite-bearing samples from outcrop adjacent to the Hodgie rare earth zone, Blue River area, east-central British Columbia.

Sample number	Sample type	Sample weight (g)	Fraction	
			Size (mm)	Weight (g)
09-SP-305	Grab	491.7	> 4	6.6
			2-4	59.3
			1-2	122.5
			<1	298.8
09-SP-306	Channel (2 m)	911.8	> 4	98.3
			2-4	107.6
			1-2	307.4
			<1	389.6
09-SP-307	Channel (1.5 m)	609.4	> 4	3.1
			2-4	35.6
			1-2	290.7
			<1	280.0

Biotite or phlogopite appears to have been the main vermiculite precursor in all samples. Vermiculite and amphibole occur mainly as individual grains; however, depending on the sample and size fraction, up to 20% of the grains may be a compound consisting of distinct (but attached) vermiculite-amphibole grains. Textural evidence suggests that limited direct conversion of amphibole or pyroxene to very fine grained vermiculite did take place, but it does not explain the origin of the vermiculite stacks 2 mm or coarser in size. Magnetite, ilmenite, pyrrhotite, zircon, ferrocolumbite, pyrochlore and olivine were identified in the Blue River carbonatites and fenites (Simandl et al., 2002), so it is possible that they could be present as minor or trace constituents. Mineralogical studies, involving polarizing microscope, x-ray diffraction and scanning electron microscope or electron microprobe, are needed. Careful study would also be required to confirm that no asbestiform minerals are present in the vermiculite-bearing raw materials.

Exfoliation Tests

All major uses of vermiculite involve expanded products; therefore, when possible, exfoliation tests are performed during the grass-roots stage of exploration. The exfoliation of vermiculite can be achieved using a number of methods, including the insertion of organic compounds (e.g., butylammonium) into vermiculite interlayers; the decomposition of H₂O₂ (hydrogen peroxide) that penetrates between vermiculite interlayers (Obut and Girgin, 2002); microwave treatment of the concentrate (Obut et al., 2003); or thermal exfoliation (Hindman, 2006). Thermal processing remains a workhorse of the vermiculite industry for high-volume markets; therefore, thermal testing remains the most popular approach used by the industry during grass-roots mineral exploration and during the screening of development projects.

Laboratory-scale thermal-exfoliation tests have been carried out on two subeconomic, very low grade BC occurrences by Morin and Lamothe (1991). While it is not entirely clear why such low-grade deposits were tested, the document provides good examples of the methodology used. The BC Ministry of Energy, Mines and Petroleum Re-

Table 2: Results of the rudimentary laboratory-scale, thermal-exfoliation tests on raw materials (without vermiculite pre-concentration) and vermiculite grade estimates, based on samples.

Sample number	Particle size (mm)	Pre-exfoliation		Post-exfoliation		Volume increase (raw; factor)	Estimate of vermiculite content (raw; wt. %)
		Volume ($\pm 0.2 \text{ cm}^3$)	Weight ($\pm 0.05 \text{ g}$)	Volume ($\pm 0.2 \text{ cm}^3$)	Heavy fraction ($\pm 0.05 \text{ g}$)		
09-SP-305	>4						
	2-4	2	2.15	7.2	0.9	3.6	58
	1-2	2	2	6.3	0.95	3.2	52
	<1	2	2.2	5.7	1.25	2.9	43
09-SP-306	>4						
	2-4	2	2.5	2.7	2.4	1.35	4
	2-4 duplicate	2	2.3	2.4	2.1	1.2	9
	1-2	2	2.7	3.7	2.15	1.85	20
	<1	2	2.65	4.3	1.9	2.15	28
09-SP-307	>4						
	2-4	2	2.8	4	2.3	2	18
	1-2	2	2.7	4.3	1.7	2.15	47
	<1	2	2.5	5	1.1	2.5	56

sources does not have the equipment required to carry out such tests. Some of the handheld, portable propane torches (air only) are able to reach an adiabatic flame temperature of 1995°C. A propane torch is not a substitute for the tests described in the previous paragraph, but it is used in the early screening of potential perlite or vermiculite ores. Rudimentary qualitative to semiquantitative expansion tests were carried out on the <1 mm, 1–2 mm and 2–4 mm size fractions of raw samples (consisting of vermiculite and gangue minerals). The results of these tests are described in Table 2.

Mini-samples of the individual size fractions, measuring 2 cm³ in volume, were weighed and then deposited in a



Figure 7. Crude laboratory set-up used to exfoliate vermiculite-bearing rock samples taken from the outcrop adjacent to the Hodgje rare earth zone, Blue River area, east-central British Columbia.

red-hot crucible. The temperature was maintained using a propane torch (Figure 7). Heating of the container continued for 3 minutes, or until the expansion ceased. When the sample cooled, the volume of the exfoliated material was measured (Figure 8; Table 2, column 5). The volume of the mini-sample after exfoliation divided by its original (pre-exfoliation) volume, in this case 2 cm³, is indicative of volume increase (Table 2, column 7).

The expanded vermiculite had a very low density and was simply floated using water (Figure 9). The floated expanded vermiculite component from each size fraction of a given sample was collected and examined under binocular microscope. It consistently exceeded 99.5% per volume. The ‘heavy minerals component’ of the same size fraction (particles denser than expanded vermiculite) was air dried and weighed (Table 2, column 6). This component consisted mainly of gangue minerals, but the fine size fractions (<1 mm in diameter) of each sample contained up to 20% of expanded vermiculite by volume. The coarse (2–4 mm) and medium (1–2 mm) size fractions of the heavy mineral component contained consistently less than 5% expanded vermiculite per volume.

A semiquantitative estimate of the vermiculite grade of specific fractions of the three samples (Table 2, column 8) was determined by subtracting the heavy mineral component after exfoliation (Table 2, column 6) from the weight of the mini-sample prior to exfoliation (Table 2, column 4).

Trace-element chemical analyses of the vermiculite raw material and/or vermiculite concentrate are required. Excessive concentrations of base metals or radioactive elements could reduce the marketability of the product. Similarly, a detailed mineralogical study would be required to ensure that no asbestiform minerals are present in the vermiculite-bearing raw materials.

Summary of Laboratory Work

No attempt was made to upgrade the unconsolidated to weakly consolidated vermiculite-bearing samples prior to testing. Results shown in Tables 1 and 2 are useful for preliminary assessments of the occurrence, in relation to other BC occurrences.

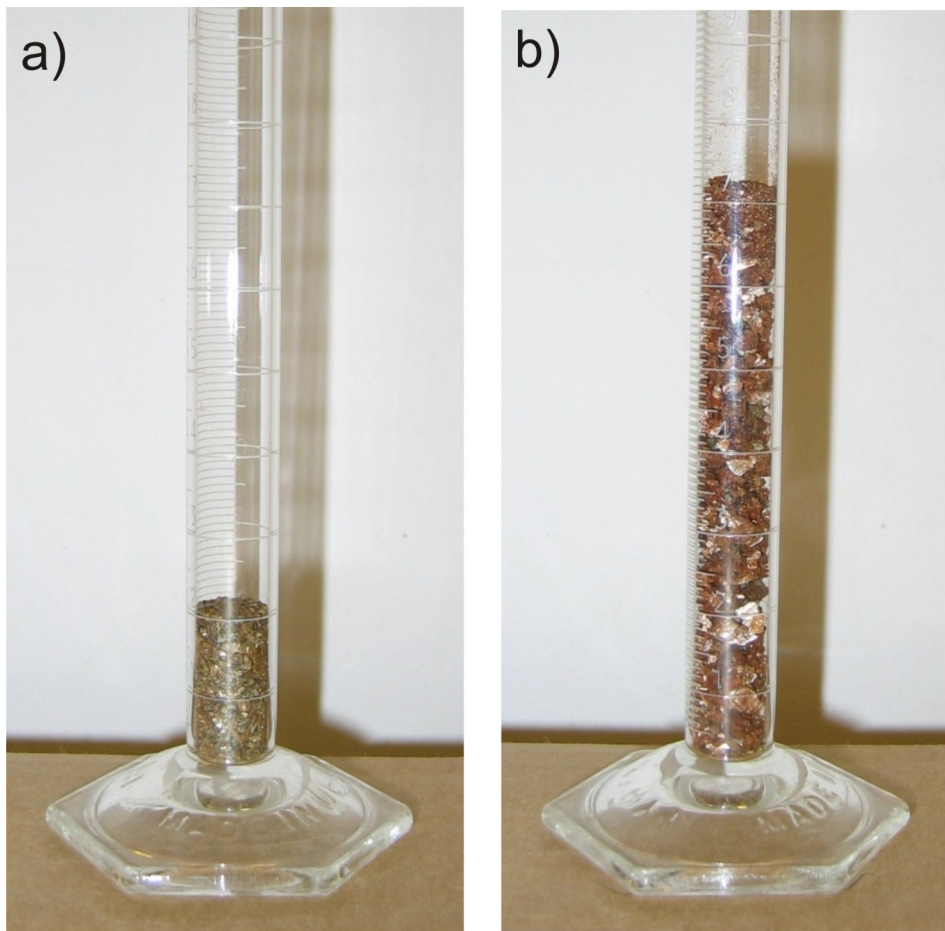


Figure 8. Change in volume caused by vermiculite exfoliation, 2–4 mm fraction of sample 09-SP-305, outcrop adjacent to the Hodgie rare earth zone, Blue River area, east-central British Columbia: **a)** pre-exfoliation, and **b)** after exfoliation.

The data confirm the following:

Vermiculite is present within the three samples.

Vermiculite grades are higher than grades reported elsewhere in the province and could locally exceed 50 wt. %.

Most of the particles composing the three samples are smaller than 2 mm.

Vermiculite content varies from sample to sample.

Vermiculite is most abundant in the coarse fraction of sample 09-SP-305 and lowest in the finest fraction. The opposite is true for samples 09-SP-306 and 09-SP-307, which have higher amphibole content than sample 09-SP-305. This is a reflection of the mineral composition of the protolith.

Mineralogical composition of each of the three samples varies according to size fraction.

Raw samples of vermiculite-bearing rock from the Blue River area exfoliate to a significant extent (Figure 10a–c); however, it is unlikely that optimal operating conditions were achieved for vermiculite exfoliation during our exfoliation experiments using the propane torch. Better results are expected if the tests are performed to the standards of the Vermiculite Institute.

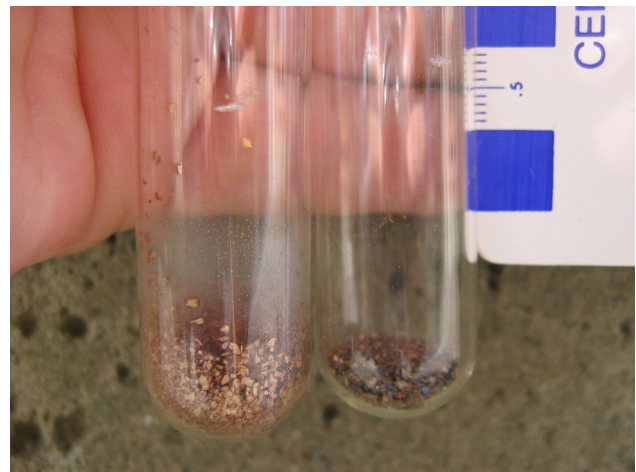


Figure 9. Separation of expanded vermiculite particles from the gangue and vermiculite-gangue composite grains of samples from outcrop adjacent to the Hodgie rare earth zone, Blue River area, east-central British Columbia; expanded vermiculite grains (left test tube) were separated by flotation (using water); composite grains, where vermiculite is attached to amphibole or other particles, have a tendency to remain within the gangue fraction (right test tube).

DISCUSSION

The vermiculite occurrence discussed in this paper may prove to be economically significant because 1) it has a relatively high vermiculite content, 2) related rudimentary exfoliation studies are encouraging, 3) there is currently no vermiculite (or perlite, the main substitute for vermiculite) production in British Columbia, and 4) the size of the surface exposure is encouraging. Evidence from the roadcuts indicates that, at least locally, carbonatites and fenites are heavily weathered (or otherwise altered) to depths in excess of 3 m. Since vermiculite is chemically inert, residual unconsolidated deposits may be found in other parts of the Blue River property. The discovery of this occurrence led to bibliographic research, which indicates that other vermiculite occurrences were reported and relatively well described in the Blue River area by McCammon (1950). These occurrences should be located and examined.

Detailed mineralogical and geochemical investigations are needed in the next stage of the investigation. Trace-element chemical analyses are required because excessive concentrations of base metals or radioactive elements could reduce the marketability of the product. Similarly, a detailed mineralogical study would be required to ensure that no asbestiform minerals are present in the vermiculite-bearing raw materials. Depending on the outcome of these mineralogical and chemical studies, more rigorous tests involving vermiculite pre-concentration and exfoliation tests may be justified and would be recommended prior to drilling or trenching.

Since the vermiculite-rich outcrops are located near the three diamond-drill holes (HO-08-1, HO-08-2 and HO-08-3) that intersect the Hodgie rare earth zone in the Blue River area, vermiculite occurrences should be analyzed for REEs. A detailed description of core (including mineralogy and geochemistry) from holes intersecting the Hodgie rare earth zone has not yet been released, and there is a possibility that it is also vermiculite rich. Vermiculite is considered by many researchers as a variety of clay. It has cation exchange capacity (CEC) in the range 100–150 milliequivalents per 100 g, more than most common clay varieties. Therefore, the remote possibility that this vermiculite mineralization also contains some REEs adsorbed (loosely bound) to the surfaces of the vermiculite laminae (analogous to the REE-bearing ionic adsorption halloysite-kaolinite ores of China) should also be investigated.

CONCLUSION

Vermiculite occurrences in the Blue River area have higher vermiculite content than any other vermiculite occurrences in British Columbia. These concentrations are comparable to the vermiculite grades in currently producing mines in other parts of the world. The response of raw vermiculite-bearing material to the exfoliation tests is encouraging. The next step should include detailed mineralogical and chemical studies. Excessive levels of base metals or radioactive elements may significantly reduce the range of potential uses for the expanded vermiculite. Similarly, detailed mineralogical study is required to establish that no asbestiform minerals are present in the vermiculite-bearing raw materials. If the outcome of these studies is positive, then rigorous metallurgical testing (vermiculite pre-concentration followed by standard exfoliation tests), mapping, trenching and drilling to establish the size and

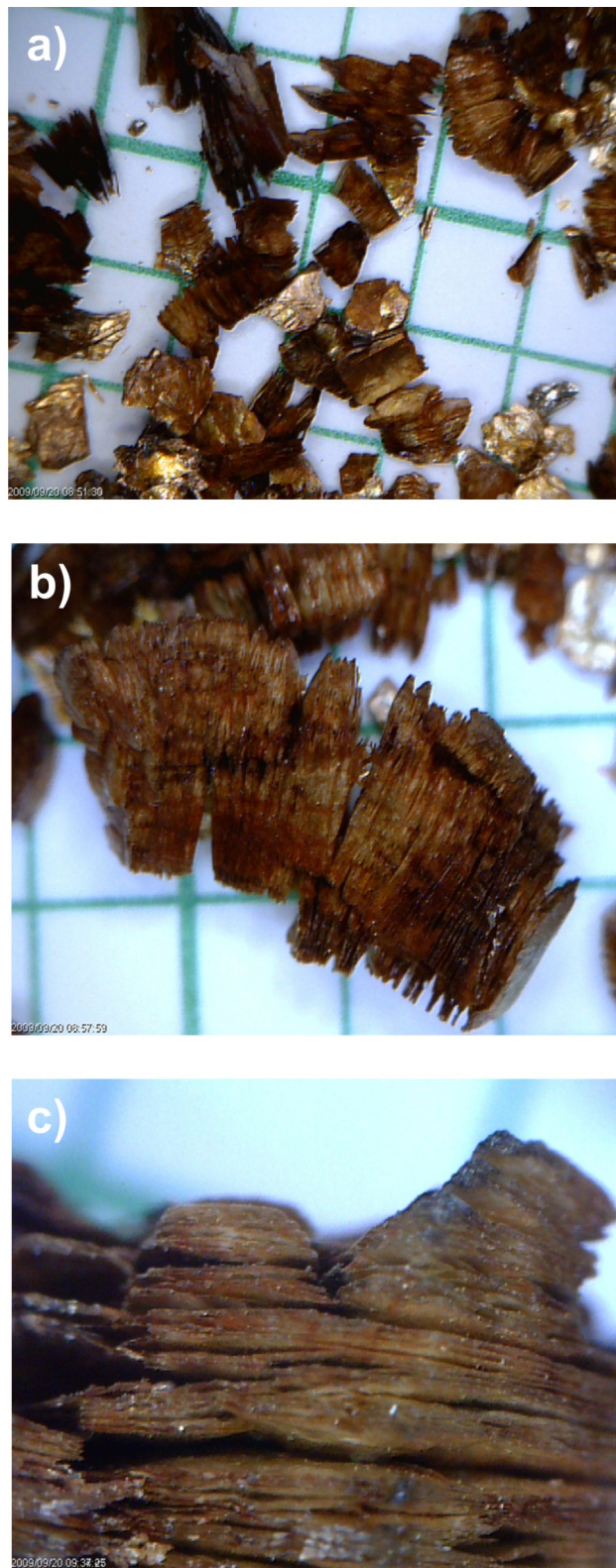


Figure 10. a) Exfoliated vermiculite-rich material derived from 2–4 mm size fraction of sample 09-SP-305, Blue River area, east-central British Columbia. b) Vermiculite particles expanding at right angles to their basal cleavage. c) Close-up of expanded vermiculite. In all three cases, the 2 mm grid is used for scale.

grade of the deposit may be warranted. Vermiculite-bearing samples should be also analyzed for REEs.

ACKNOWLEDGMENTS

The co-operation of Commerce Resources Corp. and manuscript reviews by Kirk Hancock are greatly appreciated. Ray Lett is thanked for the use of his digital microscope.

Natural Resources Canada, Earth Science Sector contribution 20090304.

REFERENCES

- Anonymous (2009): Industrial minerals; *Metal Bulletin Ltd.*, Number 501, page 69.
- Armbrustmacher, T.J., Modreski, P.J., Hoover, D.B. and Klein, D.P. (1996): Th-rare earth element vein deposits; in Preliminary Compilation of Descriptive Geoenvironmental Mineral Deposit Models, du Bray, E.A., Editor, *United States Geological Survey*, Open-File Report 95-831, pages 50–53.
- BC Geological Survey (2009): MINFILE BC mineral deposits database; *BC Ministry of Energy, Mines and Petroleum Resources*, URL <<http://minfile.ca>> [November 2009].
- Birkett, T. and Simandl, G.J. (1999): Carbonatite-associated deposits (magmatic, replacement and residual); in Selected British Columbia Mineral Deposit Profiles, Volume 3: Industrial Minerals, Simandl, G.J., Hora, Z.D. and Lefebure, D.V., Editors, *BC Ministry of Energy, Mines and Petroleum Resources*, Open File 1999-10, pages 73–76.
- Campbell, R.B. (1967): Canoe River, British Columbia; *Geological Survey of Canada*, Map 15-1967.
- Commerce Resources Corp. (2008): Development and exploration update for Blue River tantalum and niobium project in British Columbia; *Commerce Resources Corp.*, news release, December 4, 2008, 4 pages.
- Dahrouge, J. (2002): The Fir carbonatite, a potential tantalum-niobium resource; in Exploration and Mining in BC; *BC Ministry of Energy, Mines and Petroleum Resources*, pages 83–88.
- Digel, S.G., Ghent, E.D. and Simony, P.S. (1989): Metamorphism and structure of the Mount Cheadle area, Monashee Mountains, British Columbia; in Current Research, Part E, *Geological Survey of Canada*, Paper 89-1E, pages 95–100.
- Hindman, J.R. (2006): Vermiculite; in Industrial Minerals and Rocks; Kogel, J.E., Trivedi, N.C., Barker, J.M. and Krukowski, S.T., Editors, *Society for Mining, Metallurgy and Exploration Inc.*, pages 1015–1026.
- Mariano, A.N. (1989): Nature of economic mineralization in carbonatites and related rocks; in Carbonatites, Bell, K., Editor, *Unwin Hyman*, London, pages 149–176.
- McCammon, J.W. (1950): Vermiculite; in Minister of Mines, Annual Report, 1950; *BC Ministry of Energy, Mines and Petroleum Resources*, pages 229–230.
- McCammon, J.W. (1953): Lempriere; in Minister of Mines, Annual Report, 1952; *BC Ministry of Energy, Mines and Petroleum Resources*, pages 115–119.
- Modreski, P.J., Armbrustmacher, T.J. and Hoover, D.B. (1995): Carbonatite deposits; in Preliminary Compilation of Descriptive Geoenvironmental Mineral Deposit Models, du Bray, E.A., Editor, *United States Geological Survey*, Open-File Report 95-831, pages 47–49.
- Moeller, E. (2008): Vermiculite; *Mining Engineering*, Volume 60, Number 6, page 64.
- Morin, L. and Lamothe, J.-M. (1991): Testing on perlite and vermiculite samples from British Columbia; in Geological Fieldwork 1990, *BC Ministry of Energy and Mines and Petroleum Resources*, Paper 1991-1, pages 265–268.
- Mountjoy, K.J. (1992): MINFILE NTS 083D – Canoe River area and part of 083C – Brazeau; British Columbia; *BC Ministry of Energy, Mines and Petroleum Resources*, MINFILE, 133 pages.
- Obut, A. and Girgin, I. (2002): Hydrogen peroxide exfoliation of vermiculite and phlogopite; *Mineral Engineering*, Volume 15, pages 683–687.
- Obut, A., Girgin, I. and Yörükođlu (2003): Microwave exfoliation of the vermiculite and phlogopite; *Clays and Clay Minerals*, Volume 51, pages 452–456.
- Pell, J. (1994): Carbonatites, nepheline syenites, kimberlites and related rocks in British Columbia; *BC Ministry of Energy, Mines and Petroleum Resources*, Bulletin 88, 133 pages.
- Potter, M.J. (2009): Vermiculite; in Mineral Commodity Summaries, *United States Geological Survey*, pages 182–183.
- Richardson, D.G. and Birkett, T.C. (1996): Carbonatite associated deposits; in Geology of Canadian Mineral Deposit Types, Ecstrand, O.R., Sinclair, W.D. and Thorpe, R.I., Editors, *Geological Survey of Canada*, Geology of Canada, Number 8, pages 541–558.
- Simandl, G.J. (2002): Tantalum market and resources: an overview; in Geological Fieldwork 2001, *BC Ministry of Energy and Mines and Petroleum Resources*, Paper 2002-1, pages 315–320.
- Simandl, G.J., Birkett, T. and Paradis, S. (1999): Vermiculite; in Selected British Columbia Mineral Deposit Profiles, Volume 3: Industrial Minerals, Simandl, G.J., Hora, Z.D. and Lefebure, D.V., Editors, *BC Ministry of Energy, Mines and Petroleum Resources*, Open File 1999-10, pages 69–72.
- Simandl, G.J., Jones, P.C. and Rotella, M. (2002): Blue River carbonatites, British Columbia – primary exploration targets for tantalum; in Exploration and Mining in British Columbia – 2001, *BC Ministry of Energy and Mines and Petroleum Resources*, pages 73–82.
- Simandl, G.J., Irvine, M.L., Grieve, D., Lane R., Wojdak, P., Madu, B., Webster, I., Northcote, B. and Schroeter, T. (2007): Industrial minerals in British Columbia – 2006 review; *BC Ministry of Energy, Mines and Petroleum Resources*, Information Circular 2007-2, 14 pages.
- Weiss, Z., Valaskova, M., Seidlerova, J., Supova-Kristkova, M., Sustai, O., Matejka, V. and Capkova, P. (2006): Preparation of vermiculite nanoparticles using thermal hydrogen peroxide treatment; *Journal of Nanoscience and Nanotechnology*, Volume 6, pages 726–730.
- White, G.P.E. (1982): Notes on carbonatites in central British Columbia (83D/6E); in Geological Fieldwork 1981, *BC Ministry of Energy and Mines and Petroleum Resources*, Paper 1982-1, pages 68–69.
- White, G.V. (1990): Perlite and vermiculite occurrences in British Columbia; in Geological Fieldwork 1989, *BC Ministry of Energy and Mines and Petroleum Resources*, Paper 1990-1, pages 481–487.

Niobium-Thorium-Strontium-Rare Earth Element Mineralogy and Preliminary Sulphur Isotope Geochemistry of the Eaglet Property, East-Central British Columbia (NTS 093A/10W)

by Z.D. Hora¹, A. Langrová², E. Pivec³ and K. Žák²

KEYWORDS: Eaglet deposit, MINFILE 093A 046, fluorite, celestite, pyrochlore, thorite, titanbetafite, bastnaesite, sulphur isotopes

INTRODUCTION

The Eaglet fluorite property (MINFILE 093A 016) is located on the northeastern side of Quesnel Lake in east-central British Columbia in NTS area 093A/10W (Figure 1). The history, exploration activities, geological setting, petrography, mineralogy and estimated resource potential of the property have been previously described in Hora et al. (2008). That study identified several minerals not previously known from this fluorite deposit, including pyrochlore, thorite and rare earth element (REE)-enriched carbonate. In this paper, new data on the chemical composition, alteration and interrelationships of these unusual minerals have been collected. In addition, the sulphur isotope composition of celestite and common sulphide minerals was measured in several samples collected in the study area. Mineralogical and sulphur isotope studies were undertaken in Prague at the Institute of Geology, Academy of Sciences of the Czech Republic, using the methodologies described in Hora et al. (2008), and the Czech Geological Survey, Czech Republic.

NIOBIUM-THORIUM-TITANIUM-RARE EARTH ELEMENT MINERALOGY

Pyrochlore ($(\text{Na}, \text{Ca})_2(\text{Nb}, \text{Ca})_2\text{O}_6(\text{O}, \text{OH}, \text{F})$) is the dominant mineral in this group; it occurs as small ($\sim 50 \mu\text{m}$ in diameter) iso-

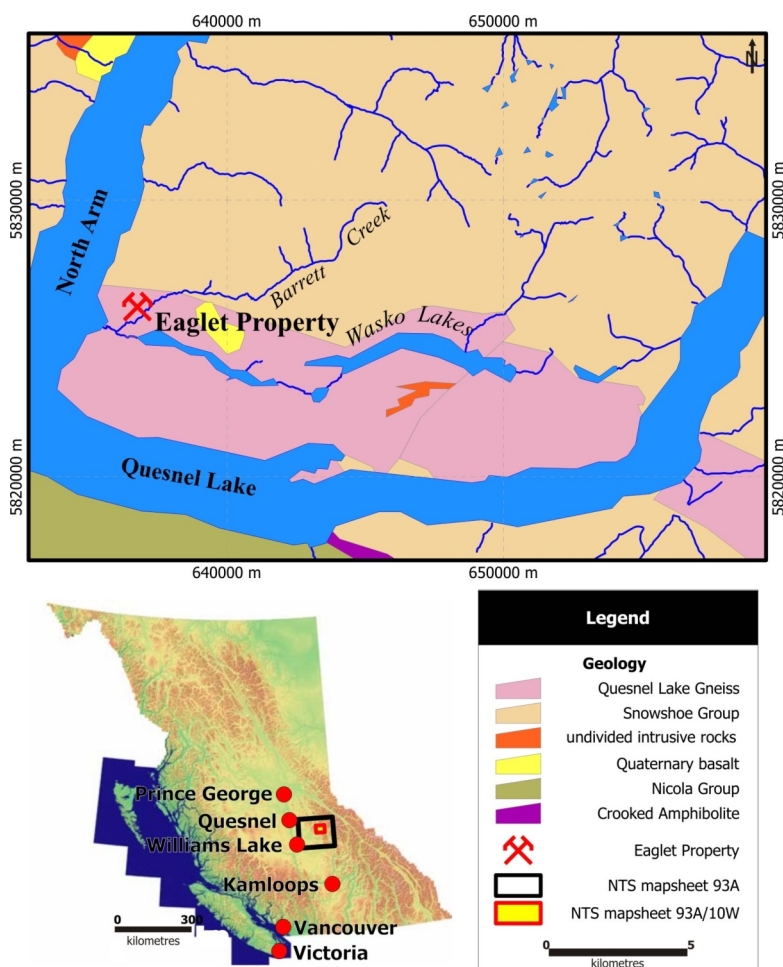


Figure 1. Location of study area, northeastern side of Quesnel Lake, east-central British Columbia.

metric grains, which commonly have partially preserved octahedron crystal habits. Pyrochlore also forms crystal-line aggregates up to $150 \mu\text{m}$ in width; these aggregates are commonly associated with zircon, kaolinite and uraninite in a matrix of K-feldspar. The most abundant elements measured by the electron microprobe are Nb, Ti (Figure 2) and U, which is as expected for pyrochlore. The pyrochlore from the Eaglet property (Table 1) also has relatively high FeO contents (up to 19.22%). Other notable observations include an inverse correlation between calcium and uranium abundances with niobium (Table 1); this is likely the result of alteration intensity (Figures 3a–d). The alteration and partial replacement of pyrochlore is especially well-de-

¹ British Columbia Geological Survey, Victoria, BC (retired)

² Institute of Geology, Academy of Sciences of the Czech Republic, Prague, Czech Republic

³ Institute of Geology, Academy of Sciences of the Czech Republic, Prague, Czech Republic (retired)

This publication is also available, free of charge, as colour digital files in Adobe Acrobat® PDF format from the BC Ministry of Energy, Mines and Petroleum Resources website at <http://www.empr.gov.bc.ca/Mining/Geoscience/PublicationsCatalogue/Fieldwork/Pages/default.aspx>.

veloped along crystal margins; its development imparts a light grey colour to the crystal margins. Uraninite and an unidentified highly hydrated mineral with 59.6% ThO₂ and 10.1% CaO occur as alteration products of pyrochlore. The identification of uraninite as an alteration product of pyrochlore is suggested by the unusual abundance of Nb, Ti, Fe and Ca (Table 1).

A carbonate mineral compound of La, Ce, Gd and Sm, probably bastnaesite ((La, Ce)CO₃F), commonly occurs in association with pyrochlore (Figures 3a–c). Bastnaesite frequently forms minor inclusions in pyrochlore (Figure 3c) and some individual bastnaesite grains range up to 10 µm in length. It is also found in cavities and fractures in other minerals such as pyrite.

Thorite (ThSiO₄) is another common mineral found in this mineral association from the Eaglet property; it occurs as isometric grains typically about 100 µm in diameter.

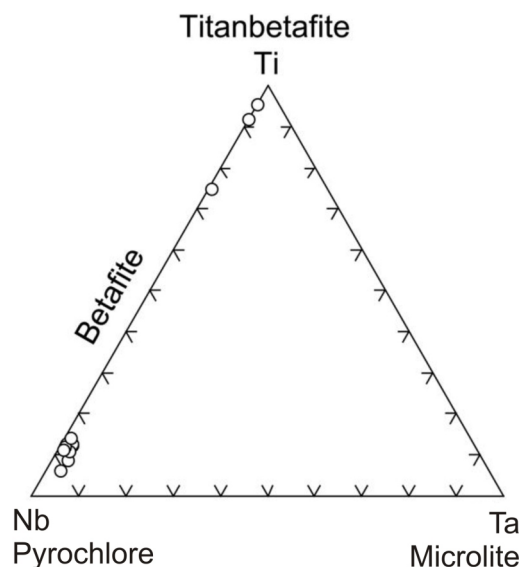


Figure 2. Ternary Ti-Nb-Ta diagram (from Godovikov, 1975) of Eaglet deposit minerals, east-central British Columbia. Points corresponding to titanbetafite were measured within one grain, whereas the cluster of points corresponding to pyrochlore represents 15 measurements in multiple adjacent grains.

Thorogummite ((Th, U)SiO₄(OH)₄; Figure 3f) commonly forms a reaction rim around a central core of thorite.

Titanbetafite, a titaniferous member of the pyrochlore family, is the least common mineral identified in samples examined from the Eaglet property (Figures 2, 3e); it is present as xenomorphic grains, which can reach up to 100 µm in length. The niobium content of titanbetafite is more variable than that of pyrochlore.

In conclusion, the Nb-Th-Ti-REE group of minerals exhibit extensive replacement reactions along their contacts with adjacent silicate minerals and alteration products. This finding suggests that the Nb-Th-Ti-REE group of minerals may represent an early stage of the mineralization process in the deposit.

SULPHUR ISOTOPE GEOCHEMISTRY

The presence of celestite (SrSO₄) has been recognized at the Eaglet property since the deposit's discovery. Although early exploration programs by Eaglet Mines Ltd. did not include analysis for strontium, the systematic inductively coupled plasma-mass spectrometry analytical work conducted later by Freeport Resources Inc. led to the discovery of the widespread distribution of celestite throughout the deposit. Values commonly in excess of 10 000 ppm Sr were reported from drillcore samples (Hora, 2005). A preliminary sulphur isotope study of celestite and several sulphide minerals (pyrite and molybdenite) was undertaken to provide a better understanding of the Eaglet deposit.

Celestite-enriched zones were separated from the samples by a combination of crushing and hand-picking; the samples were then homogenized in an agate mortar, dissolved in diluted HCl and the insoluble residuum filtered off. The dissolved sulphate was then precipitated as BaSO₄ by the addition of a solution of BaCl₂. The BaSO₄ was converted to SO₂ gas following the method outlined in Haur et al. (1973) with modifications described in Yanagisawa and Sakai (1983).

Sulphide minerals were hand-picked from crushed samples and oxidized to SO₂ following the procedure in Grinenko (1962). The sulphur isotope compositions of the prepared SO₂ gas samples were measured using a Finnigan

Table 1. Major-element content of representative minerals of niobium, thorium and uranium, Eaglet prospect, east-central British Columbia.

Oxide (%)	Pyrochlore			Titanbetafite		Thorite		Thorogummite		Uraninite
ThO ₂	0	0.01	0.37	0	0.04	73.73	71.69	66.35	66.18	0.38
TiO ₂	5.65	7.02	9.68	70.71	93.01					0.72
Nb ₂ O ₅	70.79	61.72	56.87	19.67	3.65					4.75
Ta ₂ O ₅	2.17	2.15	0.61	0.69	0.17					0
U ₂ O ₃	1.27	9.57	6.76	0	0	1.9	2.44	1.85	1.71	92.65
MnO	0.77	0	0.15	0.23	0.02					0
FeO	19.22	0.59	3.55	5.23	1.02	0.01	0.3	0.16	1.17	1.28
CaO	0.12	8.25	4.21	0.05	0.02	0.33	0.32	0.65	2.14	0.91
Na ₂ O	0	0.33	0.4	0.06	0.06					0
SiO ₂	0	0	2.58	0.42	0.04	18.33	18.19	17.07	15.07	0
Total	99.99	89.64	85.18	97.06	98.03	94.3	92.94	86.08	86.27	100.69
a.p.	4	5	11	12	13	15	16	17	18	x

Explanation: a.p., analytical points from Figure 2; x, not represented on Figure 2; empty spaces, elements not analyzed.

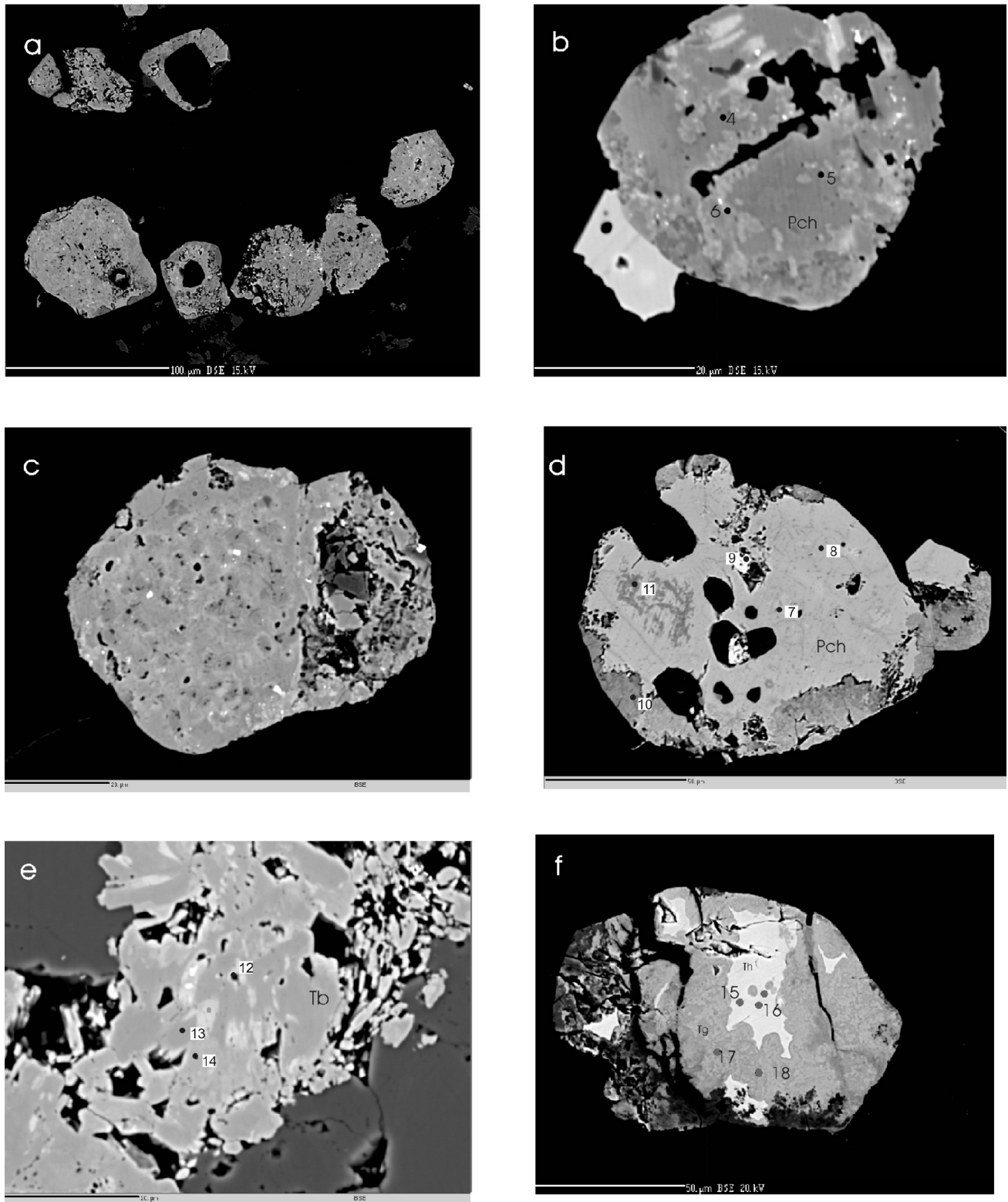


Figure 3. Scanning electron microscope photomicrographs showing **a**) partially replaced pyrochlore (Pch) crystals in host silicates with altered rims (dark shade); white dots are bastnaesite (scale bar 100 μm); **b**) corroded and altered crystal of pyrochlore; large white grain corresponds to bastnaesite; analytical points 4 and 5 (dark field), 6 (pale grey field) (scale bar 20 μm); **c**) typical occurrence of pyrochlore; small white grains correspond to bastnaesite (scale bar 20 μm); **d**) partially replaced pyrochlore rimmed by darker altered zones corresponding to altered pyrochlore; enclosed white grain (analytical point 9) is unidentified hydrated mineral close to thorianite; analytical points 7, 8, 9, 10 and 11 (scale bar 50 μm); **e**) titanbetafite (Tb) with variable contents of niobium; analytical points 12, 13 and 14 (scale bar 20 μm); **f**) thorite (Th) replaced by thorumgummite (Tg); analytical points 15, 16, 17 and 18 (scale bar 50 μm).

Table 2. Sulphur isotope data, Eaglet property, east-central British Columbia.

Sample no.	Mineral composition of the sample	$\delta^{34}\text{S}$ celestite (‰)	$\delta^{34}\text{S}$ sulphide (‰)
QL A-1	celestite, fluorite, quartz	6	
QL A-2	celestite, quartz, fluorite	7.06	
QL A-3	quartz, celestite, fluorite, feldspar	12.91	
QL A-4	celestite, quartz, fluorite, molybdenite	7.12	molybdenite: -4.81
QL A-5	celestite, fluorite, quartz, feldspar	6.87	
QL C-1	calcite, celestite, pyrite	9.86	pyrite: -4.84

MAT 251 mass spectrometer in the laboratories of the Czech Geological Survey, in Prague. Overall uncertainty in analytical measurements of ^{34}S from both sulphate and sulphide minerals is $\pm 0.2\%$. Analyses are reported relative to the Canyon Diablo troilite (CDT) standard.

RESULTS

The sulphur isotope analyses yielded the data presented in Table 2.

DISCUSSION

Measurements of ^{34}S from celestite that range between 6.00 and 12.91‰ (CDT) exclude the possibility of precipitation from metamorphic fluids mobilizing marine evaporites or of hydrothermal mobilization of sulphate minerals from evaporites of marine origin. Throughout the Earth's history, marine evaporites have had sulphate ^{34}S values greater than 10‰ (greater than 25‰ during the Late Proterozoic) and during the Mississippian, the presumed age of the Eaglet prospect host intrusion, ^{34}S values were greater than 20‰ (CDT). Only minor sulphur isotope fractionation is imparted during metamorphism of massive accumulations of evaporitic sulphate minerals or during hydrothermal mobilization of sulphate minerals followed by sulphate precipitation (in the order of a few sulphur isotopes per mil). The only exception is a high-temperature sulphur isotope exchange between sulphide and sulphate minerals, which can significantly alter the isotope composition of both minerals.

The sulphide minerals (pyrite and molybdenite) have ^{34}S values of -4.8‰ (CDT). The difference between the ^{34}S values of sulphide minerals and those of sulphate minerals is ~12–15‰. Isotope fractionation between sulphate and sulphide minerals can be used as a geothermometer (Ohmoto and Rye, 1979); when reduced and oxidized, sulphur minerals reach isotope equilibrium and the sulphide-sulphate fractionation reported here corresponds to temperatures of 450–540°C. More work is required to verify the occurrence of isotope exchange equilibrium in sulphide and sulphate minerals; in the absence of such verification, there are several ways to interpret the data:

the sulphate minerals (e.g., celestite) and sulphide minerals (pyrite and molybdenite) were formed independently, at different stages of the ore-forming process;

the sulphate minerals and sulphide minerals formed following the mobilization of sulphur from different crustal reservoirs; and

the sulphate minerals and sulphide minerals were influenced by high-temperature (~450–540°C) isotope exchange between reduced and oxidized sulphur species.

SUMMARY

In conclusion, the Nb-Th-Ti-REE group of minerals may represent an early stage of the mineralization process in the Eaglet deposit. The sulphur isotope studies allow for several interpretations of the results and more work is required to verify which interpretation applies to the Eaglet deposit.

ACKNOWLEDGMENTS

The authors would like to thank the following persons for their help in the preparation of this manuscript. M. Mihalyuk and S. Rowins provided constructive comments to improve the original manuscript, J. Pávková and Z. Korbelová provided technical assistance, V. Boehmová helped with the electron microscopy and I. Jačková operated the mass spectrometer.

REFERENCES

- Godovikov, A.A. (1975): Mineralogia; *Nedra*, Moscow, 423 pages (in Russian).
- Grinenko, V.A. (1962): The preparation of sulphur dioxide for isotopic analysis; *Zhurnal Neorganicheskoi Khimii (Russian Journal of Inorganic Chemistry)*, Volume 7, pages 2478–2483 (in Russian).
- Haur, A., Hladíková, J. and Šmejkal, V. (1973): Procedure of direct conversion of sulphates into SO_2 for mass spectrometric analysis of sulphur; *Isotopenpraxis*, Volume 9, pages 329–331.
- Hora, Z.D. (2005): Assessment report on the Eaglet property; *BC Ministry of Energy, Mines and Petroleum Resources*, Assessment Report 27823, 253 pages.
- Hora, Z.D., Langrová, A. and Pivec, E. (2008): Eaglet property revisited: fluorite-molybdenite porphyry-like hydrothermal system, east-central British Columbia (NTS 093A/10W); *BC Ministry of Energy, Mines and Petroleum Resources*, Paper 2008-1, pages 17–30.
- Ohmoto, H. and Rye, R.O. (1979): Isotope of sulfur and carbon; in *Geochemistry of Hydrothermal Deposits*, H.L. Barnes, Editor, *John Wiley and Sons*, pages 509–567.
- Yanagisawa, F. and Sakai, H. (1983): Thermal decomposition of barium-sulfate vanadium pentoxide silica glass mixtures for preparation of sulfur-dioxide in sulfur isotope ratio measurement; *Analytical Chemistry*, Volume 55, pages 985–987.

Evaluation of 'Reduced' Intrusive-Related Gold Mineralization in the Area West of Cranbrook, Southeastern British Columbia (NTS 082F/08, 16)

S.G. Soloviev¹

KEYWORDS: East Kootenay, Purcell Supergroup, Bayonne plutonic belt, intrusive-related gold, thrust fault, mineralized stockwork, coarse gold, hydrothermal alteration, geochemistry

INTRODUCTION

Gold mineralization is widespread in the vicinity of Cranbrook in southeastern British Columbia but especially abundant some 5–30 km west of the town, where many significant Au prospects have been known since the 19th and early 20th centuries (Figure 1). Since then, several exploration campaigns have been undertaken in this area, resulting in the discovery of numerous Au occurrences and delineation of local small Au resources. Recent 'peaks' in exploration occurred in 2002–2004, when Chapleau Resources Ltd. conducted massive data compilation, prospecting and rock and soil sampling programs, followed by almost 7000 m of reconnaissance, structural and delineation drilling. In 2007–2008, Ruby Red Resources Inc. also undertook significant diamond-drilling. These studies identified many new mineralized showings and demonstrated styles of Au mineralization characteristic of proximal and distal intrusive-related settings. This contributed to a better understanding of likely intrusive-related Au mineralization in southeastern BC. Gold exploration continues in the area, making it worthwhile to summarize and interpret some of the existing data.

EXPLORATION HISTORY

Placer Au was first discovered in the East Kootenay region at Wildhorse River, Moyie River, Perry Creek and Palmer Bar Creek in the 1860s, resulting in a Au rush and construction of the town of Fort Steele. Although no reliable estimate of Au production exists, the Wildhorse River is believed to have produced more than \$20 million in Au from placer mining, suggesting total Au production of approximately 1.7–2.5 million oz. (BC Ministry of Energy, Mines and Petroleum Resources, 1898). Significant placer Au production also occurred within the Perry Creek drainage and in the Moyie River basin. The East Kootenay region also underwent exploration for 'Sullivan-type' sedimentary-exhalative (SEDEX) Pb-Zn mineralization

following the discovery of the Sullivan mine in the late 19th century.

The area west of Cranbrook has undergone multiple episodes of Au exploration, beginning in the early 20th century, that led to the discovery of numerous mineral prospects. Many historical workings are present in the area. The largest of them include adits, shafts and open cuts (now caved) at the Columbia vein (MINFILE 082FSE009; BC Geological Survey, 2009), Homestake (082FSE012), Shakespeare (082FSE119), Leader (082FNE060) and other higher grade Au-bearing quartz veins ('lodes'). More recently, lode Au exploration in the area included prospecting, soil sampling, very low frequency electromagnetic (VLF-EM) surveys, geological mapping, bulldozer trenching and sampling for heavy-mineral concentrates (e.g., Troup and Wang, 1981; Holcapek, 1982). Some of the larger quartz veins were drilled, but samples returned only sporadic (although locally high-grade) intercepts of Au (Ridley and Troup, 1984; Hardy, 1986). Drilling was also conducted on the Zeus claims to the east.

In 1985–1987, Partners Oil & Minerals Ltd. established the presence of a large and strong Au-in-soil anomaly near Gold Run Lake (Brewer, 1987). Also in the mid-1980s, the old Yellow Metal prospect was explored using soil geochemistry and ground geophysics (Mark, 1986). In 1993, Consolidated Ramrod Gold Corp. expanded the soil anomaly and established its relationship to a north-north-east-striking Au-mineralized vein-shear-zone system (Klewchuk, 1994). In 1999, more detailed surface prospecting and rock geochemistry established the presence of widespread anomalous Au in bedrock, associated with quartz-pyrite stockworks and breccias. This style of Au mineralization is distinctly different from the high-grade lode Au occurrences (Klewchuk, 2000). In 2000, National Gold Corporation expanded the soil anomaly in a north-easterly-trending zone measuring 3.5 km by 2.0 km (Klewchuk, 2000, 2001). Subsequent work established this occurrence as the Zinger prospect (MINFILE 082FSE122).

In 1983–1985 and 1990–1991, significant exploration was conducted on the Bar prospect (MINFILE 082GSW068), initially targeting its base-metal potential (McDonald, 1986) and then its Au (Leask, 1992) potential. A large multi-element geochemical anomaly was identified and follow-up trenching uncovered a series of Au-mineralized zones associated with strongly altered syenite dikes. Highlights of the trenching included 4.52 g/t Au over 26.0 m, including 7.42 g/t Au over 11.0 m, 3.08 g/t Au over 18.0 m, 2.09 g/t Au over 16.0 m and 1.54 g/t Au over 30 m (Leask, 1992). The Au mineralization was traced in trenches for 280 m along strike and remained open ended. In 2002, Chapleau Resources Ltd. generally confirmed the Au grades and intervals encountered in the trenches. In addition, an extension of the mineralized structure farther

¹ International GeoSol Consulting Inc., Calgary, AB, serguei07@hotmail.com

This publication is also available, free of charge, as colour digital files in Adobe Acrobat® PDF format from the BC Ministry of Energy, Mines and Petroleum Resources website at <http://www.empr.gov.bc.ca/Mining/Geoscience/PublicationsCatalogue/Fieldwork/Pages/default.aspx>.

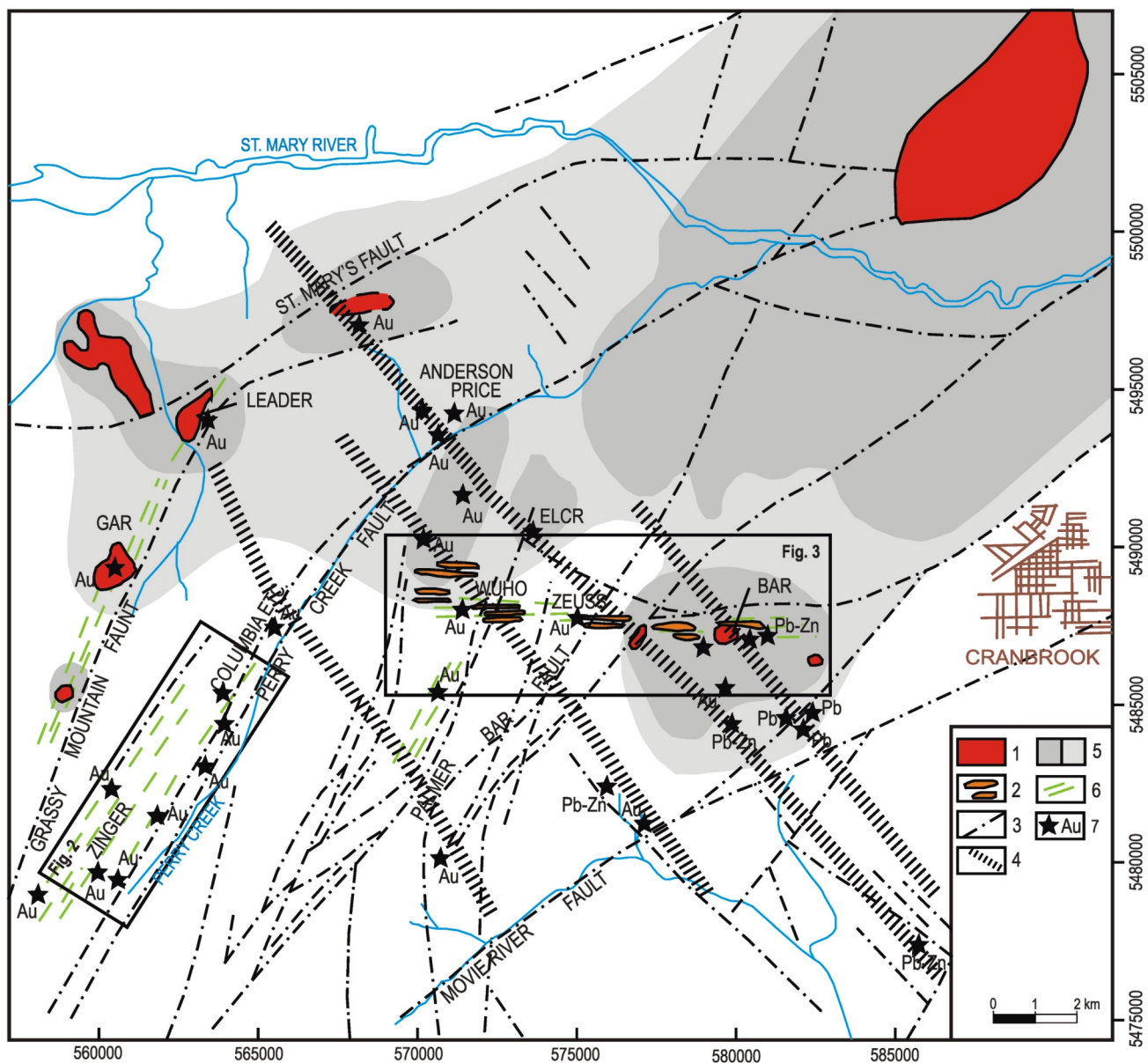


Figure 1. Geological setting of the Cranbrook area (compiled after Brown, 1998; BC Geological Survey, 2009), southeastern British Columbia, showing regional magnetic survey data (MapPlace, 2009). Legend: 1, Mesozoic (mid-Cretaceous?) quartz monzonite to granodiorite and granite intrusive rocks (Bayonne plutonic belt); 2, syenite to quartz syenite dike (not to scale); 3, major fault zone; 4, suggested concealed fault (airphoto lineament); 5, strong and moderately strong positive magnetic anomaly (total magnetic intensity); 6, large zone of quartz veining; 7, mineral occurrence.

west and east was confirmed by surface rock sampling, establishing a total strike length for the mineralized structure in excess of 1 km (Soloviev, 2003).

In 2002–2004, Chapleau Resources Ltd. conducted significant exploration work on the majority of the prospects found in the area. Reconnaissance-style and detailed follow-up prospecting and rock geochemical sampling were conducted on the Bar, Zeus, ELCR (MINFILE 082FSE117), Wuhoh, Zinger, Gar (082FSE065), Leader, Lov and other prospects, covering a total area in excess of 650 km². Detailed prospecting was carried out on the Bar, Zeus, ELCR, Wuhoh, Zinger and Gar prospects. Grid soil-geochemical sampling was conducted on three prospects (Bar, Zinger and Zeus); on Zinger, the soil sampling cov-

ered an area measuring 18 km by 3 km. The Bar and Zinger prospects were drilled (7000 m in total). In 2007–2009, Ruby Red Resources Ltd. conducted another round of exploration, which included diamond-drilling, on the Gar and Zeus prospects (e.g., Ransom, 2006; Klewchuk et al., 2007). The drilling encountered Au and Cu mineralization in zones of intense hydrothermal alteration associated with the intrusive bodies.

DISTRICT GEOLOGY AND METALLOGENY

The Cranbrook area of southeastern BC lies west of the Rocky Mountain Trench within the Purcell Anticlinorium

of the Omineca orogenic belt, a Proterozoic pericratonic terrane subjected to tectonic and magmatic activation (of distal subduction-related and/or anorogenic type) that occurred mainly in the Mesozoic (e.g., Hoy and Van der Heyden, 1988; Hoy, 1993). The area comprises an older (Precambrian) metasedimentary package and younger (Mesozoic) igneous suites.

Precambrian Metasedimentary and Igneous Rocks

The Cranbrook area is underlain by Mesoproterozoic terrigenous clastic, carbonate and minor volcanic rocks of the Purcell Supergroup that are believed to have been deposited in an intracontinental rift system (e.g., Hoy, 1993; Hoy et al., 1995; Lydon, 2007). They include the basal Aldridge Formation, composed of siliciclastic turbidites 4000 m thick and informally divided into the lower, middle and upper units. The lower Aldridge, the base of which is not exposed, comprises about 1500 m of thin- to medium-bedded argillite, wacke and quartzitic wacke, generally interpreted as distal turbidites. The Sullivan SEDEX orebody occurs at the top of this division (Lydon, 2007). The middle Aldridge contains about 2500 m of grey to rusty, dominantly medium-thick-bedded, quartzitic wacke turbidites with minor thin-bedded argillite, some of which forms finely laminated marker beds (time stratigraphic units correlated over great distances within the Purcell Basin). The upper Aldridge includes about 300 m of dark argillite and grey siltite. The Aldridge Formation is tectonically (?) overlain by the Creston Formation, consisting of quartzite and grey, green and maroon wacke up to 1800 m thick (Hoy, 1993). In turn, the Creston Formation is overlain by the Kitchener Formation, which includes oolitic limestone and dolomitic siltstone (Hoy, 1993). The Purcell Supergroup has been intruded by sills and somewhat discordant sheets and dikes of the 1443 ± 10 Ma Moyie Sill suite, which are most prominent in the lower portions of the Aldridge Formation.

Mesozoic Plutonic Suite(s)

In the Cranbrook area, the Purcell Supergroup is intruded by a number of dikes, stocks and larger plutons of mostly granodiorite, monzonite and possibly syenite composition, which are assigned to the Mesozoic. However, their age relationships are not well constrained.

The larger intrusions, composed essentially of granodiorite, likely correspond to the mid-Cretaceous Bayonne plutonic suite. As defined by Logan (2002), this suite comprises monzogranite, granodiorite, biotite granite and biotite-muscovite granite. The Bayonne suite intrusions occupy north-northeast-trending corridors in the larger north-trending magmatic belt that roughly parallels the orientation of major Cordilleran structures in the region. These plutons include the Reade Lake stock (94 Ma, U-Pb method) in the northeastern part of the area (Figure 1) and possibly the Kiakho stock (122 Ma, K-Ar method) in the southeastern part of the Bar prospect (Hoy and Van der Heyden, 1988). These stocks are alkalic, with a relative enrichment of alkali elements within the Kiakho stock. Other likely Bayonne suite intrusions in the area include the large (at least 2 km by 1 km) granodiorite to granite stock outcropping on the Gar prospect (Grassy Mountain) and the large granodiorite stock in the Palmer Bar Creek area.

The airborne magnetic survey data (MapPlace, 2009) show the presence of a large positive magnetic anomaly surrounding the Reade Lake pluton and extending roughly northeastward. This suggests that the pluton has much greater dimensions at depth and that its emplacement or modification was controlled by the northeast- to north-northeast-trending lineaments (Figure 1). The smaller stocks are also accompanied by positive magnetic anomalies that trend northeastward. In general, most of the Au and other metal occurrences in the area are located proximal to the larger positive magnetic anomalies (Figure 1), thus emphasizing the intrusive-related nature of these occurrences.

A distinct set of intrusive units occupies east-trending zones within the area. These include swarms of parallel dikes or narrow intrusive apophyses adjoining larger intrusions at depth (Figure 1). The best exposed and most studied dike swarm is traceable for 10–12 km between the Bar, Zeus and Wuho prospects. The dikes are medium- to coarse-grained porphyritic syenite or quartz syenite characterized by large phenocrysts of potassium feldspar. Drilling on the Bar prospect has demonstrated a gradual transition of these dikes into medium-grained, weakly porphyritic quartz monzonite at depth (Soloviev, 2003). Apart from this, there is no direct evidence to constrain the relationships of these ‘dikes’ to other plutons in the area. It appears, however, that the north-northeast-trending structures hosting Au mineralization and controlling the Bayonne suite intrusions are younger than the east-trending structures hosting the dikes and associated mineralization.

Tectonic and Metallogenic Setting

The oldest and best known metallogenic feature in the area is the SEDEX Pb-Zn mineralization preserved in the Mesoproterozoic sedimentary rocks. This mineralization includes the world-class Sullivan SEDEX Pb-Zn deposit, located north of the area, and a number of much smaller Pb-Zn occurrences that are hypothesized to correspond with this age and style of mineralization (Hoy et al., 1995).

Southeastern BC is underlain by continental-margin rocks of ancestral North America and various magmatic suites, suggesting it is a southern continuation of the metallogenically significant Tintina Au belt of Yukon-Alaska. This was originally pointed out by Lefebure and Cathro (1999) and Logan (2000, 2002), who emphasized that the Mesozoic (mid-Cretaceous) age and composition (mostly granodiorite) of the intrusions found in southeastern BC are similar to those of the Tombstone and other plutonic suites in the Yukon that are accompanied by intrusive-related Au mineralization. Extending the Au-W-Sn metallogenic province, or belt, 1600 km from the Yukon south to Salmo (Lefebure and Cathro, 1999; Logan, 2000, 2002) highlights the potential for similar mineralization in the Cranbrook area. This belt contains significant Au mineralization from the Cariboo and Cassiar camps along its entire length. In the south, the mid-Cretaceous Bayonne plutonic suite forms an arcuate metallogenic zone extending along the eastern edge of the Kootenay Arc from northwest of Salmon Arm through the Revelstoke, Golden and Cranbrook areas to beyond the Canada–United States border (Logan, 2002).

There are at least three structural trends in the Cranbrook area that control possible Mesozoic intrusive-related Au mineralization. First, the major north-northeast- to northeast-trending fault system that roughly parallels the

orientation of the major Cordilleran orogenic belts extends through the entire area. This system includes a number of well-exposed faults (Palmer Bar, Old Baldy, Perry Creek, Dublin and Grassy Mountain) that cut and displace Mesoproterozoic rock sequences and Mesozoic intrusions. These faults appear to follow older faults, which control the emplacement of the Mesozoic stocks arranged as north-northeast- to northeast-trending chains and mostly corresponding to magnetic features, suggesting the presence of hidden intrusions at depth. In total, this suggests long-lasting activity on these faults. Fault and deformation zones with this orientation commonly host significant occurrences of Au-bearing quartz and quartz-sulphide veins and stockworks. Typically, native Au occurs in isolation in quartz or is associated with elevated abundances of pyrite, galena and chalcopyrite (e.g., Soloviev, 2004b).

Second, east-striking faults and airphoto lineaments are also common in the area, although these faults are typically less well expressed than the north-northeast- to north-east-trending varieties or have experienced less reactivation. One of the most pronounced east-trending features occurs in the central part of the area and is marked by swarms of porphyry dikes (quartz syenite to quartz monzonite to granite). Gold mineralization is associated with this structural trend. The Au-bearing zones are characterized by intense silicification, phyllic and argillic alteration, and quartz and quartz-sulphide veins and stockworks. Gold is commonly associated with elevated contents of As, Cu and locally Bi. Some larger quartz veins (up to 3–5 m thick) contain native Au with or without pyrite. Other smaller (?), east-trending zones are present elsewhere in the area (Figure 1).

The third structural trend is oriented to the northwest. It is expressed to a lesser degree, although it can be found to control some smaller granodiorite to granite stocks, relatively small deformation zones and swarms of quartz veins. This orientation is coincident with that reported for the Vine vein (MINFILE 082GSW050), which is interpreted to be Middle Proterozoic ‘Sullivan-style feeder’ mineralization (e.g., Hoy and Pighin, 1995), although its upper age limit is not constrained. It contains abundant arsenopyrite and lesser pyrrhotite, sphalerite and galena in a gangue assemblage of quartz, sericite, calcite, chlorite and minor albite. The fault zone hosting this vein can be traced to the Bar prospect, where similar Pb-Zn-As mineralization also occurs in northwest-striking zones that apparently overprint the east-striking Au mineralization. Other northwest-striking Pb-Zn-As (+Au+Ag) veins are common in the area, suggesting that they may be part of a district-scale vein system. Although hosted by Precambrian metasedimentary rocks, these base-metal veins may have formed in response to Mesozoic magmatism. Zonation of Au and base-metal mineralization in relation to the causative intrusion is well documented for intrusive-related mineralization (Hart, 2007).

In summary, these three fault systems have likely experienced reactivation to form an interconnected structural network that acted as permeable ‘conduits’ to localize the deposition of Au and associated minerals in the area.

LOCAL GEOLOGY OF SOME AU PROSPECTS

The most studied Au occurrences include the Zinger, Gar (Grassy Mountain) and Leader prospects from the north-northeasterly mineralized trends, and the Bar, Zeus and Wuho prospects from the easterly mineralized trends. Some of these mineralized trends correspond to distinct corridors of small intrusive stocks and dikes, probably marking the fault zones that controlled magmatism and mineralization. A north-northeast-trending corridor of small granodiorite to monzonite intrusions and the Grassy Mountain fault can be traced between the Gar and Leader prospects in the western portion of the area. Farther northeast, this corridor trends toward the large northeast-elongated Reade Lake intrusion. The smaller intrusions to the southwest of the Reade Lake body might be correlative satellite bodies. At least, most of these smaller stocks lie within the large positive magnetic anomaly surrounding the Reade Lake intrusion to the southwest. The Bar, Zeus and Wuho prospects follow a swarm of easterly-trending quartz syenite (?) dikes (Figure 1).

Gar (Grassy Mountain; MINFILE 082FSE065) and Leader (MINFILE 082FNE060) Prospects

These prospects cover a broad north-northeast-trending strip of highly deformed, altered and mineralized rocks that extends for 7–8 km along the western edge of the area. This mineralized corridor is coincident with a chain of granodiorite stocks and displays a variety of auriferous mineralization styles from quartz stockworks within the intrusions and in their proximity to shear-controlled quartz-sulphide veins in more distal settings.

In particular, the Gar prospect occupies the southern part of this corridor and is represented by intense auriferous quartz to quartz-Fe-carbonate-sericite-pyrite (locally with traces of galena) stockwork veins and larger quartz veins overprinting a 2 km by 1 km stock of granodiorite to granite and adjacent metasedimentary rocks with a coincident positive magnetic anomaly. The stockwork comprises several north-northeast-striking mineralized zones that are 100–150 m in width and traceable for more than 2–3 km along strike. About 250 rock samples, collected in 2001–2004 over a large part of the stockwork, returned values of generally less than 0.5–1 g/t Au, with several values in the range of 8–12 g/t Au. The zone of structural complexity and quartz veining corresponding to the mineralized zone encountered on the Gar prospect was traced farther southwest for a distance of 3–4 km (Soloviev, 2004b). In 2007, the Gar prospect was drilled by Ruby Red Resources Inc.; drilling encountered quartz veinlets in a stockwork overprinting quartz monzonite and containing up to 0.11 g/t Au over 1 m, and quartz-sulphide veinlets containing up to 3.0 g/t Au, 394 g/t Ag and 2.4% Pb, with minor Zn and Cu (Klewchuk et al., 2007). Ransom (2006) reported a strong Mo-in-soil anomaly coincident with the stock; rock sampling also revealed locally elevated Mo values in Au-bearing and Au-free quartz veinlets (Table 1).

To the north-northeast, the zone of quartz veining was traced for 2–3 km to the Leader prospect. This prospect is represented by a narrow (averaging 0.5 m) but extended (traced for 650 m), subvertical quartz-sulphide vein in the vicinity of a porphyry granite intrusive outcropping west of

the vein. The vein contains abundant galena and chalcopyrite, along with pyrite and scheelite; it returned high Au values for its entire length, with numbers varying from 0.7 to 164 g/t Au, together with 10–1971 g/t Ag, 1.5–69.5% Pb and 6.8–10% Cu (Sookochoff, 1985). Another round of sampling in 2003 returned similarly high values: 12 of the 28 samples returned values exceeding 1 g/t Au, and six of them contained more than 10 g/t Au, the highest being 37.7 g/t Au. Many samples also returned high values of Pb (up to 19.4%), Ag (up to 675 g/t), Cu, Zn, Sb and elevated W (Soloviev, 2004b).

Zinger Prospect (MINFILE 082FSE122)

The Zinger prospect covers a broad mineralized corridor parallel to and 2–3 km east of the Gar and Leader prospects. It is apparently the largest Au prospect in the area; it incorporates numerous Au occurrences represented by auriferous quartz and quartz-sulphide veins and stockworks that are traceable for at least 8 km along strike as a continuous mineralized package some 2 km wide (Figure 2). This prospect occurs along the Perry Creek–Hellroaring Creek divide. Perry Creek is known for its large Au placers, whereas none occur on the western side of the divide. The prospect is underlain mainly by rocks of the Creston Formation and, along its extreme western edge, by the Kitchener Formation (Klewchuk, 2001; Kennedy and Klewchuk, 2002). The Kitchener Formation crops out west of the prospect along the Hellroaring Creek road, and the lowermost bedrock exposures in the western part of the prospect appear to be near the Creston–Kitchener contact. The Creston Formation consists mainly of laminated and thin-bedded argillite, medium-thick-bedded siltstone, and quartzite. A number of north-northeast-striking (i.e., bedding parallel) mafic dikes occur in the Creston Formation on the eastern flank of the prospect; however, some dikes extend into transverse east- and west-northwest-trending structures.

The major structural pattern of the prospect is defined by a series of parallel, north-northeast-trending (020°) deformation zones that are roughly parallel to bedding and together form a thick and continuous package of sheared, faulted and mineralized sedimentary rocks. The deformation zones alternate with relatively less deformed and undeformed rocks, and often occur 'en échelon'. Degree and expression of deformation also vary in different rock types: according to Klewchuk (2001), argillaceous units have responded to deformation in a more ductile manner, providing an abundance of thin continuous quartz veins, whereas quartzite and siltstone are often brecciated and form 'crackle breccia' units, with branching and merging, irregularly shaped quartz veins (Figure 3). Klewchuk (2001) described common small drag folds along the faults with west-side-up sense of the movement, suggesting thrust faulting. In addition to the linear stockwork zones, the deformation package also incorporates larger single shears striking north-northeast and typically dipping steeply to the east-southeast; they host large (up to 10–15 m thick) quartz and quartz-sulphide veins that are traceable for up to 1–2 km along strike.

The Zinger prospect incorporates at least three relatively more intensely mineralized sectors, referred to as the 'Central Zinger', 'South Zinger' and 'North Zinger' sectors, each exceeding approximately 1.5 km by 2.5 km in surface area. The structural settings and styles of mineral-

ization are somewhat different among these sectors. In particular, the Central Zinger sector is characterized by development of an auriferous linear quartz stockwork (in the western part) and massive quartz-sulphide veins (in the eastern part), both trending northeast. Numerous (several hundred) outcrop grab and chip (including channel chip) samples returned highly anomalous Au values ranging from a few hundred parts per billion to several grams/tonne and locally up to 15–25 g/t. The South Zinger ('Gold Run Lake') sector is centred about 2 km south of the Central Zinger sector and is characterized by a strong Au-in-soil anomaly more than 2 km across. The Au-in-soil values locally exceed 1 g/t, with a peak at 50–300 ppb. Although most of the area is covered by overburden and intense vegetation, limited outcrops suggest the presence of a large auriferous quartz stockwork with minor development of massive quartz veins. Some of these veins returned values up to 5–15 g/t Au, with historical data reaching 3.9 oz./ton Au in grab samples. A notable feature of the sector is the presence of east-striking mafic (lamprophyre?) dikes and numerous east-striking quartz veins. Limited drilling on the Central and Southern Zinger sectors conducted in 2003 (Soloviev, 2004a) failed to intersect the 'roots' of the intense and often high-grade Au mineralization outcropping on the surface, but did encounter alternating sequences of low-grade auriferous and barren intervals. The North Zinger sector ('Columbia–Homestake veins') is centred about 3 km north of the Central Zinger sector and is characterized by predominance of massive quartz and quartz-sulphide veins, with only minor quartz stockworks. Four or five large, northeast-striking quartz-veined deformation zones have been identified to date; some of them were traced for 2–3 km, continuing the trend on the Central Zinger sector.

The Au-bearing and barren systems of quartz (quartz-sulphide) veining found on the prospect represent four or five different structural settings (Soloviev, 2004a). First, northeast-striking (about 020°), vertical or steeply (70–85°) northwest-dipping Au-bearing quartz-sericite (plus pyrite, Fe-carbonate and occasional galena and chalcopyrite) stringers, veinlets, veins and wider pervasive alteration and stockwork zones represent the most abundant mineralization. Locally, stockworks contain up to 50 stringers per metre and form broad (up to 30–50 m wide) and extensive (up to 300–400 m in strike length) zones. The stockworks contain the most intensive and consistent Au mineralization, grading from a few hundred parts per billion to several grams/tonne Au, although barren zones are also common. Visible Au is locally present. The individual stockworks are 10–30 m in thickness and extend 300–900 m downdip. These stockworks, situated en échelon and separated by barren intervals, can be combined into at least seven to eight larger mineralized 'corridors', some of which are 200–300 m thick and traceable for 1–5 km along strike.

Secondly, north-northeast-striking (about 020°), vertical or steeply (70–85°) west-northwest-dipping, massive quartz veins (with minor sericite, pyrite and Fe-carbonate) vary in thickness from 0.5–1 m to 10–15 m. Some individual veins exhibit significant strike extent (up to 150–200 m); a number of more prominent zones hosting these veins were followed for 3–5 km. The veins are often surrounded by quartz-sericite (plus pyrite and carbonate) stockworks. Locally, these veins contain galena, sphalerite (occasionally in high concentrations—up to 20–30% together with pyrite), tennantite-tetrahedrite and sporadic ar-

Table 1. Selected compositions showing geochemical signatures of various Au-bearing and associated assemblages from the Au prospects of the western Cranbrook area, southeastern British Columbia.

Sample	UTM		Element (ppm, except where indicated as %)													
	Northing	Easting	Au	Ag	As	Ba	Bi	Co	Cu	Hg	Mo	Ni	Pb	Sb	W	Zn
Gar:																
1	5484211	564012	<0.005	<0.2	<2	30	<2	1	3	<1	213	2	2	<2	<10	<2
2	5484218	560450	0.118	0.2	<2	10	<2	1	2	<1	3	1	100	<2	<10	54
3	5484213	560453	1.035	0.5	<2	40	27	7	32	<1	1	9	56	<2	<10	7
4	5484215	560476	0.549	<0.2	2	90	3	18	16	<1	1	16	12	<2	<10	42
5	5484215	560458	0.368	0.2	3	30	30	20	18	<1	8	9	31	<2	<10	7
6	5484222	560523	9.24	11.8	8	70	32	43	60	<1	52	19	95	<2	<10	18
7	5484214	560575	0.118	0.2	<2	80	5	4	29	<1	1	5	16	<2	<10	4
Leader:																
8	5489521	563522	6.73	675	299	600	2	12	8940	23	14	18	8160	1550	300	709
9	5489525	563523	23.3	185	120	480	10	10	9430	8	6	10	4.80%	650	200	685
Zinger:																
10	5476202	559800	14.4	16.8	2	100	<2	1	337	<1	1	2	57	<2	<10	4
11	5476182	559880	23.7	26.6	<2	20	<2	1	1165	<1	<1	2	76	<2	<10	4
12	5477855	559933	16.75	78.8	<2	170	5	3	3170	1	5	10	2.56%	8	<10	2120
13	5475834	559805	3.03	9.5	<2	190	<2	1	119	<1	<1	1	1850	<2	<10	136
14	5475805	560426	0.785	3	2	40	<2	2	191	<1	<1	3	52	<2	<10	4
15	5475602	560236	3.21	1	2	200	<2	2	8	<1	2	3	111	<2	<10	276
16	5475552	560205	0.289	1.1	2	30	<2	2	26	<1	<1	2	11	<2	<10	3
17	5475005	559223	2.11	0.6	<2	20	<2	<1	8	<1	<1	1	15	<2	<10	<2
18	5475631	561045	0.006	0.6	4	40	5	2	5	<1	1	2	26	<2	540	6
19	5475625	561040	0.007	<0.2	26	40	<2	6	6	<1	1	11	16	<2	150	34
20	5475003	558801	0.66	0.2	9	10	<2	7	9	<1	30	17	10	<2	<10	3
21	5474804	560925	<0.005	<0.2	<2	40	<2	4	4	<1	40	3	3	<2	<10	6
Columbia-Shakespeare-Homestake:																
22	5479555	564205	0.764	0.2	5	210	<2	13	2	<1	1	7	<2	<2	10	4
23	5479522	564253	8.35	0.5	44	60	2	82	9	<1	2	43	7	2	10	51
24	5479116	563533	0.186	<0.2	160	20	4	417	231	<1	11	28	261	32	20	107
25	5479851	563354	3.53	0.7	8	<10	<2	8	979	<1	1	43	527	<2	<10	6
Anderson-Price:																
26	5494508	570041	19.65	34.8	9	30	24	1	53	1	8	7	1.32%	11	<10	525
27	5494492	570045	25.1	23.6	<2	<10	29	1	15	<1	4	3	1.16%	17	<10	138
ELCR:																
28	5484513	574020	11.9	1.5	8	50	94	9	192	<1	2	16	123	108	<10	20
29	5484505	574010	8.21	0.8	4	30	184	5	129	<1	1	15	88	19	<10	7
Bar:																
30	5482312	577910	14.95	12.6	3490	50	12	52	80	2	4	13	1330	16	<10	535
31	5482330	577922	7.34	531	>10000	10	990	291	137	6	12	8	>30%	618	<10	638
32	5482375	577902	2.02	5	3010	50	<2	51	77	<1	5	16	1065	15	<10	626
33	5482406	577897	2.51	8.3	>10000	320	<2	47	113	<1	6	18	1440	41	<10	691
34	5482481	578277	16.85	40	2820	10	35	2	1185	<1	28	4	1.48%	36	<10	139
35	5482350	577781	9.36	2.5	133	20	5	11	64	<1	3	6	528	<2	<10	24
36	5482341	577855	0.847	2.5	26	10	<2	2	25	<1	1	4	311	2	<10	13
37	5482374	577801	98/281	1.7	85	10	3	8	41	<1	2	4	344	<2	<10	15
38	5482435	577415	4.36	5	6	20	<2	4	5	<1	1	7	4	<2	<10	8
39	5482373	577571	0.827	0.3	9	20	<2	11	2	<1	1	4	13	<2	<10	<2
Zeus:																
40	5482505	575215	391	42.8	188	40	21	14	343	<1	3	25	101	<2	10	11
41	5482512	575235	0.088	3.3	197	10	63	66	4650	2	2	15	18	<2	<10	13
42	5482522	575240	0.117	5.2	229	<10	115	101	7050	1	7	20	3	<2	10	10
43	5482515	575223	2.84	0.6	323	10	218	4	1665	<1	2	9	28	<2	<10	11
44	5482513	575213	0.036	1.8	105	<10	318	34	6010	<1	1	16	18	2	<10	9
45	5482506	575211	2.48	16.3	125	20	9	3	149	<1	3	8	5560	9	<10	53
46	5482505	575212	5.09	76.1	1435	10	32	20	3000	1	20	19	2.00%	61	20	426
Wuho:																
47	5482602	571720	158	19	<2	<10	<2	37	6	<1	<1	19	12	1	<10	10
48	5482650	571771	0.191	<0.2	4	60	<2	7	53	<1	2	8	42	4	<10	88
49	5482616	571712	0.097	<0.2	5	140	4	13	153	<1	<1	11	18	8	<10	176
50	5484074	571018	0.071	<0.2	1015	50	<2	34	10	<1	3	192	6	<2	<10	57
51	5484075	571005	0.431	0.4	3640	50	2	39	10	<1	3	132	9	<2	<10	33
52	5484071	571016	0.008	4.9	8	40	19	36	8230	<1	<1	40	5	<2	<10	110

senopyrite and chalcopyrite, although the sulphide content generally is low. Scheelite occurs locally. Visible Au has been identified in a number of veins and stockworks. Locally, the Au-bearing quartz stockworks and veins are superimposed on the gabbroic dikes or border the dikes. These massive quartz veins ('lodes') include the Columbia vein (MINFILE 082FSE009), which averages 9–12 m thick and contains Au values as high as 50.2 g/t but typically not exceeding 9–11 g/t. Another showing, called the 'Homestake mine' (MINFILE 082FSE012), is located east of the Columbia vein; it locally contains up to 96.5 g/t Au in grab samples and one drill intersection returned 9.5 g/t Au over 1 m. To the south, the Columbia vein can be traced to the Shakespeare vein (MINFILE 082FSE119), where values up to 32 g/t Au have been reported (Brewer, 1997), and then to the Petra vein (MINFILE 082FSE121). However, Au mineralization in these veins is typically erratic.

Other structural settings appear to have less importance in controlling Au mineralization. They include the north-northeast-striking (~020°), flat to moderately (10–40°) west-northwest-dipping quartz-hematite stringers that are typically very thin (~5 mm) and form a weak stockwork (locally up to 5–10 stringers per metre but usually less) spread throughout the property but relatively more intense in its southern portion. Usually, these stringers are barren but, in a few locations, they returned up to 6 g/t Au. Also, roughly east-striking (060–070°), steeply (70–90°) south-dipping quartz (plus pyrite) veins, typically narrow (0.5–5 m thick), were traced for up to 300–400 m along strike; they bear low Au values (50–100 ppb), with just sporadic enrichment up to 10 g/t in the intersections with the north-northeast-striking stockwork zones. Finally, the west-northwest-striking (290–320°), steeply (70–90°) south-southwest-dipping, quartz-chlorite-hematite-Fe-carbonate veins and veined zones, typically narrow (from a few centimetres to 5 m), were traced for more than 1000 m along strike; they are typically barren and appear to represent the latest mineralizing event. Significant displacements of the other (including Au-bearing) mineralized zones often occurs along these veins.

Bar Prospect (MINFILE 082GSW068)

The Bar prospect (Figure 4) is remarkable due to close spatial association of Au mineralization with an intrusion and the distinct structural control of its higher grade portion by a well-expressed low-angle fault (possibly thrust fault) zone. The prospect is underlain by the Middle Aldridge quartzite wacke and the Creston quartzite, intruded by the monzonitic Kiakho stock; the monzonite forms large outcrops on the northern side of the prospect and occurs in large boulders (rubble crops) on the southern side, suggesting that the pluton underlies the entire prospect. In addition, there are several east-striking dikes, up to 60 m thick and traceable for 1 km along strike, that follow a large fault

zone. These dikes exhibit porphyry texture (with K-feldspar in phenocrysts) and are believed to be syenite or quartz syenite. As revealed by drilling, these syenite dikes adjoin (or are cut off by?) at depth a much larger pluton of weakly porphyritic to equigranular medium-grained rock visually similar to the Kiakho stock monzonite. Thus, they may be either just porphyry apophyses of the stock or older dikes preserved in the roof pendant.

The mineralization is closely associated with these syenite dikes and traceable on surface within a zone up to 60 m wide and extending for >1 km along strike. It is represented by dense quartz-sulphide stockworks and disseminations in strongly brecciated, gouged, phyllically (quartz-sericite-Fe-carbonate) and argillically altered quartz syenite (?) and adjacent sedimentary rocks. The altered rocks contain 5–10% finely disseminated sulphides (mostly pyrite and arsenopyrite); surface sampling of this material returned typically low to moderate values of 0.1–3.0 g/t Au, including 2.09 g/t Au over 16.0 m and 1.54 g/t Au over 30 m (Leask, 1992). The drilling indicated that the stockwork is present to a depth of at least 350 m; it forms a number of nearly vertical to steeply north-dipping zones up to a few tens of metres thick. The majority of drill intercepts on these stockwork zones returned low Au grades, typically 0.1–0.5 g/t Au over short intervals, which are much shorter than the total width of the zone (i.e., significant portions of the stockworks contain sulphides but no Au). Some of the stockworks exhibit a strong 'nugget effect'; however, fine disseminated Au is also common.

In contrast, much higher grade Au mineralization is hosted by a low-angle fault, possibly a thrust fault, that dips moderately steeply (40–50°) to the north and by a number of steeper 'splays' occurring along its hangingwall side (Soloviev, 2003). It is unclear whether this fault corresponds to the east-trending Cranbrook fault (previously believed to be a normal fault) or represents another (but also roughly east-striking) fault zone 'superimposed' on and displacing the Cranbrook fault. The low-angle fault cuts and displaces the intrusion, forming one of its contacts. The high-grade Au mineralization occurs in strongly brecciated massive quartz veins, often with intense cataclasis, that contain oxidized and gouged sulphides (mostly pyrite, with some galena, sphalerite and arsenopyrite), Fe-carbonate and sericite, and continues for ~150 m down dip before gradually pinching out; smaller 'swellings' are present in other parts of the structure. The best drill intercepts were as high as 10.3 g/t Au over 7.5 m, 15.3 g/t Au over 1.6 m and 38.0 g/t Au over 1.0 m; a strong 'nugget effect' is common. Remarkably, the highest grade Au mineralization in the low-angle fault corresponds to its intersection with a transverse, northwest-trending (310–320°) fault zone that lies directly along strike from the alteration and mineralization zone on the Vine prospect (MINFILE 082GSW050). This structural intersection is consistently marked by abundant northwest-striking quartz-galena veins and corresponds to

←
Notes: 1, Au-free, Mo-rich quartz veinlet; 2–7, auriferous quartz veinlets with trace sulphides (galena, etc.); 8–9, sulphide-rich quartz vein; 10–11, high-grade Au-bearing quartz veins; 12, auriferous quartz-sulphide veins; 13–21, north-northeast-striking Au-bearing quartz and quartz-sulphide stockworks and 'crackle breccia'; 22–23, Au-bearing quartz veins; 24–25, Au-bearing quartz-sulphide veins; 26–27, high-grade Au-bearing quartz-sulphide veins; 28–29, high-grade Au-bearing quartz veins with minor sulphides; 30–34, Au-bearing quartz-sulphide veins (arsenopyrite, galena, chalcopyrite, etc.); 35–37, sulphide-poor quartz veins with coarse Au; 38–39, sulphide-free quartz veins and veinlets; 40–44, Au-bearing quartz-pyrite-bornite stockworks; 45–46, northwest-striking Au-bearing quartz-galena veinlets; 47–49, quartz and quartz-pyrite veins with coarse Au; 50–51, Au-bearing quartz stockwork with arsenopyrite; 52, Au-bearing quartz-bornite veinlets. Assaying by ALS Chemex, North Vancouver, BC using atomic absorption spectrophotometry for Au and inductively coupled plasma-emission spectroscopy for other elements.

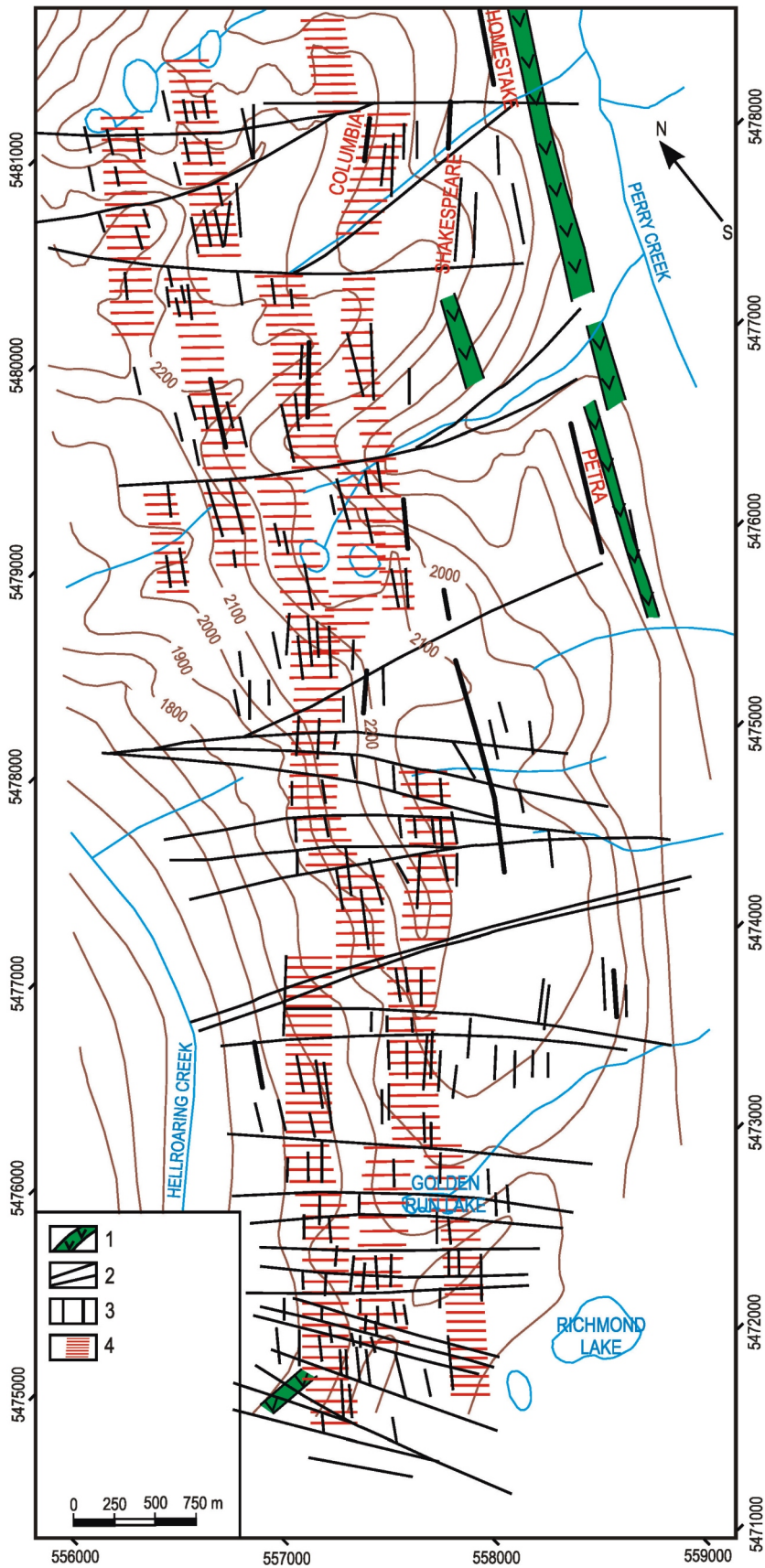


Figure 2. Geology of the Zinger and adjacent prospects (simplified after Klewchuk, 2000, 2003a, b; Soloviev, 2004a, b). Legend: 1, mafic dike; 2, fault zone; 3, zones of small and large quartz veins; 4, zone of auriferous quartz stockwork and silicification.

the widest portion of the east-striking mineralized zone, which is some 300 m in strike length. There are also thick massive quartz veins and zones of total silicification overprinting the brecciated rocks (Figure 3). Surface sampling of the mineralized material returned very high local Au grades (up to 98–281 g/t in rock grab samples and up to 7.4 g/t over 11 m in channel samples; Leask, 1992; Soloviev, 2003, 2004b). To the east and west, the mineralized zone splits into two or more parallel but narrower (<5 m thick) branches that are traceable for several hundred metres along strike; grab samples returned up to 15 g/t Au.

Zeus Prospect (Centred at UTM ~5482500N, ~575500E)

The Zeus prospect (Figure 4), located 2–4 km west of the Bar prospect, traces the immediate extension of the east-trending quartz syenite (?) dike and corresponding mineralized zone. The prospect incorporates a number of east-trending quartz syenite (?) dikes dipping 45° to the north; they are subjected to strong quartz-carbonate-sericite-pyrite and argillic alteration, and locally contain quartz and quartz-sulphide veins and stockworks. The latter are

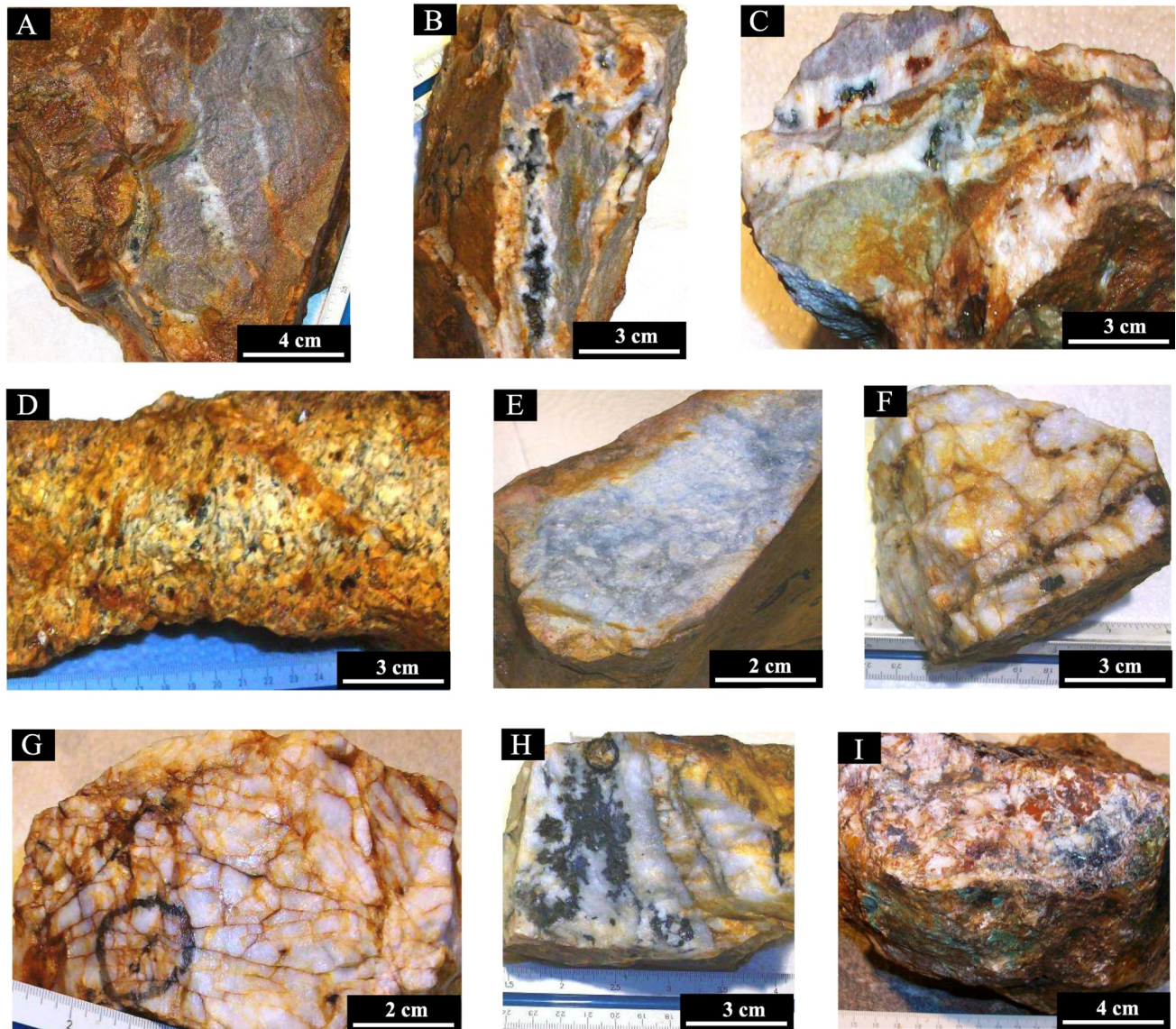


Figure 3. Various types of mineralized quartz veins and stockworks found in the area west of Cranbrook, southeastern British Columbia: **A) to C)** Au-bearing quartz and quartz-sulphide stockwork and 'crackle breccia' in silicified metasedimentary rocks, Zinger prospect; **D)** quartz veining, silicification and argillic alteration in syenite, Wuho prospect; **E)** strongly silicified and argillically altered breccia containing fragments of metasedimentary (?) rocks, Bar prospect; **F)** massive Au-bearing quartz vein with minor sulphides, ELCR prospect; **G)** massive quartz vein containing native Au with no association with sulphides, Anderson-Price prospect; **H)** massive Au-bearing quartz vein with elevated amount of sulphides, Anderson-Price prospect; **I)** massive Au-Ag-bearing quartz-sulphide vein, Leader prospect.

especially intense in those areas where the major east-trending zone is intersected by the northeast-trending district-scale Palmer Bar fault, associated with a 100 m wide mineralized zone, and by a northwest-trending fault similar to those observed on the Bar prospect and corresponding to the 'Vine vein' structural trend. These structural intersections control a number of more localized mineral showings, including the 'Quartz Pit' trench, yielding anomalous Cu, Ag and Au values (up to 10.8 g/t Au); the 'Horseshoe Pit', with massive galena samples returning 16.4 oz./ton Ag; the 'Pink Mountain' trench, yielding values up to 0.2% Cu; and the 'Quartz Float Train', with samples returning 0.01–0.258 oz./ton Au (Allen, 1984; Banting, 1988).

The drilling in 1988 identified a "large structurally controlled quartz-sulphide flooded zone along the Cranbrook Fault" (Banting, 1988), with some holes returning sporadic Au values up to 0.3 oz./ton over widths of 0.1–0.3 m and consistently anomalous Au values within the syenite dikes. The quartz-flooded zone also hosts elevated Cu values, with drill intersections of 1.4% Cu over 4.1 m and 0.57% Cu over 50.5 m. Rock sampling of quartz-pyrite-bornite mineralization with minor quartz-pyrite-galena stockwork, found in the 'Limonite pit', returned values up to 1.93 g/t Au over 2.3 m. Resampling of a 0.8 m portion returned a value of 381 g/t Au (410 g/t Au in check assay). Grid soil sampling revealed a number of other narrow, northwest-trending zones of anomalous Au values corresponding to the 'Vine vein trend' (Soloviev, 2003, 2004b). These northwest-trending zones are traceable to the ELCR prospect, located 3 km northwest of the Zeus prospect.

In 2007–2008, another drilling program returned 0.63% Cu over 57 m, together with elevated Bi (up to 130 ppm over 10 m) and Co (up to 304 ppm over 46 m). The elevated Co content corresponds to abundant pyrite in a zone of intense silicification, quartz-albite breccia, and quartz–Fe–carbonate–sericite and subsequent argillic alteration. The follow-up drilling in 2007 returned wide intercepts of elevated Cu values, with locally elevated Au (up to 3.7 g/t over 0.8 m), and the zone was interpreted to represent the uppermost parts of a buried porphyry system.

Eastern and Western Wuho Creek Areas (Centred at UTM ~5483000N and ~571500E)

The Eastern and Western Wuho Creek areas (unrecorded prospects) are located 2.0 and 4.0 km, respectively, west of the Zeus prospect (Figure 4). Both prospects cover the intersections of west-northwest- and north-northeast-trending faults, including the larger Old Baldy fault, with the east-trending structure controlling quartz syenite (?) dikes and mineralization of the Zeus and Bar prospects. A strong positive magnetic anomaly, measuring 2.0 km by 1.0 km, occurs between the Eastern and Western Wuho Creek prospects, suggesting a buried intrusion.

The Eastern Wuho Creek prospect contains abundant quartz syenite (?), quartz and quartz-sulphide float. Rock grab samples of quartz-pyrite float returned Au values of up to 2.99 g/t, 15.3 g/t and 158 g/t (Soloviev, 2004b). Interestingly, the third high-grade Au value was obtained from a series of ten samples taken from the same large quartz boulder, nine of which returned Au values below detection

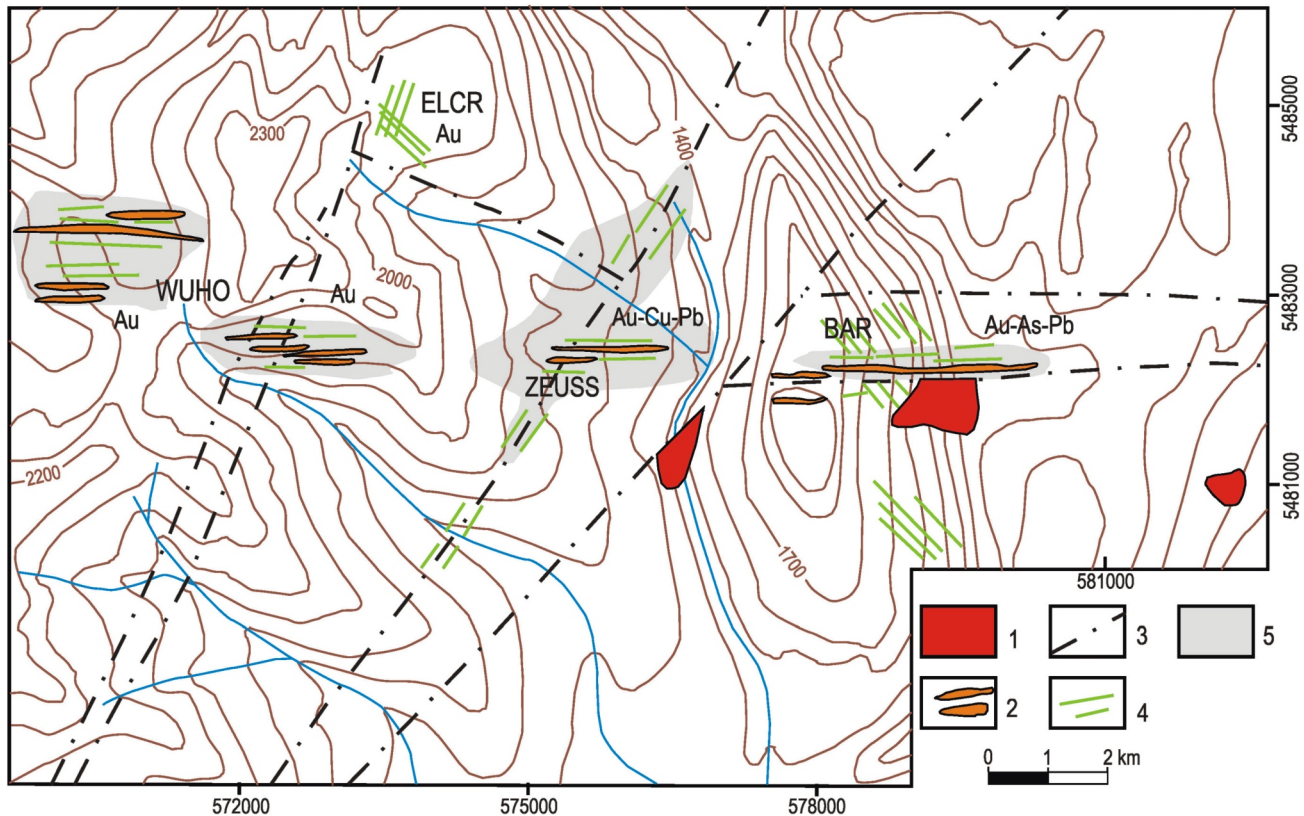


Figure 4. Geology of the Bar-Zeus-Wuho prospects: 1, Mesozoic quartz monzonite to granodiorite intrusions; 2, syenite to quartz syenite (?) dikes; 3, fault zones; 4, zones of quartz veining; 5, areas of hydrothermal alteration (silicic, phyllic and/or argillic alteration).

limit, thus indicating a very strong ‘nugget effect’. Silt sampling of a 1 km long, south-flowing tributary of Wuho Creek, which flows through the prospect, returned extremely high values of 256 and 401 g/t Au, with associated high Pb values. Panning of larger silt samples revealed numerous fine- to medium-sized (up to 3 mm by 3 mm) free Au particles associated with abundant magnetite. Prospecting identified abundant quartz-galena float upslope. The Western Wuho Creek prospect covers a large (greater than 2 km by 1 km) area of abundant quartz-syenite (?) float and rubble crop. Quartz-syenite (?) boulders, some more than 2 m across, are strongly silicified and argillically altered, with strong limonitic staining, locally intense quartz stockwork and minor quartz-magnetite veins. The rocks contain 0.4–0.6 g/t Au; a sample of quartz-magnetite vein returned 2.6 g/t Au. The intersecting north-northeast-trending structure was traced by Au-bearing quartz float for a distance of 2–3 km. Sampling has also revealed substantial Cu mineralization (Table 1). In total, the Bar, Zeus and Wuho prospects, although possibly being divided by faults and less mineralized intervals, may be the expression of a single large (traceable for >10 km along strike) mineralized zone.

ELCR (MINFILE 082FSE117) and Anderson-Price (MINFILE 082FNE056) Prospects

These prospects comprise well-expressed ‘structurally controlled’ quartz and quartz-sulphide veins in the Proterozoic metasedimentary rocks. There are typically two structural settings for the veins on each prospect: both northeast and northwest-striking veins are present, although the northeast-striking veins predominate. The veins usually occur en échelon, forming parallel swarms of two to three larger (up to 2–4 m thick) ‘pivot’ veins that locally pinch and swell (to the point of splitting into separate lenses) and are surrounded by a parallel series of much smaller veins and veinlets. At the Anderson-Price prospect, the quartz-vein zone occurs adjacent to a series of small northeast-trending granite dikes, whereas the ELCR prospect is coincident with a local strong positive magnetic anomaly measuring 1 km by 1 km (Figure 1). The Au mineralization is represented by native Au and is either associated with minor sulphides scattered through the quartz veins or occurs separately, strongly enriching selected parts of the veins (where Au grades range from many tens to a few hundred grams per tonne; Table 1).

GEOCHEMICAL SIGNATURES

As noted above, the Au mineralization found in the Cranbrook area is characterized by the presence of various mineral assemblages. The data presented in Table 1 illustrate some important geochemical features of these mineral assemblages.

These data show that at least four to five distinct Au-bearing mineral assemblages, and therefore compositional (mineralogical and geochemical) types of quartz and quartz-sulphide veins and stockworks, can be distinguished. They include

a sulphide-free Au-quartz assemblage, containing coarse native Au with variable and often high Au:Ag ratios (1:1 to 10:1, up to 100:1) but only minute amounts of sulphides. This mineralization is present on the majority of the prospects studied. As a subtype

of this assemblage, a pyrite-rich (5–20 vol. % pyrite) Au-bearing assemblage can be distinguished: it is characterized by elevated Co and Ni values associated with pyrite.

an auriferous sulphide-rich (20–50 vol. % sulphides) assemblage containing abundant sulphides (especially galena) and occasional scheelite. It is enriched in Ag, with low Au:Ag ratios varying typically from 1:1 to 1:5, and often bears elevated Bi, Sb and Zn values. The geochemical data show that galena is common not only in large quartz-sulphide veins, but also (in minor concentrations) in Au-bearing quartz stockworks (i.e., on the Zinger, Gar and other prospects).

a series of transitional assemblages containing moderate amounts (from 3–5 to 15–20 vol. %) of sulphides (and sulphosalts) and occasional scheelite. They are distinguishable by characteristic Pb-Zn-Ag (Anderson-Price prospect) or Cu-Pb-Sb (ELCR prospect) geochemical signatures, suggesting the presence of either galena or Cu-Pb sulphosalts (tennantite-tetrahedrite, etc.).

another distinct sulphide-rich (20–50 vol. % sulphides) Au-bearing assemblage containing elevated Pb and Zn values and accompanied by high Ag and As contents. This assemblage, whose Au:Ag ratio is the lowest (up to 1:100), is present on the Bar, ELCR and Zeus prospects. It closely resembles that encountered on the Vine prospect and some other Pb-Zn prospects elsewhere in the district.

a Cu-enriched (bornite-pyrite or bornite-chalcocopyrite-pyrite) Au-bearing assemblage associated with altered quartz-syenite (?) dikes or intrusive apophyses on the Zeus and Wuho prospects. The high Cu values are locally accompanied by elevated As and Bi values.

Au-bearing mineralization that also has elevated Mo and/or W values (Gar, Leader, Zinger prospects); in addition, Au-free quartz-molybdenite veinlets are locally present in the vicinity of Au-bearing stockworks (e.g., Gar). The presence of these metals provides additional evidence for the intrusive-related character of the Au mineralization, even its distal varieties.

Of special importance is the presence of more than one Au-bearing assemblage on larger prospects. In particular, both sulphide-free and sulphide-rich assemblages are present on the Bar, Zeus and Zinger prospects. Locally, these assemblages may be accompanied by Cu-rich Au-bearing mineralization. This may suggest a long-lasting mineralization event, with the formation of several successive mineral assemblages.

STYLES AND STRUCTURAL SETTINGS OF GOLD MINERALIZATION

The best evidence for a relationship between intrusive-related mineralization in the Cranbrook area and the mid-Cretaceous monzonite and granodiorite of the ilmenite-type (or ‘I-type’) Bayonne intrusive suite occurs where the mineralization is spatially associated with an intrusion. The mineralization comprises Au-bearing quartz and quartz-sulphide (plus sericite, Fe-carbonate and locally barite) veins and stockworks containing pyrite and locally pyrrhotite, as well as other sulphides and sulphosalts, including arsenopyrite, galena, sphalerite, chalcocopyrite and tetrahedrite-tennantite. Magnetite and hematite are typi-

cally absent, further suggesting the 'reduced' character of this mineralization. As previously noted, this style of Au mineralization was originally recognized in the region by Lefebvre and Cathro (1999) and Logan (2000, 2002). A specific feature of this mineralization in the Cranbrook area is the association of Au with elevated Mo and W (rather than Sn and W) values.

The data obtained on apparent intrusive-related Au mineralization in the area west of Cranbrook make it possible to illustrate the variations in mineralogy and geochemistry that occur on prospects that formed in different structural settings. These structural and compositional varieties may include:

most proximal (?) Au-Cu-Bi-As (+Co+Ni) mineralization in close spatial association with dike swarms or small intrusive apophyses and stocks. This mineralization includes zones of intense silicification, phyllic and argillic alteration, quartz and quartz-sulphide (mostly pyrite) stockworks and possibly hydrothermal breccias.

more distal Au-Cu-Pb (+W) to Au-Pb mineralization, including quartz and quartz-sulphide stockworks (locally possibly evolving into hydrothermal 'crackle' breccias) and larger veins with minor to abundant sulphides and locally scheelite. No direct relationship to significant magmatic bodies is apparent, although rare felsic to mafic dikes may be in the area.

also distal 'structurally controlled', Au-bearing quartz veins and 'sediment-hosted' Au-bearing quartz stockworks, typically with minor sulphides and local scheelite. Veins and stockworks are localized in larger fault zones. The Au-bearing quartz and quartz-sulphide veins also display a strong structural control by larger fault zones and locally attain maximum thicknesses of 10–20 m and strike lengths on the order of a few hundred metres. Steeply dipping veins predominate, although flat-lying veins in low-angle faults (possibly thrust faults) and their splays have also been mapped. The veins are commonly found in close spatial association with gabbroic dikes (Moyie sills?) and/or with apparently younger mafic (possibly lamprophyre?) dikes, locally altered to listwaenite. The veins are characterized by massive quartz, lesser Fe-carbonate and traces of sericite. Gold is found in both finely disseminated and coarse (visible) form, and is often characterized by extremely erratic distribution.

most distal (?) Au-bearing Ag-Pb-Zn mineralization, typically represented by quartz-sulphide veins in fault zones and lacking any spatial association with magmatic bodies. These veins typically contain very little Au, but their occurrence in the same structures that host other types of Au mineralization indicates reactivation (opening) of these structures and possible further enrichment of Au.

The presence and possible significance of low-grade (typically around 1 g/t Au) quartz to quartz-sulphide (quartz-Fe-carbonate-sericite-sulphide) stockworks in the area was recognized recently (e.g., Klewchuk, 2001, 2003a, b; Soloviev, 2004a, b), and the potential of some possibly low-grade, bulk-tonnage Au occurrences remains unevaluated. The stockworks occur both within the intrusions (e.g., Gar prospect) and in sediments (Zinger prospect). In both cases, however, the stockworks trace some district-scale faults, controlling chains of intrusions, that

were reactivated as post-intrusive faults. The overprinting of the intrusions and metasedimentary packages by these linear stockworks is especially visible at a larger scale. They consist of subparallel and intersecting quartz stringers forming stockwork zones that are lens-shaped, typically subvertical and situated en échelon, locally attaining maximum widths ranging from a few to several tens of metres and strike lengths of up to several hundred metres. Individual stockwork zones can be amalgamated into much wider (up to 100–200 m) and longer (up to several kilometres) quartz stockwork and alteration units that trace the fault zones. Locally, higher grade Au-bearing veins occur within the low-grade stockworks. The stockworks contain variable amounts of sulphides, mainly pyrite but locally with traces of galena and chalcopyrite; again, there is no correlation between the amount or type of sulphide mineral and the Au grade. Alternatively, some of the Au (Cu) occurrences in the area may be 'oxidized' porphyry Cu-Au deposits. The presence of Cu-Au porphyry mineralization has been suggested by Ransom (2006) for the Zeus prospect. In addition to its Cu-Au-As geochemical signature, Zeus mineralization has a close spatial relationship with probable alkalic (syenitic?) dikes, although the exact composition of these dikes requires further study. Another notable feature is the local abundance of magnetite (Wuho) and bornite (Zeus). The minerals are uncommon in both 'reduced' intrusive-related Au mineralization (e.g., Hart, 2007) and 'reduced porphyry Cu-Au' (RPCG) deposits (Rowins, 2000a), such as may occur in the historical Rossland Au camp (e.g., Rowins, 2000b). Rather, the relatively 'oxidized' character of the magmatic-hydrothermal ore fluids is typical of the Jura-Triassic suite of large alkalic porphyry Cu-Au deposits that occurs throughout central BC (e.g., Chamberlain et al., 2007).

TECHNICAL ASPECTS OF EXPLORATION

The data obtained on the Au mineralization in the Cranbrook area reveal several features that should be considered during exploration.

First, the system of faults, fractures and airphoto lineaments gives considerable structural complexity to the Au occurrences. Gold mineralization is commonly localized at 'double' or even 'triple' fault intersections that lack continuity and consistency along strike and down dip. This setting does, however, create a favourable environment for structural superimposition of multistage, and possibly much more variably aged, mineralization events. Consequently, the application of dense exploration drilling grids to reveal structural patterns that define the most favourable trends is required for future drilling.

Second, the structural controls on Au mineralization are complicated to an even greater degree by multiple syn- and post-mineralization faulting episodes. As a result, common brecciation, gouging and late surficial weathering of mineralized material cause numerous drilling issues related to core-recovery rates and down-hole deviation. Remarkably, many holes drilled in the past exhibit very low drillcore-recovery rates in mineralized zones, which means that reported Au assays, both high and low, are essentially meaningless. This is because an unknown, but potentially significant, fraction of Au (especially free native Au) was possibly removed (likely preferentially) from the mineralized rock, together with soft clay gouge and/or sandy rock

fragments. The application of modern drilling techniques that provide core-recovery rates in excess of 95% are required for effective exploration.

Third, as revealed by exploration, many Au occurrences in the Cranbrook area consist mainly of native (free) Au. It is distributed in the mineralized rock very irregularly and commonly forms larger multigrain aggregates. This irregular distribution produces a strong ‘nugget effect’ (or ‘coarse Au effect’; e.g., Stanley, 2008) in Au assays from many of the occurrences. In practical terms, this means that Au assay results are unreliable and unrepresentative where obtained on small amounts of mineralized material. Consistently, the industry-standard 30 g fire assay can be considered inadequate to represent the true Au values of these samples. The use of metallic-screen assays (‘dry’ metallic screen in sandy and solid rock material, and ‘wet’ metallic screen in clayey material), in combination with pulverization of the entire sample, is necessary in many cases. Table 2 illustrates the predominance of coarse native Au in many mineralized intervals encountered on the Bar and Zinger prospects. It is apparent that application of the metallic-screen assay method typically ‘reduces’ grades in high-grade samples and ‘increases’ grades in otherwise low-grade samples. This makes the overall Au-bearing intervals somewhat lower in grade but more consistent between samples. Regardless, the existence of a very strong ‘nugget effect’ in the samples requires the use of large-volume bulk-sampling methods to determine the true Au grades of the prospects.

DISCUSSION AND CONCLUSIONS

The data obtained from recent exploration programs highlight some important features of likely intrusion-related Au mineralization in the Cranbrook area. Possible styles of Au mineralization encountered include a) proximal intrusion-hosted and more distal auriferous quartz and quartz-sulphide stockworks; b) distal mineralized faults and deformation zones, including significant breccia; and c) most distal mineralization controlled by faults, including low-angle and possibly thrust faults, with abundant sulphide. To summarize, this proximal to distal zonation of Au mineralization styles from a causative intrusion corresponds to the reduced intrusion-related Au model proposed by Lang and Baker (2001). A difference, however, is the importance of district- and local-scale fault/deformation zones on localizing Au mineralization in the majority of Au prospects in the Cranbrook area. The variably oriented faults form a structural network over the entire area and predetermine the location of Au and other metal occurrences. Further analysis would likely reveal more distinct compositional and structural features associated with this district-scale metal zonation model.

The variety of structural styles of possible intrusion-related Au mineralization corresponds to distinct mineralogical and geochemical diversity in occurrences. These include Au:Ag ratios varying from 100:1 to 1:100, and auriferous mineral assemblages that are both sulphide-free and sulphide-rich. Mineral assemblages also contain different sulphides, with arsenopyrite and/or galena being especially abundant in many of them. Scheelite and/or molybdenite

Table 2. Selected assay results for Au mineralization from the Zinger and Bar prospects, west of Cranbrook, southeastern British Columbia, obtained by standard fire assay versus metallic-screen fire assay.

Prospect	Hole interval or sample number	Au (g/t) by standard fire assay		Au (g/t) by metallic-screen fire assay					
		Check	Total Au	Total weight of Au (mg)	Au in +100 μ m fraction	Fraction weight (g)	Au in -100 μ m fraction	Fraction weight (g)	
Zinger	GD 1463 (grab)	8.93	9.58	19.1	8.096	182.5	4.44	9.26	812.2
Zinger	GD 1432 (grab)	2.16	2.41	2.74	0.329	144.5	2.28	2.29	686
Zinger	OB 1673 (grab)	3.42	3.47	4.78	0.913	82.8	11.02	3.32	588.7
Zinger	Homestake vein (grab)	8.35	7.49	7.56	0.166	11.55	10.02	7.5	1629
Zinger	Columbia vein (grab)	3.53	2.93	5.69	1.557	269	5.79	3.36	655.5
Bar	Hole B-02-01, 10.25–11.87 m (core)	11.05	14.4	2.43	1.017	88.6	11.48	0.59	536.2
Bar	Hole B-02-01, 45.80–46.10 m (core)	3.48		9.23	1.107	95.1	11.64	6.19	328.7
Bar	Hole B-02-02, 9.28–10.26 m (core)	38	37.4	7.23	1.334	176.5	7.55	2.28	258.4
Bar	Hole B-02-02, 50.05–50.50 m (core)	0.339		7.92	2.428	187.5	12.96	1.38	355.4
Bar	Hole B-02-03, 23.60–24.09 m (core)	1.675		15.8	3.976	287	13.85	2.26	277.3
Bar	Hole B-02-03, 52.88–53.64 m (core)	0.048		8.84	2.078	104.5	19.87	3.62	364.8
Bar	Hole B-02-03, 54.65–55.47 m (core)	>10.0	0.25	1.35	0.142	7.23	19.63	1.1	468.9
Bar	Hole B-02-04A, 18.29–18.54 m (core)	16.35		7.5	2.43	829	2.93	1.73	417.6
Bar	Hole B-02-04A, 18.54–19.80 m (core)	19		5.2	5.867	345	17	2.91	2525

Note: Samples from the Homestake and Columbia veins are the same ones listed in Table 1 as numbers 23 and 25, respectively. Gold assays by ALS Chemex, North Vancouver, BC using metallic-screen methods and atomic absorption spectrophotometry.

are locally present. The presence of various sulphides makes it possible to determine pathfinder elements for different styles of Au mineralization.

Despite the significant exploration work conducted in the area, many aspects pertaining to the recognition and classification of intrusion-related Au occurrences remain controversial. Firstly, it is unclear whether Au mineralization in the Cranbrook area is related to a single plutonic suite or to multiple suites accompanied by different types (e.g., reduced intrusion-related Au; 'oxidized' and 'reduced' porphyry Au [Cu]; polymetallic skarn) and styles (e.g., veins, vein stockworks, disseminations, replacement zones) of Au mineralization. It is notable that the Tintina Au belt in the Yukon and Alaska—the type area for reduced intrusion-related Au deposits (i.e., Ft. Knox and Dublin Gulch)—incorporates at least three productive plutonic suites. These include subalkalic, alkalic and peraluminous plutonic suites (Hart, 2007). If this situation applies to southeastern BC, then it may partially explain the variability of the Au mineralization styles in the Cranbrook area.

Many other aspects and possible genetic relationships between Au mineralization and intrusions in the Cranbrook area require further study. In particular, the possible similarity of some mineral occurrences (e.g., Zeus) to Cu-Au porphyry mineralization should be investigated; if proved, this may demonstrate the presence and potential of this mineralization style in the district. Also, some structurally controlled base-metal (with minor Au) prospects traditionally regarded as Proterozoic and 'Sullivan-feeder' style must be re-examined within the context of a Mesozoic intrusion-related Au model; they may significantly increase the number of intrusion-related Au occurrences found in the area. Interestingly, these Sullivan-style occurrences may have no economic importance in terms of Sullivan-style Pb-Zn targets but may be indicative of the presence of intrusion-related Au mineralization at depth or nearby (e.g., the Vine vein; see Hoy and Pighin, 1995). In addition, it is worthwhile determining if some mafic dikes traditionally considered within the Moyie suite are, in fact, much younger (Mesozoic?) and lamprophyric in composition. Specifically, some mafic dikes on the Zinger prospect appear to be lamprophyric, which raises the question of whether lamprophyre-related Au mineralization (cf., Muller and Groves, 1997) is present in the area. For example, Au mineralization at the Taurus deposit in northwestern BC is closely associated with lamprophyre dikes (Panteleyev et al., 1997; Logan, 2000). Combined with other geological data, a better understanding of these features will help in the evaluation of reduced intrusion-related Au potential in southeastern BC.

ACKNOWLEDGMENTS

The author thanks Jim Stypula, CEO of Chapleau Resources Ltd., for support and permission to publish the data on the Au prospects found in the Cranbrook area. Eric Wiltzen, Alan Rella and Robin Sudo also provided significant support. Important assistance in the collection of field data was provided by Olexiy Baklyukov, Carl Schulze, Rick Walker, Garry Dyck and Shawn Wiltzen; data on some prospects were shared by David Pighin, Gordon Leask, Peter Klewchuk, Doug Anderson, Glen Rodgers, Paul Ransom, Craig Kennedy and other local geologists. The paper

greatly benefited from editorial reviews by Jim Logan and Steve Rowins of the BC Geological Survey.

REFERENCES

- Allen, D.G. (1984): Geological and geochemical report on the Bar property, Fort Steele Mining Division; *BC Ministry of Energy, Mines and Petroleum Resources*, Assessment Report 14061, 51 pages.
- Banting, R.T. (1988): Assessment report on the Purcell camp, Fort Steele Mining Division: Morgan South, Buck 2 and Bar properties; *BC Ministry of Energy, Mines and Petroleum Resources*, Assessment Report 17514, 265 pages.
- BC Geological Survey (2009): MINFILE BC mineral deposits database; *BC Ministry of Energy, Mines and Petroleum Resources*, URL <<http://minfile.ca>> [December 2009].
- BC Ministry of Energy, Mines and Petroleum Resources (1898): Annual report; BC Ministry of Energy, Mines and Petroleum Resources, 296 pages.
- Brewer, L.C. (1987): Geological/geochemical/geophysical report on the CND mineral claims, Fort Steel Mining Division, British Columbia; *BC Ministry of Energy, Mines and Petroleum Resources*, Assessment Report 16656, 25 pages.
- Brown, D.A. (1998): Geological compilation of Grassy Mountain (east half) and Moyie Lake (west half) map areas, south-eastern British Columbia; *BC Ministry of Energy, Mines and Petroleum Resources*, Geoscience Map 1998-3, scale 1:50 000.
- Chamberlain, C.M., Jackson, M., Jago, C.P., Pass, H.E., Simpson, K.A., Cooke, D.R. and Tosdal, R.M. (2007): Toward an integrated model for alkalic porphyry copper deposits in British Columbia; in *Geological Fieldwork 2006, BC Ministry of Energy, Mines and Petroleum Resources*, Paper 2007-1, pages 259–273.
- Hardy, J.L. (1986): Report on geology and diamond drilling, Perry Creek property, Fort Steele Mining Division; *BC Ministry of Energy, Mines and Petroleum Resources*, Assessment Report 15649, 173 pages.
- Hart, C.J.R. (2007): Reduced intrusion-related gold systems; in *Mineral Deposits of Canada: A Synthesis of Major Deposit Types, District Metallogeny, the Evolution of Geological Provinces, and Exploration Methods*, Goodfellow, W.D., Editor, *Geological Association of Canada*, Mineral Deposits Division, Special Publication 5, pages 95–112.
- Holcapek, F. (1982): Preliminary geology and evaluation report, Perry Creek gold property, Fort Steele Mining Division, British Columbia; *BC Ministry of Energy, Mines and Petroleum Resources*, Assessment Report 9850.
- Höy, T. (1993): Geology of the Purcell Supergroup in the Fernie west-half map area, SE British Columbia; *BC Ministry of Energy, Mines and Petroleum Resources*, Bulletin 84, 157 pages.
- Höy, T. and Pighin, D.L. (1995): Vine – a Middle Proterozoic massive sulphide vein, Purcell Supergroup, south-eastern British Columbia (92G/5W); in *Geological Fieldwork 1994, BC Ministry of Energy, Mines and Petroleum Resources*, Paper 1995-1, pages 85–98.
- Höy, T. and Van der Heyden, P. (1988): Geochemistry, geochronology and tectonic implications of two quartz monzonite intrusions, Purcell Mountains, south-eastern British Columbia; *Canadian Journal of Earth Sciences*, Volume 25, Number 1.
- Höy, T., Price, R.A., Legun, A., Grant, B. and Brown, D. (1995): Purcell Supergroup, geological compilation map; *BC Ministry of Energy, Mines and Petroleum Resources*, Geoscience Map 1995-1, scale 1:250 000.
- Kennedy, T. and Klewchuk, P. (2002): Assessment report on geologic mapping and rock geochemistry, Hot Sausage and HS

- Claims, Fort Steel Mining Division, British Columbia; *BC Ministry of Energy, Mines and Petroleum Resources*, Assessment Report 27025, 23 pages.
- Klewchuk, P. (1990): Report on diamond drill hole B-90-1, Bar claims, Palmer Bar Creek area, Fort Steele Mining Division; *BC Ministry of Energy, Mines and Petroleum Resources*, Assessment Report 20274, 41 pages.
- Klewchuk, P. (1994): Assessment report on road building, trenching and diamond drilling, Blue Robin property, Kamma and Perry Creek areas, Nelson and Fort Steel mining divisions, British Columbia; *BC Ministry of Energy, Mines and Petroleum Resources*, Assessment Report 23398, 59 pages.
- Klewchuk, P. (2000): Geological report on the Zinger property; *BC Ministry of Energy, Mines and Petroleum Resources*, Assessment Report 26216, 29 pages.
- Klewchuk, P. (2001): Assessment report on soil and rock geochemistry, Zinger claims, Fort Steel Mining Division, British Columbia; *BC Ministry of Energy, Mines and Petroleum Resources*, Assessment Report 26589, 28 pages.
- Klewchuk, P. (2003a): Assessment report on prospecting, geological mapping and rock geochemistry, Zinger claims, Fort Steel Mining Division, British Columbia; *BC Ministry of Energy, Mines and Petroleum Resources*, Assessment Report 27242, 69 pages.
- Klewchuk, P. (2003b): Assessment report on rock geochemistry on the Zinger property; *BC Ministry of Energy, Mines and Petroleum Resources*, Assessment Report 27090, 30 pages.
- Klewchuk, P., Anderson, D., Kennedy, S. and Pighin, D. (2007): Assessment report on geologic compilation, geologic mapping, soil and rock geochemistry, access trail construction, and trenching: Purcell block claims (Eddy, Hope, Gar, and Lov properties); *BC Ministry of Energy, Mines and Petroleum Resources*, Assessment Report 28920, 161 pages.
- Lang, J.R. and Baker, T. (2001): Intrusion-related gold systems: the present level of understanding; *Mineralium Deposita*, Volume 36, pages 477–489.
- Leask, G.P. (1992): Geologic report on the Lookout property, Fort Steele Mining Division; *BC Ministry of Energy, Mines and Petroleum Resources*, Assessment Report 22186, 39 pages.
- Lefebure, D.V. and Cathro, M. (1999): Plutonic-related gold-quartz veins and their potential in British Columbia; in Short Course on Intrusion-Related Gold, *Kamloops Exploration Group*, pages 185–219.
- Logan, J.M. (2000): Plutonic-related gold-quartz veins in southern British Columbia; in Geological Fieldwork 1999, *BC Ministry of Energy, Mines and Petroleum Resources*, Paper 2000-1, pages 193–206.
- Logan, J.M. (2002): Intrusion-related gold mineral occurrences of the Bayonne magmatic belt; in Geological Fieldwork 2001, *BC Ministry of Energy, Mines and Petroleum Resources*, Paper 2002-1, pages 237–246.
- Lydon, J.W. (2007): Geology and metallogeny of the Belt-Purcell Basin; in Mineral Deposits of Canada: A Synthesis of Major Deposit Types, District Metallogeny, the Evolution of Geological Provinces, and Exploration Methods, Goodfellow, W.D., Editor, *Geological Association of Canada*, Mineral Deposits Division, Special Publication 5, pages 581–607.
- MapPlace (2009): Southeast BC geophysics map; British Columbia Geological Survey MapPlace website, *BC Ministry of Energy, Mines and Petroleum Resources*, URL <<http://www.empr.gov.bc.ca/Mining/Geoscience/MapPlace/thematicmaps/Pages/geophysSEBC.aspx>> [December 2009].
- Mark, D.G. (1986): Geochemical/geophysical report on soil geochemistry, VLF-EM and magnetometer surveys within the Hawk 1 claim (Yellow Metal prospect), Perry Creek area, Fort Steel Mining Division, British Columbia; *BC Ministry of Energy, Mines and Petroleum Resources*, Assessment Report 15387, 31 pages.
- McDonald, J. (1986): Assessment report on geochemical soil survey on the Bar 19 mineral claim, Fort Steele Mining Division; *BC Ministry of Energy, Mines and Petroleum Resources*, Assessment Report 14823, 16 pages.
- Muller, D. and Groves, D.I. (1997): Potassic Igneous Rocks and Associated Gold-Copper Mineralization; *Springer-Verlag*, Berlin–Heidelberg–New York, 238 pages.
- Panteleyev, A., Broughton, D. and Lefebure, D. (1997): The Taurus project, a bulk tonnage gold project near Cassiar, British Columbia, NTS 104P/5; in Geological Fieldwork 1996, *BC Ministry of Energy, Mines and Petroleum Resources*, Paper 1997-1, pages 255–266.
- Ransom, P. (2006): NI 43-101 technical report on tear-2005 property (mineral claims) acquisition by Ruby Red Resources Inc. from SuperGroup Holdings Ltd. (Purcell and Rocky Mountains, Cranbrook, south-east British Columbia)/NTS 82F-82GSW; *Ruby Red Resources Inc.*, 65 pages (available on www.sedar.com).
- Ridley, J.C. and Troup, A.G. (1984): Geological, geophysical and geochemical surveys report on the Perry Creek property, Fort Steel Mining Division, British Columbia; *BC Ministry of Energy, Mines and Petroleum Resources*, Assessment Report 11802, 52 pages.
- Rowins, S.M. (2000a): Reduced porphyry copper-gold deposits: a new variation on an old theme; *Geology*, Volume 28, pages 491–494.
- Rowins, S.M. (2000b): A model for the genesis of ‘reduced’ porphyry copper-gold deposits; *The Gangue*, Issue 67, pages 1–7.
- Ruby Red Resources Inc. (2008): Ruby Red Resources – results from renewed drilling at Zeus; *Ruby Red Resources Inc.*, press release, February 26, 2008, URL <http://www.rubyredresources.com/news.html> [December 2009].
- Soloviev, S.G. (2003): Diamond drilling (phases 1 and 2) assessment report on the Bar 19 claim; *BC Ministry of Energy, Mines and Petroleum Resources*, Assessment Report 27264, 825 pages.
- Soloviev, S.G. (2004a): Assessment report on prospecting, grid soil sampling and diamond drilling on the Zinger property; *BC Ministry of Energy, Mines and Petroleum Resources*, Assessment Report 27340, 1416 pages.
- Soloviev, S.G. (2004b): Technical report and year-2003 exploration results on the Cranbrook gold project; *Chapleau Resources Ltd.*, internal report, 235 pages (available on www.sedar.com).
- Sookochoff, L. (1985): Geological evaluation report on the Leader claim group, Fort Steele Mining Division; *BC Ministry of Energy, Mines and Petroleum Resources*, Assessment Report 14112, 81 pages.
- Stanley, C.R. (2008): Missed hits or near misses: how many samples are necessary to confidently detect nugget-borne mineralization; *Geochemistry: Exploration, Environment, Analysis*, Volume 8, Number 2, pages 129–138.
- Troup, A.G. and Wong, C. (1981): Geochemistry and geophysics report, Perry Creek gold property, Fort Steele Mining Division, British Columbia; *BC Ministry of Energy, Mines and Petroleum Resources*, Assessment Report 09850, 42 pages.

Southern Nicola Project: Granite Creek Area, Southern British Columbia (Parts of NTS 092H/07, 10)

by N.W.D. Massey and S.L. Oliver¹

KEYWORDS: Nicola Group, Eastgate–Whipsaw metamorphic belt, Tulameen complex, Tulameen coal basin, mineralization

INTRODUCTION

The Southern Nicola Project area is located on the eastern boundary of Manning Park, about 15 km southwest of the town of Princeton (Figure 1), in southern British Columbia. Tectonically, the project area lies at the western edge of Quesnellia, just inboard of the bounding Pasayten fault, and includes the southernmost exposures of the Late Triassic Nicola Group.

Mapping by Rice (1947), Preto (1972) and Monger (1989) has outlined the essential distribution of Nicola Group strata in the Princeton area (NTS 092H/SE) and their relationships to younger intrusive and volcano-sedimentary sequences. To the east of the Similkameen River, rocks of the Nicola Group are assigned to the ‘eastern belt’ (Preto, 1979; Mortimer, 1987) and display an alkalic affinity; these rocks host the important porphyry and skarn deposits of the Copper Mountain area (Preto, 1972). To the west, the rocks of the Nicola Group have not been assigned to any of the three major belts, although Mortimer (1987) suggested they may belong to the calcalkaline ‘western belt’.

The western boundary of the study area is defined by the eastern edge of the Jurassic–Cretaceous Eagle Plutonic complex. Rocks adjacent to the complex, correlated with the Nicola by Rice (1947) and Monger (1989), show significant lithological differences to the immediately adjacent Nicola volcanic rocks and have been renamed the ‘Eastgate–Whipsaw metamorphic belt’ (Massey et al., 2009). This belt may be equivalent to the Late Permian–Early Triassic Sitlika–Kutcho sequences, including volcanic rocks and intrusions from the Ashcroft area (Childe et al., 1997), about 150 km north-northwest of Princeton.

Mapping in 2008 focused in the area to the southwest of Princeton (Figure 1). In 2009, mapping continued northwards from Whipsaw Creek into the Granite Creek and Tulameen River areas, concentrating on the Nicola Group rocks. Field observations were limited by lack of access or outcrop in the Arrastra Creek area and to the west of Lodestone Mountain.

PREVIOUS WORK

The area west of Princeton has a mining history dating from the discovery of placer gold in the 1860s. The first geological reports were those of Bauerman (1885), as part of the Boundary Commission Expedition of 1859–1861, and Dawson (1877). Subsequent regional mapping in the area was undertaken by Camsell (1913), Rice (1947), Preto (1972, 1979), Coates (1974) and Monger (1989). Coal-bearing units of the Princeton Group have been described by Camsell (1913), Shaw (1952), Donaldson (1973) and Evans (1978, 1985), while industrial minerals have been described by Read (1987, 2000). Comprehensive studies of the geology and petrology of the Tulameen complex have been published by Findlay (1963, 1969), Rublee (1994), Nixon (1988) and Nixon et al. (1997). No systematic mapping of Quaternary deposits, soils or terrain features has been undertaken in the area, although Hills (1962) provided some observations and discussion of the glacial and postglacial history of the area.

GEOLOGY

The results of the 2009 mapping program are summarized in Figures 2 and 3.

Stratified Units

PERMIAN (?) TO LATE TRIASSIC EASTGATE–WHIPSAW METAMORPHIC BELT

The Eastgate–Whipsaw metamorphic belt had previously been included in the Nicola Group, but is lithologically distinct. To the south, in the Eastgate area, it is quite heterogeneous, yet has been divided into three northwest-trending lithological assemblages, which show increasing metamorphic grade from east to west (Massey et al., 2009). Only the amphibolite unit continues north into the southwestern corner of the Granite Creek area. The belt is separated from schistose volcanic rocks of the Nicola Group by the Similkameen Falls fault (Massey et al., 2009), although the latter is not exposed in this area. The belt is intruded by rocks of the Eagle Plutonic complex along its western margin.

The amphibolite is overall medium grey to black, typically medium to coarse grained and well foliated, and comprises alternating mafic- and felsic-rich layers (Figure 4). It consists of black to greenish black amphibole, white feldspar, quartz and minor biotite and magnetite. The elongate amphibole minerals are usually larger than the subhedral feldspar and quartz. In some outcrops, laminae and thin layers of actinolite quartzite and actinolite-biotite quartzite oc-

¹University of British Columbia, Vancouver, BC

This publication is also available, free of charge, as colour digital files in Adobe Acrobat® PDF format from the BC Ministry of Energy, Mines and Petroleum Resources website at <http://www.empr.gov.bc.ca/Mining/Geoscience/PublicationsCatalogue/Fieldwork/Pages/default.aspx>.

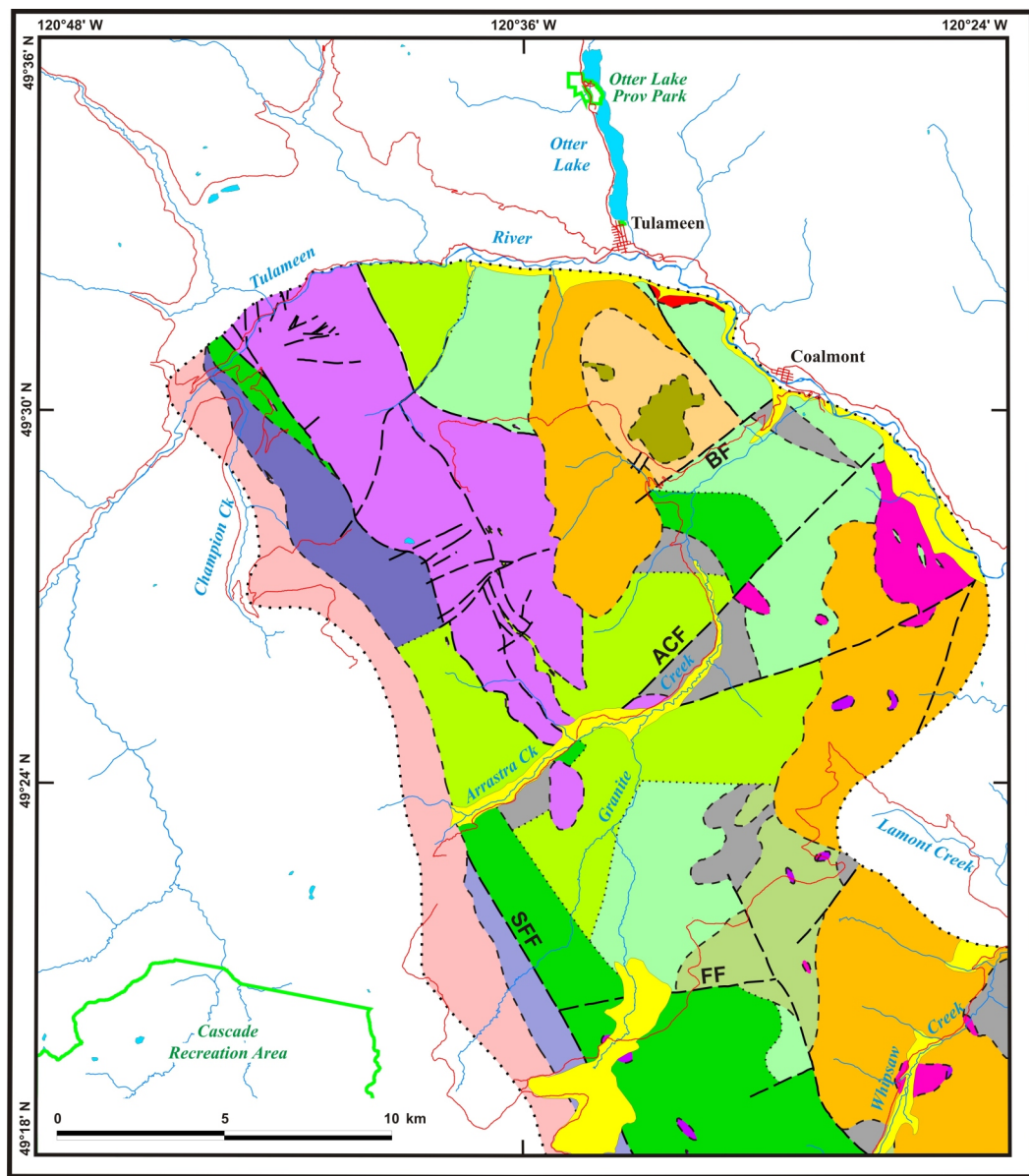


Figure 2. Geology of the Granite Creek area, southern British Columbia, from mapping done in 2009. See Figure 3 for key to geological units. Faults are shown with thick dashed lines; geological contacts with thinner dashed lines, or dotted lines where transitional or uncertain. Abbreviations: ACF, Arrastra Creek fault; BF, Blakeburn fault; FF, Frenchy Creek fault; SFF, Similkameen Falls fault.

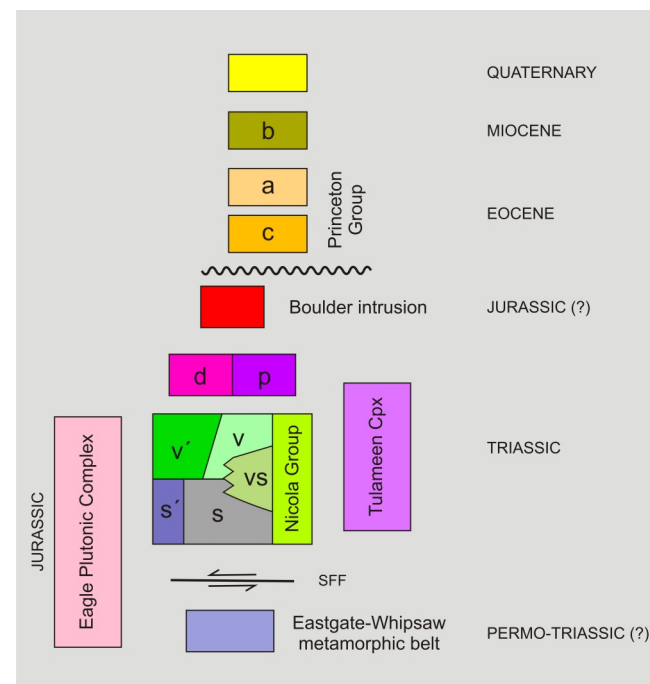


Figure 3. Geological units in the Granite Creek map area, southern British Columbia. Abbreviations: b, columnar basalt; SFF, Similkameen Falls fault; Cpx, complex. Princeton Group abbreviations: c, Cedar Formation; a, Allenby Formation. Nicola Group abbreviations: s, clastic sedimentary rocks; s', schistose metasedimentary rocks; v, volcanic rocks; vs, volcanoclastic sedimentary rocks; v', schistose volcanic rocks. Intrusive units abbreviations: d, diorite; p, pyroxenite.



Figure 4. Foliated amphibolite of the Eastgate–Whipsaw metamorphic belt, Granite Creek area, southern British Columbia (field station 09NMA04-03; UTM Zone 10, 5470528N, 658385E, NAD 83).



Figure 5. Clastic sedimentary rocks of the Nicola Group, Granite Creek area, southern British Columbia: **a)** slump structures in argillite-siltstone interbeds (field station 09NMA14-07; UTM Zone 10, 5484990N, 667162E, NAD 83); **b)** pebble conglomerate with negatively weathering limestone clasts (09NMA14-06; UTM Zone 10, 5484877N, 667157E, NAD 83).

cur interbedded with the amphibolite, which is presumably of volcanic protolith.

LATE TRIASSIC NICOLA GROUP

Rocks of the Nicola Group west of Princeton are divided into two informal lithological units, a clastic sedimentary unit and a volcanic unit. Correlation between individual outcrop areas of the two units is uncertain and they may combine several distinct stratigraphic units. Feldspathic tuff and tuffaceous sedimentary rocks, found interbedded with the clastic sedimentary unit in the Lamont main road area to the south (Massey et al., 2009), were not seen in the present map area.

The clastic sedimentary unit is dominated by black argillite interbedded with grey to green-grey siltstone and sandstone, and polymictic conglomerate. Finer grained beds are massive to laminated (Figure 5a) and may have a limy or siliceous matrix. Coarser beds can be massive, graded or laminated, and vary in thickness from millimetres to several centimetres. Layers of matrix-supported, polymictic granule to pebble conglomerate are intercalated with the finer sedimentary rocks. The clasts are dominantly clastic sedimentary, but locally include limestone (Figure 5b) and volcanic material.

In the Champion Creek area, in the northwest of the mapped area, the sedimentary rocks are strongly metamorphosed in the aureole of the Eagle Plutonic complex to produce a sequence of quartz±feldspar-rich schist with variable proportions of biotite, actinolite, garnet, muscovite and magnetite (Figure 6). Chlorite and epidote may occur as secondary alteration minerals. The schist shows marked colour banding with dark and pale layers up to several centimetres thick, although some quartzite beds can reach up to 2 m in thickness. Calcareous beds are recrystallized to buff-weathering, medium- to coarse-grained white marble. The marbles are usually massive, but can display a weak foliation delineated by quartz, chlorite or minor calcisilicate minerals.

The volcanic unit includes the interbedded pyroxene-feldspar tuff, lapilli tuff, breccia, agglomerate and tuffaceous sedimentary rocks that are characteristic of the Nicola Group in other areas (Figure 7). The rocks of this unit are light grey, weathering to green-grey with orange-stained fracture surfaces and contain lithic clasts, which vary from angular to subrounded and are typically 3–5 cm across, ranging up to 20–25 cm in breccia and agglomerate. The clasts are dominantly pyroxene-feldspar porphyritic basalt and basaltic andesite, characterized by a wide variation in proportions and sizes of phenocrysts, although aphyric basalt can also be seen. They are usually supported in a medium- to coarse-sand-sized matrix containing feldspar and pyroxene crystals, and small lithic clasts. Epidote, chlorite and calcite occur as alteration minerals in clasts and matrix, and also in veins. Quartz veins are also common.

A sequence of massive, medium grey to green, fine-grained feldspar basalt and greenstone flows occurs in the area south-east of the Granite Creek campsite. Lath-



Figure 6. Schistose metasedimentary rocks of the Nicola Group, Granite Creek area, British Columbia: **a)** thinly laminated biotite-actinolite schist (field station 09NMA01-03; UTM Zone 10, 5484828N, 650771E, NAD 83); **b)** interbedded quartzite and biotite-actinolite schist (09SOL01-10; UTM Zone 10, 5484054 N, 651703E, NAD 83); **c)** coarse actinolite needles and sheaves along a foliation plane in actinolite quartzite (09SOL02-03; UTM Zone 10, 5484382N, 651692E, NAD 83).

shaped feldspar phenocrysts 1–3 mm in size make up 5–10% of the rock. One flow also contained subhedral pyroxene phenocrysts 2–3 mm in size, with distinct blue-green feldspar in a bluish grey groundmass. Epidote and chlorite alteration is common both in the matrix and in veins.

The volcanic rocks become progressively schistose from east to west in the Fitzgerald mountain area, south of Coalmont. The tuff and lapilli tuff look massive in outcrop but display a weak foliation on broken surfaces. This foliation becomes progressively more penetrative to the west. Finer grained tuff produces bluish green-grey chlorite schist. Relict pyroxene is chloritized and varies from euhedral shapes to smeared blebs along the schistosity. Clasts in lapilli tuff and breccia are undeformed to slightly flattened. Chloritic rims may develop around the clasts, with feathering of their terminations occurring along the foliation. Similar schistose metavolcanic rocks also are found south of Arrastra Creek and in the Champion Creek area, where actinolite and biotite are developed in metavolcanic rocks in the aureole of the Eagle Plutonic complex.

PRINCETON GROUP

Eocene rocks of the Princeton Group occur in the northern (Tulameen coal basin) and eastern (Princeton basin) parts of the map area (Figure 2). They lie unconformably on the Nicola Group and related intrusive rocks. Moderate paleorelief is evident on the unconformity and was estimated at more than 300 m in the Princeton area by McMechan (1983).

Within the map area, the Princeton Group comprises a lower volcanic sequence correlated by Read (2000) with the Cedar Formation and formerly called the ‘Lower Volcanic Formation’ (Shaw 1952a, b; McMechan, 1983), and an overlying sedimentary succession referred to as the ‘Allenby Formation’. A Middle Eocene age has been suggested for these rocks based on whole-rock K-Ar dating and paleontological determinations (Church and Brasnett, 1983; Read, 2000). Field observations were restricted to outcrops of the Cedar Formation in the southwestern part of the Tulameen basin, in the Blakeburn Creek area, and on the eastern edge of the map area, from the old Rice millsite south to Bromley Creek.

In the Blakeburn Creek area, the basal unit is a distinctive fine-grained, aphyric, amygdaloidal to vuggy, massive mafic flow. It is medium grey, weathers brown to orange-brown and contains vesicles, vugs and thin veinlets infilled with milky white to clear chalcedony. This unit is overlain by a sequence of coarse-grained, grey-brown to pale brown-weathering clastic sedimentary rocks, ranging from sandstone and gritstone to pebble conglomerate. Sandstone is medium to coarse grained and includes dark lithic fragments as well as quartz and feldspar. Some beds fine upward into silty laminated tops. Conglomerate is polymictic and includes subangular to subrounded clasts of various volcanic rocks, fine-grained volcanic detritus and quartz. Clast-clast contacts are common. Carbonized plant debris was observed in one gritstone outcrop. The sedimentary sequence is overlain, in turn, by mafic to intermediate flows, which may contain some vesicles, although they are generally massive. The flows range from black to grey to buff and vary from aphyric to porphyritic. Phenocrysts include white feldspar, pink to toffee-coloured K-feldspar, pyroxene and biotite.

At the eastern edge of the map area, clastic sedimentary rocks are absent from the Cedar Formation. The volcanic rocks vary widely in type and composition, from mafic to felsic, aphyric to porphyritic, and massive to volcanoclastic. Volcanic units of intermediate composition are most common and generally display porphyritic textures. These include varieties of feldspar, feldspar-pyroxene, feldspar-

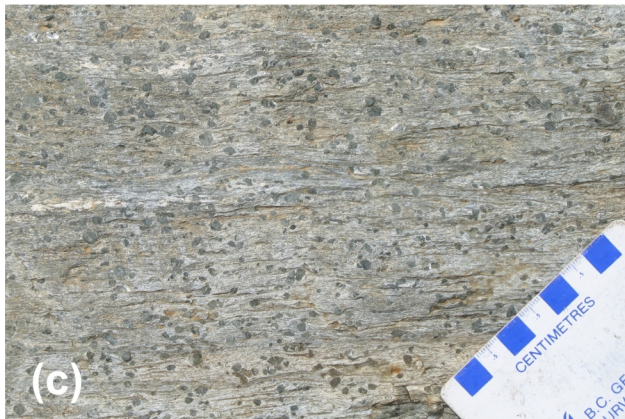


Figure 7. Volcanic and metavolcanic rocks of the Nicola Group, Granite Creek area, southern British Columbia: **a)** purple monolithic basalt breccia (field station 09NMA15-02; UTM Zone 10, 5484259N, 668284E, NAD 83); **b)** heterolithic tuff breccia (09NMA13-07; UTM Zone 10, 5483105N, 665739E, NAD 83); **c)** relict pyroxene crystals in chlorite schist (metatuff) (09NMA02-06; UTM Zone 10, 5471753N, 659170E, NAD 83); **d)** boudinaged clast in lapilli metatuff, showing notable feathering of end of clast into the schistosity (09NMA03-02; UTM Zone 10, 5472126N, 658555E, NAD 83).

hornblende and hornblende–K-feldspar andesites, megacrystic feldspar andesite and feldspar-hornblende dacite, as well as monolithic and heterolithic andesitic breccias, lapilli tuff, and pyroxene and feldspar crystal tuffs. Mafic units consist of dark grey or brown, vesicular, massive or monolithic breccia. Epidote alteration is found in the matrix of breccia, replacing feldspar phenocrysts and along fractures and veins. Chlorite infills vesicles and minor veinlets, and may be accompanied by minor calcite, quartz and zeolite.

MIOCENE COLUMNAR BASALT

Flat-lying, massive to columnar-jointed, olivine basalt flows unconformably overlie the Princeton Group in the Blakeburn area (Rice, 1947). Based on a whole-rock K-Ar determination of 9 ± 0.9 Ma (Evans, 1978; Church and Brasnett, 1983; Mathews, 1989; Breitspecher and Mortensen, 2004), these basalt flows are Miocene and therefore correlative with the Chilcotin Group. Isolated, up to room-sized blocks are also observed in the Blakeburn Creek–Newton Creek area to the west of the main outcrop areas (Figure 8). The basalt is fine- to medium-grained, black on the fresh surface, but lighter grey with orange spots on the weathered surfaces. Sparse vesicles are infilled with white quartz and zeolite. Columnar joints are well developed, although often subhorizontal due to tilting of the blocks.

Blocks up to 30 m across have also been reported in Granite Creek (Evans, 1985), which suggests that the flows were originally more extensive.



Figure 8. Large isolated block of Miocene columnar olivine basalt, Granite Creek area, British Columbia; block is approximately 2.5 m high (field station 09NMA09-14; UTM Zone 10, 5484605N, 660440E, NAD 83).

Intrusive Rocks

Several phases of intrusions occur in the map area, including: the Late Triassic ultramafic-mafic Tulameen complex, the Jurassic–Cretaceous Eagle Plutonic complex, the Jurassic (?) Boulder intrusion and minor Tertiary intrusions coeval with the Princeton Group.

LATE TRIASSIC INTRUSIONS

Tulameen ultramafic-mafic complex

The Tulameen complex is the largest Alaskan-type intrusion in British Columbia (Nixon et al., 1997). It occurs in the northwestern part of the map area, extending from Arrastra Creek to the Tulameen River (Figure 2) and north to Grasshopper Mountain. It has been described in detail by Findlay (1963, 1969), Rublee (1994) and Nixon et al. (1997). No new mapping was undertaken as part of the present study. The principal units of the complex comprise dunite, olivine clinopyroxenite, hornblende clinopyroxenite and gabbroic to dioritic and monzonitic rocks. Contacts with the surrounding Nicola Group rocks are rarely exposed and are generally faulted. However, Nixon et al. (1997) reported rafts of Nicola metasedimentary rocks intruded by gabbro and hornblende south of Blakeburn Creek. A U-Pb zircon date in the range of 204–212 Ma from a syenodiorite phase was reported by Rublee and Parrish (1990) and Rublee (1994), in agreement with older K-Ar and $^{40}\text{Ar}/^{39}\text{Ar}$ dates from hornblendes (Roddick and Farrar, 1971, 1972; McDougall, 1974), which indicates that the complex is Late Triassic, probably coeval with the surrounding Nicola Group.

Other Diorite and Pyroxenite Stocks

The Rice stock and several smaller stocks of diorite-gabbro and pyroxenite are found in the eastern part of the map area, where they intrude Nicola Group rocks or are unconformably overlain by the Princeton Group. They may be related to the Tulameen complex or to the Late Triassic Copper Mountain intrusions, further to the east.

The Rice stock is medium grey to green, coarse-grained and equigranular to slightly porphyritic gabbro to diorite. Feldspar laths are white to apple green; minor pink K-feldspar forms small interstitial crystals. Quartz is generally absent, but may be present as a minor constituent in more dioritic phases. Mafic minerals are interstitial to subhedral and include both square to lath-shaped pyroxene and tabular to needle-like hornblende, with colour indices varying from 25 to 50. Pyroxene phenocrysts up to 3–5 mm in size can impart a distinctly spotted appearance to the outcrop (Figure 9a).

An outcrop at the GD showing (Table 1), about 5 km to the west of the Rice stock, is similarly coarse-grained diorite with white to pale green plagioclase feldspar and minor pink K-feldspar. Hornblende needles range up to 1 cm in size. The diorite is notable for the presence of abundant xenoliths, including rounded, cognate pyroxenite (Figure 9b). Very coarse pegmatitic diorite, with hornblende up to 2–3 cm long, occurs in float, but was not observed in outcrop.

Coarse-grained, layered pyroxenite-gabbro-diorite occurs in an isolated outcrop 2 km south of the main Rice stock. Pyroxenite is dark green to black on fresh surfaces, weathers dark grey and contains crystals ranging up to 1 cm in size; minor white feldspar and magnetite occur intersti-

tially. Pyroxene-rich gabbro and melanodiorite are generally finer grained. The diorite also contains elongate hornblende.

JURASSIC-CRETACEOUS EAGLE PLUTONIC COMPLEX

The Eagle Plutonic complex lies along the western margin of the map area (Figure 2), intruding the Eastgate–Whipsaw metamorphic belt and Nicola Group. Greig (1989, 1992) described the complex immediately to the north. Within the map area, most outcrops belong to Greig's 'Eagle tonalite', although, in the absence of petrographic data, these were called 'biotite-granodiorite' in the field, which terminology is retained here. Greig et al. (1992) reported Middle to Late Jurassic U-Pb zircon ages for the Eagle tonalite.

The biotite-granodiorite is a syntectonic intrusion with varying texture and fabrics. A range of foliate fabrics from massive to gneissic are seen in the granodiorite. Massive phases are equigranular to seriate, varying in grain size from 3–5 mm to 5–6 mm. White feldspar forms subhedral laths. Translucent grey quartz is irregular, often interstitial to feldspar and biotite and may be smaller in grain size. Biotite is typically black and makes up 10–25% of the rock. Minor epidote, magnetite and red garnet are common. Finer grained microgranodiorite (1–2 mm grain size) is of similar

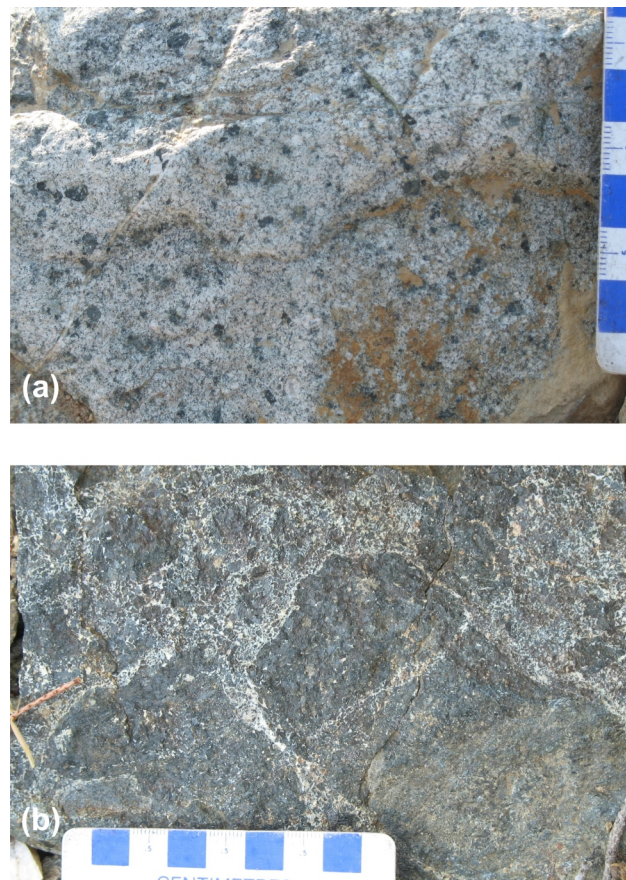


Figure 9. Triassic diorite from the Granite Creek area, southern British Columbia: **a)** pyroxene phenocrysts in diorite (field station 09NMA17-03; UTM Zone 10, 5479310N, 671135E, NAD 83); **b)** cognate pyroxenite xenoliths in diorite (09NMA18-07; UTM Zone 10, 5479715N, 666731E, NAD 83).

Table 1. Mineral occurrences in the map area (from MINFILE, 2009). Note that only the principal name is shown for each occurrence for brevity. Deposit type codes: A03, sub-bituminous coal; A04, bituminous coal; B07, bog Fe, Mn, U, Cu, Au; C01, surficial placer; D01, open-system zeolite; E06, bentonite; G06, Noranda/Kuroko massive sulphide; I01, Au-quartz vein; I02, intrusion-related Au pyrrhotite veins; I05, Ag-Pb-Zn±Au polymetallic veins; K01, Cu skarn; K04, Au skarn; K07, Mo skarn; L01, subvolcanic Cu-Ag-Au (As-Sb); L03, alkalic porphyry Cu-Au; L04, porphyry Cu±Mo±Au; M04, magmatic Fe-Ti±V oxide deposit; M05, Alaskan-type Pt±Os±Rh±Ir.

MINFILE Number	Name	Status	Commodities
Tulameen Coal Basin: Coal and industrial minerals			
092HNE094	Collin's Gulch	Past Producer	Cl, Cy
092HNE188	Fraser Gulch	Prospect	Ze
092HSE157	Basin Coal	Past Producer	Cl, Bn
092HSE228	Hayes and Vittoni	Prospect	Cl
Tulameen Complex: Cu-Pt-Cr, magnetite, olivine			
092HNE008	Jenson's	Showing	Cu
092HNE009	Sotheran	Showing	Pb, Cu, Zn, Ag
092HNE010	Britton	Showing	Cu, Ag
092HNE038	Cathy	Showing	Cu, Pt, Pd, Cr
092HNE128	D	Prospect	Cr, Pt, Cu, Ni, Ab
092HNE184	Olivine Mountain	Prospect	Pt, Cr
092HNE189	Grasshopper Mountain Olivir	Prospect	Ol
092HNE201	Asp 14	Showing	Cu
092HNE202	Copper Queen	Showing	Cu
092HNE205	H & H	Showing	Cu, Ag, Pd, Pt, Au
092HNE206	West Side	Showing	Cu, Ag, Au, Pt
092HSE034	Lodestone Mountain	Developed Prospect	Ma, Fe, Va, Pt, Ti
092HSE035	Tanglewood Hill	Developed Prospect	Ma, Fe, Ti
092HSE039	Hop	Showing	Cu, Au, Ag
092HSE095	Asp	Showing	Cu, Ag
092HSE117	Polaris 16	Showing	Cu
092HSE120	FRM 52	Showing	Cu, Pt, Pd
092HSE128	FRM 73 (99)	Showing	Cu
092HSE129	FRM 92	Showing	Cu
092HSE141	RC	Showing	Cu
092HSE142	Lode 1	Showing	Cu, Fe
092HSE159	Newton Creek Platinum	Showing	Pt, Cu
Polymetallic veins and skarn			
092HNE022	El Alamein	Past Producer	Au, Ag, Cu
092HNE097	Red Gold	Prospect	Mo, Cu, Zn, Ag, Au
092HNE209	White Gold	Showing	Zn, Ag
092HSE042	Wilmac	Showing	Cu
092HSE076	Newton Creek	Showing	Cu, Au
092HSE077	Riv	Showing	Au, Ag
092HSE105	Ski	Showing	Cu
092HSE115	Polaris	Showing	Cu
092HSE124	Goldrop	Past Producer	Zn, Cu, Pb, Au, Ag
092HSE134	GD	Prospect	Au, Cu, Ag
092HSE135	Lam	Showing	Cu
Placers			
092HNE194	Cedar Creek Placer	Past Producer	Au, Pt
092HNE195	Collins Gulch Placer	Past Producer	Au
092HNE197	Hines Creek Placer	Past Producer	Pt, Au
092HNE198	Slate Creek Placer	Past Producer	Au, Pt
092HNE199	Tulameen River Placer	Past Producer	Au, Pt, Cu
092HSE230	Granite Creek Placer	Past Producer	Au, Pt, Os, Ir, Rh, Pd, Cr, Cu
092HSE232	Newton Creek Placer	Past Producer	Au, Pt
092HSE235	Tulameen River	Past Producer	Au, Pt, Ir, Pd, Rh, Os, Ru
092HSE236	Whipsaw Creek Placer	Past Producer	Au, Pt
Other Industrial Minerals			
092HSE103	Granite Creek Gypsum	Prospect	Gy
092HSE170	Roany Creek	Past Producer	Mr

Table 1. (continued)

MINFILE Number	Latitude	Longitude	Deposit type	Zone	Easting	Northing
Tulameen Coal Basin: Coal and industrial minerals						
092HNE094	49.513890	-120.734700	A04	10	663970	5487051
092HNE188	49.513050	-120.745000	D01	10	663229	5486936
092HSE157	49.489170	-120.754200	A04, E06	10	662645	5484260
092HSE228	49.499720	-120.717200	A03	10	665285	5485514
Tulameen Complex: Cu-Pt-Cr, magnetite, olivine						
092HNE008	49.509450	-120.881700	L01, M05	10	653348	5486247
092HNE009	49.528890	-120.895000	I05, M05	10	652323	5488382
092HNE010	49.521670	-120.917500	M05	10	650717	5487533
092HNE038	49.518610	-120.906100	M05	10	651551	5487217
092HNE128	49.527220	-120.902800	M05	10	651765	5488181
092HNE184	49.519170	-120.882200	M05	10	653278	5487327
092HNE189	49.526390	-120.904200	M04	10	651667	5488085
092HNE201	49.503330	-120.854400	M05	10	655338	5485624
092HNE202	49.511110	-120.890000	M05	10	652740	5486416
092HNE205	49.530280	-120.861900	M05	10	654710	5488603
092HNE206	49.533050	-120.887200	M05	10	652873	5488861
092HSE034	49.463050	-120.836900	M05	10	656734	5481182
092HSE035	49.492220	-120.820800	M05	10	657807	5484458
092HSE039	49.455830	-120.810300	L03	10	658689	5480435
092HSE095	49.491110	-120.841100	L04	10	656342	5484293
092HSE117	49.410560	-120.789700	L04, M05	10	660326	5475446
092HSE120	49.497500	-120.891100		10	652702	5484900
092HSE128	49.433890	-120.819400	L04, M05	10	658096	5477977
092HSE129	49.434720	-120.800800	L04, M05	10	659442	5478109
092HSE141	49.489440	-120.855000	M05, L04	10	655342	5484079
092HSE142	49.486110	-120.883900	M05	10	653260	5483649
092HSE159	49.439720	-120.802200	M05	10	659325	5478662
Polymetallic veins and skarn						
092HNE022	49.539440	-120.839700	I02	10	656289	5489668
092HNE097	49.509720	-120.930800	K01, K04, K07, I05	10	649789	5486179
092HNE209	49.501390	-120.933100	I05	10	649653	5485248
092HSE042	49.375550	-120.679700		10	668424	5471795
092HSE076	49.462220	-120.736400	I05, L01	10	664022	5481304
092HSE077	49.355000	-120.601400	I01, L01	10	674183	5469688
092HSE105	49.348610	-120.604700		10	673963	5468970
092HSE115	49.405560	-120.799700		10	659617	5474869
092HSE124	49.335560	-120.626900	G06, I05	10	672395	5467468
092HSE134	49.447780	-120.699400	M05, L01, L04	10	666748	5479779
092HSE135	49.401670	-120.678100	L04	10	668456	5474701
Placers						
092HNE194	49.521670	-120.787800	C01	10	660105	5487801
092HNE195	49.532500	-120.740600	C01	10	663486	5489107
092HNE197	49.536950	-120.864700	C01	10	654488	5489339
092HNE198	49.534440	-120.822500	C01	10	657551	5489148
092HNE199	49.533610	-120.889200	C01	10	652730	5488918
092HSE230	49.456670	-120.725800	C01	10	664806	5480709
092HSE232	49.447500	-120.780000	C01	10	660911	5479573
092HSE235	49.476940	-120.629400	C01	10	671719	5483179
092HSE236	49.306390	-120.649700	C01	10	670841	5464174
Other Industrial Minerals						
092HSE103	49.481670	-120.708300	B07	10	665989	5483527
092HSE170	49.479170	-120.663300	B07	10	669257	5483349

mineral composition, although more melanocratic with up to 50% biotite.

Weakly foliated granodiorite is similar to the massive phase, except that biotite shows a marked alignment, may cluster and may also be coarser grained. In foliated phases, biotite forms penetrative sheets, or folia, that break the granodiorite into layers 1–10 cm thick. Within the layers between folia, biotite is aligned parallel to the folia. White feldspar megacrysts up to 1–2 cm can be associated with the biotite folia, giving a very distinctive spotted look to surfaces.

Massive muscovite granite, probably related to muscovite granite in the mid-Cretaceous Fallslake Plutonic suite (Grieg, 1992; Greig et al., 1992), occurs in the upper Arrastra Creek area. The granite is pinkish white to pale grey, medium to coarse grained (1–3 mm grain size) and leucocratic. It contains both pink and white subhedral feldspar laths, rounded to interstitial quartz, silvery micaceous muscovite and black biotite. Contacts between the granite and the biotite granodiorite were not observed.

JURASSIC (?) BOULDER INTRUSION

Granite of the Boulder intrusion occurs in the very northeast of the map area near Tulameen. This intrusion of still uncertain age was not visited during this present study, but has been described by Camsell (1913) and Rice (1947) as pink, coarse-grained, hornblende granite. It intrudes rocks of the Nicola Group and is, in turn, intruded by the Cretaceous Otter Lake stock.

MINOR TERTIARY INTRUSIONS

Dikes of mafic to felsic composition, coeval with the Princeton Group, occur throughout the map area. They include feldspar basalt; pyroxene, pyroxene-feldspar and hornblende±feldspar andesite porphyries; hornblende-feldspar, feldspar and aphyric dacite; and rare rhyolite.

STRUCTURE

Folds

Problematic correlation within different lithological units, the lack of regional markers and suspected facies changes within the volcanic and volcanoclastic rocks of the Nicola Group render the identification of major folds difficult. Although few bedding attitudes were observed, even in the sedimentary rocks, they generally strike northwesterly. Dips are often steep, 60–80° to both the northeast and the southwest. Bedding attitudes in the sedimentary unit immediately northeast of Roany Creek suggest that they lie in the core of a syncline. However, the volcanic rocks in the two limbs show significant lithological differences and the effects of faulting cannot be discounted.

Schistosity or cleavage in the Nicola Group rocks is subparallel to bedding, where both are observed. They strike northwesterly with variable (40–80°) southwesterly dips. Dips are more consistent, with steep inclinations (50–75°) closer to the contact with the Eagle Plutonic complex. Amphibolite of the Eastgate–Whipsaw metamorphic belt and syntectonic granodiorite of the Eagle Plutonic complex have similarly inclined schistositities.

Two schistositities are discernible in some outcrops in the Whipsaw area to the south (Massey et al., 2009). These intersect at an acute angle and it is often difficult to deter-

mine their relative order of formation; similar fabrics were rarely observed in the Granite Creek area. Occasionally observed outcrop-scale S- and Z-folds of both bedding and schistosity (Figure 10) usually show shallow plunges of 10–20° to the southeast. The age of deformation of rocks within the Nicola Group and Eastgate–Whipsaw metamorphic belt is unknown, although it is at least, in part, contemporaneous with the intrusion of the Middle to Late Jurassic Eagle tonalite.

The Tertiary Tulameen basin preserves a portion of a southeasterly plunging syncline, which has been truncated on the southeast by the Blakeburn fault (Church and Brasnett, 1983; Read, 1987). Beds are generally gently dipping (up to 35°), although they may steepen up to 63° on the western limb (Read, 1987). Princeton Group rocks in the east of the map area lie on the western limb of the Tailings syncline of the Princeton basin (Read, 1987); however, the predominantly massive volcanic rocks yield a scarcity of structural information.

Major Faults

Contacts between the Tulameen complex and the Nicola Group are reported to be ductile shears or faults (Nixon et al., 1997). The attitudes of contact faults and re-



Figure 10. S-fold in actinolite-chlorite schist of the Nicola Group metavolcanic unit, Granite Creek area, southern British Columbia (field station 09NMA03-03-01; UTM Zone 10, 5472062N, 658522E, NAD 83).

lated planar fabrics in adjacent rocks along the western margin of the Tulameen complex are parallel to the regional northwesterly trending foliations in the Nicola Group and Eagle Plutonic complex. Northeast- to easterly trending high-angle faults crosscut the Tulameen complex and may be contemporaneous with other northeasterly trending faults cutting the Nicola Group, such as the Arrastra Creek fault (Figure 2). The age of this faulting is unknown, but truncation of the Tulameen coal basin by the Blakeburn fault suggests that some of the faulting may be Tertiary.

The Eastgate–Whipsaw metamorphic belt is separated from Nicola Group volcanic rocks by the northwest-trending Similkameen Falls fault of unknown age. Though not exposed in the present field area, it is seen along Highway 3 about 1 km south of Similkameen Falls (Massey et al., 2009). The fault trace appears to be linear and is inter-

preted to be steep. It terminates easterly trending faults in the Nicola Group and also appears to acutely crosscut the three lithological assemblages of the Eastgate–Whipsaw metamorphic belt, which suggests that it postdates the Middle–Late Jurassic deformation. Both the metamorphic belt and the fault trace are terminated by muscovite granite of the Eagle Plutonic complex, which may correlate with the mid-Cretaceous Fallslake Plutonic suite, suggesting that the fault predates the mid-Cretaceous.

MINERALIZATION

Some 48 mineral occurrences are reported for the map area in the MINFILE database (Table 1; MINFILE, 2009). The most important of these are the deposits of the Late Tri-

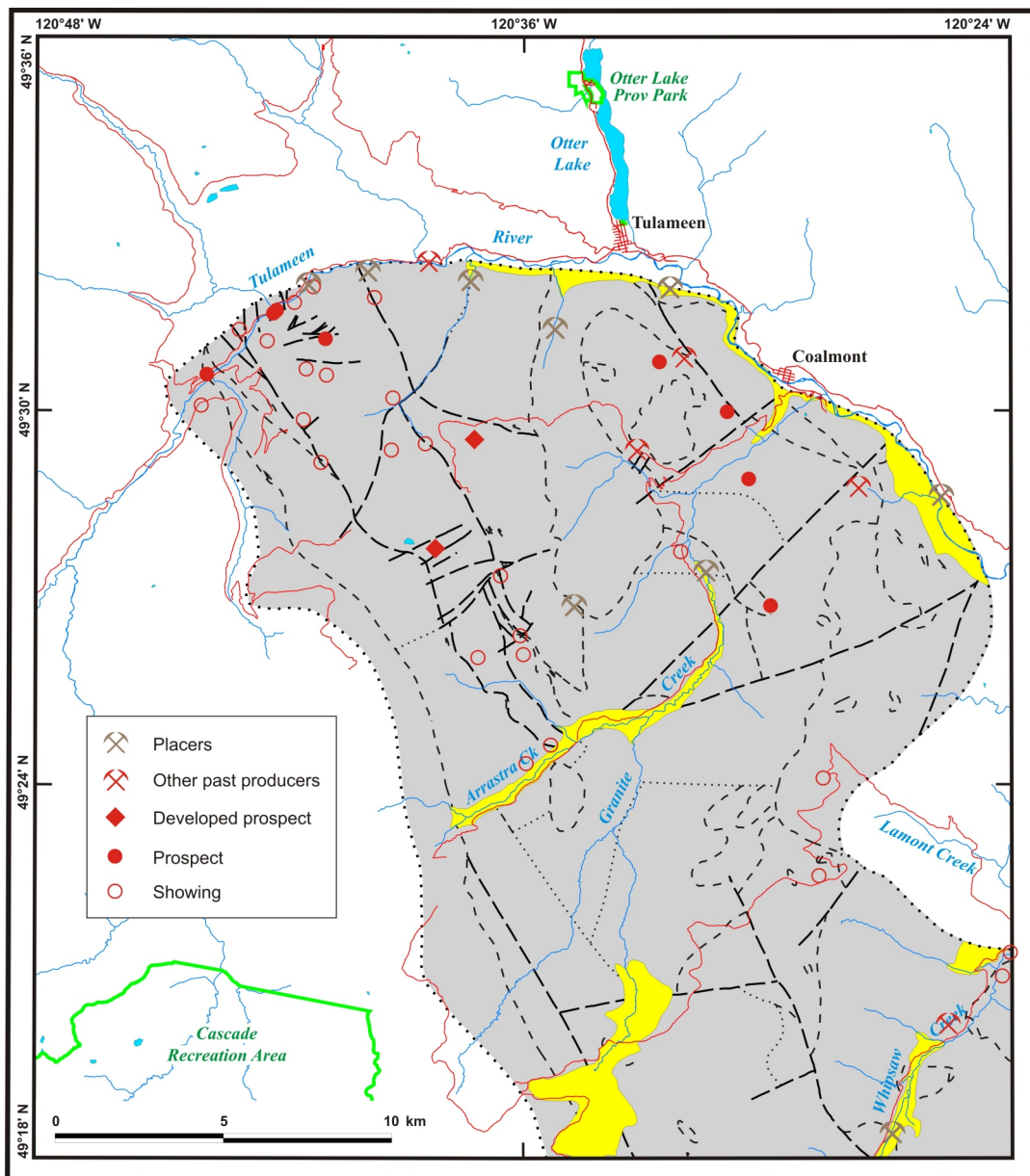


Figure 11. Locations of mineral occurrences in the map area, Granite Creek area, southern British Columbia. Geological contacts and faults in the grey map area are as in Figure 2.

assic Tulameen complex, the Tertiary Tulameen coal basin and the various gold-platinum placers.

Tulameen Complex

Twenty-two of the MINFILE occurrences lie in the northwestern corner of the map area (Figure 11) and are hosted in the Tulameen complex. Aspects of the geology and mineralization have been described by Camsell (1913), Rice (1947), Findlay (1969) and Nixon et al. (1997); four main types of deposit have been found. Chromitite in the dunite core of the complex, in the Olivine Mountain area, forms bulbous or irregular masses or thin discontinuous schlieren up to 4 m in length (Nixon et al., 1990). The chromitite can be rich in platinum group metals, although the proportion of platinum group minerals is highly variable. Minor quantities of base-metal sulphide and arsenide minerals also occur.

Magnetite forms semi-massive to massive lenses or vein-like bodies in hornblende pyroxenite in the Lodestone Mountain and Tanglewood Hill areas. The lenses vary from a few centimetres to 5.5 m thick, although they usually are less than 1 m thick. Ilmenite, minor leucoxene and sphene are intimately associated with the magnetite.

Copper mineralization is associated with a variety of hostrocks, commonly gabbro to diorite or hornblende-rich pegmatite. Mineralization is primarily chalcopyrite, pyrite and bornite, but may include minor sphalerite and galena. Whereas some silver and platinum have been reported in assays, only trace quantities of gold have been found. The mineralization occurs in lenticular or discontinuous zones within faults, fractures and quartz veins. Some hostrocks exhibit epidote-chlorite alteration, and malachite and azurite staining is also found.

Olivine from unserpentinized dunite in the Olivine Mountain–Grasshopper Mountain area may be suitable for the production of foundry sand and other refractory products (White, 1987; Hora and White, 1988).

Tulameen Coal Basin

Exploration for, and production of, coal in the Tulameen basin has proceeded sporadically since prior to 1900, when coal was first discovered near Blakeburn Creek and Collins Gulch. Summaries and details of the coal deposits and their exploration have been provided by Camsell (1913), Rice (1947), Shaw (1952), Donaldson (1973), Church and Brasnett (1983), Evans (1985) and Read (2000). From 1919 to 1940, underground coal mines extracted about 2 million tonnes from the Tulameen basin, and in the 1950s, surface mining extracted about 0.15 million tonnes (Ryan, 2004). There was renewed exploration in the Tulameen basin in the 1970s and 1980s, and a major exploration program in 1998. Small-scale production has proceeded sporadically into the 2000s.

The coal deposits are hosted in the Allenby Formation of the Princeton Group. Several coal seams are found in a shale-rich member approximately 130 to 200 m thick (the Vermilion Bluffs shale of Read, 1987), underlain by up to 120 m of sandstone, siltstone and andesitic volcanic rocks ('Hardwicke sandstone' of Read, 1987), and overlain by 580 to 700 m of sandstone and pebble conglomerate, with interbeds of shale, ash and coal in the lower sections ('Summers Creek sandstone' of Read, 1987). The coal consists of up to 30 m of coal interbedded with mudstone, bentonite

shale and sandstone. It occurs in the lower 80 m of the coal-shale member in a zone of mostly brown to grey to black fissile shale and mudstone with lesser coal and white to buff bentonite. Individual seams vary in thickness from a few centimetres to over 10 m and strike lengths, up to 2–3 km; however, correlation of seams between the two limbs of the basin is not possible. Coal rank is generally high-volatile C to B bituminous (Ryan, 2002).

Zeolite and bentonite are also known from intermediate to felsic ash-rich sedimentary units in the Allenby Formation of the Tulameen basin (Read, 2000).

Gold-Platinum Placers

Placer deposits were discovered along the Tulameen and Similkameen rivers in the 1860s, with major production starting up in the 1880s. Within the map area, the richest deposits were on Granite Creek and the Tulameen River; however, several other creeks have also attracted interest (Table 1; Figure 10). Although production at most deposits continued intermittently only into the 1930s, exploration and production along the Tulameen River continued well into the 1970s. Interest is now limited to small-scale seasonal operations.

Gold has been the main focus of interest, but significant platinum has also been extracted (Rice, 1947). Metals found along the Tulameen River tend to occur in old sinuous channels buried deep below glacial gravel, which yields only spotty values. At Granite Creek, gold- and platinum-bearing sections are generally found to occur on bedrock. These pay gravels are well indurated and cemented by a stiff clay. The gold in the placers occurs in rough, angular or slightly flattened, rarely well-flattened nuggets, some of which contain abundant white quartz. Platinum forms small rounded grains of uniform size, which are smaller than the gold nuggets and are commonly pitted. The gravel worked along the upper Tulameen River also yielded black sand consisting of magnetite and chromite as well as significant gold and platinum values. The origin of the gold and platinum in the placers is believed to be from gold veins of the Grasshopper Mountain area and the chromitite, in the dunite of the Tulameen complex in the Olivine Mountain region (Rice, 1947; Nixon et al., 1990; Levson et al., 2002).

Other Occurrences

Copper mineralization similar to that observed in the Tulameen complex is found associated with the Rice stock at the GD (MINFILE 092HSE134; MINFILE, 2009) and Lam (MINFILE 092HSE135) occurrences and in pyroxenite at the Wilmac (MINFILE 092SHE042) showing. Other mineral showings mainly consist of a variety of quartz veins with gold and sulphide minerals, and a polymetallic skarn; gypsum and marl are found in Quaternary sediments in the Granite Creek area.

ACKNOWLEDGMENTS

The authors are much indebted to Rob Marshall of Weyerhaeuser (Princeton), Todd Chamberlain of Stuwix Resources Ltd. (Merritt) and Dean Jaeger of Tolko Industries Ltd. (Merritt), for all their invaluable help and advice during the planning stages of this project. The authors also acknowledge the Canadian Mining Initiative Council for

the financial support provided to the second author. Paul Schiarizza offered invaluable comments on an earlier draft of this manuscript.

REFERENCES

- Baerman, H. (1885): Report on the geology of the country near the forty-ninth parallel of north latitude west of the Rocky Mountains; *Geological Survey of Canada*, Report of Progress 1882–83–84, Part B, pages 5–42.
- Breitspacher, K. and Mortensen, J.K. (2004): BC Age 2004A-1: a database of isotopic age determinations for rock units from British Columbia; *BC Ministry of Energy, Mines and Petroleum Resources*, Open File 2004-3.
- Camsell, C. (1913): Geology and mineral deposits, Tulameen District, British Columbia; *Geological Survey of Canada*, Memoir 26, 188 pages.
- Childe, F.C., Friedman, R.M., Mortensen, J.K. and Thompson, J.F.H. (1997): Evidence for Early Triassic felsic magmatism in the Ashcroft (92I) map area, British Columbia; in *Geological Fieldwork 1996*, *BC Ministry of Energy, Mines and Petroleum Resources*, Paper 1997-1, pages 117–123.
- Church, B.N. and Brasnett, D. (1983): Geology and gravity survey of the Tulameen coal basin (92H), in *Geological Fieldwork 1982*, *BC Ministry of Energy, Mines and Petroleum Resources*, Paper 1983-1, pages 47–54.
- Coates, J.A. (1974): Geology of Manning Park area, British Columbia; *Geological Survey of Canada*, Bulletin 238, 177 pages.
- Dawson, G.M. (1877): Report on explorations in British Columbia; *Geological Survey of Canada*, Report of Progress 1875–76, pages 233–265.
- Donaldson, J.R. (1973): The petrography of the coal from the Blakeburn strip mine in the Tulameen coal area, British Columbia; *Geological Survey of Canada*, Paper 72-39, 13 pages.
- Evans, S.H. (1978): Tulameen coal basin; in *Geological Fieldwork 1977*, *BC Ministry of Energy, Mines and Petroleum Resources*, Paper 1978-1, pages 83–84.
- Evans, S.H. (1985): Geology of the Tulameen coal basin; in *Geology in British Columbia 1977–1981*, *BC Ministry of Energy, Mines and Petroleum Resources*, pages 76–87.
- Findlay, D.C. (1963): Petrology of the Tulameen ultramafic complex, Yale District, British Columbia; PhD thesis, *Queen's University*, 415 pages.
- Findlay, D.C. (1969): Origin of the Tulameen ultramafic-gabbro complex, southern British Columbia; *Canadian Journal of Earth Sciences*, Volume 6, pages 399–425.
- Greig, C.J. (1989): Geology and geochronometry of the Eagle Plutonic complex, Coquihalla area, southwestern British Columbia, (92H6, 7, 10, 11); MSc thesis, *University of British Columbia*, 423 pages.
- Greig, C.J. (1992): Jurassic and Cretaceous plutonic and structural styles of the Eagle Plutonic complex, southwestern British Columbia, and their regional significance; *Canadian Journal of Earth Sciences*, Volume 29, pages 793–811.
- Greig, C.J., Armstrong, R.L., Harakal, J.E., Rinkle, D and van der Hayden, P. (1992): Geochronometry of the Eagle Plutonic complex and the Coquihalla area, southwestern British Columbia; *Canadian Journal of Earth Sciences*, Volume 29, pages 812–829.
- Hills, L.V. (1962): Glaciation, structures and micropalaeontology of the Princeton coalfield, British Columbia; MSc thesis, *University of British Columbia*, 141 pages.
- Hora, Z.D. and White, G.V. (1988): The evaluation of olivine sand prepared from Tulameen dunite ((92H/10); in *Fieldwork 1987*, *BC Ministry of Energy, Mines and Petroleum Resources*, Paper 1988-1, pages 381–383.
- Levson, V.M., Mate, D.J. and Ferbey, T. (2002): Platinum-group element (PGE) placer deposits in British Columbia: characterization and implications for PGE potential; in *Geological Fieldwork 2001*, *BC Ministry of Energy, Mines and Petroleum Resources*, Paper 2002-1, pages 303–312.
- Massey, N.W.D., MacIntyre, D.G., Desjardins, P.J. and Cooney, R.T. (2005): Geology of British Columbia; *BC Ministry of Energy, Mines and Petroleum Resources*, Geoscience Map 2005-3, scale 1: 1 000 000.
- Massey, N.W.D., Vineham, J.M.S. and Oliver, S.L. (2009): Southern Nicola Project: Whipsaw Creek–Eastgate–Wolfe Creek area, southern British Columbia (NTS 092H/01W, 02E, 07E, 08W); in *Geological Fieldwork 2008*, *BC Ministry of Energy, Mines and Petroleum Resources*, Paper 2009-1, pages 189–204.
- Mathews, W.H. (1989): Neogene Chilcotin basalts in south-central British Columbia: geology, ages, and geomorphic history; *Canadian Journal of Earth Sciences*, Volume 26, pages 969–982.
- McDougall, I. (1974): The $^{40}\text{Ar}/^{39}\text{Ar}$ method of K-Ar age determination of rocks using HIFAR reactor; *Atomic Energy in Australia*, Number 17, pages 9–18.
- McMechan, R.D. (1983): Geology of the Princeton Basin; *BC Ministry of Energy, Mines and Petroleum Resources*, Paper 1983-3, 52 pages.
- MINFILE (2009): MINFILE BC mineral deposits database; *BC Ministry of Energy, Mines and Petroleum Resources*, URL <<http://minfile.ca>> [November 2009].
- Monger, J.W.H. (1989): Geology, Hope, British Columbia; *Geological Survey of Canada*, Map 41-1989, scale 1:250 000.
- Mortimer, N. (1987): The Nicola Group: Late Triassic and Early Jurassic subduction-related volcanism in British Columbia; *Canadian Journal of Earth Sciences*, Volume 24, pages 2521–2536.
- Nixon, G.T. (1988): Geology of the Tulameen ultramafic complex; *BC Ministry of Energy, Mines and Petroleum Resources*, Open File 1988-25, scale 1:25 000.
- Nixon, G.T., Cabri, L.J. and Laflamme, J.H.G. (1990): Platinum-group-element mineralization in lode and placer deposits associated with the Tulameen Alaskan-type complex, British Columbia; *Canadian Mineralogist*, Volume 28, pages 503–535.
- Nixon, G.T., Hammack, J.L., Ash, C.A., Cabri, L.J., Case, G., Connelly, J.N., Heaman, L.M., Laflamme, J.H.G., Nuttall, C.N., Paterson, W.P.E. and Wong, R.H. (1997): Geology and platinum-group-element mineralization of Alaskan-type ultramafic-mafic complexes in British Columbia; *BC Ministry of Energy, Mines and Petroleum Resources*, Bulletin 93, 142 pages.
- Preto, V.A. (1972): Geology of Copper Mountain; *BC Ministry of Energy, Mines and Petroleum Resources*, Bulletin 59, 87 pages.
- Preto, V.A. (1979): Geology of the Nicola Group between Merritt and Princeton; *BC Ministry of Energy, Mines and Petroleum Resources*, Bulletin 69, 90 pages.
- Read, P.B. (1987): Tertiary stratigraphy and industrial minerals, Princeton and Tulameen basins, British Columbia; *BC Ministry of Energy, Mines and Petroleum Resources*, Open File 1987-19, scale 1:25 000.
- Read, P.B. (2000): Geology and industrial minerals of the Tertiary basins, south-central British Columbia; *BC Ministry of Energy, Mines and Petroleum Resources*, GeoFile 2000-03, 110 pages.
- Rice, H.M.A. (1947): Geology and mineral deposits of the Princeton map-area, British Columbia; *Geological Survey of Canada*, Memoir 243, 136 pages.

- Roddick, J.C. and Farrar, E. (1971): High initial argon ratios in hornblendes; *Earth and Planetary Science Letters*, Volume 12, pages 208–214.
- Roddick, J.C. and Farrar, E. (1972): Potassium-argon ages of the Eagle granodiorite, southern British Columbia; *Canadian Journal of Earth Sciences*, Volume 9, pages 596–599.
- Rublee, V.J. (1994): Chemical petrology, mineralogy and structure of the Tulameen complex, Princeton area, British Columbia; MSc thesis, *University of Ottawa*, 183 pages.
- Rublee, V.J. and Parrish, R.R. (1990): Chemistry, chronology and tectonic significance of the Tulameen complex, south-western British Columbia; *Geological Association of Canada – Mineralogical Association of Canada*, Abstracts with Programs, Volume 15, page A114.
- Ryan, B.D. (2002): Coal in British Columbia; *BC Ministry of Energy, Mines and Petroleum Resources*, URL <<http://www.empr.gov.bc.ca/Mining/Geoscience/Coal/CoalBC/Pages/default.aspx>>, [November 2009].
- Ryan, B.D. (2004): Coalbed gas potential in British Columbia; *BC Ministry of Energy, Mines and Petroleum Resources*, Petroleum Geology Paper 2004-1, 76 pages.
- Shaw, W.S. (1952a): The Princeton coalfield, British Columbia; *Geological Survey of Canada*, Paper 52-12, 28 pages.
- Shaw, W.S. (1952b): The Tulameen coalfield, British Columbia; *Geological Survey of Canada*, Paper 52-19, 13 pages.
- White, G.V. (1987): Olivine potential in the Tulameen ultramafic complex preliminary report; in *Geological Fieldwork 1986, BC Ministry of Energy, Mines and Petroleum Resources*, Paper 1987-1, pages 303–307.

Boundary Project: Geochronology and Geochemistry of Jurassic and Eocene Intrusions, Southern British Columbia (NTS 082E)

by N.W.D. Massey, J.E. Gabites¹, J.K. Mortensen¹ and T.D. Ullrich¹

KEYWORDS: Quesnel terrane, Jurassic, Eocene, McKinney Creek stock, West Kettle batholith, Mount Baldy stock, Beaverdell suite, Greenwood stock, Gidon Creek porphyry

INTRODUCTION

The Boundary Project was initiated in 2005 with the purpose of better characterizing the lithological and geochemical variations within and between the various Paleozoic sequences in the southern Okanagan region along the United States border (Massey, 2006, 2007a, b; Massey and Duffy, 2008a–c). These sequences occur within Quesnel terrane, which is dominated by Paleozoic mafic volcanic and pelitic rocks that are unconformably overlain by Triassic and Jurassic volcanic and sedimentary rocks, and intruded by various suites of Triassic, Jurassic and Eocene granitic rocks. This paper documents the results of isotopic dating and lithochemical studies on several of the granitic intrusions in the project area.

ANALYTICAL METHODOLOGY

U-Pb Zircon Dating

Uranium-lead dating of zircons was carried out at the Pacific Centre for Isotopic and Geochemical Research (PCIGR) at The University of British Columbia, using the laser-ablation inductively coupled plasma–mass spectrometry (LA-ICP-MS) method. Instrumentation employed at the PCIGR comprises a New Wave UP-213 laser-ablation system and a ThermoFinnigan Element2 single-collector, double-focusing, magnetic-sector ICP-MS. Data acquisition and reduction protocols at the PCIGR have been described by Tafti et al. (2009), and are summarized below. Zircons were hand-picked from the heavy mineral concentrate and mounted in an epoxy puck along with several grains of the Plešovice zircon standard (Sláma et al., 2007), together with an in-house, 197 Ma standard zircon, and brought to a very high polish. High-quality portions of each grain free of alteration, inclusions or possible inherited cores were selected for analysis. The surface of the mount was washed for 10 minutes with dilute nitric acid and rinsed in ultraclean water prior to analysis. Line scans rather than spot analyses were employed in order to minimize elemental fractionation during the analyses. Backgrounds were

measured with the laser shutter closed for 10 seconds, followed by data collection with the laser firing for approximately 29 seconds. The time-integrated signals were analyzed using GLITTER software (Van Achtenbergh et al., 2001; Griffin et al., 2008), which automatically subtracts background measurements, propagates all analytical errors and calculates isotopic ratios and ages. Corrections for mass and elemental fractionation were made by bracketing analyses of unknown grains with replicate analyses of the Plešovice zircon standard. A typical analytical session at the PCIGR consists of four analyses of the standard zircon, followed by four analyses of unknown zircons, two standard analyses, four unknown analyses, etc., and finally four standard analyses. The 197 Ma in-house zircon standard was analyzed as an unknown in order to monitor the reproducibility of the age determinations on a run-to-run basis. Final interpretation and plotting of the analytical results employ the Isoplot software (version 3.09; Ludwig, 2003). Interpreted ages are based on a weighted average of the individual calculated $^{206}\text{Pb}/^{238}\text{U}$ ages.

Although zircons typically contain negligible amounts of initial common Pb, it is important to monitor the amount of ^{204}Pb present in order to evaluate the amount of initial common Pb, and/or blank Pb, that is present in the zircons being analyzed. The argon that is used in an ICP-MS plasma commonly contains at least a small amount of Hg, and approximately 7% of natural Hg has a mass of 204. Measured count rates on mass 204 include ^{204}Hg as well as any ^{204}Pb that might be present, and direct measurement of ^{204}Pb in a laser-ablation analysis is therefore not possible. Instead, mass 202 is monitored; this corresponds exclusively to ^{202}Hg . The expected count rate for ^{204}Hg present in the analysis can then be calculated from the known isotopic composition of natural Hg, and any remaining counts at mass 204 can be attributed to ^{204}Pb . Using this method, it is possible to conclude that there was no measurable ^{204}Pb present in any of the analyses in this study.

Ar/Ar Dating

Biotite and hornblende for $^{40}\text{Ar}/^{39}\text{Ar}$ dating were hand-picked from fine crushed samples. Mineral separates for dating were wrapped in aluminum foil and stacked in an irradiation capsule with samples of similar age and neutron flux monitors (Fish Canyon Tuff sanidine [FCs], 28.02 Ma; Renne et al., 1998). The samples were irradiated at the McMaster Nuclear Reactor in Hamilton, Ontario for 90 MWh, with a flux of approximately 6×10^{13} neutrons/cm²/s. Analyses ($n = 45$) of 15 neutron-flux monitor positions produced errors of <0.5% in the J value. The samples were analyzed at the Noble Gas Laboratory of the PCIGR. The mineral separates were step-heated at incrementally higher powers in the defocused beam of a 10W CO₂ laser (New Wave Research MIR10) until fused.

¹ The University of British Columbia, Vancouver, BC

This publication is also available, free of charge, as colour digital files in Adobe Acrobat® PDF format from the BC Ministry of Energy, Mines and Petroleum Resources website at <http://www.empr.gov.bc.ca/Mining/Geoscience/PublicationsCatalogue/Fieldwork/Pages/default.aspx>.

The gas evolved from each step was analyzed by a VG5400 mass spectrometer equipped with an ion-counting electron multiplier. All measurements were corrected for total system blank, mass spectrometer sensitivity, mass discrimination, radioactive decay during and subsequent to irradiation, and interfering Ar from atmospheric contamination and the irradiation of Ca, Cl and K (isotope production ratios: $(^{40}\text{Ar}/^{39}\text{Ar})_{\text{K}} = 0.0302 \pm 0.00006$; $(^{37}\text{Ar}/^{39}\text{Ar})_{\text{Ca}} = 1416.4 \pm 0.5$; $(^{36}\text{Ar}/^{39}\text{Ar})_{\text{Ca}} = 0.3952 \pm 0.0004$; $\text{Ca}/\text{K} = 1.83 \pm 0.01(^{37}\text{Ar}_{\text{Ca}}/^{39}\text{Ar}_{\text{K}})$). Plateau and correlation ages were calculated using Isoplot (Ludwig, 2003). Errors are quoted at the 2 (95% confidence) level and are propagated from all sources except mass spectrometer sensitivity and age of the flux monitor.

Results of the dating studies are briefly summarized in Table 1. Complete analytical data are presented in Massey et al. (2010). Locations of samples are shown in Figure 1.

JURASSIC AND EOCENE INTRUSIONS

Greenwood Area

GREENWOOD STOCK

Several granodiorite stocks and smaller bodies in the Greenwood area have been ascribed to the Jurassic Nelson suite (Little, 1983; Fyles, 1990). The Greenwood stock

(sample 1 on Figure 1 and in Table 1) is one of these bodies, centred on the city of Greenwood. Like the other intrusions, it consists of medium- to coarse-grained, grey biotite-hornblende granodiorite to quartz diorite. It intrudes chert and basalt of the Knob Hill Complex and lies in the footwall of the western extension of the Snowshoe fault, a listric normal fault of Tertiary age (Fyles, 1990).

Results of laser-ablation determinations (Figure 2a) yield a latest Early Jurassic age of 179.9 ± 3.8 Ma. This is slightly older than the reported age of 172.5 ± 5.0 Ma for the oldest phases of the Nelson batholith (Ghosh, 1995) and suggests earlier plutonic activity in the Boundary district. It is, however, slightly younger than the volcanic rocks of the Sinemurian Elise Formation of the Rossland Group (Høy and Dunne, 1997).

GIDON CREEK PORPHYRY

The Gidon Creek porphyry (sample 5 in Figure 1 and Table 1) is well exposed in roadcuts in the Norwegian Creek and Gidon Creek areas. The porphyry intrudes Triassic Brooklyn Formation metavolcanics in the footwall of the Number 7 fault, although its relationship to the fault was not directly observed.

The sample is a leucocratic quartz-feldspar porphyry. Pink perthitic K-feldspar megacrysts are subhedral to subrounded and about 1 cm in size, ranging up to 2 cm.

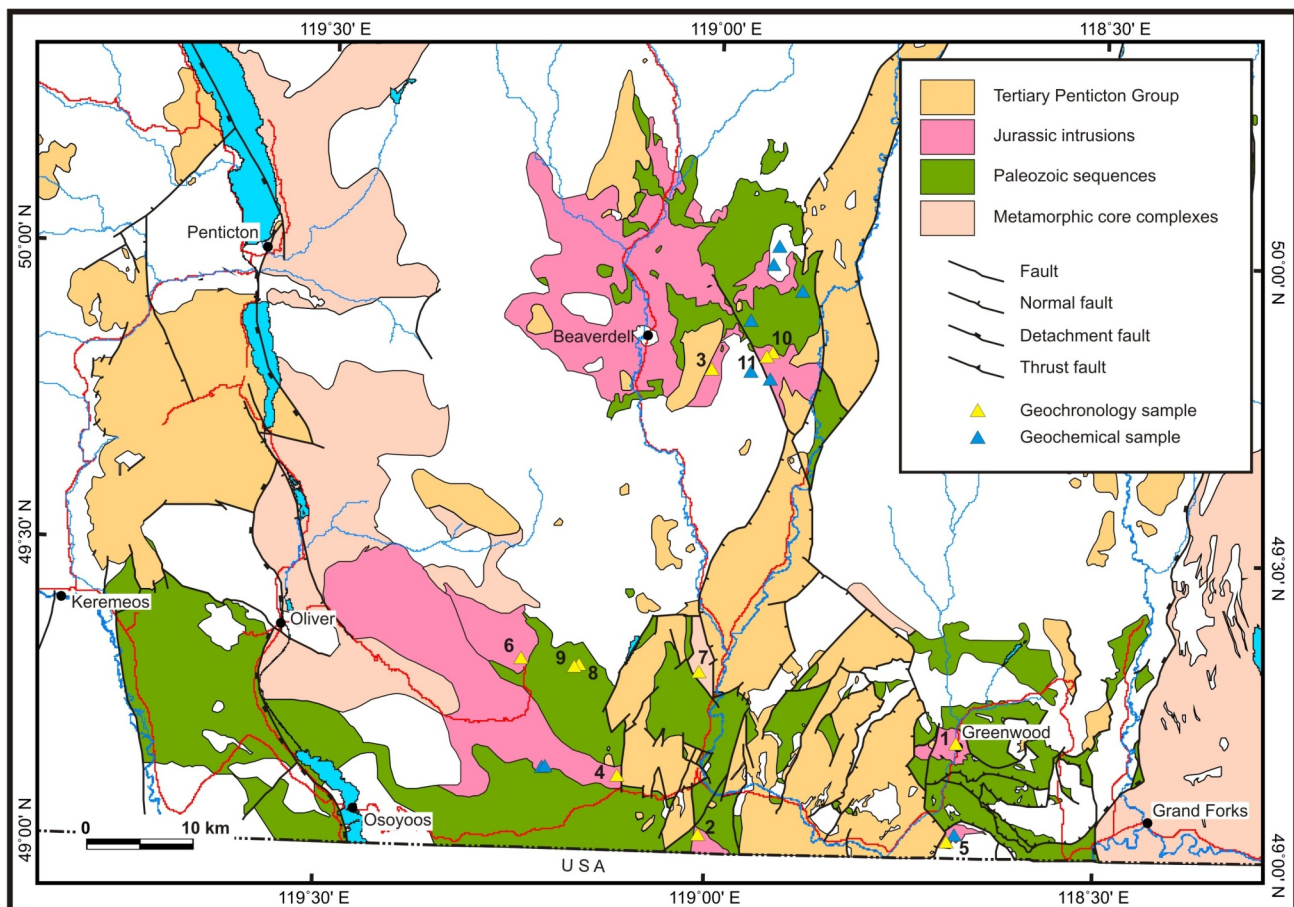


Figure 1. Regional geology of the Boundary Project area (amended from Massey et al., 2005), southern British Columbia, showing the location of samples collected for geochronology and geochemistry. Geochronological samples are numbered as in Table 1. The Paleozoic sequences include the Wallace Formation of the Beaverdell area, which may be Triassic. Only the sampled intrusions are shown on the map; others have been omitted.

Table 1. Summary of U-Pb zircon and $^{40}\text{Ar}/^{39}\text{Ar}$ ages obtained for intrusive samples collected during the Boundary Project, southern British Columbia. All UTM location data are in Zone 11, NAD83. Errors associated with individual ages are listed at the 2 level (95% confidence interval); see Massey et al. (2010) for complete analytical data.

Sample number	Map unit	Latitude	Longitude	UTM		Area	Age		Note	
		°N	°W	Northing	Easting		Ma	±		
Zircon (laser ablation)										
<i>Jurassic intrusions</i>										
1	06NMAGreenwood1	Greenwood stock (Nelson suite)	49.097050	118.680870	5439604	377298	Greenwood, Trans-Canada Trail	179.9	3.8	Some inherited zircons
2	06NMA05-01-02	Myer's Creek stock (Nelson suite)	49.016554	119.011395	5431245	352934	Old railway, west of Myncaster	157.0	1.2	
3	07NMA45-005	West Kettle batholith (Nelson suite)	49.410378	119.005005	5475009	354563	South Crystal Lake	213.5	0.9	
4	07NMA09-02	McKinney Creek stock (Nelson suite)	49.061520	119.116490	5436452	345390	Roadcut, Jolly Creek campsite	57.1	0.5	Inherited zircons ranging from 80 to ~2500 Ma
5	05NMA25-01B	Gidon Creek porphyry	49.009087	118.695168	5429850	376036	Gidon Creek	171.6	2.3	Inherited zircons ranging from 225 to 1978 Ma
6	07NMA09-01	Mount Baldy granodiorite	49.161480	119.240650	5447824	336650	South slope of ski hill	168.5	1.40	
<i>Unknown age</i>										
7	06NMA22-12A	Ed James orthogneiss	49.151378	119.017097	5446243	352916	Conkle Lake, Ed James Forest Service road	187.7	1.1	
	06NMA22-12B	Unfoliated leucogranite intrudes 06NMA22-12A	49.151378	119.017097	5446243	352916	Conkle Lake, Ed James Forest Service road	--	--	Insufficient zircons recovered
Hornblende ($^{40}\text{Ar}/^{39}\text{Ar}$)										
8	07NMA05-15-Hb	Diorite, McKinney Creek (Nelson suite?)	49.155757	119.164309	5447025	342198	Powerline, Rock Creek	--	--	No plateau age (extreme excess argon); no sensible isochron
9	07NMA05-16-Hb	Diorite, McKinney Creek (Nelson suite?)	49.154794	119.167530	5446925	341960	Powerline, Rock Creek	--	--	No plateau age; no sensible isochron
	07NMA05-16-Bio	Diorite, McKinney Creek (Nelson suite?)	49.154794	119.167530	5446925	341960	Powerline, Rock Creek	51.00	0.28	Plateau age
								51.00	0.31	Isochron
10	07NMA41-008-Hb	Crowded feldspar hornblende diorite'	49.420506	118.929211	5475992	360089	GK Property, Crouse Creek	--	--	No plateau age; no sensible isochron
11	07NMA43-010-Hb	Crowded feldspar hornblende diorite'	49.418590	118.937517	5475794	359482	GK Property, Crouse Creek	177.3	1.0	Plateau age

Plagioclase phenocrysts were also observed, although smaller than the K-feldspar. Quartz eyes are rounded and commonly 3–5 mm in size but ranging up to 10 mm. Ground-mass is a white to pale pink, finer grained mosaic of quartz, K-feldspar and plagioclase crystals. Mafic minerals are sparse, with colour index often <5%, and are mostly biotite replaced by chlorite.

The margins of the porphyry are sheared, foliation varying from trachytic to mylonitic in appearance. Where preserved, phenocrysts are broken and strung out along the foliation. Quartz shows strained extinction in thin sections. Feldspars are completely altered to sericite, epidote and chlorite.

The Gidon Creek porphyry has been correlated with the nearby Lexington porphyry (Fyles, 1990), subsequently dated at 199 Ma by Church (1992) and Dostal et al. (2001). However, the Gidon Creek quartz-feldspar porphyry is lithologically and chemically distinct from the Lexington porphyry and probably not directly correlatable (Massey, 2007c). Zircons from the Gidon Creek porphyry confirm this, yielding a Middle Jurassic age of 171.6 ± 2.3 Ma (Figure 3a). Xenocrystic zircons of several ages,

including 225 Ma, 373–363 Ma, 1689 Ma and 1978 Ma, are also present in the sample (Figure 3a; the oldest two analyses are not shown in the figure).

The porphyry may correlate with the Silver King intrusions of the Rossland area, which have similar ages (Höy and Dunne, 1997). These synkinematic intrusions show intensely sheared margins similar to those of the Gidon Creek porphyry but lack the K-feldspar megacrysts (Dunne and Höy, 1992).

Rock Creek–McKinney Creek Area

MCKINNEY CREEK GRANODIORITE

The McKinney Creek granodiorite (sample 4 in Figure 1 and Table 1) forms a linear body just north of Bridesville. It has been correlated with the Nelson intrusions (Little, 1961; Tempelman-Kluit, 1989) and intrudes rocks of the Paleozoic Anarchist schist to the north and south. However, relationships with more gneissic rocks to the west are uncertain. The stock comprises two distinct phases: an early biotite granodiorite and later porphyritic

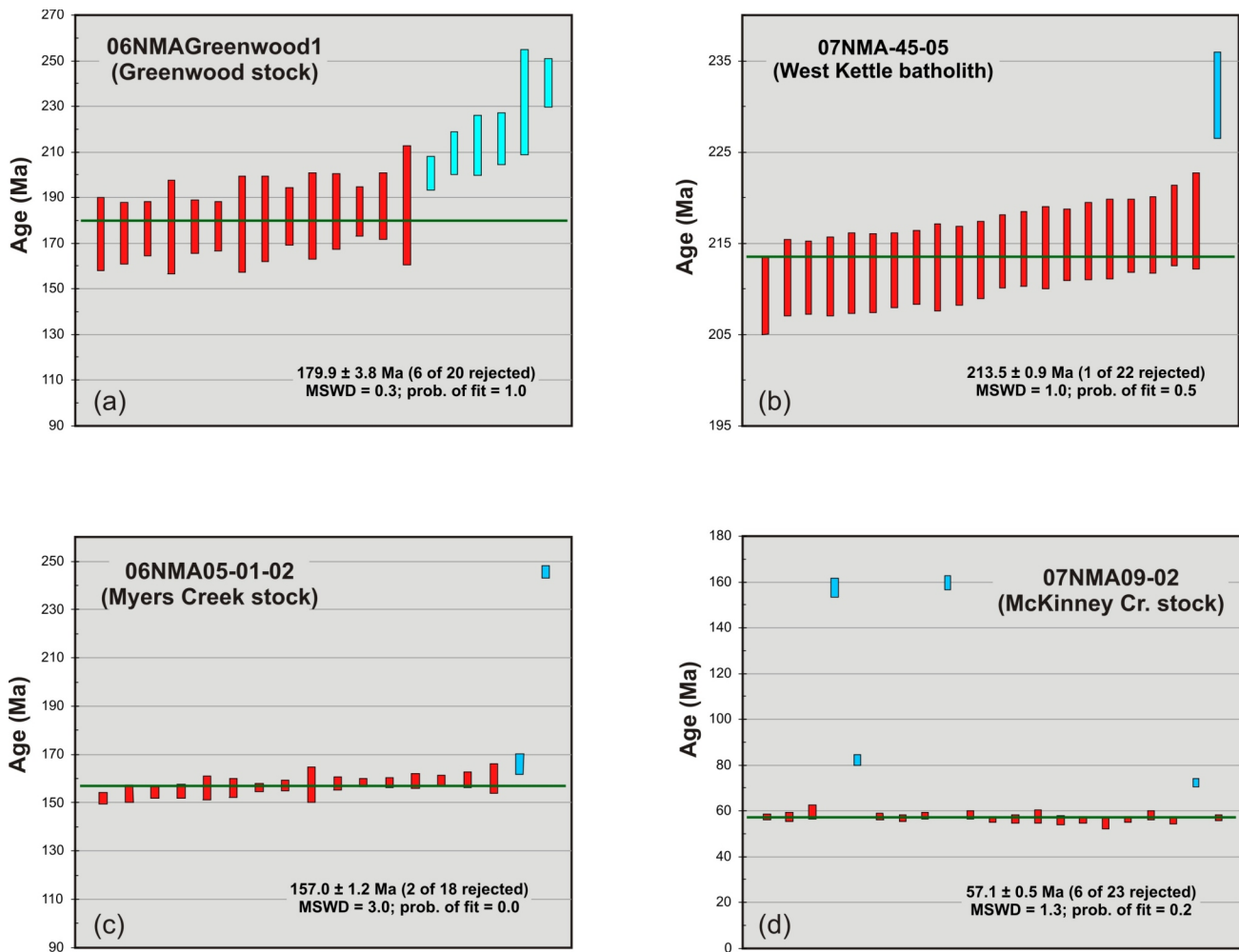


Figure 2. LA-ICP-MS zircon age determinations for 'Nelson suite' granitic bodies in the Boundary Project area, southern British Columbia: **a)** Greenwood stock, **b)** West Kettle batholith, **c)** Myers Creek stock, and **d)** McKinney Creek stock (two rejected samples >180 Ma have been omitted). See Table 1 for location data. Error bars for individual analyses and for the final weighted average ages on these and subsequent plots are shown at the 2 level. Analyses that were included in the weighted average age are shown as red bars and those that were rejected are shown as blue bars.

granodiorite. Only the biotite granodiorite was sampled for geochronometry. It is coarse grained (up to 4 mm) and white to grey. It is equigranular with typical ‘salt-and-pepper’ texture made up of white feldspar, translucent quartz and black biotite plates. Biotite also forms clots that can be up to 1 cm. Colour index averages 25. Small rounded amphibolite xenoliths are common and chlorite coats fractures and joints.

Zircons from the McKinney Creek biotite granodiorite yield a Paleocene age of 57.1 ± 0.5 Ma (Figure 2d), with some older xenocrystic zircons ranging up to about 2500 Ma (two samples not plotted in Figure 2d). This is in contrast to an age of 160.5 ± 2.0 Ma reported by Parkinson (1985), possibly within the same stock, to the northwest of Anarchist Mountain. However, it compares favourably with U-Pb ages of 62–54 Ma obtained from the Ladybird granite and is slightly older than the 52–50 Ma ages reported for the syenitic Coryell suite (Parrish et al., 1988; Ghosh, 1995). Parrish (1992b) also reported an age of 48 ± 5 Ma, based on the lower intercept of discordant U-Pb zircon determinations, for biotite granite from the Okanagan batholith in the upper Kettle River area.

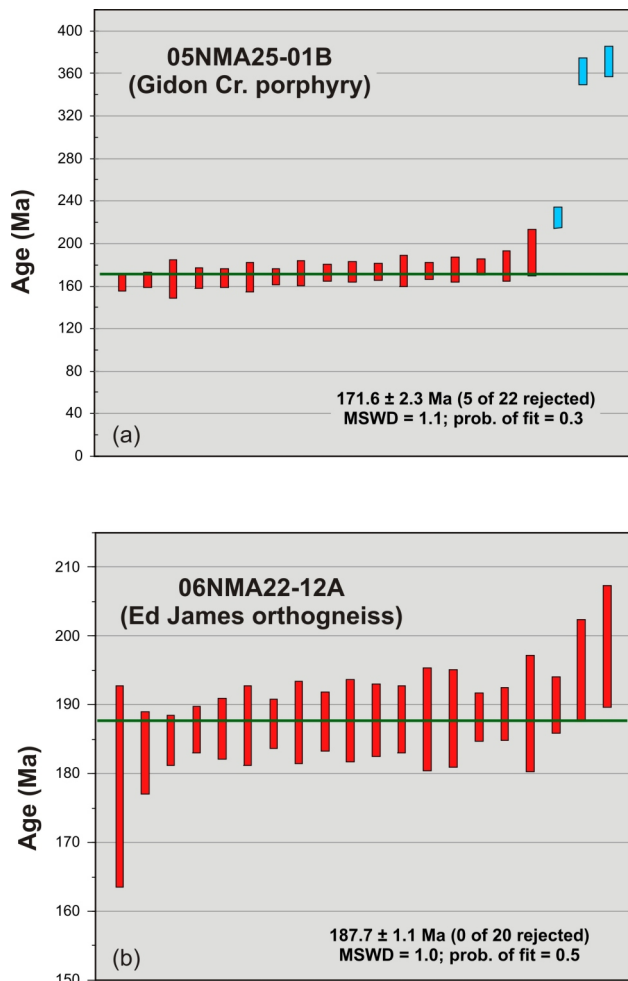


Figure 3. LA-ICP-MS zircon age determinations for felsic bodies of previously unknown age in the Boundary Project area, southern British Columbia: a) Gidon Creek porphyry (two rejected samples >100 Ma have been omitted), b) Ed James Creek orthogneiss. See Table 1 for sample locations.

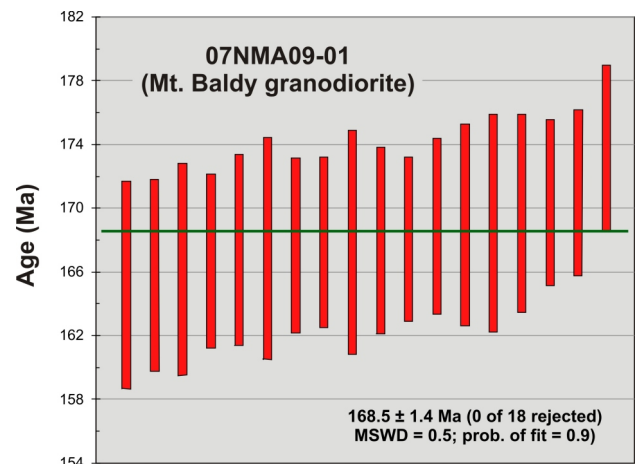


Figure 4. LA-ICP-MS zircon age determinations for the Mount Baldy stock, Boundary Project area, southern British Columbia. See Table 1 for sample locations.

MOUNT BALDY GRANODIORITE

The Mount Baldy granodiorite (sample 6 in Figure 1 and Table 1) is medium to coarse grained, ranging from 2 to 5 mm, and shows an equigranular phaneritic texture. It is light to dark grey and comprises euhedral white feldspar, irregular grey quartz and black tabular biotite. Chlorite alteration is apparent within the rock. The granodiorite is cross-cut by feldspar porphyry dikes, assumed to be Tertiary in age. Isotropic, lath-shaped hornblende may be developed in the granodiorite around some porphyry dikes. The stock is part of the Okanagan batholith (Tempelman-Kluit, 1989), a larger body of poorly constrained Jura-Cretaceous age that includes K-feldspar megacrystic granite correlated with the Eocene Coryell suite (Massey and Duffy, 2008c).

Zircons from the Mount Baldy stock yield a Middle Jurassic age of 168.5 ± 1.4 Ma (Figure 4), comparable to similar Middle Jurassic ages from the Nelson batholith and Bonnington pluton (Ghosh, 1995). It confirms the presence of Middle Jurassic magmatic products in the Okanagan batholith, although more mapping and geochronological studies are needed to adequately discriminate all its phases.

DIORITE-GABBRO

A belt of diorite occurs along the northeastern edge of the McKinney Creek map area (Massey and Duffy, 2008c), intruding rocks of the Paleozoic Anarchist schist. The unit comprises medium- to coarse-grained, black to grey diorite to gabbro that weathers dark greenish grey. The rock comprises varying quantities of equigranular greenish black hornblende and white feldspar, and occasional quartz. Shear zones are common, accompanied by flattening and stretching of minerals, white veinlets of feldspar and quartz, and chloritization. Pegmatitic diorite veins are also found. The unit is a composite intrusion with fine-grained chills between different diorite phases. These fine-grained chills are difficult to distinguish from basaltic dikes in small outcrops. Several ultramafic intrusions are spatially associated with the belt of diorite, and presumed to be genetically related.

The mafic rocks are intruded by, and included as xenoliths in, Jurassic (?) granodiorite and may be an older phase of the Nelson suite. Diorite and serpentinite are also in-

truded by the Mount Baldy granodiorite. Alternatively, the diorite and ultramafic rocks may be contemporaneous with older Jurassic ultramafic intrusions in the Greenwood area (e.g., on the Sappho property; Nixon, 2002).

Two samples of hornblende-rich diorite were collected for $^{40}\text{Ar}/^{39}\text{Ar}$ age determination (samples 8 and 9 in Figure 1 and Table 1). Unfortunately, the separated hornblendes showed excess argon and failed to yield a plateau age. However, one sample of biotite yielded a plateau age of 51.0 ± 0.3 Ma (Figure 5), representing a cooling age after the regional heating effects of Eocene magmatism and extensional tectonics. The crystallization age for the diorite remains undetermined.

MYERS CREEK QUARTZ DIORITE

The Myers Creek stock (sample 2 in Figure 1 and Table 1) is a grey to orange white quartz diorite to diorite. It is medium to coarse grained and equigranular, with a typical salt-and-pepper texture. It comprises white feldspar, colourless quartz, black flakey biotite and minor black hornblende. Mafic minerals locally form up to 30% of the rock. Like the McKinney Creek stock, the Myers Creek stock was correlated with the Nelson suite by Little (1961) and Tempelman-Kluit (1989). It is found in either faulted or intrusive contact with quartzite and metasedimentary rocks of the Anarchist schist (Massey, 2007a).

Zircons from the Myers Creek stock yielded an earliest Late Jurassic age of 157.0 ± 1.2 Ma (Figure 2c). This is significantly younger than the other Jurassic intrusions sampled in the area, and the Middle Jurassic Nelson suite with which it was previously correlated. Magmatic activity in the Late Jurassic is poorly documented in southern BC. However, similar late Middle to early Late Jurassic ages have been reported from a biotite granite phase of the Nelson batholith (158.9 ± 0.6 Ma; Sevigny and Parrish, 1993), a leucocratic gneiss remnant from the Kinnaid gneiss (156.6 ± 6.0 Ma; Ghosh, 1995) and metaporphyrphy in the Nicola horst (158.3 ± 0.6 Ma; Moore et al., 2000; 157.5 ± 0.5 Ma; Erdmer et al., 2002), suggesting that this magmatism is more common in southern BC than previously believed.

ED JAMES CREEK ORTHOGNEISS

Orthogneiss forms an inlier in the Ed James Creek area (sample 7 in Figure 1 and Table 1), lying structurally beneath the Knob Hill Complex, although the bounding fault is not exposed. Schistosity within the gneiss is flat to moderately dipping to the east, matching that in the rocks of the overlying Knob Hill Complex and suggesting an easterly-dipping extensional fault. A subvertical normal fault bounds the gneiss to the east, putting it in contact with Tertiary volcanic and sedimentary rocks. The gneiss is tentatively correlated with gneiss of the Proterozoic Grand Forks Gneiss Complex, which shares a similar structural relationship with the Knob Hill Complex in the Grand Forks area (Höy and Jackaman, 2005) and with the Vaseaux gneiss of the Okanagan Valley (Tempelman-Kluit, 1989).

Several varieties of orthogneiss are observed in the study area. A grey biotite-feldspar-quartz gneiss is most common. It is coarse grained and well foliated, with schistosity defined by the alignment of biotite porphyroblasts. White feldspar porphyroblasts, ranging up to 5 mm in longest dimension, form small augens. Biotite forms large clots, up to 2 cm in diameter, within the foliation plane, giving a spotted appearance to the rock when broken

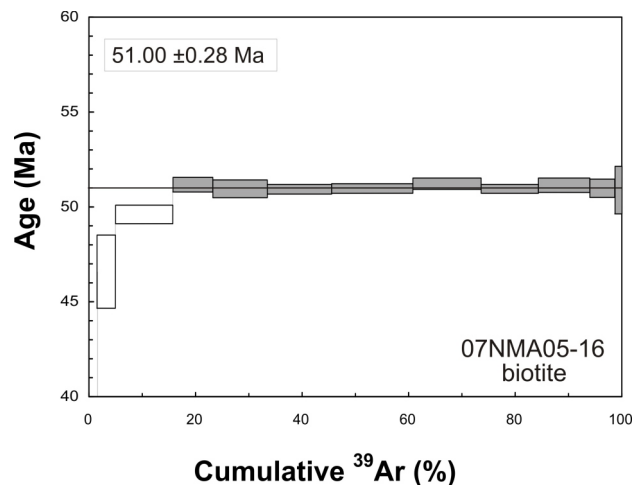


Figure 5. $^{40}\text{Ar}/^{39}\text{Ar}$ age spectrum for biotite from diorite in the McKinney Creek vicinity of the Boundary Project area, southern British Columbia. See Table 1 for sample locations. Box heights for steps in this plot are shown at the 2 level. Steps that were utilized for that plateau age calculation are filled; rejected steps are open.

appropriately. Variation in mineral proportions results in colour banding and a variation from diorite to granodiorite in composition.

The gneiss is intruded by a medium- to coarse-grained unfoliated leucogranite. The rock is composed predominantly of white feldspar and quartz with minor biotite; colour index is less than 5 and the rock occasionally shows a pinkish hue on fresh surfaces.

Zircons from the biotite-feldspar-quartz gneiss yielded an Early Jurassic age of 187.7 ± 1.1 Ma (Figure 3b). This compares to the 197–181 Ma age reported for the Fife diorite of the Christina Lake area (Acton et al., 2002), but is older than the Middle Jurassic ages reported here, and previously (Ghosh, 1995), for the Nelson batholith. Other Early Jurassic diorite and porphyry bodies occur in the Rossland area and have been correlated with volcanic rocks of the Early Jurassic Rossland Group (Fyles, 1984; Brown and Logan, 1989).

No zircons were recovered from the unfoliated leucogranite. Similar post-tectonic granitic intrusions in the Castlegar gneiss yielded early Tertiary ages (Parrish et al., 1988; Parrish, 1992a).

Beaverdell Area

WEST KETTLE BATHOLITH

The West Kettle batholith is composed of granodiorite, quartz diorite and microgranodiorite with minor aplite and pegmatite. The granodiorite is white to light grey and medium to coarse grained equigranular with a typical salt-and-pepper texture. Weathered surfaces are white to grey but can be greenish or slightly pink. The rock comprises white subhedral feldspar, translucent irregular quartz, greenish black tabular hornblende and black biotite flakes. Pink feldspar is minor. Quartz varies from about 5 to 20% or may be absent in dioritic phases. Colour index is about 10–15 but may range up to 25 in diorite and quartz diorite. Chlorite and epidote occur in veins, chlorite and iron oxides on fracture surfaces. Xenoliths of amphibolite and microdiorite are occasionally seen.

Zircons from a sample of granodiorite from the West Kettle batholith (sample 3 in Figure 1 and Table 1) yielded a Late Triassic age of 213.5 ± 0.9 Ma (Figure 2b). It compares to the similar Late Triassic age assigned to the Josh Creek diorite in the Christina Lake area by Acton et al. (2002).

Further, the West Kettle batholith has a similar calc-alkaline, volcanic-arc character and normalized rare earth element (REE) patterns that are identical to volcanic rocks of the Wallace Formation, which it intrudes (Massey, 2010). This suggests that the West Kettle batholith may be, at least in part, coeval with the Wallace Formation.

HORNBLENDE CROWDED FELDSPAR DIORITE

Bodies of diorite, quartz diorite, microdiorite and microgranodiorite intrude sedimentary rocks of the Wallace Formation east of Beavertell (samples 10 and 11 in Figure 1 and Table 1). These are medium- to coarse-grained equigranular rocks comprising white feldspar, green-black hornblende and variable amounts of quartz. One distinctive lithology, termed the 'hornblende crowded feldspar diorite' by Greig and Flasha (2005), underlies much of the GK property. This rock is characterized by abundant subrounded to subhedral lath-shaped, white feldspar crystals set in a finer grained black groundmass of acicular hornblende and feldspar. Tabular hornblende phenocrysts may also be developed. Quartz is rare or absent. The diorite is variably mineralized with up to 5% disseminated pyrrhotite, lesser pyrite and rare arsenopyrite (Greig and Flasha, 2005). The relationship of the dioritic rocks to the West Kettle granodiorite is presently unknown.

One sample yielded a good hornblende $^{40}\text{Ar}/^{39}\text{Ar}$ plateau age of 177.3 ± 1.0 Ma (Figure 6). This is significantly younger than the Late Triassic age obtained for the West Kettle batholith, and compares with that of the Nelson suite Greenwood stock.

GEOCHEMISTRY OF THE GRANITOID INTRUSIONS

Whole-rock geochemical analyses were carried out on all the dated samples, as well as other samples from the Jurassic and Eocene intrusions (Figure 1). Results are summarized in Table 2. Although only a small number of samples was analyzed, the results appear to suggest some differences between the various suites.

All samples are subalkaline, intermediate to felsic (Figure 7), and calcalkaline or high-K calcalkaline (Figures 8, 9) in character, with the exception of

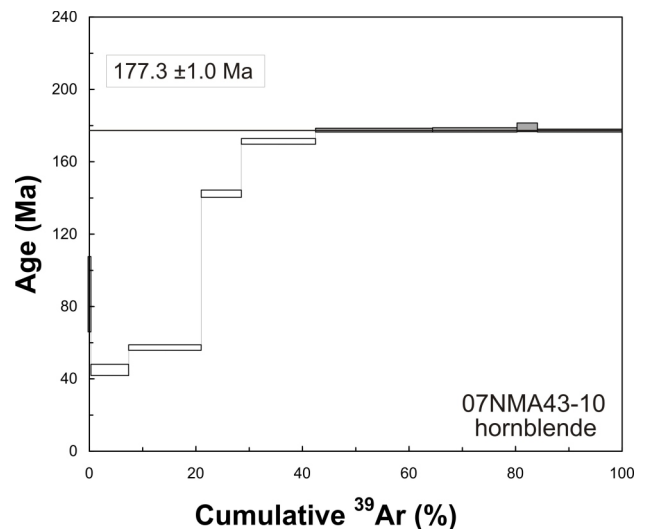


Figure 6. $^{40}\text{Ar}/^{39}\text{Ar}$ spectrum for hornblende from the 'hornblende crowded feldspar diorite' (Greig and Flasha, 2005), Crouse Creek vicinity, Boundary Project area, southern British Columbia. See Table 1 for sample locations. Box heights for steps in this plot are shown at the 2 level.

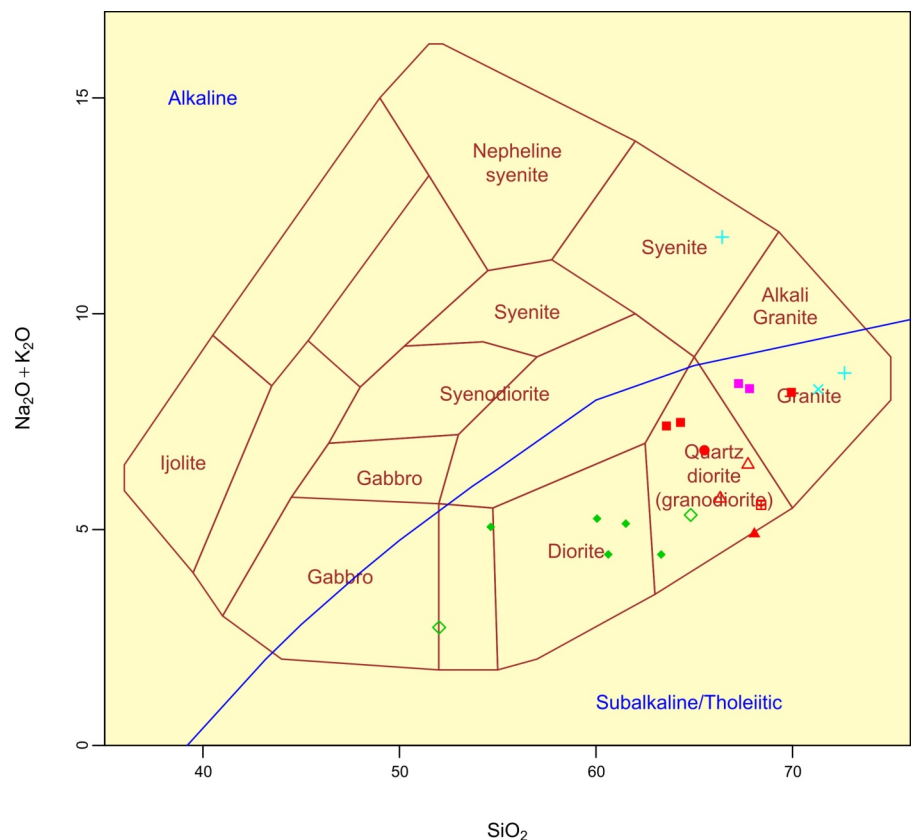


Figure 7. Total alkali versus SiO_2 plot for granitic intrusions in the Boundary Project area, southern British Columbia. Classification fields and nomenclature from Wilson (1989) after Cox et al. (1979). The alkaline-subalkaline dividing line is from Irvine and Baragar (1971). Symbols: open green diamonds, McKinney diorite; solid green diamonds, Beavertell diorite; open red triangles, Triassic West Kettle batholith; solid red triangle, Middle Jurassic Greenwood stock; red X, Middle Jurassic Mount Baldy stock; solid purple squares, Middle Jurassic Gidon Creek porphyry; red crossed square, Middle Jurassic Ed James orthogneiss; solid red circle, Late Jurassic Myers Creek stock; solid blue squares, Eocene McKinney Creek stock; blue crosses, Eocene Beavertell intrusion; blue crossed square, Eocene Ed James leucogranite.

Table 2. Whole-rock geochemical analyses for granitic intrusions in the Boundary Project area, southern British Columbia. Major elements and Rb, Sr, Ba, Y, Zr, Nb, V, Ni and Cr were determined by x-ray fluorescence (major elements on fused disc, trace elements on pressed-powder pellet) by Teck (Global Discovery) Labs. Rare earth elements, Th, Ta and Hf were determined by peroxide-fusion inductively coupled plasma–mass spectrometry at Memorial University of Newfoundland. Dashes indicate element determination below detection limit; blank values indicate elements not analyzed.

Analytical parameter	McKinney diorite ¹		McKinney Creek stock			Mount Baldy stock	Myers Creek stock	Ed James Lake orthogneiss		Gidon Creek porphyry	
	07NMA05-15	07NMA05-16	07NMA09-02	07NMA14-16	07NMA14-17	07NMA09-01	06NMA05-01-02	06NMA22-12A	06NMA22-12B	05NMA25-01B	05NMA25-03A
SiO ₂	51.38	64.36	60.92	69.09	63.42	70.61	64.30	67.50	75.96	66.62	66.03
TiO ₂	0.45	0.47	0.63	0.22	0.53	0.27	0.49	0.29	0.05	0.34	0.32
Al ₂ O ₃	15.15	16.06	16.57	15.75	16.31	15.63	15.68	16.80	13.74	16.28	16.60
Fe ₂ O ₃							1.40			1.62	1.81
FeO							2.65			1.00	0.72
Fe ₂ O ₃ t	7.74	5.17	5.58	2.38	5.03	1.60		2.86	0.50		
MnO	0.17	0.09	0.06	0.04	0.09	0.02	0.08	0.08	0.01	0.07	0.07
MgO	9.15	2.33	1.89	0.84	1.89	0.46	1.83	0.94	0.02	0.77	0.68
CaO	11.98	5.33	2.84	2.29	3.79	2.18	4.53	4.59	0.66	3.19	3.46
Na ₂ O	2.47	3.47	2.78	3.48	3.59	4.95	3.23	3.95	4.42	4.74	4.50
K ₂ O	0.23	1.83	4.31	4.60	3.79	3.22	3.48	1.55	4.07	3.38	3.73
P ₂ O ₅	0.05	0.18	0.23	0.09	0.19	0.08	0.18	0.12	0.01	0.12	0.18
BaO	0.01	0.09	0.09	0.11	0.09	0.16	0.09	0.09	0.01	0.07	0.08
LOI	1.20	0.60	3.42	0.49	0.67	0.31	1.81	0.58	0.15	1.03	1.12
Total	99.98	99.98	99.32	99.38	99.39	99.49	99.75	99.35	99.60	99.23	99.30
Rb	-	66	185	175	198	60	98	51	137	80	106
Sr	181	512	386	378	467	1084	703	560	175	1062	1087
Ba	122	870	868	1128	865	1575	869	894	99	751	836
Y	17	8	15	10	21	-	15	11	4	21	10
Zr	27	86	183	101	188	134	150	69	54	144	146
Nb	7	10	18	14	21	8	11	3	9	16	23
V	169	115	127	47	103	33	76	77	18	63	61
Ni	99	-	6	-	3	-	-	-	-	-	-
Cr	353	10	27	22	30	15		60	-		
La	1.243	15.346	36.980	30.329	49.986	36.935	29.817	7.829	3.672	19.798	18.209
Ce	3.661	25.062	68.400	54.991	91.380	67.791	54.659	14.829	8.150	35.702	34.140
Pr	0.676	2.621	7.695	5.829	9.998	7.754	6.174	1.819	0.666	4.225	4.037
Nd	4.315	9.784	28.578	19.776	35.663	28.428	22.857	7.353	1.899	16.687	16.161
Sm	1.833	1.799	5.276	3.486	6.350	4.237	4.145	1.538	0.272	3.124	3.043
Eu	0.659	0.504	1.098	0.694	1.092	0.922	1.056	0.494	0.094	0.850	0.818
Gd	2.749	1.715	4.204	2.602	5.140	2.287	3.495	1.397	0.134	2.825	2.716
Tb	0.489	0.257	0.590	0.361	0.737	0.245	0.499	0.203	0.020	0.400	0.398
Dy	3.409	1.569	3.239	1.915	4.072	1.022	2.777	1.244	0.098	2.437	2.362
Ho	0.744	0.330	0.634	0.363	0.759	0.177	0.505	0.232	0.024	0.540	0.524
Er	2.186	0.970	1.796	1.037	2.131	0.476	1.441	0.692	0.078	1.584	1.514
Tm	0.318	0.147	0.264	0.152	0.305	0.073	0.209	0.106	0.015	0.240	0.232
Yb	2.007	1.034	1.696	1.061	1.968	0.436	1.451	0.705	0.124	1.565	1.558
Lu	0.294	0.160	0.254	0.161	0.280	0.069	0.217	0.111	0.028	0.240	0.232
Hf	0.848	2.415	3.670	2.854	4.704	3.982	4.187	2.162	2.799	3.428	3.068
Ta	0.077	0.279	1.581	1.463	2.053	0.396	0.886	0.280	0.283	1.014	1.142
Th	0.212	4.182	24.408	23.439	38.029	6.195	10.043	1.492	17.562	4.405	4.701
Latitude	49.155757	49.155757	49.061520	49.069317	49.069552	49.161480	49.016554	49.151378	49.151378	49.009087	49.021726
Longitude	-119.164309	-119.164309	-119.116490	-119.206104	-119.204795	-119.240650	-119.011395	-119.017097	-119.017097	-118.695168	-118.677616
UTM Zone	11	11	11	11	11	11	11	11	11	11	11
Northing	5447025	5447025	5436452	5437505	5437528	5447824	5431245	5446243	5446243	5429850	5431227
Easting	342198	342198	345390	338871	338967	336650	352934	352916	352916	376036	377351

Table 2. (continued)

Greenwood stock	Westkettle batholith		"Crick Creek diorite"	Crowded feldspar diorite				Collier Lake stock	Unnamed stock west of Crouse Creek
	06NMAGreenwood1	07NMA28-20	07NMA45-05	07NMA27-17	07NMA33-07B	07NMA34-15	07NMA41-08	07NMA43-10	07NMA28-17
66.53	65.39	66.84	53.11	62.42	59.02	58.86	59.74	65.71	71.50
0.27	0.40	0.38	0.87	0.45	0.47	0.49	0.48	0.40	0.28
18.81	16.02	15.33	18.72	17.15	17.31	17.53	17.42	16.67	14.67
3.05	4.39	4.06	8.43	5.49	5.81	6.56	6.80	2.89	1.49
0.07	0.09	0.07	0.15	0.10	0.15	0.14	0.13	0.10	0.01
1.02	1.95	1.58	3.23	1.85	1.86	2.52	2.29	0.40	0.45
5.06	4.61	3.88	7.49	6.57	6.20	6.56	7.12	1.04	1.46
3.42	3.64	3.35	3.71	3.40	3.94	3.79	3.12	5.14	4.15
1.37	2.00	3.07	1.21	0.96	0.99	1.36	1.24	6.51	4.34
0.15	0.11	0.12	0.27	0.19	0.19	0.20	0.20	0.07	0.07
0.12	0.14	0.14	0.07	0.09	0.09	0.14	0.09	0.02	0.16
1.73	0.87	1.05	2.22	0.81	3.45	1.43	0.98	0.31	0.55
99.60	99.60	99.87	99.48	99.48	99.48	99.58	99.61	99.26	99.13
34	58	69	20	20	24	28	33	270	140
602	332	452	538	537	567	511	537	100	1050
1166	1439	1377	687	860	880	1402	853	170	1553
9	10	11	22	11	9	10	13	22	6
86	83	94	98	82	75	74	76	631	186
6	8	8	7	7	8	7	8	71	14
64	92	84	201	101	123	139	136	19	35
-	-	-	3	-	-	-	-	-	-
35	35	22	30	17	36	23	20	45	35
5.549	9.347	16.004	15.154	11.285	10.264	10.639	10.398	92.146	60.742
11.063	17.973	28.881	30.919	22.574	20.992	21.416	20.891	165.029	114.865
1.430	2.253	3.365	4.160	2.952	2.750	2.766	2.745	17.515	13.067
6.216	9.414	13.192	18.401	12.699	11.875	12.089	11.958	58.594	47.994
1.494	2.126	2.695	4.348	2.928	2.765	2.864	2.816	8.727	7.115
0.464	0.553	0.603	1.230	0.893	0.848	0.765	0.851	0.789	1.168
1.471	2.145	2.531	4.358	2.955	2.685	2.866	2.788	5.817	3.635
0.229	0.335	0.391	0.683	0.458	0.431	0.443	0.436	0.826	0.366
1.386	2.053	2.366	4.120	2.813	2.579	2.744	2.625	4.582	1.792
0.278	0.424	0.490	0.821	0.561	0.518	0.560	0.522	0.873	0.272
0.841	1.254	1.482	2.424	1.684	1.516	1.679	1.528	2.618	0.739
0.130	0.197	0.236	0.350	0.258	0.235	0.247	0.228	0.401	0.101
0.878	1.319	1.603	2.397	1.713	1.614	1.685	1.556	2.686	0.664
0.142	0.205	0.260	0.355	0.263	0.242	0.257	0.247	0.413	0.093
2.193	2.534	4.183	3.067	2.489	1.994	2.277	2.256	14.829	3.978
0.358	0.414	0.522	0.351	0.286	0.348	0.248	0.252	4.610	0.674
1.109	3.099	8.861	2.591	2.483	2.078	2.164	2.010	32.916	19.217
49.097050	49.495475	49.410378	49.473268	49.448155	49.399108	49.420506	49.418590	49.510924	49.405806
-119.680870	-118.927312	-119.005005	-118.888715	-118.955065	-118.932716	-118.929211	-118.937517	-118.920253	-118.953738
11	11	11	11	11	11	11	11	11	11
5439562	5484322	5475009	5481783	5479114	5473620	5475992	5475794	5486026	5474403
377348	360440	354563	363173	358294	359774	360089	359482	360995	358268

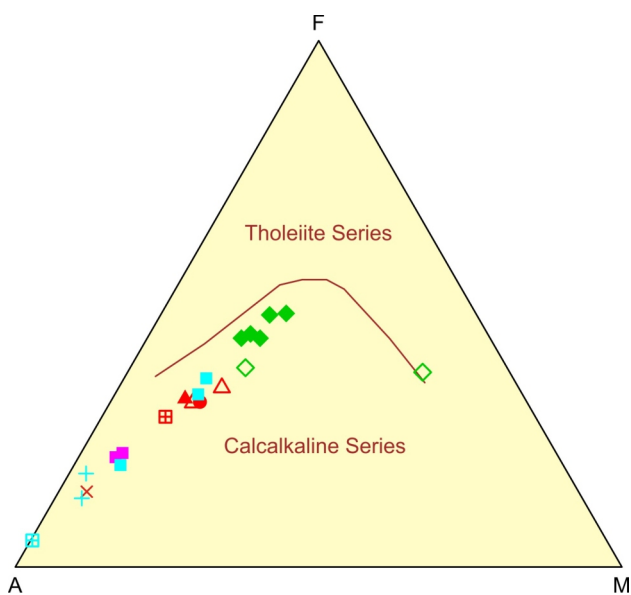


Figure 8. AFM diagram for granitic intrusions in the Boundary Project area, southern British Columbia (after Irvine and Baragar, 1971). A = Na₂O + K₂O; F = FeO_{total}; M = MgO, all as weight percent. Symbols as in Figure 7.

one McKinney Creek diorite sample (07NMA05-15), which is more mafic and tholeiitic, and the Eocene Collier Lake stock, which is alkalic. Major and trace elements, however, do show distinctions between the various suites. Triassic and Jurassic intrusions, including both the diorites and the granodiorites, show a typical volcanic-arc character (Figures 10, 11), although the Gidon Creek and Mount Baldy stocks have a late-orogenic signature.

Eocene intrusions, including the post-foliation leucogranite from the Ed James Creek area, are also distinct on geochemical plots. However, their extensional tectonic environment (Parrish et al., 1988) is poorly discriminated in Figures 10 and 11, although the alkalic Collier Creek stock does show a within-plate anorogenic character. Other samples have a character transitional between syn- and post- collisional.

Chondrite-normalized REE diagrams further demonstrate the geochemical distinction of the various suites. Diorites from both the McKinney and Beaverdell areas show typical light rare earth element (LREE)-enriched calcalkaline patterns, except for the tholeiitic sample from McKinney (07NMA-15, Figure 12a), which shows a LREE-depleted pattern. This sample also shows other trace-element characteristics that are comparable to island-arc

tholeiite, a magma type that has not been recognized previously in the Mesozoic rocks of the study area but that is present in the Paleozoic in both the Knob Hill Complex and the Anarchist schist. Further mapping and sampling are needed to adequately discriminate the components of this composite diorite body, to determine if it includes Paleozoic material.

All Jurassic intrusive suites show typical LREE-enriched calcalkaline patterns (Figures 13, 14), although they differ in absolute abundances and steepness of the REE pattern. In particular, the Middle Jurassic Mount Baldy stock is more LREE enriched than the other Jurassic samples (Figure 13b). Tertiary intrusions have higher REE contents and are more LREE enriched than the main Triassic and Middle Jurassic suites (Figure 14a). Sample 07NMA38-01, from the unnamed stock west of Crouse Creek, is from a K-feldspar megacrystic granite that was correlated with the Coryell suite (Massey and Duffy, 2008b). However, it has a normalized REE pattern similar to that of the Mount Baldy stock (Figure 13b). This intrusion has not been directly dated and may have been incorrectly designated as Eocene instead of Middle Jurassic. Further geochronological and geochemical studies are warranted.

The Ed James Creek leucogranite has the lowest REE contents of any sample and a distinct concave-upward REE pattern (Figure 14b), perhaps reflecting end-product fractionation with the removal of hornblende and the minor phases that normally host the REEs and other high-field-strength elements.

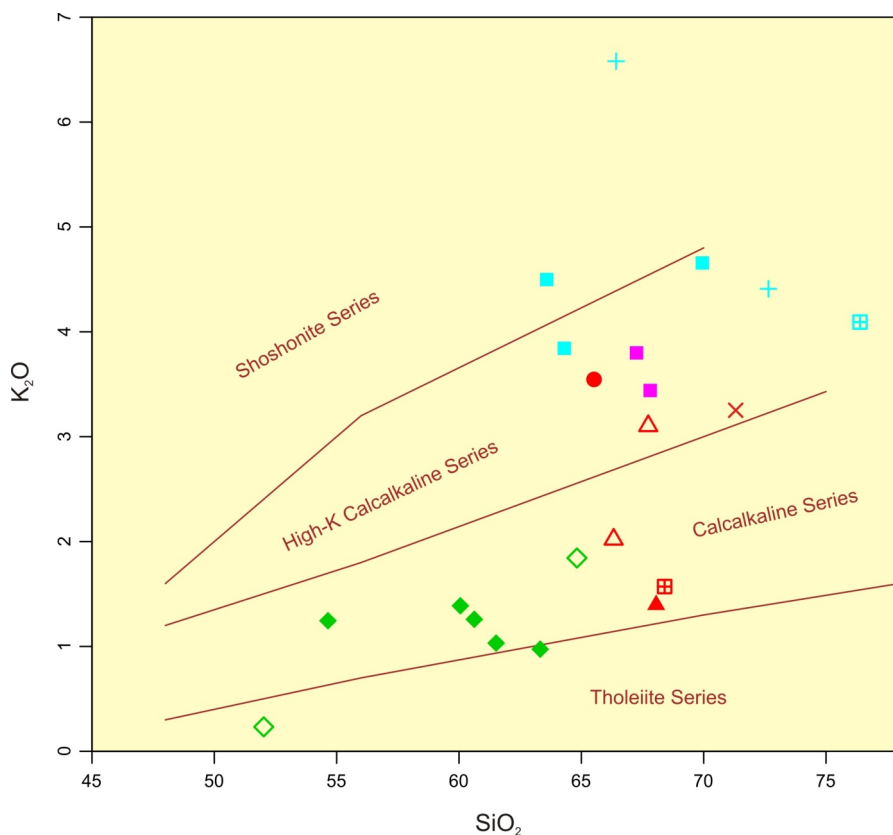


Figure 9. K₂O-SiO₂ plot for granitic intrusions in the Boundary Project area, southern British Columbia, showing fields from Peccerillo and Taylor (1976). Symbols as in Figure 7.

CONCLUSIONS

The data presented here illustrate that the magmatic history of the Boundary Project area is more complex than previously thought. Granitic intrusions in the area were previously ascribed to the Middle Jurassic Nelson suite, a poorly defined Jura-Cretaceous suite, or to the Eocene Coryell suite. New isotopic age data suggest that at least four pre-Eocene suites are present: Late Triassic (213 Ma), Early Jurassic (188 Ma), Early to Middle Jurassic (179–168 Ma) and earliest Late Jurassic (157 Ma). Although these are generally all of a similar continental arc-like geochemistry, the Mount Baldy intrusion is significantly distinct.

Eocene intrusions are present and, although they are enriched in lithophile elements, they are not all alkaline like the classic Coryell suite intrusions. More detailed mapping, coupled with systematic sampling for geochemistry and isotopic dating, is needed to confirm these results, and possibly reveal even more complications, throughout the region.

ACKNOWLEDGMENTS

The senior author is much indebted to Jim Fyles and Neil Church for all their invaluable help and advice during the planning stages of this project and subsequently. The collaboration, support and ready welcome of the Boundary District exploration community continue to be exceptional. The project would not have made progress without the indispensable assistance of Alan Duffy, Kevin Paterson, Bev Quist, Eric Westberg, Ashley Dittmar and Sean Mullan during fieldwork and in the office. Jim Logan provided a thorough review of an earlier version of this manuscript.

REFERENCES

- Acton, S.L., Simony, P.S. and Heaman, L.M. (2002): Nature of the basement to Quesnel Terrane near Christina Lake, southeastern British Columbia; *Canadian Journal of Earth Sciences*, Volume 39, pages 65–78.
- Batchelor, R.A. and Bowden, P. (1985): Petrogenetic interpretation of granitoid rock series using multicationic parameters; *Chemical Geology*, Volume 48, pages 43–55.
- Brown, D.A. and Logan, J.M. (1989): Geology and mineral evaluation of Kokanee Glacier Provincial Park, southeastern British Columbia; *BC Ministry of Energy, Mines and Petroleum Resources*, Paper 1989-5, 47 pages.
- Church, B.N. (1992): The Lexington porphyry, Greenwood mining camp, southern British Columbia: geochronology (82E/2E); in *Geological Fieldwork 1991, BC Ministry of*

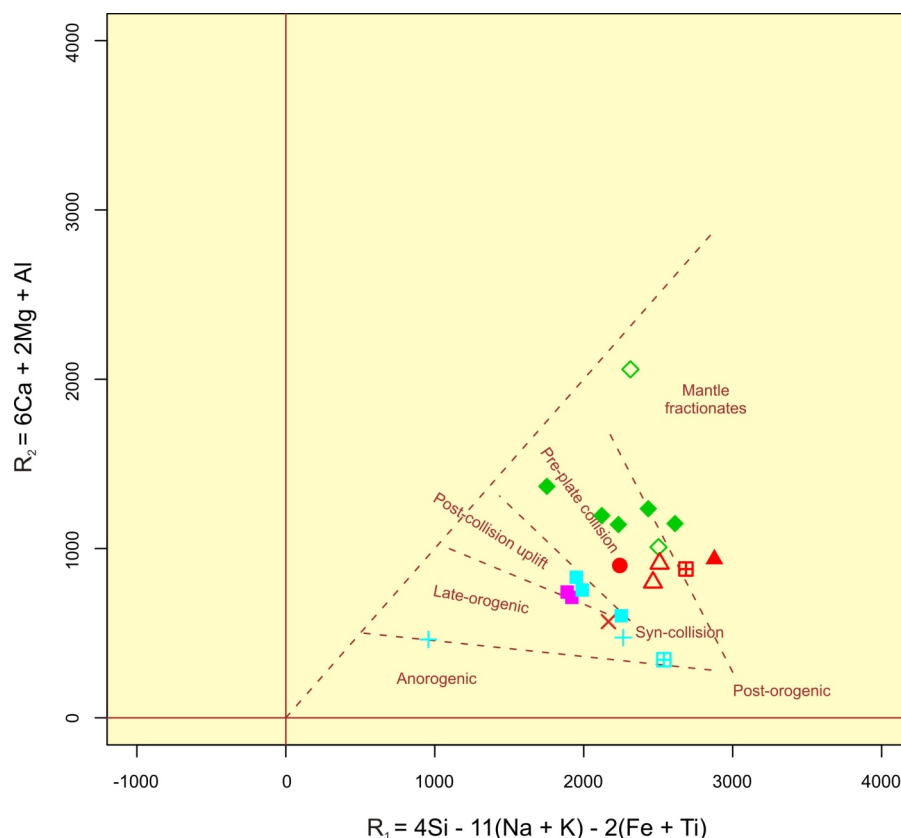


Figure 10. Major-element multi-cation plot for granitic intrusions in the Boundary Project area, southern British Columbia, with fields from Batchelor and Bowden (1985). Symbols as in Figure 7.

Energy, Mines and Petroleum Resources, Paper 1992-1, pages 295–297.

- Cox, K.G., Bell, J.D. and Pankhurst, R.J. (1979): The Interpretation of Igneous Rocks; *George, Allen and Unwin*, London, United Kingdom, 450 pages.
- Dostal, J., Church, B.N. and Höy, T. (2001): Geological and geochemical evidence for variable magmatism and tectonics in the southern Canadian Cordillera: Paleozoic to Jurassic suites, Greenwood, southern British Columbia; *Canadian Journal of Earth Sciences*, Volume 38, pages 75–90.
- Dunne, K.P.E. and Höy, T. (1992): Petrology of pre to syntectonic Early and Middle Jurassic intrusions in the Rossland Group, southeastern British Columbia (82F/SW); in *Geological Fieldwork 1991, BC Ministry of Energy, Mines and Petroleum Resources*, Paper 1992-1, pages 9–19.
- Erdmer, P., Moore, J.M., Heaman, L., Thompson, R.I., Daughtry, K.L. and Creaser, R.A. (2002): Extending the ancient margin outboard in the Canadian Cordillera: record of Proterozoic crust and Paleocene regional metamorphism in the Nicola Horst, southern British Columbia; *Canadian Journal of Earth Sciences*, Volume 39, pages 1605–1623.
- Fyles, J.T. (1984): Geological setting of the Rossland mining camp, British Columbia; *BC Ministry of Energy, Mines and Petroleum Resources*, Bulletin 74, 19 pages.
- Fyles, J.T. (1990): Geology of the Greenwood–Grand Forks area, British Columbia, NTS 82E/1, 2; *BC Ministry of Energy, Mines and Petroleum Resources*, Open File 1990-25, 61 pages.
- Ghosh, D.K. (1995): U-Pb geochronology of Jurassic to early Tertiary granitic intrusives from the Nelson-Castlegar area,

southeastern British Columbia, Canada; *Canadian Journal of Earth Sciences*, Volume 32, pages 1668–1680.

Greig, C.J. and Flasha, S.T. (2005): 2004–2005 exploration program on the GK property; *BC Ministry of Energy, Mines and Petroleum Resources*, Assessment Report 28179.

Griffin, W.L., Powell, W.J., Pearson, N.J. and O'Reilly, S.Y. (2008): Glitter: data reduction software for laser ablation ICP-MS; in *Laser Ablation ICP-MS in the Earth Sciences: Current Practices and Outstanding Issues*, Sylvester, P.J., Editor, *Mineralogical Association of Canada*, Short Course Series, Volume 40, pages 308–311.

Höy, T. and Dunne, K. (1997): Early Jurassic Rosslund Group, southern British Columbia: part I, stratigraphy and tectonics; *BC Ministry of Energy Mines and Petroleum Resources*, Bulletin 102.

Höy, T. and Jackaman, W. (2005): Geology of the Grand Forks map sheet (082E/01); *BC Ministry of Energy Mines and Petroleum Resources*, Geoscience Map 2005-1, scale 1:50 000.

Irvine, T.N. and Baragar, W.R.A. (1971): A guide to the chemical classification of the common volcanic rocks; *Canadian Journal of Earth Sciences*, Volume 8, pages 523–548.

Little, H.W. (1961): Kettle River (west half), British Columbia; *Geological Survey of Canada*, Map 15-1961, scale 1:253 440.

Little, H.W. (1983): Geology of the Greenwood map-area, British Columbia; *Geological Survey of Canada*, Paper 79-29, 37 pages.

Ludwig, K.R. (2003): Isoplot 3.09 – a geochronological toolkit for Microsoft Excel; *Berkeley Geochronology Center*, Special Publication 4, 74 pages.

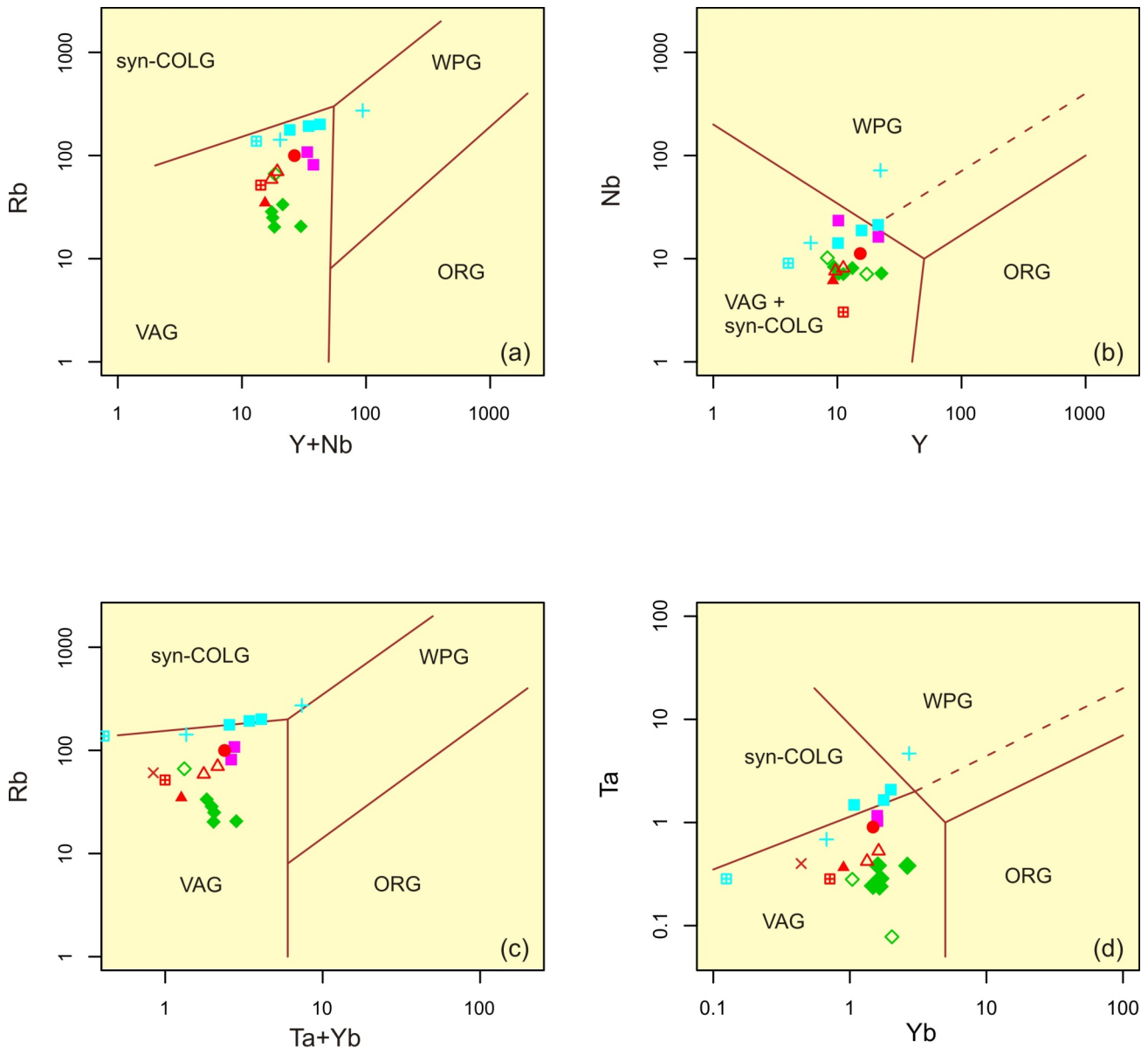


Figure 11. Trace-element discrimination diagrams for granitic intrusions in the Boundary Project area, southern British Columbia, with fields from Pearce et al. (1984). Abbreviations: VAG, volcanic-arc granites; syn-COLG, syn-collisional granites; WPG, within-plate granites; ORG, ocean-ridge granites. Symbols as in Figure 7.

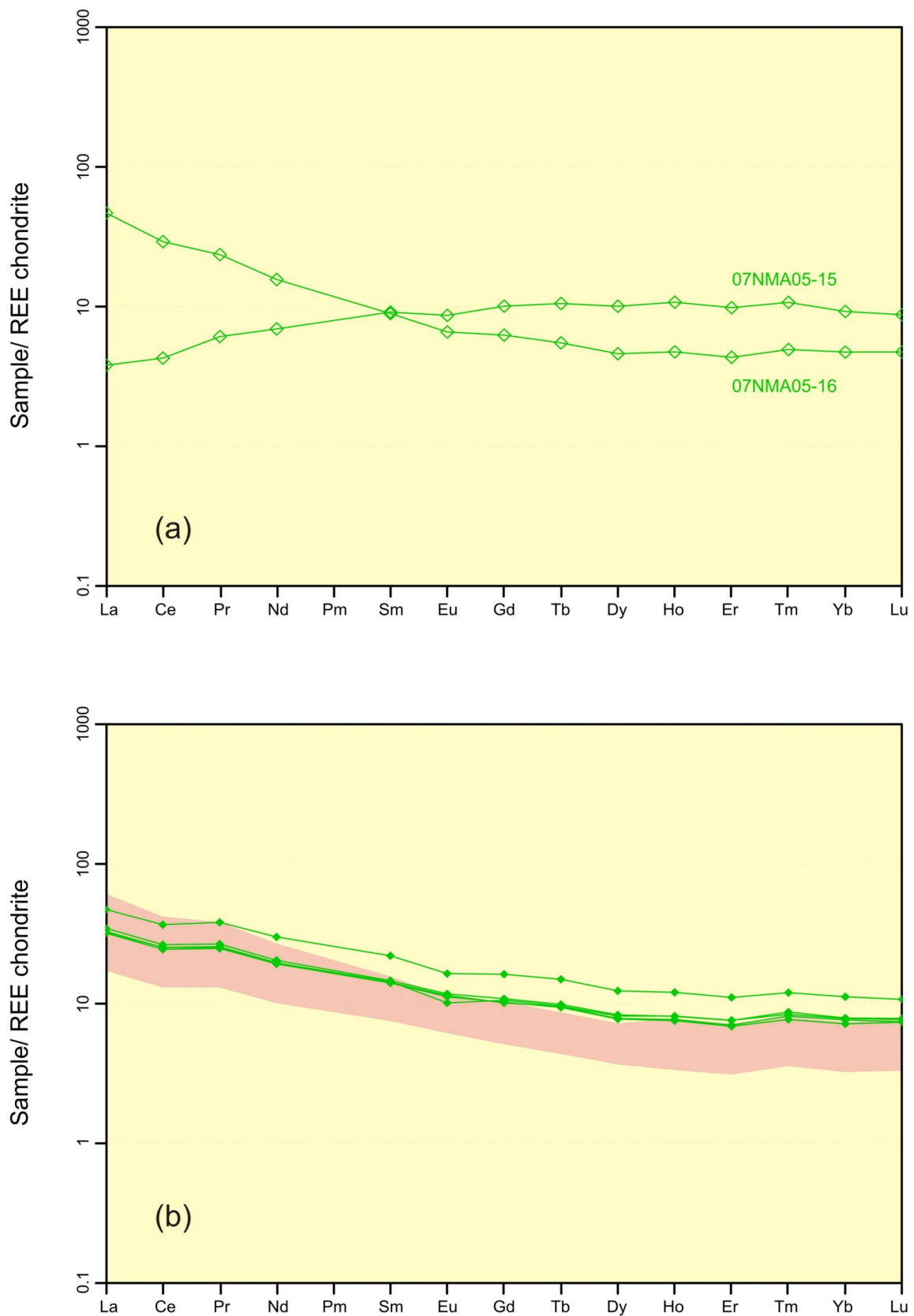


Figure 12. Chondrite-normalized rare earth element plots for diorites from the Boundary Project area, southern British Columbia (normalizing values after Nakamura, 1974): **a)** diorites from the McKinney Creek area; 07NMA05-15 is tholeiitic in composition, 07NMA05-16 is calcalkaline; **b)** diorites from the Beaverdell area; pink-shaded field is for all Triassic to Middle Jurassic granodiorites, except for the Mount Baldy stock (Figure 13).

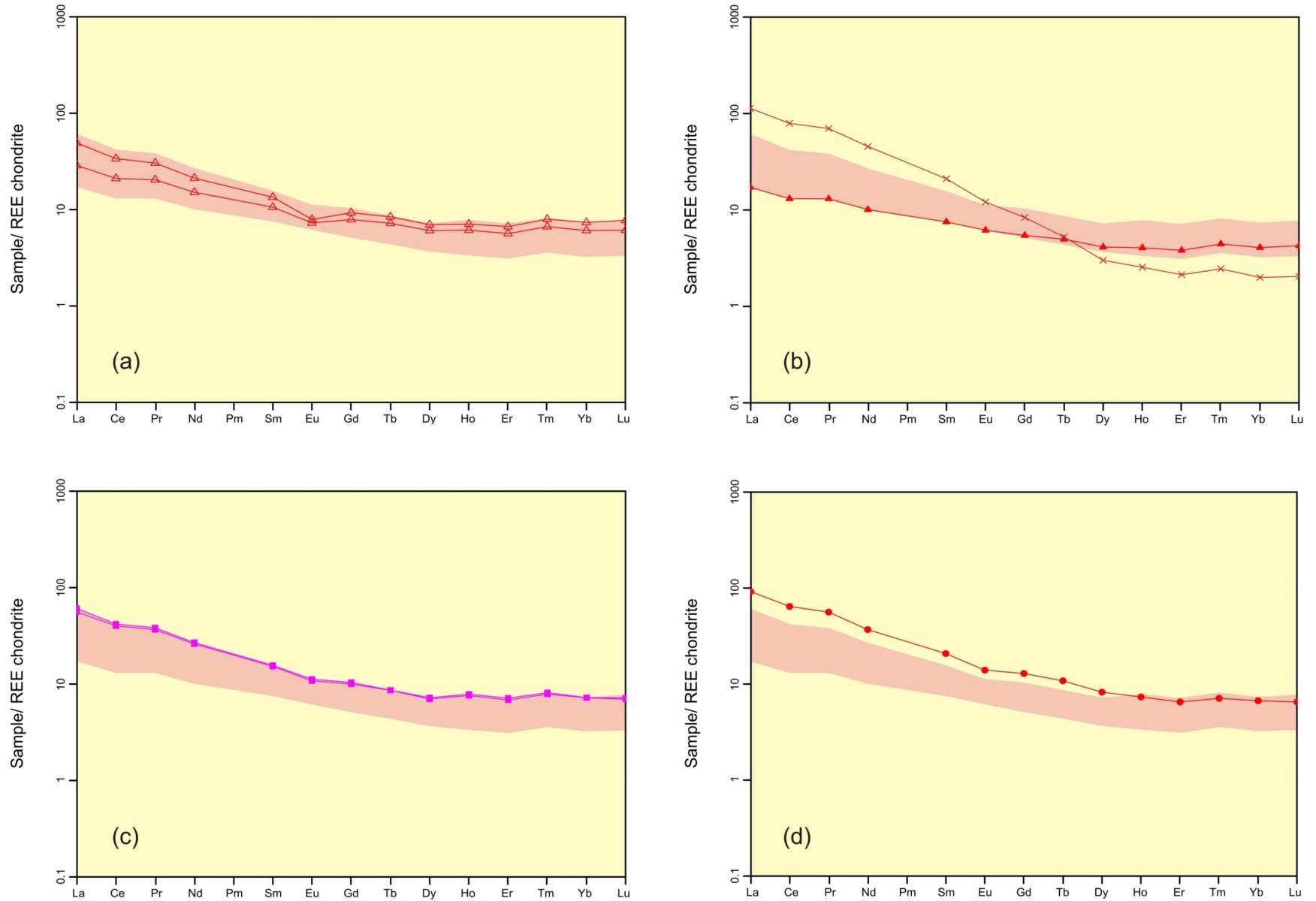


Figure 13. Chondrite-normalized rare earth element plots for Triassic and Jurassic granitic rocks in the Boundary Project area, southern British Columbia (normalizing values from Nakamura, 1974): **a)** Triassic West Kettle batholith; **b)** Middle Jurassic Greenwood stock (closed red triangles) and Mount Baldy stock (red Xs); **c)** Middle Jurassic Gidon Creek stock; **d)** Late Jurassic Myers Creek stock. For comparison, the pink-shaded field in all diagrams includes all Triassic to Middle Jurassic intrusions except the Mount Baldy stock.

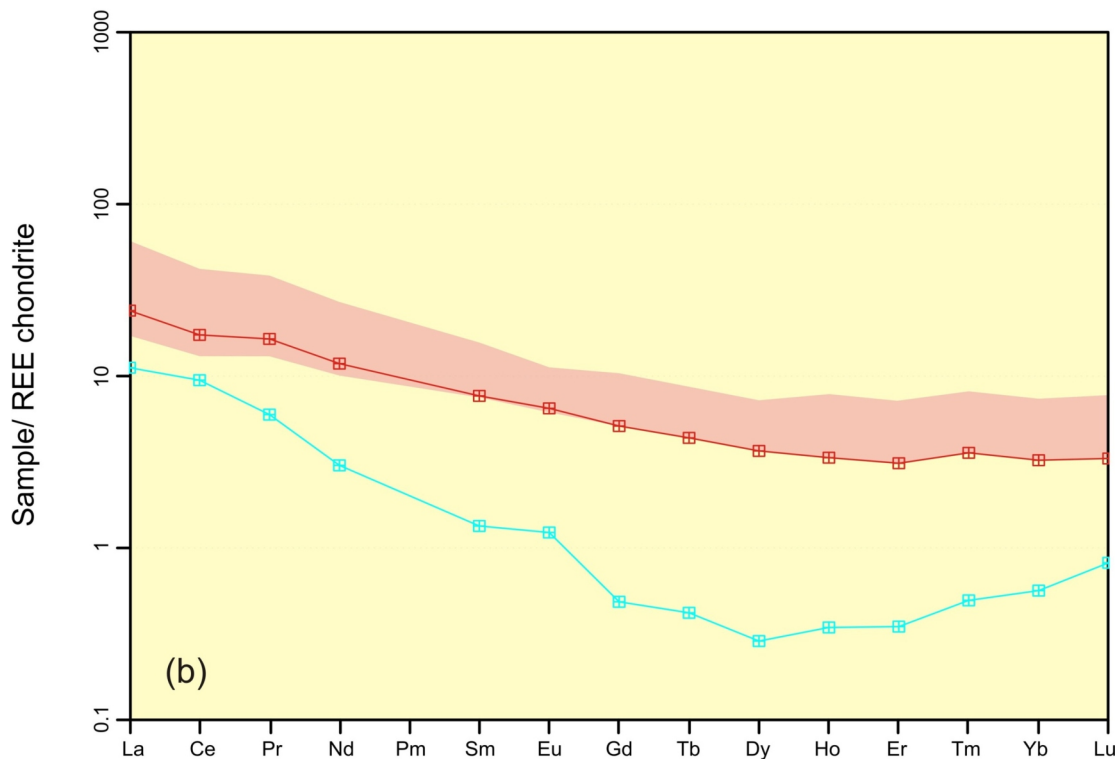
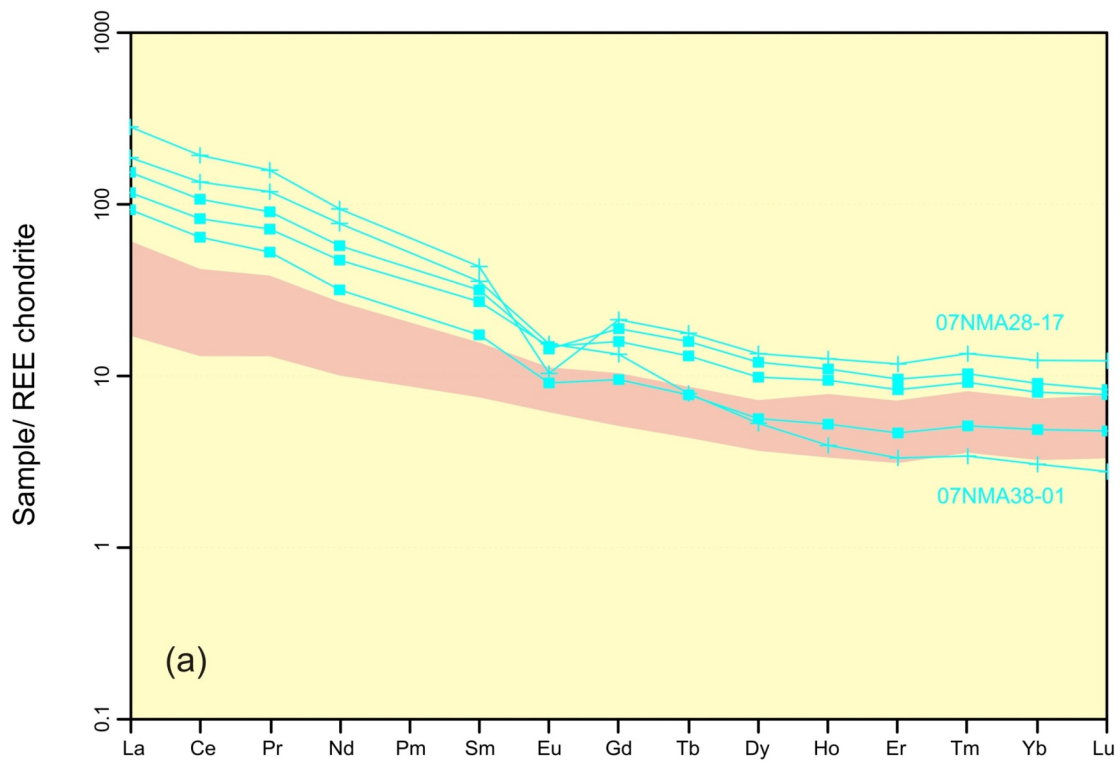


Figure 14. Chondrite-normalized rare earth element plot for rocks in the Boundary Project area, southern British Columbia: **a)** Tertiary granitic McKinney Creek stock (solid blue squares) and Beaverdell suite stocks (blue crosses; normalizing values after Nakamura, 1974); 07NMA28-17 is the alkalic Collier Creek stock and 07NMA38-01 an unnamed stock west of Crouse Creek. **b)** Early Jurassic Ed James Creek biotite-feldspar-quartz orthogneiss (red crossed squares) and undated, unfoliated leucogranite (blue crossed squares). For comparison, the pink-shaded field is for the Triassic to Middle Jurassic granodiorite, except the Mount Baldy stock (Figure 13).

- Massey, N.W.D. (2006): Boundary Project: reassessment of Paleozoic rock units of the Greenwood area (NTS 82E/02), southern British Columbia; in *Geological Fieldwork 2005, BC Ministry of Energy, Mines and Petroleum Resources, Paper 2006-1 and Geoscience BC, Report 2006-1*, pages 99–107.
- Massey, N.W.D. (2007a): Geology and mineral deposits of the Rock Creek area, British Columbia (82E/02W; 82E/03E); *BC Ministry of Energy, Mines and Petroleum Resources, Open File 2007-7*, 1:25 000 scale.
- Massey, N.W.D. (2007b): Boundary Project: Rock Creek area (82E/02W; 82E/03E); in *Geological Fieldwork 2006, BC Ministry of Energy, Mines and Petroleum Resources, Paper 2007-1 and Geoscience BC, Report 2007-1*, pages 117–128.
- Massey, N.W.D. (2007c): The Lexington porphyry revisited (NTS 82E/02); in *Geological Fieldwork 2006, BC Ministry of Energy, Mines and Petroleum Resources, Paper 2007-1*, pages 129–136.
- Massey, N.W.D. (2010): Boundary Project: geochemistry of volcanic rocks of the Wallace Formation, Beaverdell area (82E/06E, 82E/07W, 82E/10W and 82E/11W); in *Geological Fieldwork 2009, BC Ministry of Energy, Mines and Petroleum Resources, Paper 2010-1*, pages 33–42.
- Massey, N.W.D. and Duffy, A. (2008a): Boundary Project: McKinney Creek (82E/03) and Beaverdell (82E/06E, 82E/07W, 82E/10W and 82E/11W) areas; in *Geological Fieldwork 2007, BC Ministry of Energy, Mines and Petroleum Resources, Paper 2008-1*, pages 87–102.
- Massey, N.W.D. and Duffy, A. (2008b): Geology and mineral deposits of the area east of Beaverdell, British Columbia (parts of NTS 082E/6E; 082E/07W; 082E/10W; 082E/11E); *BC Ministry of Energy, Mines and Petroleum Resources, Open File 2008-9*, 1:25 000 scale.
- Massey, N.W.D. and Duffy, A. (2008c): Geology and mineral deposits of the McKinney Creek area, British Columbia (parts of NTS 082E/3); *BC Ministry of Energy, Mines and Petroleum Resources, Open File 2008-10*, 1:20 000 scale.
- Massey, N.W.D., Gabites, J.E., Mortensen, J.K., and T.D. Ullrich (2010): Boundary Project: geochronology and geochemistry of Jurassic and Eocene intrusions; *BC Ministry of Energy, Mines and Petroleum Resources, GeoFile 2010-1*.
- Massey, N.W.D., MacIntyre, D.G., Desjardins, P.J. and Cooney, R.T., (2005): Digital geology map of British Columbia, *BC Ministry of Energy, Mines and Petroleum Resources, Open File 2005-2*, DVD.
- Moore, J.M., Gabites, J.E. and Friedman, R.M. (2000): Nicola Horst: toward a geochronology and cooling history; in *Slave–Northern Cordillera Lithospheric Evolution (SNORCLE) Transect and Cordilleran Tectonics Workshop Meeting, 25–27 February 2000, University of Calgary, Calgary, Alberta.*, Cook, F. and Erdmer, P., Compilers, LITHOPROBE Report 72, LITHOPROBE Secretariat, *University of British Columbia*, pages 177–185.
- Nakamura, N. (1974): Determination of REE, Ba, Fe, Mg, Na and K in carbonaceous and ordinary chondrites; *Geochimica Cosmochimica Acta*, Volume 38, pages 757–775.
- Nixon, G.T. (2002): Alkaline hosted Cu-PGE mineralization: the Sappho Alkaline Plutonic Complex, south-central British Columbia; *BC Ministry of Energy, Mines and Petroleum Resources, Open File 2002-7*, 2 maps at 1:5000 scale.
- Parkinson, D.L. (1985): U-Pb geochronometry and regional geology of the southern Okanagan Valley, British Columbia: the western boundary of a metamorphic core complex; M.Sc. thesis, *University of British Columbia*.
- Parrish, R.R. (1992a): U-Pb ages of Jurassic–Eocene plutonic rocks in the vicinity of the Valhalla Complex, southeast British Columbia; in *Radiogenic Age and Isotopic Studies: Report 5, Geological Survey of Canada, Paper 91-2*, pages 115–134.
- Parrish, R.R. (1992b): Miscellaneous U-Pb zircon dates from southeast British Columbia; in *Radiogenic Age and Isotopic Studies: Report 5, Geological Survey of Canada, Paper 91-2*, pages 143–153.
- Parrish, R.R., Carr, S.D. and Parkinson, D.L. (1988): Eocene extensional tectonics and geochronology of the southern Omineca Belt, British Columbia and Washington; *Tectonics*, Volume 7, pages 181–212.
- Pearce, J.A., Harris, N.B.W. and Tindle, A.G. (1984): Trace element discrimination diagrams for the tectonic interpretation of granitic rocks; *Journal of Petrology*, Volume 25, pages 956–983.
- Peccerillo, R. and Taylor, S.R. (1976): Geochemistry of Eocene calc-alkaline volcanic rocks from the Kastamonu area, northern Turkey; *Contributions to Mineralogy and Petrology*, Volume 58, pages 63–81.
- Renne, P.R., Swisher, C.C., III, Deino, A.L., Karner, D.B., Owens, T., and DePaolo, D.J. (1998): Inter-calibration of standards, absolute ages and uncertainties in $^{40}\text{Ar}/^{39}\text{Ar}$ dating; *Chemical Geology*, Volume 145, pages 117–152.
- Sevigny, J.H. and Parrish, R.R. (1993): Age and origin of Late Jurassic and Paleocene granitoids, Nelson Batholith, southern British Columbia; *Canadian Journal of Earth Sciences*, Volume 30, pages 2305–2314.
- Sláma, J., Košler, J., Condon, D.J., Crowley, J.L., Gerdes, A., Hanchar, J.M., Horstwood, M.S.A., Morris, G.A., Nasdala, L., Norberg, N., Schaltegger, U., Xchoene, B., Tubrett, M.N. and Whitehouse, M.J. (2007): Plešovice zircon—a new natural reference material for U-Pb and Hf isotopic microanalysis; *Chemical Geology*, Volume 249, pages 1–35.
- Tafti, R., Mortensen, J.K., Lang, J.R., Rebagliati, M., and Oliver, J. (2009): Jurassic U-Pb and Re-Os ages for the newly discovered Xietongmen Cu-Au porphyry district, Tibet, PRC: implications for metallogenic epochs in the southern Gangdese belt; *Economic Geology*, Volume 104, pages 127–136.
- Tempelman-Kluit, D.J. (1989): Geology, Penticton, British Columbia; *Geological Survey of Canada, Map 1736A*, scale 1:250 000.
- Van Acherbergh, E., Ryan, C.G., Jackson, S.E. and Griffin, W.L. (2001): Data reduction software for LA-ICP-MS: appendix; in *Laser Ablation–ICP–Mass Spectrometry in the Earth Sciences: Principles and Applications*, Sylvester, P.J., Editor, *Mineralogical Association of Canada, Short Course Series, Volume 29*, pages 239–243.
- Wilson, M. (1989): *Igneous Petrogenesis*; *Unwin Hyman*, London.

Boundary Project: Geochemistry of Volcanic Rocks of the Wallace Formation, Beaverdell Area, South-Central British Columbia (NTS 082E/06E, 07W, 10W, 11W)

by N.W.D. Massey

KEYWORDS: Quesnellia, Triassic, Wallace Formation, Beaverdell, calcalkaline

INTRODUCTION

The Boundary Project was initiated in 2005 with the purpose of better characterizing the lithological and geochemical variations within and between the various Paleozoic sequences in the southern Okanagan region along the American border (Massey 2006, 2007; Massey and Duffy 2008a). Pre-Jurassic rocks in the Beaverdell area were assigned by Reinecke (1915) to the 'Wallace Group' (single quotation marks are used to highlight the actual term used in the paper) and correlated, in part, with Paleozoic sequences to the south, including the Anarchist schist and the Attwood 'series'. Little (1957, 1961) and Tempelman-Kluit (1989a, b) extended this work to the east and west including these rocks in the 'Anarchist Group'.

The pre-Jurassic rocks of the Beaverdell area (Figure 1), however, differ significantly from the type Anarchist schist to the south (Massey and Duffy, 2008a). They are dominated by fine- to medium-grained clastic sedimentary rocks that are essentially unmetamorphosed, though they do show extensive hornfelsing from Jurassic plutons. Limestone and greenstone members occur in the Crouse Creek area, and are stratigraphically the lowest exposed units. Significantly, there is no chert developed in the sequence. No penetrative deformation was observed, except for one small area, to the west of Crouse Creek.

Massey and Duffy (2008a) proposed to revert to Reinecke's original terminology of 'Wallace' for these rocks, though at the formation level rather than the group level. It should be noted, however, that not all of the area originally mapped as Wallace by Reinecke (1915) is actually underlain by pre-Jurassic rocks—there is a significant amount of younger intrusive material. In particular, many rocks mapped as so-called pyroxene-phyric volcanic rocks in Reinecke's Wallace are actually porphyry dikes of Tertiary age, and in one area, east of Collier Lake, pyroxene-phyric flows of the Eocene Marron Formation.

No geochronological or paleontological data are currently available for the Wallace Formation rocks and correlation is therefore difficult. As stated above, it is lithologically dissimilar to any of the Paleozoic sequences to the

south. It does, however, show some similarities to parts of the Middle–Late Triassic Brooklyn Formation of the Greenwood area (Fyles, 1990) or the Franklin Camp, though lacking the distinctive basal sharpstone conglomerate, possibly due to a lack of exposure. The Wallace Formation is intruded by the West Kettle batholith, now known to be of Late Triassic age (Massey et al, 2010).

WALLACE FORMATION

The lowest exposed unit in the Wallace Formation is the Larse Creek limestone member. Contact with the overlying greenstone member is not exposed, but the limestone is estimated to be at least 100 m thick. It is grey on weathered surfaces, varying from black to grey to white on fresh surfaces. It is massive to well bedded and laminated. Thin siliceous and minor calcsilicate veins weather with positive relief. Macrofossils are absent and conodonts have not been recovered to date.

The Crouse Creek greenstone member overlies the limestone member. This unit comprises mostly massive mafic flows, though amygdules are not uncommon. The flows are medium to dark green-grey, bluish green or black in colour. They may show bright green epidosite patches up to 30 cm across (Figure 2a) and veins of quartz-chlorite±epidote±calcite. Many flows are fine-grained and aphyric, but feldspar-phyric and pyroxene-feldspar-phyric flows are also common. Phenocrysts are 1–2 mm in size. Volcanic breccia, lapilli tuff, pyroxene lapilli tuff or chloritic metatuff (Figures 2b–d) and minor laminated limestone are found interbedded in the flows. Some volcanic breccias also contain limestone and clastic sediment clasts.

Most of the exposed Wallace Formation is typically interbedded and laminated siltstone and argillite. Siltstone beds are light buff to pale grey in colour, whereas the argillite is dark grey. Weathered surfaces may be broken with a coating of rusty oxides. Individual beds can range up to 3 cm thick with laminations of ~1–2 mm. The sedimentary rocks are often siliceous or porcelaneous and may be recrystallized due to hornfels development by Triassic and Jurassic intrusions. Occasional white, tan or grey limestone interbeds vary from several centimetres up to five metres thick. The limestone is massive and may be recrystallized due to the development of hornfels or variable silicification and skarn.

Coarser clastic beds are also found, though less common than the siltstone-argillite interbeds. Sandstone beds are grey, medium to coarse grained, and generally massive. Hornfelsed sandstone is recrystallized to feldspar-quartz-amphibole assemblages that can be difficult to discriminate from microdiorite or microgranodiorite in the field. Con-

This publication is also available, free of charge, as colour digital files in Adobe Acrobat® PDF format from the BC Ministry of Energy, Mines and Petroleum Resources website at <http://www.empr.gov.bc.ca/Mining/Geoscience/PublicationsCatalogue/Fieldwork/Pages/default.aspx>.

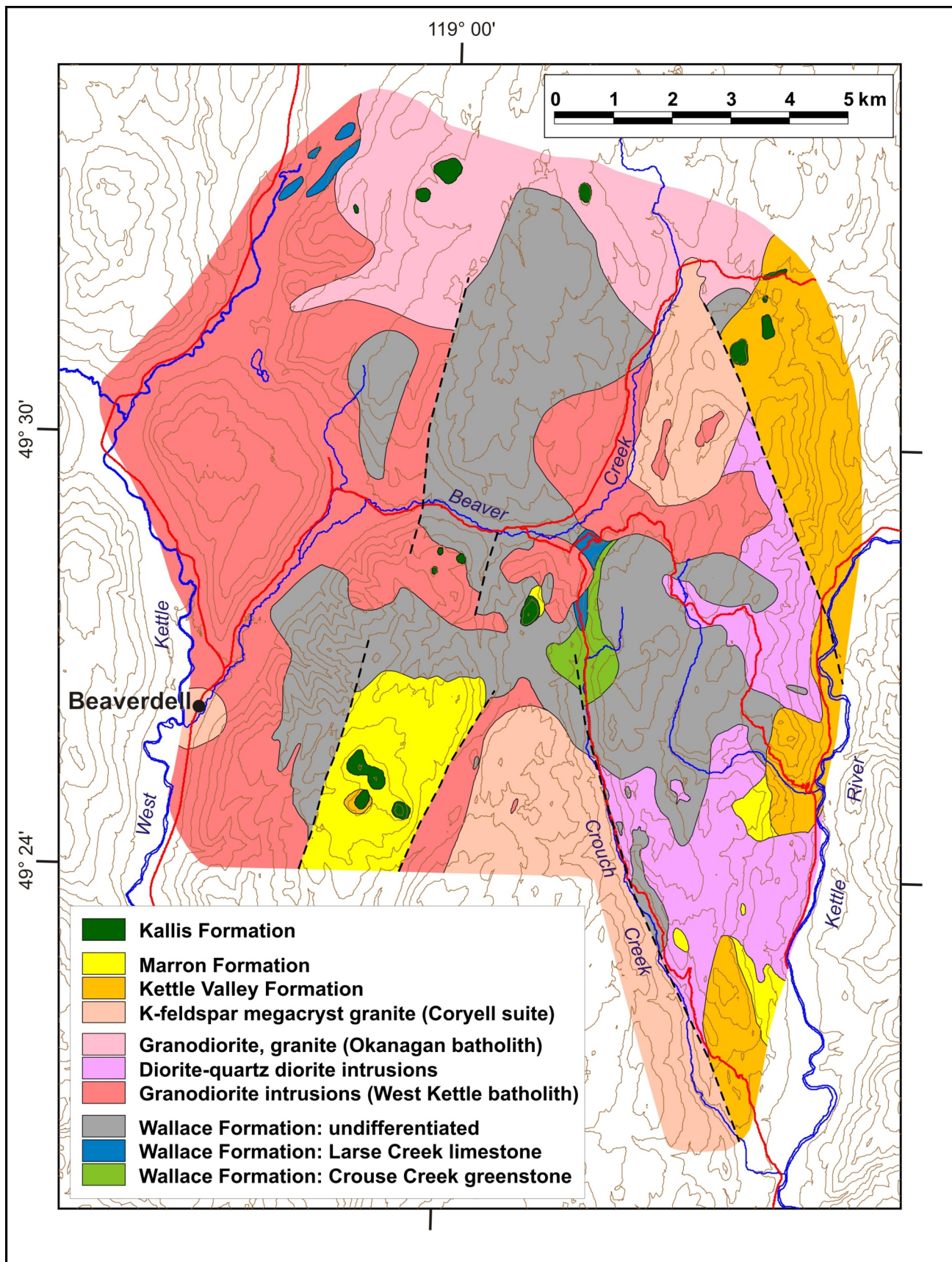


Figure 1. Geology of the area east of Beaverdell, south-central British Columbia (after Massey and Duffy, 2008b). The extent of coloured polygons shows the limit of the area mapped in 2007.

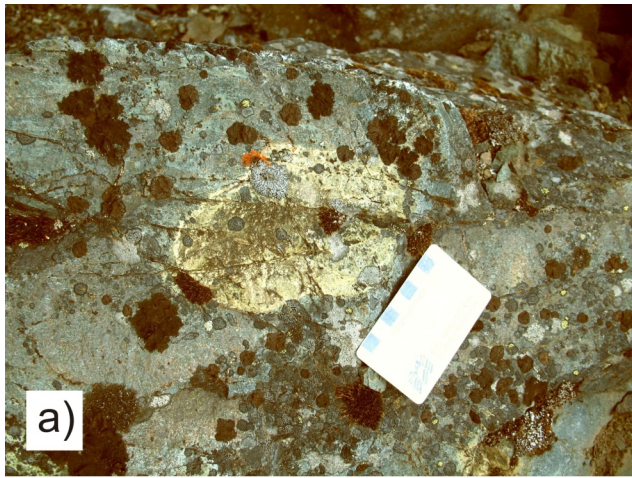


Figure 2. The Crouse Creek greenstone member of the Wallace Formation, south-central British Columbia: **a)** epidiosite patch in massive greenstone (07NMA31-01; UTM Zone 11, 5479991N, 358567E, NAD83); **b)** pyroxene crystal-lapilli tuff (07NMA32-04; UTM Zone 11, 5479062N, 358777E, NAD83); **c)** pyroxene-feldspar crystal tuff (07NMA33-02; UTM Zone 11, 5479283N, 357806E, NAD83); **d)** pyroxene crystal-lapilli tuff with rhyolite clasts (07NMA32-04; UTM Zone 11, 5479062N, 358777E, NAD83).

glomerate and pebbly sandstone have matrix-supported, rounded to subangular clasts. The clasts are dominantly of siliceous siltstone and argillite, but also can include limestone. The latter are usually larger in size. All clasts appear to be intraformational and no exotic rock types have been observed.

Fine-grained basalt is found within the sedimentary section, particularly in the area north of Canyon Creek. The basalt is aphyric, dark to medium grey in colour, weathering light grey to buff with a greenish tinge. Outcrops are massive with blocky jointing and fractures. Direct contacts were not observed, and it is unclear if the basalt forms interbedded flows or dikes.

GEOCHEMISTRY OF THE VOLCANIC ROCKS

Fourteen samples of the Crouse Creek greenstone member and six basalt samples from the clastic sediment package were analyzed for whole-rock major, minor and

trace elements. Results are summarized in Table 1. Samples range in composition from basalt to andesite and dacite (Figure 3). They show some mobility of alkali elements but generally all preserve a subalkalic, calcalkaline character (Figures 3, 4). Minor- and trace-element diagrams further confirm the formation of both suites in an arc environment, though not all diagrams successfully discriminate between calcalkaline and island-arc tholeiite basalt (Figures 5–8). A continental arc environment is suggested by both major- and trace-element data (Figures 9, 10). Extended trace-element plots show typical calcalkaline patterns with the negative Nb-Ta anomaly characteristic of volcanic arcs (Figure 11).

REGIONAL CORRELATIONS

The calcalkaline, volcanic arc character of the Wallace Formation volcanic rocks is comparable to that of the Triassic Brooklyn Formation (Dostal et al., 2001), but differs distinctly from that of the tholeiitic Paleozoic Knob Hill Complex (Massey, 2008) and Anarchist schist (Massey, un-

Table 1. Whole-rock chemical analyses for Wallace Formation volcanic rocks, south-central British Columbia. Major elements and Rb, Sr, Ba, Y, Zr, Nb, V, Ni and Cr determined by x-ray fluorescence (XRF; major elements on fused disc, trace elements on pressed-powder pellet) by Teck (Global Discovery) Labs (Vancouver). Rare earth elements (REE), Th, Ta and Hf determined by peroxide fusion–ICP-MS by Memorial University of Newfoundland (St. John’s). Dashes indicate element determinations below detection limit; blank values indicate element not analyzed.

Analytical parameter	Crouse Creek Member										
	07NMA22-13	07NMA26-05A	07NMA26-05B	07NMA31-01a	07NMA31-01b	07NMA31-04	07NMA31-08	07NMA31-12	07NMA32-01	07NMA33-03	07NMA33-04
SiO ₂	52.68	52.26	52.54	52.56	52.86	61.37	55.12	59.37	47.16	50.42	53.30
TiO ₂	0.62	0.64	0.75	0.69	0.61	0.61	0.88	0.50	0.60	0.54	0.62
Al ₂ O ₃	12.02	19.82	18.91	17.72	11.96	14.93	16.10	16.17	17.57	15.72	17.60
Fe ₂ O _{3t}	9.13	8.02	8.52	9.77	9.14	4.54	8.82	7.01	8.48	9.48	8.61
MnO	0.18	0.22	0.25	0.17	0.18	0.07	0.11	0.10	0.15	0.20	0.14
MgO	10.13	3.34	3.35	4.79	10.13	2.94	5.94	3.62	6.98	6.77	5.50
CaO	10.04	7.52	7.96	8.44	9.90	2.87	6.93	8.42	9.80	12.22	8.53
Na ₂ O	1.80	4.98	4.77	2.42	1.84	3.21	2.70	3.56	2.35	1.99	2.54
K ₂ O	1.42	1.40	0.92	1.04	1.35	3.81	0.69	0.37	0.82	0.53	1.27
P ₂ O ₅	0.33	0.20	0.24	0.20	0.33	0.29	0.17	0.15	0.18	0.16	0.17
BaO	0.07	0.08	0.02	0.07	0.08	0.20	0.07	0.03	0.08	0.05	0.09
LOI	1.43	1.34	1.43	2.12	1.61	4.89	2.44	0.44	5.43	1.38	1.56
Total	99.85	99.78	99.66	99.99	99.99	99.73	99.97	99.74	99.60	99.46	99.93
Rb	28	49	16	21	27	86	11		20	7	27
Sr	367	708	423	372	359	739	290	391	452	390	430
Ba	741	748	233	740	764	1993	684	326	782	451	877
Y	14	15	20	16	14	15	16	12	10	14	13
Zr	70	60	64	51	68	207	92	55	51	52	55
Nb	8	6	8	6	8	23	12	6	8	8	8
V	204	206	224	279	210	98	201	173	235	229	253
Co	42	22	32	33	41	20	39	38	31	38	36
Ni	15	-	-	8	13	13	8	74	102	117	45
Cr	749	17	11	33	777	48	65	248	367	404	151
La		6.383	7.440	6.794	12.131	51.696		6.691	5.850		
Ce		13.237	16.291	14.909	24.345	94.025		14.425	12.855		
Pr		2.004	2.431	2.037	3.204	10.459		1.939	1.697		
Nd		10.630	12.562	9.522	13.896	38.931		9.093	7.934		
Sm		3.020	3.658	2.614	3.081	6.097		2.048	2.010		
Eu		1.113	1.326	0.769	0.963	1.354		0.756	0.674		
Gd		3.663	4.782	2.937	3.198	4.476		2.329	2.312		
Tb		0.582	0.713	0.471	0.484	0.576		0.392	0.380		
Dy		3.833	4.597	3.131	3.037	3.220		2.484	2.436		
Ho		0.827	1.072	0.668	0.621	0.598		0.523	0.505		
Er		2.596	3.187	1.992	1.821	1.642		1.566	1.571		
Tm		0.366	0.449	0.292	0.259	0.224		0.219	0.219		
Yb		2.389	3.135	2.008	1.681	1.405		1.593	1.444		
Lu		0.365	0.467	0.322	0.260	0.231		0.230	0.223		
Hf		2.098	2.645	1.574	2.124	6.191		1.520	1.318		
Ta		0.168	0.151	0.158	0.280	0.932		0.143	0.148		
Th		0.901	0.990	1.214	2.391	11.435		1.358	1.010		
Latitude	49.456604	49.444199	49.444479	49.456109	49.456109	49.454224	49.450260	49.442010	49.440026	49.448959	49.448996
Longitude	-118.950777	-118.910477	-118.910440	-118.951612	-118.951612	-118.950781	-118.950608	-118.949914	-118.949570	-118.960509	-118.959758
UTM Zone	11	11	11	11	11	11	11	11	11	11	11
Northing	5480045	5478591	5478622	5479991	5479991	5479780	5479339	5478421	5478200	5479213	5479216
Easting	358629	361515	361518	358567	358567	358622	358623	358650	358669	357902	357957

Table 1. (continued)

Analytical parameter	Crouse Creek Member					Aphyric basalt (?) dikes					
	07NMA33-05E2	07NMA35-03	07NMA35-05	07NMA35-06	07NMA35-08	07NMA18-14	07NMA28-08	07NMA29-08	07NMA29-13	07NMA29-14	07NMA29-17A
SiO ₂	61.48	56.03	59.04	55.14	53.04	55.79	57.43	51.41	51.53	51.13	50.45
TiO ₂	0.46	0.62	0.52	0.65	0.75	0.81	0.52	0.77	0.68	0.72	0.72
Al ₂ O ₃	17.76	17.69	18.01	17.81	17.56	16.19	18.04	16.84	19.24	18.46	18.56
Fe ₂ O ₃ t	5.87	7.97	5.66	8.46	8.44	9.46	6.30	8.98	8.08	9.98	8.94
MnO	0.10	0.18	0.14	0.21	0.19	0.09	0.11	0.20	0.18	0.19	0.24
MgO	1.92	3.87	1.86	3.84	3.47	5.06	3.06	5.00	3.25	4.09	3.40
CaO	6.06	6.82	5.29	7.71	7.17	7.42	6.19	8.71	7.86	6.72	9.83
Na ₂ O	3.82	3.99	4.81	3.69	2.75	2.95	4.06	3.80	4.82	4.43	3.05
K ₂ O	0.79	0.77	1.70	0.83	1.32	0.49	2.77	1.34	0.93	1.47	0.90
P ₂ O ₅	0.20	0.27	0.27	0.27	0.28	0.12	0.34	0.34	0.23	0.29	0.23
BaO	0.08	0.06	0.13	0.05	0.13	0.02	0.16	0.08	0.04	0.10	0.07
LOI	1.31	1.71	2.30	1.04	4.56	1.58	0.80	2.17	2.61	2.15	3.15
Total	99.85	99.98	99.73	99.70	99.66	99.98	99.78	99.64	99.45	99.73	99.54
Rb	17	24	54	20	35	12	53	23	19	32	18
Sr	459	632	462	496	597	279	722	687	729	680	566
Ba	814	553	1299	549	1346	193	1645	781	439	995	743
Y	13	14	14	16	16	18	16	17	19	16	17
Zr	82	86	97	80	81	75	87	57	71	58	61
Nb	9	10	11	10	10	8	7	7	4	8	8
V	112	178	110	199	230	222	194	293	205	276	231
Co	26	27	20	28	26	36	25	26	21	24	23
Ni	-	-	-	-	-	17	6	15	4	6	4
Cr	24	26	19	19	18	76	24	44	16	28	33
La					12.8245	7.965				7.665	
Ce					26.457	16.712				15.885	
Pr					3.6315	2.277				2.206	
Nd					17.285	10.986				11.444	
Sm					3.9535	2.820				3.187	
Eu					1.161	1.042				1.074	
Gd					3.963	3.986				4.103	
Tb					0.616	0.594				0.604	
Dy					3.629	3.847				3.878	
Ho					0.895	0.873				0.867	
Er					2.6485	2.650				2.621	
Tm					0.3695	0.393				0.352	
Yb					2.3945	2.541				2.543	
Lu					0.337	0.375				0.389	
Hf					2.071	2.732				2.099	
Ta					0.3175	0.403				0.136	
Th					1.8165	1.381				1.109	
Latitude	49.449362	49.393454	49.390055	49.388879	49.386997	49.479276	49.460473	49.437396	49.437550	49.437930	49.438132
Longitude	-118.958177	-118.924602	-118.922569	-118.921878	-118.920446	-119.010463	-118.932273	-118.898797	-118.894089	-118.894896	-118.887550
UTM Zone	11	11	11	11	11	11	11	11	11	11	11
Northing	5479254	5472976	5472594	5472462	5472251	5482679	5480440	5477813	5477822	5477866	5477875
Easting	358072	360347	360485	360532	360630	354371	359981	362342	362684	362627	363160

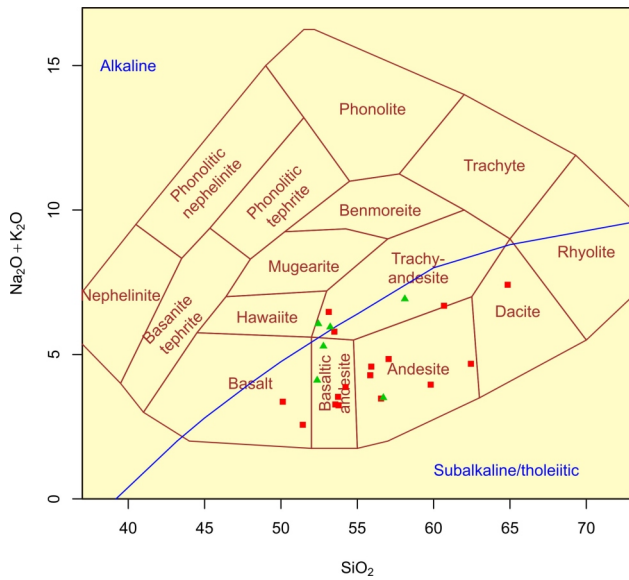


Figure 3. Total alkali elements versus SiO₂ (anhydrous weight percent) plot for Wallace Formation volcanic rocks, south-central British Columbia. Classification fields and nomenclature after Cox et al. (1979). The alkaline-subalkaline dividing line after Irvine and Baragar (1971). The Crouse Creek greenstone member is indicated by red squares; the aphyric basalt (dikes?) in clastic sedimentary rocks is indicated by green triangles.

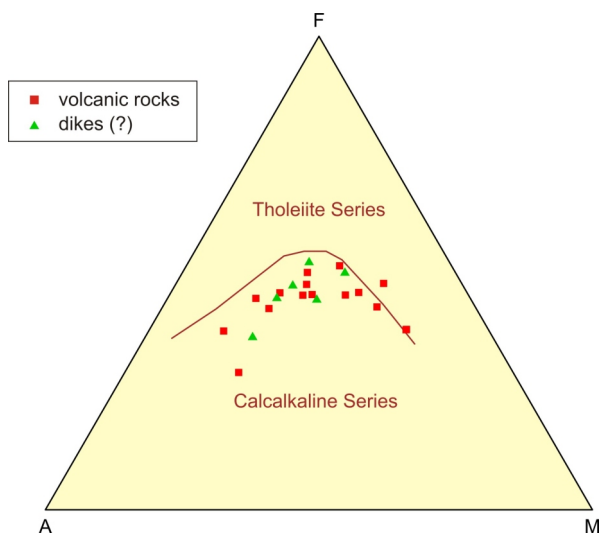


Figure 4. AFM diagram for Wallace Formation volcanic rocks, south-central British Columbia, after Irvine and Baragar (1971); A = Na₂O + K₂O; F = FeO_{total}; M = MgO, all as anhydrous weight percents. Symbols are as in Figure 3.

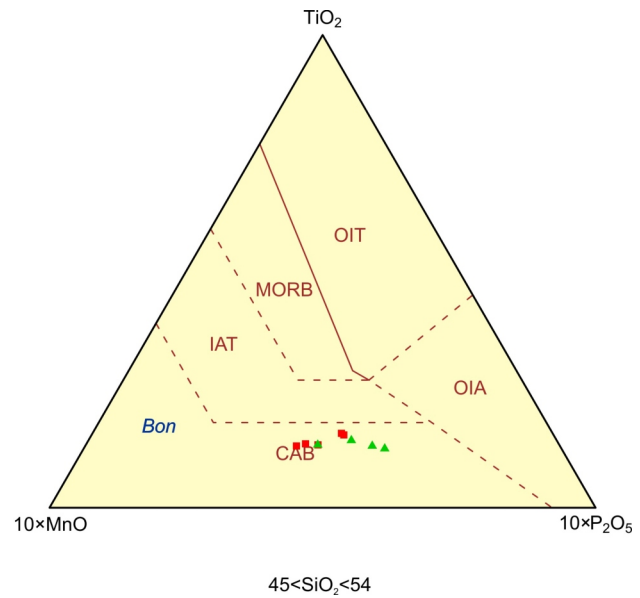


Figure 5. MnO-TiO₂-P₂O₅ (anhydrous weight percent) discrimination diagram for Wallace Formation volcanic rocks, south-central British Columbia, after Mullen (1983). Abbreviations: Bon, boninite; CAB, calcalkaline basalt; IAT, island-arc tholeiite; MORB, mid-ocean-ridge basalt; OIA, ocean-island alkali basalt; OIT, ocean-island tholeiite. Symbols are as in Figure 3. Only basaltic samples with 12 < CaO + MgO < 20 wt. % are shown.

published data, 2006–2009). Further, the Late Triassic West Kettle batholith, which intrudes the Wallace Formation, has a similar calcalkaline, volcanic arc character and identical normalized REE patterns to Wallace Formation volcanic rocks (Massey et al, 2010). This suggests that the West Kettle batholith may, at least in part, be coeval with the Wallace Formation.

The correlation of the basalt dikes (?) found within the clastic sedimentary rocks of the Wallace Formation is still uncertain. They are indistinguishable from the Crouse Creek greenstone member in nearly all geochemical diagrams and are most likely contemporaneous and consanguineous. However, if indeed they are intrusive, they may be younger in age. Comparison with Middle Jurassic diorite of the area shows the latter, though similarly calcalkaline (Massey et al., 2010), has steeper REE (Figure 12) and extended trace-element patterns (Figure 11c), which suggests they are not consanguineous. Similar comparisons can be made with the Early Jurassic Elise Formation (Höy and Dunne, 1997). Correlation with volcanic rocks of the nearby Tertiary Pentiction Group is also unlikely as the latter are alkalic in character.

ACKNOWLEDGMENTS

The author is much indebted to Jim Fyles and Neil Church for all their invaluable help and advice during the planning stages of this project and since. Acknowledgments also go to Alan Duffy, Kevin Paterson and Bev Quist for their indispensable assistance during fieldwork and in the office. The collaboration, support and ready welcome of the Boundary District exploration community continue to be exceptional. Steve Rowins expertly reviewed an earlier version of this manuscript.

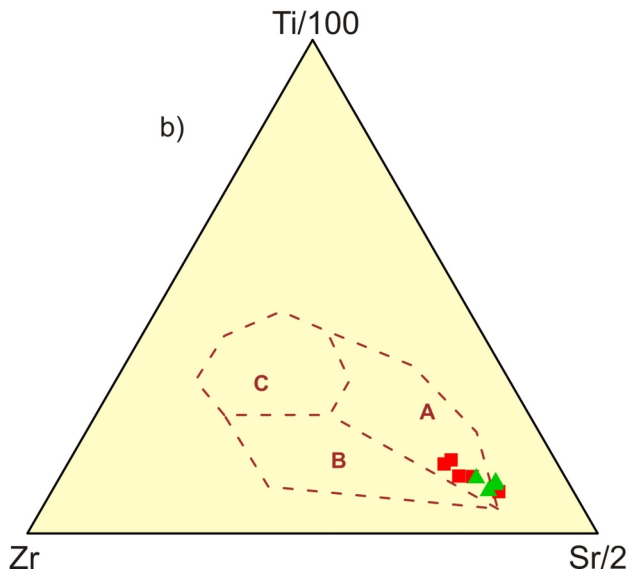
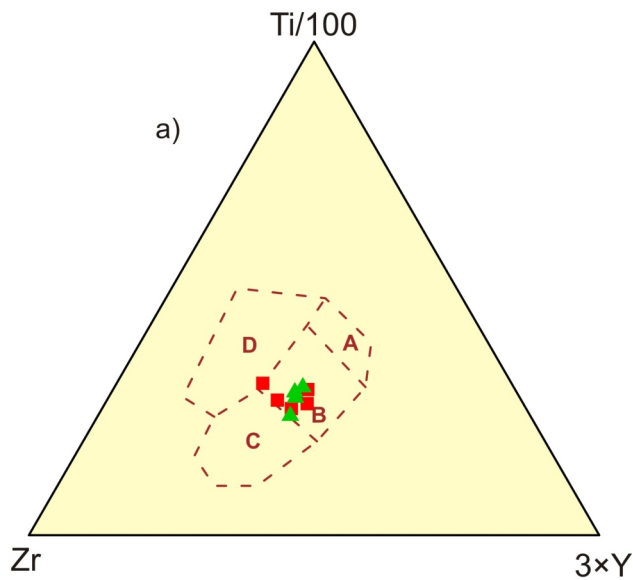


Figure 6. Trace-element discrimination diagrams for Wallace Formation volcanic rocks, south-central British Columbia, after Pearce and Cann (1973). Symbols are as in Figure 3. Only basaltic samples with $12 < \text{CaO} + \text{MgO} < 20$ wt. % are shown: **a)** Ti-Zr-Y diagram; A, island-arc tholeiites; B, mid-ocean ridge basalts, island-arc tholeiites and calcalkaline basalts; C, calcalkaline basalts; D, within-plate basalts; **b)** Ti-Zr-Sr diagram; A, island-arc tholeiites; B, calcalkaline basalts; C, mid-ocean-ridge basalts.

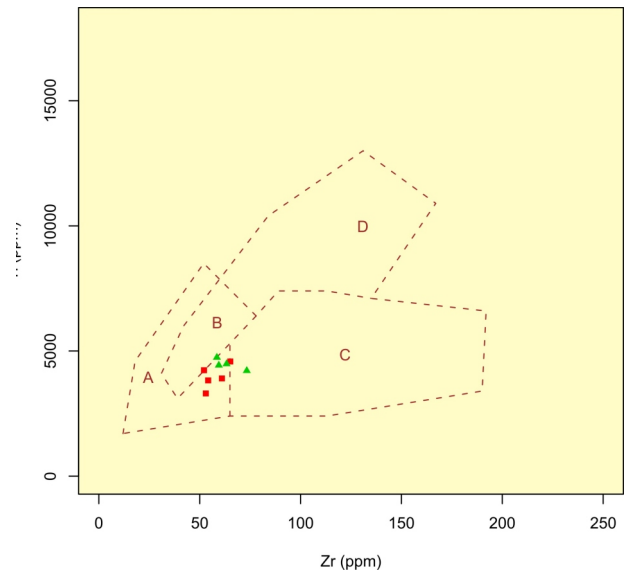


Figure 7. Zr-Ti discrimination diagram for Wallace Formation volcanic rocks, south-central British Columbia, after Pearce and Cann (1973). A, island-arc tholeiites; B, mid-ocean ridge basalts, island-arc tholeiites, calcalkaline basalts; C, calcalkaline basalts; D, within-plate basalts. Symbols are as in Figure 3. Only basaltic samples with $12 < \text{CaO} + \text{MgO} < 20$ wt. % are shown.

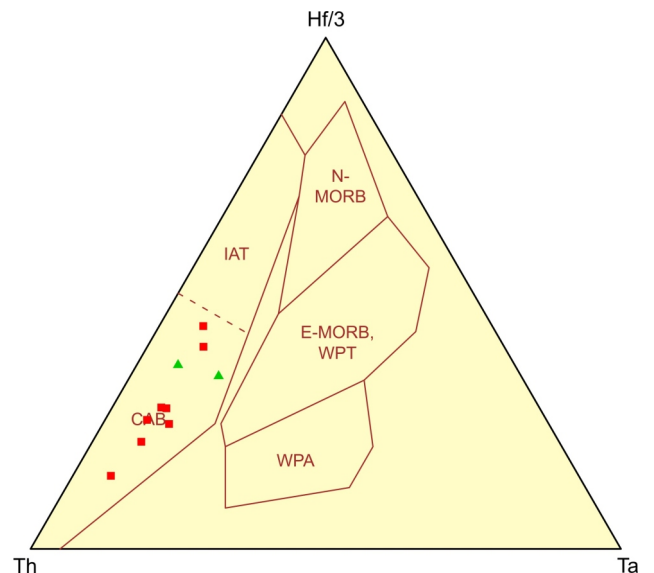


Figure 8. Th-Hf-Ta discrimination diagram for Wallace Formation volcanic rocks, south-central British Columbia, after Wood (1980). Abbreviations: CAB, calcalkaline basalt; E-MORB, enriched mid-ocean-ridge basalts; IAT, island-arc tholeiite; N-MORB, normal mid-ocean ridge basalts; WPA, within-plate alkali basalt; WPT, within-plate tholeiite. Symbols are as in Figure 3. Only basaltic samples with $12 < \text{CaO} + \text{MgO} < 20$ wt. % are shown.

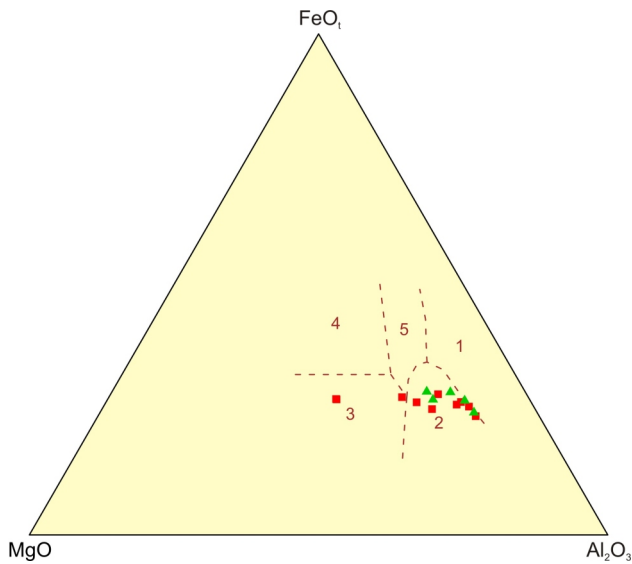


Figure 9. MgO-FeO₁-Al₂O₃ (anhydrous weight percent) discrimination diagram for Wallace Formation volcanic rocks, south-central British Columbia, after Pearce et al. (1977). 1, spreading centre island; 2, island-arc and active continental margin; 3, mid-ocean-ridge basalt; 4, ocean island; 5, continental flood basalts. Symbols are as in Figure 3. Only samples of intermediate composition, 51 < SiO₂ < 56 wt. %, are plotted.

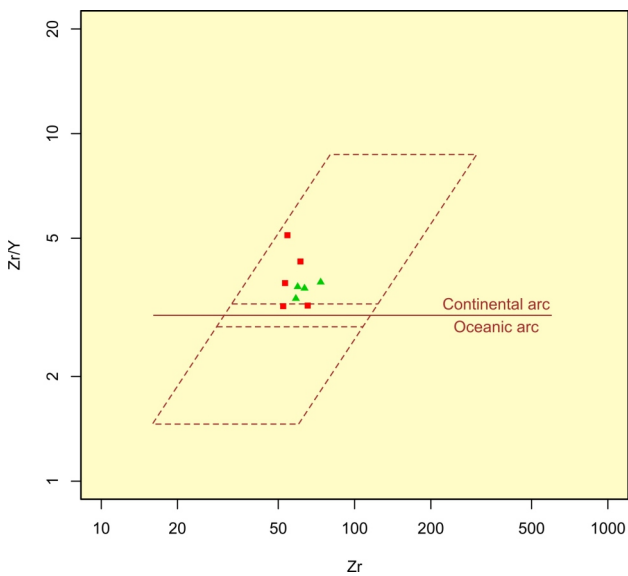


Figure 10. Zr-Zr/Y discrimination diagram Wallace Formation volcanic rocks, south-central British Columbia, after Pearce (1983). Fields of continental (upper) and oceanic-arc (lower) basalts separated on the basis of a Zr/Y value of 3. Field of overlap between the two basalt types indicated. Symbols are as in Figure 3. Only basaltic samples with 12 < CaO+MgO < 20 wt. % are shown.

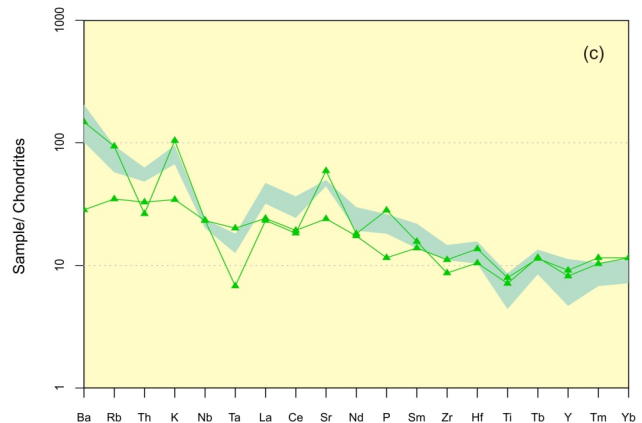
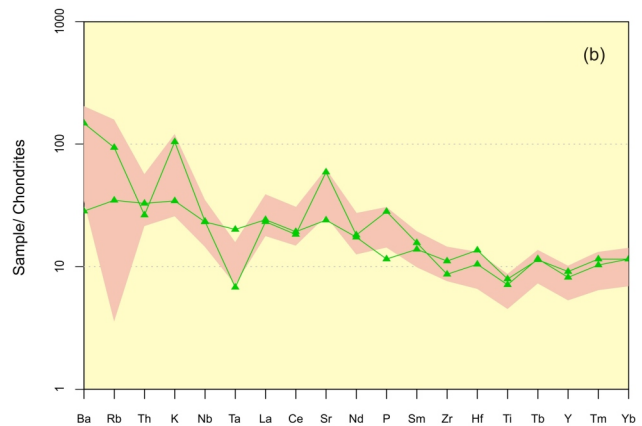
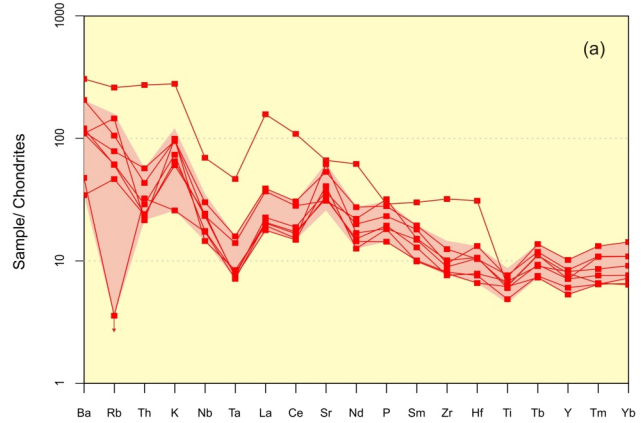


Figure 11. Trace-element concentrations normalized to chondrite, after Thompson (1982), samples from south-central British Columbia: **a)** Crouse Creek member volcanic rocks; only samples with the complete range of determined elements are plotted; the pink shaded field shows the range for all samples except for dacite sample 07NMA31-04; **b)** aphyric basalts (dikes?) in clastic sedimentary rocks; only samples with the complete range of determined elements are plotted; the pink shaded field as in a); **c)** aphyric basalts (dikes?) in clastic sedimentary rocks compared to Jurassic diorite of the Beaverdell area (pale green shaded field; Massey et al., 2010).

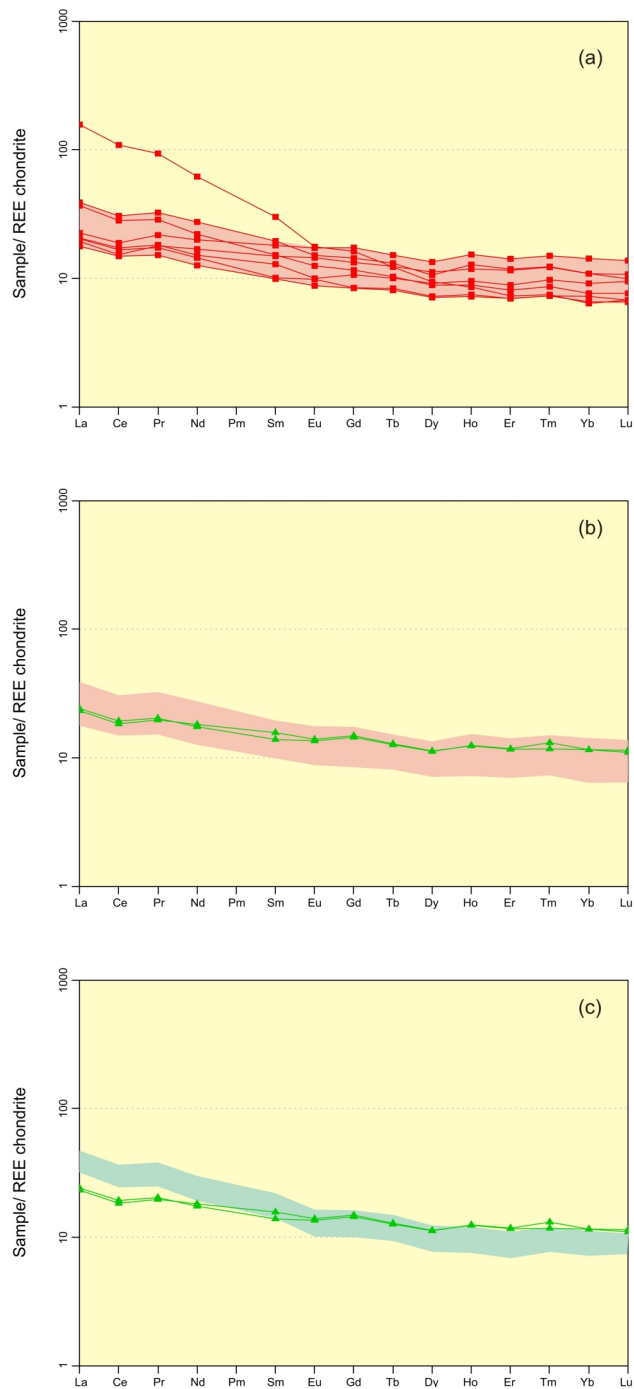


Figure 12. Rare earth element abundances normalized to chondrite (after Nakamura, 1974): **a)** Crouse Creek member volcanic rocks; the pink shaded field shows the range for all samples except for the dacite sample 07NMA31-04; **b)** aphyric basalts (dikes?) in clastic sedimentary rocks; the pink shaded field as in a); **c)** aphyric basalts (dikes?) in clastic sedimentary rocks compared to Jurassic diorite of the Beaverdell area, pale green shaded field (Massey et al., 2010).

REFERENCES

- Cox, K.G., Bell, J.D. and Pankhurst, R.J. (1979): The Interpretation of Igneous Rocks; *George, Allen and Unwin*, London.
- Dostal, J., Church, B.N. and Höy, T. (2001): Geological and geochemical evidence for variable magmatism and tectonics in the southern Canadian Cordillera: Paleozoic to Jurassic suites, Greenwood, southern British Columbia; *Canadian Journal of Earth Sciences*, Volume 38, pages 75–90.
- Fyles, J.T. (1990): Geology of the Greenwood–Grand Forks area, British Columbia, NTS 82E/1, 2; *BC Ministry of Energy, Mines and Petroleum Resources*, Open File 1990-25, 19 pages.
- Höy, T. and Dunne, K.P.E. (1997): Early Jurassic Rossland Group, southern British Columbia: part I, stratigraphy and tectonics; *BC Ministry of Energy, Mines and Petroleum Resources*, Bulletin 102, 124 pages.
- Irvine, T.N. and Baragar, W.R.A. (1971): A guide to the chemical classification of the common volcanic rocks; *Canadian Journal of Earth Sciences*, Volume 8, pages 523–548.
- Little, H.W. (1957): Kettle River (east half), British Columbia; *Geological Survey of Canada*, Map 6-1957, scale 1:253 440.
- Little, H.W. (1961): Kettle River (west half), British Columbia; *Geological Survey of Canada*, Map 15-1961, scale 1:253 440.
- Massey, N.W.D. (2006): Boundary Project: reassessment of Paleozoic rock units of the Greenwood area (NTS 82E/02), southern British Columbia; in *Geological Fieldwork 2005*, *BC Ministry of Energy, Mines and Petroleum Resources*, Paper 2006-1 and *Geoscience BC*, Report 2006-1, pages 99–107.
- Massey, N.W.D. (2007): Boundary Project: Rock Creek area (82E/02W; 82E/03E); in *Geological Fieldwork 2006*, *BC Ministry of Energy, Mines and Petroleum Resources*, Paper 2007-1 and *Geoscience BC*, Report 2007-1, pages 117–128.
- Massey, N.W.D. (2008): The Knob Hill Complex—a Paleozoic supra-subduction zone ophiolite in southeastern British Columbia?; *Cordilleran Tectonics Workshop 2008*, Program and Abstracts, page 35.
- Massey, N.W.D. and Duffy, A. (2008a): Boundary project: McKinney Creek (82E/03) and Beaverdell (82E/06E, 82E/07W, 82E/10W and 82E/11W) areas; in *Geological Fieldwork 2007*, *BC Ministry of Energy, Mines and Petroleum Resources*, Paper 2008-1, pages 87–102.
- Massey, N.W.D. and Duffy, A. (2008b): Geology and mineral deposits of the area east of Beaverdell, British Columbia (parts of NTS 082E/6E; 082E/07W; 082E/10W; 082E/11E); *BC Ministry of Energy, Mines and Petroleum Resources*, Open File 2008-9, scale 1:25 000.
- Massey, N.W.D., Mortensen, J.K., Gabites, J. and Ullrich, T.D. (2010): Boundary project: geochronology and geochemistry of Jurassic and Eocene intrusions; in *Geological Fieldwork 2009*, *BC Ministry of Energy, Mines and Petroleum Resources*, Paper 2010-1, pages 43–58.
- Mullen, E.D. (1983): MnO/TiO₂/P₂O₅: a minor element discriminant for basaltic rocks of oceanic environments and its implication for petrogenesis; *Earth and Planetary Science Letters*, Volume 62, pages 53–62.
- Nakamura, N. (1974): Determination of REE, Ba, Fe, Mg, Na and K in carbonaceous and ordinary chondrites; *Geochimica et Cosmochimica Acta*, Volume 38, pages 757–775.
- Pearce, J.A. (1983): Role of the sub-continental lithosphere in magma genesis at active continental margins; in *Continental Basalts and Mantle Xenoliths*, Hawkesworth, C.J. and Norry, M.J., Editors, *Shiva*, Nantwich, pages 230–249.
- Pearce, J.A. and Cann, J.R. (1973): Tectonic setting of basic volcanic rocks determined using trace element analyses; *Earth and Planetary Science Letters*, Volume 19, pages 290–300.

- Pearce, T.H., Gorman, B.E. and Birkett, T.C. (1977): The relationship between major element chemistry and tectonic environment of basic and intermediate volcanic rocks; *Earth and Planetary Science Letters*, Volume 36, pages 121–132.
- Reinecke, L. (1915): Ore deposits of the Beaverdell map-area; *Geological Survey of Canada*, Memoir 79, 172 pages.
- Tempelman-Kluit, D.J. (1989a): Geological map with mineral occurrences, fossil localities, radiometric ages and gravity field for Pentiction map area (NTS 82/E) southern British Columbia; *Geological Survey of Canada*, Open File 1969.
- Tempelman-Kluit, D.J. (1989b): Geology, Pentiction, British Columbia; *Geological Survey of Canada*, Map 1736A, scale 1:250 000.
- Thompson, R.N. (1982): British Tertiary volcanic province; *Scottish Journal of Geology*, Volume 18, pages 49–107.
- Wood, D.A. (1980): The application of a Th-Hf-Ta diagram to problems of tectonomagmatic classification and to establishing the nature of crustal contamination of basaltic lavas of the British Tertiary volcanic province; *Earth and Planetary Science Letters*, Volume 50, pages 11–30.

Redefining the Southern Nicola Group: Petrographic and Structural Characterization of the Eastgate-Whipsaw Metamorphic Belt, Southern British Columbia (NTS 092H/02E)

by S.L. Oliver¹, K.A. Hickey¹ and J.K. Russell¹

KEYWORDS: Nicola Group, Eastgate-Whipsaw metamorphic belt, Manning Park, Princeton, Quesnel terrane

INTRODUCTION

The Late Triassic–Early Jurassic Nicola Group in south-central British Columbia and its northern continuation, the Takla Group, constitute the volcanic arc that defines the extent of the Quesnel terrane (Figure 1). It hosts economically significant alkalic porphyry copper-gold deposits, including those at Copper Mountain, Highland Valley, Mount Milligan and Mount Polley. Past geological mapping of the Nicola Group by Rice (1947), Preto (1972), Mortimer (1987) and Monger (1989) established its distribution and divided it into three differing belts. However, the southwesterly portion of the Nicola Group, south of the town of Princeton, on the eastern boundary of Manning Park, was not assigned to any of the three major belts, although Mortimer (1987) suggested it may be a part of the calcalkaline western belt.

Rocks adjacent to the Jurassic–Cretaceous Eagle Plutonic complex, along the margin of Manning Park, differ significantly from other nearby Nicola Group outcrops and have been assigned to the Eastgate–Whipsaw metamorphic belt by Massey et al. (2009a). Key differences between this area and the supposed affiliated Nicola Group include higher metamorphic grade in the metamorphic belt (upper greenschist to lower amphibolite facies, compared to lower greenschist in typical Nicola), stronger deformation, differing rock types and the presence of several volcanogenic massive sulphide (VMS) deposits not usually seen in Nicola rocks (e.g., the Red Star and S and M VMS properties). There is a notable resemblance in lithology, metamorphism and setting with the Permo–Triassic Sitlika–Kutcho Formation, a known VMS-hosting unit (e.g., Kutcho Creek), emplaced along the margins of the Quesnel and Cache Creek terranes; the Sitlika has been shown to extend south as far as Ashcroft (NTS 092I), only 150 km northwest (along strike) of this ‘suspect’ metamorphic belt. This ongoing MSc project is focused on a detailed geological analysis of the poorly documented metamorphic belt; this paper is reporting preliminary observations on the petrography of the metamorphic rocks and overall structure of the belt.

¹University of British Columbia, Vancouver, BC

This publication is also available, free of charge, as colour digital files in Adobe Acrobat® PDF format from the BC Ministry of Energy, Mines and Petroleum Resources website at <http://www.empr.gov.bc.ca/Mining/Geoscience/PublicationsCatalogue/Fieldwork/Pages/default.aspx>.

RECENT WORK

Mapping in 2008 focused on determining the boundaries and constraining the rock types between definite Nicola Group exposures, units of the metamorphic belt and the Eocene Princeton Group. The metamorphic belt has been divided into three general units (Massey et al., 2009a): the eastern amphibolite belt, the central quartzite belt and the western metavolcanic-metasedimentary belt (Figure 2). The metamorphic belt’s bounding contacts and the contacts between the three compositional belts all strike in a northerly direction. A dominant foliation, also northerly trending and parallel to the contacts, has been noted across the belt striking, on average, towards 165° and dipping increasingly steeply towards its western edge. Although few contacts are exposed, a definite fault contact, named the Similkameen Falls fault, was mapped between augitephyric, mildly to undeformed Nicola Group volcanic rocks and the eastern edge of the metamorphic belt, making a lithofacies gradation somewhat less likely, as previously believed (Rice, 1947; Preto, 1972; Monger, 1989). Mapping in 2009 helped to further constrain the limits of the belt, which abruptly pinches out to the north where it is intruded by muscovite granite of the Eagle Plutonic complex (Massey and Oliver, 2010).

PETROGRAPHY

Select samples from the 2008 field season were used to study the petrography of the mapped units (Figure 2). The petrographic descriptions presented here (listed in Table 1) are discussed in order starting from westerly samples and moving to the east. The samples studied are categorized according to the three generalized units within the Eastgate–Whipsaw metamorphic belts: the amphibolite belt, the quartzite belt and the metavolcanic-metasedimentary belt (Massey et al., 2009a). These sample groupings may be subject to reinterpretation based on subsequent mapping and ongoing petrographic and petrochemical studies.

The intense metamorphism and deformation experienced by this belt have overprinted any primary textures that once existed in the rocks. The only possible relict texture noted in the field is the bedding boundaries between differing compositional layers, which often strike sub-parallel to the dominant 165° foliation in the metamorphic belt. However, this bedding may not reflect the original orientation, depending on the extent to which the metamorphic and deformation events have mobilized and transposed these relations. This has yet to be determined.

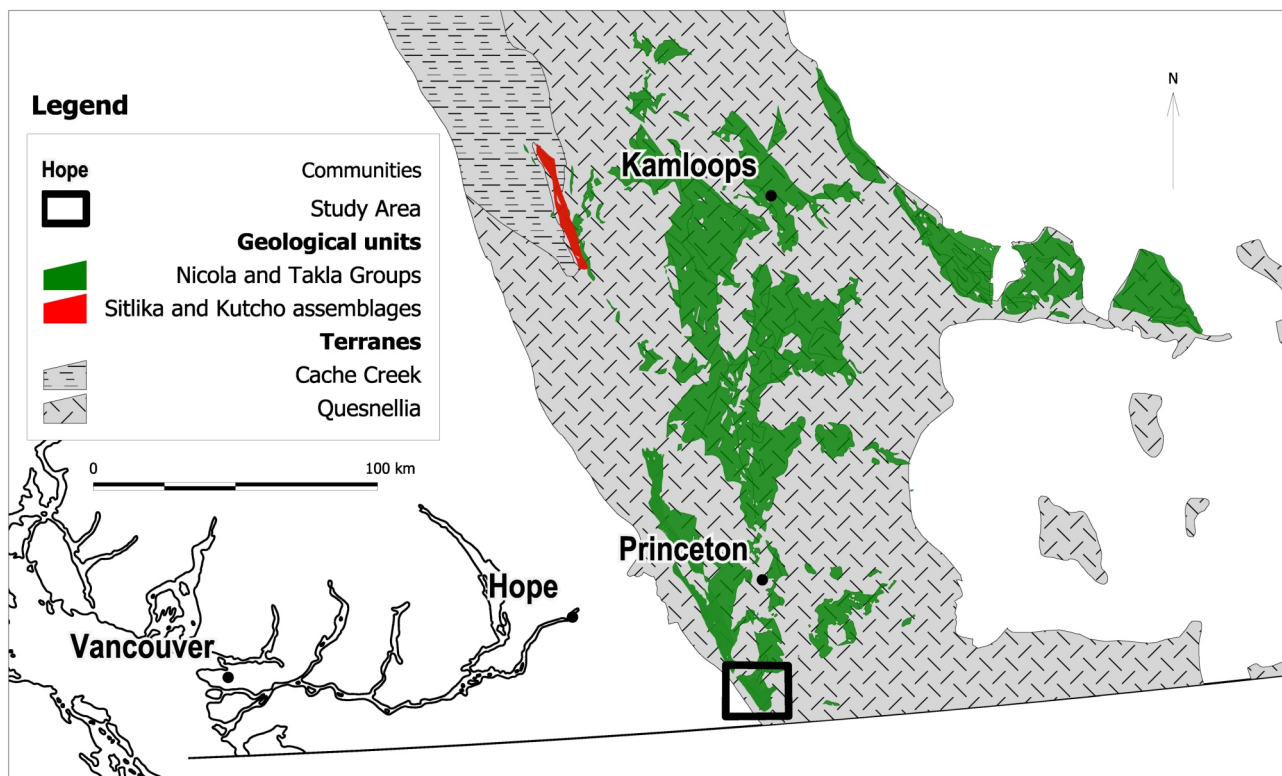


Figure 1. Location of study area, southwestern margin of Quesnellia, southern British Columbia.

Amphibolite Belt

There are several examples of amphibole-rich rock types within the Eastgate–Whipsaw metamorphic belt. The most consistent is a belt of northwest-trending rocks, tens of metres wide, on the westernmost edge of the metamorphic belt (Figure 2), in contact with the Eagle Plutonic complex. In outcrop, the belt is composed of black, actinolite+epidote-rich schistose rocks, which occur across the entire western unit. Between the 1–3 cm thick, dark layers are thin bands (only a few millimetres thick) of white quartzofeldspathic material. These two compositionally variable layers have distinct, although gradational, boundaries (Figure 3).

The felsic layers are composed of plagioclase, some quartz, interstitial calcite and minor actinolite and epidote. The fine grain size precludes the determination of relative proportions of plagioclase to quartz. The dark layers consist predominantly of poikiloblastic euhedral actinolite, epidote granules, anhedral oxides, magnetite, minor secondary biotite associated with the amphibole and small amounts of fine-grained, interstitial feldspathic material. Although the gradual grading in composition between the layers may be indicative of a primary lithological control, a clear protolith cannot be determined since both para- and ortho-amphibolites commonly display this banded feature (Evans and Leake, 1960). Further study into the variation of chemical trends (Leake, 1964) and the distributions, and contents, of major and trace elements (Shaw and Kudo, 1965) of the amphibolite will be undertaken to aid in determining the nature of the protolith.

AMPHIBOLITE INTERBEDS IN QUARTZITE UNITS—QUARTZITE BELT CONTACT

Amphibole-rich interbeds in quartzite were mapped at the boundary between the amphibolite belt and the quartzite belt (Figure 4). It has been noted in the literature that thin bands of amphibole-rich layers are commonly found in metamorphosed sedimentary rocks and are thought to be associated with chemical reactions rather than simple depositional features (Preto, 1970). It is likely that observations on closed-system metasomatic influences made by Orville (1969) on similar interbeds do not apply here since no significant calcareous sedimentary units were observed in the area. Further investigation using chemical analysis will help to better understand their formation.

Quartzite Belt

East of the amphibolite belt is a thick package of siliceous metamorphic rocks. The common, monomineralic samples are categorized as biotite quartzite (Figure 5) and occur in the southwestern section of the quartzite belt. The orange-white samples in this area all have a fine-grained, sugary texture with the minor platy biotite aligned parallel to the regional foliation. Moving away from the southwestern corner of the quartzite belt, either in an easterly or northerly direction, the composition in the quartzite belt units begins to vary. The mineralogy of the rock units to the north and east is changed by the appearance of actinolite, some garnet, oxides and, on the far-eastern side of the quartzite belt, chlorite. The ratio of siliceous material to the other mineral components decreases to such a degree that, on the eastern edge of the quartzite belt, the rock units are

Table 1. Common rock types in the Eastgate–Whipsaw metamorphic belt, southern British Columbia.

Belt unit	Description
Amphibolite belt	act+ep+pl+bio+qz+cal schist
Quartzite belt	
major units	bt qte bt+mag qte bt qtz-schist bt+act qtz-schist qtz+act+bt schist
minor units	chl+ilm+czo+ap qtz-schist with relic qtz clasts act+ep+pl+bt+qtz+cal schist act+pl/qtz+ep+chl+bt+ilm schist
Metavolcanic-metasedimentary belt	
mafic units	act+ep+cal+pl/qtz+ilm+bt schist (metabasite)
low mica units	bt+oxide+ep+ms qtz/fel-schist with pl porphyroclasts and qtz relics (metarhyolite) chl+bt qtz/pl-schist with sericitized pl porphyroclasts and qtz relics qtz/fel-schist with minor bt+chl, pl porphyroclasts and cumulophyric clusters of pl+bt+chl+oxide
low to no potassium units	qtz+chl+ilm schist with relic qtz clasts and ap porphyroblasts
micaceous units	qtz+ms+chl+ilm+ap schist with relic qtz clasts qtz/fel=chl+ep+act+bt schist with pl porphyroclasts and minor relic qtz clasts qtz/fel+act+chl±bt+ms+ilm schist with pl porphyroclasts and minor relic qtz clasts act+qtz/fel+chl+mag+bt schist

Abbreviations: act, actinolite; ap, apatite; bt, biotite; cal, calcite; chl, chlorite; czo, clinozoisite; ep, epidote; fel, feldspar; ilm, ilmenite; mag, magnetite; ms, muscovite; pl, plagioclase; qtz, quartz; qte, quartzite

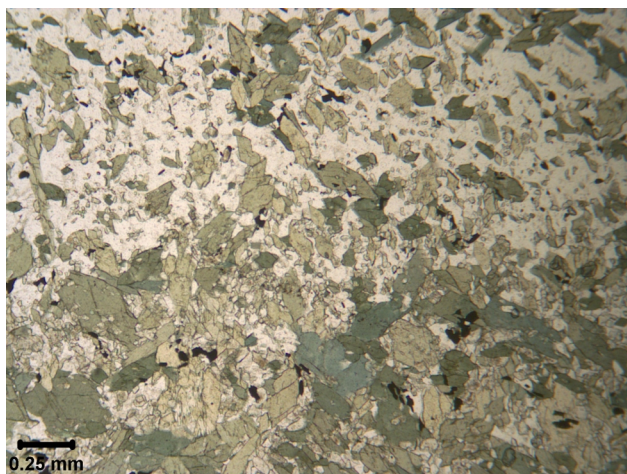


Figure 3. Thin-section photomicrograph of a mafic layer in amphibolite grading into a more felsic layer, Eastgate–Whipsaw metamorphic belt, southern British Columbia (field station 08SOL24-01, UTM Zone 10, 5445656N, 672513E, NAD 83).



Figure 4. Outcrop photo of an amphibolite interbedded in a quartzite unit, Eastgate–Whipsaw metamorphic belt, southern British Columbia (field station 08NMA17-06, UTM Zone 10, 5442201N, 675785E, NAD 83).

no longer proper quartzite but quartz-schist. The strike of the schistosity also varies slightly in the southeastern corner of this belt by veering away from 165° and striking closer to 190°, this change has been interpreted as indicating the presence of a possible fold (Massey et al., 2009a).

More typically in outcrop, the composition of the unit will be consistent, changing gradually over tens of metres, although there are some examples of layered outcrops where the units will vary slightly in composition over thick-

nesses of 0.5–1 m. However, the typical trend in bulk compositional change is occurring gradually over the distance of the quartzite belt.

CHLORITE QUARTZ-SCHIST INTERBED

In the north-central section of the quartzite belt (Figure 2), the units are still quartz rich and predominantly actinolite+biotite+magnetite bearing, but also contain significant aluminum-, potassium-, calcium- and iron-bearing



Figure 5. Outcrop photo of a biotite-quartzite, Eastgate–Whipsaw metamorphic belt, southern British Columbia (field station 09THS02-02, UTM Zone 10, 5441526N, 675973E, NAD 83).

phases. Moving towards the east in the northern section of the map area, interbedded units lacking any potassium-bearing phases become increasingly abundant. These thin (10–20 cm thick) interbeds are equigranular, fine-grained chlorite+ilmenite quartz-schist with minor apatite+clinozoisite. They are interlayered between actinolite+biotite+chlorite quartz-schist (Figure 6) and seem to have sharp contacts between the differing compositions still containing potassium-bearing mineral phases.

The lack of potassium possibly reflects a change to a more volcanic source or, at least, to a reduced sedimentary input. Further to the east, chlorite continues to be a significant mineral phase in the schist layers, along with variable amounts of actinolite and biotite.

MAFIC SCHIST

Also along the boundary between the quartzite belt and the metavolcanic-metasedimentary belt (Figure 2), there is a cropping-out of a few thick beds of massive amphibole-rich rocks, often 5–10 m thick. Their mineralogy includes actinolite, epidote, ilmenite, plagioclase, calcite and quartz, with lineations defined by the more elongate minerals. In thin section, some of the samples are texturally and compositionally similar to the western margin amphibolite, as they have layers of differing composition and a significant quartzofeldspathic component (see Figure 3). They are also heterogeneous and contain thin plagioclase-, quartz- and calcite-rich layers within more mafic bands rich in actinolite and epidote. However, this mafic schist in hand

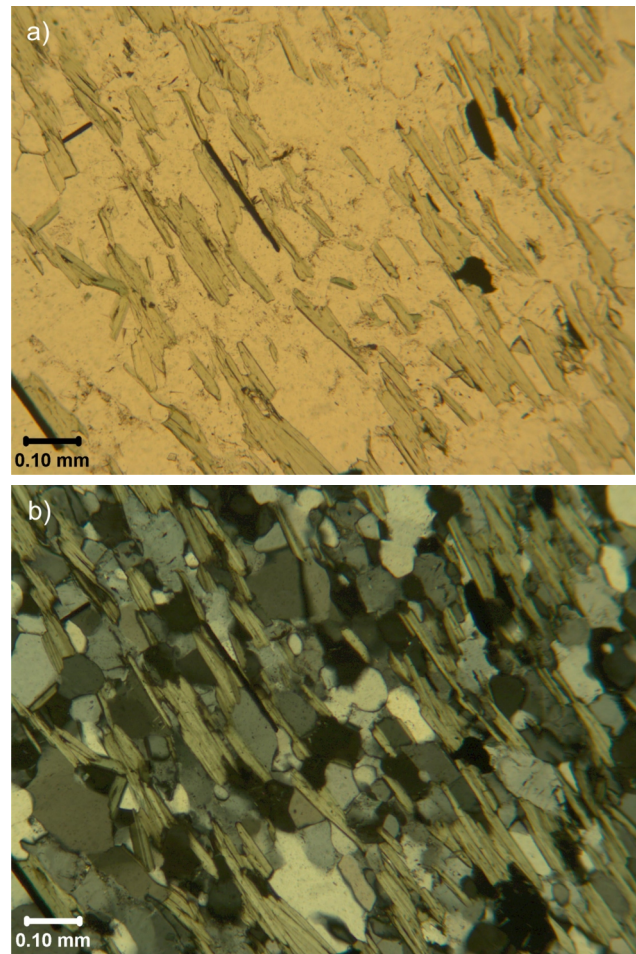


Figure 6. Thin-section photomicrographs of a chlorite-ilmenite quartz-schist unit found between units of actinolite+biotite+chlorite quartz-schist, Eastgate–Whipsaw metamorphic belt, southern British Columbia: a) plain-polarized light thin section; b) cross-polarized light thin section (field station 08SOL24-02, UTM Zone 10, 5445666N, 673032E, NAD 83).

sample does not appear black and schistose like the amphibolite to the west, but rather much more grey-green, hard and massive.

Two other outcrops of mafic schist along this central boundary are more mafic in composition, being fine-grained, massive and mostly homogeneous. In order of abundance, it is composed of actinolite, epidote plagioclase, calcite and quartz. Small, flat planes of chlorite+biotite clusters approximately a few millimetres thick and 10–15 cm wide are found sporadically in outcrop. In both outcrop and thin section, these units look like typical greenstones.

Metavolcanic-Metasedimentary Belt

The eastern side of the metamorphic belt is made up of a variety of schists of differing compositions (Figure 2). Unlike the quartzite belt, the metavolcanic-metasedimentary belt does not appear to have any obvious compositional trend. The Red Star VMS deposit (067 on Figure 2) occurs in the north-central area of the belt, where units proximal to the deposit have a felsic composition. As the outcrops become more distant from the deposit, in either a southwest-

erly or southeasterly direction, their compositions often become increasingly mafic. The variation in composition seems to occur in clusters of more felsic schist surrounded by more common intermediate to mafic schist. A full description of each common rock type found in this belt is given below.

QUARTZ-CHLORITE SCHIST

Similarly to the interlayers found in the quartzite belt, a few outcrops found in this belt also lack potassium, forming quartz+chlorite schist with quartz and plagioclase porphyroclasts. Some units have no biotite or muscovite at all, while others have only small amounts (1% or less). The typical mineral assemblage for this unit is a chlorite quartz-schist with minor apatite, ilmenite and clinozoisite. In outcrop, this unit is a green schist with visible porphyroclasts. The fine-grained schist matrix is typically equal parts chlorite to quartzofeldspathic material. Two units of this composition were mapped, one of them in the very northeastern edge of the belt, while the second originated directly in the Red Star showing itself (067 on Figure 2).

In the sample from the Red Star showing, the porphyroclasts of quartz are recrystallized and the relict shapes often appear quite round. However, the plagioclase porphyroclasts are fresh-looking, euhedral laths with sharp edges. The well-defined foliation, expressed particularly by chlorite in this unit, wraps around the quartz and plagioclase porphyroclasts. Their appearance suggests that the quartz-eyes and plagioclase laths were present before the development of that particular foliation. Whether the plagioclase crystals are definitely porphyroclasts or porphyroblasts will require a detailed study into the specific chemistry of the feldspars.

FELDSPATHIC UNITS

Feldspathic units are found as thick packages proximal to the Red Star showing (067 on Figure 2) on the northeastern side of the study area (red and pink dots on Figure 2). In outcrop, the units are light in colour, often white or a light pink with minor green siliceous bands. They either have very thin planes (less than 0.5 mm thick) of biotite, muscovite and chlorite defining the foliation or lack micaceous layers and a penetrative foliation, only showing alignment in minor amounts of platy minerals. The matrix is fine grained to very fine grained and even though dynamic recrystallization has affected the texture, the differing grain sizes is likely due to a primary grain-size influence. The finer grained units have undergone more alteration, since the plagioclase porphyroclasts and the matrix are more sericitized. Grain boundary migration can often be noted in the matrix, while some are so fine grained that they become mylonitic. All of the units have relatively large (3–4 mm) porphyroclasts of plagioclase (3–5% of rock) that are rounded and mantled by biotite, chlorite and recrystallized quartzofeldspathic material (Figure 7). The plagioclase porphyroclasts have undergone some form of deformation since they have developed subgrain boundaries. There are also occasional relict quartz porphyroclasts (1% of rock) that are now coarsely recrystallized. Cumulophyric clusters of feldspar, anhedral oxides, calcite and biotite, on the order of 3–4 mm in width, are also commonly found (Figure 7).

QUARTZ+FELDSPAR+CHLORITE+EPIDOTE SCHIST

This unit is a more mafic version of the feldspathic units described above. Dynamically recrystallized, blue quartz porphyroclasts and brittle deformed, plagioclase porphyroclasts, with red oxide in cracks, are found in a matrix of fine-grained recrystallized plagioclase, quartz, chlorite, epidote and some biotite (Figure 8). Biotite is usually located on the outer edge of the plagioclase porphyroclasts and is often being replaced by chlorite. The feldspars have developed microfaults, and actually have sections broken off and pulled apart; the subsequent cracks are filled with oxides and give the plagioclase crystals an orange-pink appearance. A fabric is apparent in this rock due to mineral alignment, but this unit does not tend to break on even planes.

MUSCOVITE+CHLORITE QUARTZ-SCHIST

Some schist in the volcanic package has a more felsic composition and forms muscovite+chlorite quartz-schist with notable blue-hued quartz-eye porphyroclasts.

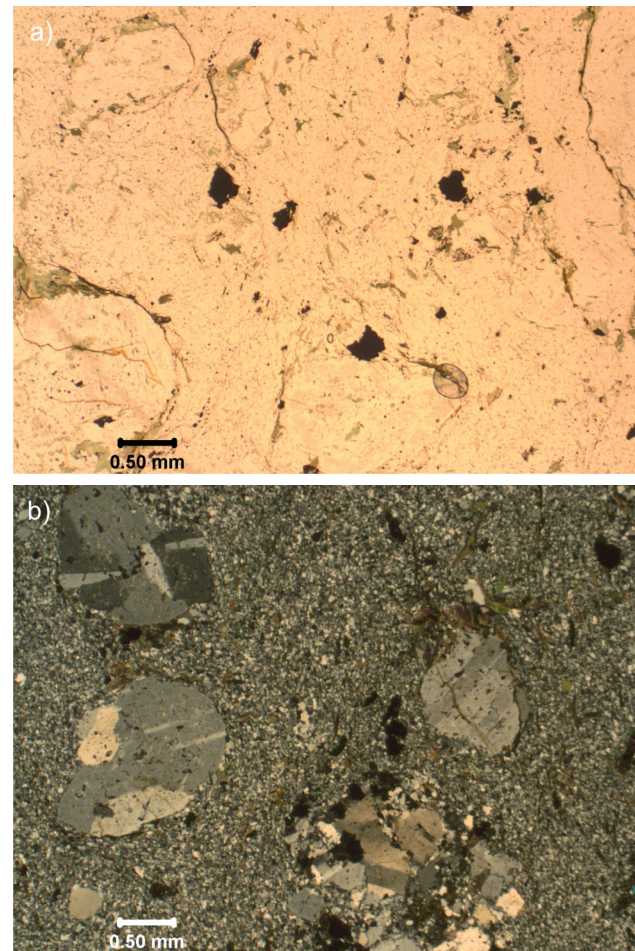


Figure 7. Thin-section photomicrographs of a feldspathic unit in the metavolcanic-metasedimentary belt of the Eastlake–Whipsaw metamorphic belt, southern British Columbia: **a)** plain-polarized light thin section showing porphyroclasts and cumulophyric clusters; **b)** cross-polarized light thin section (field station 08NMA21-01, UTM Zone 10, 5447289N, 675398E, NAD 83).

Using the mineralogy and presence of feldspar porphyroclasts as evidence, the eastern side of the metamorphic belt appears to be composed of volcanic or volcanoclastic rocks with varying amounts of clastic input. The majority of the schist contains a significant amount of feldspathic material (55–70% in the matrix). The unit's matrix has undergone significant dynamic recrystallization, judging by the grain sizes and textures on the grain boundaries. Finer grain sizes, combined with the grain boundary recrystallization textures, suggest that some samples are perhaps mylonitic. It is difficult to tell based solely on this grain size as it may be reflecting the primary grain size of the protolith rather than just how extensive recrystallization may have been.

ALTERATION

There has also been irregular alteration occurring in certain areas of the belt, as shown by sericitized feldspar porphyroclasts 7 m away from a similar outcrop with relatively fresh feldspar. Extensive veining does occur in clusters proximal to known showings, for example Red Star and Knobb Hill (067 and 069 respectively on Figure 2), with associated oxidization. Alteration is also noted near the fault

in the form of sericitization and secondary calcite associated with calcite veining, and near the Red Star showing in the form of sericitization and oxidization.

STRUCTURE

As well as the dominant northwest-trending foliation noted throughout the belt, a secondary schistosity was observed in some outcrops (Figure 9a). The strikes appear to be similar in the field, with the weaker foliation having a slightly steeper dip. Moving east to west across the metamorphic belt, the dip of the primary foliation tends to steepen. Observation of thin sections consistently reveals both foliations in samples. Crenulation cleavage is present in many schists with adequate mica and/or chlorite (Figure 9b). In the more felsic micaceous schist, the dominant schistosity consists mostly of muscovite while the weaker, older schistosity is associated with chlorite and muscovite. The more mafic schist commonly displays two lineations through two orientations of actinolite needles, one overprinting the other. Another phase of actinolite also occurs which cuts across the foliations. These actinolite needles have grown at a later stage and have not been affected by any deformation likely to have caused them to align.

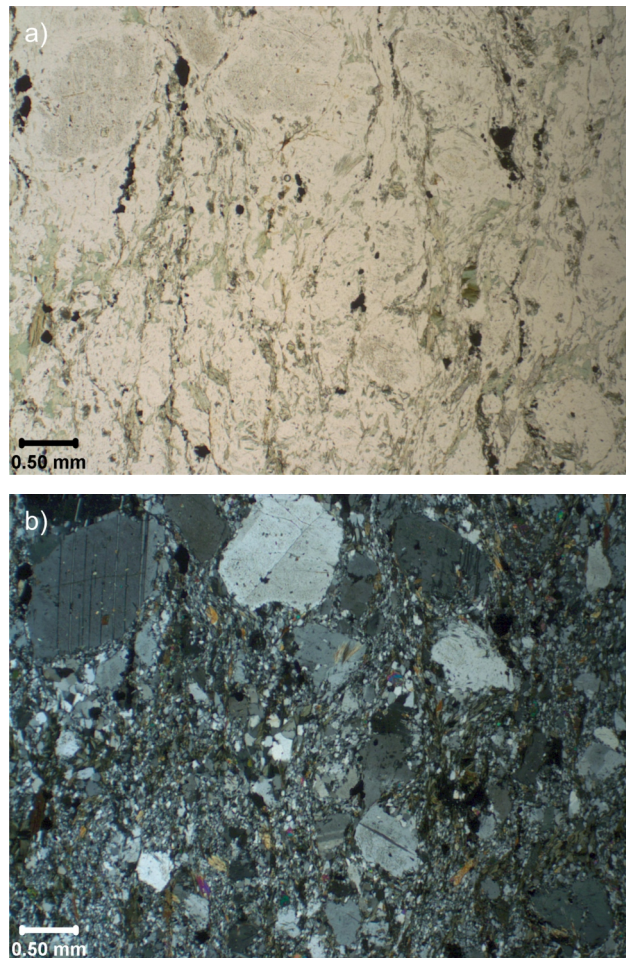


Figure 8. Thin-section photomicrographs of a quartz+ feldspar+chlorite+epidote schist with sericitized plagioclase porphyroclasts from the Eastlake–Whipsaw metamorphic belt, southern British Columbia: **a)** plain-polarized light thin section; **b)** cross-polarized light thin section (field station 08SOL23-04, UTM Zone 10, 5446993N, 674351E, NAD 83).

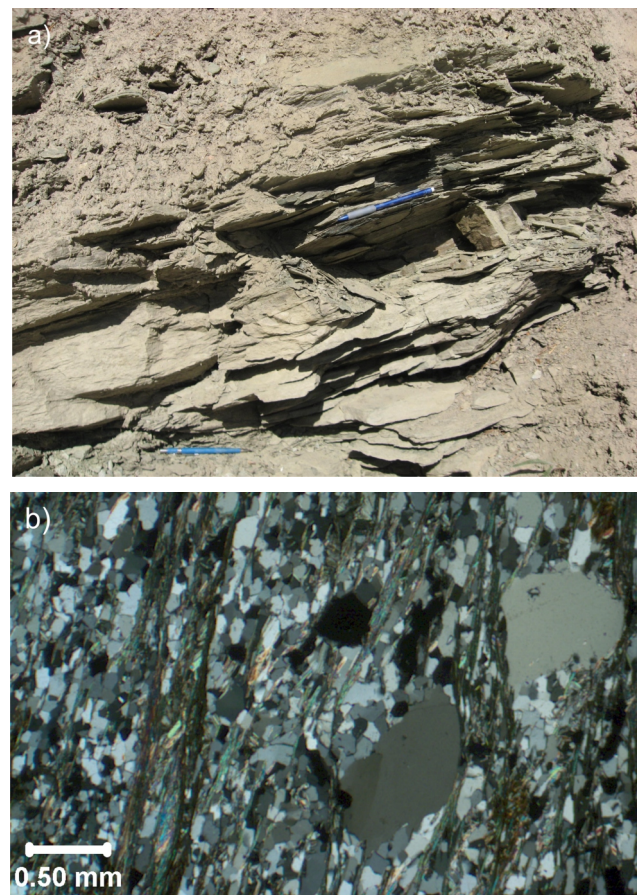


Figure 9. Structural features of the Eastlake–Whipsaw metamorphic belt, southern British Columbia: **a)** outcrop photo of acutely intersecting schistosity in muscovite quartzite (field station 09THS03-01, UTM Zone 10, 5444706N, 676242E, NAD 83); **b)** thin-section photomicrograph of a crenulation cleavage in a chlorite quartz-schist (field station 08SOL24-02, UTM Zone 10, 5445666N, 673032E, NAD 83).

Many samples rich in quartz have undergone grain reduction due to grain boundary migration. Even larger relict quartz porphyroclasts will have recrystallized into several smaller grains, blurring or removing any primary textures. Plagioclase porphyroclasts often have minor strain shadows on their edges, but have not formed new grains within their original margins. However, they do have some deformation textures in the form of subgrain boundary rotation and sometimes microfaults, forming domino-type fragments (for further reading on domino-type fragments, see Passchier and Trouw, 2005). Sometimes the porphyroclasts are slightly rectangular and occur obliquely to the direction in which the foliation is aligned, causing the mantled minerals to develop what appears to be opposite shear senses (Figure 10).

Finer grained matrix material includes quartz and feldspar that have undergone recrystallization, which causes the two minerals not only to be fine grained, but also similar in appearance and difficult to distinguish from one another. The rock types containing higher amounts of grain-size reduction are consistently the rock types with the highest ratio of feldspathic material in them.

There has been some brittle failure noted in a chlorite quartz-schist sample collected on Highway 3, in a location adjacent to the Similkameen Falls fault. In thin section, the sample has a milled texture, with all grains, including porphyroclasts, being well-rounded and quite small. The fine-grained matrix has calcite veining, higher amounts of interstitial calcite and significant anhedral oxide material. It seems likely that movement on the fault is milling material in the schist, breaking down the softer mica. The fault could also be acting as a conduit for carbonate-bearing fluids, altering and veining the wallrock.

A third deformation structure, as yet only observed in the field, is visible in certain rock types, in particular a metachert (UTM Zone 10, 5447048N, 674136E, NAD 83). The fold itself is an open fold that maintains constant bed thickness throughout the bend. Striations are seen on the micaceous layers, indicating movement similar to a deck of cards. This style of folding is characteristic of the brittle regime and is thus much different from the other types of



Figure 10. Thin-section photomicrograph of a mantled relict porphyroclasts showing shear textures in an actinolite+chlorite+felspar/quartz+biotite schist, Eastlake–Whipsaw metamorphic belt, southern British Columbia (field station 08SOL22-04, UTM Zone 10, 5446268N, 676013E, NAD 83).

strain discussed above, which have all been ductile; this folding style has only been noted in two locations, which may mean it is only a localized event.

Stereonet Projections

Upon plotting all available structural data measured in the study area, several significant facts can be noted. All foliations and schistosity sit in a single, moderately defined cluster (Figure 11a). In outcrop, there is evidence for two foliations that are further proven through thin section study, showing evidence of crenulation cleavages and two directions of alignment in elongate minerals. However, upon first inspection, there is no obvious distinction between the possible two foliations in the scatter of poles. Since the two foliations strike in similar directions and differ in dip direction mostly, the two clusters would likely overlap, which would make it difficult to extrapolate one from the other. It is worth noting that by using a statistical density contouring analysis on the many pole measurements plotted, two separate clouds are crudely drawn (Figure 11b). In order to truly determine where the separation between the clusters lies on the stereonet projection, many more data points would have to be obtained. The two sets of diamonds (purple and green) are from two separate outcrops where both schistosity were measurable. Both outcrops have the stronger schistosity defined by muscovite and dip more steeply ($69\text{--}90^\circ$). The weaker schistosity is shallower for both ($35\text{--}38^\circ$) and defined by chlorite and muscovite. The green diamonds both correlate well with the statistical clusters, each one relating to one of the two clusters. The two purple diamonds, however do not correlate as closely; one purple diamond does plot within the density cluster, while the other lies just outside of the perimeter (Figure 11b). The lineations align well on a plane, but without knowing what surface the lineations were measured on, the two apparent clusters are not easily explained. The bedding orientations sit parallel to the foliations, suggesting that a form of transposition has occurred. Since few of the units seem to have preserved the deformation textures well, further study into microstructures must be undertaken. Minor units have been sampled, which are high in graphite and have preserved all stages of microfolds well. Thin sections of such samples were not prepared in time for this publication, but will be added to the data in the future. It is definitely significant to note that all the measurements do lie on the same strike planes.

SUMMARY

In order to compare variation in the metamorphic grade across the Eastgate–Whipsaw metamorphic belt, the mineralogy of the more mafic units was analyzed to determine what mineral assemblage is stable. According to Spear (1993), the diagnostic greenschist assemblage is made up of chlorite+albite+zoisite+actinolite+quartz+carbonate+titanite, while the diagnostic amphibolite assemblage is made up of hornblende+plagioclase±quartz±ilmenite. The metamorphic mineralogy observed in samples across the belt is generally consistent with the epidote–actinolite grade. A more detailed study will be undertaken using the scanning electron microscope to better understand the variations in the solid solutions and link those compositions to more specific pressures and temperatures.

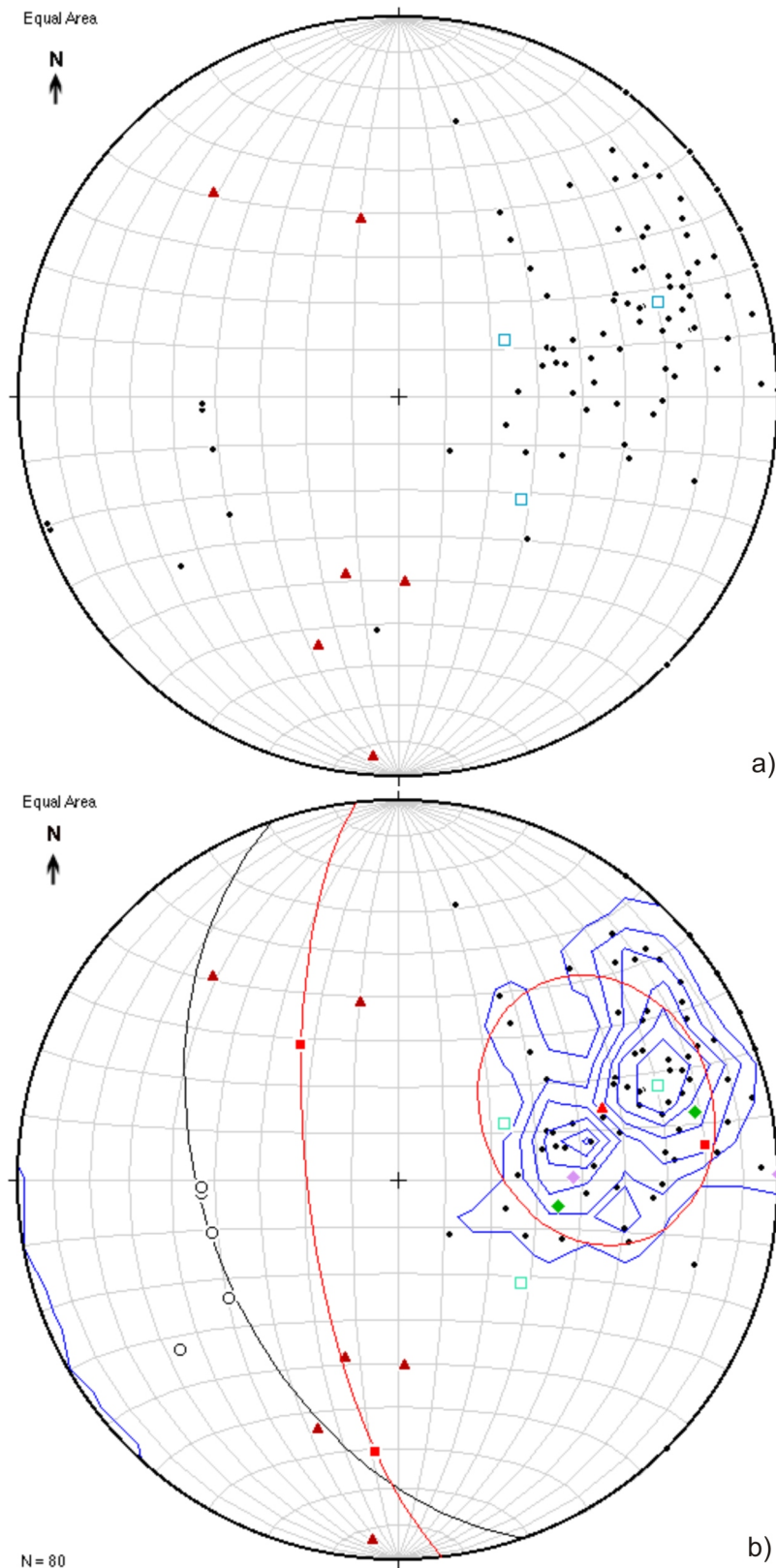


Figure 11. Stereonet projections of structural data from the Eastgate–Whipsaw metamorphic belt, southern British Columbia: **a)** all structural data: black dot, pole to foliation/schistosity; empty green squares, pole to bedding; red triangle, lineation; **b)** statistical contouring: blue contours, 1% density contours; empty blue squares, pole to bedding; red triangle, average pole to foliation/schistosity; empty black circle, cleavage; red square and great circle, average great circle and pole of lineation; black great circle, plane to average foliation/schistosity pole; green and purple diamonds, two schistosities measured at same outcrop (field station 08SOL11-03, UTM Zone 10, 5446508N, 675562E, NAD 83 and field station 08SOL11-10, UTM Zone 10, 5446401N, 675934E, NAD 83).

The main compositional trend is noted in the quartzite belt. This trend goes from west to east and undergoes an addition of calcium and a decrease in potassium in the mineral phases.

The belt has undergone at least three different stages of deformation, culminating in crenulated cleavages and then even-layered folding, which must have occurred at shallow depths later in the deformation history since it overprints the foliations.

ACKNOWLEDGMENTS

We would like to acknowledge Dave Lefebure and Nick Massey of the BC Geological Survey for their continuing support and encouragement during this project. The Canadian Mining Initiative Council provided valuable financial support to the senior author during the summer of 2009. Nick Massey reviewed an earlier draft of this manuscript.

REFERENCES

- Evans, B.W. and Leake, B.E. (1960): The composition and origin of the striped amphibolites of Connemara, Ireland; *Journal of Petrology*, Volume 1, pages 1337–1363.
- Leake, B.E. (1964): The chemical distinction between ortho- and para-amphibolites; *Journal of Petrology*, Volume 5, pages 238–254.
- Massey, N.W.D. and Oliver, S.L. (2010): Southern Nicola project: Granite Creek area, southern British Columbia (parts of NTS 092H/07, 10); in Geological Fieldwork 2009, *BC Ministry of Energy, Mines and Petroleum Resources*, Paper 2010-1, pages 59–72.
- Massey, N.W.D., Vineham, J.M.S. and Oliver, S.L. (2009a): Southern Nicola Project: Whipsaw Creek–Eastgate–Wolfe Creek area, southern British Columbia (NTS 092H/01W, 02E, 07E, 08W); in Geological Fieldwork 2008, *BC Ministry of Energy, Mines and Petroleum Resources*, Paper 2009-1, pages 189–204.
- Massey, N.W.D., Vineham, J.M.S. and Oliver, S.L. (2009b): Geology and mineral deposits of the Whipsaw Creek–Eastgate–Wolfe Creek area, British Columbia (NTS 092H/01W, 02E, 07E, 08W); *BC Ministry of Energy, Mines and Petroleum Resources*, Open File 2009-8, scale 1:30 000.
- Monger, J.W.H. (1989): Geology, Hope, British Columbia; *Geological Survey of Canada*, Map 41-1989, scale 1:250 000.
- Mortimer, N. (1987): The Nicola Group: Late Triassic and Early Jurassic subduction-related volcanism in British Columbia; *Canadian Journal of Earth Sciences*, Volume 24, pages 2521–2536.
- Orville, P.M. (1969): A model for metamorphic differentiation origin of thin-layered amphibolites; *American Journal of Science*, Volume 267, pages 64–86.
- Passchier, C.W. and Trouw, R.A.J. (2005): *Microtectonics*; Springer, Germany, 366 pages.
- Preto, V.A.G. (1970): Amphibolites from the Grand Forks quadrangle of British Columbia, Canada; *Geological Society of America*, Bulletin, Volume 81, pages 763–782.
- Preto, V.A. (1972): Geology of Copper Mountain; *BC Ministry of Energy, Mines and Petroleum Resources*, Bulletin 59, 87 pages.
- Rice, H.M.A. (1947): Geology and mineral deposits of the Princeton map-area, British Columbia; *Geological Survey of Canada*, Memoir 243, 136 pages.
- Shaw, D.M. and Kudo, A.M. (1965): A test of the discriminant function in the amphibolite problem; *Mineralogical Magazine*, Volume 34, pages 423–435.
- Spear, F.S. (1993): *Metamorphic Phase Equilibria and Pressure-Temperature-Time Paths*; *Mineralogical Society of America*, Washington, DC, 799 pages.

Age of Mineralization and 'Mine Dykes' at Copper Mountain Alkaline Copper-Gold-Silver Porphyry Deposit (NTS 092H/07), South-Central British Columbia

by M.G. Mihalynuk, J. Logan, R.M. Friedman¹ and V.A. Preto²

KEYWORDS: Copper Mountain, alkalic porphyry, Cu-Au-Ag deposit, mineralization, alteration, geochronology, isotopic age, U-Pb zircon, U-Pb titanite, ⁴⁰Ar/³⁹Ar, Quesnel Arc

INTRODUCTION

Underground mass mining techniques have enabled profitable extraction of the deep portions of porphyry deposits at minesites worldwide. Often considered a relatively new innovation, block caving was originally developed for copper mining in Utah in 1906 (Barger and Schurr, 1944). Examples of block cave mining of copper porphyry deposits include the recently decommissioned San Manuel Cu mine in Arizona, and the currently active alkalic Cu-Au-Ag Ridgeway deposit in New South Wales, Australia. Profitable underground mining of large tonnage, low-grade deposits combined with the recent strength in metal commodity prices has prompted deep exploration of porphyry deposits in British Columbia, especially within the prolific Quesnel terrane (Figure 1). For example, in the Iron Mask batholith near Kamloops, New Gold Inc. has outlined 44.4 million tonnes at a grade of 0.98% Cu, 0.72 g/t Au and 2.27 g/t Ag (New Gold Inc., 2007) beneath the former Afton pit and has started development. Copper Mountain Mining Corporation has similarly demonstrated the potential for subsurface extensions to mineralization that was extracted from open pits at Copper Mountain, about 15 km south of Princeton, in south-central BC (Figure 2).

In 2009, the company reported a resource of 470.8 million tonnes grading 0.311% Cu (0.15% Cu cut-off; O'Rourke, 2008) adjacent to, and beneath, the proposed 'super pit' (Figure 3; Holbek, 2009). Current plans are to extract 211.2 million tonnes at 0.361% Cu from the super pit (Chance et al., 2009). This resource of more than 1 billion kilograms Cu adds significantly to historical production between 1908 and 1996 of ~650 million kilograms of Cu, nearly 16 million grams Au and over 648 million grams Ag (BC Geological Survey, 2009; MINFILE 092HSE001). In addition, largely untested magnetotelluric targets extend

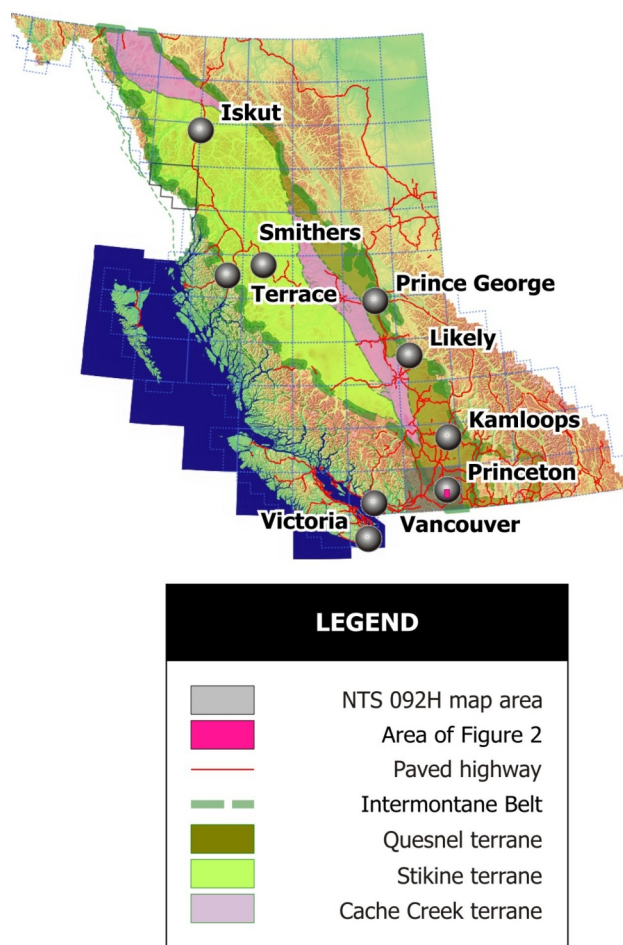


Figure 1. Location of the Copper Mountain area south of Princeton, south-central British Columbia. The area covered by Figure 2 is shown on top of the southern part of the Princeton town symbol.

1000 m below the lowest planned super pit levels (Holbek, 2007, 2009).

Large capital expenditures are required for deep exploration and development, so a clear and accurate exploration model is particularly desirable. To this end, we initiated a geochronological investigation of the mineralizing system at Copper Mountain in 2006. Our principal objective was to test the assertion that mineralization at Copper Mountain was coeval with the emplacement of the Lost Horse Intrusions of the Copper Mountain intrusive suite (e.g., Figure 4; Preto, 1972). However, existing geochronometric determinations place the age of mineralization in the Early Jurassic

¹Pacific Centre for Isotopic and Geochemical Research, The University of British Columbia, Vancouver, BC

²Preto Geological Inc., Sooke, BC

This publication is also available, free of charge, as colour digital files in Adobe Acrobat® PDF format from the BC Ministry of Energy, Mines and Petroleum Resources website at <http://www.empr.gov.bc.ca/Mining/Geoscience/PublicationsCatalogue/Fieldwork/Pages/default.aspx>.

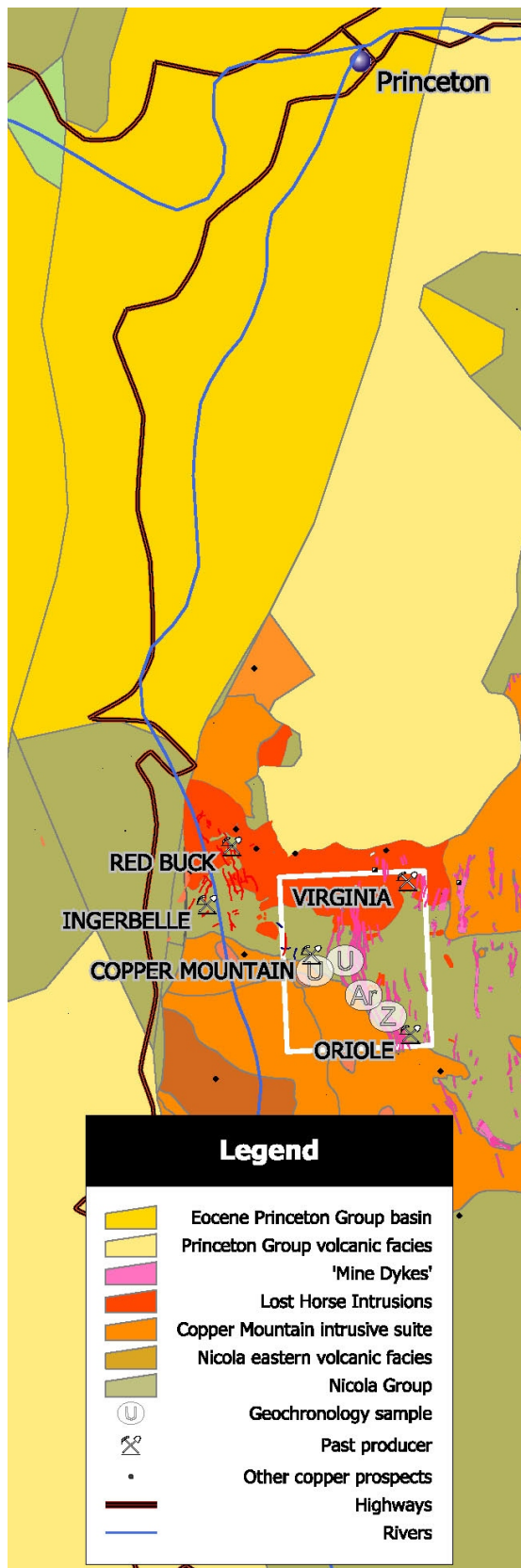


Figure 2. Regional geological map of the Copper Mountain area, south-central British Columbia, incorporating mapping by Preto (1972) and compilations by Preto et al. (2004) and Massey et al. (2005).

(192 ± 16 Ma and 198 ± 14 Ma; Breitsprecher and Mortensen, 2004; recalculated from Preto, 1972 and Farquharson and Stipp, 1969, respectively), while the best crystallization age data on phases of the mineralized Copper Mountain suite intrusive rocks place them in the Late Triassic (Figure 4; Mortensen et al., 1995; $202.7 \pm 4.4/-0.5$ Ma, 200.3 ± 2.1 Ma and 204 ± 6 Ma). Based on these data, and in consideration of their full error limits, between -14 and 33 m.y. (median, 7 m.y.) elapsed between intrusion and mineralization of the Copper Mountain stock. Even without considering error envelopes, the means of these datasets suggest that 7 m.y. elapsed, which is far greater than is typical for the main mineralizing event in porphyry deposits (McInnis et al., 2005) and raises the question of a separate, younger mineralizing intrusion.

Geochronometric data from various workers have been combined together with new data as part of an investigation of Mesozoic copper porphyry deposits in BC under the direction of J. Logan (Logan and Mihalynuk, 2005a, b; Logan and Bath, 2006; Logan et al., 2007). This work has shown that increased geochronometric precision on intrusive and mineralizing events reveals them to be coeval, within the resolution of the geochronometric technique applied. Additionally, the new data show that, with a few notable exceptions, all alkalic copper porphyry deposits in the Canadian Cordillera are part of a metallogenic epoch in the latest Triassic (together with numerous calcalkalic deposits, such as Highland Valley; e.g., Ash et al., 2007). Herein we affirm both the addition of the Copper Mountain alkalic porphyry to this epoch and the original assertion of Preto (1972), that intrusion and mineralizing events are essentially synchronous at Copper Mountain.

LOCATION AND GEOLOGICAL SETTING

Copper Mountain is located within the Quesnel Arc (Figure 1), a crustal terrane that accreted to ancestral North America (ANA) or a crustal ribbon that lay adjacent to ANA in Early Jurassic time (ca. 186 Ma; Nixon et al., 1993). Subduction of ancient Pacific Ocean crust to form the proto-Quesnel and conjoined Stikine arcs is believed to have begun in the Devonian (e.g., Brown et al., 1996; Mihalynuk, 1999; Logan and Koyanagi, 2000). Arc growth continued sporadically with a significant pulse in the Late Triassic. Near the end of this magmatic pulse, a prolific metallogenic event is manifest as a chain of alkalic Cu-Au±Ag-Mo porphyry deposits along the arc axes. Intrusions allied with mineralization at Copper Mountain were recognized by Preto (1972, 1979) as part of this well-endowed magmatic suite.

Mineralization at Copper Mountain is mainly focused at the margins and between the polyphase Copper Mountain stock (to the south) and the Lost Horse Intrusions (to the north). Intervening country rocks that host the bulk of the mineralization locally display protolith textures of andesitic to basaltic lapilli tuff and breccia belonging to the Late Triassic Nicola Group. Intense hydrothermal alteration of these rocks generally displays the following petrogenesis:

- 1) biotite flooding
- 2) extensive albite-epidote metasomatism
- 3) K-feldspar and scapolite veining

SAMPLES FOR AGE DETERMINATION

Four samples were selected for isotopic age determination. Two samples from mineralized veins that contain medium-grained crystals of titanite were collected for U-Pb determination. Because of the relatively high closure temperature for lead diffusion in titanite at 660–700°C (Scott and St-Onge, 1995), relatively straightforward isotopic age determinations were anticipated from the mineralization in these two vein samples. In addition, coarse-grained euhedral biotite was extracted from an archival specimen of museum-quality massive bornite-chalcocopyrite-biotite from the Big Lead to provide a $^{40}\text{Ar}/^{39}\text{Ar}$ cooling age on mineralization from a spectacular ‘glory hole’ (now mined out).

The fourth sample, a relatively unaltered representative sample of the ‘Mine Dyke’ swarm (Figures 3, 5), was collected to date the late, cross-cutting intrusions. We are not aware of any published crystallization age for the ‘Mine Dyke’ swarm; existing ages are cooling ages, mainly K-Ar and fission-track determinations.

Titanite-Bearing Veins

Titanite occurs in dominantly south-trending, planar sets of K-feldspar veins. Vein mineralogy includes coarse, chloritized biotite, malachite-stained bornite and chalcocopyrite, epidote and titanite (Figure 6). White alteration envelopes are interpreted as albite; no bladed scapolite was observed.

These veins were sampled at the margin of the Copper Mountain stock (MMI06-32-5) along the haul road south of Pit 1 (Figure 3) and midway between the Copper Mountain stock and the main body of Lost Horse Intrusions, on the north rim of Pit 2 (MMI06-32-3). They probably belong to the ‘ore fractures’ reported by Preto (1972). Where the veins of pegmatitic biotite–K-feldspar–copper sulphides, called ‘ore fractures’, thickened to 30 cm or more, they were historically exploited by miners from glory holes. One especially rich glory hole, known as the Big Lead, was located in what is now the central part of Pit 3.

Big Lead Massive Bornite-Biotite

Massive bornite–chalcocopyrite–biotite±K-feldspar of the Big Lead was sampled by V.A. Preto in 1969. The sample was taken from the subsidence area over shallow stopes and glory holes, which was located near what is now the middle of Pit 3 (see Plate XIII in Preto [1972] for a historical perspective). This archival sample contains beautiful, euhedral booklets of coarse, vitreous biotite within massive copper sulphide. Such textural equilibrium suggests simultaneous growth of the idiomorphic biotite crystals and chalcocopyrite from a magmatic-hydrothermal fluid. Idiomorphic biotite enclosed in bornite is reported at other high-grade porphyry deposits such as Grasberg, where they are interpreted as coarse-grained replacements of mafic phenocrysts (Pollard et al., 2005).

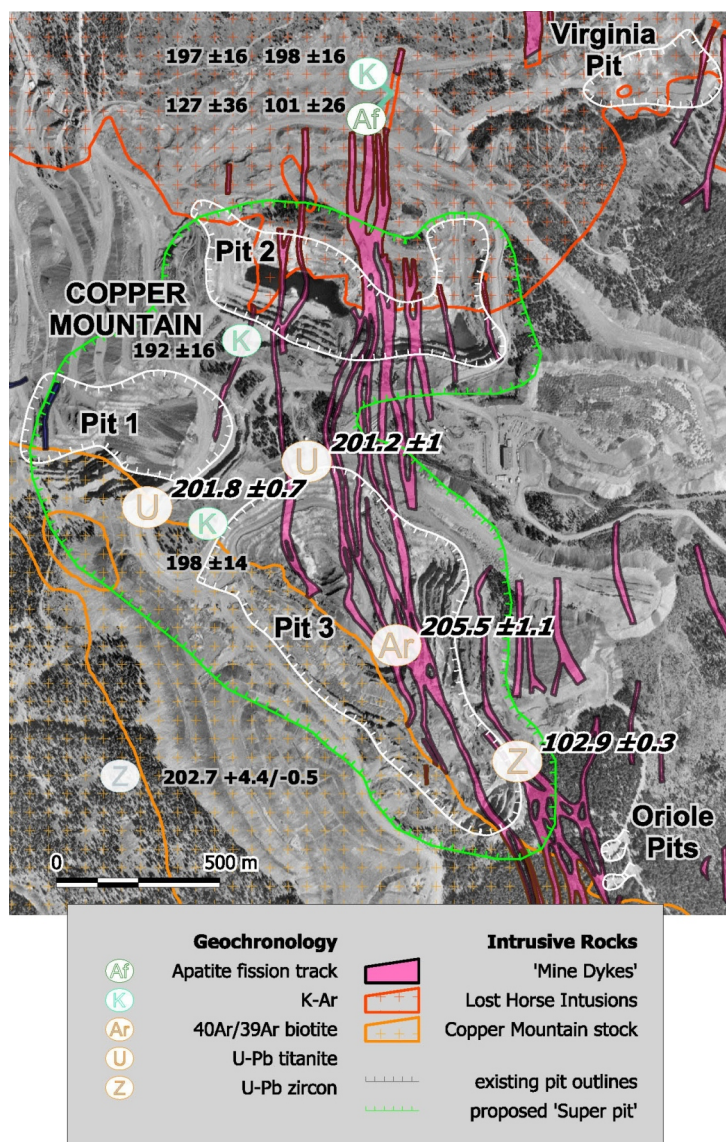


Figure 3. Locations of geochronological samples collected as part of this study (large symbols) and those collected previously by other authors (smaller symbols) as reported in the database compiled by Breitsprecher and Mortensen (2004), Copper Mountain area, south-central British Columbia. Geological contacts and underlying imagery are adapted from Preto et al. (2004). The proposed ‘super pit’ outline is from Chance et al. (2009). Values on the map are in Ma.

‘Mine Dyke’ Swarm

The ‘Mine Dykes’ are white to yellow-orange weathering, blocky to flaggy and relatively recessive (Figure 5). They dip steeply and anastomose, generally conforming to a strong north-northeast trend with a few orthogonal exceptions (Figures 2, 3, 5). Preto (1972) reported their compositional range as trachyte to rhyolite. Medium-grained, grey quartz eyes are conspicuous (7%), and coarse-grained probable K-feldspar relicts are replaced by greasy green clay. Matrix material is a bleached, fine-grained aplite with ~1% magnetite and traces of pyrite. In general, the dikes are strongly clay- and carbonate-altered and only ghosts of former feldspar phenocrysts remain.

U-PB GEOCHRONOLOGY METHODS

Sample preparation and analytical work for both the U-Pb and the $^{40}\text{Ar}/^{39}\text{Ar}$ isotopic ages presented herein was conducted at the Pacific Centre for Isotopic and Geochemical Research (PCIGR) at the Department of Earth and Ocean Sciences, The University of British Columbia.

Titanite was handpicked from samples MMI06-32-3 and 32-5. Picked samples were microscopically evaluated to ensure purity (Figure 7). Pink, brown and greenish grain fragments of moderate clarity were selected for analysis. Titanite sample aliquots analyzed are shown in Figure 7. Uranium-lead isotopic age determinations were obtained by thermal ionization mass spectroscopy (U-Pb ID-TIMS) with results listed in Table 1 and plotted in Figure 8.

Zircon was separated from the ‘Mine Dyke’ sample MMI06-32-4 using standard mineral separation techniques (crushing, grinding, Wilfley wet shaker table, heavy liquids and magnetic separation), followed by hand picking. Air-abraded single zircon grains were analyzed (Figure 7). Uranium-lead isotopic age determinations were obtained by U-Pb ID-TIMS with results listed in Table 2 and plotted in Figure 9. Details of both the mineral separation and analytical techniques are presented in Logan et al. (2007).

U-PB GEOCHRONOLOGY RESULTS

All data overlap concordia at the 2 σ confidence level and quoted ages are based on Ludwig concordia interpretations (Figures 8, 9) for all three samples (Tables 1, 2). The two mineralized vein samples that contain titanite were analyzed in three (MMI06-32-3) or four (MMI06-32-5) fractions. Analytical results from the fractions can be interpreted in two ways. If the data from the two widely separated copper sulphide–epidote–K-feldspar-titanite veins are part of the same mineralizing event, then the data may be considered collectively, in which case a pooled concordia age for the two dated titanite samples yields 201.6 ± 0.6 Ma (mean square of weighted deviates [MSWD] = 1.16, probability = 0.28). However, we prefer the more conservative approach, and consider the age of the mineralizing event as some time(s) between the 2 σ error envelopes of 200.2–202.5 Ma.

Four single zircon fractions were analyzed from the ‘Mine Dyke’ sample. Error envelopes for the individual analyses mutually overlap on concordia. Together they providing a tight age determination of 102.85 ± 0.25 Ma, with a MSWD of 1.8 and probability of concordance of 0.18 (Figure 9). We recommend using a slightly more conservative best age of 103 ± 0.3 Ma.

$^{40}\text{Ar}/^{39}\text{Ar}$ AR COOLING AGE

The $^{40}\text{Ar}/^{39}\text{Ar}$ isotopic age determinations were obtained by the laser-induced step-heating technique. Details of the analytical techniques are presented in Logan et al. (2007). Gas measurements obtained during each of the heating steps are presented in Table 3. Consideration of the entire release spectrum produces a total release integrated age of 192.98 ± 0.95 Ma (Table 3), which is not geologically meaningful. Low-temperature steps should be rejected (Figure 10) because loosely bound argon has been partially lost. A resultant, robust plateau produced by the higher-temperature steps 8 through 14 represents 71.8% of the

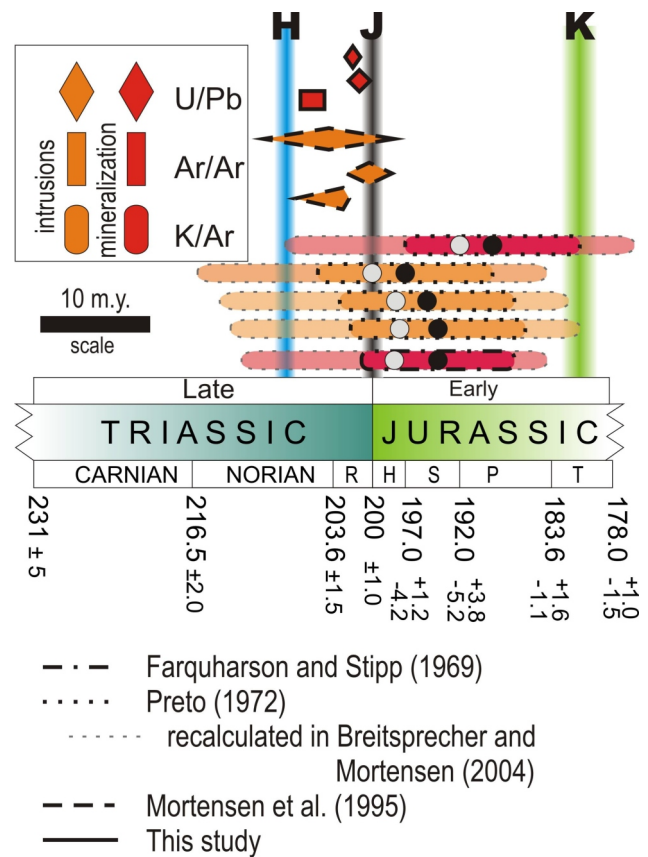


Figure 4. Geological timeline showing age determinations from the mineralizing system at Copper Mountain, south-central British Columbia. Triassic-Jurassic boundaries from time scales discussed in the text are H = Harland et al. (1982), J = Pálffy et al. (2000) and K = Kulp (1961). Abbreviations: H, Hettangian; P, Pliensbachian; R, Rhaetian; S, Sinemurian; T, Toarcian. Time scale is from Okulitch (2002), which incorporates the Jurassic time scale of Pálffy et al. (2000).

^{39}Ar released. This plateau provides the best interpreted age of 205.5 ± 1.1 Ma (1 σ , including J-error of 0.5%). The MSWD for this determination is 0.29, with a probability of 0.94. Initial $^{40}\text{Ar}/^{36}\text{Ar}$ is 277.6, lower than the atmospheric value of 295.5.

DISCUSSION OF AGE DETERMINATIONS

Extensive intrusion of the Copper Mountain area by the swarm of ‘Mine Dykes’ has reset the isotopic systems with low closure temperatures. For example, fission-track cooling ages for the Lost Horse Intrusions and dikes are reported by Christopher (1973) as ranging from 100 to 127 Ma (with uncertainties on the order of ± 25 Ma—see Figure 3 for specific examples). These dates reflect the annealing of apatite within the Late Triassic intrusions where they are intersected by the dike swarm. The U-Pb age reported herein, 102.9 ± 0.3 Ma, is the first crystallization age from the ‘Mine Dyke’ swarm, and is concordant with the fission track ages. It is identical, within error, to the age of the Verde Creek quartz monzonite, which is dated by K-Ar biotite as 100 ± 8 Ma and 102 ± 8 Ma (Breitsprecher and Mortensen, 2004; recalculated from Preto, 1972 as 98

± 4 Ma and 101 ± 4 Ma). The ‘Mine Dykes’, however, are observed to cut the Verde Creek pluton (Preto, 1972) and must, at least locally, be younger. Interestingly, the northerly trending dike swarm parallels the straight western margin of the 20 km long Verde Creek pluton, which is located immediately east of the area outlined by the southern half of Figure 2.

Isotopic age determination of mineralization at Copper Mountain has relied largely upon cooling ages or imprecise fission track techniques (Figures 3, 4). Although a robust U-Pb zircon age from the Copper Mountain stock yielded $202.7 +4.4/-0.5$ Ma, 200.3 ± 2.1 Ma and 204 ± 6 Ma (Figure 4; Mortensen et al., 1995), age determinations from mineralization have historically been by techniques susceptible to isotopic disturbance. This is particularly problematic in the mine area where extensive intrusion by the younger ‘Mine Dykes’ heated the surrounding country rocks. Such cooling ages include K-Ar biotite determinations on the Copper Mountain stock and mineralized veins



Figure 5. Light-coloured ‘Mine Dykes’ cutting dark, hydrothermally altered Nicola Group volcanic strata within Pit 3, Copper Mountain, south-central British Columbia. View is to the southeast. The location of sample MMI06-32-4 is just visible on the far pit wall (red arrow).

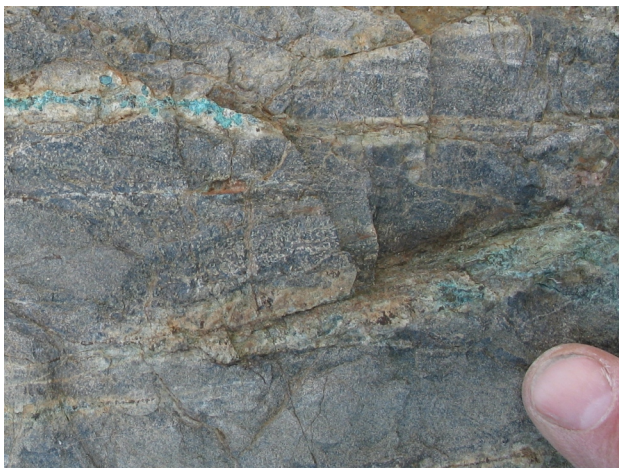


Figure 6. Pegmatitic mineralized K-feldspar veins containing copper carbonate–stained biotite–chalcopyrite–bornite–epidote–titanite, Copper Mountain, south-central British Columbia. The light-coloured halo is probably due to albite alteration.

that yielded a mean age of 193 ± 7 Ma (Sinclair and White, 1968), and those on the pegmatitic sulphide veins and Lost Horse and other intrusions that yielded a “mean age of 193.5 ± 8 Ma” (Preto, 1972). Consistency of these two datasets and the time scale calibration of the day (Kulp, 1961) placed the intrusions and mineralization within the

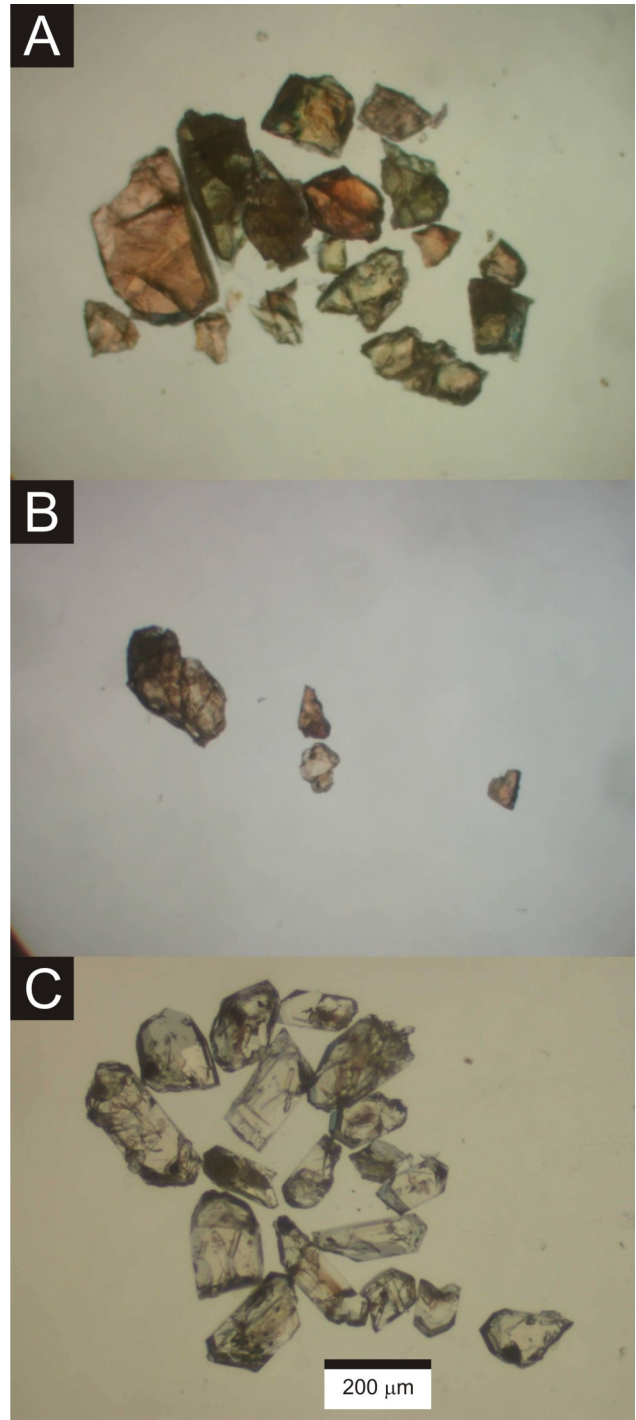


Figure 7. Titanite grains analyzed from samples from Copper Mountain, south-central British Columbia: **A)** titanite from sample MMI06-32-3; field of view is ~ 2 mm; **B)** titanite from sample MMI06-32-5; field of view is ~ 2 mm; **C)** zircon separate from sample MMI06-32-4 prior to abrasion (200 μ m scale bar).

Table 1. U-Pb thermal ionization mass spectrometry analytical data for titanite from mineralized veins in samples MMI06-32-3 and MMI06-32-5, Copper Mountain, south-central British Columbia.

Fraction ¹	Wt (mg)	U ² (ppm)	Pb ³ (ppm)	Pb ⁴		Pb ⁶ (pg)	Th/U ⁷	Isotopic ratios $\pm 1\sigma$, % ⁸			r ⁹	% ¹⁰ discordant ⁹	Apparent ages $\pm 2\sigma$, Ma ⁸		
				²⁰⁶ Pb/ ²⁰⁴ Pb	Pb*/Pb _c ⁵			²⁰⁶ Pb/ ²³⁸ U	²⁰⁷ Pb/ ²³⁵ U	²⁰⁷ Pb/ ²⁰⁶ Pb			²⁰⁶ Pb/ ²³⁸ U	²⁰⁷ Pb/ ²³⁵ U	²⁰⁷ Pb/ ²⁰⁶ Pb
MMI06-32-3															
T1	19	139.4	5.5	319.2	5.90	17.3	1.183	0.031843 \pm 0.20	0.221415 \pm 1.09	0.05043 \pm 1.01	0.4880	6.1	202.07 \pm 0.8	203.09 \pm 4.0	214.9 \pm 46.1/47.4
T2	26	58.4	2.3	234.1	4.24	13.7	1.196	0.031564 \pm 0.20	0.213294 \pm 1.75	0.049009 \pm 1.65	0.5322	-35.6	200.33 \pm 0.8	196.31 \pm 6.2	148.3 \pm 75.5/79.2
T3	13	75.7	3.1	189.7	3.48	11.2	1.341	0.0317 \pm 0.26	0.223142 \pm 2.54	0.051053 \pm 2.41	0.5546	17.6	201.18 \pm 1.0	204.52 \pm 9.4	243.2 \pm 107.4/115
MM06-32-5															
T1	66	80.6	7.6	137.7	5.58	88.3	7.449	0.03209 \pm 0.436	0.226608 \pm 1.50	0.051215 \pm 1.25	0.6762	19.0	203.62 \pm 1.8	207.39 \pm 5.6	250.5 \pm 56.4/58.4
T2	52	114.9	10.5	266.3	11.35	47.4	7.130	0.031856 \pm 0.176	0.217481 \pm 1.68	0.049514 \pm 1.60	0.5363	-17.6	202.15 \pm 0.7	199.81 \pm 6.1	172.3 \pm 72.9/76.3
T3	68	165.8	12.0	779.3	27.41	29.0	4.967	0.031746 \pm 0.092	0.220232 \pm 0.34	0.050314 \pm 0.29	0.6308	3.9	201.47 \pm 0.4	202.1 \pm 1.2	209.5 \pm 13.4/13.5
T4	84	60.0	5.7	201.3	8.52	54.3	7.450	0.031939 \pm 0.284	0.220755 \pm 1.10	0.050129 \pm 0.94	0.6451	-0.8	202.67 \pm 1.1	202.54 \pm 4.0	201 \pm 43.1/44.3

¹Fraction ID: T1, T2, etc. All analysed titanites were fragments taken from veins.²U blank correction of 0.2 pg \pm 20%; U fractionation corrections were measured for each run with a double ²³³⁻²³⁵U spike.³Radiogenic Pb; all raw Pb data corrected for fractionation of 0.23%/amu \pm 20% determined by repeated analysis of NBS-982 reference material.⁴Measured ratio corrected for spike and Pb fractionation.⁵Radiogenic Pb/common Pb, including ²⁰⁸Pb.⁶Total common Pb in analysis based on blank isotopic composition: ²⁰⁶Pb/²⁰⁴Pb = 18.5 \pm 3%, ²⁰⁷Pb/²⁰⁴Pb = 15.5 \pm 3%, ²⁰⁸Pb/²⁰⁴Pb = 36.4 \pm 0.5%.⁷Model Th/U derived from radiogenic ²⁰⁸Pb and the ²⁰⁷Pb/²⁰⁶Pb age of fraction.⁸Corrected for fractionation, blank (5 pg, based on procedural blanks) and common Pb, the latter with a composition based on Stacey-Kramers model Pb at 200 Ma (Stacey and Kramers, 1975).⁹Correlation coefficient.¹⁰Discordance in % to origin.**Table 2.** U-Pb thermal ionization mass spectrometry analytical data for zircon from the 'Mine Dyke' sample MMI06-32-4, Copper Mountain, south-central British Columbia.

Fraction ¹	Wt (mg)	U ² (ppm)	Pb ³ (ppm)	Pb ⁴		Pb ⁶ (pg)	Th/U ⁷	Isotopic ratios $\pm 1\sigma$, % ⁸			r ⁹	% ¹⁰ discordant ⁹	Apparent ages $\pm 2\sigma$, Ma ⁸		
				²⁰⁶ Pb/ ²⁰⁴ Pb	Pb*/Pb _c ⁵			²⁰⁶ Pb/ ²³⁸ U	²⁰⁷ Pb/ ²³⁵ U	²⁰⁷ Pb/ ²⁰⁶ Pb			²⁰⁶ Pb/ ²³⁸ U	²⁰⁷ Pb/ ²³⁵ U	²⁰⁷ Pb/ ²⁰⁶ Pb
MMI06-32-4															
A	16	217.46	3.6	832.6	13.4	4.2	0.467	0.016087 \pm 0.15	0.107795 \pm 0.61	0.0486 \pm 0.57	0.39466	20.1	102.88 \pm 0.3	103.95 \pm 1.2	128.6 \pm 26.6/27
B	14	126.93	2.1	541.5	8.6	3.4	0.447	0.016129 \pm 0.5	0.108037 \pm 1.2	0.04858 \pm 1.1	0.487005	19.3	103.15 \pm 1	104.17 \pm 2.4	127.6 \pm 49.3/50.9
C	5	386.9	6.5	261.2	4.1	7.9	0.552	0.01604 \pm 0.28	0.105135 \pm 1.4	0.047537 \pm 1.2	0.492711	-34.7	102.58 \pm 1	101.5 \pm 2.6	76.3 \pm 58.2/60.4
D	4	669.44	11.0	380.4	5.8	7.4	0.424	0.016103 \pm 0.2	0.10663 \pm 0.9	0.048024 \pm 0.8	0.448427	-2.5	102.98 \pm 0.5	102.88 \pm 1.8	100.5 \pm 39.1/40

¹All grains air abraded; all single grains processed and analysed, except where noted by number of grains after fraction ID.²U blank correction of 0.2 pg \pm 20%; U fractionation corrections were measured for each run with a double ²³³⁻²³⁵U spike.³Radiogenic Pb; all raw Pb data corrected for fractionation of 0.23%/amu \pm 20% determined by repeated analysis of NBS-982 reference material.⁴Measured ratio corrected for spike and Pb fractionation.⁵Radiogenic Pb/common Pb, including ²⁰⁸Pb.⁶Total common Pb in analysis based on blank isotopic composition: ²⁰⁶Pb/²⁰⁴Pb = 18.5 \pm 3%, ²⁰⁷Pb/²⁰⁴Pb = 15.5 \pm 3%, ²⁰⁸Pb/²⁰⁴Pb = 36.4 \pm 0.5%.⁷Model Th/U derived from radiogenic ²⁰⁸Pb and the ²⁰⁷Pb/²⁰⁶Pb age of fraction.⁸Fractionation, blank and common Pb corrected; Pb procedural blanks were \sim 2.0 pg and U $<$ 0.2 pg. Common Pb compositions are based on Stacey-Kramers model (Stacey and Kramers, 1975)

Pb at the interpreted age of the rock: MMI06-32-4 – 103 Ma.

⁹Correlation coefficient.¹⁰Discordance in % to origin.

Late Triassic period, which extended to 181 Ma (K on Figure 4). Both the mineralized veins and intrusions cut rocks that contain meagre but significant fossil collections yielding Late Triassic ages. Penecontemporaneous country rocks and intrusions seemed consistent with evidence for a near-surface intrusive environment. Such evidence includes porphyritic textures and breccia bodies indicative of low confining pressures (Preto, 1972). However, a time scale revision in 1982 (Harland et al., 1982; H on Figure 4) pushed the Triassic-Jurassic boundary back to 208 Ma, providing for a ~15 m.y. lag between deposition of arc strata and intrusion. A subsequent revision of the Jurassic time scale for the Canadian Cordillera (Pálffy et al., 2000; J on Figure 4), moderated the 1982 Triassic-Jurassic boundary revision, placing the new boundary at 200 ± 1.0 Ma. Fol-

lowing the time scale revision in 2000, the Copper Mountain story was: intrusion around 202 Ma, in the Late Triassic, followed by mineralization around 193 Ma, in the Early Jurassic. In light of typical durations for hypogene ore formation, which range from 0.01 to 0.1 m.y. for Cu±Mo±Au porphyry deposits worldwide (McInnis et al., 2005) the lag time of nearly 10 m.y. seemed unreasonable, and most

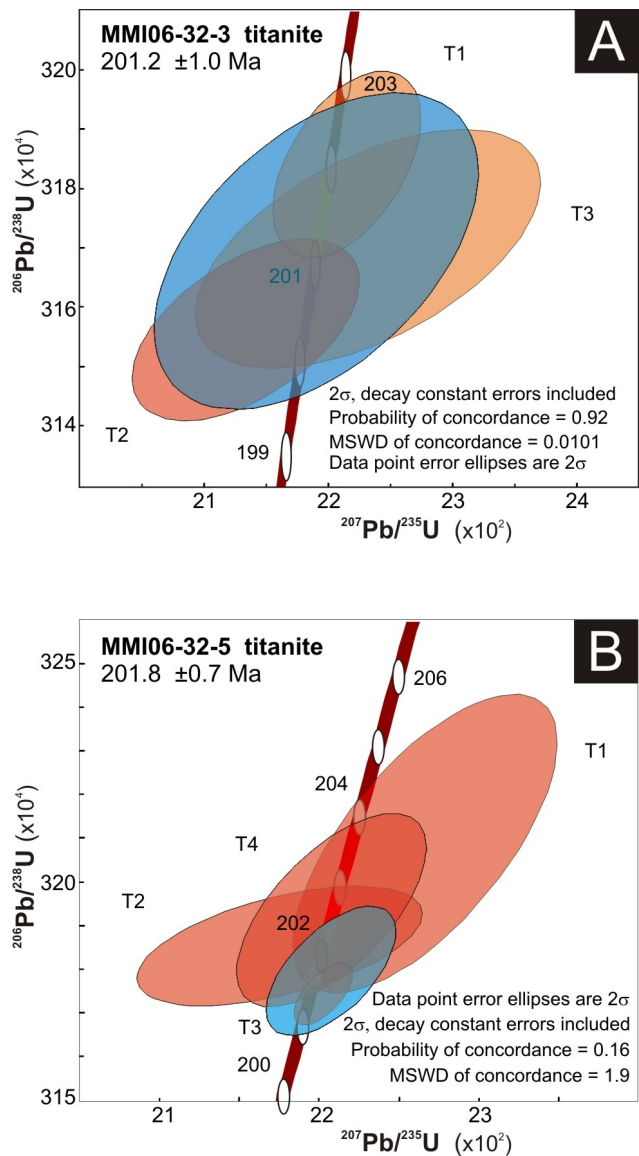


Figure 8. Concordia plots for U-Pb thermal ionization mass spectrometry data for samples from Copper Mountain, south-central British Columbia: **A)** sample MMI06-32-3; **B)** sample MMI06-32-5. 2 error ellipses for individual analytical fractions are red. Blue ellipses represent the best estimate concordia age of the sample. Concordia bands include 2 errors on U decay constants.

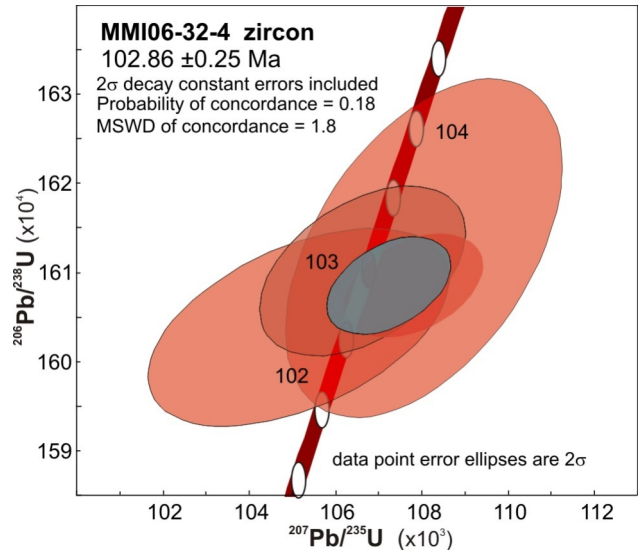


Figure 9. Concordia plot for U-Pb thermal ionization mass spectrometry data for the 'Mine Dyke' sample, MMI06-32-4, Copper Mountain, south-central British Columbia. 2 error ellipses for individual analytical fractions are in red. The blue ellipse represents the best estimate concordia age of the sample. Concordia bands include 2 errors on U decay constants.

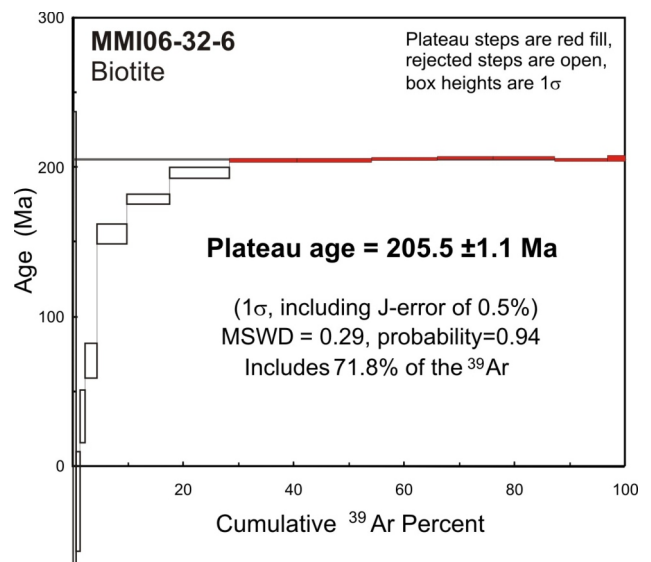


Figure 10. Step-heating Ar gas release spectra for euheedral biotite from sample MMI06-32-6, Big Lead, bornite-biotite ore, Copper Mountain, south-central British Columbia. Plateau steps are filled; rejected steps are open. Box heights at each step are 1σ. Rising low-temperature steps to the robust plateau at 205.5 ± 1.1 Ma indicate a deficit of loosely bound Ar.

Table 3. $^{40}\text{Ar}/^{39}\text{Ar}$ step heating gas release data from sample MMI06-32-6, a centimetre-thick slice of a sample of the Big Lead glory hole biotite-bornite mineralization, Copper Mountain, south-central British Columbia.

MMI06-32-6	Biotite										
Laser Power (%)	Isotope Ratios	$^{38}\text{Ar}/^{39}\text{Ar}$	$^{37}\text{Ar}/^{39}\text{Ar}$	$^{36}\text{Ar}/^{39}\text{Ar}$	Ca/K	Cl/K	% ^{40}Ar atm	f ^{39}Ar	$^{40}\text{Ar}^*/^{39}\text{ArK}$	Age (in Ma)	
2	363.182±0.012	0.344±0.046	0.085 ±0.076	1.308 ±0.022	0.961	0.018	103.47	0.2	-12.772 ±7.318	-255.28 ±157.12	
2.2	100.783± 0.008	0.224 0.026	0.065 ±0.059	0.354 ±0.019	1.58	0.033	101.28	0.92	-1.319 ±1.822	-24.76 ±34.42	
2.4	41.627 ±0.008	0.131 0.030	0.164 ±0.018	0.147 ±0.023	4.343	0.02	95.47	0.71	1.835 ±0.958	33.88 ±17.52	
2.73	40.243 ±0.005	0.115 0.018	0.027 ±0.053	0.127 ±0.018	0.623	0.018	90.23	2.1	3.880 ±0.664	70.91 ±11.90	
3.2	30.272 ±0.004	0.078 0.015	0.013 ±0.035	0.074 ±0.018	0.307	0.011	70.93	5.5	8.736 ±0.398	155.89 ±6.80	
3.4	21.238 ±0.004	0.059 0.015	0.007 ±0.044	0.039 ±0.017	0.176	0.009	52.04	7.67	10.114 ±0.201	179.29 ±3.39	
3.6	16.366 ±0.012	0.048 0.022	0.004 ±0.045	0.018 ±0.023	0.086	0.007	31.42	11.06	11.149 ±0.195	196.67 ±3.25	
3.8	13.820 ±0.004	0.041 0.013	0.002 ±0.058	0.008 ±0.026	0.044	0.006	15.33	12.27	11.622± 0.079	204.57 ±1.32	
3.9	13.110 ±0.006	0.038 0.013	0.002 ±0.054	0.005 ±0.025	0.033	0.005	10.64	13.46	11.637 ±0.078	204.81 ±1.30	
4	12.476 ±0.004	0.036 0.019	0.001 ±0.069	0.003 ±0.038	0.016	0.005	5.73	11.83	11.677 ±0.061	205.48 ±1.01	
4.1	12.338 ±0.004	0.036 0.023	0.002 ±0.087	0.003 ±0.046	0.017	0.005	4.32	10.07	11.713 ±0.065	206.08 ±1.08	
4.2	12.291 ±0.004	0.035 0.021	0.002 ±0.076	0.003 ±0.036	0.016	0.005	4.01	11.16	11.712 ±0.060	206.06 ±0.99	
4.2	12.233 ±0.004	0.035 0.017	0.002 ±0.060	0.003 ±0.048	0.01	0.005	4.02	9.56	11.648 ±0.063	204.99 ±1.05	
4.4	12.445 ±0.005	0.037 0.029	0.004 ±0.079	0.005 ±0.068	0.03	0.005	4.54	3.49	11.712 ±0.110	206.07 ±1.83	
Total/Average	16.998 ±0.001	0.046±0.003	0.064 ±0.001	0.020 ±0.003	0.117	0.011		100	11.669 ±0.028		

J-error = 0.010331 ±0.000010

Volume ^{39}ArK = 1157.55

Integrated Date = 192.98 ±0.95

Volumes are $1 \times 10^{-13} \text{cm}^3 \text{NPT}$

Neutron flux monitors: 28.02 Ma FCs (Renne et al., 1998)

Isotope production ratios: ($^{40}\text{Ar}/^{39}\text{ArK}$) = 0.0302 ±0.00006, ($^{37}\text{Ar}/^{39}\text{ArCa}$) = 1416.4 ±0.5, ($^{36}\text{Ar}/^{39}\text{ArCa}$) = 0.3952 ±0.0004, Ca/K=1.83 ±0.01($^{37}\text{ArCa}/^{39}\text{ArK}$).

likely attributable to the large errors of the age determinations from mineralization (Figure 4).

Our sampling of mineralization includes titanite-biotite-bearing veins in the margin of the Copper Mountain stock and those equidistant between the Copper Mountain stock and the body of Lost Horse Intrusions (Figure 3). In addition to this spatial variability, we have used two different techniques: U-Pb titanite and $^{40}\text{Ar}/^{39}\text{Ar}$ biotite dating with closure temperatures of 660–700°C (Scott and St-Onge, 1995) and 300–450°C (McDougall and Harrison, 1999), respectively. These techniques are more robust than the K-Ar biotite technique used in the past. Our results for the titanite-bearing veins, 201.2 ±1.0 Ma and 201.8 ±0.7 Ma, are identical, within error, to the crystallization ages reported by Mortensen et al. (1995). If there is any systematic difference in the ages of intrusion and mineralization, its measurement is beyond the resolution of the geochronometers available to us. This contemporaneity of intrusion and hypogene mineralization is consistent with the results of similarly robust datasets elsewhere within the Cordilleran belt of alkalic porphyry deposits (e.g., Iron Mask and Mt. Polley; Logan et al., 2007), and results from other porphyry systems globally (McInnis et al., 2005). Our new data provide a tight integration of the Copper Mountain deposit with the ca. 205–200 Ma alkalic Cu-Au porphyry event that stretches the length of the Canadian Cordillera.

ACKNOWLEDGMENTS

T. Ullrich conducted and interpreted the $^{40}\text{Ar}/^{39}\text{Ar}$ analyses. H. Lin carried out mineral separations and provided assistance with mass spectrometry; R. Lishansky assisted with grain selection, abrasion and in the clean lab. G. Nixon provided digital data from Geoscience Map 2004-3 to aid construction of Figures 2 and 3. Access to the pits at

Copper Mountain was granted by J. Cullen of Envirogreen Technologies Ltd. An earlier draft of this manuscript was reviewed by S. Rowins.

REFERENCES

- Ash, C.H., Reynolds, P.H., Creaser, R.A. and Mihalynuk, M.G. (2007): $^{40}\text{Ar}/^{39}\text{Ar}$ and Re-Os isotopic ages for hydrothermal alteration and related mineralization at the Highland Valley Cu-Mo deposit (NTS 0921), southwestern British Columbia, in *Geological Fieldwork 2006, BC Ministry of Energy, Mines and Petroleum Resources*, Paper 2007-1, pages 19–24.
- Barger, H. and Schurr, S. (1944): The mining industries, 1899–1939: a study of output, employment, and productivity; *The National Bureau of Economic Research*, Publication Number 43, 447 pages.
- BC Geological Survey (2009): MINFILE BC mineral deposits database; *BC Ministry of Energy, Mines and Petroleum Resources*, URL <<http://minfile.ca>> [December 2009].
- Breitsprecher, K. and Mortensen, J.K. (2004): BC Age 2004A-1: a data base of isotopic age determinations for rock units from British Columbia; *BC Ministry of Energy, Mines and Petroleum Resources*, Open File 2004-03.
- Brown, D.A., Gunning M.H. and Greig, C.J. (1996): The Stikine Project: geology of western Telegraph Creek map area, northwestern British Columbia (104G/5, 6, 11W, 12 and 13), *BC Ministry of Energy, Mines and Petroleum Resources*, Bulletin 95, 176 pages.
- Chance, A.V., Giroux, G.H., Holbek, P.M., Martin, T., Murray, D., O'Rourke, J.C., El Sabbagh, M. and Thompson, I.S. (2009): Technical report on the Copper Mountain Project, Princeton, British Columbia; *Copper Mountain Mining Corp.*
- Christopher, P.A. (1973): Application of K-Ar and fission track dating to the metallogeny of porphyry and related mineral deposits in the Canadian Cordillera; *Canadian Journal of Earth Sciences*, Volume 10, pages 846–851.

- Farquharson, R.B. and Stipp, J.J. (1969): Potassium-argon ages of dolerite plugs in the south Cariboo region, British Columbia; *Canadian Journal of Earth Sciences*, Volume 6, pages 1468–1470.
- Harland, W.B., Cox, A.V., Llewellyn, P.G., Pickton, C.A.G., Smith, A.G. and Walters, R. (1982): *A Geological Time Scale 1982*; Cambridge University Press, Cambridge, 131 pages.
- Holbek, P. (2007): Titan 24 Deep Earth Imaging identifies large target areas; *Copper Mountain Mining Corporation*, press release, December 4, 2007, URL <http://www.cumtn.com/sitemanager/_pdf_news/0701204_CMMC_News_Release.pdf> [December 2009].
- Holbek, P. (2009): Copper Mountain 2008 exploration drill program final results; *Copper Mountain Mining Corporation*, press release, January 21, 2009, URL <http://www.cumtn.com/sitemanager/_pdf_news/080121_CMMC_explore_results_release.pdf> [December 2009].
- Kulp, J.L. (1961): Geologic time scale; *Science*, Volume 133, Number 3459, pages 1105–1114.
- Logan J.M and Bath, A.B. (2006): Geochemistry of Nicola Group basalt from the central Quesnel Trough at the latitude of Mount Polley (NTS 093A/5, 6, 11, 12), central BC; in *Geological Fieldwork 2005*, BC Ministry of Energy, Mines and Petroleum Resources, Paper 2006-1, pages 83–98.
- Logan J.M. and Koyanagi V.M. (1994): Geology and mineral deposits of the Galore Creek area (104G/3, 4); BC Ministry of Energy, Mines and Petroleum Resources, Bulletin 92, 96 pages.
- Logan, J.M. and Mihalynuk, M.G. (2005a): Porphyry Cu-Au deposits of the Iron Mask batholith, southeastern BC; in *Geological Fieldwork 2004*, BC Ministry of Energy, Mines and Petroleum Resources, Paper 2005-1, pages 271–290.
- Logan, J.M. and Mihalynuk, M.G. (2005b): Regional geology and setting of the Cariboo, Bell, Springer and northeast porphyry Cu-Au zones at Mount Polley, south-central British Columbia; in *Geological Fieldwork 2004*, BC Ministry of Energy, Mines and Petroleum Resources, Paper 2005-1, pages 249–270.
- Logan, J.M., Mihalynuk, M.G., Ullrich, T. and Friedman, R.M. (2007): U-Pb ages of intrusive rocks and $^{40}\text{Ar}/^{39}\text{Ar}$ plateau ages of copper-gold-silver mineralization associated with alkaline intrusive centres at Mount Polley and the Iron Mask batholith, southern and central British Columbia; in *Geological Fieldwork 2006*, BC Ministry of Energy, Mines and Petroleum Resources, Paper 2007-1, pages 93–116.
- Massey, N.W.D., MacIntyre, D.G., Desjardins, P.J. and Cooney, R.T. (2005): Digital geology map of British Columbia: whole province; BC Ministry of Energy, Mines and Petroleum Resources, GeoFile 2005-1, scale 1:250 000, URL <<http://www.empr.gov.bc.ca/Mining/Geoscience/PublicationsCatalogue/GeoFiles/Pages/2005-1.aspx>> [December 2009].
- McDougall I. and Harrison, T.M. (1999): *Geochronology and thermochronology by the $^{40}\text{Ar}/^{39}\text{Ar}$ method*, 2nd Edition; Oxford University Press, New York, 269 pages.
- McInnes, B.I.A., Evans, N.J., Fu, F.Q., Garwin, S., Belousova, E., Griffin, W.L., Bertens, A., Sukarna, D., Permadewi, S., Andrew, R.L. and Deckart, K. (2005): Thermal history analysis of selected Chilean, Indonesian and Iranian porphyry Cu-Mo-Au deposits; in *Super Porphyry Copper and Gold Deposits—A Global Perspective*, Porter, T.M., Editor, PGC Publishing, Adelaide, Volume 1, pages 27–42.
- Mihalynuk, M.G. (1999): Geology and mineral resources of the Tagish Lake area, northwestern British Columbia (NTS 104M/8, 9, 10E, 15, 104N/12W); BC Ministry of Energy, Mines and Petroleum Resources, Bulletin 105, 217 pages.
- Mortensen, J.K., Ghosh, D.K. and Ferri, F. (1995): U-Pb geochronology of intrusive rocks associated with copper-gold porphyry deposits in the Canadian Cordillera; in *Porphyry Deposits of the Northwestern Cordillera of North America*, Canadian Institute of Mining, Metallurgy and Petroleum, Special Volume 46, pages 142–158.
- New Gold Inc. (2007): New Afton feasibility study indicates potential to develop one of Canada's largest underground metals mine and one of its lowest cost gold producers; *New Gold Inc.*, press release, April 2, 2007, URL <<http://www.newgoldinc.com/MediaCentre/NewGoldNews/PressReleaseDetail/2007/NewAftonFeasibilityStudyIndicatesPotentialtoDeveloponeofCanada039sLargestUndergroundMetalsMineandoneofitsLowestCostGoldProducers/default.aspx>> [December 2009].
- Nixon, G.T., Archibald, D.A. and Heaman, L.M. (1993): $^{40}\text{Ar}/^{39}\text{Ar}$ and U-Pb geochronometry of the Polaris Alaskan-type complex, British Columbia: precise timing of Quesnelia–North America interaction; *Geological Association of Canada–Mineralogical Association of Canada*, Joint Annual Meeting, Program with Abstracts, page 76.
- Okulitch, A.V. (2002): Geological time chart, 2002; *Geological Survey of Canada*, Open File 3040.
- O'Rourke, J. (2009): 2008 drilling significantly increased resource and produces improved mine plan and agreements with Mitsubishi Materials Corporation progressing; *Copper Mountain Mining Corporation*, press release, April 16, 2009, URL <http://www.cumtn.com/sitemanager/_pdf_news/090416_CMMC_PR.pdf> [December 2009].
- Pálffy, J., Smith, P.L. and Mortensen, J.K. (2000): A U-Pb and $^{40}\text{Ar}/^{39}\text{Ar}$ time scale for the Jurassic; *Canadian Journal of Earth Sciences*, Volume 37, pages 923–944.
- Pollard, P.J., Taylor, R.G. and Peters, L. (2005): Ages of intrusion, alteration, and mineralization at the Grasberg Cu-Au deposit, Papua, Indonesia; in *A Special Issue Devoted to Giant Porphyry-Related Mineral Deposits*, *Economic Geology and the Bulletin of the Society of Economic Geologists*, Volume 100, Number 5, pages 1005–1020.
- Preto, V. (1972): Geology of Copper Mountain, British Columbia; BC Ministry of Energy, Mines and Petroleum Resources, Bulletin 59, 87 pages.
- Preto, V.A. (1979): Geology of the Nicola Group between Merritt and Princeton, British Columbia; BC Ministry of Energy, Mines and Petroleum Resources, Bulletin 69, 90 pages.
- Preto, V.A., Nixon, G.T. and Macdonald, E.A.M. (2004): Alkaline Cu-Au porphyry systems in British Columbia: Copper Mountain; BC Ministry of Energy, Mines and Petroleum Resources, Geoscience Map 2004-3.
- Renne, P.R., Swisher, C.C., Deino, A.L., Karner, D.B., Owens, T.L. and DePaolo, D.L. (1998): Intercalibration of standards, absolute ages and uncertainties in $^{40}\text{Ar}/^{39}\text{Ar}$ dating; *Chemical Geology*, Volume 145, pages 117–152.
- Scott, D.J. and St-Onge, M.R. (1995): Constraints on Pb closure temperature in titanite based on rocks from the Ungava orogen, Canada: implications for U-Pb geochronology and P-T-t path determinations; *Geology*, Volume 23, Number 12, pages 1123–1126.
- Sinclair, A.J. and White, W.H. (1968): Age of mineralization and post-ore hydrothermal alteration at Copper Mountain, BC; *Canadian Institute of Mining, Metallurgy and Petroleum Bulletin*, Volume 61, Number 673, pages 633–636.
- Stacey, J.S. and Kramers, J.D. (1975): Approximation of terrestrial lead isotope evolution by a two-stage model; *Earth and Planetary Science Letters*, Volume 26, pages 207–221.

British Columbia's Property File: Project Update and a Case Study of an Integrated MapPlace Analysis of a Target Hidden in the Files

by K.D. Hancock and N.D. Barlow¹

KEYWORDS: Property File, database, mineral occurrence, MINFILE, integrated research, exploration target, MapPlace, QUEST Project, geochemistry, RGS, catchment basins

INTRODUCTION

The British Columbia Geological Survey (BCGS) is the provincial agency responsible for the mineral resources of the province of BC. As part of its overall mandate, the BCGS has developed the MapPlace website as its primary research and information source. MapPlace comprises numerous integrated databases and applications related to the geology and mineral resources of the province. Property File is one part of this system.

The BCGS Property File is an extensive collection of mineral development documents from throughout the province. Documents within the collection date back to 1852 and are often the only extant copies of the items. The documents have been collected primarily by BCGS staff, but also come from industry donations. Within the files, there is much original information that is not available elsewhere. Until 2009, this information was only accessible in hard copy at the Ministry's library in Victoria. The Property File project was initiated in 2005 to index and make the documents available online. In 2008, the first group of files, comprising approximately 3400 documents, was posted to the web.

Further work on Property File documents in 2009 by Purple Rock Editing, as part of the Geoscience BC QUEST project, added a significant number of documents to the website. During the course of document cataloguing, a number of previously unrecorded mineral occurrences were catalogued and several anomalous locations were identified. This report uses one of the anomalous locations to develop a case study for the use of MapPlace to generate an exploration target based on the Property File information.

REVIEW OF THE PROPERTY FILE DATABASE AND APPLICATION

History

It became apparent to BCGS staff that it was difficult to deal with mineral occurrence related information that did not fit with the other, more standardized files/databases like MINFILE or the Assessment Report Indexing System (ARIS). The BCGS staff recognized the relative importance of the information but needed a repository for it. Thus, Property File was born as an adjunct to the Ministry's library. The information was collected and stored on an ad hoc basis and there was no standardization of what was collected. Nonetheless, the information contained was and is still useful. With the advent of MINFILE, the collected documents were generally sorted and stored by MINFILE number with a catch-all designation of a general file associated with each 1:250 000 map sheet. These documents became the classic (or library) collection used extensively by generations of mineral industry clients.

Over the years, as files were added to Property File, two issues became apparent. The first was that this information was located only in Victoria. Industry and other clients had to travel to Victoria to view the materials. Second, over the years, items went missing and thus were lost from the public domain. As many of the documents are now the only extant copies, the BCGS recognized that there needed to be a better way to store and retrieve the files to increase their accessibility and security.

In 2005, the BCGS began designing a web-based system to store, retrieve and display the information contained in Property File. Associated with this was a recognition that the system could leverage off the already powerful and well-used MINFILE database and eventually be integrated into MapPlace. The design and build of the system began in 2007 and the initial roll-out started in 2008. To date there are over 9000 individual documents available online with approximately 20 000 more scanned, indexed and in the process of being added to the database.

The documents are scanned at high resolution and quality checked to ensure all information in the original document is visible in the scanned copy. All documents are then available to the public as Adobe Acrobat® PDFs, which are downloadable free of charge. The scanned documents are available as black and white, greyscale or full colour as dictated by the original. Also, on all maps and map-like documents larger than 11 by 17 in., a digital reference scale has been inserted so that scales can be checked for printing or plotting purposes and for those without included scales, it can be calculated back from reference points on the ground. The scanning contractor developed a unique method to digitally insert the map reference. These

¹ Purple Rock Editing, Victoria, BC

This publication is also available, free of charge, as colour digital files in Adobe Acrobat® PDF format from the BC Ministry of Energy, Mines and Petroleum Resources website at <http://www.empr.gov.bc.ca/Mining/Geoscience/PublicationsCatalogue/Fieldwork/Pages/default.aspx>.

requirements and innovations have increased the utility of the digital documents over their hard-copy originals.

Sources of Information

The primary sources for the documents are BCGS staff, who collect the items in the course of their work. Other major sources include donations from exploration companies, prospectors and other individuals. Other major inputs have come from companies that closed or downsized exploration offices in BC, such as Falconbridge Limited, Chevron Corporation (Chevron), Cyprus-Anvil Mining Corporation, Placer Dome Inc., Rimfire Minerals Corp. and Inmet Mining Corporation. Other significant collections have come from individuals and include: all the Prospector's Assistance Program reports, 1994–2001; Western Exploration Co. Ltd. (Charles Starr file); Tom Kirk's J & L file; Ken Dawson; Dennis Gorc; and the Cam Stephens family bequest. The total number of documents in Property File in its entirety is estimated at 100 000, with about two-thirds currently having limited to no indexing. The balance is either posted to the web, is ready for posting or is in progress. The BCGS is receiving donations on an ongoing basis and welcomes documents for inclusion in Property File. Information on donations is on the Property File home page at <http://www.empr.gov.bc.ca/Mining/Geoscience/PropertyFile/Pages/default.aspx>.

Types of Documents in Property File

Twenty-four types of documents are catalogued in Property File. They include reports, letters, notes, field notes, memos, maps of all kinds, mine plans, securities documents, photos, thin sections and other items. These documents are items in the public domain and are available for general use. Other items in Property File are subject to copyright regulations, including news clippings, theses, excerpts from journals and special publications. Work is progressing on getting the copyright issues solved and having these items posted.

Property File Search Function

Primary access to the Property File is through the search tool that is available at <http://propertyfile.gov.bc.ca/>. All items are coded with MINFILE references and this is probably the most powerful search field (Figure 1). Items that refer to a large area are typically coded by an NTS 1:250 000 map sheet general reference (e.g., 093K GEN), which was specially developed for this project. Author/title indexing, document date, type and collection name can also be used to filter the searches.

The search results page is presented in tabular format and includes the MINFILE number, document title, collection name and the document file size. Clicking on the document title takes the client to the metadata page for the document and includes a link to the PDF document. Clicking on the document file size links the client directly to the PDF document. Clicking on any of the headers sorts the results in ascending order of that header.

Integration with MINFILE

Property File is also cross-linked with MINFILE. The linking process is ongoing and at the time of writing, several hundred MINFILE occurrences are cross-linked. In those that are linked, the 'EMPR PF' coded reference listings in the MINFILE bibliography are linked to the metadata pages for specific documents in Property File. This works in a similar manner as the ARIS assessment report links in MINFILE.

CASE STUDY OF HIDDEN TARGETS IN PROPERTY FILE AND INTEGRATION WITH MAPPLACE ANALYSIS

Roundtop Mountain/Black Stuart Mountain Target, NTS 093A/14

Property File contains a plethora of documents, largely produced by exploration geoscientists. In the course of processing the documents, contract geologists noted that there

Property File Document Search

The screenshot shows a search interface for the Property File. At the top, there is a header with the text 'PROPERTY FILE'. Below this is a search form with two columns of input fields. The left column contains: 'Collection:' with a dropdown menu set to 'All'; 'MINFILE No.:', 'Document No.:', 'Project:', 'Title:', 'Author:', and 'Document Type:' with a dropdown menu. The right column contains: 'Map Sheet:', 'Date From:' and 'To:' with date pickers, 'Area:', and 'Keywords:'. Below the search fields is a 'Search' button. At the bottom right of the page, there is a link for 'Property File Home Page'.

Figure 1. British Columbia's Property File search page as viewed on the website (<http://propertyfile.gov.bc.ca/>).

were many projects that were not related to any MINFILE occurrences. Also, some projects were at a reconnaissance level and interesting targets were apparently never followed up. This case study highlights one of these finds and includes an integrated review using MapPlace to evaluate a potential exploration target.

Research by Barlow et al. (2010) as part of the QUEST project examined 2619 documents in Property File that relate to areas within the QUEST and QUEST-West areas. These documents were catalogued, scanned and posted to the Property File website. In the course of the work, numerous regional documents were processed. Upon the examination of the documents during processing, a number of interesting items were identified. One set of these came from the Chevron collection and was part of a regional stream-sediment sampling program called the Cordilleran Sediments Program (Dillon, 1980). Two regions were examined as part of the project: Quesnel Lake–Barkerville and Chetwynd. This project was designed to find base-metal targets with the following elements analyzed: Cu, Pb, Zn, Ag, Au, As, Ba, Fe, Mn, Mo and V. The summary report was prepared by Dillon (1980) and is Property File document number 840311. The reconnaissance geochemical survey in NTS map area 093A/14 is Property File document number 840322 and the detailed follow-up map is Property File document number 840327 (Figure 2).

The initial phase of the Cordilleran Sediments Program sampled a widespread number of creeks in the Barkerville to Quesnel Lake region. Ninety-three sites were sampled in the NTS 093A/14 map area. Initially, samples were collected for heavy-mineral concentrate analysis. From these, several anomalous-element value groups were identified, including two in the Roundtop and Black Stuart mountain areas. Significant anomalous values included >500 ppm Pb, >500 ppm Zn and >3.5 ppm Ag. Maximum values were 2540 ppm Pb, 2080 ppm Zn and 6.2 ppm Ag.

Follow-up sampling focused on adjacent creeks, with 206 additional sites, and the silt-sized fraction of the samples were analyzed (Figure 2). For this aspect of the project, only Cu, Pb, Zn, Ag and Ba were examined. In this case, similar element values were detected. However, significantly higher values were returned from Nolaka Creek, east of Roundtop Mountain; an unnamed creek due west of Black Stuart Mountain; and Kimball Creek, northeast of Black Stuart Mountain. In Nolaka Creek, Pb values ranged from 21 to 113 ppm and Zn values ranged from 63 to 2615 ppm with eight samples at the head of the creek ranging from 525 to 2615 ppm Zn. The highest values for both elements are clustered together at the head of the creek. On Kimball Creek, the detailed sampling revealed a cluster of 14 Zn values with a range from 575 to 3080 ppm. Lead values were elevated slightly above background in the same area. On the unnamed creek, nine samples extending from top to bottom ranged from 530 to 2620 ppm Zn. Five samples, all from the head of the creek adjacent to the peak of Black Stuart Mountain, were in excess of 1500 ppm Zn. Dillon (1980) recognized the significance of the sampling results and commented on it in his report.

Integrated MapPlace Analysis

The following is an example of how MapPlace can provide an analysis to supplement the information contained in Property File. As MapPlace information is spatially defined, the map-based interface can provide a visual superimposition of multiple datasets and increase the utility of individual datasets and applications such as MINFILE, ARIS, Mineral Titles Online, regional geology and base-map data.

Base-map information on MapPlace shows the region is rugged and mountainous. Slopes are steep with generally narrow valleys. There are numerous streams within a net-

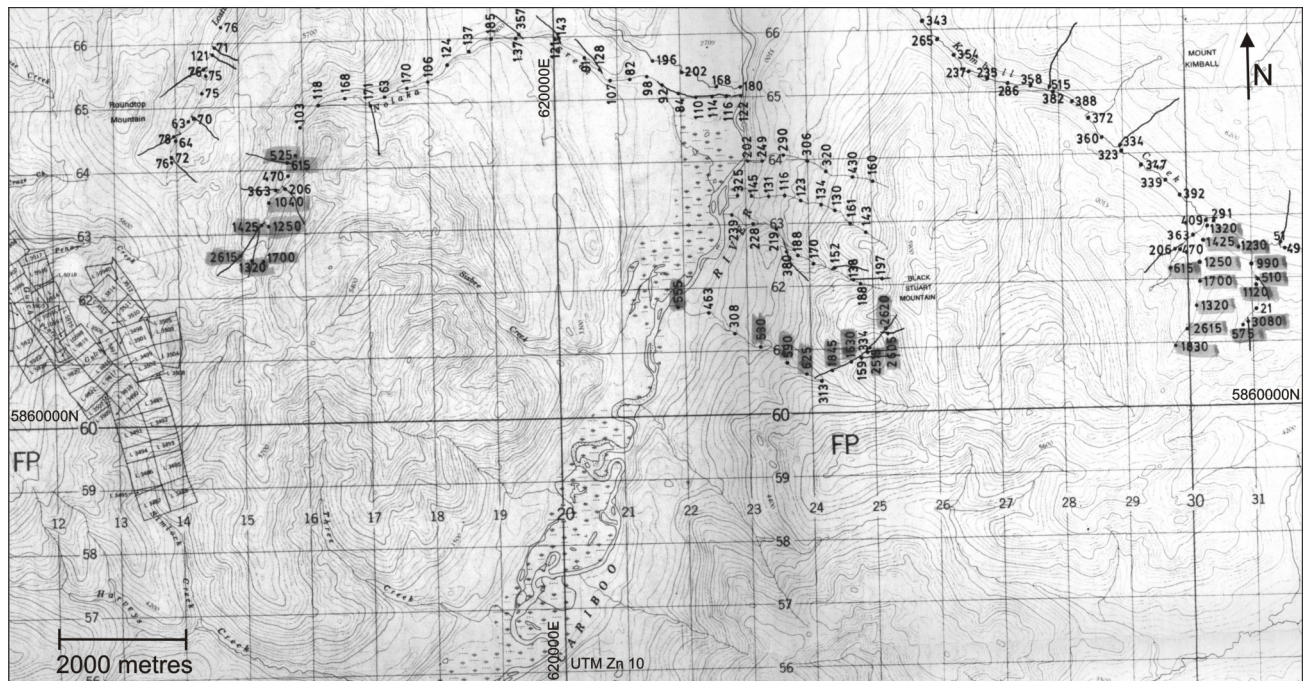


Figure 2. Image clip from the detailed follow-up sampling program map by Dillon (1980), Cariboo Lake, British Columbia. The numeric values are Zn concentrations in ppm. Shading of anomalous values reflects the original highlighting on the map.

values is associated with the one known mineral occurrence generated from the original geochemical survey and is discussed below.

Mineral exploration work in the area has largely been focused on placer gold of the Cariboo/Barkerville mining camp and associated hard-rock gold veins. This is shown by the significant number of known metallic mineral occurrences in MINFILE that are located primarily along Cunningham Creek west of Roundtop Mountain and down to the Cariboo River. At the top of Roundtop Mountain, there are two industrial minerals occurrences, one of quartzite and the other of limestone. Between Roundtop and Black Stuart mountains there are no mineral occurrences recorded. This is the area that hosts the stream samples with elevated Zn, Pb and Ag concentrations, according to Dillon (1980).

Mineral assessment reports (housed in the ARIS database) follow the same pattern as the MINFILE occurrences. Reports along Cunningham Creek in the vicinity of Roundtop Mountain range in age from 1976 to 2009. The majority of work has been on both the placer and hard-rock gold occurrences. It is noteworthy that there have been minor amounts of work on Pb-Zn veins/open space fillings and several W showings in the area. Again, however, there has been no recorded work east of Roundtop Mountain. The one exception has been some work on Zn-Pb showings east of Black Stuart Mountain and is associated with some of the results identified by Dillon (1980).

The acquisition of mineral titles has also focused largely on the Cunningham Creek corridor. At the time of writing, most of the ground was staked. Analysis with the Mineral Titles tool in the Exploration Assistant map, however, shows that several large blocks of claims have a common owner and have an anniversary date of early 2010.

Other related research indicates that the original staking was part of an area play to the northwest and so the tenure may not be related to local mineralization. Also, when the work by contract geologists originally identified the Property File information above, a significant part of the Roundtop–Black Stuart mountain area was open ground. At the time of writing, this area had been staked. This may be a reflection of the active and dynamic exploration situation in the region.

East of Black Stuart Mountain is a single mineral occurrence that was discovered and developed in association with Dillon’s survey work. The occurrence is named the Comin’ Thru Bear showing (MINFILE 093A 148). Teck Explorations Ltd. performed a geochemical survey, geological mapping and diamond drilling program on the property in 1981 (Assessment Report 9819; Luvang and Reed, 1981). Lead-zinc mineralization was identified in several locations, which were trenched and subsequently some sites were drilled. Geological mapping by Greenwood (1981) identified the mineralization as diagenetic Pb-Zn mineralization in open spaces within chert-carbonate of the Mural Formation. This stratigraphic designation is inconsistent with the later, revised stratigraphy of Struik (1988) and more closely resembles his chert-carbonate unit assigned to the Black Stuart Group. Mapping, trenching and drilling did not find any economic mineralization but Greenwood (1981) concluded that there was potential for more to be found elsewhere within the Mural Formation.

SUMMARY OF THE CASE STUDY AND INTEGRATED ANALYSIS

This case study is based on a set of documents from Property File. The information was recognized as signifi-

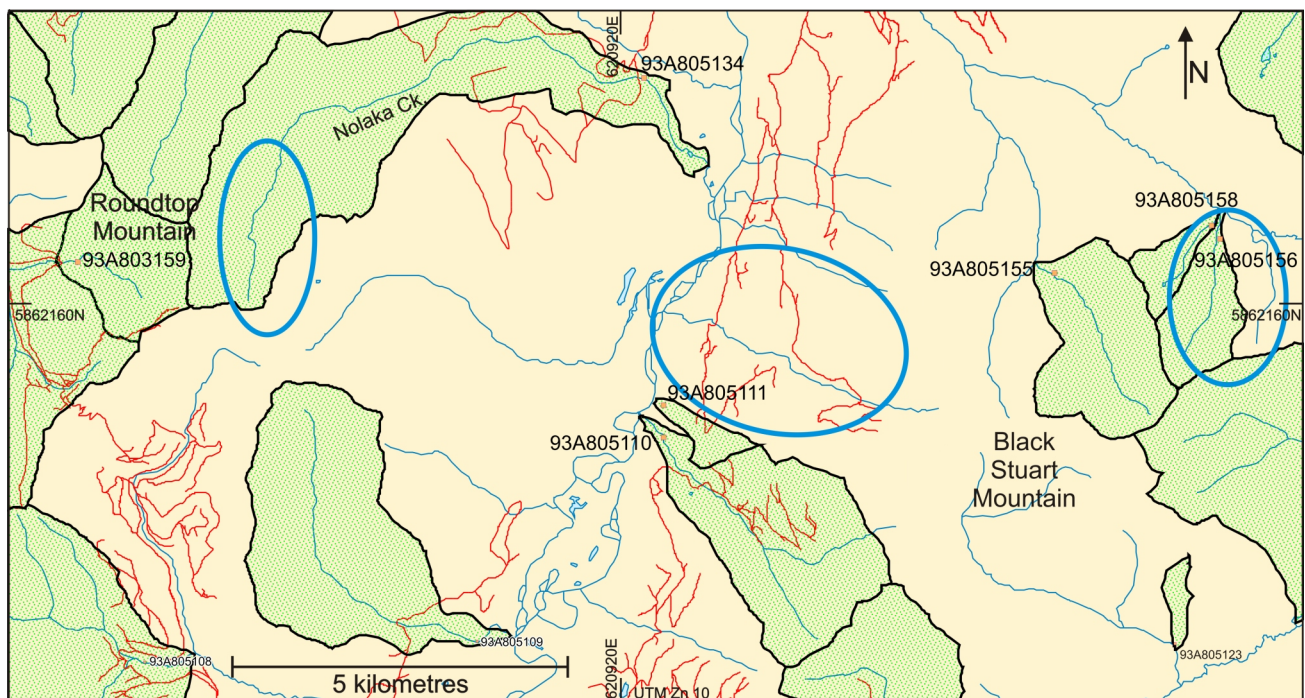


Figure 4. Area of interest, Cariboo Lake, British Columbia, with the Catchment Basins in green shading and the RGS sample locations labelled with a Master Identification number. Blue ellipses show the outline of where the anomalous Zn values from Dillon (1980) are grouped. Image outline is the same as the previous maps.

cant but had limited context. By using MapPlace, multiple datasets could be quickly reviewed and examined to evaluate the context of the original document. MapPlace provided access to several specific mineral-related datasets including MINFILE, ARIS, Mineral Titles Online, BCGS geology, airphotos and base mapping. By superimposing the different datasets, a comprehensive review could be developed. As this information is all web-based and free to use, the review could be done anywhere by anyone with Internet access.

The review of the available information allowed known mineralization and its characteristics to be identified. From there, the review identified a general region between Roundtop Mountain and Black Stuart Mountain that hosts prospective geology for Pb-Zn mineralization. The tenure situation in the region is fluid and there exists potential for areas to become free for staking on an ongoing basis. Should that not be the case, either an existing tenure holder or an outside operator could establish a business agreement with the title holder (e.g., a property option) and could follow-up on this kind of research. The ultimate value of Property File information is its record of work, which can provide a basis for future mineral development work.

ACKNOWLEDGMENTS

The authors wish to recognize the considerable input of work into the Property File project by K. Flower, S. Sweeney, G. Robinson and J. Barlow. L. Groseth of Camirage Imaging Services and J. Weger of Docupointe Services provided high-quality scanning services with often delicate, archival documents. Retired Director of the Resource Information Section, BCGS, G. McArthur provided the ini-

tial concept and impetus for the project. The authors thank all the companies and individuals that have contributed material to the Property File. Also, R. Booth, of the BC Ministry of Energy, Mines and Petroleum Resources, Health and Safety Branch, kindly supplied over 3000 scans of mine plans for the database's Mine Plans collection. L. Jones and T. Demchuk provided peer reviews of this paper.

REFERENCES

- Barlow, N.D., Flower, K.E., Sweeney, S.B., Robinson, G.L. and Barlow, J.R. (2010): QUEST and QUEST-West Property File: analysis and integration of Property File's Industry File documents with British Columbia's MINFILE (NTS 093, 094A, B, C, D, 1031); in *Geoscience BC Summary of Activities 2009, Geoscience BC, Report 2010-1*, pages 175–188.
- Dillon, E.P. (1980): Cordilleran sediments, geochemical stream sediment program, Quesnel Lake–Barkerville area; *Gulf Minerals Canada Limited*, unpublished report, BC Ministry of Energy, Mines and Petroleum Resources Property File, document number 840311, 55 pages, URL <<http://propertyfile.gov.bc.ca/searchresult.aspx?mn=&tt=&dn=840311&ar=&fd=&td=&kw=&cl=&nt=&pj=&dt=&aa>> [December 2009].
- Greenwood, H.J. (1981): Geology of the Teck Corporation prospect “Comin’ Thru Bear”; in *Assessment Report 9819, BC Ministry of Energy, Mines and Petroleum Resources*, pages 3–19.
- Luvang, G. and Reed, A.J. (1981): Assessment Report on the Comin’ Thru Bear property; *BC Ministry of Energy, Mines and Petroleum Resources*, Assessment Report 9819, 81 pages.
- Struik, L.C. (1988): Structural geology of the Cariboo Gold Mining District, east-central British Columbia; *Geological Survey of Canada*, Memoir 421, 100 pages plus maps.

Preliminary Review of the Effect of Analytical Method Variability on Regional Geochemical Survey Data, British Columbia

by R.E. Lett and W. Jackaman¹

KEYWORDS: geochemistry, regional geochemical surveys, aqua-regia digestion, inductively coupled plasma-mass spectrometry analysis

INTRODUCTION

Regional geochemical drainage sediment data is commonly levelled before contouring to compensate for spatial and temporal variations that can be introduced by using different sample media and analytical methods. Linear 'edge effects' in the form of a visible 'step' along the common boundary between two adjacent survey maps are often revealed in large-scale contoured regional geochemical maps and can reflect merging of source data from separate surveys, each carried out at different times. The British Columbia regional geochemical survey (RGS) is an example of a large database populated by stream, lake-bottom and moss-mat sediment sample geochemistry data from over 50 individual surveys carried out since 1976, using several laboratories and analytical methods (Lett, 2005). As part of the Canada-wide National Geochemical Reconnaissance (NGR) program, the BC RGS has been carried out to conform to sample collection, quality control, sample preparation and sample analysis standards that were established by the Geological Survey of Canada (Garrett, 1974).

The protocol for analysis of the -80 mesh size (<0.177 mm) drainage sediment fraction to determine a range of geochemical pathfinder elements (e.g., As, Cu, Pb, Mo, Hg, Zn) is historically an aqua-regia (HCl-HNO₃) digestion followed by atomic absorption spectrophotometry (AAS) or, more recently, inductively coupled plasma-mass spectrometry (ICP-MS). Ideally, analyses produced by this protocol should be comparable from survey to survey allowing for variations due to routine sampling and analytical errors. In practice, however, subtle differences in the analytical method, especially the conditions of the digestion techniques used, introduce an additional variable into element determinations. Past studies have examined the geochemical effects of analyzing regional drainage sediment samples for elements with different methods. For example, Day et al. (1988) compared Ag, As, Cd, Co, Cu, Fe, Mo, Mn, Pb, Sb and Zn values of sediment samples determined using a Lefort aqua-regia (3HNO₃:HCl) digestion followed by AAS with values for the same elements determined by Lefort aqua-regia digestion followed by inductively cou-

pled plasma-emission spectrometry (ICP-ES). They found that there were statistically different concentrations for all of the elements, except Co, determined by the two methods.

This paper will illustrate three situations common to established regional geochemical survey programs that may introduce analytical variability. The first example compares element data from regional geochemical survey sample analyses. Initially, the samples were analyzed with aqua-regia digestion followed by AAS and later the archived sediment samples were reanalyzed with a HCl-HNO₃-H₂O digestion followed by ICP-MS. The second example briefly comments on a comparison of results for a control reference standard analyzed by aqua-regia digestion followed by ICP-MS at a single laboratory for two analytical projects completed in different years. The final example summarizes the results of analyzing Canada Centre for Mineral and Energy Technology (CANMET) reference materials by an aqua-regia digestion followed by ICP-MS at different laboratories for a range of elements commonly reported from regional drainage surveys. It is emphasized that for all three examples, the analytical results and discussions reported in this paper are very preliminary. They are intended to illustrate that these types of data complexity are inherent to the design and structure of RGS programs that have been conducted over many years.

METHODS COMPARISON: REANALYSIS OF RGS SAMPLES FROM NTS MAP AREA 093J

During 1985, stream sediment and water samples were collected from 1088 sites at an average density of one sample per 13 km² throughout the 14 770 km² of NTS map area 093J (McLeod Lake; Figure 1), central BC. The air-dried sediment samples were sieved through a -80 mesh (<0.177 mm) and ball milled. A total of 1152 sediment samples, duplicate samples and standard reference materials were analyzed at a commercial laboratory for Ag, As, Cd, Cu, Co, Hg, Fe, Mo, Mn, Ni, Pb, Sb, V, and Zn by an aqua-regia digestion followed by AAS. Original geochemical survey results were reported in Geological Survey of Canada Open File 1216 (Geological Survey of Canada, 1986). In 2005, archived stream sediment samples from the survey were reanalyzed at a second commercial laboratory for 37 elements, including those listed above, by leaching a 1 g sample with a HCl-HNO₃-H₂O (2:2:2, volume of solute per volume of solvent [v/v]) mixture at 95°C for one hour and then measuring the concentration of the 37 elements in the diluted solution by ICP-MS (Lett and Bluemel, 2006). The original As, Cd, Cu, Co, Hg, Fe, Mo, Mn, Ni, Pb, Sb, V and Zn values from 1986 can be compared statistically with archived sample determinations to establish if there are differences between the two datasets. A two-sample t-test is

¹ Noble Exploration Services Ltd., Sooke, BC

This publication is also available, free of charge, as colour digital files in Adobe Acrobat® PDF format from the BC Ministry of Energy, Mines and Petroleum Resources website at <http://www.empr.gov.bc.ca/Mining/Geoscience/PublicationsCatalogue/Fieldwork/Pages/default.aspx>.

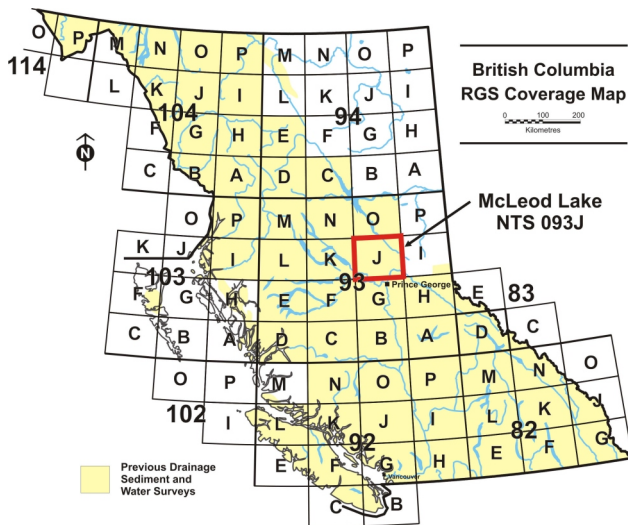


Figure 1. Location of the NTS 093J regional geochemical survey (RGS) area, British Columbia.

applied to determine if there is a difference at the 0.05% significance level between the population means for aqua-regia digestion and AAS compared to HCl-HNO₃-H₂O digestion and ICP-MS measured values. Silver was not included in the test because there is a large difference between the AAS and ICP-MS detection limits. An analysis of variance (F-test) is applied before the t-test to establish if the two populations have an equal or unequal variance. Once equality or inequality of variance is established, the appropriate t-test is applied to test the null hypothesis (*H₀*) that there is no significant difference between element population means (Davis, 1973). In Table 1, the t-test results for the 1986 aqua-regia digestion and AAS determined elements compared to the 2006 HCl-HNO₃-H₂O digestion and

Table 1. Summary of a t-test to determine if there is a difference at the 0.05% significance level between the population mean for elements (in 1152 stream sediment samples from NTS 093J, central British Columbia) determined by aqua-regia digestion followed by atomic absorption spectrophotometry (AAS) compared to means for the same samples reanalyzed by HCl-HNO₃-H₂O digestion followed by inductively coupled plasma-mass spectrometry (ICP-MS). A blue to red bar indicates a significant difference whereas a green bar indicates no difference. A red bar shows the higher of the two means. All values except Fe have been logarithmically transformed before statistical analysis.

Element	AAS	ICP-MS	AAS Mean	ICP-MS Mean
As (ppm)			4.5	4.7
Cd (ppm)			0.4	0.46
Co (ppm)			10	11
Cu (ppm)			24	24.61
Fe (%)			2.14	2.22
Hg (ppb)			141	132
Mn (ppm)			741	747
Mo (ppm)			2	1.06
Ni (ppm)			36	39.3
Pb (ppm)			5	7.5
Sb (ppm)			0.4	0.33
V (ppm)			37	40
Zn (ppm)			72	74.5

ICP-MS values are summarized. A blue to red bar (low to high) indicates a significant difference between the means whereas a green bar indicates no difference. A comparison of the population means listed in Table 1 shows that they are generally very similar, allowing for differences in method detection limit. However, the t-test indicates that there is a statistical difference between the population means for 9 of the 13 elements and that only Cu, Fe, Mn and V results from 1986 appear to be comparable to the 2006 data.

YEAR TO YEAR COMPARISON: ANALYSIS OF REFERENCE MATERIAL FROM THE QUEST SURVEY AREAS

A similar pattern of statistical differences can also be observed when comparing control reference sample data that was reported by the same laboratory, but determined in different years. Data used in this study comprised a single standard that had been randomly inserted 77 times into the sample sequence of two separate Geoscience BC data-reanalysis projects in two years (Jackaman, 2008, 2009). Each analytical project included element determinations (by aqua-regia digestion followed by ICP-MS) for several thousand samples originating from a number of previous RGS programs. For most of the elements, t-test results indicated a difference in population means that was considered statistically significant with the exception of Au, Mn and Mo. In terms of their scientific significance with regards to exploration geochemistry, only the mean differences for Ag and Hg were found to be sufficiently large that they could have an adverse influence when interpreting merged data from several sources. These results suggest that combining data from different surveys into a single analytical package for large-scale reanalysis projects helps reduce the analytical variability commonly associated with complex geochemical datasets.

INTERLABORATORY COMPARISON: ANALYSIS OF REFERENCE STANDARD BY AQUA-REGIA DIGESTION FOLLOWED BY ICP-MS

Partial dissolution of minerals in stream sediment and soil samples by aqua-regia digestion followed by ICP-MS analysis is now commonly available commercially for routine determination of up to 50 ore-indicator and pathfinder elements, including Ag, As, Cd, Co, Cu, Fe, Hg, Mo, Mn, Ni, Pb, Sb, V and Zn. Acid digestion methods and ICP-MS analysis have been previously reviewed by Chao and Sanzalone (1992) and Hall (1992). While aqua-regia digestion is sufficiently aggressive to completely dissolve native Au and most mineral sulphides, it will only partially release metals from mineral oxides and rock-forming aluminosilicate minerals. The amount of metal liberated by the acid mixture from oxide, silicate and refractory minerals can vary depending on the reaction conditions such as digestion temperature, digestion time and operating conditions of the instruments used to measure element concentrations in the solution. Consequently, identical samples, when analyzed by different laboratories using an aqua-regia digestion followed by a combination of ICP-ES and ICP-MS, may return slightly different element concentrations from each laboratory. The disparity between element values detected by different laboratories in the same sample may be small

and have negligible effect on the ability to distinguish element anomalies within data generated from detailed, property-scale surveys. However, the small differences become more critical when attempting to merge and level large-scale survey analytical data from several independent sources. Consequently, it was decided to have several laboratories analyze geochemical standard reference materials for Ag, As, Cd, Co, Cr, Cu, Fe, Hg, Mn, Mo, Ni, Pb, Sb, V and Zn using aqua-regia digestion followed by ICP-MS and then compare the results reported.

Sample Batch Preparation and Geochemical Analysis

A batch of samples, consisting of CANMET stream sediment standards STSD-1, STSD-3 and STSD-4, was assembled for analysis. A single bottle of each CANMET standard was homogenized for two hours in a roller mixer, the contents of the bottle decanted on a clean paper sheet and 4–5 g aliquots measured into three groups of pre-numbered Ziploc® bags. The standards were then assembled in random order and assigned a unique, blind identification number to create three identical sample batches. Each batch was submitted to a commercial laboratory for routine aqua-regia digestion followed by ICP-MS. The analytical method requested at each laboratory was that routinely used to generate regional geochemical survey data for the BC Geological Survey (BCGS) and Geoscience BC (Jackaman, 2009).

Results of the Geochemical Analysis

Statistical analysis of the reported geochemical data for the standards is in progress and final results will be reported in a future publication. For this reason, only preliminary results will be presented and discussed in this paper. Mean and percent relative standard deviation (%RSD) have been calculated from eight, repeat, random determinations of each of the CANMET drainage sediment standards (STSD-1, STSD-3, STSD-4). The samples were analyzed for elements including those noted above. Table 2 lists the mean and %RSD values for the elements in standard STSD-1 determined by each laboratory, along with the corresponding CANMET recommended mean value reported by Lynch (1990), for a concentrated HCl-HNO₃ digestion followed by ICP-MS. Most of the mean values for elements reported by the laboratories are within 15% of the CANMET recommended mean value. However, the mean value reported by individual laboratories may be higher or lower depending on the element determined in STSD-1. Among likely reasons for the variations observed between laboratory reported and recommended means for elements in STSD-1 are differences in the detection limit reported by a laboratory for some of the elements and the conditions of the analytical method used, including the digestion procedure. Analytical precision, based on the %RSD values, is

commonly better than 5% for most of the elements in STSD-1. Larger %RSD values, greater than 5%, for Ag, Mo and Hg can be explained by a higher detection limit for these elements reported by some of the laboratories and the influence of a wider range of high or low outlier values on calculated precision.

CONCLUSIONS

Comparison of geochemical data from identical regional stream sediment samples analyzed first by an aqua-regia digestion followed by AAS and then later by HCl-HNO₃-H₂O digestion followed by ICP-MS reveals small, but statistically significant differences between the population mean values for 9 of the 13 elements determined. There are also statistically significant differences between the population mean values for the majority of elements measured from year to year in sediment reference standards by aqua-regia digestion followed by ICP-MS at one laboratory.

CANMET standard reference materials have been analyzed repeatedly by aqua-regia digestion followed by ICP-MS at several commercial laboratories. Precision (%RSD) for most of the elements reported from the aqua-regia digestion followed by ICP-MS analysis are within limits ($\pm 15\%$) that are generally accepted as satisfactory for routine geochemical exploration purposes. However, differences between mean values reported by each laboratory for a reference standard suggest that the raw data from different laboratories, while of good quality, should be used with caution when merged and processed to display large regional geochemical patterns.

ACKNOWLEDGMENTS

The authors appreciate constructive comments on a preliminary draft of this paper by Tania Demchuk, BCGS.

Table 2. Mean and relative standard deviation (%RSD) for elements in Canada Centre for Mineral and Energy Technology (CANMET) sediment standard STSD-1, determined by laboratories A, B and C by an aqua-regia digestion followed by inductively coupled plasma-mass spectrometry. The CANMET recommended means for STSD-1 are from Lynch (1990).

Element	Lab A Mean	Lab B Mean	Lab C Mean	CANMET Mean	Lab A %RSD	Lab B %RSD	Lab C %RSD
Ag (ppb)	308	268	328	300	6.9	4.9	3.4
As (ppm)	18.9	20.6	20.9	17	2.2	2.3	2.7
Cd (ppm)	0.93	1.08	0.86	0.8	4.2	4.7	3.4
Co (ppm)	13.4	13.9	13.6	14.00	1.6	2.9	2.7
Cr (ppm)	24.4	28.6	26.1	28.00	2.6	2.5	2.4
Cu (ppm)	31.63	37.94	34.40	36.00	2.2	2.3	2.5
Fe (%)	3.53	3.39	3.28	3.50	1.7	1.8	2.6
Hg (ppb)	112	101	109	110.00	3.3	5.0	6.0
Mn (ppm)	3810	3729	3499	3740	1.3	2.5	2.7
Mo (ppm)	0.97	0.99	1.02	2	5.9	2.0	2.7
Ni (ppm)	16.9	21.1	19.6	18	2.9	3.1	2.4
Pb (ppm)	33.86	38.11	32.48	34	4.5	3.3	3.9
Sb (ppm)	2.27	2.46	2.31	2	2.4	3.9	3.6
V (ppm)	44	46	45	47	3.4	2.3	2.8
Zn (ppm)	157.08	166.68	158.88	165	2.4	2.8	2.6

REFERENCES

- Chao, T.T. and Sanzolone, R.F. (1992): Decomposition techniques; *Journal of Geochemical Exploration*, Volume 44, pages 65–106.
- Davis, J.C. (1973): Statistics and data analysis in geology; *John Wiley and Sons*, New York, 550 pages.
- Day, S.J., Matysek, P.F. and Johnson, W.M. (1988): The regional geochemical survey: evaluation of an ICP-ES package; in *Geological Fieldwork 1987, BC Ministry of Energy, Mines and Petroleum Resources*, Paper 1988-1, pages 503–508.
- Garrett, R.G. (1974): Field data acquisition methods for applied geochemical surveys at the Geological Survey of Canada; *Geological Survey of Canada*, Paper 74-62, 36 pages.
- Geological Survey of Canada (1986): National Geochemical Reconnaissance - British Columbia regional geochemical survey - McLeod Lake (NTS 93J); *Geological Survey of Canada*, Open File 1216 and *BC Ministry of Energy, Mines and Petroleum Resources*, Regional Geochemical Survey 15.
- Hall, G.E.M. (1992): Inductively coupled mass spectrometry in geoanalysis; *Journal of Geochemical Exploration*, Volume 44, pages 201–250.
- Jackaman, W. (2008): QUEST Project sample reanalysis; *Geoscience BC*, Report 2008-3.
- Jackaman, W. (2009): QUEST-West Project sample reanalysis (NTS 93E, 93F, 93L, 93M); *Geoscience BC*, Report 2009-5.
- Lett, R.E.W. (2005): Regional geochemical survey database on CD; *BC Ministry of Energy, Mines and Petroleum Resources*, GeoFile 2005-17, CD-ROM.
- Lett, R.E.W. and Bluemel, B. (2006): A reanalysis of regional geochemical stream sediment samples from the McLeod Lake area (NTS map sheet 93J); *BC Ministry of Energy, Mines and Petroleum Resources*, GeoFile 2006-9.
- Lynch, J. (1990): Provisional element values for eight new geochemical lake sediment and stream sediment reference materials. LKSD-1, LKSD-2, LKSD-3, LKSD-4, STSD-1, STSD-2, STSD-3, STSD-4; *Geostandards Newsletter*, Volume 14, pages 153–167.